The Journal of American Science

ISSN 1545-1003

Volume 6 - Number 7 (Cumulated No. 28), July 1, 2010, ISSN 1545-1003

Marsland Press, Michigan, The United States

The Journal of American Science

The ***Journal of American Science*** is an international journal with a purpose to enhance our natural and scientific knowledge dissemination in the world. Any valuable paper that describes natural phenomena and existence or any reports that convey scientific research and pursuit is welcome. Papers submitted could be reviews, objective descriptions, research reports, opinions/debates, news, letters, and other types of writings that are nature and science related. All the manuscripts will be processed in a professional peer review. After the peer review, the journal will make the best efforts to publish all the valuable works as soon as possible.

Introductions to Authors

1. General Information

(1) Goals: As an international journal published both in print and on internet, *The Journal of American Science* is dedicated to the dissemination of fundamental knowledge in all areas of nature and science. The main purpose of *The Journal of American Science* is to enhance our knowledge spreading in the world. It publishes full-length papers (original contributions), reviews, rapid communications, and any debates and opinions in all the fields of nature and science.

(2) What to Do: *The Journal of American Science* provides a place for discussion of scientific news, research, theory, philosophy, profession and technology - that will drive scientific progress. Research reports and regular manuscripts that contain new and significant information of general interest are welcome.

(3) Who: All people are welcome to submit manuscripts in any fields of nature and science.

(4) Distributions: Web version of the journal is opened to the world. The printed journal will be distributed to the selected libraries and institutions. For the subscription of other readers please contact with: editor@americanscience.org or americansciencej@gmail.com or editor@sciencepub.net

(5) Advertisements: The price will be calculated as US$400/page, i.e. US$200/a half page, US$100/a quarter page, etc. Any size of the advertisement is welcome.

2. Manuscripts Submission

(1) Submission Methods: Electronic submission through email is encouraged and hard copies plus an IBM formatted computer diskette would also be accepted.

(2) Software: The Microsoft Word file will be preferred.

(3) Font: Normal, Times New Roman, 10 pt, single space.

(4) Indent: Type 4 spaces in the beginning of each new paragraph.

(5) Manuscript: Don't use "Footnote" or "Header and Footer".

(6) Cover Page: Put detail information of authors and a short title in the cover page.

(7) Title: Use Title Case in the title and subtitles, e.g. "**Debt and Agency Costs".**

(8) Figures and Tables: Use full word of figure and table, e.g. **"Figure 1.** Annul Income of Different Groups**", Table 1. Annual Increase of Investment".**

(9) References: Cite references by "last name, year", e.g. "(Smith, 2003)". References should include all the authors' last names and initials, title, journal, year, volume, issue, and pages etc.

Reference Examples:

Journal Article: Hacker J, Hentschel U, Dobrindt U. Prokaryotic chromosomes and disease. Science 2003;301(34):790-3.

Book: Berkowitz BA, Katzung BG. Basic and clinical evaluation of new drugs. In: Katzung BG, ed. Basic and clinical pharmacology. Appleton & Lance Publisher. Norwalk, Connecticut, USA. 1995:60-9.

(10) Submission Address: editor@sciencepub.net, Marsland Company, P.O. Box 21126, Lansing, Michigan 48909, The United States, 517-980-4106.

(11) Reviewers: Authors are encouraged to suggest 2-8 competent reviewers with their name and email.

2. Manuscript Preparation

Each manuscript is suggested to include the following components but authors can do their own ways:

(1) Title page: including the complete article title; each author's full name; institution(s) with which each author is affiliated, with city, state/province, zip code, and country; and the name, complete mailing address, telephone number, facsimile number (if available), and e-mail address for all correspondence.

(2) Abstract: including Background, Materials and Methods, Results, and Discussions.

(3) Key Words.

(4) Introduction.

(5) Materials and Methods.

(6) Results.

(7) Discussions.

(8) References.

(9) Acknowledgments.

Journal Address:
Marsland Press
PO Box 180432, Richmond Hill, New York 11418, USA
Telephones: 347-321-7172; 718-404-5362; 517-349-2362
Emails: editor@americanscience.org; americansciencej@gmail.com; sciencepub@gmail.com
Websites: http://www.americanscience.org; http://www.sciencepub.net; http://www.sciencepub.org

The Journal of American Science

ISSN 1545-1003

Volume 6, Issue 7

Cover Page, Introduction, Contents, Call for Papers, am0607

The following manuscripts are presented as online first for peer-review, starting from May 1, 2010.

All comments are welcome: editor@americanscience.org

Welcome to send your manuscript(s) to: americansciencej@gmail.com.

CONTENTS

	content was between 2.1 g/100g in soybean and 7.2 g/100g in lima bean. The seed of soybean was least in concentrations of phytic acid, trypsin inhibitor, saponin and oxalate whereas significant ($P<0.05$) variations were observed among the under-utilized grain legume (UGL) seeds for these anti-nutrients. The metabolizable energy (ME), Organic matter digestibility (OMD) and short chain fatty acids (SCFA) of the UGL seeds differed ($P<0.05$) significantly. The ME was between 8.8 and 12.1 MJ/Kg, OMD was between 49.6 and 80.5% while the SCFA ranged from 0.7 to 1.2 mmol. Gas production characteristics revealed that methanogenesis was low in jack beans (35 ml) and highest in soybean (48.7 ml), potential gas production, b, was between 23.4 ml in lima bean and 38.5 ml in soybean. The rate of substrate fermentation was lowest in jack bean and highest soybean. It is concluded that among the UGL seeds investigated Lima bean, pigeon pea and jack bean seeds are unsuitable as feed resources for ruminant livestock. [Journal of American Science 2010;6(7):1-7]. (ISSN: 1545-1003). **Keywords:** Degradation coefficients, gas fermentation, secondary metabolites, under-utilized grain legume seeds	
2	**Application of Elovic and Bhattacharya/Venkobacharya Models to Kinetics of Herbicide Sorption by Poultry Based Adsorbent: A GCMS External Standard Approach.** Itodo Adams Udoji[1],FunkeWosilat Abdulrahman[2],Lawal Gusau Hassan[3],S.A.Maigandi[4],Happiness Ugbede Itodo[5] [1]Department of Applied Chemistry, Kebbi State University of Science and Technology, Aliero, Nigeria [2]Department of Chemistry, University of Abuja, Nigeria [3]Department of Pure and Applied Chemistry, Usmanu Danfodiyo University, Sokoto, Nigeria [4]Faculty of Agriculture, Usmanu Danfodiyo University, Sokoto, Nigeria [5]Department of Chemistry, Benue State University, Makurdi, Nigeria *itodoson2002@yahoo.com* **Abstract:** Three kinetic models were utilized in analyzing the removal of Atrazine from herbicide solution by its adsorption onto acid treated Poultry dropping Activated carbon. The forecasted pseudo-first order (with K_1=0.00921min^{-1}) was proven unfit in predicting the adsorption rate by the Bhattacharya and Venkobacharya rate constant which is approximately the same (k_a= -0.009212min^{-1}) but opposite in sign to the former. The linearity of (U)T shows that atrazine molecule has great accessibility to the adsorbent molecule .Desorption constant by the Elovic model was estimated as 12.987g/mg. Other parameters investigated to increase linearly with contact time include the fractional attainment at equilibrium(Ca/Co),equilibrium constants(Kc), sorption efficiency (%RE) and Gibbs free energy (-ΔG). [Journal of American Science 2010;6(7):8-18]. (ISSN: 1545-1003). **Key words:** *Poultry dropping, Kinetics, Herbicide, Sorption, Activated carbon.GC/MS*	Full Text
3	**GC/MS Batch Equilibrium study and Adsorption Isotherms of Atrazine Sorption by**	Full Text

Activated H_3PO_4 - Treated Biomass.

Itodo Adams Udoji[1],Funke Wosilat Abdulrahman[2],Lawal Gusau Hassan[3],S.A.Maigandi[4],Happiness Ugbede Itodo[5]
[1]Department of Applied Chemistry, Kebbi State University of Science and Technology, Aliero, Nigeria
[2]Department of Chemistry, University of Abuja, Nigeria
[3]Department of Pure and Applied Chemistry, Usmanu Danfodiyo University, Sokoto, Nigeria
[4]Faculty of Agriculture, Usmanu Danfodiyo University, Sokoto, Nigeria
[5]Department of Chemistry, Benue State University, Makurdi, Nigeria
itodoson2002@yahoo.com

Abstract: Acid modified abundant lignocellulose Agricultural wastes, Sheanut shells (SS/A) was used to develop activated carbon and applied to removal of Agrochemical(Atrazine) from a multicomponent herbicide solution. A GCMS which can separate, detect and measure the target (sorbate) was applied to estimate equilibrium phase atrazine. Generated data were tested with 3 isotherm models.Extent of fitness follows the order Freundlich (R^2=0.994)>Langmuir (R^2=0.977)>BET (R^2=0.894) implying that surface coverage is more of heterogeneous. Freundlich adsorption capacity was valued at 0.045 x10^{-3} K_F (units in mgg^{-1} ($1mg^{-n(n)}$). Study of the effect of initial sorbate concentration (%RE) revealed that adsorption efficiency increases linearly with time in a range of 46.08% (for SS/A/5gdm^3) to 66.324 (for SS/A/25gdm^3).Generally,t he GCMS quantitation via external standard methods shows that sorted waste could be a potential source of active filter for atrazine sorption. [Journal of American Science 2010;6(7):19-29]. (ISSN: 1545-1003).

Keywords:: Sheanut shells; Atrazine; Activated carbon; GCMS

4

An Assessment of Fluid Inclusions Composition Using the Raman Spectroscopy at Daleishan Goldfield, Dawu County, Hubei Province, P.R. China.

Full Text

Diarra Karim [1*], Hanlie Hong [2]

[1]China University of Geosciences, Wuhan, 430074, China
[2] Faculty of Earth Sciences, China University of Geosciences, Wuhan, 430074 (Hubei province), China
[*]Corresponding Author: E mail: bn_cogem@yahoo.fr

Abstract: The purpose was to assess fluid inclusions composition in the Goldfield, Hubei province, China. The laser Raman spectroscopy was used as an analytical tool. The results show that water and carbon dioxide (70 %), and quartz (10 %) are the primary and secondary compositions of most of the inclusions, respectively. A number of three phase inclusions were low and inclusion size varies from 1 to 27µm. The density of CO2 fluid inclusions measured in quartz mineral varied from 0.61 to 0.96 g/cm3. No traces of other gases such as hydrogen (H2), ethylene (C2H2), ethene (C2H4), benzene (C6H6), hydrogen sulphide (H2S) and carbon monoxide (CO) were observed, confirming epithermal origin of the deposit (quartz ± calcite± adularia ± illite assemblage). In Daleishan goldfield, according to inclusion composition, vapor and liquid may be main agent transports for gold in epithermal systems as well as for silver. [Journal of American Science 2010;6(7):30-37]. (ISSN: 1545-1003).

Key words: Auriferous veins, Raman spectroscopy, inclusions fluids, Daleishan Goldfield, quartz

5

Early-age compressive strength assessment of oil well class G cement due to borehole pressure and temperature changes

Mojtaba Labibzadeh [1], Behzad Zahabizadeh [1], Amin Khajehdezfuly [1]
[1.] Department of Civil Engineering, Faculty of Engineering, Shahid Chamran University, Ahvaz, Iran
Labibzadeh_m@scu.ac.ir

Abstract: Development of high early-age compressive strength oil well cement is an important task in the oil well cement design. Achievement of suitable early-age compressive strength of oil well cement ensures both the structural support for the casing and hydraulic/mechanical isolation of borehole intervals. Holding this issue in mind, in this research, the effect of pressure and temperature changes inside the borehole on the class G oil well cement compressive strength has been studied. In the proposed work, in contrast to the mostly previous studies which considered some certain temperatures and atmospheric pressure in their tests, the effects of contemporary pressure and temperature changes on the early-age compressive strength of oil well cement have been investigated. Using a non-destructive method, the compressive strength of 48 hours cured cement samples under progressive changing of simultaneously pressures and temperatures coincident to a real oil well data were measured and recorded continuously at predefined intervals during this 48 hours period time. The case study was an oil well located in Darquain region of Khuzestan province in Iran. Obtained results showed that 8 and 12 hours aged samples have a maximum compressive strength in a certain combination of pressure and temperature, 51.7 MPa and 121°C, whereas 24, 45 and 48 hours aged samples have a minimum point in their compressive strength curve at 17.2 MPa and 68°C and a maximum point at 41.4 MPa and 82°C. All the samples show the significant reduce (up to approximately 70%) in compressive strength after the 51.7 MPa and 121°C point. Considering the case study oil well profile of borehole pressure and temperature changes, this tested class G cement is recommended to use in cementing job from ground level down to the almost 4000 m below the surface. [Journal of American Science 2010;6(7):38-47]. (ISSN: 1545-1003).

Keywords: Compressive Strength, Oil Well, Cementing, borehole Pressure and Temperature

Full Text

6

Influence of Oil Well Drilling Waste on the Engineering Characteristics of Clay Bricks

Medhat S. El-Mahllawy* and Tarek A. Osman
Raw Building Materials Technology and Processing Research Institute
Housing and Building National Research Center, Egypt
Email: medhatt225@yahoo.com

Abstract: Huge quantities of oil-based mud waste were produced during oil we

Full Text

	drilling operations in Egypt. These quantities are environmental hazards an usually disposed in open pits that constructed during drilling operations. Thes pits, approximately 50 years old, resemble an extreme environmental and healt hazards integrated with fire and dangerous sinking risks. Consequently, the mai objective of this paper is to explore the influence of oil well drilling wast basically oil based mud waste, on the engineering characteristics of th manufactured environmentally friendly, sufficient performing red clay buildin brick. Compositions of the used materials as well as physico-mechanic characteristics of fired briquettes were investigated. The laboratory resu demonstrate that the water absorption, bulk density, efflorescence an compressive strength of the fired briquettes are met the acceptable limits Egyptian Standard No. 204-2005 for clay masonry units used for load and no load bearing walls construction. The reuse of this waste material in the buildin industry will contribute to the protection of the environment through gre advantages in waste minimization and beneficial income to the communit through the utilization process in building industry. [Journal of American Scien 2010;6(7):48-54]. (ISSN: 1545-1003). **Keywords:** Oil-based mud, clay brick, physico-mechanical properties, bearing walls construction	
7	**Mass Multiplication of *Celastrus paniculatus* Willd - An Important Medicinal Plant Under *In Vitro* Conditions using Nodal Segments** Devi Lal and Narender Singh* Department of Botany, Kurukshetra University,Kurukshetra, Haryana, India—136119. nsheorankuk@yahoo.com **Abstract:** A rapid clonal propagation system has been developed for *Celastrus paniculatus* (Celastraceae) an important medicinal plant under *in vitro* conditions. Nodal explants from mature plant of this species were collected and cultured on MS medium supplemented with various concentrations (0.5, 1.0 and 2.0 mg l^{-1}) of cytokinins (BAP and Kn) and auxins (IAA, NAA and 2, 4-D) alone and in various combinations under controlled condition of 16 hours of photoperiod and 8 hours dark period at a temperature of 25±2ºC. The maximum number of shoots (8.9±0.5) along with hundred per cent bud break was recorded in the MS medium supplemented with 1.0 mg l^{-1} BAP. Most of the combinations of cytokinins with IAA induced the formation of less number of shoots. The *in vitro* regenerated shoots were excised aseptically and implanted on full and half strength MS medium without or with growth regulators (IAA, NAA and IBA) at the concentrations of 0.5 and 1.0 mg l^{-1} for rooting. MS half strength medium supplemented with 0.5 mg l^{-1} NAA proved best with hundred per cent rooting. The regenerated plantlets were successfully acclimatized in pots containing sterilized soil and sand mixture (3:1). The plantlets were then transferred to the field conditions. Seventy per cent of the regenerants survived well. [Journal of American Science 2010;6(7):55-61]. (ISSN: 1545-1003). **Key words*:*** Micropropagation, nodal segments, multiple shoots, *Celastrus paniculatus.*	Full Text
8	**Fatigue Analysis of Hydraulic Pump Gears of**	Full Text

JD 955 Harvester Combine Through Finite Element Method

Hassan seyed Hassani [1], Ali Jafari [2*], Seyed Saed Mohtasebi [2] and Ali Mohammad Setayesh [3]
[1.] Msc Student in Mechanic of Agricultural Machinery, University of Tehran, Karaj, Iran.
e-mail: hshasani@yahoo.com
[2.] Members of Scientific Board of Faculty of Engineering & Agricultural Technology, University of Tehran, Karaj, Iran.
[*] Corresponding author, Phone number: e-mail: jafarya@ut.ac.ir
[3.] Department of Research & Development, ICM Company, Arak, Iran.

Abstract: Throughout the present research, the gears fatigue of the hydraulic pump in JD 955 harvester combine was investigated through the finite element method and using contact analysis for precise determination of the contact region of the engaged teeth so that their lifespan was estimated. The reason for performing this research was to study the intended gears behaviour affected by fatigue phenomenon due to the cyclic loadings and to consider the results for more savings in time and costs, as two very significant parameters relevant to manufacturing. The results indicate that with fully reverse loading, one can estimate longevity of a gear as well as find the critical points that more possibly the crack growth initiate from. For the investigated gears, the most critical points were detected as nodes numbered 36573 and 37247. Furthermore, the allowable number of load cycles and using fully reverse loading was gained 0.9800E+07. It is suggested that the results obtained can be useful to bring about modifications in the process of the above-mentioned gears manufacturing. [Journal of American Science 2010;6(7):62-67]. (ISSN: 1545-1003).

Key words: Harvester combine; Fatigue; Longevity; Finite element; Optimization; Contact analysis

9

Subsurface Geophysical Estimation of Sand Volume in Ogudu Sandfilled area of Lagos, Lagos, Nigeria.

Adeoti Lukumon [1], Oyedele K. Festus [1] and Adegbola R. Bolaji [2]
[1.]Department of Geosciences University of Lagos, Lagos Nigeria
[2.]Department of Physics, Lagos State University, Lagos Nigeria.

lukuade@yahoo.com, kayodeunilag@yahoo.com

Abstract
Surface geophysical survey was carried out using Electrical resistivity and induced polarization methods to estimate volume of sand deposits for the purpose of development/exploitation via dredging in Agboyi area of Lagos State .The study area was divided into square, rectangular, triangular and trapezoidal cells before conducting the geophysical survey. A total of 125 Vertical electrical sounding (VES) data were collected using Schlumberger electrode configuration with an electrode spacing varying between 100 and

Full Text

400m. Five wells were also drilled for the collection of soil samples with a view to mapping the litho-logical variations of the subsurface strata. The combination of Vertical electrical sounding (VES) data, Induced Polarization (IP) data and well log data were used in inferring the litho-logical units of each geo-electric layer within the study area. The geo-electric sections delineate three to five subsurface layers, which include sand, sandy clay/ clayed sand, and clay. The 2-D and 3-D Isopach maps show the distribution of sand with thickness ranging between 0.5m and 7.0m.The volume of sand within each cell was calculated and the results were summed to give a total volume of 165596.5712m^3 of sand as against 1.5million m^3 projected. Hence, the analysis shows that the study area is devoid of enough sands for the purpose of development/exploitation via dredging. [Journal of American Science 2010;6(7):68-77]. (ISSN: 1545-1003).

Keywords: Vertical Electrical sounding (VES); Geoelectric Section; Lithological

10

Cell surface hydrophobicity (CSH) of *Escherichia coli*, *Staphylococcus aureus* and *Aspergillus niger* and the biodegradation of Diethyl Phthalate (DEP) via Microcalorimetry.

Alhaji Brima Gogra [a,d], Jun Yao [a,*], Edward H. Sandy [a], ShiXue Zheng [b], Gyula Zaray [c], Zheng Hui [b]

[a] State Key Laboratory of Biogeology and Environmental Geology of Chinese Ministry of Education, School of Environmental Studies and Sino-Hungarian Joint Laboratory of Environmental Science and Health, China University of Geosciences, 430074 Wuhan, PR China.

[b] State key Laboratory of Agricultural Microbiology, College of Life Science and Technology, Huazhong Agricultural University, 430070 Wuhan, PR China.

[c] Department of Chemical Technology and Environmental Chemistry, Eötvös University, H-1518 Budapest, P.O. Box 32, Hungary.

[d] Department of Chemistry, School of Environmental Sciences, Njala University, Sierra Leone.

* Corresponding author. E-mail address: yaojun@cug.edu.cn (J. Yao) or abgogra@yahoo.co.uk (A. B. Gogra)

Abstract: This work was focused on investigating the occurrence of cell surface hydrophobic (CSH) character among diethyl phthalate (DEP)-degrading microbes (*Escherichia coli*, *Staphylococcus aureus*, and *Aspergillus niger*) by evaluating the effect of DEP on microbial cell surface hydrophobicity and to investigate any relationship between cell surface hydrophobicity and the ability of such microbes to degrade DEP using microcalorimetry and other methods. In this study, a TAM III multi-channel microcalorimeter, at 28 ^{o}C, was used to measure the minimum inhibitory concentration (MIC) of DEP and the DEP biodegradation efficiency by fitting the thermogenic curves and integrating the area limited by these curves, respectively. Using MATHS (microbial adhesion to hydrocarbons) assay, CSH of the microbial cells was determined as a measure of their adherence to the hydrophobic n-octane. From

Full Text

the experimental data, *S. aureus* was found to be the most efficient DEP degrader and *E. coli* the least and that *S. aureus* showed high, whilst *E. coli* and *A. niger* showed moderate hydrophobicity and autoaggregation abilities. There were positive correlations between microbial cell surface hydrophobicity and autoaggregation ability, DEP biodegradability, IC_{50} values for the tested strains. [Journal of American Science 2010;6(7):78-88]. (ISSN: 1545-1003).

Keywords: Hydrophobicity, *Escherichia coli*, *Staphylococcus aureus*, *Aspergillus niger*, Microcalorimetry, Diethyl phthalate, Autoaggregation, IC_{50}.

11

Effect of planting dates and different levels of potassium fertilizer on growth, yield and chemical composition of sweet fennel cultivars under newly reclaimed sandy soil conditions

Full Text

Abou El-Magd, M. M. *Zaki, M. F.* and Camilia Y. Eldewiny**
* Department of Vegetable Res., National Research Centre (NRC), Dokki, Cairo, Egypt
**Department of Soil and Water Use, National Research Centre (NRC), Dokki, Cairo, Egypt.

Abstract: Two field experiments were conducted at the Agricultural research Station, National Research Centre, El-Nobaria province, El Beheira Governorate, Egypt, during the two successive winter seasons of 2007/2008 and 2008/2009 on sweet in an area of newly reclaimed soil to study the effect of transplanting dates and different rates of potassium salphate fertilizer on vegetative growth, yield, quality and chemical content of six sweet fennel cultivars (cvs. Dolce, Zefa Fino, Selma, Fino, De Florance and Zwejahrig). Transplanting dates were early (15th September) and late (1st October) combined with four rates of potassium salphate,i.e. 0, 45, 60 and 75 kg K_2O/ fedd.(Feddan = 0.40 ha.). Results indicated that transplanting dates differed statistically in their effect on the vegetative growth of sweet fennel plants. The highest vegetative growth expressed as plant height, leaves number /plant, fresh and dry weight of the total plant and its organs, bulb dimensions (thickness, width and length); total green yield and macro-nutrients content in leaves and bulbs (N, P and K) were obtained by early plantation (15th September). On the other hand, lower values of vegetative growth, green yield and quality of bulbs were obtained in the late plantation (1st October). Results summarized that sweet fennel cultivars as mentioned previously differed statistically in their vegetative growth, bulb dimensions and total green yield as well as chemical content in leaves and bulbs of sweet fennel plants. Zwejahrig cultivar was superior in its vegetative growth expressed as plant height; leaves number; fresh and dry weight of the total plant and its organs; bulb dimensions (thickness, width and length); total green yield and macro-nutrients (N, P and K) content in leaves and bulbs compared with other cultivars. On the other hand, the lowest values were recorded by cvs. Dulce and Zefa Fino. With respect to potassium fertilizer rates, results reveal that sweet fennel plants treated with 75 kg K_2O/ fed. showed higher vegetative growth parameters (plant length, leaves number and bulb dimensions, thickness, width and length), fresh and dry weight of leaves, bulbs and total plant; total green yield; physical bulb quality (flatten, cylinder and elongated shape ratios) and macro-nutrients content (N, P and K) in tissues of sweet fennel leaves and bulbs than

	he lower rates of potassium. The results indicated that combined effect of ransplanting dates and cultivars of sweet fennel caused significant increases in egetative growth, green yield, bulb quality and chemical contents. The highest egetative growth, yield and quality as well as chemical contents were btained by cv. Zwejahrig combined with early date. The interaction effect etween cultivars and rates of potassium fertilizer gave a significant increase in egetative growth, bulb yield and chemical constituents. The highest values ere obtained by adding the highest potassium rate (75 kg K_2O / fed.) to cv. wejahrig plants. The highest values were obtained by early date combined ith the highest potassium rate (75 kg K_2O/ fed.). In addition, the highest egetative growth with the maximum total green yield was obtained under the ombination of cv. Zwejahrig in early date and the highest potassium rate. Journal of American Science 2010;6(7):89-105]. (ISSN: 1545-1003). **Key words**: Sweet fennel; Cultivars; Sowing dates; Potassium mineral fertilizer; N; P; K; Green yield and quality; Chemical content	
12	**An Expertise Recommender System for Web Cooperative Production** Muhammad Aslam[1], Ana Maria Martinez Enriquez[2], Muhammad Tariq Pervez[3], Zakia Saeed[4] [1]Department of CS & E, U.E.T., Lahore, Pakistan [2]Department of CS, CINVESTAV-IPN, Mexico [3]Department of CS, Virtual University Shadman Campus, Lahore, Pakistan [4]Faisalabad Institute of Cardiology(FIC), Faisalabad, Pakistan tariq_cp@hotmail.com **Abstract:** This paper focuses on providing dedicated expertise recommender system to enhance awareness among group members, working in a distributed cooperative environment. Normally, coauthors lack the information about the production capabilities of their colleagues. As a result of this lack, when they need assistance for the production of complex objects (formulae, figures, style sheets, etc.) they ask their colleagues for help, consequently the authoring process is disturbed. On the other hand, personal referrals may not be useful due to human biasing, liking, and disliking. The existing expertise recommender systems work on user profiles containing user qualification, experience, and history of solved problems. These systems require manual database updation which can be performed by only skilled person. We treat the issue by developing an expertise recommender system which is in-charge to seamlessly observe user activities and to auto detect a possible human expert of elaborated productions on the basis of a generic criterion. Whenever, a participant is deduced as a novice having some production problem, the developed system recommends him/her the presence of an expert with whom the novice can communicate. The entire goal is to enhance awareness coordination among collaborator activities and hence to generate a consistent shared production. [Journal of American Science 2010;6(7):106-112]. (ISSN: 1545-1003). **Keywords:** Knowledge based systems, presence awareness, collaborative information filtering, recommender systems	Full Text
13	**Impact Of Emission Uniformity On Nutrients Uptake And Water And Fertilizers Use**	Full Text

Efficiency By Drip Irrigated 15 Years Old Washington Novel Orange Trees Grown On A Newly Reclaimed Sandy Area.

EL-Hady O.A[1]., S.M.Shaaban[2] and A.A.M., Mohamedin[3].
[1]Soils & Water use Dept. National Research Centre, Cairo, Egypt
[2]Water Relations and Field Irrigation Dept. National Research Centre, Cairo, Egypt
[3] Field Drainage Dept., Soils, Water and Environment Research Institute, Agriculture Research Center, Giza, Egypt
dr_mona_zaki@yahoo.co.uk

Abstract A two successive years (2008- 2009) completely randomized field experiment with four replications on ≈ 15 years old Washington novel orange trees was conducted in a drip irrigated newly reclaimed sandy area at Wadi El-Mollak, Ismailia governorate. Field emission uniformity (Eu) and absolute field emission uniformity (Eua) were determined for the area under study to be 85.6% for Eu and 86.8% for Eua. The irrigation system at the studied area could be considered as good. Although the uniformity of irrigation at the area under sandy has exceeded 85%, great differences were estimated between the discharge of the drippers that adversely affected the uniformity of growth, nutrients uptake, yield and both water and fertilizers use efficiency by the trees. With this respect, differences among the annual amounts of irrigation water received by the trees and consequently fertilizers dissolved in it have reached 43.1%. accordingly, significant variations were calculated to be 27.8% for leaf area, 26.7% for the dry weight of the leaves and 40.6% for obtained yield. Content of nutrients in the leaves of trees that received the maximum amount of irrigation water were higher than those of trees that received the minimum amounts by 18.3, 22.0, 25.8, 18.4 and 30.4% for N, P, K, Ca and Mg, respectively. Consequently, relative uptake of these nutrient took the same trend. Positive differences in this parameter were 45.3, 49.0, 51.8, 46.6 and 56.4% for the aforementioned nutrients, respectively. Values of water and fertilizers use efficiency by the trees were also greatly affected by the uniformity of irrigation. Higher amounts of irrigation water and applied fertilizers adversely affected both parameters. Improving the uniformity of emission of the trickle irrigation system to be more than 90% will lead to uniform fertigation. Uniform production (quantity and quality of fruits for each tree) is expected. [Journal of American Science 2010; 6(7):113-119]. (ISSN: 1545-1003).

Key Words: Trickle irrigation, Field emission uniformity, Sandy soil, novel orange, Water use efficiency, Nutrients uptake, Fertilizers use efficiency

14

Physiological Responses of Fennel (*Foeniculum Vulgare* Mill) Plants to Some Growth Substances. The Effect of Certain Amino Acids and a Pyrimidine Derivative

M. E. El-Awadi and Esmat A. Hassan*

Full Text

Botany Department, Division of Agricultural and Biological Research National Research Centre, Dokki, 12311, Cairo, Egypt.
*el_awadi@yahoo.com

Abstract: In the Green house of the Botany Department (winter season 2007/08-2008/09) fennel seeds (*Foeniculum vulgare* Mill), from Department of Medicinal and Aromatic Plants, were cultivated after 3 hours soaking in the amino acids methionine and tryptophan and in the pyrimidine derivative material (SG93) provided by the Department of The Pharmaceutical Industry, each at 100 and 500mg/l. Growth measurements and chemical analyses of the plant were carried out at juvenile and fruiting stages, i.e. age of 84 and 119 days respectively. The pre-sowing seed treatment with the growth substances; methionine, tryptophan and the pyrimidine derivative (SG93) resulted in significant increases in plant height, number of leaves, number of branches, fresh and dry weight of shoots, number of umbels per plant, weight of seeds per umbel and per plant , in comparison to control. The pre-sowing seed treatments led to an elevation of leaf photosynthetic pigments` content, total protein, total phenolic compounds in the shoots and in the yielded seeds as well as in the percentage of fixed and essential oils as compared to the control. The highest content of the essential oil percentage was obtained as a result of seed-soaking treatment in methionine at 100mg/l concentration. In this connection, anethol represented the major component of such a percentage. [Journal of American Science 2010; 6(7):120-125]. (ISSN: 1545-1003).

Key words: Essential oil, *Foeniculum vulgare,* growth, growth substances, productivity

15

Vegetative Growth and Chemical Constituents of Croton Plants as Affected by Foliar Application of Benzyl adenine and Gibberellic Acid

Soad, M.M. Ibrahim, Lobna, S. Taha and M.M. Farahat
Department of Ornamental Plant and Woody Trees, National Research Centre, Dokki, Cairo, Egypt

Abstract A pot experiment was conducted during 2008 and 2009 seasons at National Research Centre, Dokki, Cairo, Egypt, Research and Production Station, Nubaria. The aim of this work is to study the effect of foliar application with benzyl adenine (BA) at (50, 100 and 150 ppm) and gibberellic acid (GA_3) at (100, 150 and 200 ppm) on the vegetative growth and some chemical constituents of croton plants. Most of the criteria of vegetative growth expressed as plant height, number of branches and leaves/plant, root length, leaf area and fresh and dry weights of stem, leaves and roots were significantly affected by application of the two factors which were used in this study.All foliar applications of BA and GA_3 separately promoted all the aforementioned characters in this study, as well as chemical constituents i.e. Chl. (a and b), carotenoids, total soluble sugars, total indoles ,total soluble phenols and N, P and K content compared with control plants. The highest recorded data were obtained in plants treated with GA_3 200 pm for all chemical constituents and growth parameters, except stem diameter and number of branches/plant, and N, P and K % while BA 150 ppm gave the

Full Text

	highest stem diameter and number of branches and N, P and K % and content. [Journal of American Science 2010;6(7):126-130]. (ISSN: 1545-1003). **Keywords**: croton plant, benzyl adenine (BA) , gibberellic acid (GA3)	
16	**Ability of Immobilized Starter Cells and Metabolites to Suppress the Growth Rate and Aflatoxins Production by *Aspergillus flavus* in Butter** Kawther El-Shafei; *Eman M. Hegazy and Zeinab I. Sadek* Dairy Department and Food Toxicology and Contaminants Department, National Research Centre, Dokki, Egypt. *E-mail address: zozok1@yahoo.com **Abstract:** Antifungal activity of lactic acid bacteria (LAB)starter cultures, *Lactococcus lactis* ssp. *lactis* and *Leuconostoc mesenteroides* and their metabolites in single and mixed cultures were found to inhibit spoilage and aflatoxin production by *Aspergillus flavus* in butter ,and have potential as bio-preservative agents. Also, treating cream before churn with free cells culture proved to give the greatest antifungal control upon *A. flavus* growth and aflatoxin production; while the use of immobilized cells showed lower activity, then the immobilized metabolites of the mixed culture. In cream artificially contaminated with aflatoxin (B_1, B2, G_1andG_2) treated with immobilized cells or immobilized metabolites of the mixed cultures revealed a reduction of the concentration of aflatoxins recovered from butter made from this cream. The study indicated that the use of lactic acid bacteria and their metabolites in cream or butter have the potential to be as food-grade bio-preservatives for extending the shelf-life of butter and combating the problem of moulds and associated toxins. [Journal of American Science 2010;6(7):131-138]. (ISSN: 1545-1003).	Full Text
17	Development of Doubled Haploid Wheat Genotypes Using Chromosome Eliminating Technique and Assessment under Salt Stress *A. Y. Amin[1] and G. Safwat[2,3] and G., El-Emary[4] 1 Department of Plant Physiology, Faculty of Agriculture, Cairo University, Giza, Egypt 2 Horticulture Research Institute, Agriculture research Centre, Doki, Giza, Egypt 3 Faculty of Biotechnology, October University of Modern Sciences and Art, Egypt 4 Institute of Efficient Productivity, Zagazig University.	Full Text

Abstract: The chromosome elimination technique is an efficient method by which beneficial characters for salt tolerance can be combined within a short time and a large number of doubled haploid (DH) genotypes with desirable variability can be produced. In the present study 120 spring wheat DH genotypes has been developed using the wheat (*Triticum aestivum L.*) x millet (*Pennisetum glaucum*) crosspollination method with the F1 cross between Kharchia (Indian cultivar) one of the most cultivar recorded as salt tolerance worldwide and Sakha 93 (Egyptian breeding cultivar) cultivated in saline soil and recommended for newly reclaim lands, north area of Egypt. Under normal conditions the DHs agronomical traits (i.e. flowering time, number of spikelets per spike (NSPS), plant height, spike length and 1000 grain weight) distribution was normal and significant transgressive segregation was observed. ANOVA analysis showed significant differences among DH genotypes for all agronomical traits, and the DH 11, 22, 57, 98, 106, 111 and 118 lines found to have better yield characters SNPS, spike length and 1000 grain weight than the parents under non-saline condition. The 120 DHs and both parents were grown in hydroponics culture medium, with the concentration of NaCl : $CaCl_2$ 4:1 being 150mM. Some of those DHs showed much high in responses to growth under salinity than both parents. The variances between DH lines were significant for Na^+ and Cl^- ions, leaf Fresh weight (lfw), leaf dry weight (ldw), leaf 2 extension rate before salt additions (LE-b), leaf 4 extension rate after salt additions (LE-a), number of spikes per plant (SNPP), number of spikelets per spike (NSPS), number of grains per plant (GN) and grain weight per plant (GW), and non-significant for K^+ ion and water percentage (W%). Overall the mean values for the DHs were higher than the parents values under salt stress, for the DH 3, 12, 38, 57 and 96 genotypes mid-values of LE-a were close to the average of LE-b under non-saline conditions. A significant negative correlation was determined between Na content and yield parameters i.e. SNPP, NSPS, GN and GW. In contrast it was positively correlation with W%, which might indicates that better yield characters of DH lines i.e. 10, 25, 42, 57, 68, 96, and 114 than parents under salt conditions may be due mainly to better exclusion of Na from the shoots.
[Journal of American Science 2010;6(7):139-148]. (ISSN: 1545-1003).
Keywords:- doubled haploid , chromosome elimination, salinity, Triticum aestivum L, breeding

18

A New Method for Fabrication and Laser Treatment of Nano-Composites

Hebatalrahman. A
Housing & Building National Research Centre (HBRC), Egypt.
Hebatalrahman@naseej.com

Abstract: A new method for manufacturing of nano-composites was invented; a new technique calls Composite material machine with four strokes was established. Composite material machine is a machine for manufacturing of both plastic and metals matrix composites independent on size, type, and volume fraction of fillers. The machine works in four strokes, each of which worked separately. It depends on the material. The four stokes can be controlled to work in schedule controlled by the main control unit connected to the computer, the machine also work manually. The final products were treated by laser irradiation to improve mechanical properties without any significant

Full Text

	change in composition. The new technique is cheap, qualified and simple design. The technique was full automated and has been transferred to industry successfully. [Journal of American Science 2010;6(7):149-154]. (ISSN: 1545-1003). **Keywords:** Fabrication, parameters, nanocomposite, laser irradiation, nanoparticles, reinforcement	
19	**Optimized Conditions for Increasing *Escherichia coli* Resistance to p-Hydroxybenzoic Acid** Mohamed M. Aboulwafa[1], *Ramadan A. El Domany[2], Riham M. Shawky[2] and Shima M. A. Ibrahim[2] Microbiology & Immunology Department, Faculty of Pharmacy, Ain Shams University[1], and Microbiology & Immunology Department, Faculty of Pharmac Helwan University[2] *E-mail: Rdomanii@yahoo.com **Abstract:** The present study aimed at increasing resistance of *Escherichia coli* to p-hydroxybenzoic acid (pHBA) through manipulation of different environmental and physiological factors. According to the study, different incubation temperatures, pHs, agitation rates and medium components were tested to characterize *E. coli* resistance to pHBA in shake flask and a laboratory fermentor. Genetic analysis using PCR of four representative *E. coli* isolates showed that *yhcP* gene was detected in both sensitive and resistant wild isolates of natural sources, a finding that stressed the importance of studying different environmental, physiological and genetic factors affecting the regulation of *yhcP* gene. MIC of pHBA against *E. coli* strain BW25113 that has the YhcP efflux pump showed a 64 fold increase by changing the growth medium from nutrient broth to basal medium containing 2% peptone and 2.6% glucose and keeping the pH constant at 8. Increased resistance of *E. coli* to pHBA could provide an effective solution to the toxicity of acid to the producing host bacterial cell which in turn will help to increase production of this molecule for commercial use. [Journal of American Science 2010;6(7):155-169]. (ISSN: 1545-1003). **Keyword:** *Escherichia coli*, p-hydroxybenzoic acid, environmental, physiological factors, *yhcP* gene	Full Text
20	**Immunomodulation of Hepatic Morbidity in Murine *Schistosomiasis mansoni* Using Fatty Acid Binding Protein** Ibrahim Rabia[1]; Eman El-Ahwany[2]; Wafaa El-Komy [1] and Faten Nagy[2] [1]Parasitology [2]Immunology Department,Theodor Bilharz Research Institute,Giza, Egypt. dr_mona_zaki@yahoo.co.uk **Abstract:** Hepatic fibrosis and portal hypertension are responsible for morbidity in schistosomiasis *mansoni*.The objective of this study was to evaluate the possible anti-morbidity effect of fatty acid binding protein (FABP) of *Schistoma mansoni* when given to mice before infection. Multiple small doses of FABP were injected intra-peritoneally into experimental animals (100	Full Text

	µg of purified FABP followed 2 weeks later by two booster doses of 50 µg each at weekly intervals) and the experimental design included 3 groups of 15 mice each; the first group received FABP (immunized group), the second group was injected with the 3 doses of FABP one week prior to infection with 100 *S.mansoni* cercariae (immunized-infected group) and the third group served as infected control. Data revealed reduction in CD4+ cells and increase in CD8+ cells of hepatic granuloma in FABP-immunized infected group, resulting in significant decrease in CD4+/CD8+ ratio, in comparison to infected control group; the serum cytokine levels of both TNF-alpha and IFN-gamma were also significantly decreased. Histopathological examination of liver revealed remarkable increase in percent of degenerated ova within hepatic granuloma which decreased in diameter (12%). In this study, significant reductions in worm burden (46%) and tissue egg loads (42.8% and 50% for hepatic and intestinal ova respectively) were observed in addition to decreased percent of immature stages with increase in percent of dead ova in Oogram pattern .This work could present a trial contributing to shaping the severity of hepatic morbidity. [Journal of American Science 2010;6(7):170-176]. (ISSN: 1545-1003). **Key words:** Schistosomiasis. – fatty acid binding protein – immunization. – histopathology	
21	# Fault Determination Using One Dimensional Wavelet Analysis S. Morris Cooper, Liu Tianyou, Innocent Ndoh Mbue *Institute of Geophysics and Geomatics, China University of Geosciences, Wuhan 430074, China;* smorriscpr@gmail.com **Abstract:** Faults play an important role in mineral exploration and volcanic activities. Their identification, a major problem in the world of geosciences, is significant to both geologists and geophysicists. Multiscale wavelet analysis, a powerful tool for filtering and denoising, has been applied to solve many problems in geophysics. Wavelet transforms have advantages to traditional Fourier methods in analyzing physical situations where the signal contains discontinued and sharp spikes. In this paper we advance the use of one dimensional multiscale wavelet for the identification of faults from potential field data. The method is based on the power of the discrete wavelet utilizing the concept of breakline and discontinuity (edge detection) and uses the Daubachies wavelet. The method is applied to synthetic data and real potential field data from Dagang, southern China yielding very good results. [Journal of American Science 2010;6(7):177-182]. (ISSN: 1545-1003). **Keywords:** Wavelet decomposition, Fault, Potential field, Dagang Oilfield	Full Text
22	# The Empirical Mode Decomposition (EMD), a new tool for Potential Field Separation S. Morris Cooper[1], Liu Tianyou[2], Innocent Ndoh Mbue[3] [1, 2] Institude of Geophysucs and geomatics, China University of Geosciences, Wuhan [3] Faculty of Earth Sciences, State Key Laboratory for Geological Processes and	Full Text

	Mineral Resources, China University of Geosciences, Wuhan E-mail: smorriscpr@gmail.com **Abstract:** In this paper we are proposing the use of the Empirical Mode decomposition method as a tool for potential field data separation. The empirical mode decomposition (EMD) is a new data analysis method suitable to process non-stationary and nonlinear data. Its power to filter and decompose data has earned it a high reputation in signal processing. Its decomposition results in what is called "Residual", which is similar to the regional anomaly of a potential field data. This residual does not require any preset parameters unlike contemporary field separation methods. The method is applied to a magnetic data from the Jianshandian mine in Hubei, China enabling us to construct a 2.5D inverse model inferring the existence of deep ore deposits. The method is effective at separating both local and regional data from magnetic data. [Journal of American Science 2010;6(7):183-187]. (ISSN: 1545-1003). . **Keywords:** Empirical Mode decomposition (EMD), Intrinsic Mode Functions (IMF), potential field separation, Jianshandian Mine	
23	# Remote Sensing Data Dissemination and Management: Potential of Replication and Provenance Techniques Tauqir Ahmad [1], Abad Ali Shah [2] Department of Computer Science University of Engineering and Technology, Lahore tauqir_ahmad@hotmail.com abad_shah@uet.edu.pk **Abstract:** With the proliferation of computer technology in almost every sphere of life such as e-government, health care and services sector, there is an increased reliance on digital data. More recently, satellite and remote sensing data has gained importance owning to its applications in real time decisions for GIS, military and strategic needs, and, surveillance and security systems. However, real time access to the digital repositories most of which are web based is plagued by various management and dissemination issues. In data intensive domains such as scientific computations, bioinformatics and e-commerce, replication and provenance have been used successfully for improved performance of data sources by handling the issues of availability, discovery, reliability, authenticity and consistency. In this paper we argue that remote sensing data dissemination and management share common issues and problems with the data intensive domains mentioned above. We also suggest that replication and provenance techniques offer a promising solution to remove the bottleneck of data dissemination and management for real time decision making based on remote sensing data. [Journal of American Science 2010;6(7):188-198]. (ISSN: 1545-1003). **Keywords**: Remote sensing data, data dissemination, data management, replication, provenance	Full Text
24	Potential field Investigation of the Liberia Basin, West Africa	Full Text

	S. Morris Cooper Institute of Geophysics and Geomatics China University of geosciences Email: smcooper2002@yahoo.com **Abstract:** Euler deconvolution is a useful tool for providing estimates of the localities and depth of magnetic and gravity sources. Wavelet analysis is an interesting tool for filtering and improving geophysical data. The application of these two methods to gravity and magnetic data of the Liberia basin enable the definition of the geometry and depth of the subsurface geologic structures. The study reveals the basin is sub-divided and the depth to basement of the basin structure ranging from 5km at its Northwest end to 10km at its broadest section eastward. [Journal of American Science 2010;6(7):199-207]. (ISSN: 1545-1003). **Keywords:** Wavelet transform, Euler deconvolution, Potential field, Liberia basin	
25	Joint magnetic and seismic interpretation; Determining Depth and Orientation of Volcanic Rock in the Qikou Depression, China S. Morris Cooper, Liu Tianyou [1] Institute of Geo physics and Geomatics, China University of Geosciences Wuhan, China smorriscpr@gmail.com **Abstract:** Identification of volcanic rocks is important in both the oil and gas industry since they may serve as either hindrance or source rocks. Their exploration in deep layer, especially when judging their geological properties, is usually difficult, even for 3-D seismic method. However, these special geological bodies vary distinctly in density, susceptibility and resistivity, which laid a foundation for adopting comprehensive geophysical prospecting techniques to solving this kind of problems. In this paper we use integrated geophysics method to construct a 2.5d inverse model of an igneous rock in the Qikou depresson, eastern China. The model was constrained by a seismic straitigraphic model based on reflection coefficient and well data. The combination of seismic and magnetic data for the inversion of volcanic rocks produces a much clearer understanding as to the orientation of said rocks as demonstrated in this paper. [Journal of American Science 2010;6(7):208-212]. (ISSN: 1545-1003). **Keywords:** Reflection coefficient, seismic data, magnetic data, modeling, Qikou depression	Full Text
26	**Non-insect benthic phytomacrofauna and organism-water quality relations in a tropical coastal Ecosystem: impact of land based pollutants.**	Full Text

C.A. EDOKPAYI, R.E.UWADIAE and C. E.NJAR (In memoriam)
Benthic Ecology Unit, Department of Marine Sciences, University of Lagos, Akoka, Lagos, Nigeria.
Email: eferoland@yahoo.com. Tel: +2347059497190.

Abstract. The impact of land based pollutants on the non-insect benthic phytomacrofauna and water quality in Epe lagoon was investigated between September, 2004 and February, 2005. Five study stations impacted by land based pollutants were selected upstream along the course of the Lagoon. The study showed that land based pollutants caused a decrease in dissolved oxygen and pH and an increase in biochemical oxygen demand (BOD) and phosphates. Significant differences in these parameters were established among the stations sampled. A post hoc test indicated that stations 2, 3, and 4 were mostly impacted by pollutants. A generally low taxa population and diversity were recorded in this study. Eight taxa were identified from a total of 65 individuals collected from the five stations along the lagoon. No organism was recorded in station 3.The analyses showed that the overall abundance of fauna differed significantly among the stations. Analysis of variance showed that the abundance of Lymnaeidae was significantly higher ($P<0.05$) than those of the other families. The dominance of the taxa Lymnaeidae was a clear indication of pollution which resulted in a decline and total elimination of other benthic macroinvertebrates, which are intolerant of the effects of polluting effluents. This study suggests that the response of benthic phytomacrofauna is important in the study of impacted aquatic systems. [Journal of American Science 2010;6(7):213-220]. (ISSN: 1545-1003).

Keywords: phytomacrofauna, water quality, tropical coastal ecosystem.

27

Rare Plants Protection Importance and Implementation of Measures to Avoid, Minimize or Mitigate Impacts on their Survival in Longhushan Nature Reserve, Guangxi Autonomous Region, China.

Dado Toure*, J. Ellis Burnet*, Zhou Jianwei*
*China University of Geosciences (Wuhan), School of Environmental Studies
Wuhan, Hubei. 430074. Lumo Lu. P.R.China
touredado@yahoo.fr , cactais@gmail.com

Abstract: Longhushan reserve is a karst forest of very high geological and biological quality. Located in South of China, Guangxi Region, the area reflects the high diversity of Guangxi, which biological resources are among the first in China, and ranks first among the Chinese provinces in terms of rare species of plants. The present research was undertaken to examine the ecosystems within the forest, and generate awareness about the importance of rare plant species in order to stimulate the conservation role of Governments, administrators and population. A field survey was conducted, plant species were recorded from 17 quadrats, geological and soil samples were collected to examine some of their chemical and physical characteristics significance on the vegetation. During the survey, 152 plant species were recorded, 35 species were found as dominant canopy and substrata species, and 12 species were identified as endangered. Within those endangered species, 6 are included in

Full Text

	the International Union for Conservation of Nature and Natural Resources (IUCN) red list for endangered species and 3 are endemic. Analysis of geological and soil samples revealed that dolomite appears to be the factor that impacted species distribution, while rare plants and dominant species responded differently to soil type, PH, moisture and organic matter (OM) content. Which lead to say that in the reserve each karst environment is unique due to its localized conditions, geological and soil properties, land use practices, climatic conditions, hydrological and geomorphologic status. The results also pointed out the evidence of karst ecosystem fragility which makes the vegetation formation or restoration slow and difficult process. Therefore, plant species protection especially endangered species is fundamental in the area because their conservation is central not only to biodiversity conservation but also to the preservation of karst ecosystems. [Journal of American Science 2010;6(7):221-238]. (ISSN: 1545-1003). **Key words**: Rare plants Protection; Longhushan; avoidance, minimization/mitigation measures; Impact	
28	**BIOMIMETIC SYNTHESIS OF GUIDED-TISSUE REGENERATION HYDROXYAPATITE/POLYVINL ALCOHOL NANOCOMPOSITE SCAFFOLDS: INFLUENCE OF ALIGNATE ON MECHANICAL AND BIOLOGICAL PROPERTIES.** E. TOLBA[1], B. M. ABD-ELHADY[1], B. ELKHOLY[1], H.ELKADY[2],M. ELTONSI[3] [1.] Biomaterial Department, National Research Center, Cairo, Egypt. [2.] Civil Engineering Department, National Research Center, Cairo, Egypt. [3.] Physics Department, Faculty of science, El-Mansoura University, El-Mansoura, Egypt hala.elkady@gmail.com **Abstract:** This paper presents a part of a major research, in which HA/PVA/alginate scaffolds -with different alginate compositions -up to 20wt% were fabricated by a modified freeze-extraction method. This method includes the physical cross-linking of PVA and chemical cross-linking of the alginate. Characterization of the prepared scaffolds was performed by morphology observations using scanning electron microscopy (SEM). Different physical properties – as porosity and density-were measured. It was noticed that by increasing alginate composition scaffolds exhibited highly porous, open-cellular pore structures with almost porosity about 90%, regardless of alginate composition and the pore sizes from about 150 to about 300μm.The In Vitro bioactivity and biodegradability of nano-composite scaffolds were investigated by incubation in simulated body fluid (SBF) and water under osteoclastic resorption conditions, respectively. The in-vitro bioactivity test indicating the higher bone-bonding ability of the biomimetically synthesized a scaffold that is awarded by the fast formation of bonelike apatite on their surfaces within one day. Also The addition of alginate to HA/PVA scaffolds increased the biodegradability compared with that one without alginate. Mechanical behavior of scaffolds was investigated under axial loading. Scaffolds stress strain behavior, maximum true stress, and elastic moduli, were calculated. It was	Full Text

found that increasing alginate content from 0 to 20% by weight, decreased the compressive modulus from 85.3 to 44.7 MPa, whereas the maximum compressive strength decreased from 6 to 5 MPa. Finally, it was concluded that the proposed scaffolds expressed promising performance, despite of the resulting degradation in their mechanical behavior. The obtained compressive strength and modulus of elasticity were still within satisfactory limits. [Journal of American Science 2010;6(7):239-249]. (ISSN: 1545-1003).

Keywords: Tissue re-generation, Poly(vinyl), composites, scaffolds

29

Chlorpyrifos (from different sources): Effect on Testicular Biochemistry of Male Albino Rats.

Afaf, A. El-Kashoury* and Hanan, A. Tag El-Din**

* Department of Mammalian and Aquatic Toxicology, Central Agricultura Pesticides Laboratory, Agricultural Research Center, Giza, Egypt.
** Chemistry Department, Hormonal Lab., Animal Health Research Institute, Dokki, Giza, Egypt.
drofscience@ymail.com

Abstract

Organophosphates are known primarily as neutrotoxins. However, reactive oxygen species (ROS) caused by organophosphates may be involved in the toxicity of various pesticides. Therefore, in this study we aimed to investigate the toxic effects of three trade names of chlorpyrifos (CPF) pesticide, from different local manufactures [chlorozan (K) pestpan (W) and pyriban (H)] on testicular weight , testicular oxidative stress and some testicular biochemical parameters in male albino rats. **Methods:** Three compounds (K, W and H) were administrated orally to rats at dose of 23.43, 21.40 and 17.43 mg/kg b.w., respectively (which represent the 1/4 LD_{50}) with 5 doses per week for 28 days. Twenty-four hours after the last treatment the rats were sacrificed using anesthetic ether. Testes were collected , cleaned and weighed. Right testes were fractionated and supernatant of testicular homogenate was obtained by centrifugation, lipid peroxidation (LPO), total glutathione, activities of alkaline and acid phosphatases, lactate dehydrogenase and total protein were measured. Moreover, the left tests were histologically examined. **Results :** The testes weights were significantly decreased in (W) group only . Chlorpyrifos treatments (K, W and H) alter markedly the testicular lipid peroxidation (LPO) levels, while, the decline in the total glutathione (GSH) was occurred only in (W and H) groups, in comparing with the control group. Also, there was significant decrease in the activities of alkaline and acid phosphatase (ALP and ACP) and lactate dehydrohenase (LDH) in all treated groups . Total protein (TP) level exhibited an elevation in testicular tissue in comparison with the control group. Treatment-dependent histopathological changes were seen in testes of CPF-W group only. **Conclusion:** Chlorpyrifos (CPF) alters testicular functions possibly by induction of testicular oxidative stress and inhibition of the activities of marker enzymes, thereby disrupting male reproduction. [Journal of American Science 2010;7(7):252-261]. (ISSN: 1545-1003).

Keywords: Chlorpyrifos; rats; lipid peroxidation; total glutathione; acid and alkaline phosphatase; lactate dehydrogenase; total protein ; tests

Full Text

30

Issues In Interacting With GIS In Hydrocarbon Exploration Industry

Muhammad Shaheen [1], Muhammad Shahbaz [2], Zahoor ur Rehman [3], M. Sarshar Aurangzeb[4]

[1,2,3.] University of Engineering & Technology Lahore, Punjab Pakistan
[4] Pakistan Accumulators Pvt. Ltd. Pakistan
[1] shaheen@uet.edu.pk, [2] m.shahbaz@uet.edu.pk, [3] xahoor@gmail.com, [4] sarshar_zeb@yahoo.com

Abstract: Technology changed the scenarios in past few decades. Recent developments in the processing power and storage capacity revolutionized the industrial development and even troubleshooting. There was a time when basic computational tools were very slow or even unavailable in industry but now state of the art tools and technologies can envisage exploring virtual reality. In energy sector, world is desperately looking for large reserves of fossil fuels along with other reserves. The efforts in hydrocarbon discovery phase deplete lots of resources resulting in either a very small sized reservoir or in failure. Geographic information system (GIS) along with related technology of remotely sensed satellite images, information system skeleton, graphical user interfaces (GUIs) and analytical tools can also be used for automated hydrocarbon explorations. GIS is operated by GIS analysts who have specialized skills in geo-spatial technologies. Therefore the exploration companies especially in the developing countries of the world do not rely on the capabilities of GIS and remote sensing. The reasons are concluded to be. (1). Interface of GIS is not friendly for non-specialist and/or novice user. (2). Accuracy of spatial data is not convincing for accuracy-critical tasks. (3). Unavailability of standards of spatial / non-spatial data display. The paper addresses the issues in interacting with GIS for hydrocarbon exploration and proposes enhanced model of Geographic Information System (GIS) for making it a reliable technology in any part of the world in hydrocarbon discovery phase. [Journal of American Science 2010;6(7):262-271]. (ISSN: 1545-1003).

Keywords: Geographic Information System (GIS), Usability, Interactivity, Human-GIS Interaction, Positional Accuracy, Hydrocarbon Exploration, Backpropogation Neural Network

Full Text

31

Surgical Site Infections and Associated Risk Factors in Egyptian Orthopedic Patients

[1]Khaleid M. Abdel-Haleim, [2]Zeinab Abdel-Khalek Ibraheim, [3]Eman M. El-Tahlawy

Departments of [1]Orthopedic Surgery, [2] Medical Microbiology and Immunology, Cairo University,
[3]Departement of environmental health, National Research Center, Egypt
we.za.2007@hotmail.com

Abstract: Background:Surgical site infections (SSIs) were identified on inpatient surgical wards, and most were associated with cardiac, abdominal, and orthopedic surgery. SSIs surveillance data are the foundation of effective infection control programs. **Aim of the work**:This study was conducted to estimate the risk factors and major pathogens involved in SSIs in orthopedic

Full Text

ward in a public hospital in Cairo, Egypt. **Materials and Methods**:During a 9-months period; a total of 93 consecutive orthopedic surgery patients were followed prospectively for 30 days after surgery. Risk factors for SSIs development were assessed for each patient. Swabs from infected surgical wounds were inoculated into routine culture media. Isolates were identified to the species level, and antimicrobial resistance patterns were determined. **Results:**The present study detected an overall SSIs rate of 25.8% (from 4.1% in clean wound to 66.7% in dirty contaminated wounds). Surveillance of risk factors of SSI, defined age**,** obesity (Body mass index "BMI" > 25), smoking, length of stay in hospital, class of wound, number of persons in the operating room, duration of operation and National Nosocomial infections surveillance (NNIS) index as independent risk factors for SSIs development. Microbiological study of infected surgical sites detected 47 pathogens. *S. aureus* was isolated most frequently 42.6%, Coagulase negative staphylococci "CoNS" and Enterococci were detected in 10.6% and 6.4% of isolates respectively. *K. pneumonia, P. aeruginosa, K. oxytoca, E. coli and A. baumannii* were detected in percentages of 14.9%, 10.6%, 4.3%, 4.3% and 2.1% of isolates respectively. *Candida albicans* was also detected in 4.3% of isolates. Antimicrobial susceptibility testing of isolates detected Oxacillin resistant S.aureus (ORSA) in 65% of *S. aureus* isolates. Enterococcus species resistance to vancomycin (VA) was 33.4%, and that to ampicillin (AMP) was 66.7%. Fluoroquinolones (FQs) resistance was detected in 20% of *P. aeruginosa* isolates. Extended-spectrum cephalosporin resistance (ESBLs) was detected in 50% of *K. oxytoca* isolates, 40% of *P. aeruginosa* and 28.6% of *K. pneumonia* isolates. Carbapenem resistance was detected only in *K. pneumonia* isolates (14.2%). **Conclusion:**We concluded that incidence of SSIs in orthopedic patients in Egypt is higher than that reported in some developing countries. *S. aureus* is the most common pathogens associated with orthopedic SSIs. ORSA, VA-resistant Enterococcus species, ESBLs producing *Klebsiellae* species and *P. aeruginosa*, as well as FQs resistant *P. aeruginosa and* carbapenem resistance *K. pneumonia* pose an ongoing and increasing challenge to the antimicrobial policy in our hospital. In orthopedic surgery unit risk factors for SSIs that may represent points of intervention including; limiting the number of personnel entering the operating room, improving NNIS risk index of patients and reduction of duration of surgery. In the era of restricted hospital budgets and increased bacterial resistance, long-term surveillance of SSIs rates and follow-up of compliance may provide a way to improve performance at low costs. [Journal of American Science 2010;6(7):272-280]. (ISSN: 1545-1003).

Key words; Surgical site infections (SSIs); Risk factors of SSIs; *S. aureus*, Oxacillin resistant S. aureus (ORSA); Extended-spectrum cephalosporin resistance (ESBLs); Carbapenem resistance

For back issues of *the Journal of American Science*, click here.

Emails: editor@americanscience.org; americansciencej@gmail.com

Nutritive evaluation of some tropical under-utilized grain legume seeds for ruminant's nutrition.

*Festus Tope Ajayi, Sikirat Remi Akande, Joseph Oluwafemi Odejide[1] and Babajide Idowu

Institute of Agricultural Research and Training, Obafemi Awolowo University,
Moor Plantation, Ibadan, Nigeria.
[1]Federal College of Agriculture, Moor Plantation, Ibadan, Nigeria.
ajayiajay@yahoo.com

Abstract: This study was undertaken to evaluate the nutritional potential of seeds of African yam bean (*Sphenostylis stenocarpa*), Lima bean (*Phaseolus lunatus*), Bambara groundnut (*Vigna subterranean*), sword bean (*Canavalia gladiata*), jack bean (*Canavalia ensiformis*), pigeon pea (*Cajanus cajan)*, Lablab (*Lablab purpureus*) and soybean (*Glycin max*) for feeding livestock using in-vitro techniques. The crude protein of the seeds ranged from 18.8% in jack bean to 33.5% in soybean. The neutral detergent fibre (NDF) was between 16.4% in soybean and 23.2% in African yam bean. Soybean was lowest (4.5%) in acid detergent lignin (ADL) compared to other legumes investigated. Tannin content was between 2.1 g/100g in soybean and 7.2 g/100g in lima bean. The seed of soybean was least in concentrations of phytic acid, trypsin inhibitor, saponin and oxalate whereas significant ($P<0.05$) variations were observed among the under-utilized grain legume (UGL) seeds for these anti-nutrients. The metabolizable energy (ME), Organic matter digestibility (OMD) and short chain fatty acids (SCFA) of the UGL seeds differed ($P<0.05$) significantly. The ME was between 8.8 and 12.1 MJ/Kg, OMD was between 49.6 and 80.5% while the SCFA ranged from 0.7 to 1.2 mmol. Gas production characteristics revealed that methanogenesis was low in jack beans (35 ml) and highest in soybean (48.7 ml), potential gas production, b, was between 23.4 ml in lima bean and 38.5 ml in soybean. The rate of substrate fermentation was lowest in jack bean and highest soybean. It is concluded that among the UGL seeds investigated Lima bean, pigeon pea and jack bean seeds are unsuitable as feed resources for ruminant livestock. [Journal of American Science 2010;6(7):1-7]. (ISSN: 1545-1003).

Keywords: Degradation coefficients, gas fermentation, secondary metabolites, under-utilized grain legume seeds.

1. Introduction

Inadequate nutrition all year round is one of the major causes of low productivity of ruminants in sub-Sahara Africa (Osuji et al. 1995). Majority of ruminant livestock in tropical Africa are raised on natural pastures which decline rapidly in quality during the dry season (Ajayi, 2007). During the dry season, poor nutrition of animals results in irregular growth and weight loss. Supplementation of forage legumes to grass or crop residue based diets of ruminants increases the weight and productivity of the animals (Babayemi et al. 2006).

Under-utilized grain legume seeds are potential sources of supplement in ruminant livestock diet. African yam bean (AYB) (*Sphenostylis stenocarpa* Hochst ex A Rich), Lima bean (*Phaseolus lunatus*), Bambara groundnut (*Vigna subterranean*), sword bean (*Canavalia gladiata*), jack bean (*Canavalia ensiformis*), pigeon pea (*Cajanus cajan*), and lablab (*Lablab purpureus*) are under-utilized grain legumes that posses high crude protein content between 22 and 37% (Adeparusi 2001; Fasoyiro et al. 2006). These legumes are widely grown in Nigeria and in other West African countries like Ghana, Cameroon, Cote d'lvore and Togo (Klu et al. 2001).The major constraint to the utilization of these legumes is the long hour of cooking. However, the seeds could be relevant in ruminant livestock nutrition. Although, anti-nutritional factors were reported in these legumes (Borget 1992), ruminants can tolerate some anti-nutrients because of their rumen ecology.

A lot of seeds are produced from these legumes and is likely that some of the seeds possess defaunating property. The seeds with high protein contents combined with defaunating activities could result in greater microbial protein flow into the small intestine thus providing the host animal with more protein (Odeyinka 2004). This study was designed to evaluate the nutrient contents, organic matter digestibility, metabolizable energy, short chain fatty acids and

degradation coefficients of Lima bean, Bambara groundnut, sword bean, African yam bean, jack bean, pigeon pea, and Lablab *in-vitro* for ruminant livestock nutrition.

2. Materials and Methods

Rumen liquor was collected from three West African dwarf goats through suction tube prior to morning feeding. The goats were fed concentrate feeds consisting of 20% maize, 20% corn bran, 25% wheat offal, 20% palm kernel cake, 10% groundnut cake, 4% oyster shell, 0.5% common salt, 0.25% fish meal and 0.25% grower premix. In addition, *Gliricidia sepium* and *Panicum maximum* forages were fed to the goats *ad libitum* for 7 days prior to rumen liquor collection. The liquor was filtered through three layers of cheese cloth, mixed and stirred with a buffered mineral solution ($NaHCO_3$ + Na_2HPO_4 + KCl + NaCl +$MgSO_4.7H_2O$ +$CaCl_2.2H_2O$ (1.4, v/v) under continuous flushing with carbondioxide.

Two hundred milligrams of ground samples of the UGL seeds were weighed into 100ml syringes with lubricated pistons. Thirty mls of the mixed buffered solution and rumen liquor was added to the samples in the syringes, stirred gently, clipped and placed in the incubator at 39^{o}C. Gas production rates were recorded at 3, 6,9,12,15,18,21 and 24 hour. At the end of 24 hour incubation, 4mls of NaOH was added to the substrate in each syringe to determine the methane production. Rates and extent of gas production were determined for each substrate from linear equation $\mathbf{Y = a + b (1 - e^{-ct})}$ described by Ørskov and McDonald (1979) where **Y** = volume of gas produced at time't', **a** = intercept (gas produced from soluble fraction), **b** = Potential gas production (ml/g DM) from insoluble fraction, **c** = gas production rate constant (/h) for the insoluble fraction, **t** = incubation time. The metabolizable energy (MJ/Kg) and organic matter digestibility were estimated from the volume of gas produced after 24 hr of incubation (GP, ml/g) and the proportion of crude protein as established by Menke and Steingass (1988):
OMD = 24.91 + 0.7222 GP + 0.0815CP ME = 2.2 + 0.1357GP + 0.0057CP+ $0.0002859CP^2$. Short chain fatty acids were calculated as described by Getachew et al. (1999).

Chemical Analysis

Ground samples of seeds were analyzed for nitrogen by the Micro-kjeldahl method. Crude protein was obtained by multiplying N by 6.25. Dry matter (DM), Ether extract (EE) were determined according to AOAC (1990) methods. Nitrogen free extract was obtained by calculation while neutral detergent fibre (NDF), acid detergent fibre (ADF) and acid detergent lignin (ADL) were determined by method of Van Soest et al. (1991). Saponin, phytate and trypsin inhibitors were analyzed by methods of Okwu and Josiah (2006), Maga (1983) and Kakade et al. (1969) respectively while tannin and oxalates were determined by method of Beutler et al. (1980).

Statistical Analysis

Data obtained were analyzed by ANOVA and significant differences between means were compared using Duncan (Duncan 1955) multiple range test with the aid of SAS/STAT program (SAS 1998).

3. Results and Discussion

The dry matter of the UGL seeds ranged from 63.6% in sword bean to 70.3% in AYB. Crude protein (CP) ranged from 18.8% in Jack bean to 33.5% in soybean (Table 1). The ether extract (EE) was between 2.4% and 10.1% in pigeon pea/lima bean and soybean respectively. The neutral detergent fibre (NDF) ranged from 44.2% in lima bean to 50.1% in lablab. Acid detergent fibre (ADF) was between 16.4% and 23.2% in soybean and AYB respectively. Acid detergent lignin (ADL) ranged from 4.3% in lima bean to 6.8% in jack bean. The nitrogen free extract (NFE) was between 10.6% and 17.3% in lima bean respectively. The DM values obtained in this study for the UGL seeds were slightly lowered than those reported (Fasoyiro et al. 2006) for Bambara groundnut, Lima bean, AYB, pigeon pea and soybean. The CP values obtained however, correspond with values earlier reported (Odeyinka 2004; Fasoyiro et al. 2006).

Tannin contents of the UGL seeds ranged from 3.5g/100g in lablab to 7.2 g/100g in Lima bean while that of soybean was 2.1 g/100g. Tannin forms strong insoluble complexes with proteins and divalent metals which results in poor digestibility and palatability in monogastrics (Adeparusi 2001; Ologhobo et al. 2003). However, sheep and cattle can tolerate 2-5%

dietary tannin ((Diagayete and Hugg 1981) while goats can tolerate about 9% tannin in their diets (Nastis and Malecheck 1981). Tannin is water–soluble phenolic metabolite concentrated beneath the testa of the seed and can be removed by soaking in water. Tannin contents were removed from sorghum (Nyachoti et al. 1997) and African yam bean (Adeparusi 2001) by soaking in water all night. Phytate concentration was highest in pigeon pea (16.2 mg/g) and lowest in soybean (10.3 mg/g). Phytin chelates metals such as Calcium, phosphorus, copper, magnesium and iron and forms complexes with proteins in legumes thereby reducing the nutritive value (Adeparusi 2001). Phosphorus deficiency occurs in animals when phytin combines with phosphorus. It is reported that soaking and boiling for ten minutes completely removed phytin in seed (Reddy et al. 1982). Trypsin inhibitor (TI) ranged from 12.0 Tiu/mg in soybean to 22.6 Tiu/mg in Bambara groundnut. It has been shown that all night soaking followed by boiling for ten minutes totally eliminates TI (Borge 1992) The concentration of saponin was highest in jack bean and sword bean (1.8 and 1.7 g/100g respectively) and lowest in soybean (0.8 g/100g).

Saponin containing seeds reduces methane production in the rumen by suppressing protozoa which influences butyrate production during rumen methanogenesis. The higher the contents of saponin in seed, the lower the volume of methane produced in the rumen. Methane production is loss of energy derivable from a feedstuff by the animal. Sword bean and jack bean with high saponin contents had low methane production whereas soybean with low content of saponin had the highest production of methane. Since methanogenesis is energy loss, it is essential that livestock diets should be balanced with a rich energy source (Ajayi 2007). Oxalate content ranged from 0.1 mg/100g in soybean to 0.9 mg/100g in lablab. Oxalate contents obtained in seeds of jack bean and lima bean was similar to reported values (Ologhobo et al., 2003). Oxalates have been implicated to impair magnesium metabolism in forages (Oke 1969). However, soaking in water all night before boiling for ten minutes eliminates oxalate content in seed.

Metabolizable energy (8.8 – 13.4 MJ/Kg) obtained for the UGL seeds are adequate for daily maintenance and production of ruminants. The ME of seeds was far above the 2.32 MJ/Kg reported for confined goats with liveweight of 10 kg (Steele 1996). The OMD obtained (49.6 – 77.2%) were higher than 45.0 – 60.8% reported (Juarez-Reyes et al. 2004) and 35.8 – 42.06% reported (Ajayi and Babayemi 2008). The variations observed in OMD and SCFA of these legumes were due to the level of secondary metabolite in them; especially tannin. High secondary metabolite in a feedstuff lowers the OMD and SCFA. Higher values of OMD and SCFA were observed in lablab and soybean. Gas fermentation and methane production of the legumes showed a progressive rise in gas volume as incubation time increased to 24 hr. The increase volume of gas reflects increase digestion of feedstuffs (Menke and Steingass 1988) and production of SCFA which is energy source for host animal (Hoffmann et al. 2003). It was observed that the seeds having high secondary metabolite had the least gas production at the end of incubation (24 hr). Higher gas is produced when substrate is fermented to acetate or butyrate. However, lower gas production is associated with propionate production (Ngamsaeng et al. 2006). The variations observed in the methane production in the legumes were due to the saponin contents of the legumes. Jack bean and sword bean with higher saponin contents had the least methane production values. This observation corroborates earlier findings that saponin containing seeds showed the ability to reduce rumen methane and butyrate production (Babayemi et al. 2004).

The gas production coefficients of the UGL seeds differed ($P<0.05$) significantly (Table 5). The potential gas production, *b* varied from 23.4 ml/g in Lima bean and jack bean to 37.3 ml/g in lablab; soybean had the highest value of 38.5 ml/g. The observed values for gas production in AYB, pigeon pea, sword bean and Bambara groundnut were not significantly ($P<0.05$) different. The total volume of gas produced, Y, ranged from 18.4 ml/g in jack bean to 32.6 ml/g in lablab. The rate of substrate fermentation among the UGL seeds was between 1.4 $\%h^{-1}$ in jack bean and 21.5$\%h^{-1}$ in lablab; soybean seed had the highest rate of fermentation (23.2$\%h^{-1}$). Higher gas production coefficients were recorded (Odeyinka 2004) for *Clitoria ternatea, Centrosema pubescens, Leucaena leucocephala, Macroptillium artropurpureum Clitoria ternatea, Centrosema pubescens, Leucaena leucocephala, Macroptillium* than values observed in this study.

The secondary metabolites in the UGL seeds could be responsible for the low values.

Table 1: Proximate composition of some under- utilized grain legume seeds and soybean.

Seed	DM	CP	EE	NDF	ADF	ADL	NFE
Lima bean	65.8c	21.4d	2.4c	44.2c	21.7b	4.3d	17.3a
African yam bean	70.3a	25.2b	3.1bc	48.6ab	23.2a	6..0b	11.7c
Pigeon pea	68.7ab	21.6d	2.4c	48.3ab	19.2c	5.8c	13.2bc
Sword bean	63.6d	22.7c	3.6b	49.5a	20.6bc	6.2b	12.0c
Jack bean	69.4a	18.8e	3.3b	49.8a	22.3a	6.8a	11.4c
Lablab	67.6b	22.5c	3.6b	50.1a	22.5a	5.8c	10.6c
Bambara groundnut	67.5b	19.4e	2.8c	46.3b	19.8c	6.1b	14.8b
soybean	67.3b	33.5a	10.1a	45.2c	16.4d	4.5d	15.6b
SEM	1.01	0.74	0.55	0.86	0.89	0.22	1.20

[abc] = Means in the same column with different superscripts differ significantly (P<0.05).
DM = Dry matter, CP = crude protein, CF = crude fibre, EE = Ether extract, NDF= Neutral detergent fibre, ADF = Acid detergent fibre, ADL = Acid detergent lignin, NFE = Nitrogen free extract. SEM = standard error of the mean.

Table 2: Secondary metabolite of seeds of some under-utilized grain legumes and soybean.

Seed	Tannic acid (g/100g)	Phytic acid (mg/g)	Trypsin inhibitor (Tiu/mg)	Saponin (g/100g)	Oxalates (mg/100g)
Lima bean	7.2a	13.6c	17.2c	1.5b	0.5b
African yam bean	5.4b	14.9ab	14.5d	1.2b	0.3c
Pigeon pea	4.3bc	16.2a	19.2b	1.4b	0.7ab
Sword bean	5.7b	14.4b	18.7b	1.7a	0.6b
Jack bean	4.5b	13.7c	16.4c	1.8a	0.8a
Lablab	3.5c	15.7a	19.7b	1.3b	0.9a
Bambara groundnut	4.9b	14.8ab	22.6a	1.4b	0.7ab
soybean	2.1d	10.3d	12.0e	0.8c	0.1d
SEM	0.58	0.42	1.22	0.20	0.11

[abc] = Means in the same column with different superscripts differ significantly (P<0.05). SEM = standard error of the mean.

Table 3: Metabolizable energy, Organic matter digestibility and short chain fatty acid of under-utilized grain legume seeds.

Seed	Metabolizable Energy (MJ/Kg)	Organic matter Digestibility (%)	Short chain fatty acid (mmol)
Lima bean	8.8d	49.6f	0.7b
African yam bean	13.4a	66.9d	0.7b
Pigeon pea	11.5bc	71.1c	0.7b
Sword bean	10.4bcd	70.4c	0.8b
Jack bean	8.9d	60.9e	0.8b
Lablab	12.1ab	80.5a	1.1a
Bambara groundnut	10.0cd	60.0e	0.9b
soybean	11.9ab	77.2b	1.2a
SEM	0.51	3.27	0.12

[abc] = Means in the same column with different superscripts differ significantly (P<0.05). SEM = standard error of the mean.

Table 4: Gas fermentation (ml/g) and methane production of some under-utilized grain legume seeds.

Seed	Hour of incubation (hr)			
	12	18	24	CH_4 (ml)
Lima bean	24.0b	31.5d	36.0d	40.0bc
African yam bean	20.0d	35.5c	39.5c	45.3b
Pigeon pea	23.5b	38.0b	40.1c	42.0b
Sword bean	26.0a	34.0c	40.0c	36.4c
Jack bean	23.5b	31.5d	41.0c	35.0c
Lablab	29.0a	44.5a	50.5b	43.7b
Bambara groundnut	19.0c	31.5d	40.7c	43.2b
Soybean	27.0a	38.0b	55.0a	48.7a
SEM	0.80	1.12	1.30	2.14

[abc] = Means in the same column with different superscripts differ significantly (P<0.05). SEM = standard error of the mean.

Table 5: *In-vitro* gas fermentation characteristics of under-utilized grain legume seeds

Seed	Y (ml)	b (ml)	c (h^{-1})
Lima bean	20.9c	23.4d	0.020d
African yam bean	22.0c	30.6b	0.062bc
Pigeon pea	22.0c	27.0c	0.028d
Sword bean	27.5b	30.4b	0.087b
Jack bean	18.4c	23.5d	0.014e
Lablab	32.6a	37.3a	0.215a
Bambara groundnut	25.7b	33.0b	0.083b
soybean	31.4a	38.5a	0.232a
SEM	2.86	1.31	0.006

[abc] = Means in the same column with different superscripts differ significantly (P<0.05). SEM = standard error of the mean.

4. Conclusion

The productivity of livestock can be enhanced by adequate nutrition in quality and quantity. The seeds of African yam bean, Bambara groundnut, sword bean and lablab are suitable as supplements for ruminants. However, seeds of Lima bean, jack bean and pigeon pea are unsuitable as legume supplements and if it has to be used at all, minimal quantity should be used in diets of livestock. There is need to further research on the inclusion level of these UGL seeds when used as supplements in diets of livestock.

Corresponding Author
Dr. Ajayi Festus Tope
Livestock Improvement Programme
Institute of Agricultural Research and Training, Obafemi Awolowo Universiy
P.M.B. 5029, Moor Plantation, Ibadan, Nigeria
E-mail: ajayiajay@yahoo.com

References

1. Adegbola AA (1985) Proceedings of theNational Conference on Small Ruminant Production, Zaria, Nigeria pp 85-99.
2. Adeparusi EO (2001) Effect of processing on some minerals, anti-nutrients and nutritional composition of African yam bean. Journal of Sustainable Agriculture and Environment 3: 101-108.
3. Ajayi FT (2007) Nutritional Evaluation of guinea grass (*Panicum maximum* cv Ntchisi) intercropped with some legumes for west African dwarf goats. Ph.D Thesis. University of Ibadan, Ibadan.
4. Ajayi FT, Babayemi OJ and Taiwo AA (2008) Effects of supplementation of

Panicum maximum with four herbaceous forage legumes on performance, nutrients digestibility and nitrogen balance in West African dwarf goats. Animal Science Journal 79: 673-679.

5. Ajayi FT and Babayemi OJ (2008) Comparative *in-vitro* evaluation of mixtures of *Panicum maximum* cv Ntchisi with stylo (*Stylosanthes guianensis*), lablab (*Lablab purpureus*), centro (*Centrosema pubescens*) and histrix (*Aeschynomene histrix*). Livestock Research for Rural Development 20 (6) art. # 83.
6. AsJuarez-Reyes, Nevarez-Carrasco G, Cerrillo-soto MA (2004) Chemical composition, energy content, intake and in-situ crude protein degradability of the forage consumed by goats in a thorn scrubland in semi arid region of north Mexico. Livestock Research for Rural Development 16 (1) art. # 3
7. AOAC (1990) Official Methods of Analysis, 15th edition, Washington, D.C., USA; Association of Official Analytical Chemist, pp 69-88.
8. Babayemi OJ, Demeyer D and Fievez V (2004) In-vitro rumen fermentation of tropical browse seeds in relation to their content of secondary metabolites. Journal of Animal and Feed Science 13 (1): 32-34.
9. Babayemi OJ, Ajayi FT, Taiwo AA, Bamikole MA and Fajimi AK (2006) Performance of West African dwarf goats fed *Panicum maximum* and concentrate diets supplemented with lablab (*Lablab purpureus*), leucaena (*Leucaena leucocephala*) and Gliricidia (*Gliricidia sepium*) foliage. Nigerian Journal of Animal Production 33: 102-111.
10. Bamikole MA, Babayemi OJ, Arigbede OM and Ikhatua UJ (2003) Nutritive value of *Ficus religiosa* in West African dwarf goats. Animal Feed Science and Tech. 10920: 1-9.
11. Bamikole MA Ikhatua UJ, Anota B and Omaduvie F (2003) Feed intake, feed utilization and weight gain of West African dwarf goat fed varying proportions of *Ficus religiosa* and *Panicum maximum.* Proceedings of the 28th Annual Conference of the Nigerian Society of Animal Production, held in I.A.R.&T., Obafemi Awolowo University, Moor Plantation, Ibadan, March 16-20. pp 274-278.
12. Borget M (1992) Food Legumes. The tropical Agriculturist, CTA, Macmillan Press Limited, London, pp 103.
13. Diagayete M and Huss W (1983) Tannin contents of African pasture plants: Effects on analytical data and *in-vitro* digestibility. Animal Research and Development 15: 79-80
14. Duncan DB (1955) Multiple Range and Multiple F-test. Biometrics 11: 1-42.
15. Fasoyiro SB, Ajibade SR, Omole AJ, Adeniyan ON and Farinde EO (2004) Proximate, minerals and anti-nutritional factors of some under-utilized grain legumes in south western Nigeria. Nutrition and Food Science 36: (1) 18-23.
16. Getachew G, Makkar HPS and Becker K (1999) Stoichiometric relationship between short chain fatty acid and *in-vitro* gas production in presence and absence of polythene glycol for tannin containing browses. EAAP satellite Symposium. Gas production: fermentation kinetics for feed evaluation and to assess microbial activity. 18-19 August Wageningen, the Netherlands.
17. Hoffmann EM, Muetzel S and Becker K (2003) Effects of *Moringa oleifera* seed extraction on rumen fermentation *in-vitro*. Archives of Animal 57: 65-81.
18. Kakade ML, Simon N and Leiner IE (1969) An evaluation of natural vs synthetic for measuring the antitryptic activity of soybean samples. Cereal Chemistry 46: 518-526
19. Klu GYP, Amoatey HM, Bansa D and Kumaeja FK (2001) Cultivation and use of African yam bean (*Sphenostylis stenocarpa* ex A Rich) in the Volta region of Chana. The Journal of Food Technology in Africa 6 (3)
20. Maga JA (1983) Phytate: Its chemistry, occurrence, food interactions, nutritional significance and methods of analysis. Journal of Agriculture and Food chemistry 30: 1-9
21. Menke KH and Steingass H (1988) Estimation of the energetic value from chemical analysis and *in-vitro* gas production using rumen fluid. Animal Research and Development 28: 7-55.
22. Mupangwa JF, Ngongoni NT, Topps JH and Hamudikuwanda H (2000) Effects of supplementing a basal diet of *Chloris gayana* hay with one of three protein-rich legume hays of *Cassia rotundifolia, Lablab purpureus* and *Macroptilium atropurpureum* forage on some nutritional parameters in

goats. Tropical Animal Health and Production 32: 245-256.
23. Nastis AS and Matechek JC (1981) Digestion and utilization of nutrients in Oak browse by goats. Journal of Animal Science 52: 283-288.
24. Ngamsaeng A, Wanapat M and Khampa S (2006) Evaluation of local tropical plants by in-vitro rumen fermentation end-products. Pakistan Journal of Nutrition 5 (5): 414-418.
25. Nwokolo E (1987) A nutritional assessment of African yam bean (*Sphenostylis stenocarpa* ex A.Rich) Harms and Bambara groundnut (*Voandzeia subterranean L*) Journal of Food Science and Agriculture 41: 123-129.
26. Nyachoti CM, Atkinson J and Leeson L (1997) Sorghum tannin: A review. World poultry Science Journal 53: 1-21.
27. Odeyinka SM, Hector BL, Ørskov ER and Newbold CJ (2004) Assessment of the nutritive value of the seed of some tropical legumes as feeds for ruminants. Livestock Research for Rural Development 16 (9) Art. # 69
28. Oke OL (1969) Oxalic acids in plants and in nutrition. World Review of nutrients Diet. 10: 262-302.
29. Okwu DE and Josiah C (2006) Evaluation of the chemical composition of two Nigerian medicinal plants. African Journal of Biotechnology 5(4): 357-361.
30. Ologhobo A, Mosenthin R and Alaka OO (2003) Products from under-utilized plant seed as poultry feed ingredients. Tropical Journal on Animal Science 6 (1): 101-110.
31. Osuji PO, Fernandez-Rivera S and Odenyo A (1995) Improving fibre utilization and protein supply in animals fed poor quality roughages: In Rumen Ecology Research Planning (eds) Wallace, R.J and Lahlou-kassi, A. International Livestock Research Institute, Addis Ababa, Ethiopia pp 1-22.
32. Ørskov ER and McDonald I (1979) The estimation of protein degradability in the rumen from incubation measurements weighted according to the rate of passage. Journal of Agriculture Science. Cambridge 92: 499-503
33. Reddy NR, Sathe SK and Salukhe DK (1982) Phytates in legumes and cereals. Advance Food Research 28: 1-92.
34. SAS (1998) Statistical Analytical Systems Institute, SAS/STAT User's Guide. Statistics, SAS Institute, Cary. North Carolina, USA. 943
35. Steele M (1996) Goats: The Tropical Agriculturist. Macmillan CTA, Netherlands. Pp 125.
36. Van Soest PJ, Robertson JB and Lewis BA (1991) Methods for dietary fibre, neutral detergent fibre and non-starch polysaccharides in relation to animal nutrition. Journal of Dairy Science 74 (10): 3583-3597.

2/04/2010

Application of Elovic and Bhattacharya/Venkobacharya Models to Kinetics of Herbicide Sorption by Poultry Based Adsorbent: A GCMS External Standard Approach.

Itodo Adams Udoji[1],FunkeWosilat Abdulrahman[2],Lawal Gusau Hassan[3],S.A.Maigandi[4],Happiness Ugbede Itodo[5]

[1]Department of Applied Chemistry, Kebbi State University of Science and Technology, Aliero, Nigeria

[2]Department of Chemistry, University of Abuja, Nigeria

[3]Department of Pure and Applied Chemistry, Usmanu Danfodiyo University, Sokoto, Nigeria

[4]Faculty of Agriculture, Usmanu Danfodiyo University, Sokoto, Nigeria

[5]Department of Chemistry, Benue State University, Makurdi, Nigeria

itodoson2002@yahoo.com

Abstract: Three kinetic models were utilized in analyzing the removal of Atrazine from herbicide solution by its adsorption onto acid treated Poultry dropping Activated carbon. The forecasted pseudo-first order (with K_1=0.00921min^{-1}) was proven unfit in predicting the adsorption rate by the Bhattacharya and Venkobacharya rate constant which is approximately the same (k_a= -0.009212min^{-1}) but opposite in sign to the former. The linearity of (U)T shows that atrazine molecule has great accessibility to the adsorbent molecule .Desorption constant by the Elovic model was estimated as 12.987g/mg. Other parameters investigated to increase linearly with contact time include the fractional attainment at equilibrium(Ca/Co),equilibrium constants(Kc), sorption efficiency (%RE) and Gibbs free energy (-ΔG). [Journal of American Science 2010;6(7):8-18]. (ISSN: 1545-1003).

Key words: *Poultry dropping, Kinetics, Herbicide, Sorption, Activated carbon.GC/MS*

1. Introduction

Herbicide in the soil and water contains ingredients that are poisonous to human and other organism. Atrazine for example is the most widely used agricultural herbicide The application of Agro-chemicals such as herbicides and pesticides is an indication that the mechanism and magnitude of herbicide spreading after application continues to be an active area of research. Past studies was built on a strong case that atrazine is hazardous and unsafe to both human and ecosystem. Some of these studies found that the herbicide, atrazine disrupt the production and functionality of human hormones and a higher incidence was reported for cases of cancer in humans and laboratory animals (Zhongren *et al.*, 2006). The sorption of herbicide aqueous phase by activated carbon has been reported (Agdi *et al*.,2000; Zhongren *et al.*, 2006). Applicable methods for herbicide removal include a combination of biological, chemical and physical processes. Adsorption evolved as the most effective, less expensive physical process for herbicide removal. The most commonly used adsorbent has been activated carbon. It is relatively costly hence, suitability of activated carbon from locally available agricultural by-product is sorted (Agdi *et al.*, 2000), owing to their economic advantages. Taking into account the specific properties (high cellulosic content, high porosity, low density, weak conductivity etc). Some agro-wastes were selected with the aim of optimizing the effective abatement condition in a cost effective fashion to remove herbicides. The use of active carbon was prescribed by USEPA as the best available technology for the removal of (USEPA,2002)

In the United States, a predicted 8.6 billion broilers will be produced in 2004 ,generating approximately 9 million metric tons of manure. Broiler management involves their confinement in concentrated animal facilities which usually results in excessive localized land application of this manure due to over production. This situation may pose a threat to public

health and the environment because of potential contamination of air, ground and surface water sources via run-off and odor releases. Other manure uses, beside land application, such as burning for fuel recovery or land filling, produce low-value alternatives (Isabel *et al.*,2005).

There was report on Pseudo-second-order kinetic for adsorption of methylene blue on papaya seeds activated carbon and on the adsorption of dyes on activated carbon prepared from sawdust (Malik, 2004).

Choice of equipment: The gas chromatographic technique is at best a mediocre tool for qualitative analysis. It is best used with other technique to answer the question of what is present in a sample. Besides the simplicity of the instrument, ease of operation, GC also provides the answer to how much? It is an excellent quantitative analytical tool in quantifying micrograms in a litre or one volume in millions of volumes (Robert and Eugene, 2004).The sample herbicide (containing atrazine) is a multicomponent mixture containing atrazine (test sample) and other organochlorine moieties, which are very similar to atrazine. Secondly, the GC column has a very high efficiency which was claimed to be in excess of 400,000 theoretical plates. The column is about 100m long, a very dispersive type of stationary phase retaining the solute approximately in order of increasing boiling point. Helium carrier gas was selected since it can realize high efficiencies with reasonable analysis time (Raymond, 2003). The quantitative principle of GC depends on the fact that the size of the chromatographic peak is proportional to the amount of material (Robert and Eugene, 2004).Peak size is the size of chromatographic peak is proportional to the amount of material contributing to the peak. It is the measure from height and area of the peak while Peak height is proportional to the amount of material contributing to the peak if nothing in the system changes that could cause a change in the width of the peak between sample and standard.

Equilibrium is a phenomenon when the rate of adsorption and the rate of desorption are equal (Cooney, 1999). This is also the case when the effluent exiting an adsorption column contains pollutants at greater concentrations than is allowed. With a column system the adsorbent is said to be "spent."The relationship between the amount of adsorbate adsorbed onto the adsorbent surface and the equilibrium concentration of the adsorbate in solvent at equilibrium at a constant temperature may be estimated by various adsorption isotherm models.The amount of Dye at equilibrium, q_e was calculated from the mass balance equation given in equation 1 by Hameed et al.,(2006).

$$q_e = (C_O - C_e)\, V/W \quad \text{……..(1)}$$

where C_o and C_e are the initial and final Dye concentrations (mg/L) respectively. V is the volume of dye solution and M is the mass of the acid catalyzed Poultry waste sorbent (g). while t is the equilibrium contact time, when q_e = qt, equation 1 is expressed as equation 2 below:

$$q_t = (C_o - C_t)V/W - \quad - \quad (2)$$

where $q_e = q_t$ and C_t is the concentration at time t. The percent dye removal (RE %) was calculated for each equilibration by the expression presented as equation 3

$$R\,E(\%) = (C_0 - C_e)/Co \times 100 - \quad - \quad (3)$$

Where R (%) is the percent of dye adsorbed or removed. The % removal and adsorption capacities were used to optimize the activation condition.(Maryam *et al.*, 2008). The test were done at a constant temperature of 25 ± 2^0C.(Rozada *et al.*,2002).

Rate and extent of adsorption: Adsorption is often confused with absorption, where the substance being collected or removed actually penetrates into the other solid (Reynolds and Richards, 1997). Activated carbon uses the physical adsorption process whereby attractive Van der Waals Forces pull the solute out of solution and onto its surface (Reynolds and Richards, 1997).Kinetics of adsorption is one of the important characteristics defining the efficiency of adsorption (Anirudhan and Krishnan, 2003). According to Demirbas *et al.*, (2004), the study of adsorption dynamics describes the solute uptake rate and evidently the rate control the resident time of adsorbate uptake at the solid-solution interface. The adsorption rate constant can be used to compare the performance of activated carbons (Dianati-Tilaki and Ali, 2003).Several models have been used by a number of authors to ascertain the kinetics and mechanism of adsorption onto activated carbon surface. Among several kinetic models employed for rate studies include Apparent first order (Ana *et al.*,2009), Pseudo First and second order models (Hameed,2009), Elovic equation (Badmus *et al.*, 2007; Chen and Clayton, 1980), Battacharya/Venkobacharya model (Omoniyi and

Patricia,2008;Ho *et al.*,1995), Intraparticle diffusion model (Shrihari et al.,2005;Itodo *et al.*,2009a) e.t.c.

Thermodynamic constant and sorption feasibility: The change in Gibbs free energy (ΔG) For the adsorption can be investigated from the relationships in equation 4 and 5 below (Itodo *et al.*, 2009a; Namasivayan and Kavitha, 2007).

$$\Delta G = - RT \ln K_c \quad - \quad - \quad (4)$$

$$K_c = C_a/C_e \quad - \quad - \quad (5)$$

Where K_c = equilibrium constant, C_a is the solid phase concentration of equilibrium (i.e. concentration of adsorbent adsorbed onto the adsorbent), C_e is the equilibrium concentration of dye (unabsorbed concentration of dye in the solution). T is the temperature in Kelvin, R is the ideal gas constant ($Jmol^{-1}k^{-1}$). C_a (mg/g) and C_e (mg/l) are the concentration of dye at the solid phase (adsorbed) and at equilibrium (unabsorbed) phase respectively.

This present study reports atrazine sorption, not in a micro quantity but within range that could account for both the topical and systemic poisoning reportedly associated with atrazine (Raymond, 2003).

2. Materials and methods

Brand name herbicide (atrazine® presumably 2-chloro-4-ethylamino-6-isopropylamino-1,3,5-trazine) with assay of 50% atrazine was procured from a retailer's stand of the Agro-chemical wing of Sokoto central market, Nigeria. Stock standard solution (25g/L) was prepared and from which ranges of working standard were prepared in chloroform and stored in the dark. This was employed as adsorbate, used in this analysis. Zinc Chloride (98+ %) and Ortho Phosphoric acid obtained from prolabo chemicals were used as chemical activants while Chloroform was used as solvent. Hydrochloric acid (0.1M) and distilled water were used as washing agents.

Sample collection and preparation of activated carbon: Poultry droppings, PD (as the raw material for the production of activated carbon) were collected from Labana farms, Aliero in Kebbi state. The raw materials were pretreated as earlier described elsewhere (Zahangir *et al.*,2008;Itodo *et al* .,2009a and b). For thermo chemical (heat/chemical) activation, methods by Itodo *et al.*, 200a and 2009b;Turoti *et al.*,2007 were used after slight modifications. The samples (activated carbon produced) were crushed and sieved using <2mm aperture size sieve.

Preparation of Atrazine standard :5g of substrate was diluted to the mark of $100cm^3$ volumetric flask. This concentration of 50g/L herbicide is equivalent to 25g/L or 25,000ppm atrazine stock.

Batch equilibrium kinetic studies: Accurately 0.1g of home based activated carbon was mixed with $10cm^3$ of the 25g/L atrazine solution. The residual concentration of atrazine in solution (C_e in g/L) was measured after different stirring and interaction times (60, 120, 180, 240, and 300mins). The equilibrium phase herbicide was analyzed using a GC/MS. External standard method was used to calibrate the machine beforehand (Min and Yun,2008;Agdi *et al.*,2000).

GC/MS Conditioning: A gas chromatography equipped with a mass spectrophotometer detector (with a model GCMS QP2010 plus Shimadzu, Japan) was used in this analysis. The column was held at 60^oC in injection volume of 1µL and then programmed to 250^oC. it was set at a start m/z of 40 and end m/z of 420.The detector (mass spectrophotometer) was held at 250^oC above the maximum column temperature. The sample size was 1µL, which was split 100^{-1} onto the column and so the total charge on the column was about 1. Helium was used as the carrier gas at a linear velocity of 46.3cm/sec and pressure of 100.2kPa. Ionization mode is electron ionization (EI) at a voltage of 70eV. In this analysis, Amplification and resolution for test herbicide was achieved by adjusting the threshold to 6000 (Itodo *et al.*,2009c). Thus, worse interference and solvent peaks were screened out leaving majorly the deflection of target compound (atrazine) as it was made pronounced on the chromatogram. Baseline disturbance was linked to either hydrocarbon impurities. Impure carrier gas can also cause baseline instability (Robert and Eugene, 2004).It can be corrected by changing the purifier when pressure drops reaches 10 – 15 pSi routinely monitoring the pressure. Sorption efficiency of an adsorption process was defined based on the fractions of extracted and unextracted sorbates (Robert and Eugene, 2004; Itodo *et al.*,2009c).

Calibration curve for GC/MS analysis: A three point calibration curve was made from 1.0, 5.0 and 10.0g/L atrazine solution. These standards were run chromatographically under ideal conditions. A direct relationship between the peak height or size and concentration of target was established. The unknown

was extrapolated graphically (Robert and Eugene, 2004).

3.Results

Experimental results were fitted into Elovic and Bhattacharya/Venkobacharya kinetic model. The integrated and linearized expression were given as equations below.

Effects of contact time on sorption efficiency (%RE): The results from 1 shows the equilibrium phase concentration at any time (C_t). The mass of the unadsorbed sorbates reduces (from 0.0693 – 0.0571) as contact time increases from 60 – 300 minutes. This implies that the removal efficiency increases (from 72.032% - 77.1325%) with time. Table 1 therefore presents the effects of sorbate –sorbent contact time on the sorption efficiency.

Table 1: Adsorption experimental data of atrazine uptake by fixed mass of PD-Sorbents at different contact time, using GC/MS.

Biosorbent	Co(g/dm^3)	Ct (g/dm^3)	Ca (g/dm^3)	% RE	Ads mass (g)	q_t (mg/g)	Kc	-ΔG
PD/A/60	25	6.925	18.008	72.032	0.1801	1.801	2.600	2384.428
PD/A/120	25	6.205	10.795	75.180	0.1879	1.879	3.029	2765.536
PD/A/180	25	6.065	18.935	75.740	0.1894	1.894	3.122	2844.001
PD/A/240	25	5.865	19.135	76.540	0.1914	1.914	3.263	2951.233
PD/A/300	25	5.707	19.293	77.172	0.1929	1.929	3.381	3039.882

PD/A/60 – Poultry droppings, treated with, H_3PO_4interacted with Atrazine solution for 60 minute. PD/A/300 – Poultry droppings, treated with, H_3PO_4interacted with Atrazine solution for 300 minute.

Chromatograms presented as Figures 1 to 5 were typical of charts obtained for the equilibrium phase concentration analyzed using GC/MS. Analysis was carried out after filtration at the 60,120,180,240 and 300th minutes contact time. As interaction time increases, equilibrium concentration reduces. This implies an increase in adsorbed sorbate concentration with time.

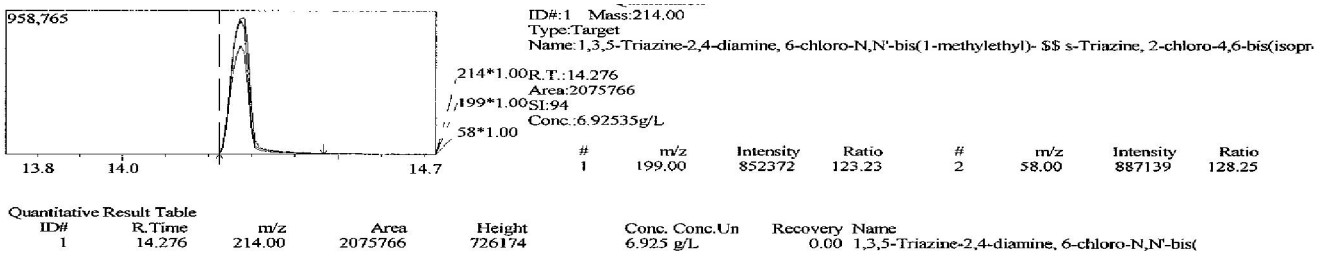

Figure 1: GC/MS chromatogram, quantitative measurement and spectral information of equilibrium phase atrazine after adsorption onto PD/A/60min sorbent

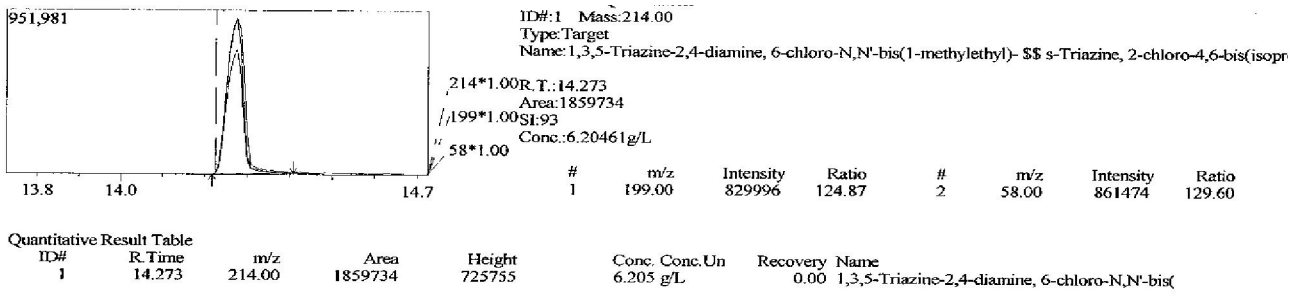

Figure 2: GC/MS chromatogram, quantitative measurement and spectral information of equilibrium phase atrazine after adsorption onto PD/A/120min sorbent

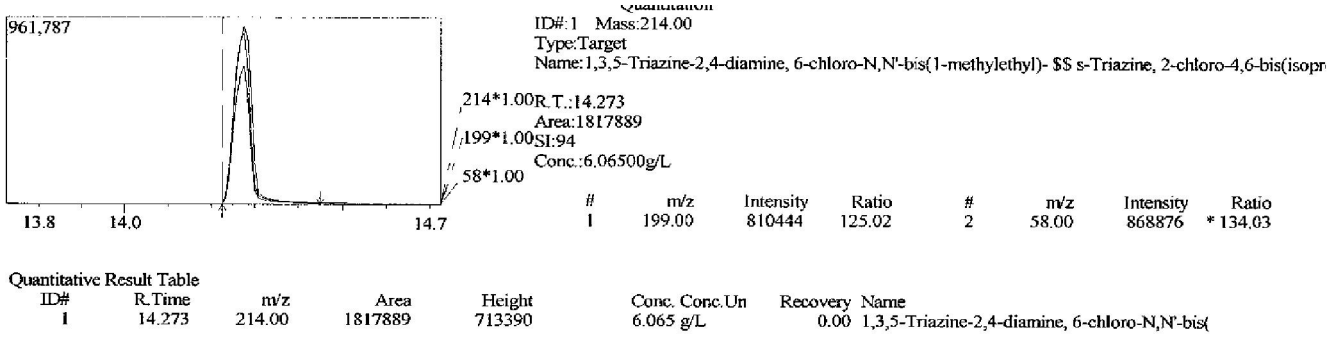

Figure 3: GC/MS chromatogram, quantitative measurement and spectral information of equilibrium phase atrazine after adsorption onto PD/A/180min sorbent

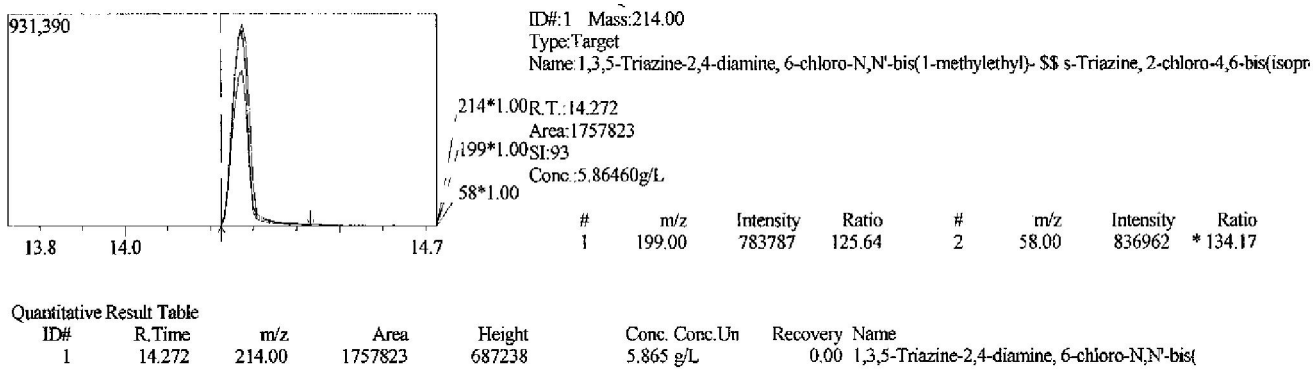

Figure 4: GC/MS chromatogram, quantitative measurement and spectral information of equilibrium phase atrazine after adsorption onto PD/A/240min sorbent

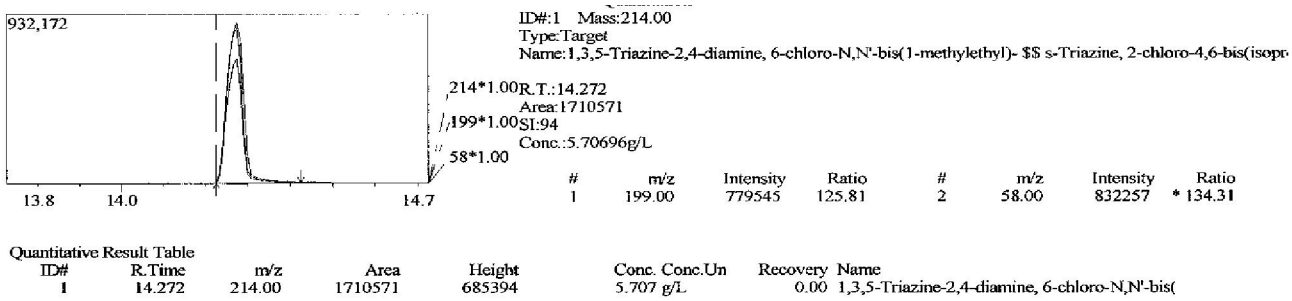

Figure 5: GC/MS chromatogram, quantitative measurement and spectral information of equilibrium phase atrazine after adsorption onto PD/A/300min sorbent

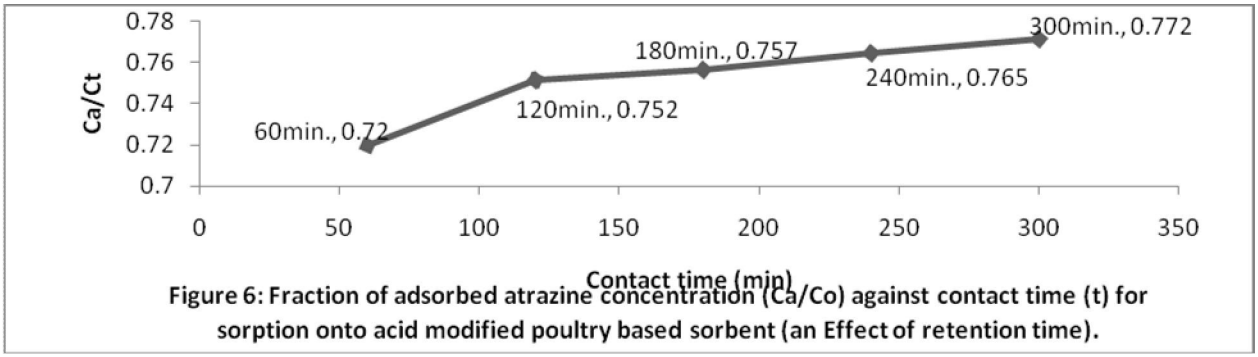

Figure 6: Fraction of adsorbed atrazine concentration (Ca/Co) against contact time (t) for sorption onto acid modified poultry based sorbent (an Effect of retention time).

4. Discussions

The fraction of Atrazine uptake at a given time was presented (Figure 6). The rise was pronounced from the 60th to 120th minutes After which the increase steadily adds from 0.752 to 0.772. i.e for every one portion of sorbate,0.772 part was adsorbed at the 300th minutes. This is the fractional attainment at equilibrium (Ca/Co).

Effect of contact time on sorption feasibility: The negative value of ΔG at a given temperature indicate spontaneous nature of adsorption (Namasivayan and Kavitha, 2007).The more negative the value of ΔG, the more spontaneous the nature of adsorption(Itodo *et al.*,2009b).As the thermodynamic equilibrium constant becomes more positive with time, the negative ΔG value increases (Figure 7). That is, ΔG becomes more negative with interaction time. Hence, the adsorption of dye onto chemically modified poultry droppings becomes more spontaneous with time.

The changes imposed on atrazine uptake by energy changes were investigated. ΔG values estimated in this analysis were all negative. This is an indication of a feasible adsorption. The trend of increase in negative ΔG with time follows the fashion PD/A/60minutes (-2384.400) < PD/A/120mins (-2765.536) < PD/A/180mins (-2841.001) < PD/A/240mins (-2951.233) < PD/A/300mins (-3039.882) units in kJ/mol. This implies that as the contact time increases, ΔG becomes more negative. This result tends to an increase adsorption over time.

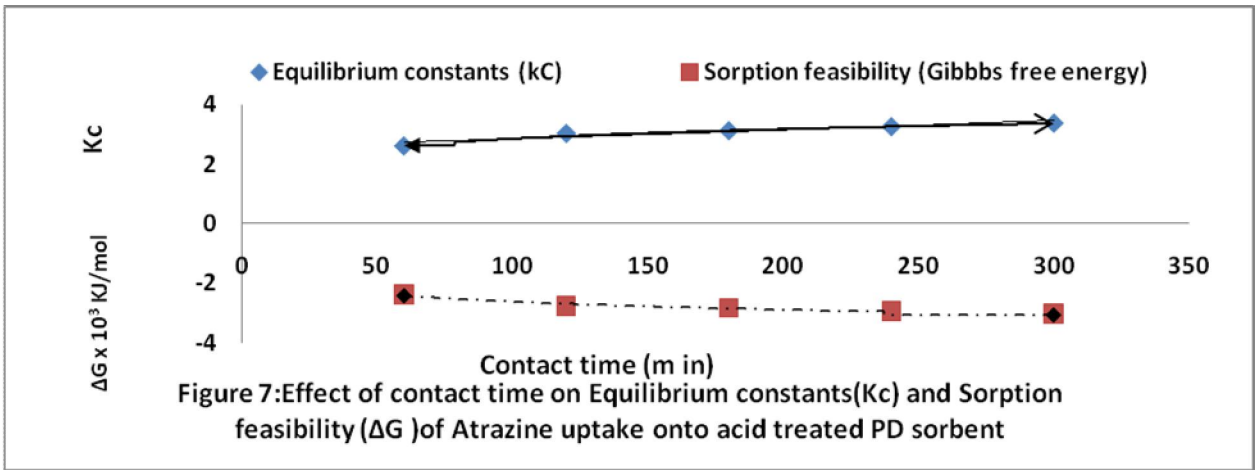

Figure 7:Effect of contact time on Equilibrium constants(Kc) and Sorption feasibility (ΔG)of Atrazine uptake onto acid treated PD sorbent

The more negative the value of ΔG, the more spontaneous is the adsorption. The thermodynamic equilibrium constant (Kc) was studied with interaction time. Kc is a measure the ratio of sorbate (atrazine) in the solid phase (adsorbed) to that in the equilibrium phase (unadsorbed). The magnitude of Kc is determined by the relative affinity of the adsorbent for the adsorbate. For good adsorption, a positive and large Kc value is reported. Table 1 revealed that as contact time increases. The amount of atrazine attracted by the PD-adsorbent increases. This is an indication of good adsorption. The values of Kc at 60, 120, 180, 240 and 300minutes interaction time are 2.600, 3.029, 3.122, 3.263 and 1.929 respectively. It thus follows that as the Kc value increases, ΔG value becomes more negative. This is due to the thermodynamic relationship between the two parameters.

Table 2: kinetic experimental data of atrazine uptake onto PD/A-sorbent by fixed mass of PD-Sorbents at different contact time, using GC/MS.

t(min)	lnt	$t^{1/2}$	Ct	q_t x10^{-3}	$1/q_t$ x10^{-3}	t/q_t x10^{-3}	ln (Ca/Ct)
60	4.094	7.746	6.925	1.801	0.555	33.315	0.9755
120	4.787	10.954	6.205	1.879	0.532	63.864	1.108
180	5.193	13.416	6.065	1.894	0.528	95.037	1.138
240	5.481	15.492	5.865	1.914	0.522	125.392	1.183
300	5.704	17.321	5.707	1.929	0.518	155.521	1.218

Bhattacharya and Venkobacharya equation is also a pseudo-first order equation given as equation 6 and 7 (Omoniyi and Patricia,2008;Ho *et al.*,1995

$\log [1 - (U)T] = (K_{ad}/2.303)t$ -- (6)

Where $U(T) = (C_i - C_t)/(C_i - C_e)$ - - (7)

C_i, C_t are initial concentration and concentration at time t respectively, K_{ad} is the rate constant and C_e is the concentration at equilibrium. Figure 8 is a straight line with high correlation coefficient, R^2 in the range of 0.968 which indicates acceptability of the model for the sorption process.

Table 3: Bhattacharya and Venkobacharya equation experimental data for atrazine uptake by PD - biosorbent

T(min)	C_i	C_t	C_i-C_t	C_i-C_e	U(T)= C_i-C_t/ C_i-C_e	Log[1-U(T)]
60	25	6.925	18.008	19.293	0.933	-1.174
120	25	6.205	18.795	19.293	0.974	-1.585
180	25	6.065	18.935	19.293	0.981	-1.721
240	25	5.865	19.135	19.293	0.992	-2.097
300	25	5.707	19.293	19.293	1.000	----

The Bhattacharya and Venkobacharya plots (Figures 8) also gave a linear plot. It is evidence that B & V value of K_{ad} (-0.009212min^{-1}) is approximately the same with the Lagergren K_{ad} value (0.00921min^{-1}) but of opposite sign. This validity test further reaffirms the unfit of the experimental data by the Lagergren model of pseudo-first order kinetic. The high values of (U)T (0.933,0.974,0.981,0.992 and 1.000) from Table 3 shows that atrazine molecules have greater accessibility to the adsorbent surfaces. The kinetic theory behind Figure 8 is that it can be used to explain the sorption process in terms of adsorption being controlled by film-diffusion or particle-diffusion (Ho *et al.,* 1995; Omoniyi and Patricia, 2008). The linearity of the Figures 8 indicate that the adsorption of atrazine is controlled by particle -diffusion. Linearity of the diffusibility plot showed that the Pseudo-first order equation proposed was inadequate in describing the adsorption study. The B&V negative rate constant (Ka= -0.009212 min^{-1}) which is of the same value to a positive value for the Lagergren Pseudo first order rate constant given on Table 4 further suggest a second order kinetics since the statistical sum of error (%SSE) and precision test based on q_e for the first order kinetics are large and poor respectively.The integrated and linearized pseudo-first order kinetic model expression was given by Lagergren, (1898) in Ho and Mckay,(1999) is given as equation 8

$$\text{Log}\,(q_e - q_t) = \log q_e - (k_1/2.303)\,t \quad \text{--} \quad \text{-(8)}$$

Table 4: Bhattacharya and Venkobacharya experimental constants of atrazine uptake onto PD/A-sorbent by fixed mass of Sorbents at different contact time, using GC/MS

Kinetic model	Relationship (y =)	R^2	Constants	Values
B & V model			Ka(min^{-1})	-0.009212
	-0.004x-0.918	0.968	C	-0.919
			U(T)	0.933-1.00
Pseudo First order model	-0.004x – 0.630	0.974	k_1(min^{-1})	0.00921
			q_e(cal)(mgg$_{-1}$)	0.234
			q_e(exp)(mgg^{-1})	1.929
			%SSE	0.758

Table 5: Elovic model experimental constants of atrazine uptake onto PD/A-sorbent by fixed mass of PD-Sorbents at different contact time, using GC/MS.

Kinetic model	Relationship (y =)	R^2	Constants	Values
Elovic equation	0.077x + 1.494	0.946	β (g/mg)	12.9870
			α	1.9345
			1/ β	0.077

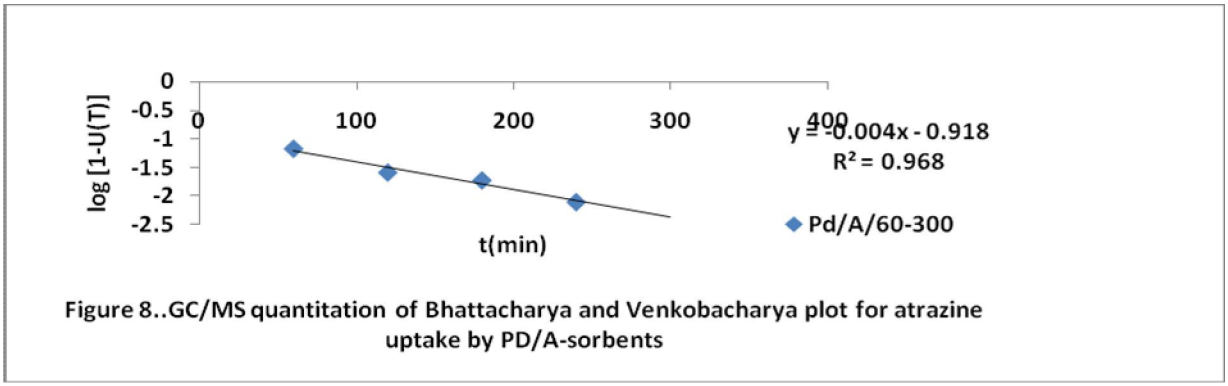

Figure 8..GC/MS quantitation of Bhattacharya and Venkobacharya plot for atrazine uptake by PD/A-sorbents

Elovic Equation: Elovic equation was developed to describe the kinetics of chemisorption of a sorbent onto solid. The parameter, α, represents the rate of chemisorption at zero coverage and the parameter, β, is related to the extent of surface coverage and the activation energy of chemisorption (Badmus *et al.*, 2007;Chen and Clayton,1980). q_t (mgg^{-1}) is the amount adsorbed at time, t. while α and β are constant during the experiment. The constant, α can be regarded as the initial rate since dq_t/dt tends to α as qt tends to zero (Badmus *et al.*, 2007).

The Elovic equation is generally expressed as equation 9 (Juliade *et al*., 2008)

$$dq_t/dt = \alpha \exp(-\beta q_t) \quad \text{---} \quad (9)$$

α is the initial adsorption rate, β is the desorption constant (g/mg),q_t is the amount of sorbate adsorbed at time, t.

To further simplify the equation for correlation regression estimation, Dermibas *et al.*, (2004) assumed $\alpha \beta t >>> t$. After applying boundary condition $q_t = 0$ at t=0 and $q_t = q_t$ at t = t, the equation becomes as expressed in 10;

$$q_t = 1/\beta \ln(\alpha\beta) + 1/\beta \ln(t) \quad \text{---} \quad (10)$$

A plot of q_t versus ln(t) yield a linear plot with a slope of (1/β) and intercepts of (1/β) ln (αβ). Elovic plot obtained in this analysis was presented as Figure9.

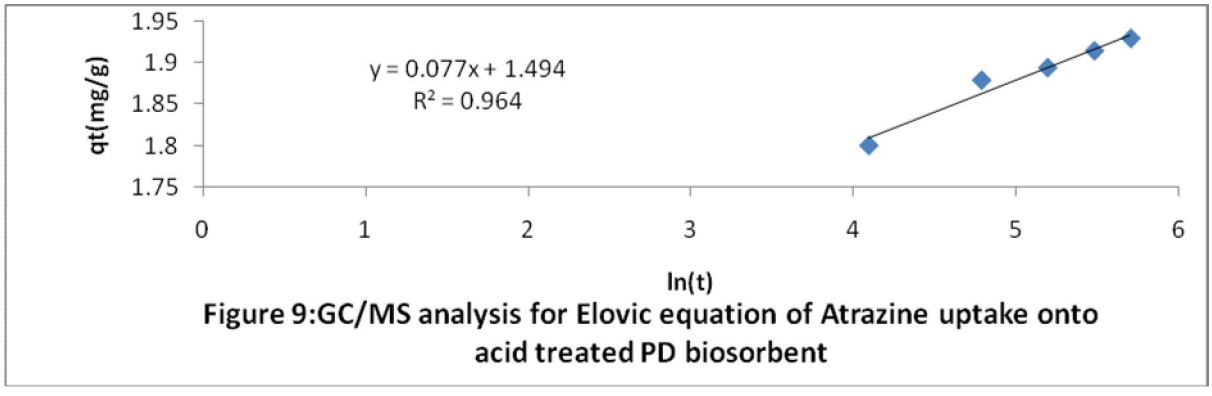

Figure 9:GC/MS analysis for Elovic equation of Atrazine uptake onto acid treated PD biosorbent

In this analysis, the parameter, representing the desorption constant (β) was estimated as 12.987 g/mg while the value reported for the initial adsorption rate (α) is 1.93453 mg/g/min. Subjecting the kinetic data into this model gave a fitness with a correlation coefficient, R2 = 0.946. This implies that this model, like any other kinetic models could be applicable in describing the solute uptake rate and idea on probable control of resident time of adsorbent and possible prediction of desorption.

In Conclusion, an external standard preparation, followed by GC/MS quantitation proves a good option for analyzing the quantity of single analyte from a multicomponent system such as atrazine from either herbicide or pesticide. Investigation of the derived PD activated carbon, using the two ways activation scheme with acid (H3PO4) was found to be worthwhile. The fractional attainment at equilibrium (Ca/Co), estent of feasibility (ΔG), equilibrium constants (Kc) and sorption feasibility (%RE) all presented values that increases linearly with interaction time adsorption for a kinetic study of 60min-300min. Contact time. A second order kinetic process was predicted since validity test relating the Bhattacharya / Venkobacharya and Lagergren Pseudo first order rate constant disagree (as does the %SSE and precision validity test). The adsorption of atrazine is governed by particle diffusion while high level of (U)T shows that atrazine molecules has accessibility to the adsorbent.

Acknowledgements:

Authors are grateful to the Department of Pure and Applied Chemistry of both Usmanu Danfodiyo University, Sokoto and Kebbi state University of Science and Technology, Aliero, Nigeria for supervisory guidance and to NARICT, Zaria for GCMS Analysis.

Corresponding Author:

Dr. Itodo Udoji Adams

Department of Applied Chemistry,

Kebbi state University of Science and Technology,

P.M.B 1144, Aliero, Kebbi state, Nigeria

E-mail: itodoson2002@yahoo.com

TEL: +2348073812726, +2348039503463

REFERENCES

1.Agdi K, Bouaid A, Martin E, Fernandez H, Azmani A, Camara C. Removal of atrazine from environmental water by diatomaceous earth remediation method. Journal of Environmental monitor 2000; 2: 420-423.

2.Ana S, Joao P, José M, Jose B, Carvalho C, Ania O.Waste-derived activated carbons for removal of ibuprofen from solution: Role of surface chemistry and pore structure. Bioresource Technology.2009; 100 : 1720–1726.

3.Anirudhan TS, Krishnan KA. Removal of Cd2+ from aqueous solution by Steam-activated sulphurised carbon prepared from sugar-cane bagasse pith: Kinetics and equilibrium studies. Water. 2003; 29(2):147-156.

4.Badmus MA, Audu TO,Anyata BU. Removal of Pb (++) ion from industrial waste water. Turkish J. Eng. Env. Science. 2007; 31 (1):

5.Bansode R, Losso J, Marshall E, Rao M,Portier J. Adsorption of volatile organic compd by pecen and almond shell based activated carbon. Bioresource Technology 2003; 90. (2):175-184.

6.Chen SH, Clayton W. Application of Elovic equation to the kinetics of phosphate release and adsorption on soil. J. soil Sc. Soc. Am. 1980; 44 (1): 265-268.

7.Cooney, David O. Adsorption Design for Wastewater Treatment. First Edn. Lewis. Publishers, CRC Press LLC, Boca Raton, Florida,1999.

8.Dermibas, E; Kobya, M; Senturk, E. and Ozkan, T. (2004). Adsorption kinetics for the removal of Cr (vi) from aqueous solutions on the activated carbon prepared from agricultural wastes. Journal of water. 30 (4): 533-539.

9.Dianati T, Ramazan A. Study on removal of cadmium for activated carbon preparation and application for the removal from water environment by adsorption on GAC, BAC and Biofilter. Diffuse Pollution Conference, Dublin,2003.

10.Dinesh M, Charles U, and Pittman T. Arsenic removal from waste water using adsorbent;A critical review.2007 Elsevier B.V, 2007:16-42

11.Hameed BH, Din AM, Ahmad AL. Adsorption of methylene blue onto Bamboo based activated carbon: kinetics and equilibrium studies. Hazardous materials. 2006;137(3):695- 699

12.Hetric J, Parker R, Pisigan J, Thurman N. Progress

report on estimating pesticide concentration in drinking water. 2000. Retrived on 10/07/009 from http://www.epa.gov/sapoly/sap/meetings/2000 /september/sepoo_sap_dw_0907.pdf

13.Ho YS, Mckay G. Pseudo second order model for sorption processes. Journal of water. 1999; 34:451-465.

14.Ho YS, John D A, Foster CF.Water Resources, 1995; 29: 1327.

15.Isabel M, Wayne, M. The ultimate trash to treasure: poultry waste into toxin – grabbing char. Agricultural research . 2005; 306 (1): 127-43.

16.Itodo AU, Abdulrahman FW, Hassan LG, Maigandi SA, Happiness UO. Thermodynamic equilibrium, kinetics and adsorption mechanism of industrial dye removal by chemically modified poultry droppings activated carbon.Nigerian Journal of Basic and Applied Science. 2009a;17(1):38-43.

17. Itodo AU, Abdulrahman FW, Hassan LG, Maigandi SA, Happiness UO. Batch kinetic studies of bioremediation of textile effluent via Heavy metal and dye adsorption. International journal of chemical sciences.2009b;2 (1):27-33.

18. Itodo AU, Abdulrahman FW, Hassan LG, Maigandi SA, Itodo H.U. Gas Chromatographic Prediction of Equilibrium Phase Atrazine after Sorption onto Derived Activated Carbon. Int'nal Journal of Poultry Science. 2009c; 8(12):1174-1182. Retrieved on 20/01/2010 from http://www.pjbs.org/ijps.htlm.

19. Malik, R; Ramteke, D. and Wate, S. Adsorption of Malachite green on groundnut shell waste based activated carbon. Waste management. 2006; 27 (9): 1129-1138.

20.Maryam k, mehdi A, Shabnam T, Majdeh M, Hamed k. Removal of Pb, Cd Zn and Cu from industrial waste water by carbon developed from Walnut, Hazelnut, Almond and Apricot Stones. Harzadous material .2008;150:322-327.

21.Monika J, Garg V, Kadirvelu k. Chromium (VI) removal from aqueous solution, using sunflower stem waste. J. Hazardous materials 2009;162:365 – 372.

22. Namarsivayan C, Kavitha D. Removal of congo red from water by adsorption onto activated carbon prepared from Coir pith.Dye and pigments.2007; 54:47-58.24.

23.Omoniyi P, Patricia D. Kinetics of the removal of ovalbumin from wine model solution. CSN Conference proceeding. 31st int'l Chemical Society of Nigeria conf/exh. Held on 22nd – 26 sept, 2008: 75-80.

24. Raymond, P.W. Principle and practice of chromatography. First edition. Chrom. Edn. Bookseries, 2003;19 – 26. Retrieved from http://www.library4science.com/enla.html.

25.Robert, L. and Eugene, F. Modern practice of chromatography. 4th Edn. Wiley interscience. John Wiley and sons Inc. New Jersey, 2004; 425.

26.Rozada F, Calvo F, Garcia A., Martin V, Otaro M. Dye adsorption by sewage sludge based activated carbon in batch and fixed bed system. Bioresource technology 2003; 87 (3): 221 – 230.

27.Shrihari V, Madhan S, Das A. kinetics of phenol sorption by Raw Agrowastes. Applied Sciences. 2005;6 (1): 47-50.

28.USEPA. Revised Preliminary Human health risks assessment for Atrazine. Office of Pesticide Programs, Washington D.C. 2002; 28.

29.Zahangir A, Suleyman A, Noraini K. Production of activated carbon from oil palm empty fruit Bunch for Zn removal.

Bul.conference proceedings 12th int.water Tech conf. IWTC12 Egypt. 2008; 373-383

30.Zhongren Y, James E, Kishore R, Gary B, Marv P, Ding L, Benito M. Chemically Activated Carbon on a Fibre glass Substrate for removal of trace atrazine from water. Material Chemistry. 2006;16: 3375-3380.

2/1/ 2010

GC/MS Batch Equilibrium study and Adsorption Isotherms of Atrazine Sorption by Activated H_3PO_4 - Treated Biomass.

Itodo Adams Udoji[1],Funke Wosilat Abdulrahman[2],Lawal Gusau Hassan[3],S.A.Maigandi[4],Happiness Ugbede Itodo[5]

[1]Department of Applied Chemistry, Kebbi State University of Science and Technology, Aliero, Nigeria

[2]Department of Chemistry, University of Abuja, Nigeria

[3]Department of Pure and Applied Chemistry, Usmanu Danfodiyo University, Sokoto, Nigeria

[4]Faculty of Agriculture, Usmanu Danfodiyo University, Sokoto, Nigeria

[5]Department of Chemistry, Benue State University, Makurdi, Nigeria

itodoson2002@yahoo.com

Abstract: Acid modified abundant lignocellulose Agricultural wastes, Sheanut shells (SS/A) was used to develop activated carbon and applied to removal of Agrochemical(Atrazine) from a multicomponent herbicide solution. A GCMS which can separate, detect and measure the target (sorbate) was applied to estimate equilibrium phase atrazine. Generated data were tested with 3 isotherm models.Extent of fitness follows the order Freundlich (R^2=0.994)>Langmuir (R^2=0.977)>BET (R^2=0.894) implying that surface coverage is more of heterogeneous. Freundlich adsorption capacity was valued at 0.045 x10^{-3} K_F (units in mgg^{-1} ($1mg^{-n(n)}$). Study of the effect of initial sorbate concentration (%RE) revealed that adsorption efficiency increases linearly with time in a range of 46.08% (for SS/A/5gdm^3) to 66.324 (for SS/A/25gdm^3).Generally,t he GCMS quantitation via external standard methods shows that sorted waste could be a potential source of active filter for atrazine sorption. [Journal of American Science 2010;6(7):19-29]. (ISSN: 1545-1003).

Keywords:: Sheanut shells; Atrazine; Activated carbon; GCMS.

1.Introduction

Water pollution by Organochlorine and Organophosphorus pesticide and herbicides are worldwide ecoproblem, particularly in the Agricultural regions. Among the different pollutants of aquatic ecosystem include; Herbicides, especially triazines .They are considered as priority pollutants since they are harmful to organism even μgL^{-1} levels. These pesticides or herbicides constitute a diverse group of chemical structures exhibiting a wide range of physiochemical properties (Agdi *et al.*, 2000). Atrazine (2-chloro-4-, amino-6-isopropylamino-s-triazine) and related substituted chlorotriazine compound,2-chloro-4,6-bis(ethylamino)-s-triazine) finds extensive use as herbicides (Shimabukoro,1967).They are widely used for the control of broadleaf and grassy weeds. Contrary to expectations, these compounds reduce the rate of CO_2 fixation in plants and act as inhibitors of hill reaction during photosynthesis. Unfortunately too, it is also widely detected in water supplies **(**Itodo *et al.*, 2009a**).** Herbicide in the soil and water sometime contains ingredients that are poisonous to human and other organism. Atrazine for example is the most widely used agricultural herbicide The application of Agro-chemicals such as herbicides and pesticides is an indication that the mechanism and magnitude of herbicide spreading after application continues to be an active area of research. Paramount interest on which this research focuses is their removal. Industries cannot afford the conventional waste water treatment chemicals like Alum, Ferric chloride, polymer flocculants and coal based activated carbon because they are cost intensive (Namasivayan and kavitha, 2009).

Disposal of Agricultural by – product is currently a major economic and ecological issue, and the conversion of these Agro products to adsorbent, such

as activated carbon represents a possible outlet (Malik *et al.*, 2006). This measure, to some extent, agrees with the concept of zero emission" as

proposed to be an idea of reducing environmental impact produced by discarded waste products and increase the effective and repeated utilization of resources Various carbonaceous material, such as coal, lignite, coconut shell, wood and peat are used in the production of commercial activated carbon (Bansode *et al.*, 2003). The Shea Tree is a sacred tree from the Sahel region in Africa. The shells are known to be poor source of energy while its biodegradation takes time. its menaces cuts across eye sores, space occupancy to injurious nature due to its strength and sharpness(Itodo *et al.*,2009a).

Among the conventional techniques for removing dissolved sorbates (heavy metals, dyes, organics etc.) include electrodialysis, phytoextraction (Myroslav *et al.*,2006). Others include ultrafilteration, reverse osmosis, chemical precipitation, ion exchange, carbon adsorption, evaporation and membrane adsorption. Most of this methods are expensive and ineffective when applied to low strength wastes with heavy metal concentration less than $100mgL^{-1}$ .Non conventional methods, studied for sorbate uptake include the use of wood, fullers earth, fired clay, fly ash, biogas waste slurry, waste orange peels, chitin, silica etc (Namasivayan and kavitha, 2009). Adsorption is the adhesion of a chemical substance (adsorbate) onto the surface of a solid (adsorbent). The most widely used adsorbent is activated carbon (Reuben and Miebaka, 2008).

Activated carbons are high porosity, high surface area material manufactured by carbonization and activation of carbonaceous materials, which find extensive use in the adsorption of pollutants from gaseous and liquid streams (Itodo *et al.*,2009a). Commercial sources activated carbon appear to be made from a variety of activating agents, and binders (USDA, 2002). According to Gimba *et al.*, (2004), a wide range of activating agents can be used. These include Acid, Inorganic Salts, Organic Salts, Bases, Steam, CO_2, Cyanides, Dolomite. Others include Boric acid, Calcium hydroxide, Calcium phosphate, Nitric acid Ortho phosphoric acid, Potassium carbonate, Potassium sulfide, Potassium thiocyanate, Sodium hydroxide, Sodium phosphate, Sulphur, Sulphur dioxide, Sulfuric acid and Zinc chloride (Gimba *et al.*, 2004).

Adsorption isotherm: Isotherm are empirical relationship used to predict how much solute can be adsorbed by activated carbon (Steve and Erika, 1998). Chilton *et al.*,(2002) defined Adsorption isotherm as a graphical representation showing the relationship between the amount adsorbed by a Unit weight of adsorbent (eg activated carbon) and the amount of adsorbate remaining in a test medium at equilibrium. It maps the distribution of adsorbable solute between the liquid and solid phases at various equilibrium concentration (Chilton *et al.*, 2002).The adsorption isotherm is based on data that are specific for each system and the isotherm must be determined for every application. An adsorption isotherm beside providing a panorama of the course taken by the system under study in a concise form indicate how efficiently a carbon will allow an estimate of the economic feasibility of the carbons' commercial application for the specific solute (Chilton *et al.*, 2002).The three well known isotherms are (a) Freundlich (b) Langmuir and (c) BET adsorption isotherm (Steve and Erika, 1998).

Equilibrium is a phenomenon when the estent of adsorption and of desorption are equal (Cooney, 1999). This is also the case when the effluent exiting an adsorption column contains pollutants at greater concentrations than is allowed. With a column system the adsorbent is said to be "spent."The relationship between the amount of adsorbate adsorbed onto the adsorbent surface and the equilibrium concentration of the adsorbate in solvent at equilibrium at a constant temperature may be estimated by various adsorption isotherm models.

Choice of Equipment: The sample herbicide (containing atrazine) is a multicomponent mixture containing atrazine (test sample) and other organochlorine moieties, which are very similar to atrazine. Secondly, the GC column has a very high efficiency which was claimed to be in excess of 400,000 theoretical plates. The column is about 100m long, a very dispersive type of stationary phase retaining the solute approximately in order of increasing boiling point. Helium carrier gas was selected since it can realize high efficiencies with reasonable analysis time (Raymond, 2003).

2.Material and Methods

Sample collection: Presumably 2-chloro-4-ethylamino-6-isopropyl amino-1,3,5-triazine with specification of 50% atrazine was procured from a retailer's stand of the agro-chemical wing of Sokoto central market, Nigeria. Zinc Chloride (98+ %) and Ortho Phosphoric acid obtained from prolabo chemicals were used as chemical activants while Chloroform was used as received.Hydrochloric acid (10%) and distilled water were used as washing agents. Shea nut shells (SS) were obtained from waste hip sites at Rikoto- Zuru,in Kebbi state,Nigeria.

Sample treatment and preparations: The method of sample treatment by Fan *et al*., (2003); Itodo *et al* .,(2009a&b) were adopted. The samples were washed with plenty of water to removes surface impurities and sundried , then, dried in an oven at $105^{O}C$ overnight (Omonhenle *et al.*,2006). The samples were separately pounded/ grounded followed by sieving with a <2mm aperture sieve. The less than 2mm samples were stored in airtight containers. About 3g of each pretreated biosolid (< 2mm mesh size) were introduced into six (6) different clean and pre weighed crucibles. They were introduced into a furnace at $500^{O}c$ for 5 minutes after which they were poured from the crucible into a bath of ice block. The excess water was drained and the samples were sun dried. This process was repeated until a substantial amount of carbonized samples were obtained (Gimba *et al.*,2004).The carbonized sample was washed, using 10% HCl to remove surface ash, followed by hot water wash and rinsing with distilled water to remove residual acid (Fan *et al*., 2003) the solids were then sun dried, then, dried in the oven at $100^{O}C$ for one hour . Accurately weighed 2g each of already carbonized samples were separately mixed with $2cm^3$ of each 1M activating agent (H_3PO_4 and $ZnCl_2$). The samples were introduced into a furnace, heated at $800^{O}c$ For 5 minutes. The activated samples were cooled with ice cold water. Excess water was drained and samples were allowed to dry at room temperature (Gimba *et al*., 2004,). The above procedure was repeated for different residual time (5min and 15 min).Washing of the above sample was done with 10% HCl to remove surface ash, followed by hot water and rinsing with distilled water to remove residual acid (Fan *et al*, 2005). Washing was completed when pH of the supernatant of 6-8 was ascertained (Ahmedna *et al.,* 2000). The sample were dried in an oven at $110^{O}C$ overnight and milled or grounded, followed by filtration to different mesh size and stored in air tight container.

Atrazine standard solution for equilibrium studies: For the sorption/equilibrium studies, several concentrations viz; 10, 20, 30, 40 and 50g/L Herbicide equivalent of 5, 10, 15, 20 and 25g/L Atrazine was prepared by respectively dissolving 0.25, 0.5, 0.75, 1.0 and 1.25g of herbicide into a conical flask, poured gently into a $25cm^3$ volumetric flask, homogenized and made to the mark with chloroform (i.e. 5,000ppm – 25,000ppm atrazine).A three point calibration curved based on external standard method was prepared with the GC/MS run.

External standardization (Calibration) for GC/MS: Techniques of external standardization entails the preparation of standards at the same levels of concentration as the unknown in the same matrix with the known. These standards are then run chromatographically under ideal conditions as the sample. A direct relationship between the peak size and composition of the target component is established and the unknown was extrapolated graphically.This technique allows the analysis of only one component in the same sample. Peak size is plotted against absolute amount of each component or its concentration in the matrix (Robert and Eugene, 2004). A three point calibration curve was made from 1.0, 5.0 and 10.0g/L atrazine solution. These standards were run chromatographically under ideal conditions. A direct relationship between the peak height or size and concentration of target was established. The unknown was extrapolated graphically (Robert and Eugene, 2004).The column was held at $60^{o}C$ in injection volume of 1µL and then programmed to $250^{o}C$. it was set at a start m/z of 40 and end m/z of 420.The detector (mass spectrophotometer) was held at $250^{o}C$ above the maximum column temperature. The sample size was 1µL, which was split 100^{-1} onto the column and so the total charge on the column was about 1. Helium was used as the carrier gas at a linear velocity of 46.3cm/sec and pressure of 100.2kPa. Ionization mode is electron ionization (EI) at a voltage of 70eV. In this analysis, Amplification and resolution for test herbicide was achieved by adjusting the threshold to 6000. Thus, worse interference and solvent peaks were screened out leaving majorly the deflection of target compound (atrazine) as it was made pronounced on the chromatogram. (Robert and Eugene, 2004).

Blank samples containing only the adsorbate solution were used to determine if the experimental process considerably reduces the concentration of the pollutant. It was found that significant amounts of the adsorbate were not lost in the procedure. Procedural blank was obtained by interacting the solvent with same gram of Carbon (Eva *et al.*, 2008).

Batch equilibrium experiment: 5g of substrate was diluted to the mark of $100cm^3$ volumetric flask. This concentration of 50g/L herbicide is equivalent to 25g/L or 25,000ppm atrazine stock. $10cm^3$ of the atrazine solution was interacted with 0.1g of each sorbent and allowed to stand for 12hours. The mixture was filtered and the filtrate was analyzed with a gas chromatography (coupled with a mass spectrophotometer detector) for atrazine equilibrium phase concentration (Min and Yun,2008;Agdi *et al*.,2000).

The amount of atrazine at equilibrium, q_e was calculated from the mass balance equation given in equation 1 by Hameed *et al.*,(2006).

$$q_e = (C_O - C_e)\, V/W \quad \text{.....(1)}$$

where C_o and C_e are the initial and final Dye concentrations (mg/L) respectively. V is the volume of dye solution and M is the mass of the acid catalyzed Poultry waste sorbent (g). while t is the equilibrium contact time, when q_e = qt, equation 1 will be expressed as equation 2 below:

$$q_t = (C_o - C_t)v/w \quad \text{.....(2)}$$

where $q_e = q_t$ and C_t is the concentration at time,t. The percent dye removal (RE %) was calculated for each equilibration by the expression presented as equation 3

$$R\,E(\%) = (C_0 - C_e)/Co \times 100, \quad \text{.....} \quad (3)$$

Where RE (%) is the percent of dye adsorbed or removed. The % removal and adsorption capacities were used to optimize the activation condition. The test were done at a constant temperature of 27 ± 2^0C.(Rozada *et al.*,2002). The equilibrium concentration of atrazine (herbicide), q_e and Adsorption efficiency (% Removal) were estimated. The extent of atrazine removal (by difference) from chloroform spiked with 25g/L of atrazine was expressed as equation 3 (Hameed *et al.*,2006)

3.Results

The chromatogram shown as Figure 1 stands for unadsorbed sorbate out of the 5g/dm^3 atrazine which was interacted with SS/A sorbent. The chromatogram was characterized by a baseline disturbance. This is caused by either hydrocarbon impurities or by impure carrier gas (Robert and Eugene, 2004).The former could be linked to the fact that the sorbate concentration (5g/dm^3) is too low for the 0.1g carbon dose. Unoccupied pore size could as well, lead to desorption of the sorbate with a resultant poor percentage removal (46.08%).

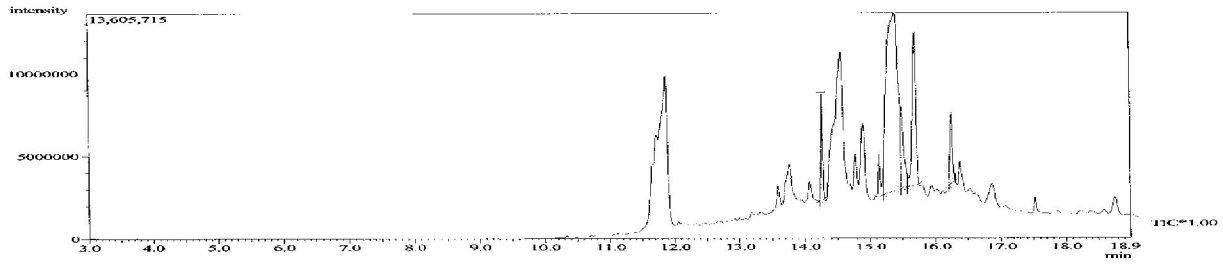

Figure 1: GC/MS chromatogram of equilibrium concentration atrazine after adsorption onto SS/A/5gL^{-1} sorbent (*Carrier gas-Helium 100.2kpa,Column temperature –60^{o}c,Injection temperature-250^{o}c,Injection volume—1µL,Flow rate-1.61mL/min, Injection method- split, Linear velocity- 43.6cm/sec.*)

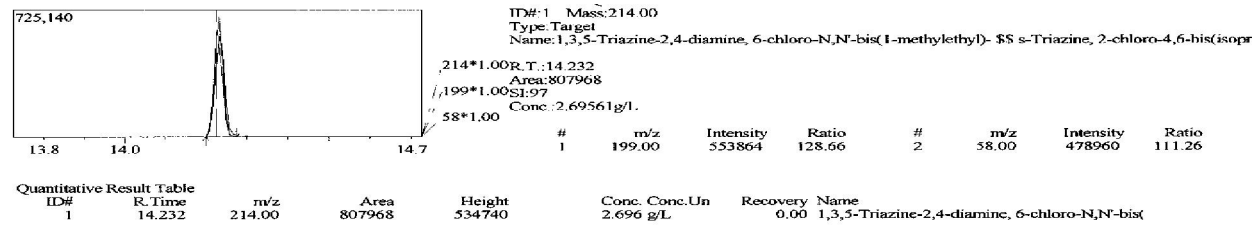

Figure 2: GC/MS chromatogram, quantitative measurement and spectral information of equilibrium phase atrazine after adsorption onto SS/A/5gL^{-1} sorbent

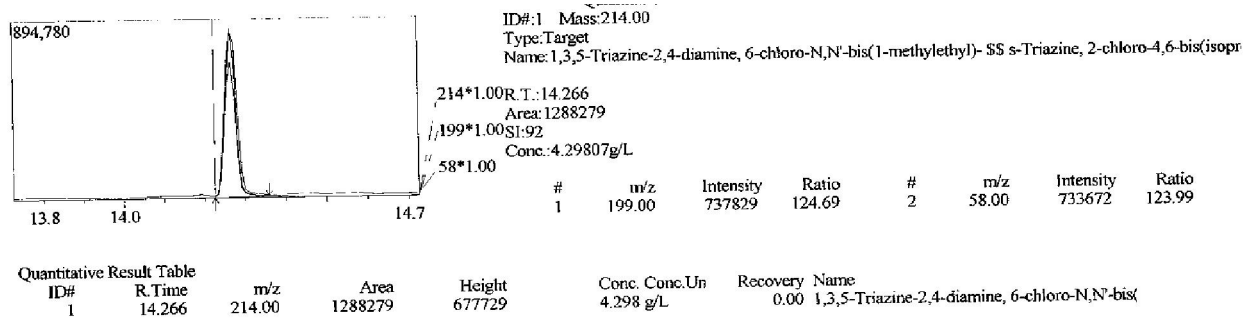

Figure 3: GC/MS chromatogram, quantitative measurement and spectral information of equilibrium phase atrazine after adsorption onto SS/A/10gL^{-1} sorbent

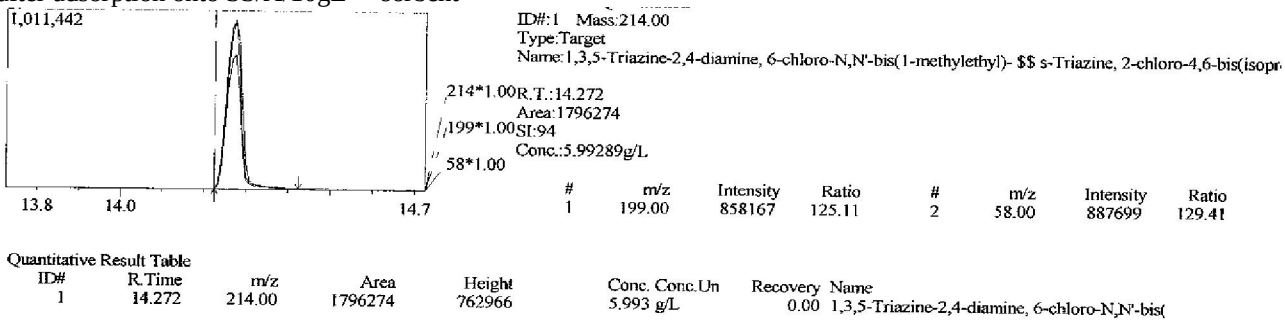

Figure 4: GC/MS chromatogram, quantitative measurement and spectral information of equilibrium phase atrazine after adsorption onto SS/A/15gL^{-1} sorbent

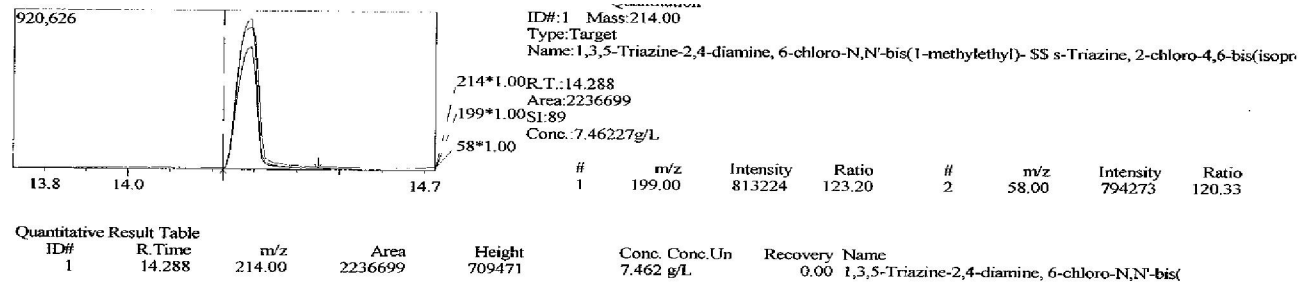

Figure 5: GC/MS chromatogram, quantitative measurement and spectral information of equilibrium phase atrazine after adsorption onto SS/A/20gL^{-1} sorbent

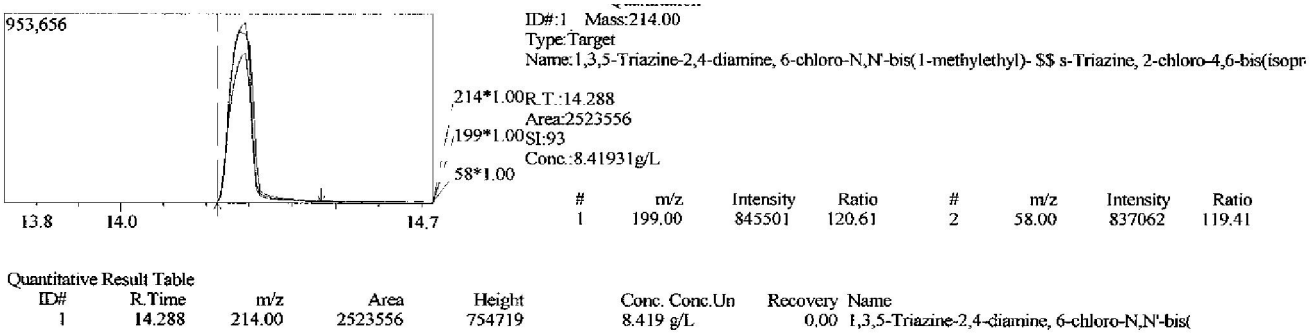

Figure 6: GC/MS chromatogram, quantitative measurement and spectral information of equilibrium phase atrazine after adsorption onto SS/A/25gL^{-1} sorbent
Equilibrium experimental data from figures 2to 6 were treated as Table 1

Table 1: Adsorption experimental data of atrazine uptake by fixed mass of SS-Sorbents at different initial sorbate concentration, using GC/MS

Sorbent	Co (g/dm^3)	Ce (g/dm^3)	Ca (g/dm^3)	% RE	Ads.m ($mg.10^{-3}$)	q_e ($mg/g \times 10^{-3}$)	Kc	ΔG (kJ/mol)
SS/A/5	5	2.696	2.304	46.08	0.0230	0.230	0.854	+393.941
SS/A/10	10	4.298	5.702	57.02	0.0570	0.570	1.327	-705.381
SS/A/15	15	5.993	9.007	60.047	0.0901	0.901	1.503	-1016.670
SS/A/20	20	7.462	12.558	62.69	0.1254	1.254	1.680	-1294.989
SS/A/25	25	8.419	16.581	66.324	0.1658	1.658	1.969	-1691.330

SS/A/5 -Sheanut shells, treated with H_3PO_4,interacted with Atrazine for 15 minute contact time, **SS/A/5** -Sheanut shells, treated with H_3PO_4,interacted with Atrazine for 15 minute contact time,

4. Discussions

Effect of initial atrazine concentration on removal efficiency:Table 1 presents the role played by initial sorbate concentration and its effect on sorption efficiency. The highest percentage atrazine removal was observed with the interaction of 0.1g atrazine with $10Cm^3$ of a 25g/L atrazine solution. Hence, out of 25g/L, 20g/L, 15g/L, 10g/L and 5g/L initial atrazines concentration, a total of 16.581, 12.538, 9.007, 5.702 and 2.696g/L atrazine was attracted onto the sheanut shell (SS) bioadsorbent. These accounts for a 66.324, 62.69, 60.007, 57.020 and 46.080% removal efficiency respectively. Findings in this research showed that for the selected time (1hour interaction) and within the 0.1g sorbent dose on $10Cm^3$ sorbate solution, (i) Adsorption efficiency increases with initial sorbate concentration.

(ii) Adsorption within the low sorbate concentration (5 – 10g/dm^3) range could possibly be followed by desorption. Hence, a less than 50% adsorption was investigated.

(iii) Adsorption of fairly high concentrated atrazine (15 – 25g/L) could be governed by a multilayer adsorption with resultant intraparticle attraction.In light of this, sorption efficiency or percentage sorbate uptake is greater than 60%.

Sorption isotherm modeling

The GC/MS quantitative results were fitted into 3 different isotherm models. These isotherms were used to investigate mode of surface coverage (Langmuir, Freundlich and BET models), while sorption capacity and intensities were investigated with Langmuir and Freundlich models only.

Table 2: batch adsorption isothermal experiment data of herbicide (atrazine) uptake by SS at different initial concentration, using GC/MS quantitation

biosorbent	Ce	log Ce	ln Ce	1/Ce	log(1+ 1/Ce)	$q_e \times 10^{-3}$	$1/q_e$	Log q_e
SS/A/5	2.696	0.431	0.993	0.371	0.137	0.230	4347.836	-3.638
SS/A/10	4.298	0.633	1.458	0.233	0.091	0.570	1754.386	-3.244
SS/A/15	5.993	0.778	1.791	0.167	0.067	0.901	1109.878	-3.045
SS/A/20	7.462	0.873	2.010	0.134	0.055	1.254	794.448	-2.902
SS/A/25	8.419	0.925	2.130	0.119	0.052	1.658	603.136	-2.780

SS/A/5 -Sheanut shells, treated with H_3PO_4,interacted with Atrazine for 15 minute contact time, **SS/A/5** -Sheanut shells, treated with H_3PO_4,interacted with Atrazine for 15 minute contact time,

The Freundlich isotherm: The Freundlich isotherm model was chosen to estimate the adsorption intensity of the sorbent towards the adsorbent. It is an empirical equation employed to describe the isotherm data and presented on Table 2.

The Freundlich model is by far the most utilized isotherm model in wastewater treatment. It has been reported that data for the adsorption involving adsorbates within a liquid phase is best fitted using the Freundlich model (Cooney, 1999). The Two-Parameter Freundlich model relates the sorbed phase

concentration to an equilibrium concentration of the adsorbate .The equation, which has a wide use in effluent or water treatment application, is given in logarithm form as equation (4) Hameed *at al.,* (2006)

$\log q_e = \log k_f + 1/n \log C_e$ - (4)

The Freundlich model implies that the energy distribution for the adsorption sites is exponential in nature (Cooney, 1999). The rates of adsorption and desorption vary with the adsorption energy of the sites and there is a possibility for more than one monomolecular layer of adsorptive coverage. The Freundlich model also does not require that the surface coverage must approach a constant value corresponding to one complete monolayer, as C_e gets larger. At high concentrations, the equation would fail to fit experimental (Cooney, 1999).

The values of K_f, the binding constant and n, the exponent, are shown the values of K_f and n determine the steepness and curvature of the isotherm (Igwe and Abia, 2007). The Freundlich equation frequently gives an adequate description of adsorption data over a restricted range of concentration, even though it is not based on the theoretical background. Apart from homogeneous surface, the Freundlich equation is also suitable for a highly heterogeneous surface and an adsorption isotherm lacking a plateau, indicating a multi-layer adsorption (Igwe and Abia, 2007).The values of 1/n, less than unity is an indication that significant adsorption takes place at low concentration but the increase in the amount adsorbed with concentration becomes less significant at higher concentrations and vice verse (Igwe and Abia, 2007). The higher the K_f value, the greater the adsorption intensity (Igwe and Abia, 2007). Figure 7 is the Freundlich isotherm plot for atrazine removal by SS sorbents.

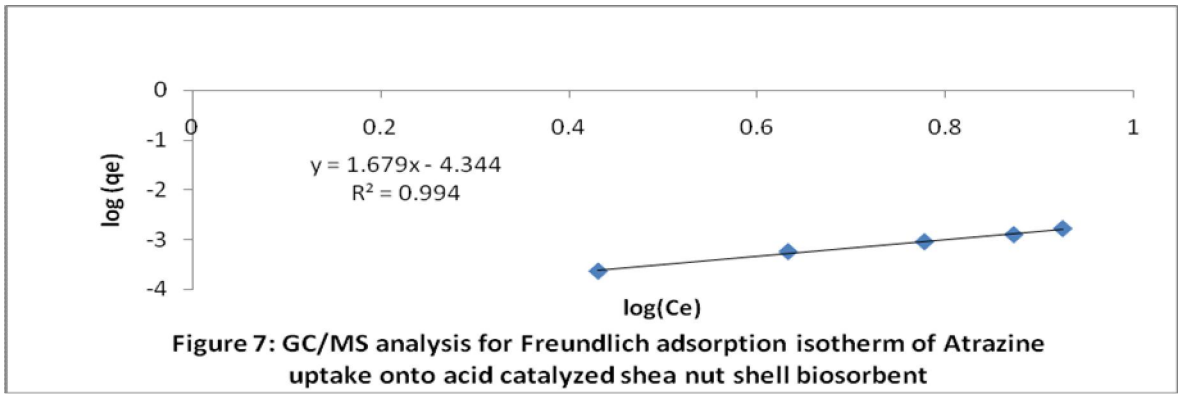

Figure 7: GC/MS analysis for Freundlich adsorption isotherm of Atrazine uptake onto acid catalyzed shea nut shell biosorbent

Langmuir isotherm: The affinity between the biomass and the different sorbates was quantified by fitting the obtained sorption values to the Langmuir isotherm model

$q = bC_e q_{max}/(1=bC_e)$ - (5)

Where q_{max} is the maximum sorption uptake and b the, Langmuir constant, which establishes the relationship between sorption and desorption rate. According to the Langmuir equation; adsorption is modeled as equation (6) below (Hameed , 2009).

$1/q_e = 1/k_a q_m . 1/C_e + 1/q_m$ - - (6)

A plot of $1/q_e$ against $1/C_e$ gave the slope, $1/K_a q_m$ and intercept, $1/q_m$.

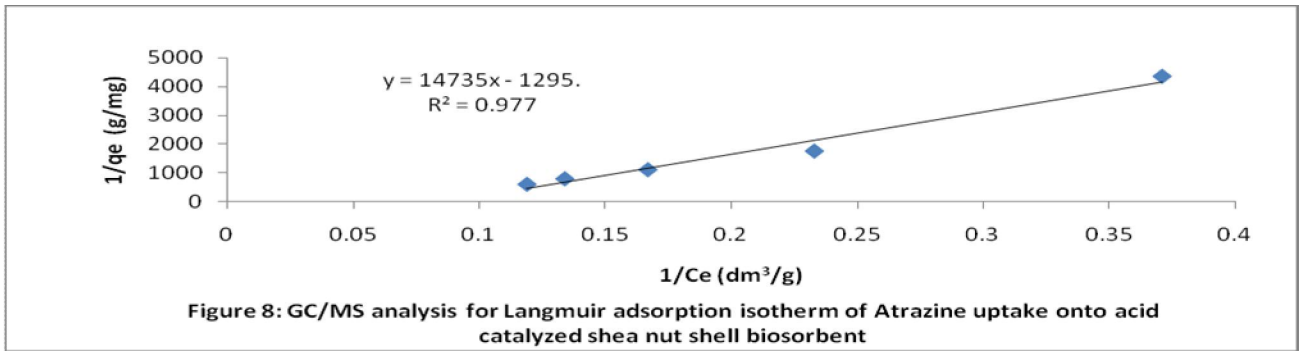

Figure 8: GC/MS analysis for Langmuir adsorption isotherm of Atrazine uptake onto acid catalyzed shea nut shell biosorbent

The model assumes monolayer adsorption onto a surface containing a finite number of adsorption sites of uniform strategies with no transmigration of adsorbate in the plane surface (Hameed *et al.*, 2006). A confirmation of the fitness of experiment data into Langmuir isotherm model indicates the homogenous

nature of the adsorbent surface. The result will also demonstrate the formation of monolayer coverage of dye molecule at the outer layer of the adsorbent (Hammed *et al.*, 2006). The essential characteristic of the Langmuir isotherm can be expressed in term of a dimensionless equilibrium parameter (R_L) defined as equation (7) by Hameed *at al.*, (2006) It is a dimensionless equilibrium parameter .

$R_L = 1/1+KaC_o$ - - (7)

Where R_L is the magnitude that determine the feasibility of the adsorption process . K_a= Langmuir constant related to energy of adsorption. while C_o is the highest initial dye concentration in the series of concentrations. The value of R_L =1 shows linear Langmuir adsorption, RL >1 and <1 are unfavourable and favourable adsorption respectively while adsorption is irreversible when $R_L = 0$

It is well known that the Langmuir equation is intended for a homogeneous surface. A good fit of this equation reflects monolayer adsorption (Igwe and Abia, 2007). Results obtained in the analysis were presented in Table3.

From Table 3, it is evidence that Langmuir isotherm predict favorable absorption as depicted from Langmuir R_L and Freundlich 1/n > 1, implying a cooperate adsorption.1/n is an indication of a measure of surface heterogeneity (Dinish *et al.*, 2007). adsorption become more heterogeneous as 1/n tends to zero). Another parameter for selecting the best of isotherms is the correlation coefficient values, R^2. Table 3 revealed that the Langmuir R^2 value (0.977) is higher than that obtained for Freundlich isotherm (0.994) .it thus implies that the adsorption process is well patterned by the Langmuir Isotherm: this, we can conclude with high proximity that adsorption is monolayer and on to a surface containing finite number of adsorption sites or uniform strategy of adsorption .This model also predicts that there is no transmigration of adsorbate in the plain of the surface (Hammed *et al.*, 2006).

Table 3: Freundlich, Langmuir and BET isotherms experimental constants of herbicide (atrazine) uptake by SS at different initial concentration, using GC/MS

Isotherms	Relationship (y =)	R^2	Parameters	Values.
Freundlich	1.679x4.344	0.994	1/n	1.679
			k_f	0.596
				0.045×10^{-3}
Langmuir	14735x-1295	0.977	q_m(mg/g)	-0.772×10^{-3}
			K_a(Lmg-1)	0.0879
			R_L	0.3127
BET	4032x-1393	0.894	BQ^O	-0.718×10^{-3}
			B	-1.895
			Q^O	0.379×10^{-3}

Beside the fact that adsorption isotherm described how the solute interact with the adsorbent, it is also used to optimize the use of adsorbent and to explain the adsorption capacity, intensity, and certain energy parameter. Freundlich k_f (0.0453×10^{-3}) and Langmuir q_m (0.772×10^{-3}) are measures of the adsorption capacity and maximum adsorption capacity respectively. It follow that q_m value is greater than K_F. This is in good agreement with earlier work conducted by this team (Itodo *et al.*, 2009b). K_F (units in mgg^{-1} ($1mg^{-n(n)}$) is defined as the distribution coefficient and represents the quantity of dye, adsorbed onto the activated carbon for a unit equilibrium concentration. It should not be unknown that 1/n ranging between 0 and 1 is a measure of adsorption Intensity. Hence, 1/n < 1 and > 1 are indication of normal and cooperative adsorption respectively. It thus implies that the adsorption of atrazine onto sheanut shell biosorbent is a cooperative type of adsorption which could be linked to the nature of adsorbate (a multicomponent sample), atrazine in herbicide moiety (Hameed *et al.*, 2006). The Langmuir, constant related to energy of adsorption, K_a is 0.0879 Lmg^{-1}

Brunauer-Emmet-Teller (BET) Theory: This theory was proposed in 1938 by Brunauer – Emmett – Teller. It relates to the formation of multilayer on adsorbent surface. According to the theory, the rate of adsorption onto the bare surface equals the rate of evaporation from the first layer of adsorbate. The inherent assumptions in the BET theory which are important to note are; (i) No interaction between neighboring adsorbed molecules

and (ii) The heat evolved during the filling of second and subsequent layers of molecules equals the heat of liquefaction. Neither of these assumptions is strictly valid, but despite this, the BET equation has been widely applied as a semi-empirical tool for the investigation of the characteristics of porous adsorbent. The BET isotherm has an empirical equation which reduces to the Langmuir model when the limit of adsorption is monolayer. Weber,(1972) presented the BET equation as 8 :

$q_e = (BC_eQ^O) /(C_i-C_e)[1+(B-1)(C_e/C_i)]$ ------ (8)

C_i = saturation concentration of the solute, C_e = measured concentration in solution at equilibrium, Q^o = number of moles of solute adsorbed per unit weight of adsorbent in forming a complete monolayer on the surface, q_e = number of moles of solute adsorbed per unit weight at concentration C_e, *B* = a constant expressive of the energy of interaction with the surface. To facilitate the application to experimental data, the equation could be transformed to the linear form as equation 9.

$C_e/(C_i.C_e)\ q_e = 1/BQ^o + [(B-1)/BQ^o][C_e/C_i]$ --------(9)

A plot of $C_e/(C_i.C_e)\ q_e$ versus C_e/C_i gives a straight line with Slope = $(B-1)/BQ^o$ and Intercept = $1/BQ^o$ (Figure 9) .This is for data which fits into the BET model (Weber, 1972).

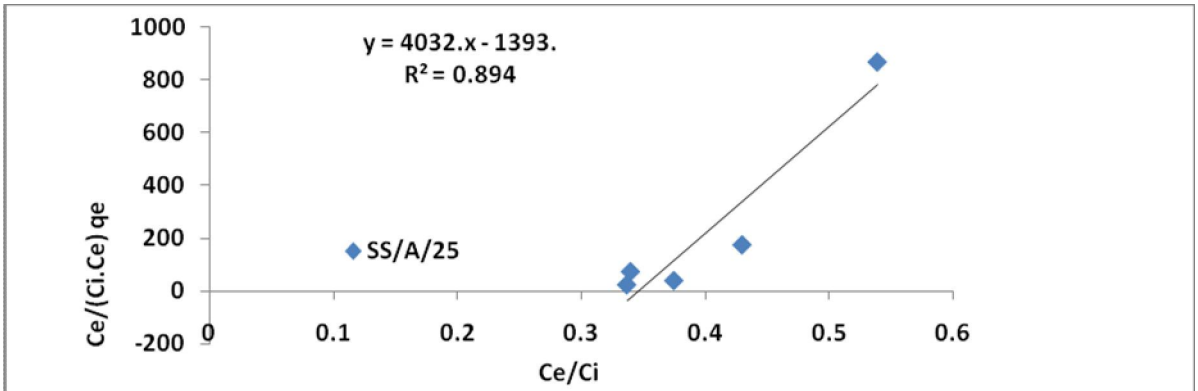

Figure 9: BET isotherm plot of atrazine uptake by SS/A/25 using GC/MS quantitation

From the analysis, the number of moles of solute adsorbed per unit weight of adsorbent in forming a complete monolayer on the surface was reported as $Q^o = 0.379x10^{-3}$

In Conclusion, a critical view of the present investigation shows that acid modified poultry waste based biosorbent is an effective absorbent for removal of Atrazine removal (with% RE range of over 66.324%)

Adsorption was studied using aqueous herbicide (atrazine) as adsorbate through fixed mass of adsorbent in batch. Sheanut shell activated carbon matrix gave a sorption efficiency (% removal) values which increases linearly with increase initial sorbate concentration from 46.08-66.324% for a 5-25g/dm^3 initial sorbate concentration. Adsorption efficiency of a given sorbate concentration is non linear as concentration increases. A GC/MS quantitation, using an external standard method gave values which were fitted into five different isotherm models. Langmuir isotherm gave best fit (High R^2 = 0.977), favorable against the Freundlich model which presented linear R^2 value (R^2 =0.994) and a constant $^{1/}_{n}$ representing surface heterogeneity, $^{1/}_{n}$ = 1.679 which implies a cooperative (not normal) adsorption ($^{1/}_{n}$ >1). It thus implies that adsorption of atrazine onto acid catalyzed sheanut shell is best explained as one on a uniform strategies of adsorption (Monolayer) and predicts that there is no transmigration of adsorbate in the plane of the surface.

Acknowledgements:

Authors are grateful to the Department of Pure and Applied Chemistry of both Usmanu, Danfodiyo University, Sokoto and Kebbi state University of Science and Technology, Aliero, Nigeria for supervisory guidance and to NARICT, Zaria for GCMS Analysis.

Corresponding Author:

Dr. Itodo Udoji Adams

Department of Applied Chemistry,

Kebbi state University of Science and Technology,

P.M.B 1144, Aliero, Kebbi state

Nigeria

E-mail: itodoson2002@yahoo.com

TEL: +2348073812726, +2348039503463

References

1.Agdi K, Bouaid A, Martin E, Fernandez H, Azmani A, Camara C. Removal of atrazine from environmental water by diatomaceous earth remediation method. Journal of Environmental monitor 2000; **2**: 420-423.

2.Ahmedna M, Marshal W, Rao M.Production of Granular activated carbon from selected Agric by products. Bioresource and Technology 2000; **71**(2): 113 – 123.

3.Bansode R, Losso J, Marshall E, Rao M,Portier J. Adsorption of volatile organic compd by pecen and almond shell based activated carbon. Bioresource Technology 2003; **90**. (2):175-184.

4.Chilton, N; Jack, N; Losso, N; Wayne, E. and Marshall, R. Freundlich adsorption isotherm of Agricultural by product based powered Activated carbon in Geosmin water system. Bioresoruce Technology 2002; **85** (2): 131-135

5.Cooney, David O. Adsorption Design for Wastewater Treatment. First Edn. Lewis. Publishers, CRC Press LLC, Boca Raton, Florida,1999.

6.Dinesh M, Charles U, Pittman T. Arsenic removal from waste water using adsorbent;A critical review.Elsevier 2007; B.V :16-42

7.Eva, C.L; Daniela, M.N; Vincenta, M. and Antonio, G.R. Interaction of Phenol, aniline and P-nitrophenol on activated carbon surface as detected by TPD. J. carbon 2008;**46**(6): 870-875.

8.Fan, M; Marshall, W; Daugaard, D. and Brown, C. Steam activation of chars produced from oat hulls Bioresource technology 2003; **93** (1):103-107.

9.Gimba C, Ocholi O, Nok A. Preparation of A.C from Agricultural wastes II. Cyanide binding with activated carbon matrix from groundnut shell. Nigerian journal of scientific research 2004; **4** (2): 106-110.

10.Hameed BH. Evaluation of papaya seed as a non conventional low cost adsorbent for removal of MB. Hazardous materials 2009 ;**162:**939-944.

11.Hameed BH, Din AM, Ahmad AL. Adsorption of methylene blue onto Bamboo based activated carbon: kinetics and equilibrium studies. Hazardous materials**.** 2006;**137**(3):695- 699

12.Igwe JC, Abia AA. Maize cob and husk as adsorbent for removal Cd, Pb and Zn ions from waste water. The physical science 2003; **2**: 83-94.

13.Itodo AU, Abdulrahman FW, Hassan LG, Maigandi SA, Abubakar MN. Activation Chemistry and kinetic studies of shea nut shells biosorbent for textile waste water treatment. Journal of research in Science, Education, Information And Communication Technology 2009a;**1**(1):168-177.

14.Itodo AU, Abdulrahman FW, Hassan LG, Happiness UO; Uba A, Sadiq IS. Enhanced Cr (vi) adsorption from textile effluent by two lignocellulosic acid catalyzed nut shells. paper presented at the 32nd international Chemical Society of Nigera (CSN) conference held on 5th-9th /10/2009 at Bauchi, Nigeria

15.Malik, R; Ramteke, D. and Wate, S. Adsorption of Malachite green on groundnut shell waste based activated carbon. Waste management. 2006; **27 (9):** 1129-1138.

16.Min C, Yun Z. Rapid method for analysis of organophosphorus pesticide in water:Bulletin application note. Agilent Technology, USA 2008;19-21.

17.Myroslav S, Boguslaw B, Arthur T, Jacek N. Study of the selection mechanism of heavy metals adsorption on clinoptilolite. J. Colloid and interface Science. 2006; **304** (1): 21-28.

18.Namarsivayan C, Kavitha D. Removal of congo red from water by adsorption onto activated carbon prepared from Coir pith.Dye and pigments.2007; **54**:47-58.

19.Omomnhenle, S; Ofomaja, A. and Okiemen, F.E. Sorption of methylene blue by unmodified and

modified citric acid saw dust. Chemical society of Nigeria 2006; **30** (1 & 2): 161- 164.

20.Raymond, P.W. Principle and practice of chromatography. First edition. Chrom. Edn. Bookseries, 2003;19 – 26. Retrieved from http://www.library4science.com/enla.html.

21.Reuben N.O, Miebaka J.A. Chromium (VI) adsorption rate in the treatment of liquid phase oil based drill cuttings. Africa journal of Environmental Sci and Tech. 2008;**2** (4): 68 - 74.

22.Robert, L. and Eugene, F. Modern practice of chromatography. 4th Edn. Wiley interscience. John Wiley and sons Inc. New Jersey, 2004; 425.

23.Rozada F, Calvo F, Garcia A., Martin V, Otaro M. Dye adsorption by sewage sludge based activated carbon in batch and fixed bed system. Bioresource technology 2003; **87** (3): 221 – 230.

24.Shimabukoro R.H. Atrazine metabolism and herbicidal selectivity. plant physiol. 1967;**42**:1269-1276.

25.Steve K, Erika T, Reynold, T., Paul M. Activated carbon :A unit operations and processes of activated carbon. Environmental engineering 2nd edn. PWS Publishing Co. 1998; 25, 350, 749.

26.USDA,.Activated Carbon processing. Review by National organic standard board panel 2002; 1-23

27.Weber WJ. physiochemical processes for water quality control. Wiley inter.science, London. 1972; 199 – 245.

28.Yoshiyuki S, Yutaka K. Pyrolysis of plant, animal and human waste: Physical and chemical characterization of the pyrolytic product. Bioresource Technology 2003;**90** (3): 241-247.

2/1/ 2010

An Assessment of Fluid Inclusions Composition Using the Raman Spectroscopy at Daleishan Goldfield, Dawu County, Hubei Province, P.R. China.

Diarra Karim [1*], Hanlie Hong [2]

[1]China University of Geosciences, Wuhan, 430074, China
[2] Faculty of Earth Sciences, China University of Geosciences, Wuhan, 430074 (Hubei province), China
[*]Corresponding Author: E mail: bn_cogem@yahoo.fr

Abstract: The purpose was to assess fluid inclusions composition in the Goldfield, Hubei province, China. The laser Raman spectroscopy was used as an analytical tool. The results show that water and carbon dioxide (70 %), and quartz (10 %) are the primary and secondary compositions of most of the inclusions, respectively. A number of three phase inclusions were low and inclusion size varies from 1 to 27µm. The density of CO2 fluid inclusions measured in quartz mineral varied from 0.61 to 0.96 g/cm3. No traces of other gases such as hydrogen (H2), ethylene (C2H2), ethene (C2H4), benzene (C6H6), hydrogen sulphide (H2S) and carbon monoxide (CO) were observed, confirming epithermal origin of the deposit (quartz ± calcite± adularia ± illite assemblage). In Daleishan goldfield, according to inclusion composition, vapor and liquid may be main agent transports for gold in epithermal systems as well as for silver. [Journal of American Science 2010;6(7):30-37]. (ISSN: 1545-1003).

Key words: Auriferous veins, Raman spectroscopy, inclusions fluids, Daleishan Goldfield, quartz.

1. INTRODUCTION

Interest in study of fluid inclusions in the Earth Sciences goes back to works of the founding father of fluid inclusions, Sorby (1858) whom described samples from ore deposits containing fluid inclusions and drew conclusions concerning ore formation. The modern science of fluids inclusion geochemistry grew principally out of pioneering work on hydrothermal ore deposits more than 50 years ago (Roedder, 1958). The plethora of researches on fluid inclusions composition in mineral deposits is a testimony to this concern (K.A.A. Hein et al. (2006) have linked mineral and fluid inclusion paragenetic studies at The Batman deposit, Mt. Todd (Yimuyn Manjerr) goldfield, Australia; Yunshuen Wang et al. (1999) proved that fluid inclusion data indicate that the hydrothermal fluids are related to ore deposition of the high sulfidation Au–Cu deposits at Chinkuashih, Taiwan; Campbell and Panter (1990) showed, using infra-red microscopy, that inclusions in quartz intergrown with cassiterite and wolframite had different microthermometric properties to those hosted by the ore minerals themselves; Roedder, 1984; Van den Kerkhof et al. (2001) provided standard criteria for the recognition of primary, pseudo-secondary and secondary inclusions.

However, poorly developed spectroscopic methods and microthermometry often characterized most of the methods used in field investigations. During the last 20 years, analytical techniques to include the laser Raman spectroscopy (*MOLE, (1976) and LABRAM or the system 1000/2000/3000 Renishaw (1997) are the first and the newest Raman microspectrometers)* have improved significantly as has the quality of data obtained (Roedder, 1984; Pasteris *et al.*, 1987; Li Binglun et al., 1986; Lu Huang Zhang et al., 1990; Rosso et al., 1995; 1997; Yamamoto et al., 2006; 2007).

In geology, Raman spectroscopy is used for testing of materials, and especially for analysis of materials in inclusions; Raman spectroscopy provides an efficient, non-destructive and sensitive tool allowing for an assessment of fluid inclusions composition and estimation of the pressures (Wopenka *et al.*, 1990; Burke A.J. E., 2001, Rosso et al., 1995; Yamamoto et al., 2006; 2007).

Studies on fluid inclusions composition in mineral deposits, especially gold deposits in China have a long history (Roedder, E., 1967, 1977a, 1979; Anderson et al., 1981, 1995; M.R., Bodnar et al., 1985 T.J., Kuehn, et al., 1989, 1991, 1994; Groves, D.I. *et al.* 1992; Heinrich, C.A et al., 1992; Sheng Jify et al., 1995; Xiao Long, et al. 2005; Roedder, E., et al. 1997; Audetat, A., et al., 1985; 1998; Hedenquist, J.W., et al., 1998*).* In Daleishan goldfield Dawu County, many researches have been carried out since 1973. However, such studies focused on characteristics (dimension, morphology, etc) of quartz veins, texture and structure of ore minerals, genesis and model of deposit, geochemistry characteristics of lamprophyre and ore, etc. (Geological Party of Ordos Basin Northeast, Hubei Province, 1973-2009; Li Jiangzhou *et al.* 1990; Hong Hanlie *et al.* 1997; 2008; 2009 Zhou Hanwen *et al.*, 1998; Du Dengwen *et al.* 2008; 2009). Studies on compositions of fluid inclusion, are still in their

juvenile and taking into consideration the fact that climate change may upset natural processes in the crust, there is need for up to date information, to serve as guide in exploration and mining planning and improved interpretation of gold ore formation. It is within this context that this study was conducted.

The purpose of this study was therefore assessing fluid inclusions composition at Daleishan Goldfield, Dawu County, Hubei Province, China, using Raman Spectroscopy. A better understanding of information on inclusion composition, through quartz mineral, over time should elucidate effective modeling and hence, the trapping of conditions of fluid inclusions and gold transport conditions in the region and beyond.

2. MATERIALS AND METHODS

2. Materials and Methods

2.1 Study Area

The study area *or Daleishan* Goldfield (longitude *114°08′37″N and latitude 31°29′08″ S)* is located in Dawu County, Hubei Province, in central China. Daleishan goldfield including two (2) gold deposits namely, Baiyun and Dapoding, is also located in Daleishan dome center, which uplifts between Dabieshan and Tongbai Mountains. Dapoding gold district is at present the biggest gold deposit discovered in northeast Ordos *Basin (5.14 and 56.76 t of gold and silver, respectively, Hong Hanlie et al. 2009) whereas Baiyun gold deposit has mined out.* Both deposits belong to (3) three ore zones of Hubei province: the Tongbai-Dabieshan Mountains polymetallic zone, the Dawu-Hong'an copper-silver zone, and the Daleishan Mountain goldfield. (Fig. 1).

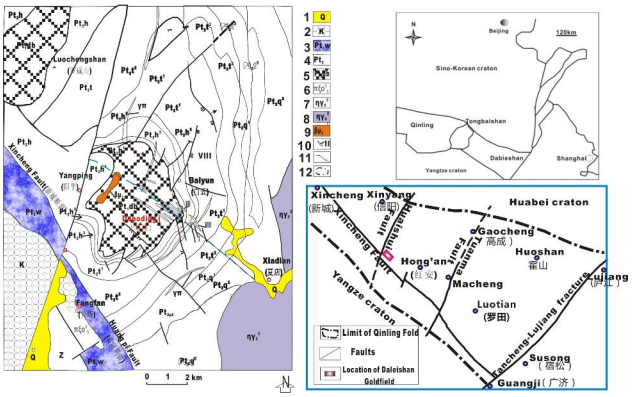

Fig 1. Simplified Geological Map of Daleishan Goldfield, modified after Du et al., 2009

The prospect temperate climate belongs to continental subtropical season; sun is shining adequately; rainfall is abundant and frost period is short; humidity rate and mean temperature are 0.93 and 15.9^0 C, respectively. Also, highest and lowest temperatures observed in June and January are 40 and -16.5°, respectively. Although rainy season is relatively short, from mid-June to mid-July, annual mean rainfall is 328.0mm; north and south are wind directions during winter and summer respectively. Deposit district is constituted by a range of low-to high mountains, following WNW and ENE directions; peak and lowest altitudes, above sea level, are 626.2 and 65.80 m, respectively.

Main rocks distributed, in the district, are (1) Lower Proterozoic metamorphic complex rocks of Dabieshan Mountain, and (2) Middle Proterozoic rocks of Hong'an. Lower Proterozoic metamorphic complex rocks of Dabieshan Mountain cover Daleishan dome center while surrounding rocks are consisted of rocks of Hong' an; the two groups of rocks show parallel structures in conformable contact. Lamprophyre and granite porphyry dikes, distributed along faults of different directions, are developed; rocks of different magmatic periods, namely granite of Yanshanian period that is related to gold (silver) mineralization, outcrop in the gold district.

At Daleishan goldfield, with 5.14 and 56.76 tons gold and silver, respectively, two ore types are dominant: gold-hosted-quartz vein and gold-hosted-altered rocks; gold grade is *4-11.63 g/t*. Vein ore mineral, according to statistics, consists of quartz (60%), k-feldspar (15%), sericite (15%), sulphide (8%) and other minerals (2%). Ore-forming phase include hydrothermal mineralization period and supergene ore-forming phase, respectively. Gold and silver are useful component of Dapoding gold deposit. Gold (silver) mineralization distribution is strictly controlled by Daleishan dome and faults of WNW and NNE directions. Even if lamprophyres have intimate relation with gold mineralization controlled by Dabie rocks, hydrothermal fluid, meteoric water and other fluids contributed significantly to formation of ore-forming mass.

2.2. Sampling Design

The samples studied here are from two gold deposits (1) Baiyun and (2) Dapoding that form Daleishan goldfield. Because gold mineralization is related to quartz veins, nine (9) hand picking samples, a least 1 kg weight, were collected, in July 2008, from three (3) of thirteen (13) auriferous veins of the goldfield, from core to rim. Two veins of Baiyun gold deposit district, No I and II, and one vein (No X) of Dapoding deposit were selected. On the whole, 5, 2 and 1 samples were collected from veins No I, II and X, respectively.

Double-polished (50-150µm) and ordinary standard thin sections of quartz were prepared at Sample Pre-treatment Bureau of China University of Geosciences, Wuhan, China. Five (5) double-polished sections (1--1;1-2-1; 1-3-1;2-1and 10-1-1) and 10 standard thin sections, four (4) from vein No I (1-2-1;1-3-1; 1-3-2; 1-4-1), four (4) from vein No 2 (2-2-1;2-2-2; 2-2-3;2-2-4), and two (2) from vein No X (10-1-1;10-1-2), sections were prepared using epoxy and resins.

2.3. Data collection and Analyses

First, microscopic observations were done, on double-polished, thin sections on Linkam THM SG600 infra-red microscope in order to collect information such as type, morphology, size, liquid-vapor ratio, distribution, origin of inclusions. Simultaneous pictographs of inclusions were taken. Main host- mineral of inclusions were determined too. All data collected were reported in table (Table 1). Each thin section or polished section was carefully examined in paying attention to different types of inclusion present, namely (1) CO_2 inclusion (2) three phase inclusion, and (3) liquid vapor phase inclusion. Representatives of each type of inclusion were selected, described, and pictures were taken under polarized-light. Infra-red microscope Linkam THM SG600 Microscope could not make composition analysis of individual inclusions, so Raman spectroscopy, Renishaw RM-1000, was selected for that. Because of limitations imposed by the minimum of sampling volume of the Raman system, only inclusions with a diameter above 5µm were selected for Raman analysis. Therefore, composition analysis has been carried out on a total of seven (7) inclusions, from 3 thin sections (1-2-1, 2-2-1 and 10-1-2) were selected.

Secondly, thin sections selected for Raman analysis were cleaned using ethanol in order to avoid surface fluorescence which can be due to incompletely dissolved remnants of epoxy and resins used in the preparation of samples.

Analysis of single fluid inclusions and solid inclusions were do using the Raman spectroscopy Renishaw RM-1000 System equipped with a microscope stage, built at State Key Laboratory of Geological Processes and Mineral Resources, located at China University of Geosciences (Wuhan). Excitation was provided by 514.5nm line of Argon-ion laser at 3.4mW, focused to a spot size of 1.5µm. Spectra were measured with spectrometer entrance slits at 12.5µm. Scanning power efficiency of fluid inclusion composition and solid inclusions are 10W, 5-20nW, respectively; counting time is 20s. First scanning is carried out from 0 to 4000 cm -1, and then second and third scanning are carried out according to peak reduced resolution zone. Data consisted of wavelength (cm^{-1}) and Raman counts that can be processed with softwares such as Excel 2007, Origin 8.0, and SPSS 17.0 for building spectrum. Raman signal from fluid-inclusion were recorded on computer screen (Fig.4), the background subtracted using Lorenz Method. For the qualitative analysis of Raman active species (identification) in fluid inclusions, only the Δv values of their characteristics are necessary species presence can be confirmed by their particular peaks in the spectrum.

3. RESULTS

3.1. Inclusion studies

Inclusion petrography, according to data collected from various inclusions under microscope, indicates that inclusions inside quartz grains are usually developed; 3 types of inclusions are notified according to their characteristics (1) CO_2 inclusion (2) three phase inclusion, and (3) liquid vapor phase inclusion., occupying large proportion, Liquid vapor two-phase is followed by single CO_2 phase, whereas a few numbers of three phase inclusion have been reported, particularly in inclusions from veins no I and II. Inclusions are, inside quartz mineral, usually are grouped, aligned or randomly distributed; their morphology is regular and present primary origin (Fig.2).

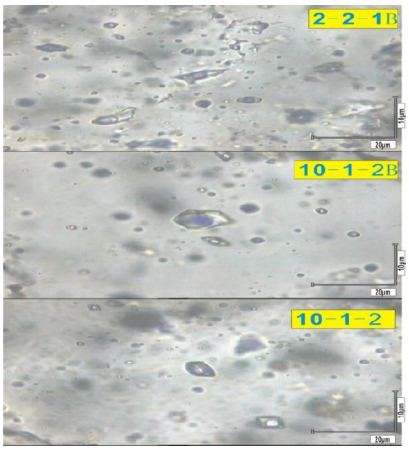

Figure.2. Photomicrographs of fluid inclusions in quartz, during Raman spectrometry analysis, from The Daleishan goldfield, Hubei Province, China.
Source : Authors' research

CO_2 inclusions present two (2) phases, with 40 to 70 % of total inclusion occupied by vapor; their sizes vary from 4 to 8µm and this type of inclusions present circular form.

Three phase inclusion usually present H_2O (l) + CO_2 (l) + CO_2 (g) (Fig.2D); its size varies from 7 to 25µm. Even though spherical, ellipsoidal, and lozenge shapes characterize most of three phase inclusion, a few numbers present regular forms. CO_2 volume, occupies at least 50% of total volume, numerous CO_2 volume up to 80% are also found.

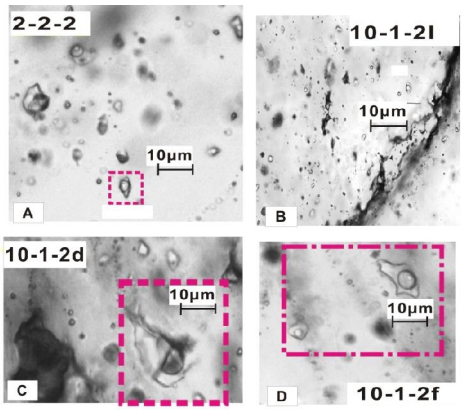

Fig.3. Examples of fluid inclusions in quartz from Daleishan goldfield. (A) sample2-2-2; isolated three phase primary inclusions with negative crystal faces; some are connected (right corner). (B) Sample 10-1-2l; CO_2 inclusion, liquid vapor, and three phases located along fractures; some inclusions are connected. (C), (D) and Samples 10-1-2d;10.-1-2f, large primary three phase inclusions with negative crystal faces, in the background- minute trails of planar inclusions for (D).All pictographs are from polarized light of Linkam THM-SG 600
Source : Authors' research

Consisting main inclusion in quartz mineral grain, liquid vapor inclusions regroup vapor bubble. Vapor liquid ratio varies between 40 and 60 % and can reach 80 %. Liquid vapor two phase inclusions present ellipsoidal, spherical and circular shapes whereas a few numbers, of the same type of inclusions present irregular shapes with size varying from 4 to 7µm.

Inclusions sizes of samples collected from veins no I and II are smaller than those of auriferous vein no X. Auriferous vein no X was mined, when samples were collected meanwhile veins no I and II were been mined out.

3.2. Inclusion composition by Raman spectroscopy analysis

Tests have been carried out on different types of inclusions (CO_2 vapor, vapor liquid and three phase inclusions) collected from different auriferous quartz veins of the deposit. Results indicated that water and dioxide carbon (CO_2) (Fig.2) are and main contents of all types of inclusions, namely three phase inclusions, liquid vapor two phase inclusion, liquid phase inclusion and vapor phase inclusion. The Raman spectra of water (broad bands of several hundred cm^{-1}) present two peaks at 3219 and at 3657 cm^{-1} , representing H_2O liquid and H_2O vapor, respectively (Dubessy *et al*.,1992; Chen *et al* 1990). Raman spectra showed no trace of other gases such as H_2, C_2H_2, C_2H_4, C_6H_6, H_2S and CO, etc as well as SO_4^{2-} and HCO_3 ions. Fluid inclusions studied here are almost all primary inclusions.

According to Raman spectroscopy analysis on inclusions, high content of water and dioxide (CO_2) is one characteristic of ore-fluid composition at Daleishan goldfield (Dapoding and Baiyun gold deposits). Obtained Raman spectra of CO_2 (v_1 : 1383 cm^{-1} and $2v_2$: 1279 cm^{-1}) have a downshift, from common Fermi diad of CO_2 (v_1 : 1388 cm^{-1} and $2v_2$: 1285 cm^{-1}), of 5 and 6 cm^{-1} ,respectively.

However, one inclusion, from sample 10-1-2A, in addition of CO_2 spectra, shows spectra of quartz inclusion at 464 and at 1160 cm^{-1}. The first spectrum of quartz, at 464 cm^{-1}, have only a downshift of 1cm^{-1} of the strongest peak of quartz, 466 cm^{-1} whereas the second spectrum of quartz (1160 cm^{-1}) represents one of the relatively strongest peaks of quartz (128, 206, 1082, and 1160 cm^{-1}). CO_2 spectra obtained with multi-channel from small inclusions (<20µm) in quartz always contain the Δv= 1160cm^{-1} peak of quartz.

Raman spectra, of seven (7) fluid inclusions, selected according to their types (CO_2 inclusions, three phase inclusion, and liquid vapor inclusions), provided water, CO_2 and quartz. Dominant Raman shift of dioxide carbon in relic inclusion assemblage of quartz ranged between 1383 cm^{-1} and 1279cm^{-1}, and 464 cm^{-1} in quartz （Fig.4） . A large proportion of inclusions, examined under Raman spectroscopy, contain water and CO_2 (70 %), and quartz (10 %) of total inclusions meanwhile a few inclusions, in addition to water and dioxide carbon (CO_2), are quartz. A total of 45 inclusions were examined under a microscope and data about size, type, morphology, liquid-vapor ratio, distribution and origin of inclusions, collected (Table 1). The sizes vary from 1 to 27µm (Fig. 5).

The Δv value of CO_2 was 104 cm^{-1} ($2v_2$-v_1; Yamamoto and Kagi, 2006; 2007)) making the densities of CO_2 fluid inclusion vary from 0.61 to 0.96 g/cm^3.

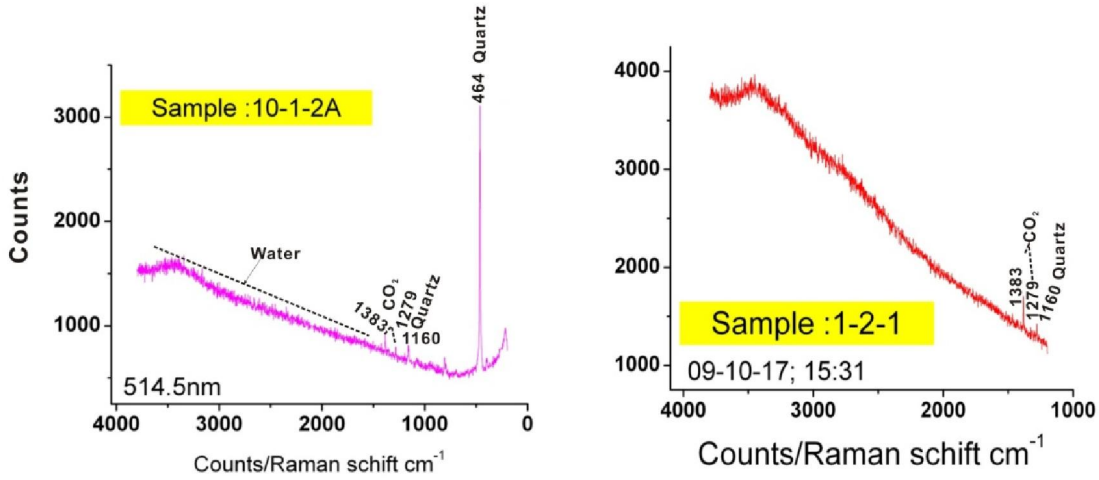

Fig.4 Raman spectrum of some inclusion
Source : Author's research

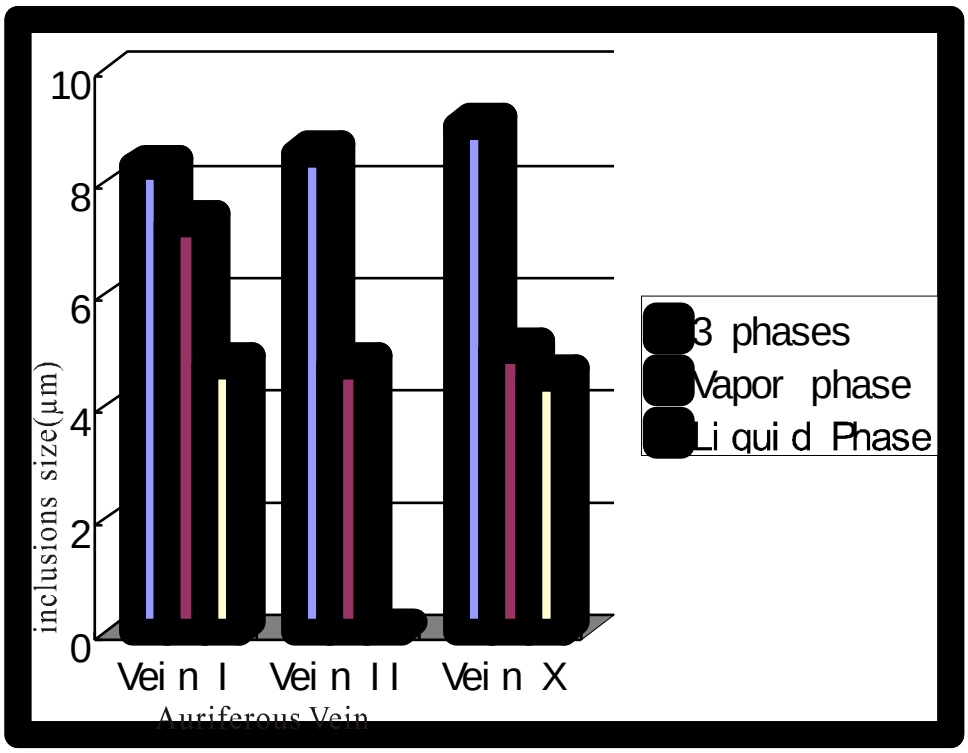

Fig.5 Mean size of different types of inclusions from different auriferous veins
Source : Authors' research

Table 1: Documentation Table of Inclusions

Vein no	Sample number	Phase type	Size (μm)	Vapor liquid ratio	distribution	Main minerals	Genesis	Photo no
X	FI-10-1-2	3 phases	5-7	3∶2∶5	group	quartz	primary	10-1-2k
II	FI-2-2-1	3 phases	6-8μm	3:1:6	group	quartz	primary	FI-2-2-1a
I	FI-1-2-1	Thunder vapor phase	4	6:4	Group	Idem	primary	1-2-1a
I	FI-1-2-1	Pure liquid phase	2	6 : 4	group	idem	primary	1-2-1b

Source: Author's research

4. Discussion

According to previous research achievements, Daleishan goldfield is an epithermal deposit that ore – forming depth is from 0.5 to 1.65 km below the water table (Geological Bureau in charge of Ordos Basin Northeast, Hubei Province, 1995). The deposit is principally linked to magmatism of Yanshanian period adamellite, where the magmatic input is entrained in and diluted by a structurally controlled or topographically driven large scale geothermal system. Epithermal deposits composed of this assemblage form in geothermal systems in volcanic arcs and rifts and result from the deep circulation of meteoric water, in Dabie Group rocks and Hong'an Group formations driven principally by a shallow intrusion. Deep down, the chloride-dominated waters are near neutral and contain reduced S-species adularia and platy calcites as deposits. During boiling of the ascending fluid, dissolved CO_2 and H_2S are partitioned into e vapor, which rises to the surface and condenses into the cool ground water, forming CO_2 –rich ground water, forming CO_2- rich or H_2S-rich steam-heated water. The CO_2 –rich or H_2S ground water is concentrated along the shallow margins of the up flow zones, where carbonate mineral-rich assemblage forms. In addition, because molecular interactions are stronger between CO_2 and H_2O for the system H_2O–CO_2- CH_4 (Dubessy *et al.*1999) may evaporate during magmatic process.

Co/Ni ratio of pyrite, superior to 1, suggests that gold mineralization is related to deep process. Only a limited number of species in fluid inclusions can be analyzed quantitatively, namely the polyatomic gas species and very few polyatomic gas species and polynuclear species in solution ($^{12}CO_2$, CH_4, N_2, H_2S, C_2H_2, SO_2, CO, NH_3, etc.) (Roedder, 1990). Therefore, further analyses such as LA-ICP–MS or PIXE, of inclusions, are needed for tracking other components like major and minor ions (Na, k, Ca, Mg, Cl, Mg, Li, Al, Fe, B, Ba, P) in liquid species or for quantitative analyses of solid species. Fluid inclusion composition provided by Raman spectroscopy suggests that dioxide carbon (CO_2), consisting main component, may play important role in gold (silver) mobilization and transport, from deep to the near-surface at Daleishan goldfield.

5. Conclusion

Raman spectra, of seven (7) fluid inclusions, present peaks of water, dioxide (CO_2) and quartz species. A large proportion of inclusions, examined under Raman spectroscopy, contain water and CO_2 (> 70% of total inclusions) whereas a few inclusions, in addition to water and CO_2, have quartz. Fluid, transporting gold (silver) mineralization may induced by intrusion of adamellite and syenite dated Yanshanian period, and has reached Daleishan dome, consisted mainly by Dabie metamorphic rocks through Hong'an formation. Sizes of inclusion from mined out veins (vein No I and II) are smaller than those from a mined vein (Vein No X), confirming an ultimate relationship between gold mineralization mobilization, transport and deposition, and inclusion sizes.

In Daleishan goldfield, according to inclusion composition, vapor and liquid may be main agent transport for gold silver in epithermal systems like at concentration (Bajo de la Alumbrera (Argentina) and Grasberg (Indonesia) porphyry copper-gold deposits (Ulrich et al. 1999) where parts-per-million levels of gold have been discovered in vapor.

ACKNOWLEGMENTS

This work would not have been possible without the logistical support of Geological Bureau in charge of Ordos Basin Northeast, Hubei province, China, and we would like to thank Xu Zhiqian, Du Dengwen, both from this bureau, for providing data for some of our figures and reports and for guiding as during field trip. Raman spectroscopy analyses and microscopic observations under Linkam THM-SG 600 of inclusions were conducted at the facilities of Prof. He Mochun at China University of Geosciences, Wuhan, China to whom we express our gratitude.

REFERENCES

[1] Anthony, E., Williams, J., Robert, J. Bowell and Artashes, A. M. , 2009. Gold in Solution. Elements, 5, 281–287. Doi: 10.2113/gselements.5.5.281

[2] Audétat, A., D., Günther, Christoph, A. H., 1998. Formation of a Magmatic-Hydrothermal Ore Deposit: Insights with LA-ICP-MS Analysis of Fluid Inclusions. Science, 279, 5359, 2091-2094.Doi: 10.1126/science.279.5359.2091

[3] Shao Jielian, 1988. Prospecting Mineralogy of Gold Deposit. China University of Geosciences Press, 1988: pp : 38-45 (in Chinese). ISBN 7-5625-1564-6

[4] Ernst, A.J. Burke, 2001. Raman microspectrometry of fluid inclusions. Lithos, 55, 139–158. Doi: 10.1016/S0024-4937 (00)00043-8

[5] Hedenquist, J.W., Reyes, A.G., Simmons, S.F., Taguchi, S., 1992.The thermal and geochemical structure of geothermal and epithermal systems: a framework for interpreting fluid inclusion data. Eur. J. Mineral. 4, 989–1015. ISSN 0935-1221.

[6] Hein, K.A.A., K., Zaw , T., P. Mernagh, 2006. Linking mineral and fluid inclusion paragenetic studies: The Batman deposit, Mt. Todd (Yimuyn Manjerr) goldfield, Australia, Ore Geol. Reviews, 28, 180–200. Doi: 016/j.oregeorev.2005.05.001 www.elsevier.com/locate/oregeorev

[7] Heinrich, C.A., Ryan, C.G., Mernagh, T.P., Eadington, P.J., 1992. Segregation of ore metals between magmatic brine and vapor: a fluid inclusion study using PIXE microanalysis. Econ. Geol., 87, 1566–1583. Doi:10.2113/gsecongeo.87.6.1566 [8] [8] Junji, Yamamoto, H. Kagi, 2003. Micro-Raman densimeter for CO_2 inclusions in mantle-originated fluid inclusions. Chem. Let. 35, 1333-1339

[9] J. Yamamoto, Hiroyuki Kagi, Yoko Kawakami, Naoto Hirano, Masaki Nakamura, 2007. Paleo-Moho depth determined from the pressure of CO_2 fluid inclusions: Raman spectroscopic barometry of mantle- and crust-derived rocks. Earth and Plan. Sc. Lett., 253, 369–377. Doi: 10.1016/j.epsl.2006.10.038

[10] J. Yamamoto, H. Kagi, 2003. Extended micro-Raman densimeter for CO2 inclusions in mantle-originated fluid inclusions. Chem., Lett., 35, 1333-1339.

[11] Lattanzi, P., Curti, E., Bastogi, M., 1989. Fluid inclusion studies on the gold deposits of the Upper Valle Anzasca, northwestern Alps, Italy. Econ. Geol., 84, 1382–1397. Doi: 10.2113/gsecongeo.84.5.1382

[12] Lattanzi, P., 1991. Applications of fluid inclusions in the study and exploration of mineral deposits. Eur. J. Mineral., 3, 689–701. ISSN 0935-1221

[13] Liu, J., Zheng, Zheng, M., Liu, J. and Su, W., 2000. Geochemistry of the La' erma and Qiongmo Au-Se deposits in the western Qinling Mountains, China. Ore Geol. Rev., 17, 1, 91-111. Doi : doi:10.1016/S0169-1368(00)00008-1

[14] Nakamoto, K., 1997. Infrared and Raman spectra of inorganic and coordination compounds. Part A : theory and applications in inorganic chemistry, pp: 401-408. Wiley-Interscience, New York ISBN : 9780471743392

[15] Pasteris, J. D., Wopenka, B., Seitz J.C., 1988. Practical Aspects of Quantitative Laser Raman microscope spectroscopy for the study of fluid inclusions Geoch. Cosmochim Acta, 52: 979-988. Doi:10.1016/0016-7037(88)90253-0

[16] Roedder, E., 1984. Fluid inclusions, Review in Min. Mineralogical Association of America, 12: 644 http://rimg.geoscienceworld.org/

[17] Roedder E., 1990. Fluid inclusions Analysis-Prologue and Epilogue. Geoch. Cosmochim Acta, 54: 495-507. Doi: 1 0.1016/0016-7037(90)90347-N

[18] Rusk, B.G. and Reed, M.H., 2002. Scanning electron microscope-cathodoluminescence of quartz reveals complex growth histories in veins from the Butte porphyry copper deposit. Montana. Geology, 30,727-730. Doi: 10.1130/0091-7613(2002) 030<0727:SEMCAO> 2.0.CO;2

[19] Shepherd, T.J., Ranbin, A.H., Alderton, D.H.M., 1985. A Practical Guide to Fluid Inclusion Studies. pp: 239. Blackie, Glasgow. ISBN : 0412006014 Takahashi, R., Matsueda, H., Okrugin,V.M and Ono,S.,2007. Epithermal gold-silver

mineralization of the Asachinskoe deposit in South Kamchatka. Russia. Resour. Geol.,57(4), 354-373 (in press).

[20] Takahashi, R., Müller, A., Matsueda, H., Okrugin, V.M., Ono, S., Van den Kerkhof, A.M., Kronz A., Thor, H. Hansteen, Andreas Klügel, 2008. Fluid Inclusion thermobarometry as a tracer for Magmatic Processes. Review in Min. Mineralogical Association of America, 69: 648 http://rimg.geoscienceworld.org/

[21] Andreeva, E.D, 2008. Cathodoluminescence and trace element in quartz: clues to metal precipitation mechanisms at the Asachinskoe gold deposit in Kamchatka.in " origin and evolution of natural diversity. Proceedings of the International Symposium The Origin and evolution of the natural diversity , 1-5 October 2007", H. Okada, S.F. Mawatari, N. Suzuki, P. guatam,eds.Sapporo,175-184. http://hdl.handle.net/2115/38463

[22] Wang, L., J. Zhenmin, H., Mouchun, 2002. Raman spectrum Study on Quartz Exsolution in Omphacite of Eclogite and its Tectonic Significance. Journal of China Univ., 14 (2): 119-126. ISSN 1002-0705

[23] Wark, D.A., Hildreth, W., Spear, F. S., Cherniak, D.J., Watson, E.B.,2007. Pre-eruption recharge of the Bishop magma system. Geology, 35, 235-238. Doi: 10.1130/G23316A.1;

[24] Wiebe, R.A., Wark, D.A, Hawkins, D.P., 2007. Insights from quartz cathodoluminescence zoning into crystallization of the Vinalhaven granite, coastal Maine. Mineral. Petrol., 154, 439-453; Doi :10.1007/s00410-007-0202-z

[25] Watt, G.R., Wright, P., Galloway, S., McLearn, C., 1997. Catholuminescence and trace element zoning in quartz phenocrysts and xenocrysts. Geochim. Cosmochim. Acta, 61, 4337-4348. Doi: 10.1016/S0016-7037(97)00248-2

[26] Wilkinson, J.J., Boyce, A.J., Earls, G., Fallick, A.E., 1999. Gold remobilization by low temperature brines: evidence from the Curraghinalt gold deposit, Northern Ireland. Econ. Geol., 94, 289–296. Doi: 10.2113/gsecongeo.94.2.289

[27] Wilkinson, J.J., 2001. Fluid inclusions in hydrothermal ore deposits. Lithos, 55,229–272. Doi: 10.1016/S0024-4937(00)00047-5

[28] William, D. Carlson, Emily A. McDowell, Masaki Enami, Tadao Nishiyama and Takashi Mouri, 2009. Laser Raman microspectrometry of metamorphic quartz: A simple method for comparison of metamorphic pressures—Corrigendum. American Mineralogist, 94, 291–1292. Doi: 10.2138/am.2009.549

[29] Xiaoming S., Y., Zhang, Dexing X., Weidong S., G., et al., 2009. Crust and mantle contributions to gold-forming process at the Daping deposit, Ailaoshan gold belt, Yunnan, China. Ore Geology Reviews 36, 235 – 249. Doi:10.1016/j.oregeorev.2009.05.002

[30] Y., B. Wu, S., Gao et al., 2009. U-Pb age, trace element, and Hf isotope composition of zircon in quartz vein from eclogite in the west Dabie Mountains: constraints on fluid during early exhumation of ultra-high pressure rocks. American Mineralogist, 94, 303-312. Doi: 10.2138/am.2009.3042

3/1/2010

Early-age compressive strength assessment of oil well class G cement due to borehole pressure and temperature changes

Mojtaba Labibzadeh [1], Behzad Zahabizadeh [1], Amin Khajehdezfuly [1]

[1.] Department of Civil Engineering, Faculty of Engineering, Shahid Chamran University, Ahvaz, Iran
Labibzadeh_m@scu.ac.ir

Abstract: Development of high early-age compressive strength oil well cement is an important task in the oil well cement design. Achievement of suitable early-age compressive strength of oil well cement ensures both the structural support for the casing and hydraulic/mechanical isolation of borehole intervals. Holding this issue in mind, in this research, the effect of pressure and temperature changes inside the borehole on the class G oil well cement compressive strength has been studied. In the proposed work, in contrast to the mostly previous studies which considered some certain temperatures and atmospheric pressure in their tests, the effects of contemporary pressure and temperature changes on the early-age compressive strength of oil well cement have been investigated. Using a non-destructive method, the compressive strength of 48 hours cured cement samples under progressive changing of simultaneously pressures and temperatures coincident to a real oil well data were measured and recorded continuously at predefined intervals during this 48 hours period time. The case study was an oil well located in Darquain region of Khuzestan province in Iran. Obtained results showed that 8 and 12 hours aged samples have a maximum compressive strength in a certain combination of pressure and temperature, 51.7 MPa and 121°C, whereas 24, 45 and 48 hours aged samples have a minimum point in their compressive strength curve at 17.2 MPa and 68°C and a maximum point at 41.4 MPa and 82°C. All the samples show the significant reduce (up to approximately 70%) in compressive strength after the 51.7 MPa and 121°C point. Considering the case study oil well profile of borehole pressure and temperature changes, this tested class G cement is recommended to use in cementing job from ground level down to the almost 4000 m below the surface. [Journal of American Science 2010;6(7):38-47]. (ISSN: 1545-1003).

Keywords: Compressive Strength, Oil Well, Cementing, borehole Pressure and Temperature

1. Introduction

Among all operation being performed during oil or gas well drilling, the wellbore tubing and cementing can certainly be known as the most important activities. Durability and efficiency of well production rate depend a lot on the degree of success of this stage. In tubing operation, wellbore is covered by special steel pipe string segments (casing) and consequently at cementing stage, annulus between casing string and well-rock (Formation) are filled with a certain compound of cement grout. This compound could be makeup from different ingredients with different percentage of weight with respect to the weight of cement in the grout mixture. For example, A cement slurry is comprising as follows: an aluminous cement the alumina content of which is at least 30%; a microsilica with a granulometry in the range 0.1 to 20 μm the percentage of which is less than 35% by weight with respect to the weight of cement; mineral particles with a granulometry in the range 0.5 to 500 μm the percentage of which is less than 35% by weight with respect to the cement, the percentage of said particles remaining below the percentage of said microsilica; a hydrosoluble fluidifying agent the percentage of which is in the range 0.2% to 3% with respect to the weight of cement; a retarding agent to control the setting time of the slurry; water in a quantity of at most 40% with respect to the cement (Asadi, 1983) .

The cement grout is gradually being set over a certain time interval (usually after several hours or several days) and converts to a stiff cement sheath. Cement sheath must be able to resist against to the pressure of formation consists of pore pressure and fracture pressure. Sum of these two pressures is called the in-situ pressure or total pressure. Furthermore, cement sheath must be able to withstand against to hydrostatic pressure due to drilling fluids inside the casing string, thermal loads due to temperature rise from surface to the bottom of the well and also periodic loads due to various operations inside the well consist of cement hydration, hydrocarbon production, stimulation treatments, pressure integrity tests of cement and casings that they can change pressure and temperature exposed on the cement sheath after placement in annulus (Abbaszadeh, 2005, Ravi et al. 2007, Al-Suwaidi et al. 2008). Monitoring wellbore

temperature is one of the most important factors controlling the chemical reaction and performance results of a cementing operation. In oil well cementing, the cement slurry placed at total depth is subject to progressively increasing temperature from the time it is mixed on the surface and pumped into the well until the time the cement cures and the formations adjacent to the wellbore return to their ultimate static pressure. Circulating and static temperatures both affect cement design. Circulating temperature is the temperature the slurry encounters as it is being pumped into the well. Static temperature is the formation heat to which the slurry will be subjected after circulation is stopped for a set period of time. Designers should know the bottom hole static temperature (BHST) to design and assess long-term stability, or rate of compressive strength development for the cement slurry. Determining BHST is especially important in deep well cementing, where the temperature differential between the top and bottom of the cement can be great. Generally, cement sensitivity increases as the BHST increase (Abbaszadeh, 2005). In the oil and gas industry, two types of compressive strength for cement are defined. Early-age compressive strength is the compressive strength of cement at initial times after the preparation and placement of cement grout into the wellbore and long-term compressive strength is the compressive strength of cement after completion of hydration process and exploitation of the well and or even after several years of the well production operation. Development of high early-age compressive strength oil well cement is an important task in the oil well cement design (Di Lullo, 2000). Achievement of suitable early-age compressive strength of oil well cement ensures both the structural support for the casing and hydraulic/mechanical isolation of borehole intervals (Di Lullo, 2000). When the cement grout is produced and pumped into the wellbore, the cement slurry starts changing from a true fluid into a semi solid set material with measurable compressive strength at beginning of the gel formation and the fluid starts undergoing hydrostatic pressure through shear strains and gel gradually gains its strength. The static gel strength which occurs due to decrease in volume leads to reduction in pressure. The transition phase is very critical, because under this condition cement column starts to support itself and does not transfer a major part of the hydrostatic pressure to the flow zone and so a longer transition phase allows a longer time for the volume to decrease (Johnstone et al., 2008). This phenomenon which leads to more gas leaking thorough the cement column is known as gas migration and caused inefficiency of cementing operation. Gas migration can be prevented by reducing the time of transition phase and in other words by speed up the development of cement compressive strength (Johnstone et al., 2008, Pedam, 2007). Another important time at initial times after cementing to note is the Wait-On-Cement (WOC) time; this is defined as the time at which compressive strength begins to develop in the slurry right after the time when the static gel-strength development ends. In other words, WOC time is the time that takes along to cement gains minimum compressive strength, equal to 3.45 MPa (500 Psi) according to API (American Petroleum Institute), for resisting the shocks caused by drilling operation at later stages. Delays in strength development cause significant amounts of lost time due to the need to WOC. Thus, drilling operations cannot proceed and the rig must sit idle until the cement is deemed hard enough to continue (Di Lullo, 2000, Pedam, 2007, Nelson, 1999). Compressive strength of cement in the long-term is important and necessary against the conditions encountered within the well, in addition to the early-age compressive strength. Hard cement must be able to cover well's casing strings and link them to the formation. Also, hard cement cause stability of wellbore and protects of casing strings against external pressures resulting from earth floors, which may even cause the pipes will be broken and against electrolysis and corrosion caused by corrosive waters underground and sour hydrocarbons or straight contact with stratums; and prevents of fluid migrations between formations and unwanted pollution of valuable hydrocarbons (Asadi, 1983). A three-step approach, outlined in Figure 1, can help operators in properly cementing a well that can produce hydrocarbons safely and economically (Ravi et al., 2007, Reddy et al., 2005). Step 1 is the engineering analysis. The outcome of the engineering analysis is to help provide the optimum cement sheath properties needed to withstand the well operations. Step 2 is cement slurry design and testing for providing a cement system that can match or exceed the cement-sheath properties evaluated in Step 1. Examples of the cement-sheath properties that should be tested in Step 2 are:

- Compressive strength
- Tensile strength
- Young’s modulus
- Poisson’s ratio
- Plasticity parameters

In addition, the laboratory-measured values from Step 2 are a part of the input variables for the engineering analysis (Step 1) to evaluate the cement-sheath integrity. To help achieve zonal isolation, Step 1 and 2 should be followed by Step 3, effective

cement slurry placement and monitoring during the life of the well (Ravi et al., 2007, Reddy et al., 2005).

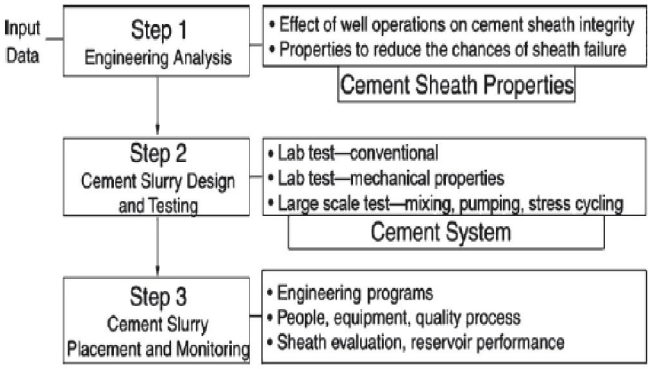

Figure1. Steps in cementing an oil well

The subject of this paper is related to step 2 in figure 1 and deals with the importance of early-age compressive strength development and its role in the degree of success of a cementing operation by evaluating the behavior of cement in terms of compressive strength under conditions of pressure and temperature changes within the well at initial times after starting operation. The main aim of the authors of this research is to achieve an optimum safety depth for injection of class G cement into the oil wells located in Darquain region of Khouzestan province of Iran in order to prevent the gas migration during well construction time and improve the safety factor in construction stage.

The main difference between this research and previous works which will be briefly mentioned in the following is that in the foregoing studies pressure was assumed constant and temperature was set to be varied. But in the present work, the pressure and temperature are set to be changed according to real conditions in the borehole, and these effects on the early-age compressive strength of cement is investigated.

1.1 Literature review

Assessment of the various treatment aspects of the cement considering the application and its impression within the oil and gas wells, always has been attended by researchers. Some of the scientists have been studied the water and additives effect on cement mechanical properties without considering the effect of pressure or temperature inside the well bore. (Dahab and Omar, 1989) prepared a cement slurry mixture mostly used in the Saudi Arabia country using sea water, fresh water and distilled water. They deduced through their investigations that cement which prepared with sea water shows more compressive strength than the other two types of grout in 1, 2 and 3 curing times. Also their evaluation on effect of additives such as calcium chloride, lignosulfonate and bentonite on the cement slurry indicated that in a certain concentration of each of these additives, cement compressive strength increases with increasing in the curing time; but in a fixed time, compressive strength is diminished with increasing concentration of each of these additives (Dahab and Omar, 1989). Lecolier, 2007 studied long-term curing time condition effects of water, salt water and crude oil on cement compressive strength. Results from the first mold (containing water) illustrated that during the first six months, the mechanical strength change is not significant. But after a year, the compressive strength slowly starts to decrease. Results of the second mold (containing salt water) which the curing fluid in it was renewed every month showed that during the first four months compressive strength is similar to the situation that curing fluid was not change. After four months, compressive strength started to severe decrease. After a year, reduced in the compressive strength was about 50 percent. But in the third case unlike what was observed in two previous tests, compressive strength remains stable over time. This could be due to the absence of acidic compounds in the crude oil (Lecolier, 2007). Some of the others add the effect of temperature factor in their studies. For example, in 1999, Noik and Rivereau compared behavior of four various compounds of cement class G at 120°C, 140°C and 180°C. Their target was the evaluation of silica sand effects on cement slurry. Their experiments demonstrated that at 180°C temperature, compressive strength values without silica was very low and would be increase with addition of silica to the cement slurry (Noik and Rivereau, 1999). Mirza, 2002 examined the effect of fly ash on cement properties. This research exerted that the use of fly ash at cement mixture in 20°C temperature and atmospheric pressure causes a reduction in the 28 and 91 day compressive strengths, compared to the reference grout having an equivalent value of water to cement ratio; But as the grout matures, the difference between the increase in strength of the reference grout and the fly ash grout decreases (Mirza, 2002). Another group of scientists consider some certain combination of temperature and pressure in their work: Jennings, 2005 tested a combination of cement containing hollow ceramic

spheres at 1.14 gr/cm3 cured for one year at 149°C and 20.7 MPa and found that the provided sample has unaccepted decline in compressive strength. The highest registered of compressive strength in one week was 7.19 MPa; and after a year of curing has decreased to 7.3 MPa. This combination declined 81% in 11.75 months when curing at 149°C and 20.7 MPa (Jennings, 2005). Also, Al-Yami, 2007 and 2008 tested another low-density blend of cement class G, aluminum silicate, crystalline silica, hollow glass microspheres and water at 1.12 gr/cm3. First in 2007, he cured this combination at 66°C and 12.4 MPa; in this case, the compressive strength continued to develop over more than one month, but then stabilized after 2 and 3 months as the system reached equilibrium. The final compressive strength of this combination after curing for 3 months at 66°C and 12.4 MPa was 15.15 MPa (Al-Yami et al., 2007). Then in 2008, he examined this mixture at 127°C and 20.68 MPa; the compressive strength in this pressure and temperature conditions was stable over the three months test period, too. The final compressive strength after curing for 3 months at 127°C and 20.68 MPa was 9.94 MPa, which significantly exceeds the recommended values of 3.45 Mpa according to API to hold many casings in place (Al-Yami et al., 2008).

2. Material and Methods

2.1. Pressure and temperature conditions inside the proposed wellbore

Pressure and temperature conditions required for curing samples of cement, were selected in accordance with actual well conditions of Darquain region located 40 Km north of Abadan city along the west bank of Karun River in Khuzestan province of Iran. Considering the given static temperature gradient in our proposed drilled borehole (Darquain wellbore) temperature values in various depths of the well has been calculated. These data have been measured by instruments inside a real oil well at April 2009.

According to Figure 3, the pressure values inside the wellbore and around it (inside the formation) are both functions of depth variable, and should be noted. The value of hydrostatic pressure inside the wellbore can be directly calculated with Equation 1 (Abbaszadeh, 2005).

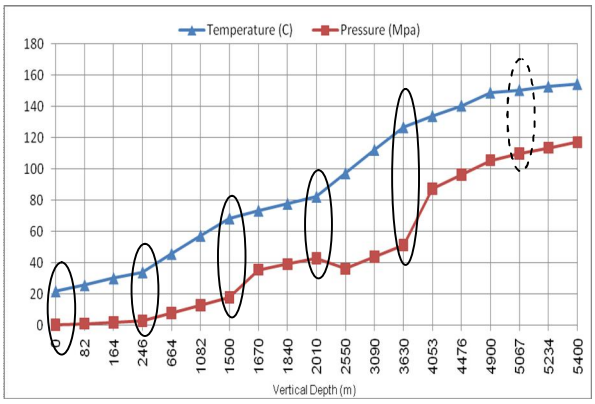

Figure 2.Temperature and pressure changes in depths of studied oil well-April 2009

$$P_{Hyd} = 9.807 \times \gamma_{Mud} \times TVD$$

Where, P_{Hyd}= hydrostatic pressure (Pa)
γ_{Mud}= drill mud density (Kg/m3)
TVD= total vertical depth (m)

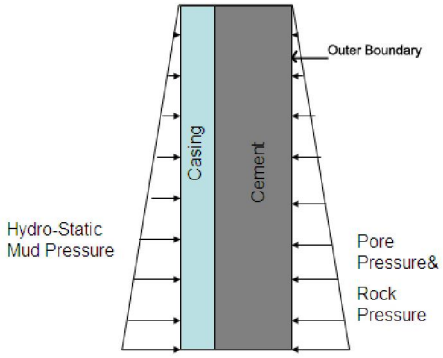

Figure 3. Schematic of pressures around and inside the wellbore

In the outer boundary we encounter two types of pressures, the rock pore pressure and the overburden pressure. The resultant pressure acts horizontally toward the wellbore (Abbaszadeh, 2005). Pressure in the outer boundary always must be in equilibrium with hydrostatic pressure due to drilling fluids. Imbalance between the two pressures mentioned can lead to gas blow out of annulus between casing and formation (if in-situ pressure be more than hydrostatic pressure) or lead to crush the around stones and fluid loss (if hydrostatic pressure be more than in-situ pressure).

When cement slurry pumps into the annulus, it creates hydrostatic pressure equivalent to mentioned pressures until is in the liquid phase. Therefore, pressure which cement encountered inside the well at curing time and after hardening is in-situ pressure in the outer boundary that should be equal to hydrostatic pressure of drilling fluid within the well. Hence, considering given values of mud density in various depths of studying well, pressure values were calculated using the Equation.1 and used for cement samples test in the laboratory to create pressures in accordance with actual conditions inside the well. Pressure changes have been showed in Figure 2.

According to Figure 2, six different points of pressure and temperatures conditions inside the well were selected for curing cement samples. The pressure at the sixth point is not real because of the limitation of the serviceability of the test machine. These points are surrounded by ellipses in figure 2.

Cement mechanical failure may be caused by stresses induced by condition variations in borehole such as:

- Pressure integrity test
- Pressure increase due to gas production
- Change in mud weight after cement placement
- Stimulation treatments
- Temperature Changes

Cement compressive failure may be occurred if the cement is placed between two casings or across a hard formation and the radial stresses exceeds the cement rupture strength (Al-Suwaidi, 2008).

Benchmarked points are ambient pressure and temperature; pressures of 2.8 MPa, 17.2 MPa, 41.4 MPa, 51.7 MPa and 51.7 MPa; and corresponding temperatures of 38°C, 68°C, 82°C, 121°C and 149°C. As stated earlier, the reason for same pressure at the last two points was limitation of pressure increase over this amount due to laboratory safety conditions.

2.2. Design of Cement Slurry

Slurry blend consists of cement class G, additives and water. There are currently eight classes of API Portland cements, designated A through H. They are arranged according to the depths, to which they are placed, and the pressures and temperatures to which they are exposed (Nelson, 1999, API, 1997). In oil well drilling industry class G and H well cements are known as basic well cements, because no additions other than calcium sulfate or water, or both, shall be inter-ground or blended with the clinker during manufacture of these well cement classes. Hence, with addition of appropriate additives such as accelerators and retarders can change their setting time to cover a wide range of well depths, pressures and temperatures (Asadi, 1983, Nelson, 1999). The main phases of class G cement clinker are consists of 50% Tricalcium Silicate (C3S), 30% Dicalcium Silicate (C2S), 5% Tricalcium Aluminate (C3A) and 12% Tetracalcium Aluminoferrite (C4AF) (Asadi, 1983).

Additives which used in cement composition are selected based on the test pressure and temperature conditions. Calcium Chloride (CaCl2) used as accelerator for reducing the setting time of cement slurry at ambient pressure and temperature and D-013 used as retarder for increase the setting time of cement slurry at high pressures and temperatures (Asadi, 1983). Considering the aim of this research, the additives which had the least possible effect on cement compressive strength were used; at the same time these additives would be able to provide relatively acceptable conditions of rheological properties and setting time close to slurries conditions used in application.

Calcium Chloride was added in cement slurry at ambient pressure and temperature in concentration of 1% by weight of cement (BWOC). D-013 was added in cement slurries in concentration of 0.1% BWOC for curing at (17.2 MPa and 68°C) and in concentration of 0.3% BWOC for curing at (41.4 MPa and 82°C), (51.7 MPa and 121°C) and (51.7 MPa and 149°C) conditions. Researches done in the past showed moderate retardation had minimal effect on the static cement properties (i.e. properties that measured under static temperature such as compressive strength) (Pedam, 2007). Considering this issue in mind and for prevention of additives effects on cement compressive strength in order to determine the true effect of pressure and temperature on the cement, the maximum value of retarder used in cement slurry was determined in concentration of 0.3% BWOC.

Also, cement slurries density in the all tests was considered as 1.84gr/cm3, which this density is placed in the density range of neat cement slurries (the density of neat cement slurries are between 1.79 gr/cm3 to 1.92 gr/cm3). Cement slurries with density lower than 1.79 gr/cm3 are called low-density cements and with density more than 1.92 gr/cm3 are called high-density cements. The water to cement ratio (WCR) was determined as 0.5 in all cases.

2.3. Measurement of Cement Compressive Strength

By measuring the change in velocity of an acoustic signal, the Ultrasonic Cement Analyzer (UCA) provides a continuous non-destructive method of determining compressive strength as a function of time, according to API (API, 1997, Instruction Manual, 2007). The UCA measures the delay time of an ultrasonic wave pulse through the sample; using set equations, this velocity is converted to uniaxial compressive strength and recorded. The basis on which this setup works is the fact that the ultrasonic compressive wave transit time, density of the substance which the wave is traveling through it and the compressive strength of the substance are inter-related (Pedam, 2007). Figure 4 shows this device and its different parts.

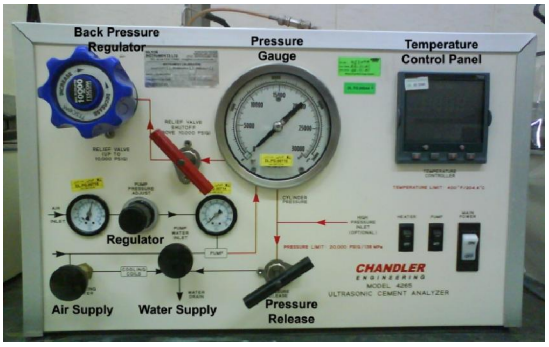

Figure 4. Different Parts of UCA Device

Since over 90 % of the total compressive strength typically develops in oil field cements at 48 hours after blending time the time interval for measuring strength in this study was determined as 48 hours. It is worth to note that this is the minimum time recommended before running bond logs to evaluate zonal isolation (Di Lullo, 2000).

3. Results and Discussions

3.1. Curing Conditions: Ambient Pressure and Temperature (0.1 MPa, 22°C)

Before considering the results of UCA, we introduce test results under ambient pressure and temperature conditions. Under these conditions cubic molds with dimensions of 5.08 cm were used. After the curing of samples at 24 and 48 hours, they were axially compressed using hydraulic press setup and the compressive strength of samples was measured. Obtained results are summarized at Table 1. In this case, compressive strength is computed as the division of final force exerted to samples to their surface area. In each curing time, three samples were implemented and average values of the compressive strength of samples were calculated and recorded as the total compressive strength in the corresponding time.

Table 1. Compressive strength values at ambient pressure and temperature

Curing Time (Hr)	Compressive Strength	
	PSI	MPa
24	1588	10.95
48	2400	16.55

Respect to the fact that the UCA device provides compressive strength values by the pounds per square inch (PSI), in this sections both strength units; MPa (SI system) and PSI are used. It can be derived from the table 1 that compressive strength of the proposed cement after 48 curing hours is increased approximately up to 150 percent in comparison to the corresponding value after 24 curing time under ambient pressure and temperature.

3.2. Curing Conditions: 2.8 MPa (400 PSI) and 38°C

In this test, results show (Figure 5) that the minimum gel strength equal to 0.34 MPa (50 PSI) is achieved at 05:55:00 and minimum acceptable cement compressive strength equal to 3.4 MPa (500 PSI) according to API is executed at 10:28:00. Also, the maximum compressive strength is observed equal to 14.24 MPa (2066 PSI) at 47:43:42. Figure 5 indicates that under these conditions trend of obtained compressive strength curve is increasing, and after reaching to the maximum value, in the last 17 minutes duration of the test, it continues nearly constantly. By comparison of corresponding results introduced in figure 5 and table 1, it can be deduced that the cement compressive strength after 24 hours of curing time is not altered under 400 PSI and 38°C, but the mentioned value is decreased about 14% after 48 hours of curing time. By the author opinion, this observed reduction can be result of the fact that the accuracy of two measurement instrument is not the same and can be neglected.

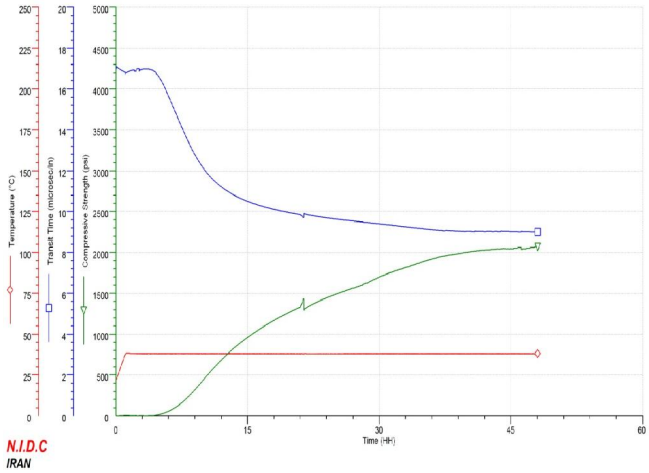

Figure 5. Changes of Compressive Strength at 2.8 MPa and 38°C

3.3. Curing Conditions: 17.2 MPa (2500 PSI) and 68°C

In this situation, results reveal (Figure 6) that the minimum gel strength is reached at 06:16:00 and minimum acceptable cement compressive strength according to API is measured at 08:37:00.The maximum compressive strength equal to 12.72 MPa (1845 PSI) is measured at 47:27:30. Figure 6 demonstrates that in these conditions similar to previous case, trend of compressive strength envelope curve is increasing and after reaching to the maximum value, in the residual 33 minutes to the end of test, it continues constantly. In this case, the time of reaching to the peak of the green curve is shorter. The final compressive strength of cement under these conditions is measured equal to 12.72 MPa (1844 PSI).

3.4. Curing Conditions: 41.4 MPa (6000 PSI) and 82°C

Results in this state indicated (Figure 7) that the minimum gel strength was achieved at 01:59:30 and minimum acceptable cement compressive strength according to API was observed at 02:49:30. Furthermore, the maximum compressive strength equal to 18.91 MPa (2742 PSI) was happened at 44:35:30. Figure 7 shows that under these qualifications compressive strength trend are increasing too, But with this difference that values of compressive strength in the early hours is much more and minimum of compressive strength is achieved much sooner than other two cases. After reaching the maximum value of compressive strength, strength decreases slightly and then in the 3 residual hours to the end of the test, it ongoing uniformly. The final compressive strength of cement under these conditions was measured equal to 18.82 MPa (2730 PSI).

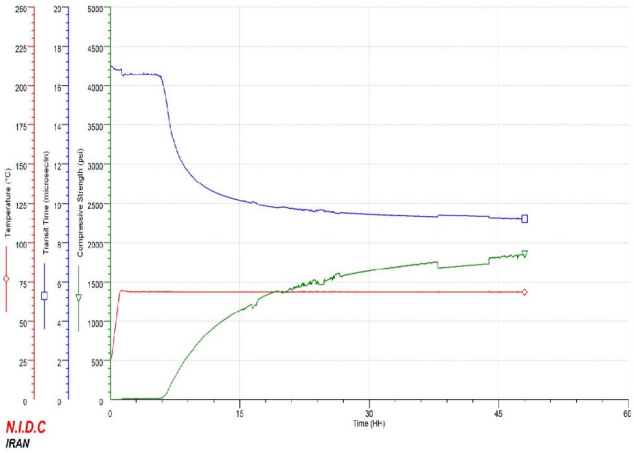

Figure 6. Changes of Compressive Strength at 17.2 MPa and 68°C

3.5. Curing Conditions: 51.7 MPa (7500 PSI) and 121°C

In this mood of the test, results proved (Figure 8) that the minimum gel strength was overtaken at 00:50:30 and minimum acceptable cement compressive strength according to API was reached at 02:05:30. The maximum compressive strength equal to 17.71 MPa (2569 PSI) was achieved at 17:20:00. Figure 8 shows that under these conditions cement compressive strength develops more rapidly and with much higher value than previous tests. After reaching the maximum value, compressive strength unchanged over the 1 hour and 10 minutes, then strength started decreasing and this decreasing trend was continued to the end of the test. The final compressive strength of cement under these situations was measured equal to 16.40 MPa (2383 PSI).

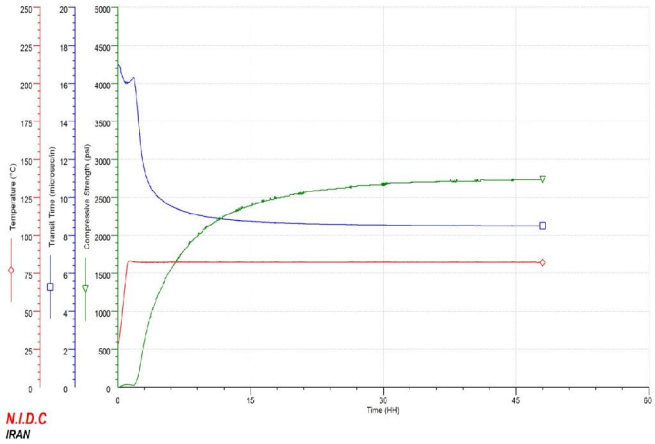

Figure 7. Changes of Compressive Strength at 41.4 MPa and 82°C

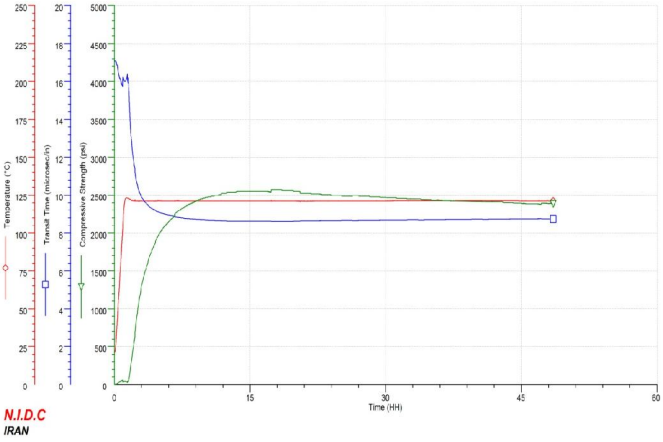

Figure 8. Changes of Compressive Strength at 51.7 MPa and 121°C

3.6. Curing Conditions: 51.7 MPa (7500 PSI) and 149°C

Outcomes illustrate thorough Figure 9 that the minimum gel strength was overtaken at 00:55:30 and minimum acceptable cement compressive strength according to API was caught up at 01:28:30. Also, the maximum compressive strength was achieved equal to 7.99 MPa (1159 PSI) at 03:31:00. Furthermore, Figure 9 shows which under these conditions compressive strength of cement sample develops more rapidly than the all previous cases and therefore was reached in the shorter time to the maximum value of strength. After that compressive strength reached to the maximum value, strength started decreasing and continues in this fashion to the end of the test. The final compressive strength of cement under these conditions was measured equal to 4.59 MPa (666 PSI). It is important to remember that this condition does not exist inside the wellbore and the real state is 110 MPa and 149°C**.**

As it was mentioned before, this is due to limitation of serviceability of the UCA machine test.

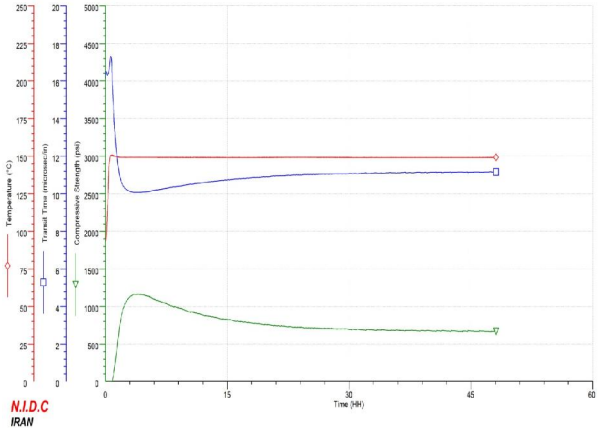

Figure 9. Changes of Compressive Strength at 51.7 MPa and 149°C

In Figures 5 to 9, green lines indicate cement compressive strength changes with time; blue lines show transit time of compression wave into cement samples and red lines show temperature value in each test. Pressure values have been set up on UCA device and were not shown in figures. Compression wave transition velocity increases with change of cement slurry density as it converts into gel state and then into hard material; so with the elongation of the test time, wave transition time becomes shorter. Temperature stays constant after reaching to required value at one hour.

4. Conclusion

It was revealed from table 1 and figures 5 through 8 that when pressure and temperature contemporary increases from (0.1 MPa, 22°C) to (51.7 MPa and 121°C) the early-age compressive strength of proposed class G cement used in our study increases. The rate of this increase is intensified

with the appearance of higher pressure and temperature. Faster development of early-age compressive strength can lead to reduction in transition phase time. This can be reduced the potential of gas migration through the cement column placed inside the oil well through the initial times (48 hour) and develops the safety factor of the project during construction . But from (51.7 MPa and 121°C) to (51.7 MPa and 149°C) it can be seen that compressive strength reduces significantly. Although this state does not occurred in the wellbore and the pressure is not changed through theses two last states, but the author believes on in accordance to literatures (Lecolier et al, 2007, Noik, and Rivereau, 1999) because of the high temperatures in this range the compressive strength would be reduced inside the wellbore in actual situation. So, it can be say that the class G oil well cement can be used in the Darquain region oil wells from surface to the depth equal to approximately 3600m safely but for the deeper depths this type of cement is not be recommended.

Acknowledgements:

Authors are grateful to the National Iranian Drilling Company (NIDC) for their cooperation to carry out this work and to Zarchi, M. for his aid in formatting the paper.

Corresponding Author:
Dr. Mojtaba Labibzadeh
Head of Civil Department,
Faculty of Engineering, Shahid Chamran University,
Ahvaz, Iran.
E-mail: labibzadeh_m@scu.ac.ir

References

1. Asadi, B. Oil Well Cementing. In: First Edition, Central Printery of Oil Company, Ahwaz, Iran, 1983.
2. Abbaszadeh, M. Detecting and Modeling Cement Failure in High Pressure/High Temperature Wells, Using Finite Element Method. M.Sc. Thesis, A & M University, Texas, U.S.A., 2008.
3. Ravi, K., et al.A Comparative Study of Mechanical Properties of Density-Reduced Cement Compositions. SPE Drilling & Completion, 2007: 22(2): 119-126.
4. Al-Suwaidi, A.S., et al. A New Cement Sealant System for Long-Term Zonal Isolation for Khuff Gas Wells in Abu Dhabi. Paper SPE 117116 Presented at the International Petroleum Exhibition and Conference, Abu Dhabi, U.A.E., 2008:3-6.
5. Di Lullo, G., and Rae, Ph. Cements for Long Term Isolation – Design Optimization by Computer Modelling and Prediction. Paper IADC/SPE 62745 Presented at the Asia Pacific Drilling Technology, Kuala Lumpur, Malaysia, 2000:11-13.
6. Pedam, S.K. Determining Strength Parameters of Oil Well Cement. M.Sc. Thesis, the University of Texas at Austin, U.S.A., 2007.
7. Johnstone, K., et al. Cementing Under Pressure in Well-Kill Operations: A Case History from the Eastern Mediterranean Sea. SPE Drilling & Completion, 2008: 23(2): 176-183.
8. Nelson, E.B. Well Cementing. Schlumberger Educational Services, Sugar Land, Texas, 1999.
9. Reddy, B.R., et al. Cement Mechanical Property Measurements under Wellbore Conditions. Paper SPE 95921 Presented at the Annual Technical Conference and Exhibition, Dallas, Texas, U.S.A., 2005: 9-12.
10. Dahab, A.S., and Omar, A.E. Rheology and Stability of Saudi Cement for Oil Well Cementing. J. King Saud Univ., Riyadh, Eng. Sci., 1989: 1(1, 2): 273-286.
11. Lecolier, E., et al. Durability of Hardened Portland Cement Paste used for Oilwell Cementing. Oil & Gas Science and Technology, Rev. IFP, 2007: 62(3): 335-345.
12. Noik, Ch., and Rivereau, A. Oilwell Cement Durability. Paper SPE 56538 Presented at the Annual Technical Conference and Exhibition, Houston, Texas, 1999: 3-6.
13. Mirza, J., et al. Basic Rheological and Mechanical Properties of High-Volume Fly Ash Grouts. Construction and Building Materials, 2002: 16(6): 353-363.
14. Jennings, S.S. Long-Term High-Temperature Laboratory Cement Data Aid in the Selection of Optimized Cements. Paper SPE 95816 Presented at the Annual Technical Conference and Exhibition, Dallas, Texas, U.S.A., 2005: 9-12.
15. Al-Yami, A.S., et al. Long-Term Evaluation of Low-Density Cement: Laboratory Studies and Field Application. Paper SPE 105340 Presented at the 15th Middle East Oil & Gas Show and Conference, Kingdom of Bahrain, 2007:11-14.
16. Al-Yami, A.S., Nasr-El-Din, H.A. Long-Term Evaluation of Low-Density Cement, Based on Hollow Glass Microspheres, Aids in Providing Effective Zonal Isolation in HP/HT Wells: Laboratory Studies and Field Applications. Paper SPE 113138 Presented at the Western Regional and Pacific Section AAPG Joint Meeting, California, U.S.A., 2008.

17. API Recommended Practice 10B. Recommended Practice for Testing Well Cements. Exploration and Production Department, 22nd Edition, 1997.
18. Instruction Manual. Ultrasonic Cement Analyzer. OFI Testing Equipment Inc., Houston, Texas, U.S.A., 2007.

4/1/2010

Influence of Oil Well Drilling Waste on the Engineering Characteristics of Clay Bricks

Medhat S. El-Mahllawy* and Tarek A. Osman

Raw Building Materials Technology and Processing Research Institute
Housing and Building National Research Center, Egypt
E.mail*: medhatt225@yahoo.com

Abstract: Huge quantities of oil-based mud waste were produced during oil well drilling operations in Egypt. These quantities are environmental hazards and usually disposed in open pits that constructed during drilling operations. These pits, approximately 50 years old, resemble an extreme environmental and health hazards integrated with fire and dangerous sinking risks. Consequently, the main objective of this paper is to explore the influence of oil well drilling waste, basically oil based mud waste, on the engineering characteristics of the manufactured environmentally friendly, sufficient performing red clay building brick. Compositions of the used materials as well as physico-mechanical characteristics of fired briquettes were investigated. The laboratory results demonstrate that the water absorption, bulk density, efflorescence and compressive strength of the fired briquettes are met the acceptable limits of Egyptian Standard No. 204-2005 for clay masonry units used for load and non-load bearing walls construction. The reuse of this waste material in the building industry will contribute to the protection of the environment through great advantages in waste minimization and beneficial income to the community through the utilization process in building industry. [Journal of American Science 2010;6(7):48-54]. (ISSN: 1545-1003).

Keywords: Oil-based mud, clay brick, physico-mechanical properties, bearing walls construction

1. INTRODUCTION

The conventional process of drilling oil and gas wells uses a rotary drill bit that is lubricated by drilling fluids and muds. As the drill grinds downward through the rock layers, it generates large amounts of drilling fluid waste and ground-up rock known as drilling cuttings.

Drilling fluid systems typically consist of bentonite and a range of additives mixed with water (water based mud; WBM) or hydrocarbon (oil-based mud; OBM). Oil-based muds were developed for situations and commonly used allover the world where WBMs could not provide enough lubrication or other desired characteristics.

The phrase "oil-based mud" was an accurate description of drilling mud containing diesel oil. It is commonly used 10 years ago, but had obvious negative connotations and was, in need, a serious source of pollution in a large number of countries.

Drill cuttings are made up of ground rock coated with a layer of drill fluids. Most drill cuttings are managed through disposal, although some are treated and beneficially reused. Before the cuttings can be reused, it is necessary to ensure that the hydrocarbon content, moisture content, salinity, etc. of the cuttings are suitable for the intended use of the material. However, the treated cuttings can be reused as construction material and used in various ways as fill material, cover material at landfills, aggregate, and filler in concrete, bricks or blocks manufacturing [1 & 2].

On the other hand, drilling fluids play an important role in traditional well drilling. However, the fluids become contaminated by their use. At the end of the drill job, they must be disposed of or processed for recycling.

Pollution problems caused by oil and other contaminates in waste drilling fluids were recognized over 0 years ago in the Gulf of Mexico and since the development of the North Sea oil and gas fields in the 1970s, have become a major political issue in Western Europe.

Bernrdo et al. [3] used oil well-derived drilling waste (muddy and rocky) and electric arc furnace slag as alternative raw materials in clinker production. It was concluded that the manufacturing process of waste–based clinkers was environmentally compatible and related cements were similar in performance to common hydraulic binders.

In Egypt, a large number of oil wells drilling companies are worked and large quantities of pollutants generated. Till now the use of oil well drilling liquid waste in brick industry has received comparatively little attention by researchers and engineers, but there is an increasing interest towards the searching of new industries which are able to give a usable product characterized by environmental compatibility.

The studied waste in this article (oil-based mud) is located in Belayium oil field, Egypt, owned by Petrobel. The field has approximately 100 offshore and 113 onshore wells. A part of regular drilling operations

during the construction of these wells and work-over, huge quantities of oil-based mud were produced. These quantities are environmental hazards and usually disposed in open pits that were constructed during drilling operations. These pits, approximately 50 years old, resemble an extreme environmental and health hazards integrated with fire and dangerous sinking risks.

This paper is focused on the evaluation of engineering characteristics of a clay brick used oil well drilling waste as a utilization process of the used slurry pollutant in a beneficial industry.

2. MATERIAL AND METHODS

2.1 Raw Materials

The materials used in this study are Belbeis clay (BLC) and oil-based drilling mud waste (OBMW). The used materials are described briefly as follows.

2.1.1 Belbeis clay sample

The investigated sample was taken from Belbeis quarries area, El-Sharkia Governorate, Egypt. The collected sample is pale grey colour, massive and damped. The sample belongs to deposits of Late Miocene age [4].

2.1.2 Oil-based drilling mud waste

This waste material was supplied by Belayium Petroleum Company (Petrobel), the oldest and largest oil and gas production company in Egypt. The OBMW originally was taken from Belayium oil wells field which is located on the eastern side of the Gulf of Suez, about 180 km south of Suez. Belayium is one of the major production fields in Egypt, The supplied waste sample is slurry, dark brown colour and has an amount of petroleum product.

2.2 Methods and Techniques

The used materials were characterized by X- ray diffraction (XRD) and X-ray fluorescence (XRF) techniques for determining the mineralogical composition and major element oxides, respectively.

For studying the clay sample by XRD, the sample was dried then extremely fine grounded to achieve a good XRD pattern. The ground Belbeis clay sample (BLC) also requires pre-treatments to be analyzed by XRD. This step is to remove undesirable coatings and cementing materials, either to improve the diffraction characteristics of the sample or to promote dispersion during size fractionation. To complete the sample preparation, the clay fraction (< 2μm) was separated, precipitated, and mounted on three glass slides. Three diffractograms were obtained according to Moore and Reynolds's method [5]. The used XRD apparatus was of X'pert Pro type (Netherlands). The analysis was run at 40 kV and 40 mA using Cu Kα radiation in the range 2θ ranged from 3º-38º. The interpretation of the obtained phases was achieved by X'Port high score PDF-2 database software on CD-Release 2006. The semi- quantitative estimation of the clay minerals was calculated on the basis of Johns's method [6]. The chemical analysis was carried out using Philips PW 1400 XRF as well as following the test method described in the American Society for Testing and Materials [7]. The pH value was measured at 20ºC by an electronic pH meter (Jenway 3510, UK) following the test method reported in the ASTM [8].

2.3 Sample Preparation and Briquettes Processing

The natural status of the BLC and OBMW samples used in this study were damped and slurry, respectively. So, the BLC is dried in an electrical dryer for 48 h at 110ºC where the other material is thermally treated at 300ºC for 24 h to release the high content of aromatic hydrocarbons. After the drying process, all the materials were first ground by a traditional jaw crusher then sieved until the fractions passing through 1 mm screen. Designed mixes from the raw materials were homogenized using a cylindrical mixer during 10 min, and then mixed with water to the desired suitable consistency (the forming water used belongs to the soft mud process). The mixtures are then hand molded in a 5 cm side length iron cube. After demolding, the shaped green briquettes left for about 2 weeks in a protected place at room temperature, then dried in a dryer and left inside for 24 h at 110ºC. Finally, the dried briquettes were fried in a controlled electrical furnace at 800º, 850º and 900ºC with a gradually heating rate of 2ºC/min and held for 2 h (soaking time).

2.4 Mixture Formulations

In order to investigate the influence of addition of the oil-based drilling mud waste on the engineering characteristics of the clay building brick for using in construction of load and non-load bearing walls, three mixes were designed on the basis of partial replacement of clay material denoted as M0, M1, M2 and M3. Each mix containing variable content of the waste, 0 % (M0, reference mix), 10 % (M1), 20 % (M2) and 30 mass % (M3) was added to the raw investigated clay (Table 1).

2.5 Laboratory Tests

To evaluate the engineering properties of the fired briquettes of the different mixes, the water absorption, bulk density, efflorescence and dry/wet compressive strength were determined according to ASTMs [9 & 10]. At least 3 fired briquettes were used in each test for all categories and the average values were calculated.

3. RESULTS AND DISCUSSION

3.1 Textural, Mineralogical and Chemical Compositions

The studied BLC sample is a plastic, very fine grained claystone of a well sorted class as mentioned from a pervious study of El-Mahllawy [11]. Table (2) summarizes the mineralogical composition of the used raw materials. The studied clay is composed mainly of quartz with minor contents of plagioclase and calcite as non-clay minerals. In the clay fraction (fraction <2μm) montmorillonite is the major mineral, kaolinite and illite are the moderate and minor clay minerals, respectively. In the ignited OBM waste, the main crystalline phase identified is barite and anhydrite (basically it was gypsum before the thermal treatment process at 300ºC). Also, it is identified peaks of a moderate content of andradite mineral.

The chemical composition of the raw materials used as shown in Table (3) shows that the clay sample matches an average limit of the most common Egyptian clay compositions (composed mainly of SiO_2, Al_2O_3 and Fe_2O_3 rather than a minor content of other oxides). The pH value refers to neutral material. The ignited waste material is composed of SiO_2 as a major oxide, CaO incorporated with BaO as a moderate oxide, minor contents of Al_2O_3 and SO_3, and traces of other major oxides. The pH value indicates a slightly alkaline material. Moreover, a typical formulation for an oil based mud stated by Balson [12] is listed in Table (4).

The chemical composition of the oil-based mud waste is conformed by the XRD as the presence of main mineral sources for the identified major element oxides. Barite ($BaSO_4$) mineral as a weighting material is used in substantial quantities to increase the density of oil mud. Pure barium sulfate is never used and commercial product is preferred which is associated with calcium sulfate, in the form of gypsum, and other minerals may occur along with barite. Lime, in different forms, is essential in the OBM. It neutralizes fatty acids in the fluid mud, stabilizes the emulsion when present in excess, and controls alkalinity. In the oil fields, it also neutralizes acid gases (H_2S and/or CO_2).

3.2 Physical Characteristics

The average values of water absorption, bulk density, and efflorescence for the briquettes made from assorted mix combinations and fired at different temperatures are displayed in Table (5). The influences of the waste addition on the engineering characteristics of the fired briquette as a function of firing temperatures are graphically illustrated in Fig. (1).

The obtained results and the discussion may summarize as follows:

- The water absorption values increase with waste contents, and decrease with firing temperature.
- The bulk density values decrease with the waste content and increase with firing temperature.
- Efflorescence degree for the briquettes fired at 900ºC increases with the waste material content.
- The overall rate of the water absorption, bulk density and efflorescence for all mixes at firing temperatures ranges are within the acceptable limits of the Egyptian Code, ECP, [13].
- The fired briquettes made from mix 0 (no waste added) show a product of better quality than those made from different waste contents with clay.
- The results of water absorption and bulk density are mainly attributed to increasing of glassy phase formation, the main source is clay material, with increasing the firing temperature and clay content causing closing of some open pores within the fired body [14] or decreasing in total-pore space in the structure [15]. The formed glassy phase by the capillary action and surface tension infiltrates the open pores of the structure and cause densification of the ceramic bodies [16].
- The increasing of water absorption and decreasing of bulk density with the waste content means that the OBM waste is mainly remained inert at the tested temperatures.
- The efflorescence values for the briquettes fired at 900ºC of different mixes increase with the waste content indicating to increasing of salts that is moved upwards briquettes surfaces by the capillary action and precipitated after placing in the distilled water.

3.3 Mechanical Characteristics

The average values of the dry and wet compressive strength for the briquettes of different mixes fired at 800º, 850º and 900ºC are listed in Table (6) and graphically illustrated in Fig (2). It is obvious to note that the compressive strength values increase with firing temperature and decrease with waste content. The possible reason for these trends is due to the increase in binding forces, clay material is the main source for the binding materials in the fired briquettes, as well as the formation of more liquid which fill pore spaces remaining and strengthen the briquette body [17].

It was observed that in all mixes, even those with a high waste content (M3), the fired briquettes achieve compressive strength within the acceptable limits prescribed in the Egyptian Code [13] for the clay bricks used either as non-load or load bearing walls.

Table (1): The composition of the raw mixes (mass %)

Mix no.	Mix proportion, %	
	BLC	OBMW
M0 (reference mix)	100	0
M1	90	10
M2	80	20
M3	70	30

Table (2): The mineralogical composition and semi-quantitative minerals of the used materials based on XRD.

Material	Mineralogical composition		Semi-quantitative percentage (SQ, %)	Chemical formula
	Non-clay minerals	Clay minerals		
Belbeis clay	- Calcite - Plagioclase - Quartz	 - Montmorillonite - Kaolinite - Illite	- 6.0 - 2.5 - 64.5 - 62.0 - 30.0 - 8.0	- $CaCO_3$ - $(Na,Ca)(Si,Al)_4O_8$ - SiO_2 -$(Na,Ca)_{0,3}(Al,Mg)_2Si_4O_{10}(OH)_2 \bullet n(H_2O)$ - $Al_2Si_2O_5(OH)_4$ - $(K, H_3O)(Al,Mg,Fe)_2(Si,Al)_4O_{10}[(OH)_2,(H_2O)]$
Oil-based mud waste	- Barite - Anhydrite - Andradite		- 49.0 - 39 .0 - 12 .0	- $BaSO_4$ - $CaSO_4$ - $Ca_3Fe^{3+}{}_2Si_3O_{12}$

SQ percentage was calculated for the clay minerals in the clay fraction

Table (3): The chemical composition and pH value of the materials used

Material	Oxide content, %									pH	LOI %
	SiO_2	Al_2O_3	Fe_2O_3	TiO_2	CaO	MgO	Na_2O	K_2O	SO_3		
Bebies clay	50.77	18.27	8.59	1.31	0.72	3.03	1.67	1.13	0.14	14.37	7.0
Ignited oil-base mud waste	60.02	3.83	5.71	Nil	22.1*	0.71	1.64	1.09	4.11	0.79	8.5

LOI: Loss on Ignition (*) sign means also includes BaO content

Table (4): Typical formulation of an oil-based mud

Component	Concentration, kg/m^3
Base oil	375.4
Lime	17.1
$CaCl_2$ salt	75.2
Fresh water	210.2
Weighting material (Barite)	940.3

Table (5): The mean values of water absorption, bulk density and efflorescence of the fired briquettes of the different formulated mixes

Mix code	Water absorption %			Bulk density g/cm^3			Efflorescence %
	800 °C	850 °C	900 °C	800 °C	850 °C	900 °C	
M0	10.81	8.55	7.75	1.70	1.76	1.81	8 Light
M1	12.48	11.14	10.50	1.67	1.72	1.76	12 Moderate
M2	13.65	12.72	11.12	1.66	1.68	1.72	19 Moderate
M3	14.23	13.91	12.46	1.64	1.66	1.69	25 Moderate
Egyptian code: 204 - 2005	Clay brick as non-load bearing walls: < 20 % Clay brick as load bearing walls : < 16 %			--- > 1.6			< 50 % < 50 %

Table (6): The mean of compressive strength of the fired briquettes as function of firing temperatures

Mix code	Dry compressive strength kg/ cm^2			Wet compressive strength kg/ cm^2		
	800 °C	850 °C	900 °C	800 °C	850 °C	900 °C
M0	165.4	202.8	241.8	142.0	170.1	204.5
M1	155.5	190.3	231.9	131.2	156.1	190.0
M2	139.7	156.4	189.1	109.2	130.3	158.8
M3	114.1	128.3	165.6	90.6	111.9	124.4
Egyptian code: 204 - 2005	Clay brick as non-load bearing walls: --- Clay brick as load bearing walls : ---			Clay brick as non-load bearing walls: 40 Clay brick as load bearing walls : 80		

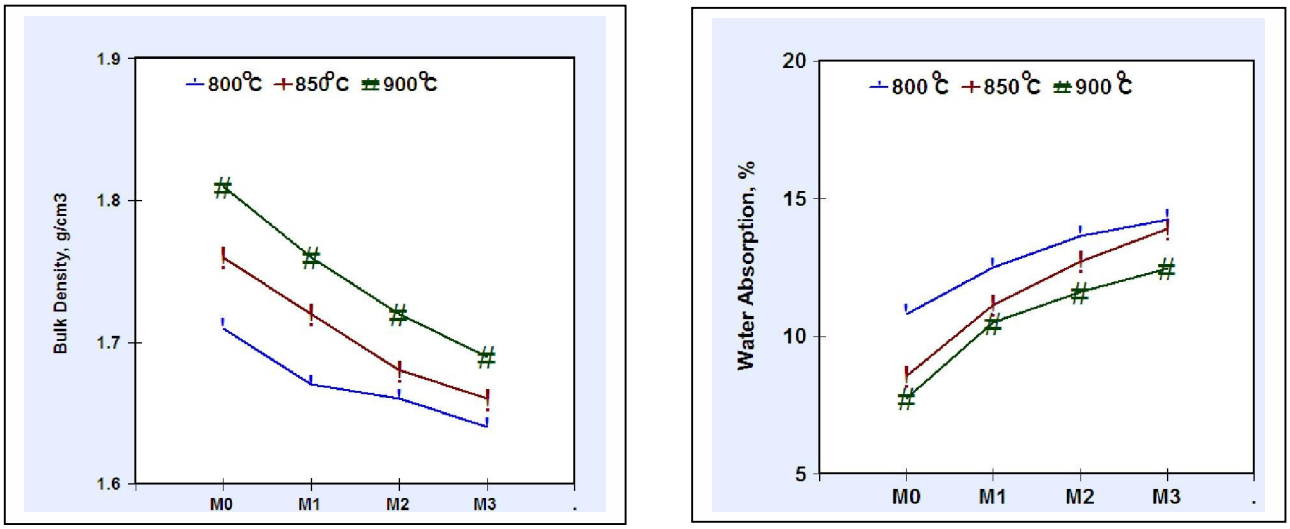

Fig. (1): Water absorption and bulk density as a function of OBM waste content as well as firing temperatures.

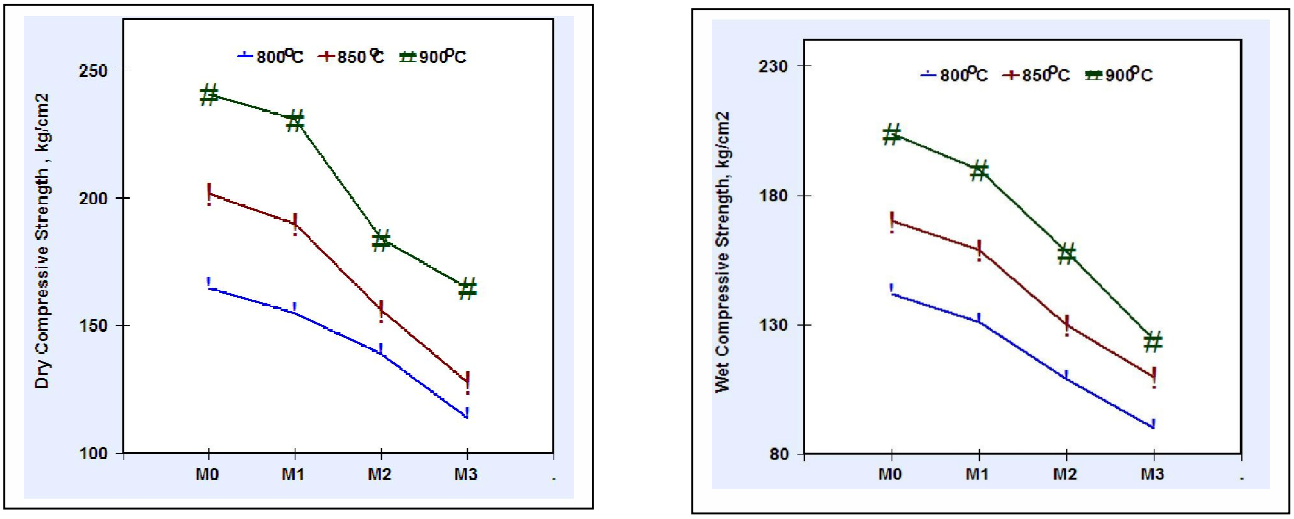

Fig. (2): Dry and wet compressive strength of fired briquettes as a function of OBM content as well as firing temperatures.

4. CONCLUSION AND RECOMMENDATIONS

This paper presented the results of the research study on the influence of the oil-based mud waste as a partial substitution for the Belbeis clay material on the engineering characteristics of fired clay bricks. Based on the experimental investigations reported in this paper, the following conclusions and recommendation are drawn:

1- The clay burnt briquettes containing oil-based mud waste prepared from the different mixes exhibited good engineering characteristics, with regards to water absorption, bulk density, efflorescence and mechanical strength.

2- The incorporation of the used waste with the clay raw material is modified relatively the production process of the red clay building manufacture.

3- The experimental results showed clearly that the oil-based mud waste in the making red clay building brick seems to be an interesting recycling destination for this abundant waste. This is very important because the incorporation of the referred waste in ceramic bodies can be a technological solution to the negative environmental impact caused by oil well drilling sector.

4- The ability to handle the extruded clay bricks from the all formulated mixes in an industrial scale is recommended to be investigated. It is expected to be positive income.

5- In terms of the environmental performance, it is worth mentioning that it is recommended to establish an environmental profile analysis data for the waste material.

6- The fired briquettes fabricated from the four mix combinations can be used as appropriate raw material resource to produce a load and non-load bearing walls suitable for civil constructions.

REFERENCES

1- Linchen Ta. An innovation utilization of drilling wastes as building materials. E& P Environmental and Safety Conference. 5-7 March, Texas, USA; 2007

2 - Greaves C, Lawson R, Hayes S, Boyle F. Reuse of cuttingsage options for the recycling of drill cuttings. SPE 80583, SPE / EPA/ DOE Exploration and Production Environmental Conference. San Antonio, TX, March 10-12; 2003

3- Bernardo G, Marroccoli M, Noobili M, Telesca A, Valenti G. The use of oil well-derived drilling waste and electric arc furnace slag as alternative raw materials in clinker production. J. Resources Conservation & Recycling 2007; 52: 95-102.

4- Said R. The geology of Egypt. A. A. Balkema Publisher, Netherlands;1990.

5 - Moore DM, Reynolds RC. X-ray diffraction and the identification and analysis of clay minerals. 2nd ed. Oxford: Pergamon Press; 1997.

6- Johns WD, Grim RE, Bradley W F. Quantitative estimation of the clay minerals by diffraction methods. J Sed Petrol 1954; 24: 242-251.

7- ASTM D 7348. Standard test methods for loss on ignition (LOI) of soil combustion residues. Annual Book of ASTM Standards, USA, 05.06; 2008.

8- ASTM D4972. Standard test method for pH of soils. Annual Book of ASTM Standards, USA, 04.08. 2007.

9- ASTM C67-09. Standard test method for sampling and testing bricks and structural clay tile. Annual Book of ASTM Standards, USA, 04.05; 2002.

10- ASTM C20. Standard test methods for apparent porosity, water absorption, apparent specific gravity and bulk density of burned refractory brick and shapes by boiling water. Annual Book of ASTM Standards, USA, 15.01; 2000.

11- El-Mahllawy M. The composition and ceramic properties of Egyptian shale deposits and their possible utilization as building materials. Ph.D. Thesis, Fac Sci. Zagazig Univ. Egypt ; 2004.

12- Balson T, Craddock H, Dunlop J, Frampton H, Payne G, Reid P. Chemistry in the oil industry VII, performance in a challenging environment, The Royal of Chemistry, UK; 2001.

13- ECP. Egyptian code for designing and execution of building works, Code no. 204. Housing and Building National Research Center, Egypt; 2005.

14 - Bhatngar JM, Geol RK. Thermal changes in clay products from alluvial deposits of the Indo-gangetic plains. J. Construction and Building Materials 2002; 16:113-122.

15 - Demir I, Orhan M. Reuse of waste bricks in the production line. J. Building and Environment 2003; 38 (1): 1451-1455.

16 - Moreira JM, Manhase JP, Holand JN. Processing of red ceramic using ornamental rock powder waste. J. Materials Processing Technology 2008; 196: 88-93.

17- Weng CH, Lin DF, Chiang PC. Utilization of sludge as brick material. Advances in Environmental Research 2003; 7: 679-685.

4/4/2010

Mass Multiplication of *Celastrus paniculatus* Willd - An Important Medicinal Plant Under *In Vitro* Conditions using Nodal Segments

Devi Lal and **Narender Singh***
Department of Botany, Kurukshetra University,Kurukshetra, Haryana, India—136119.
nsheorankuk@yahoo.com

Abstract: A rapid clonal propagation system has been developed for *Celastrus paniculatus* (Celastraceae) an important medicinal plant under *in vitro* conditions. Nodal explants from mature plant of this species were collected and cultured on MS medium supplemented with various concentrations (0.5, 1.0 and 2.0 mg l^{-1}) of cytokinins (BAP and Kn) and auxins (IAA, NAA and 2, 4-D) alone and in various combinations under controlled condition of 16 hours of photoperiod and 8 hours dark period at a temperature of 25±2ºC. The maximum number of shoots (8.9±0.5) along with hundred per cent bud break was recorded in the MS medium supplemented with 1.0 mg l^{-1} BAP. Most of the combinations of cytokinins with IAA induced the formation of less number of shoots. The *in vitro* regenerated shoots were excised aseptically and implanted on full and half strength MS medium without or with growth regulators (IAA, NAA and IBA) at the concentrations of 0.5 and 1.0 mg l^{-1} for rooting. MS half strength medium supplemented with 0.5 mg l^{-1} NAA proved best with hundred per cent rooting. The regenerated plantlets were successfully acclimatized in pots containing sterilized soil and sand mixture (3:1). The plantlets were then transferred to the field conditions. Seventy per cent of the regenerants survived well. [Journal of American Science 2010;6(7):55-61]. (ISSN: 1545-1003).

Key words*:* Micropropagation, nodal segments, multiple shoots, *Celastrus paniculatus.*
Abbreviations: BAP-6-benzylamino purine, Kn-Kinetin, IAA-indole-3-acetic acid, 2,4-D- 2,4-dichlorophenoxy acetic acid, NAA-α-naphthalene acetic acid, IBA-indolebutyric acid.

Introduction

Celastrus paniculatus Willd. (Celastraceae) commonly known as Malkangni, Jyotishmati, Bitter sweet is a rare and endangered important medicinal plant with vine like habit reaching up to a height of 10 meters. It is distributed through out India up to an altitude of 1200 meters, mainly in deciduous forests. The species is vulnerable in Western Ghat of South India (Rajesekharan and Ganeshan, 2002). Seeds of this plant are the source of an Ayurvedic drug Jyothismati used in treating rheumatism, gout and neurological disorder. *Celastrus paniculatus* is well known for its ability to improve memory (Nadkarni, 1976). Pharmacological studies suggested that the oil obtained from the seeds possess sedative and anticonvulsant properties (Gatinode et al., 1957). Seed oil has also been found to be beneficial to psychiatric patients (Hakim, 1964) and increased the intelligence quotient of mentally retarded children (Nalini et al., 1986). The seed oil is useful for treating abdominal disorders, beriberi and sores. Leaf sap is an emmenagogue and antidote for opium poisoning (Warrier et al., 1994). Bark is reported to be abortifacient, depurative and a brain tonic and taken internally for snake bite (Govil, 1993). Root-bark extract also shows antimalarial activity (Rastogi and Mehrotra, 1998). The powdered root is considered useful for the treatment of cancerous tumors (Parotta, 2001). Chemical constituents of seeds as revealed by phytochemical analysis were sesquiterpene alkaloids like celapagine, celapanigine and celapanine (CSIR, 1992).

The conventional method of propagation of this medicinally important plant is through seeds. Poor seed viability and germination (11.5%) restricts the use of seeds in multiplication (Rekha *et al*., 2005). Indiscriminate over exploitation from natural sources to meet the growing demand by pharmaceutical industry coupled with low seed viability, lack of vegetative propagation methods and insufficient attempts for replenishment of wild stock of this medicinally important plant species have contributed to its threatened status. So realizing the threat of extinction and to meet the growing need of pharmaceutical industry, a mass multiplication protocol was developed for its better future supply.

Materials and methods

Nodal explants from mature plants growing in wild near Kurukshetra city were collected. The explants were initially washed with teepol under running tap water. Finally these were surface sterilized under aseptic conditions with freshly prepared 0.1% (w/v) mercuric chloride solution for 3-5 minutes and then given a dip in absolute alcohol. After this, these explants were washed with sterilized double distilled water 4-5 times. The surface sterilized explants (10 mm long) were inoculated on MS medium (Murashige and Skoog, 1962) containing 3% (w/v) sucrose and 0.8% (w/v) agar-agar supplemented with 0.5, 1.0 and 2.0 mg l^{-1} cytokinins (BAP and Kn) and auxins (IAA, NAA and 2, 4-D) individually as well as in various combinations. The cultures were incubated in culture room under controlled condition of 16 hours of photoperiod and 8 hours dark period at a temperature of 25 ± 2ºC. The intensity of light was approximately 2000 lux. The *in vitro* regenerated shoots were excised aseptically and implanted on full and half strength MS medium without or with growth regulators (IAA, NAA and IBA) at the concentrations of 0.5 and 1.0 mg l^{-1} for rhizogenesis.

The rooted plantlets were taken out from rooting medium and washed several times with sterile distilled water to remove the traces of agar-agar. The plantlets were then transferred to pots containing soil and sand mixture (3:1). The plantlets were initially irrigated with half strength (salts only) MS medium without sucrose on alternate days. The plantlets were exposed to the natural conditions for 3-4 hours daily after 10 days of transfer. After about 30 days the plants were transferred to bigger pots in greenhouse and were maintained under natural conditions of day length, temperature and humidity. Finally the plants were transferred to the field conditions. Statistical analysis was done by using the formula:

$$SE = \pm \sqrt{\frac{(X^2)}{n(n-1)}}$$

SE = Standard error

X = deviation of mean

n = number of replicates (Snedecor, 1956)

Results and discussion

The medium devoid of growth regulators failed to induce the formation of shoot buds. Similarly, no shoot buds developed in *Peganum harmala* (Saini and Jaiwal, 2000) and *Crataeva nurvala* (Walia et al., 2003) on MS basal medium. It has been suggested that the growth regulators applied externally during *in vitro* studies might disturb the internal polarity and change the genetically programmed physiology of explants resulting in organogenesis.

Figure 1.Callus induction from nodal explant on MS medium with 0.5 mg l^{-1} NAA.

Figure 2.Callus induction from nodal explant on MS medium with 1.0 mg l^{-1}2,4-D

Table 1. Effect of cytokinins and auxins supplemented individually on nodal explants.

Growth regulators (mg l^{-1})	Bud break (%)	Average No. of days required for bud break	No. of shoots (Mean±SE)
MS control	–	–	–
BAP			
0.5	90	14.0	6.5±0.3
1.0	100	14.0	8.9±0.5
2.0	70	30.4	5.4±0.2
Kn			
0.5	70	18.6	1.0±0.0
1.0	100	25.0	1.0±0.0
2.0	100	25.0	3.1±0.2
IAA			
0.5	50	35.3	1.0±0.0
1.0	30	43.7	1.0±0.0
2.0	20	45.5	1.0±0.0
NAA			
0.5	–	–	–
1.0	–	–	–
2.0	–	–	–
2,4-D			
0.5	–	–	–
1.0	–	–	–
2.0	–	–	–

– **No Bud break**

In the present investigation, bud break was observed in MS medium supplemented with 0.5 and 1.0 mg l^{-1} BAP after 14 days of inoculation while it was delayed at higher concentration of BAP (2.0 mg l^{-1}). In the MS medium fortified with 0.5 mg l^{-1} Kn, bud break was noticed after 18.6 days of inoculation whereas, it occurred after 25 days of inoculation in the media with 1.0 and 2.0 mg l^{-1} Kn. The supplementation of auxins in place of cytokinins further delayed the process. No bud break was observed in MS medium supplemented with 0.5, 1.0 and 2.0 mg l^{-1} NAA and 2, 4-D but only callus formation took place (Table-1) (Figure 1&2). In most of the combinations of IAA with BAP and Kn, the number of days required for bud break increased with increase in concentration of IAA (Table-2&3). The development of axillary shoots was accompanied by basal callusing of the explants. However, this remains undifferentiated. Same type of observations were made by Dhawan and Bhojwani (1985), Kackar *et al.* (1991) and Nandwani and Ramawat (1991) working with *Leucaena leucocephala, Prosopis cineraria* and *P. juliflora*, respectively.

Table 2.-Effect of BAP and IAA supplemented in combinations on nodal explants.

Growth regulators	Concentration (mg l^{-1})	Bud break (%)	Average No. of days required for bud break	No. of shoots per explant (mean±SE)
BAP+IAA	0.5+0.5	100	25.4	5.3±0.17
	0.5+1.0	100	30.6	3.8±0.20
	0.5+2.0	60	32.3	2.6±0.13
BAP+IAA	1.0+0.5	100	12.7	6.9±0.28
	1.0+1.0	80	14.0	4.3±0.08
	1.0+2.0	70	14.0	3.1±0.12
BAP+IAA	2.0+0.5	100	10.0	7.8±0.07
	2.0+1.0	90	10.0	3.4±0.14
	2.0+2.0	70	10.0	2.3±0.04

Table 3. Effect of Kn and IAA supplemented in combinations on nodal explants.

Growth regulators	Concentration (mg l^{-1})	Bud break (%)	Average No. of days required for bud break	No. of shoots per explant (Mean±SE)
Kn+IAA	0.5+0.5	80	20.0	1.0±0.0
	0.5+1.0	70	25.7	2.9±0.15
	0.5+2.0	60	32.8	2.2±0.11
Kn +IAA	1.0+0.5	90	18.2	1±0.0
	1.0+1.0	70	22.3	1±0.0
	1.0+2.0	60	30.7	1±0.0
Kn +IAA	2.0+0.5	100	20.0	1±0.0
	2.0+1.0	80	24.5	1±0.0
	2.0+2.0	60	26.8	1±0.0

Figure 3.Shoot formation from nodal explant on MS medium with 1.0 mg l^{-1} BAP

When the growth regulators were applied individually, hundred per cent bud break was observed in MS medium supplemented with BAP (1.0 mg l^{-1}) and 1.0 and 2.0 mg l^{-1}Kn. Only fifty per cent bud break was noticed in the medium fortified with 0.5 mg l^{-1} IAA. The increase in concentration of IAA resulted in the decrease in per cent bud break (Table-1). Among the various combinations of BAP and Kn with IAA, hundred per cent bud break was noticed in 0.5 mg l^{-1} BAP + 0.5 mg l^{-1} IAA, 0.5 mg l^{-1} BAP + 1.0 mg l^{-1} IAA, 1.0 mg l^{-1} BAP + 0.5 mg l^{-1} IAA and 2.0 mg l^{-1} BAP + 0.5 mg l^{-1} IAA. It has been found that increase in concentration of IAA resulted in reduced percent bud break (Table-2&3).

Figure 4. Shoot formation from nodal explant on MS medium with 1.0 mg l^{-1} Kn

Figure 5.Development of roots on half strength MS medium with + 0.5 mg l^{-1}NAA

Multiple shoot formation was recorded in all concentrations of BAP while in case of Kn, it occurred only in 2.0 mg l^{-1} treated MS medium. BAP was found more efficient than Kn with respect to initiation and subsequent proliferation of axillary buds. Similar observations have been made in many species like *Rotula aquatica* (Sebastian et al., 2002), *Cinnamomum camphora* (Babu et al., 2003) and *Mamordica charantina* (Agarwal and Kamal, 2004). BAP was also an efficient growth regulator for shoot multiplication in *Chlorophytum borivilianum* (Sharma and Mohan, 2006) and *Cyphomandra betacea* (Chakraborty and Roy, 2006). Medium supplemented with 1.0 mg l^{-1} BAP induced maximum shoots (8.9) per nodal explant while medium supplemented with Kn resulted in a reduced number of shoots albeit with longer internodes (Figure 3&4). Similar results were also reported in *Rotula aquatica* (Martin, 2002). No multiple shoot formation was observed in IAA treated explants (Table-1). Most of the combinations of BAP and Kn with IAA tested in nodal explant culture, induced the formation of less number of shoots (Table-2&3). Higher concentrations (>0.05 mg l^{-1}) of IAA and NAA induced callusing and inhibited shoot formation. These results presumably indicated a threshold level of endogenous auxin in the explants (Julliard et al., 1992).

The *in vitro* regenerated shoots were excised aseptically and implanted on full and half strength MS medium without or with growth regulators (0.5 and 1.0 mg l^{-1} NAA, IAA and IBA) for rhizogenesis. Excised shoots failed to develop roots on both full and half strength MS medium without growth regulators. Although root formation with callusing at the shoot base occurred in all concentrations of NAA, IAA and IBA, but more callus formation was observed in MS full strength medium. Moreover, this callus formation increased with increase in concentration of auxins. Induction of roots was noticed after 14.2 days of implantation in the medium with 0.5 mg l^{-1} NAA. It got delayed in other media. MS half strength medium supplemented with 0.5 mg l^{-1} NAA proved best with hundred per cent rooting and very less callusing at the base (Figure 5) followed by IBA and IAA (Table-4). The efficacy of NAA at lower concentrations under *in vitro* rooting of shoots has been reported in various medicinal plants like *Verbascum thapsus* (Turker et al., 2001) and *Santolina canescens* (Casado et al., 2002). Peeters et al. (1991) found that NAA was taken up six times faster than IAA, and Van der Krieken et al. (1993) reported that IBA was taken up four times faster than IAA. Consequently, the efficacy of rooting in the presence of NAA may be due to its faster uptake. This may be due to the variation in the route of auxin uptake (De-Klerk et al., 1997). Similarly, Singh and Lal (2007) also achieved root induction on MS medium fortified with 0.5 or 1.0 mg l^{-1} of NAA in *Leucaena leucocephala*.

Figure 6. Plantlet transferred to pot

Figure 7.Plantlet transferred to field conditions

Table 4. Effect of various auxins on root formation.

Growth regulators (mg l^{-1})	Root induction (%)	Avg. No. of days required for root induction	Remarks
MS full strength without growth regulators	–	–	–
MS half strength without growth regulators	–	–	–
MS full strength+ NAA 0.5	90	14.2	C+++, stout, white
MS full strength+ NAA 1.0	80	15.3	C+++, stout, white
MS full strength+ IAA 0.5	70	16.5	C+++, thin
MS full strength+ IAA 1.0	60	17.6	C+++, thin
MS full strength +IBA 0.5	80	17.2	C++, thin
MS full strength +IBA 1.0	60	17.4	C++, thin
MS half strength+ NAA 0.5	100	12.2	C+, stout, white
MS half strength+ NAA 1.0	80	14.8	C++, stout white
MS half strength+ IAA 0.5	80	16.3	C++, thin, white
MS half strength+ IAA 1.0	70	17.4	C++, thin, white
MS half strength+ IBA 0.5	90	16.8	C++, thin, white
MS half strength+ IBA 1.0	70	17.2	C+,thin, white

C+= normal callus formation, C++ = moderate callus formation, C+++ = vigorous callus formation
- No root formation

The regenerants with well developed roots were transferred to sterilized soil and sand mixture (3:1) in earthen pots placed in growth chamber at 25 ± 2ºC. The roots were gently pulled out of the medium and immersed gently in running tap water. Medium particles sticking to the root system were carefully removed with fine brush. High humidity was maintained for the initial 20 days by using beakers. The plantlets were initially irrigated with half strength MS medium(salts only) without sucrose on alternate days. The plantlets were exposed to 3-4 hours daily to the conditions for natural humidity after 10 days of transfer. After about 30 days the plants were transferred to bigger pots in greenhouse and were maintained under natural conditions of day length, temperature and humidity. Finally the plants were transferred to the field conditions. Seventy per cent of the regenerants survived well (Figure 6&7). Therefore, the protocol could be used for the mass multiplication of this highly important medicinal plant species in a short duration. It will cater to the growing needs of pharmaceutical industry and also a mean for germplasm conservation and large scale plantation.

Acknowledgements

The authors are grateful to Kurukshetra University, Kurukshetra and U.G.C., New Delhi, India for financial assistance.

Corresponding Author:
Dr.Narender Singh
Associate Professor,
Department of Botany,
Kurukshetra University,
Kurukshetra,Haryana 136119,India.
E-mail: nsheorankuk@yahoo.com

References

1 Agarwal M and Kamal R. *In vitro* clonal multiplication of *Momordica charantia* L. Indian J. Biotech.2004. 3: 426-430.
2.Babu KN , Sajina A, Minoo D, John CZ Mini PM , Tushar KV , Rema J and Ravindran PN. Micropropagation of camphor tree (*Cinnamomum camphora*). Plant Cell Tiss. Org. Cult. 2003. 74: 179-183.
3.Casado JP, Navarro MC , Utrilla MP , Martinez A and Jimenez J. Micropropagation of *Santolina canescens* Lagasca and *in vitro* volatiles production by shoot explants. Plant Cell Tiss. Org. Cult. 2002 .69: 147-153.

4 Chakraborty S and Roy SC Micropropagation of *Cyphomandra betacea* (Cav.) Sendt., a potential horticultural and medicinal 2006.
5 CSIR. Wealth India-raw material. Council for Scientific and Industrial Research(CSIR), New Delhi, 1992. vol.3.pp 412-413.
6.De-Klerk GJ , Brugge JT and Marinova S. Effectiveness of indoleacetic acid,indolebutyric acid and naphthaleneacetic acid during adventitious root formation *in vitro* in Malus Jork 9. Plant Cell Tiss. Org. Cult. 1997. 49: 39-44.
7 Dhawan V and Bhojwani S. *In vitro* vegetative propagationof *Leucaena leucocephala*(Lam.)de Wit. Plant Cell Rep. 1985 .4: 315-318.
8.Gatinode BB, Raiker KP, Shroff FN and Patel JR. Pharmacological studies with malkanguni, an indigenous tranquilizing drug (preliminary report). Current Practice. 1957. 1: 619-621.
9.Govil JN. Medicinal plants: New Vistas of Research, Part-2 ,1993. 393.
10.Hakim RA A trial report on Malkanguni oil with other indigenous drugs in the treatment of psychiatric cases. In: Gujrat State Branch,I.M.A. Med. Bulletin. 1964. pp 77-78.
11 Julliard J , Sosountzov L, Habricot Y and Pelletier G. Hormonal requirement and tissue competency for shoot organogenesis in two cultivers of *Brassica napus*. Physiol. Plant 1992. 84: 512.
12.Kackar NL , Solanki KR , Singh M and Vyas SC. Micropropagation of *Prosopis cineraria.* Indian J. Exp. Biol. 29: 1991. 65-67.
13.Martin KP. Rapid *in vitro* multiplication and *ex vitro* rooting of *Rotula aquatica* Lour., a rare rhoeophytic woody medicinal plant. Plant Cell Rep. 2002. 67: 547-548.
14. Murashige T and Skoog F. A revised medium for rapid growth and bioassays with tobacco tissue cultures. Physiol. Plant. 1962. 15: 473-497.
15.Nadkarni AK. In: Nadkarni's Indian Materia Medica, . Popular Prakashan, Bombay, India. 1976.pp. 1: 296
16.Nalini K, Aroor AR , Kumar KB and Rao A. Studies on biogenic amines and metabolites in mentally retarded children on *Celastrus* oil therapy. Alternative medicine . 1986. 1: 355-360.
17.Nandwani D and Ramawat KG . Callus culture and plantlets formation from nodal explants of *Prosopis juliflora* (Swartz) DC. Indian J. Exp. Biol. 1991. 29**:** 523-527.
18.Parotta JA. Healing plants of peninsular India. CABI, New York. 2001.
19.Peeters AJM , Gerads W , Barendse GWM and Wullems GJ *In vitro* flower bud formation in tobacco: interaction of hormones. Plant Physiol .1991. 97: 402-408.
20.Rajesekharan PE and Ganeshan S. Conservation of medicinal plant biodiversity – an Indian perspective. J. Med. Arom. Plant. Sci.2002. 24: 132-147.
21Rastogi RP and Mehrotra BN.Compendium of Indian medicinal plants, vol.5. National Institute of Science Communication (NISCOM), New Delhi. 1998.
22.Rekha K , Bhan MK , Balyan SS and Dhar AK Cultivation prospects of endangered species *Celastrus paniculatus* Willd. Nat. Prod. Rad. 2005. 4: 483-486.
23.Saini R and Jaiwal PK . *In vitro* multiplication of *Peganum harmala*- an important medicinal plant Indian J. Exp.Biol. 2000. 38: 499-503.
24.Sebastian DP , Benjamin S and Hariharan M . Micropropagation of *Rotula aquatica* Lour – An important woody medicinal plant. Phytomorphology. 2002.52: 137-144.
25.Sharma U and Mohan JSS. *In vitro* clonal propagation of *Chlorophytum borivilianum* Sant. et Fernand., a rare medicinal herb from mature floral buds along with inflorescence axis. Indian J. Exp. Biol. 2006.44: 77-82.
26.Singh N and Lal D. Growth and organogenetic potential of calli from some explants of *Leucaena leucocephala* (Lam.) de Wit. International J. Tropical Agriculture. 2007. 25: 389-399.
27.Snedecor GW . Statistical method applied to experiments in agriculture and biology. Iowa State College Press, Ames, 1956. pp. 534.
28.Turker AU , Camper ND and Gurel E . *In vitro* culture of common mullein (*Verbascum thapsus* L.). In Vitro Cell Dev. Biol. Plant. 2001.37: 40-43.
29.Van der Krieken WM , Breteler H , Visser MHM and Mavridou D . The role of conversion of IBA into IAA on root regeneration in apple: introduction of a test system. Plant Cell Rep.1993. 12: 203-206.
30.Walia N , Sinha S and Babbar SB Micropropagation of *Crataeva nurvala*. Biol. Plantarum. 2003. 46 : 181-185.
31.Warrier PK , Nambiar VPK and Ramankutty C . Indian medicinal plants- A compendium of 500 species . Orient Longman, Madras. 1994.vol 2, pp- 47.

2/11/2010

Fatigue Analysis of Hydraulic Pump Gears of JD 955 Harvester Combine Through Finite Element Method

Hassan seyed Hassani [1], Ali Jafari [2*], Seyed Saed Mohtasebi [2] and Ali Mohammad Setayesh [3]

[1.] Msc Student in Mechanic of Agricultural Machinery, University of Tehran, Karaj, Iran.
e-mail: hshasani@yahoo.com
[2.] Members of Scientific Board of Faculty of Engineering & Agricultural Technology, University of Tehran, Karaj, Iran.
[*] Corresponding author, Phone number: e-mail: jafarya@ut.ac.ir
[3.] Department of Research & Development, ICM Company, Arak, Iran.

Abstract: Throughout the present research, the gears fatigue of the hydraulic pump in JD 955 harvester combine was investigated through the finite element method and using contact analysis for precise determination of the contact region of the engaged teeth so that their lifespan was estimated. The reason for performing this research was to study the intended gears behaviour affected by fatigue phenomenon due to the cyclic loadings and to consider the results for more savings in time and costs, as two very significant parameters relevant to manufacturing. The results indicate that with fully reverse loading, one can estimate longevity of a gear as well as find the critical points that more possibly the crack growth initiate from. For the investigated gears, the most critical points were detected as nodes numbered 36573 and 37247. Furthermore, the allowable number of load cycles and using fully reverse loading was gained 0.9800E+07. It is suggested that the results obtained can be useful to bring about modifications in the process of the above-mentioned gears manufacturing. [Journal of American Science 2010;6(7):62-67]. (ISSN: 1545-1003).

Key words: Harvester combine; Fatigue; Longevity; Finite element; Optimization; Contact analysis

1. Introduction

Gears have a wide variety of applications as a power transmission factor in engineering consumption. Spur gears are utilized as the simplest ones for power transmission in parallel shafts. Helical gears in gearboxes and engines tolerate heavy loads and are too sensitive to axial non-adjustments so that edge contact of teeth or inconsistent transmission of power would arise noise (Tsay, 1988). However it is possible to modify the gear teeth and create some optimum point in order to stay clear of edge contact (Chen, and Chung-Biau, 2002). Litvin (1997) suggested a concept for altering teeth of helical and worm gears. Applying a large number of force cycles on gears makes them experience iterative and fluctuating stresses, which lead in fatigue phenomenon in gears. Abrupt ruptures ascribed to such an incident are very dangerous and damaging. Therefore, fatigue culprits should be inspected carefully. American gear manufacture association classifies gear fatigues into five categories of wear, surface fatigue, plastic flow, teeth breakage and rupture.

Gears in which rupture occurs, contact and flexure stresses are paid more attention in analysis. (Arikan and Tamar, 1992; Roa and Muthuveerappan, 1993). Contact stresses which arise from contact forces and geometry are very important and vital so that these stresses are determinative of gears life. Contrary to teeth flexibility which plays an essential and significant role in contact load distributed through engaged teeth, contact flexibility has less effect (Hedlund and Lehtovaara, 2006). Finite element method (FEM) is a modern way for fatigue analysis and estimation of the component longevity and is decent for various toothed structures (Chen and Chung-Biau, 2002), which has the following advantages compared to the other methods.

1. Through this method, we can access the stress/strain distribution throughout the whole component which enables us to find the critical points authentically.

2. This achievement seems so useful particularly when the component doesn't have a geometrical shape or the loading conditions are sophisticated.

3. The influential component factors are able to change such as material, cross section conditions etc. Component optimization against the fatigue is performed easily and quickly.

4. Analysis is performed in a virtual environment without any necessity for prototype construction (Lo and Bevan, 2002). Totally these qualities, lead to savings in time and cost.

955 Combine manufactured by ICM Company is the most common combine in Iran so that more than 90% of combines which have been ranged in light class of combine classification are of this kind. This combine has two hydraulic circuits which are

principal circuit (dividing valve circuit) and steering circuit. The principal circuit operates three actuators connecting with height control of both cutting platform and reel, also moves variable sheave in order to vary ground speed, and steering circuit steers the machine. The only common point of two circuits is their pump which actually is the most important component of the system. Moreover, the majority of the problems and damages in the hydraulic system of the intended combine are arisen from it, so it requires special attention. The effect of fatigue ascribed to force cycles has not inspected on the above-mentioned hydraulic pump yet. Therefore, ICM Company due to improving the intended combine in line with meeting customers' needs and attracting their satisfaction defined it as a research project with the cooperation of University of Tehran. In this paper behaviour of the hydraulic pump gears of 955 harvester combine, from the fatigue point of view, is investigated through the ANSYS software.

Tao et al (2009) using strain–life based fatigue analysis methods investigated the effect of overload and different loading sequences in random spectra on fatigue damage. Mao (2007) employed an accurate non-linear finite element method on the gear fatigue wear reduction through micro-geometry modification method. Chaari et al. (2009) presented an original analytical modelling of tooth cracks and carried out a comparison with finite element model in order to validate the analytical formulation. Kramberger et al. (2004) examined the bending fatigue life of thin-rim spur gears of truck gearboxes. Asi (2006) undertook failure analysis of a helical gear used in gearbox of a bus, which was made from AISI 8620 steel. Park et al. (2010) evaluated the effects of defect blowholes of the gear carrier of tracked vehicle transmission in terms of stress distribution by finite element analysis and observed fatigue striations which are the typical features of fatigue failures by a scanning electron microscope. Kramberger et al. (2004) presented A computational model for the determination of service life of gears with regard to bending fatigue in a gear tooth root.

2. Materials and Methods

Fatigue phenomenon is a complicated subject which seems to be not known a lot. The best theory for the explanation of fatigue phenomenon proposal is the strain-life theory which is used for the fatigue strength estimation. But for the application of this theory there must be some assumptions made for the ideal state, so it results in some uncertainties. Rupture due to the fatigue is usually occurred in discontinuities or where we have the stress concentration. When in these places the existing stress, exceeds the allowed amount, the plastic strain will takes place. For the ruptures resulted from the fatigue, there must be some plastic cyclic strains. So, It was needed to seek for the component behavior during the cyclic deformations. Monsoon-koffin suggested the Equ.1 to present the relationship between fatigue life and the total strain. (Shigley and Mischke, 2001).

$$\frac{\Delta\varepsilon}{2}=\frac{\sigma_F}{E}(2N)^b+\varepsilon_F(2N)^c \quad (1$$

Where $\Delta\varepsilon$ is the total stress, N is the fatigue longevity, E is the Young's modulus, b and c are the exponents of fatigue strength and fatigue elasticity, and finally σ_F and ε_F are the coefficient of fatigue strength and elasticity respectively.

In fatigue analysis of gears, it is initially required to determine the precise contact location of two engaged teeth through contact analysis. Then assume the loading condition thoroughly reversible, the alternate loading will be iterated so much time so that the consumption life of gears would be acquired (Jahed, 2004). In order to establish, the maximum amount of applied force on the gears first the pump power was determined using the following equation.

$$P = (\frac{\Delta P_{PC}\times Q_{PC}}{60}+\frac{\Delta P_{SC}\times Q_{SC}}{60}) \times 1/\eta \quad (2$$

Where:

P = pump power (Mw)

ΔP = produced pressure by pump (MPa), subscripts PC and SC indicates principal and steering circuits of the combine respectively.

Q = flow rate (L min^{-1})

η = total efficiency of the pump which is 75% in respect to the investigated pump.

Calculating the pump power, the produced torque would be acquired 43.6 N.m. Furthermore, considering the effect point of the applied force, its amount was gained through the Eq. 3.

$$F = r \times T \quad (3$$

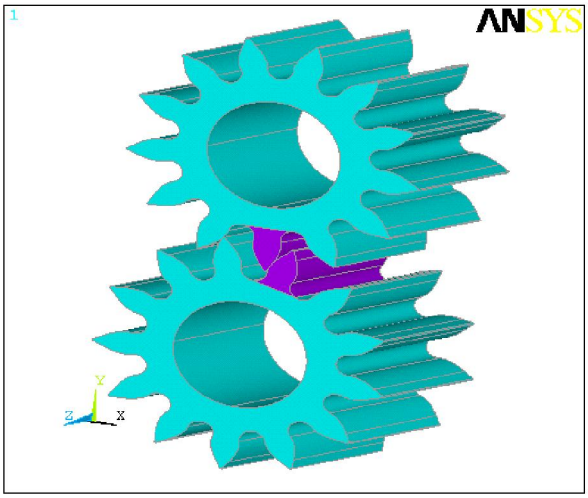

Figure 1. The thorough model of the hydraulic pump gears in 955 combine

After getting the normal and tangential force on the contact region through the resultant force, as Figure1 demonstrates the gears geometry was modelled thoroughly in order to have a real shape of the teeth engagement.

The necessary parameters for determining the gears material and their dimensional specifications are presented in Table 1 and 2 respectively.

Table 1. Properties of material used in hydraulic pump gears*

Specification	Amount
Density	7850 Kg/m^3
Hardness	59 HRC
Tensile Strength	1460 MPa
Yield Strength	1195 MPa
Modulus of Elasticity	205 GPa
Shear Modulus	80 GPa
Poisson's Ratio	0.292
Friction Coefficient	0.08

Table 2. Dimensional specifications of hydraulic pump gears*

Feature	Measurement(mm)
Base Diameter	34.03
Pitch Diameter	38.12
Hole Diameter	19.77
Pressure angle	18
Tooth number	13
Tooth width	19

*Material properties and dimensions presented in Table 1 & 2 are of the most typical and common pump used in the hydraulic system of the intended combine.

In order to reduce the elements in the insensitive places of the model whose meshing conducted with the mapped method. Therefore, simply elements around immediate area of the engagement place considered small adequately. Structural three-dimensional elements of SOLID 45 were utilized in the large majority of the model and for accessing much more precision surrounding the engagement area, 20-node elements of SOLID 95 were employed for the two engaged teeth.

The reason for choosing this element was to illustrate the geometrical parts of a complicated mechanical component clearly so that enables us to gain more authentic results based on the high techniques of fatigue life calculation. In addition to contact surfaces were meshed using elements TARGET 170 and CONTA 174 on the elements of SOLID 95 for the contact analysis (Figure 2).

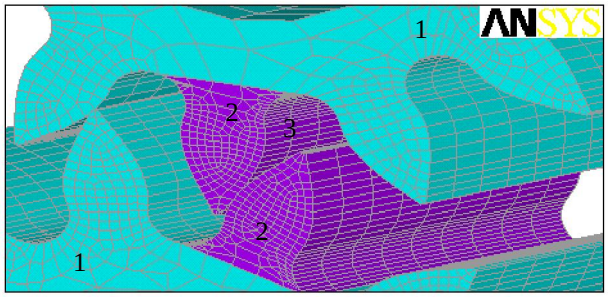

Figure 2. Elements utilised for meshing the intended gears
1. SOLID 45; 2. SOLID 95; 3. CONTA 174; 4. TARGET 170 (The opposite surface of 3)

In order to analyze the model, contact analysis was performed initially, in a way that the engaged surface of the drive and the driver gears were investigated as the contact and the target surfaces respectively. The objective of the first load step was to observe the interference contact stresses of the driven and drive gears and as represented in Figure 3 resulted in determining the contact region precisely. Then the boundary conditions were defined, exerting the pressure forces.

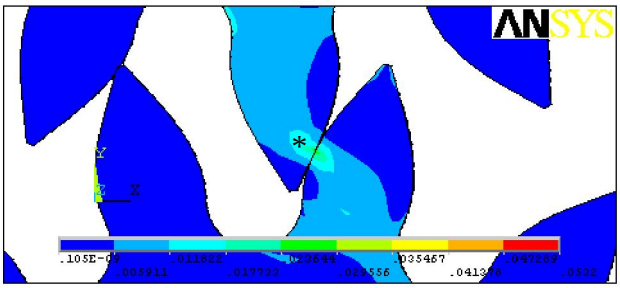

Figure 3. Determination of exact contact region through the contact analysis

Afterwards, some compressive forces, exactly with the same magnitude but in the reverse direction substituted the pressure forces and solution was done again. In every phase of loading by entering to the POST1 processor, the Von Misses stresses were activated and the critical points were determined. These nodes as shown in Figure 3 and Figure 4 are characterized with the numbers 40356 and 39145 (nodes on the engaged tooth of drive gear) and 36573 and 37247 (nodes on the engaged tooth of driven gear) through the compressive loading while nodes

numbered as 36928 and 39153 (nodes on the engaged tooth of drive gear) and 36573 and 37247 (nodes on the engaged tooth of driven gear) were the results of tension loading. After determination of these critical points, they were elected as the points for fatigue investigation. Filling the fatigue parameter blanks, the S-N data collected from the fatigue test of the certain alloy were imported into the software. The stress concentration factor was taken 1.25 which was a representative of a difference between the real model and the operating condition with the sample under the test in fatigue test[4]. Eventually a 10^6 force cycles were exerted to the model and partial consumption rate which indicated the number of exerted cycles to allowed ones for each node was gained.

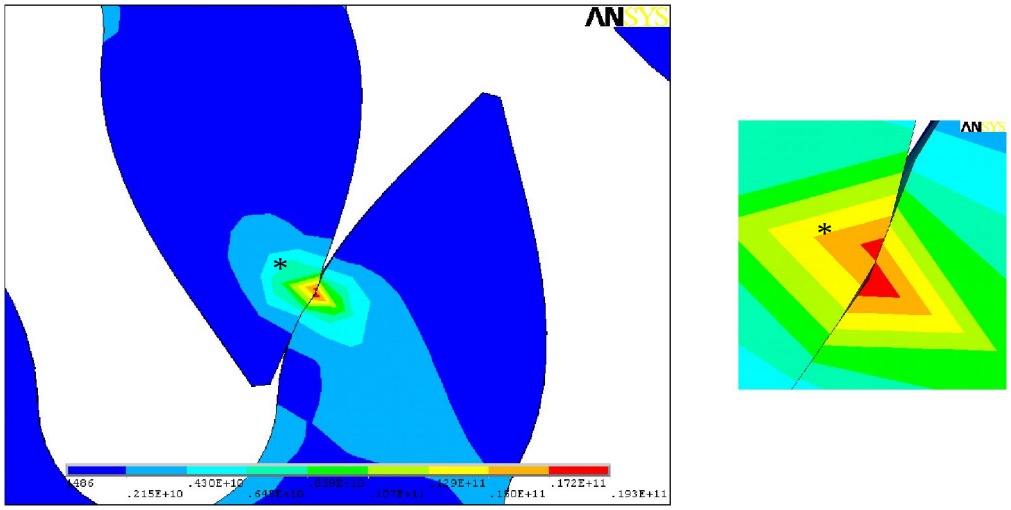

Figure 4. The stresses on the contact region of the engaged teeth due to the pressure loading

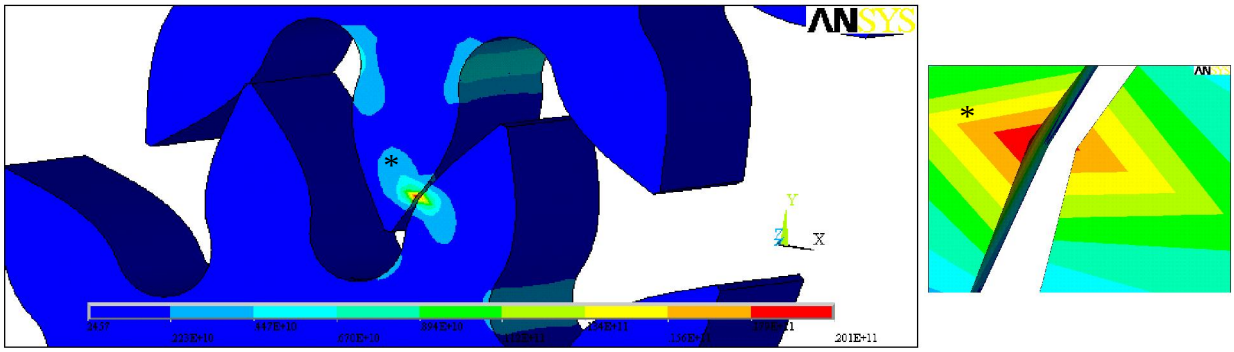

Figure 5. The stresses on the contact region of the engaged teeth due to the tensional loading

3. Result and Discussion

In the fatigue analysis of the pump gears through loading ascribed to contact analysis, determined while engagement of two teeth about 40 nodes in the contact region for which an event including two loadings were taken into account. For this purpose, applied torque on the shaft of drive gear calculated 43.6 N.m and consequently the applied force on the contact zone gained 2412.703 N. Therefore, considering the fact that pressure angle in the contact region is 18˚, normal and tangential forces were acquired 2294.617 and 745.566 N respectively. With applying loads the maximum stress created in pressure loading whose results are shown in Figure 4, was 19.3 GPa while in tension, the amount of stress (Figure 5), was gained 20.1 GPa. With this method the critical points of the model were identified as nodes numbered 40356, 39145, 36573 and 37247 in pressure loading and 36928, 39153, 36573 and 37247 in tension one. As the results demonstrate nodes 36573 and 37247 were critical through both loadings. Then considering 10^6 as the number of exerted cycles

on the model and applying fatigue sets, fatigue rate were acquired for each node (Figure 6).

PERFORM FATIGUE CALCULATION AT LOCATION: 1-6
*** POST1 FATIGUE CALCULATION ***
NODE: 39153, 36928, 40356,36573,37247, 39145
EVENT/LOADS: 1/1 AND 1/2
CYCLES USED/ALLOWED = 0.1000E+07/ 0.9800E+07 = PARTIAL USAGE = 0.10204
CUMULATIVE FATIGUE USAGE = 0.10204

Figure 6. Fatigue calculation results on the critical nodes

As shown Partial consumption rate, which indicates the number of exerted cycles to allowed ones was gained 0.102 for all the nodes. Furthermore based on the partial consumption rate definition, the number of allowed cycles of force achieved 0.9800E+07. Since the analysis carried out on only two teeth of gears, extending the results to the whole model, there would be 78 critical nodes (considering 13 teeth for each gear) which are subject to earlier fatigue in proportion to other ones.

4. Conclusion

By the finite element analysis method and the assistance of ANSYS software, It would be feasible to analyze the different machine parts from varied aspects such as fatigue and consequently save the time and the cost. The way through which loadings defines are effective on the results achieved. Therefore, they should fit as much as possible the real conditions. Moreover, since the fatigue analysis requires some static analysis, thus definition of the boundary conditions should be according to real circumstances. Stress concentration factors indicated the difference between the real and the working condition. regarding the hydraulic pump gears of 955 combine, the most critical nodes were identified 36573 and 37247 ones and the number of allowed cycles of applying force with the totally reverse loading was gained 0.9800E+07 cycles which increases through decline of stress concentration factor.

Acknowledgement

This paper is derived due to an applied research in the frame of applied research proposals defined between University of Tehran and Mine & Industry Ministry with contract number: 450/51027041. Hereby I really appreciate all the contribution and cooperation that Department of R & D of ICM Company particularly Eng. Setayesh made in order to this research is done.

Corresponding Author:
Dr. Ali Jafari
Faculty of Engineering & Agricultural Technology,
University of Tehran, Karaj, Iran.
Phone number: 00989123483037
E-mail: jafarya@ut.ac.ir

Hassan Seyed Hassani
Faculty of Engineering & Agricultural Technology,
University of Tehran, Karaj, Iran.
Phone number: 00989123572613
E-mail: hshasani@yahoo.com

References

1. Asi O. Fatigue failure of a helical gear in a gearbox. J Eng Failure Analysis 2006;13(7):1116-1125.
2. ANSYS. ANSYS user guide Version 12. ANSYS Inc 2009.
3. Aslantaşand K, Taşgetiren S. A study of spur gear pitting formation and life prediction. J Wear 2004;257(11): 1167-1175.
4. Arikan MAS, Tamar M. Tooth contact and 3-D stress analysis of involute helical gears, ASME. Intel Power Transmission and Gearing Conf 1992;43(2):461–468.
5. Chen YC, Chung-Biau Tsay CB. Stress analysis of a helical gear set with localized bearing contact. Finite Elements in Analysis and Design 2002;38:707–723.
6. Chaari F, Fakhfakh T, Haddar M. Analytical modelling of spur gear tooth crack and influence on gearmesh stiffness. Euro J Mech - A/Solids 2009;28(3):461-468.
7. Can Y, Misirli C. Analysis of spur gear forms with tapered tooth profile. J Materials & Design 2008;29(4):829-838.
8. Hedlund J, Lehtovaara A. Modeling of helical gear contact with tooth deflection. J Tribology Intel 2006;40:613–619.
9. Jahed H, Noban MR, Eshraghi MA. Finite Element ANSYS. 2nd ed. University of Tehran Press. Tehran, Iran. 2004.

10. Kramberger J, et al. Numerical calculation of bending fatigue life of thin-rim spur gears. J Eng Fracture Mech 2004;71(4-6):647-656.
11. Kramberger J, Šraml M, Glodež S, Flašker J, Potrč I. Computational model for the analysis of bending fatigue in gears. J Computers & Structures 2004;82(23-26):2261-2269.
12. Lo SHR, Bevan A. Fatigue analysis of a plate-with-a-hole specimen and a truck exhaust bracket using computer-based approach. Intel j Eng Sim (IJES) 2002;4(2).
13. Litvin FL, Kim DH. Computerized design, generation and simulation of modified involute spur gears with localized bearing contact and reduced level of transmission errors. ASME J Mech 1997;119:96–100.
14. Lanoue, F., Vadean, A. and Sanschagrin, B. 2008. Finite element analysis and contact modeling considerations of interference fits for fretting fatigue strength calculations, Simulation Modeling Practice and Theory, 17(10): 1587-1602.
15. Mao K. Gear tooth contact analysis and its application in the reduction of fatigue wear. J Wear 2007;262(11-12): 1281-128.
16. Park S, Lee J, Moon U, Kim D. Failure analysis of a planetary gear carrier of 1200HP transmission. J Eng Failure Analysis 2010;17(2):521-529.
17. Roa CRM, Muthuveerappan G. Finite element modelling and stress analysis of helical gear teeth, J. Comput. Struct., 1993;49(6):1095–1106.
18. Sfakiotakis VG, Anifantis N K. Finite element modeling of spur gearing fractures. J Finite Elements in Analysis and Design 2002;39(2):79-92.
19. Shigley J E, Mischke C R. Mechanical Engineering Design. Chapter7. McGraw-Hill, New York. 2001.
20. Tsay CB. Helical gears with involute shaped teeth: geometry, computer simulation, tooth contact analysis and stress analysis. ASME J Mech Transmissions Automation 1988;110:482–491.
21. Tao JX, Smith S, Duff A. The effect of overloading sequences on landing gear fatigue damage. Intel J Fatigue 2009;31(11-12):1837-1847.

2/18/2010

Subsurface Geophysical Estimation of Sand Volume in Ogudu Sandfilled area of Lagos, Lagos, Nigeria.

Adeoti Lukumon [1], Oyedele K. Festus [1] and Adegbola R. Bolaji [2]
[1]·Department of Geosciences University of Lagos, Lagos Nigeria
[2]·Department of Physics, Lagos State University, Lagos Nigeria.
lukuade@yahoo.com, kayodeunilag@yahoo.com

Abstract
Surface geophysical survey was carried out using Electrical resistivity and induced polarization methods to estimate volume of sand deposits for the purpose of development/exploitation via dredging in Agboyi area of Lagos State .The study area was divided into square, rectangular, triangular and trapezoidal cells before conducting the geophysical survey. A total of 125 Vertical electrical sounding (VES) data were collected using Schlumberger electrode configuration with an electrode spacing varying between 100 and 400m. Five wells were also drilled for the collection of soil samples with a view to mapping the litho-logical variations of the subsurface strata. The combination of Vertical electrical sounding (VES) data, Induced Polarization (IP) data and well log data were used in inferring the litho-logical units of each geo-electric layer within the study area. The geo-electric sections delineate three to five subsurface layers, which include sand, sandy clay/ clayed sand, and clay. The 2-D and 3-D Isopach maps show the distribution of sand with thickness ranging between 0.5m and 7.0m.The volume of sand within each cell was calculated and the results were summed to give a total volume of 165596.5712m^3 of sand as against 1.5million m^3 projected. Hence, the analysis shows that the study area is devoid of enough sands for the purpose of development/exploitation via dredging. [Journal of American Science 2010;6(7):68-77]. (ISSN: 1545-1003).

Keywords: Vertical Electrical sounding (VES); Geoelectric Section; Lithological

1.0. Introduction

Lagos state is one of the heartbeats of economic activities in Nigeria because of the presence of many industries, ports (air and sea), etc. The population of the state is now becoming explosive that many people could not afford decent accommodation while those that could afford pay exorbitantly. Thus, congestion makes suitable sites to become very scarce in urban areas. This now informed the study of some abundant areas in coastal part via geophysical methods in order to quantify the volume of sand for reclamation purposes.

Geophysical methods are often used in site investigation to determine the overburden thicknesses and map subsurface conditions prior to excavation and construction. Electrical resistivity and seismic exploration methods are the most common techniques used for this purpose (Kurthenecker 1934; Moore 1952; Drake 1962; Early and Dyer 1964; Burton 1976; kearey and Brooks 1984; Olorunfemi and Meshida 1987). There are many methods of electrical surveying, some make of naturally occurring fields within the Earth while others require the introduction of artificially generated currents into ground. These comprise the spontaneous of self-potential (SP) method, induced polarization (IP) method and electrical resistivity methods. Although more labour intensive, the electrical resistivity method is more viable for deep subsurface investigation (Reynolds, 1997). Electrical resistivity method is routinely used in engineering and hydrogeological investigations to investigate the shallow subsurface geology.

The study was carried out at Agboyi village which is considered to be one of the Islands in the coastal part of Lagos. About 1.5million m^3 of sand was envisaged for reclaiming part of the area by the proponents. The Electrical resistivity and induced polarization methods were employed because VES gives low resistivity values for both saline sand and clay but in contrast, induced polarization method differentiate both i.e, saline sand typifies low induced polarization (poor chargeability) while clay depicts high induced polarization (medium to high chargeability). In view of the nature of the geology of the study area, the combination of

both methods in delineating the subsurface could not be overemphasized.

2.0. Materials and Methods

2.1. Site and Geology

The area of study (Figure 1**)** is an Island with a swampy terrain having daily rising and falling of tides. It is accessible by road from Oworonsoki-Ojota axis expressway and from Ojota via the overhead bridge. A canoe is required to get to the site because of a canal which traverses the area and empties into the lagoon. Some of the visible activities include fishing, sand dredging and transportation via canoe. The geology of the study area can be described broadly as a sedimentary basin, which thickens from North to South (Down dip) and from East to West. The littoral and lagoon deposits of recent sediments underlie the study area. The area shares the geologic characteristics of coastal environments in Nigeria which include the presence of clays, shale deposits, sandstones and pebbles. Hence, the study area is characterized by unconsolidated sands, clays and mud with a varying proportion of vegetable matter, along the coastal areas while the alluvial consist of the coarse, clayey, unsorted sands with clay lenses and occasional beds.

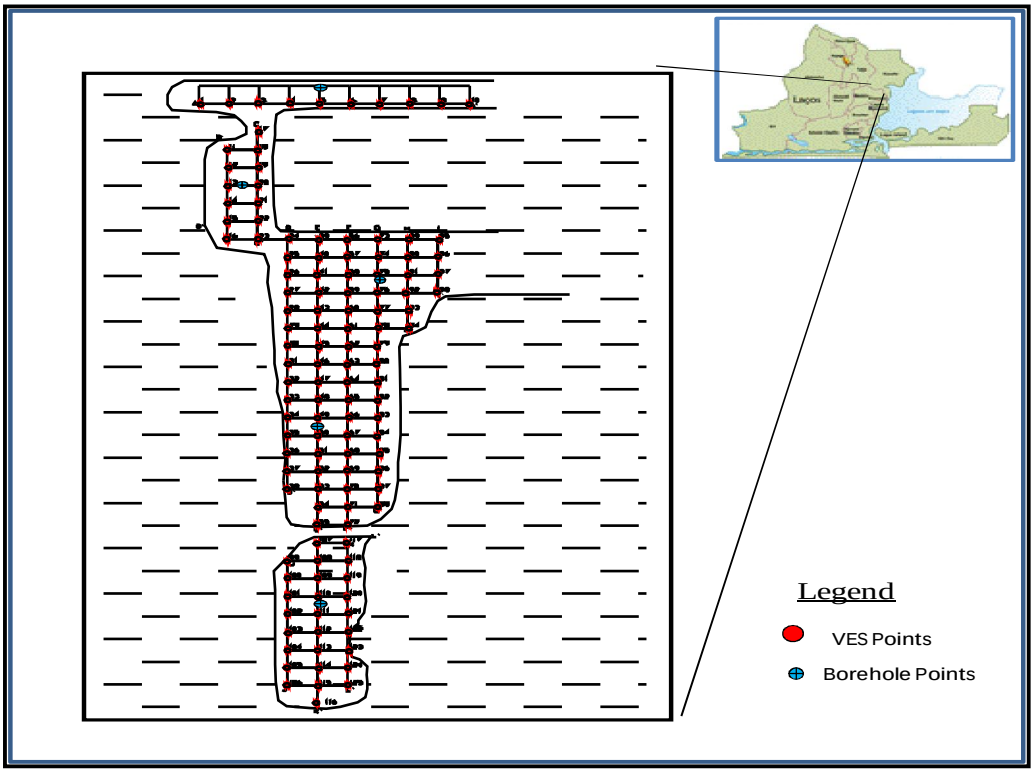

Figure 1: Base Map of Study Area

2.2. Data Acquisition

The study area was divided into square, rectangular, triangular and trapezoidal cells and geo referenced by Garmin Etrex model Global Positioning System (GPS) handset with a view to determining the longitude, latitude and elevation of the VES locations (figure 1). ABEM Terrameter SAS 1000 and PASI Tarrameter were used for the data acquisition. A total of 125 Vertical electrical sounding (VES) data were collected using the Schlumberger electrode array with electrode spread (AB) varying from 2.0m to a maximum of 400m. The electrical chargeability and resistivity measurements were taken simultaneously. The essential idea behind the vertical sounding used in this study area assume conductivity variation with depth only, is such that as the resistance between the current and potential electrode is increased, the current

filament passing across the potential electrode carries a current fraction that has returned to the surface after reaching increasing deeper depth (Telford et. al., 1976). Five wells were also drilled for the purpose of correlation with sounding results.

3.0. Results

Sounding curves were interpreted qualitatively and quantitatively. The qualitative interpretation involved evaluation of curves for estimation of volume of sand deposit in the studied area. Quantitative interpretation of the curves involves partial curve matching using two layer Schlumberger master curves and the auxiliary K, Q, A and H curves. Outputs were modelled using computer iterations. WinGLink software was utilized for the iterations. The results of qualitative interpretation of 125 VES data are characterized by HA, QHA, QH and KH curves. The results of the cuttings from the five wells drilled revealed the subsurface strata as sand, clay, clayed sand and sandy clay at various depths (Table 2).

Samples of the resistivity and IP curves are respectively shown in Figures 2 & 3. One of geoelectric sections beneath the VES is shown in Figures 4**.** Summary of some of the interpreted VES data is presented in Table 1. 2-D Isopach Map (Figure 5), 3-D Isopach Map in South-Eastern View **(**Figure 6), and Isopach Map in North-Western View (Figure 7) are presented. The estimated volume of sand within each cell is shown Table 3.

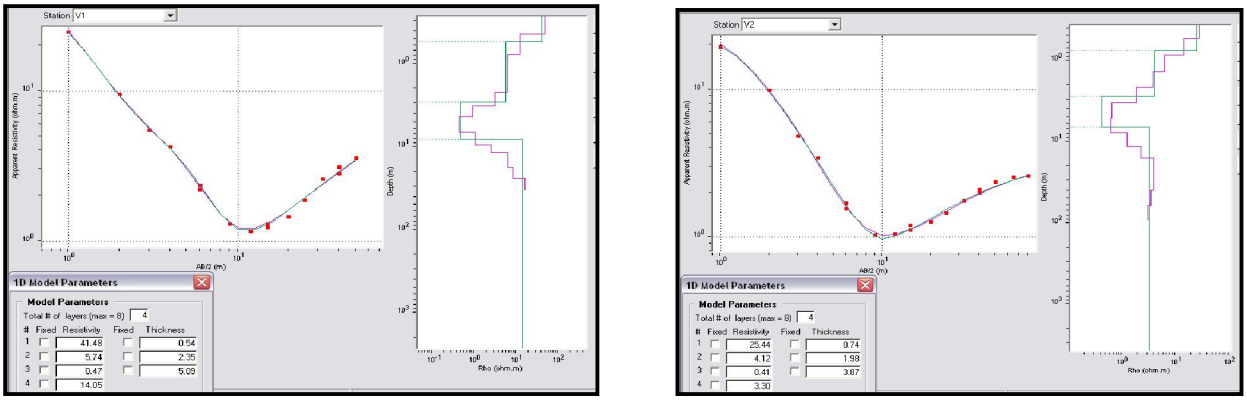

Figure: 2 Sample of resistivity field curves

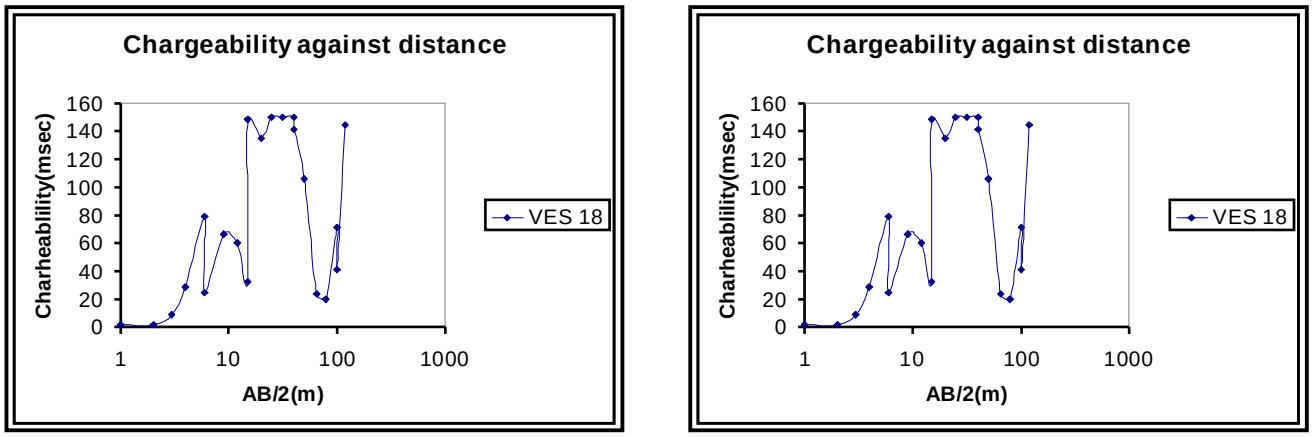

Figure 3: Sample of Induced Polarization curves

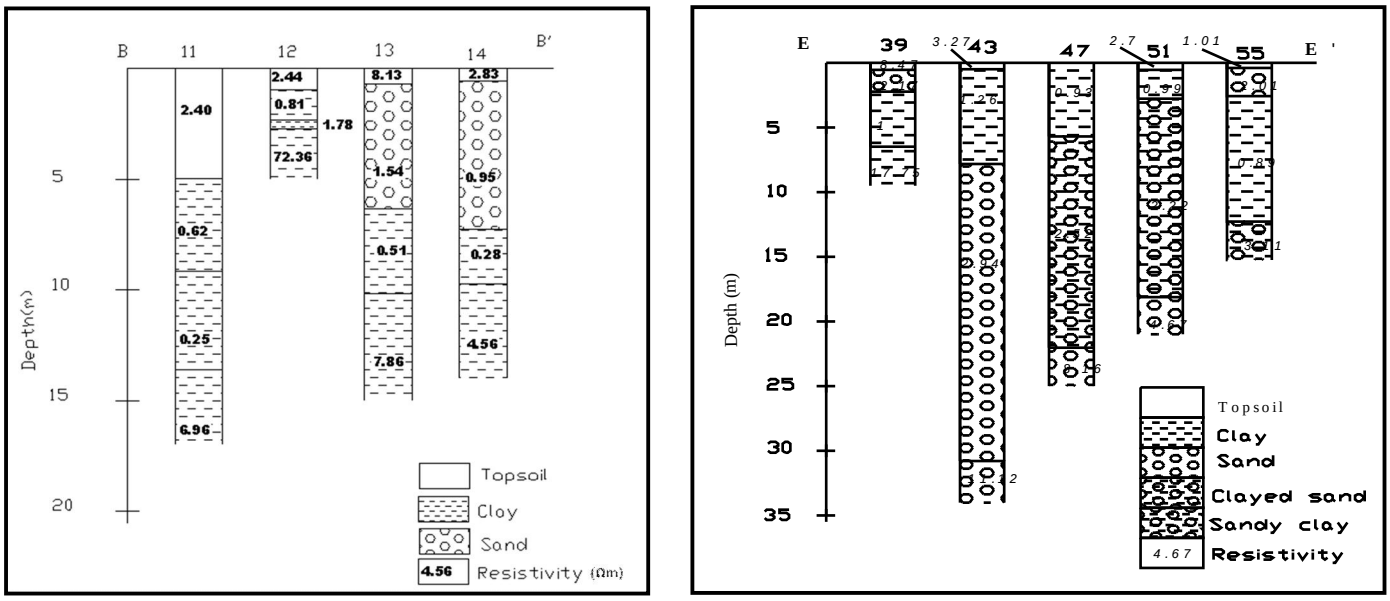

Figure 4: Sample of Geo-electric sections Along traverses BB' and EE'

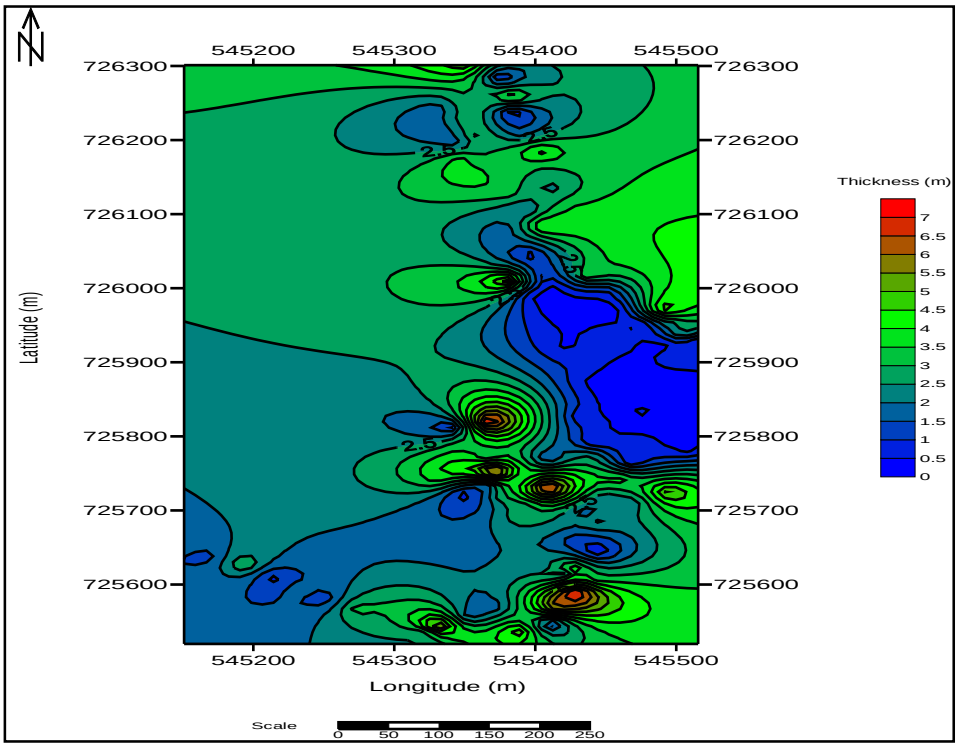

Figure 5: 2D Isopach Map of Agboyi-Ogudu, Lagos State

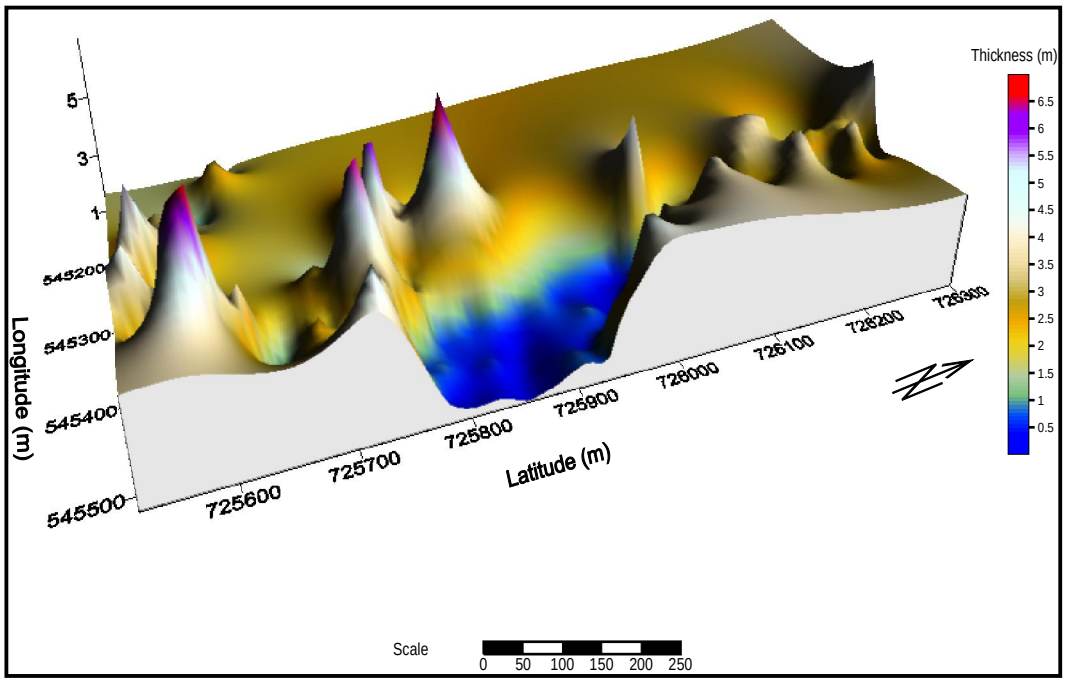

Figure 6: 3D Isopach Map (South-Eastern View) of Agboyi-Ogudu, Lagos State.

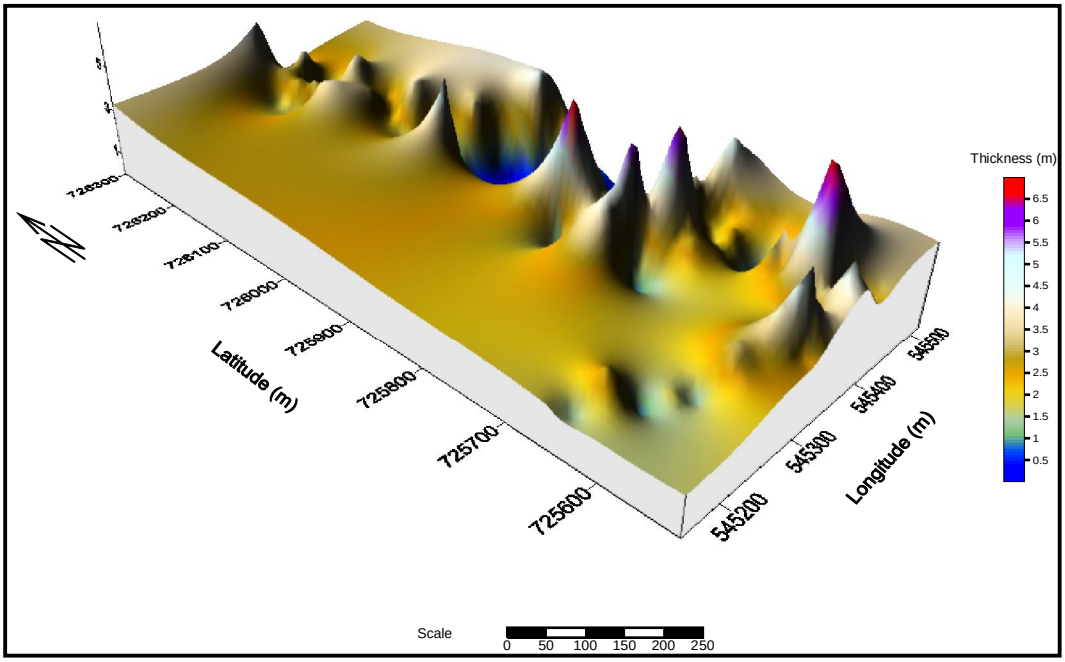

Figure 7: Isopach Map (North-Western View) of Agboyi-Ogudu, Lagos State.

Table 1. True Resistivity and Horizon Depths.

VES Number	Number of Layers	Resistivity(Ωm)	Thickness(m)	Depth(m)	Lithology
1	1	36.16	0.54	0.54	Topsoil (Sand)
	2	7.85	2.55	3.09	Sand
	3	0.16	5.09	8.18	Clay
	4	5.63	---	---	Clay
2	1	25.44	0.74	0.74	Topsoil (Sand)
	2	4.12	1.98	2.73	Sand
	3	0.41	3.87	6.59	Clay
	4	3.30	---	---	Clay
3	1	41.48	0.62	0.62	Topsoil (Sand)
	2	5.74	2.19	2.81	Sand
	3	0.47	14.75	17.56	Clay
	4	14.05	---	---	Clay
4	1	204.54	0.47	0.47	Topsoil (Sand)
	2	5.15	2.79	3.26	Sand
	3	0.88	14.37	17.63	Clay
	4	29.16	---	---	Clay
5	1	95.83	0.57	0.57	Topsoil (Sand)
	2	3.63	0.53	1.10	Sand
	3	1.46	18.52	19.62	Clay
	4	4.10	---	---	Clay
6	1	74.37	0.47	0.47	Topsoil (Sand)
	2	5.02	1.39	1.86	Sand
	3	1.26	3.76	5.62	Clay
	4	8.35	---	---	Clay
7	1	190.9	0.43	0.43	Topsoil (Sand)
	2	84.81	0.29	0.72	Sand
	3	4.95	2.97	3.69	Sand
	4	9.53	14.20	17.89	Clay
	5	5.20	---	---	Clay
8	1	28.04	0.58	0.58	Topsoil (Sand)
	2	3.36	2.54	3.12	Sand
	3	1.19	11.22	14.34	Clay
	4	9.69			Clay
9	1	5.73	1.26	1.26	Topsoil (Sand)
	2	0.91	3.24	4.50	Sand
	3	1.52	15.94	20.44	Clay
	4	2.16	---	---	Clay

Table 2: Borehole log

Sample	Depth(m)	Lithology
1	0 – 0.15	Brownish Clay (with plant roots)
2	0.15 – 1.50	Brownish- grey clay
3	2.25 - 3.0	Medium to coarse grained sand(light grey)
4	3.50 – 4.25	Fine sandy clay (light grey)
5	4.50 – 5.25	Fine - medium sandy clay (compacted)
6	5.25 – 6.0	Dark grey clay
7	6.0 – 6.75	Dark grey clay
8	6.75 – 7.5	Dark grey clay
9	7.50 – 8.25	Dark grey clay
10	8.25 – 9.00	Dark grey clay
11	9.0 – 9.75	Dark grey clay (compact)
12	9.75 – 10.25	Dark grey clay (compact)
13	10.25 – 11.00	Dark grey clay (compact)
14	11.00 – 11.75	Dark grey clay (compact)
15	12.00 – 12.55	Dark grey clay (compact)
16	12.55 – 13.25	Dark grey clay (compact)
17	13.50 – 14.25	Dark grey clay (compact)

4.0. Discussion

4.1. Geo-electric Sections

The well log data of the borehole drilled, induced polarization and VES data were used to infer geoelectric layers. These were later used to draw the geoelectric sections AA', BB', CC', DD', EE', FF', GG', HH', II', JJ', KK' and LL'. The layer resistivities and thicknesses indicate four to five subsurface layers. The topsoil is made up of sand, clay and clayed sand. The sand has resistivity values which vary from 0.53 to 90.60 ohm-m with layer thickness 0.2-7.25m. The clay shows resistivity contrast 0.93-9.13ohm-m with layer thickness between 0.23m and 6.00m while clayey sand has thickness and resistivity value of 1.59m and 2.16 ohm-m respectively.

Sand, clay and sandy clay constitute the second geoelectric layer. The sand has layer thickness and resistivities values that vary from 0.34-5.67m and 0.98-120.34 ohm-m respectively. The clay has resistivity values that range from 0.6-1130ohm-m and thickness values that vary between 0.73-7.89m. The resistivities in sandy clay vary from 0.35 to 1.55ohm-m with earth thickness 0.74-6.99m.

The third horizon is symptomatic of clay, sandy clay, and sand. The clay has resistivity values between 0.16 and 28.73ohm-m while its thickness varies from 0.15 to 17.43m. In some of the VES data, thickness could not be determined because the current terminated within this layer. Clayeysand/sandy clay region have 1.71-21.30m layer thickness with resistivity values ranging from 0.71ohm-m to certained because the current terminated within this region. The sand exhibits resistivity values 0.59-96.44ohm-m and its thickness falls between 3.89 and 3.19m.

Table 3: Estimation of volume of sand within each cell

VES Points	Average Thickness(m	Area(m^2)	Volume(m^3)
1,2,3,4,5	2.5560	3283.2428	8391.9686
6,7,8,9,10	1.7440	4530.8750	7901.8460
1,2,17	2.9000	1025.3820	2973.6078
11,12,18,19	2.3450	2060.8662	4832.7312
12,13,19,20	2.8225	1333.5017	3763.8085
13,14,20,21	4.7775	1333.5017	6370.8044
14,15,21,22	4.5225	1333.5017	6030.7614
15,16,22,23	2.6225	1575.9565	4132.9459
24,25,39,40	1.9300	947.0893	1827.8823
25,26,40,41	2.2100	694.5321	1534.9159
26,27,41,42	3.3900	694.5321	2354.4638
27,28,42,43	3.0025	694.5321	2085.3326
28,29,43,44	1.0525	694.5321	730.9950
29,30,44,45	0.4650	694.5321	322.9574
30,31,45,46	0.3950	694.5321	274.3402
31,32,46,47	0.2450	694.5321	170.1604
32,33,47,48	0.1625	694.5321	112.8615
33,34,48,49	0.5775	694.5321	401.0923
34,35,49,50	0.6375	694.5321	442.7642
35,36,50,51	1.0650	694.5321	739.6767
36,37,51,52	1.5525	694.5321	1078.2611
37,38,52,53	2.1575	694.5321	1498.4530
38,53,54,55	2.9550	719.7827	2126.9579
39,40,56,57	2.4000	947.0893	2273.0143
40,41,57,58	3.4800	625.0000	2175.0000
41,42,58,59	4.1825	625.0000	2614.0625
42,43,59,60	2.5575	625.0000	1598.4375
43,44,60,61	1.1050	625.0000	690.6250
44,45,61,62	0.6050	625.0000	378.1250
45,46,62,63	0.4950	625.0000	309.3750
46,47,63,64	0.2450	625.0000	153.1250
47,48,64,65	0.1800	625.0000	112.5000
48,49,65,66	0.5150	625.0000	321.8750
49,50,66,67	0.6375	625.0000	398.4375
50,51,67,68	0.5125	625.0000	320.3125
51,52,68,69	0.3850	625.0000	240.6250
52,53,69,70	0.5100	625.0000	318.7500
53,54,70,71	1.2875	625.0000	804.6875
54,55,71,72	1.8400	625.0000	1150.0000
56,57,73,74	2.5150	947.0893	2381.9296
57,58,74,75	4.0450	625.0000	2528.1250
58,59,75,76	3.8700	625.0000	2418.7500
59,60,76,77	2.3300	625.0000	1456.2500
60,61,77,78	1.5575	625.0000	973.4375
61,62,78,79	0.7250	1055.6889	765.3745
62,63,79,80	0.7000	1055.6889	738.9822
63,64,80,81	0.5350	1055.6889	564.7936
64,65,81,82	0.4500	1055.6889	475.0600
65,66,82,83	0.5600	1055.6889	591.1858

VES Points	Average Thickness(m)	Area(m^2)	Volume(m^3)
66,67,83,84	0.6225	1055.6889	657.1663
67,68,84,85	0.5625	1055.6889	593.8250
68,69,85,86	0.4325	1055.6889	456.5854
69,70,86,87	1.7150	1055.6889	1810.5065
70,71,87,88	2.3375	1055.6889	2467.6728
71,72,88	1.3833	544.4569	753.1654
73,74,89,90	1.6425	947.0893	1555.5942
74,75,90,91	3.6725	625.0000	2295.3125
75,76,91,92	3.7175	625.0000	2323.4375
76,77,92,93	2.5175	625.0000	1573.4375
77,78,93,94	3.5475	625.0000	2217.1875
89,90,95,96	2.5425	1414.3200	3595.9086
90,91,96,97	4.0475	889.0011	3598.2320
91,92,97,98	3.5600	889.0011	3164.8439
92,93,94,98	3.7325	1181.9269	4411.5422
99,107,108	3.1933	1212.2743	3871.1959
99,100,108,109	2.7375	889.0011	2433.6405
100,101,109,110	2.9750	889.0011	2644.7783
101,102,110,111	3.3950	889.0011	3018.1587
102,103,111,112	3.0100	889.0011	2675.8933
103,104,112,113	2.9725	889.0011	2642.5558
104,105,113,114	2.6750	889.0011	2378.0779
105,106,114,115	1.8950	889.0011	1684.6571
107,108,117,118	2.5425	1288.0414	3274.8453
108,109,118,119	2.7000	944.5637	2550.3220
109,110,119,120	3.4750	944.5637	3282.3589
110,111,120,121	3.4850	944.5637	3291.8045
111,112,121,122	2.8625	944.5637	2703.8136
112,113,122,123	2.3750	625.0000	1484.3750
113,114,123,124	2.3750	944.5637	2243.3388
114,115,124,125	2.6550	944.5637	2507.8166
106,115,125,116	2.9075	1575.9565	4582.0935
Total			**165596.5712**

The fourth substratum layer denotes clay, sandy clay/clayed sand and sand. The clay, sandy clay/clayedsand and sand have resistivity values that vary from 1.18-28.81ohm-m, 3.11-89.64ohm-m, and 2.13-31.30ohm-m respectively. The layer thicknesses could not be determined because the current terminated within those zones except in some parts of clay region where VES 8 and VES 20 have layer thicknesses of between 7.38 and 17.89m.

The fifth identified layer is diagnostic sections AA', CC', DD', and FF'. The resistivity values in clay vary from 0.11-25.64ohm-m while those in clayey sand/sandy clay ranging between 4.78 and 5.92ohm-m. Their earth thickness could not be determined because the current terminated within these horizons. 97.59ohm-m in some of the VES. Also, the earth thickness of some VES could not be as

4.2. Isopach Maps

The 2-D Isopach map in Figure 5 shows the distribution of the sand in the area investigated with thickness ranging from 0.5 to almost 7.0m. The 3-D Isopach map along South-Eastern view of the study area (Figure 6) shows the distribution of the trough and peak of the sand. The thickness of the sand ranges from 0.5m to

almost7.0m. The 3-D Isopach map along the North-Western view of the area investigated shows the distribution of the trough and peak of the sand with thickness between 0.5m and almost 7.0m (Figure 7).
The analysis of both 2-D and 3-D Isopach maps show that the sand thickness varies from 0.5m to almost 7.0m.

4.3. Volume of sand

The study area was divided into square, rectangular, triangular and trapezoidal cells. The volume of sand within each cell was calculated as shown in Table 3. Hence, these results were summed to give a total volume of 165,596.5712m^3 of sand.

Corresponding Author:
Dr. Adeoti, L. and Dr. Oyedele, K..F
Department of Geosciences,
University of Lagos, Lagos, Nigeria.
lukuade@yahoo.com, kayodeunilag@yahoo.com

References

1. Adeyemi, P. A (1972). Sedimentology of Lagos lagoon, Unpublished special BSc thesis,Obafemi Awolowo University,Ife-Ife Osun State, Nigeria.
2. Burton, A.N (1976). The use of geophysical methods in engineering geology, Part 1: Seismictechniques, Ground Engineering
3. Drake, C.L (1976). Geophysics and engineering, Geophysics 27: 193-197
4. Durotoye, A.B (1975). Quaternary sediments in Nigeria. In: Kogbe CA (ed) Geology of Nigeria. Elizabeth Press, Lagos, pp 431-451
5. Early, K.R, Dyer, K.R. (1964). The use of resistivity survey in foundation site underlain by Karst dolomite Geotechnique 14: 341-348
6. Emery, K.O.E, Uchupi, J.P, Brown, C, Mascle, J. (1975). Continental margin off Western 59: Africa-Angola to Sierria Leone. America Association of Petroleum Geologist, Bulletin 2209-2265
7. Ghost, D.P (1971). Inverse filter coefficients for the computation of apparent resistivity standard curves for ahorizontal stratified earth. Geophysical Prospecting19:749-775.
8. Halstead, L.B (1971). The shoreline of lake Kainji, a preliminary survey, Journal of MiningGeology 6: 1-22
9. Jones, G.P.A (1960). Sedimentary study of the Ngalda gravels, Bauchi province, N E JonesNigeria, Record of Geological survey, Nigeria, 29-40
10. Jones. H.A and Hockey, E.D (1964). The geology of part of south-western Nigeria. Geological survey, Nigeria Bulletin 31: 1-. 101
11. Keary, P. Brooks, M. (1984). An introduction to geophysical exploration. Blackwell Scientific Publication, Oxford, pp198-217

3/01/2010

Cell surface hydrophobicity (CSH) of *Escherichia coli*, *Staphylococcus aureus* and *Aspergillus niger* and the biodegradation of Diethyl Phthalate (DEP) via Microcalorimetry.

Alhaji Brima Gogra [a,d], Jun Yao [a,*], Edward H. Sandy [a], ShiXue Zheng [b], Gyula Zaray [c], Bashiru M. Koroma [d], Zheng Hui [b]

[a] State Key Laboratory of Biogeology and Environmental Geology of Chinese Ministry of Education, School of Environmental Studies and Sino-Hungarian Joint Laboratory of Environmental Science and Health, China University of Geosciences, 430074 Wuhan, PR China.

[b] State key Laboratory of Agricultural Microbiology, College of Life Science and Technology, Huazhong Agricultural University, 430070 Wuhan, PR China.

[c] Department of Chemical Technology and Environmental Chemistry, Eötvös University, H-1518 Budapest, P.O. Box 32, Hungary.

[d] Department of Chemistry, School of Environmental Sciences, Njala University, Sierra Leone.

* Corresponding author. E-mail address: yaojun@cug.edu.cn (J. Yao) or abgogra@yahoo.co.uk (A. B. Gogra)

Abstract: This work was focused on investigating the occurrence of cell surface hydrophobic (CSH) character among diethyl phthalate (DEP)-degrading microbes (*Escherichia coli*, *Staphylococcus aureus*, and *Aspergillus niger*) by evaluating the effect of DEP on microbial cell surface hydrophobicity and to investigate any relationship between cell surface hydrophobicity and the ability of such microbes to degrade DEP using microcalorimetry and other methods. In this study, a TAM III multi-channel microcalorimeter, at 28 ^{o}C, was used to measure the minimum inhibitory concentration (MIC) of DEP and the DEP biodegradation efficiency by fitting the thermogenic curves and integrating the area limited by these curves, respectively. Using MATHS (microbial adhesion to hydrocarbons) assay, CSH of the microbial cells was determined as a measure of their adherence to the hydrophobic n-octane. From the experimental data, *S. aureus* was found to be the most efficient DEP degrader and *E. coli* the least and that *S. aureus* showed high, whilst *E. coli* and *A. niger* showed moderate hydrophobicity and autoaggregation abilities. There were positive correlations between microbial cell surface hydrophobicity and autoaggregation ability, DEP biodegradability, IC_{50} values for the tested strains. [Journal of American Science 2010;6(7):78-88]. (ISSN: 1545-1003).

Keywords: Hydrophobicity, *Escherichia coli*, *Staphylococcus aureus*, *Aspergillus niger*, Microcalorimetry, Diethyl phthalate, Autoaggregation, IC_{50}.

1. Introduction

To satisfactorily define hydrophobicity has not been very easy, though this effect has been investigated for so many decades ago. Many researchers have tried to proffer its definition: the thermodynamists defined it from a thermodynamic view (Edsall, 1992) and the microbiologists defined it from a phenomenological view (Kauzmann, 1959; Doyle, 2000). Breslow (1991) observed that, hydrophobicity is the tendency of apolar species to aggregate in aqueous medium so as to decrease the hydrocarbon-water/oil-water interfacial area. The inability of non-polar compounds like phthalic acid esters (PAEs) to dissolve in aqueous medium has been associated with the hydrophobicity of these compounds, in fact, making the term misleading; the London dispersion interactions between molecules of water and non-polar compounds are favourable and quite substantial. Reviews by Doyle (2000) and Karplus (1997) attempted to throw light on hydrophobicity in terms of both biology and chemistry. Adherence of a microorganism to a surface may occur through hydrophobic effect provided the associating sites have sufficiently high densities of non-polar areas. Microorganisms, including bacteria and fungi have adopted ways to use the hydrophobic effect to adhere to surfaces. Hydrophobic microorganisms, in particular, are capable of adhering to the oil-water interface, and of utilizing oil components as a source of energy for growth and metabolism (Marshall, 1991). Duncan-Hewitt, (1990) observed that, there exist compelling rationales to believe that the hydrophobic effect (attributed to cell wall proteins and lipids) may be the driving force for the adhesion of most microbes.

Miyoshi (1895) was the first to describe the ability of microorganisms to consume organic compounds as sole carbon source, by reporting the microbial utilization of paraffins. A great diversity of different microbes (bacteria, fungi, yeast and moulds) capable of degrading organic compounds (such as PAEs, and other oily-liquids) in the environment

occurs. Bacteria belong to a group of the 'best bio-degraders' of organic compounds (Olivera et al., 2003; Chao et al., 2006) including oily-liquids and other hydrocarbons; in this study, diethyl phthalate, DEP, and n-octane. Unfortunately, little or no information is available on the simultaneous degradation of both pollutants and without focusing on the relationship between extent of degradation achieved and cell surface hydrophobicity (CSH), which seems to be an avoided topic especially in systems containing more than one carbon source.

CSH influences the direct contact of cell with hydrocarbon droplets and is hence, one of the major factors affecting the degradation of hydrophobic compounds (Chao et al., 2006; Prabhu and Phale, 2003; Al-Tahhan et al., 2000). This factor is of paramount importance for cell survival, as it controls the process of association between the cells and other surfaces. The rate of biodegradation of organic compounds is dependent upon several other physicochemical and biological parameters. For instance, PAEs with shorter alkyl-chains (like diethyl phthalate, DEP; dibutyl phthalate, DBP) are relatively easily biodegraded than phthalate esters with longer alkyl-chains, such as di-(2-ethylhexyl)-phthalate (DEHP) (Chang et al., 2004; Chao et al., 2006). So it's expected that DEP is more easily biodegraded than DBP. The poor solubility of PAEs in water is potentially one of the commonest physicochemical properties which hinders their rates of biodegradation in the environment, which effect makes PAEs poorly bio-available, and thus hampers their microbial degradation (Rosenberg et al., 1992; Bouchez et al., 1995; Efroymson and Alexander, 1995; Churchill et al., 1999). Bioavailability of hydrophobic organic compounds, a physicochemical parameter critical in the overall rate of compound degradation, is a function of phase solubility and solution transport processes. For chemical and physical compatibility between and/or among the organisms and the hydrophobic DEP and n-octane substrates, the microbes must possess cell surface hydrophobicity, hence, leading to enhanced mutual interactions between and/or among them (Busscher et al., 1995), which consequently, would lead to increased dispersion and greater bioavailability of DEP substrates, and enhanced utilization. Therefore, the ubiquitous occurrence of hydrophobic cell surface property among strains of DEP-degrading population of microorganisms will be a favourable feature for DEP contamination bioremediation activity in any environmental matrix. Potentially, the rate-limiting step in biodegradation of hydrophobic compounds is the ability of the compounds to be solubilized and transported into microbial cells capable of metabolizing them. Though there exist among microorganisms, direct contact and DEP-solubilization mechanisms for substrate uptake but their relative contribution in a population of DEP degraders is yet unknown. Therefore, the aim of this study was to investigate the effect of microbial CSH on the degradation of DEP by exploring any existing relationship between CSH and the ability of such microbes (two bacterial strains, *Escherichia coli* and *Staphylococcus aureus*; and a fungal strain, *Aspergillus niger*) to degrade this compound by monitoring their growth on media amended with DEP, using a combination of microcalorimetry and other methods.

2. Materials and Methods

2.1 Microorganisms

The DEP-degrading microorganisms employed in this study were wild strains of *Escherichia coli* (a Gram-negative, facultative anaerobic and non-sporulating bacterium), *Staphylococcus aureus* (a Gram-positive, facultative anaerobic coccus), and *Aspergillus niger* (a filamentous ascomycete fungus) and were all provided by the National Key Laboratory of Agromicrobiology, Huazhong Agricultural University (Wuhan, PR China).

2.2 Media preparations

Peptone culture medium (commonly known as Luria Broth, LB, culture medium) was used to incubate the bacteria, *E. coli* and *S. aureus* and was prepared by adding 10.0g Peptone and 5.0g sodium chloride (NaCl) to a 1000mL measuring cylinder containing 5.0g Beef Extract and was made to the mark with distilled water. The medium, at pH 7.2, was then sterilized in high-pressure steam in an autoclave at 121^{o}C for 30 minutes.

Potato sucrose medium (PSM), used to incubate the fungus, *A. niger*, was prepared by adding 20.0mg D-Glucose to a filtrate, obtained by boiling 200.0mg peeled potato slices in 1000mL distilled water for 30 minutes. The volume of the medium was adjusted to 1000mL with distilled water, with no pH adjustment; and was also sterilized in high-pressure steam in an autoclave at 121^{o}C for 30 minutes.

2.3 Preparation of microbial cell suspensions

For inoculum preparations, a loop full of each of the microorganisms was subcultured by inoculating them into 10 mL each of their respective sterile medium and incubated on a horizontal orbital shaker (FM FUMA, PR China) at 37^{o}C with orbital shaking 200 rev min^{-1} (rpm) for 12–18 hours, prior each measurement. The culture was then used as a source of inoculum for the experiments carried out in this work.

2.4 Reagents and their preparations

n-octane (obtained from Sinopharm Chemical Reagent Company Limited, PR China) and diethyl phthalate (DEP); obtained from Tianjin Standard Science and Technology Company Limited, PR China] were used in this work. A 5mL stock solution of 5000 μg mL^{-1} of an analytical grade 99.0% DEP was prepared by thoroughly mixing 0.0223mL DEP with 4.978mL ethanol (95%±5) and stored in the refrigerator. Ethanol was used as solvent because of the low solubility of DEP in water and that it has been widely used as a depolymerizing agent catalyzing the depolymerization of compounds of the DEP family. All chemicals were used as received without further purification. In each microcalorimetric determination, five concentrations (S_o) of DEP (0, 50, 100, 200 and 300 μg mL^{-1}) were prepared as standards from the stock DEP solutions and pipetted into separate conical flasks and/or test ampoules (whereupon most of the added ethanol was removed through 15 minutes volatilization with the aid of HDL APPARATUS clean bench).

2.5 Minimum Inhibitory concentration (MIC) of DEP

The MIC of DEP (defined as the minimum concentration of DEP at which microbial growth was inhibited) for each of the three microbial cultures was separately determined from the half inhibitory concentration, IC_{50}, values (inhibitory concentrations of causing a 50% decrease of microbial growth rate) obtained microcalorimetrically (see Section 2.6) by inoculating a series of 4 mL test ampoules each containing 2 mL air, 2 mL of each respective medium and various concentrations (0 – 300 μg mL^{-1}) of DEP with individual culture prepared as above. The IC_{50} value is determined at 50% of the growth inhibitory ratio (I) obtained by

$$I = [(k_0 - k_C)/k_0] \times 100\%, \quad (1)$$

where k_0 and k_C are the rate constants of the blank/control (0 μg mL^{-1}) and the DEP-containing sample of dose C, respectively. DEP at 25 % of the MIC concentrations was used to determine its effect on cell surface hydrophobicity (CSH) and autoaggregation of the three microbial cultures, and DEP degradation.

2.6 Calorimetry and analytical methods

Enthalpy changes of microbial growth processes can be computed through microcalorimetry, quantifying continuously the exchange of heat between the growth system and the environment. In this study, a TAM III (the third generation thermal activity monitor) multi-channel microcalorimeter (Thermometric AB, Järfälla, Sweden), in the isothermal (constant temperature) mode, was employed to measure continuously the heat production rate from microbial respiration (which is measured as microbial activity) or thermal activities of the wide variety of processes taking place in the test sample (mixture of culture medium and varied concentrations of the compound) contained in the cleaned and sterilized 4mL stainless steel ampoules placed in the instrument in terms of heat, heat flow and heat capacity (Wadsö, 1997; Yao et al., 2008) at 28 ^oC. Each of the hermetically closed (by teflon sealing discs) sample ampoules contained 2mL of nutrient medium, varied doses of DEP, a loop of cell suspension and 2mL of headspace (air). The aim of the ampoule closure was to ensure the control of evaporation yet allowing oxygen and carbondioxide transfer (Critter and Airoldi, 2001). The cell concentration of inoculums for bacteria and fungus was controlled to be equal for the purpose of comparison. The culture medium (i.e., 2mL nutrient medium plus microorganisms) in the reference ampoule serves as blank/control in all the determinations. The performance and details of the instrument's construction are described in its users' manual.

The values of the total heat generated or total thermal effect (Q_T), peak-heat output power (P_{Max}), and peak-time (t_{Max}, related to the maximum position in the P-T curves, Figure 1(a)-(c),) of the growth process for each experiment (from the start of the growth-process until data collection was ended) was computed by integrating the area limited by the P-T curves (Prado and Airoldi, 2000; Critter et al., 2002); also computed from the curves were the value of the microbial growth rate constant (k) and the generation time (t_G). The quantification procedures for these parameters are well established in Hashimoto and Takahashi (1982). The thermogenic (P-T) curves generated from all the experiments illustrate typical patterns of all the phases of the exponential microbial growth-process reactions in environmental matrices (Kimura and Takahashi, 1985; Nuñez et al., 1994): *lag*, *exponential/log growth* (exponential increase of the heat evolution rate), *stationary* and *death phases* (decline of the P–T curve due to the microbial death) and hence obey the first-order thermokinetic relation (Equation 2) at the log phase of growth,

$$S_t = S_o \exp(-kt) \quad (2)$$

where t is the time period, k is the growth rate constant, S_o and S_t represent concentrations of DEP at times 0 and t, respectively. The biodegradation kinetics of organic compounds has been described by so many models and the first-order kinetics has been utilized often to describe their biodegradation process

at low dosages (Zeng et al., 2004). The degradation rate of the DEP by the strains, expressed as relative rate of degradation (δ), could be determined using S_t and S_0 [Equation (2)] via Equation (3) as the DEP dose utilized divided by the original DEP dose, multiplied by 100.

% DEP degradation (δ) = [1-(S_t/S_0)] x 100% = ($\Delta S/S_0$) x 100%, (3)

2.7 DEP treatment and preparations of blanks and samples.

In order to investigate the extent to which 50 µg mL^{-1} (i.e., about 25 % of the MIC concentrations) of DEP could be used as a source of carbon and energy for the microbes under aerobic growth conditions, shake flask experiments were performed. Each culture was grown individually in 150 mL of respective medium in 250 mL Erlenmeyer flasks on the same shaker used for inoculum preparation, with and without 50 µg mL^{-1} DEP for the evaluation of the effect of these compounds on growth, dissolved oxygen (DO), and autoaggregation. At the end of the 24 hours' incubation of the flasks in dark at 28^{o}C, flasks were taken in turn at predetermined times and assayed for cell autoaggregation ability, and DO concentration as described Section 2.8 and the remaining culture medium was centrifuged, using TGL–16M (PR China), at 5000 rpm for 20 minutes to obtain cell pellet, which was used to evaluate the effect of DEP on microbial cell surface hydrophobicity (CSH), as described in Section 2.9.

2.8 Cells autoaggregation assay.

The microbial strains were inoculated in 250 mL Erlenmeyer flasks containing 150 mL each of either LB (for the bacteria) or PSM (for the fungus) culture and initial concentration of DEP made at 50 µg mL^{-1}. Absorbance of the cultured media of the microbial cells, grown with (as test samples) or without (as controls or blanks) 50 µg mL^{-1} DEP, was monitored as described below to observe the effect of DEP on autoaggregation ability. After 24-hour incubation at 28^{o}C in the dark, the cultured medium was vortexed for 15s and allowed to stand at room temperature for 120 minutes, and changes in absorbance were monitored, by taking 3.5 mL inoculated culture medium into quartz cuvette cell at 660 nm using the Spectrumlab 725s Spectrophotometer (Lingguang Ltd., Shanghai, PR China). Autoaggregation ability was determined as percent autoaggregation ($\%A_{Ag}$) using the formula (Equation 4)

$\%A_{Ag}$ = [1-(A/A_o) x 100, (4)

where A_o and A are the absorbances of the cultured media at 0 and 120 minute intervals, respectively. Strains with $\%A_{Ag}$ ≥70%, between 50 and 70% and <50% can arbitrarily been designated as highly, moderately and low autoaggregating, respectively.

2.9 Microbial cell surface hydrophobicity (CSH) assay

Hydrophobicity of the microbial cell suspensions prepared as above was determined, using MATHS (microbial adhesion to hydrocarbons) assay, as a measure of their adherence to the hydrophobic hydrocarbon (n-octane) following the procedure described previously by Rosenberg et al., (1983). After 24-h incubation, microbial cells were concentrated and harvested during the exponential growth phase by centrifugation (5000 x rpm for 20 minutes, TGL–16M, PR China); washed twice with phosphate buffered saline (PBS: 7.6g NaCl, 1.9g $Na_2HPO_4.7H_2O$, 0.7g $NaH_2PO_4.2H_2O$ per liter, pH 7.2, which is a hydrophilic solution), resuspended in the same buffer and the absorbance measured at 660 nm (A_1). Five milliliters (5 mL) of microbial suspension and 1 mL n-octane (i.e., the assay mixture) were mixed for 120s by vortexing to ensure thorough mixing and then incubated for 1h without shaking to insure that the two solutions had separated into biphasic state. The absorbance of the lower hydrophilic (aqueous) layer was measured again (A_2) by recording the changes in absorbance of microbial suspensions due to microbial adhesion to n-octane at 660 nm using the Spectrumlab 725s Spectrophotometer. Microbial cell surface hydrophobicity was expressed as percentage adherence ($\%Adh$) and calculated using the formula (Equation 5)

$\%Adh$ = [1-(A_2/A_1)] x 100, (5)

Strains with $\%Adh$ ≥70%, between 50 and 70% and <50% can arbitrarily been classified as highly, moderately and low hydrophobic, respectively.

2.10 Statistical analyses

Experimental values were obtained through three parallel experiments. Means and standard deviations of generated triplicate data were determined using Originlab Scientific Graphing and Analysis software (OriginPro 7.5). This tool was also used to evaluate the differences between cultures, and the effect of DEP by statistically determining the significance at the P<0.0001 level of difference between treatments and the correlation coefficient (R>0.99).

3. Results and Discussions

In this study, the minimum inhibitory concentration (MIC) for the three microbial cultures, ranging between 127.84 and 197.37 µg mL^{-1} (Table 1), is considered as the least concentration of DEP at which microbial growth was inhibited. Twenty-five percent (25%) of the highest MIC value (i.e., sub-inhibitory dose) was approximated to 50 µg mL^{-1}.

3.1 Microcalorimetry; the growth thermogenic (power-time, P-T) curves at varied doses of DEP at 28 °C.

The third generation multi-channeled thermal activity monitor (TAM) III (Thermometric AB, Järfälla, Sweden) in the isothermal mode, was employed to generate the IC_{50} values from the metabolism of DEP by the three strains by continuously measuring the heat production rate, from the microbial respiration or thermal activities of the wide variety of processes taking place in the test sample, in terms of heat, heat flow and heat capacity at 28 °C. The P-T curves for the growth of these strains in the presence of different doses of DEP (used as the sole carbon and energy source) were shown in Figure 1; all of them depicting, more or less, lag, exponential, stationary and death phases. From these curves, important parameters, including k (the microbial growth rate constant), were computed (Table 1). From Figure 1, it can be seen that DEP has an obvious inhibitory action on the growth of these strains. The IC_{50} value (regarded as the inhibiting dose capable of causing a 50% decrease of the growth rate) was determined at 50% of the inhibitory ratio (I) obtained via Equation 1 and by extrapolating C versus I plot (linear relationship). The sub-inhibitory DEP dose (50 µg mL^{-1}) used to investigate the hydrophobicity and autoaggregation ability of the strains was determined by considering the maximum of 25% of the three sought IC_{50} values. The k, I and IC_{50} values were presented in Table 1, with correlation coefficients (R) greater than 0.99. The k values, decreasing with increase in the DEP doses, show that DEP has potential antimicrobial activity even though it was almost completely biodegraded in these experiments (see δ values in Table 1). The IC_{50} values (*E. coli*, 197.37 µg mL^{-1}; *S. aureus*, 154.43 µg mL^{-1}; and *A. niger*, 127.84 µg mL^{-1}) indicated that *A. niger* and *E. coli* are, respectively, the most sensitive and most tolerant microbes to DEP. The DEP degradation efficiencies (δ) recorded for *E. coli*, *S. aureus*, and *A. niger* ranged between 51.9 - 93.5, 91.9 – 99.8 and 59.8 – 99.9%, respectively; making *S. aureus* (mean DEP Degradation, δ, = 96.18%) the most efficient DEP degrader and *E. coli* (mean DEP Degradation, δ, = 83.83%) the least.

With increasing DEP doses the time for the appearance of the peaks on each curve (t_{max} values, Table 1) increased and their heights (P_{max} and Q_T values, Table 1) decreased correspondingly; with little or diminishing peaks on curves for DEP doses of 200 and 300 µg mL^{-1}. These trends suggest that DEP has inhibitory effect (with increasing dose) on the strains as a consequence of the increased maintenance requirements due to irreparable harm to the cellular envelope (Tiehm, 1994; Chen et al., 2000). The growth curves of these strains have two characteristic peaks; which may suggest that these strains might have adopted two ways of metabolism. The presence or absence of oxygen (O_2) is very significant for microbial growth, hence influencing the ways of microbial metabolism. In this experiment, the volume of O_2 (the headspace) in the test ampoule is approximately 2.0 mL and this is only a limited amount of O_2 to be consumed by the strain in the system. The strains adopted one way of metabolism (aerobic) at the start of the experiment and when the O_2 is used up, the microbes may have adjusted themselves and adopted another metabolic way (anaerobic); which may explain the presence of two peaks. It's worthy to note that the heights of the second peaks increased greater than the first at lower and medium DEP doses and little or shrinking peaks on curves for higher DEP doses (200 and 300 µg mL^{-1}). Therefore, we may conclude that the first way of metabolism has been greatly influenced than the second way and that in the second way of metabolism, these facultative strains must have consumed DEP or/and subsequently its related degradation intermediates (monoethyl phthalate, MEP; phthalic acid, PA; and Protocatechuic acid) that may have accumulated during the primary degradation of DEP, as sources of carbon and energy needed for their continued growth for a definite time. Biodegradation of DEP (Kurane et al., 1978) follows the proposed degradative pathway [Equation (6)].

DEP → MEP → PA → Protocatechuic acid →→ CO_2 + H_2O (through TCA Cycle) **(6)**

which entails systematic cleavage of the ester bond to produce the phthalate monoester and then phthalic acid which is further metabolized and goes through the tricarboxylic acid (TCA) cycle to produce carbon dioxide (CO_2) and water (H_2O) (Wang et al., 1995).

3.2 Microbial cell surface hydrophobicity and autoaggregation of the investigated strains.

For computing microbial CSH, a quantitative method base on adherence to liquid hydrocarbon was recently illustrated. The ease of this technique lends itself to the rapid screening of numerous microbial samples. Three microbial strains were investigated for the effect of DEP on their

Table 1. Enumerative microcalorimetric experimental results of the effects of increasing doses of DEP on the growth of the three microbial strains at 28° C.

Strains	Dose (μg mL^{-1}) (C)	moles DEP (S_o) (10^{-4} mol) L^{-1}	P_{max} (μW)	t_{max} (min)	Q_T (J)	$k(10^{-3}$ $min^{-1})$	R	t_G (min)	Moles DEP (ΔS) (10^{-4} mol) L^{-1}	DEP Degradation (δ) (%)	I (%)	IC_{50} (μg mL^{-1})
E. coli	0	0.00	193.23	1944	10.50	1.62	0.9965	428	0.00	0.0	0.00	197.37
	50	2.25	186.73	1808	10.07	1.51	0.9928	459	2.10	93.5	6.79	
	100	4.50	159.37	2090	10.29	1.26	0.9983	550	4.18	92.8	22.22	
	200	9.00	161.29	2574	14.41	1.38	0.9983	502	8.74	97.1	14.81	
	300	13.50	12.00	600	0.20	1.22	0.9960	568	7.01	51.9	24.69	
S. aureus	0	0.00	145.28	1439	9.76	2.61	0.9990	266	0.00	0.0	0.00	154.43
	50	2.25	203.81	1198	12.97	2.07	0.9913	335	2.06	91.6	20.69	
	100	4.50	191.48	1751	12.77	1.68	0.9991	413	4.26	94.7	35.63	
	200	9.00	134.10	3686	27.51	1.15	0.9905	603	8.87	98.6	55.94	
	300	13.50	39.27	4106	7.52	1.51	0.9987	459	13.47	99.8	42.15	
A. niger	0	0.00	224.25	224	13.03	4.24	0.9959	164	0.00	0.0	0.00	127.84
	50	2.25	277.01	2247	12.05	3.35	0.9986	207	2.249	99.9	20.99	
	100	4.50	239.08	1914	11.90	1.33	0.9982	521	4.15	92.2	68.63	
	200	9.00	32.06	1627	2.33	0.56	0.9978	1238	5.38	59.8	86.79	
	300	13.50	-	-	-	-	-	-	-	-	100.00	

hydrophobicity (CSH) by measuring microbial adhesion to n-octane [Figure 2 (b)]; and on their autoaggregation abilities [Figure 2 (a)]. There were significant differences in the means of CSH (*E. coli*, 64.90%; *S. aureus*, 78.25%; and *A. niger*, 51.30%) and of the autoaggregation abilities (*E. coli*, 63.00%; *S. aureus*, 78.25%; and *A. niger*, 56.25%) amongst the strains without DEP treatment. Without DEP treatment, *S. aureus* showed high (Ljungh et al., 1985), whilst *E. coli* (Ljungh and Wadström, 1983) and *A. niger* (Wessels, 1997) showed moderate hydrophobicity and autoaggregation abilities. The fungal stain (*A. niger*) showed a lower CSH and autoaggregation values than those of the bacterial strains (*E. coli* and *S. aureus*), illustrating that remarkable differences might exist due to bacterial and fungal surface composition and structure (strain-specific characteristics). The effects of adding DEP to the respective medium on autoaggregating ability and CSH include decreased autoaggregation ability (*E. coli*, 35.00%; *S. aureus*, 58.00%; and *A. niger*, 23.00%) and a corresponding decrease in CSH of the strains (*E. coli*, 43.85%; *S. aureus*, 59.40%; and *A. niger*, 31.70%) [Figure 2 (a) and (b)]. When compared with the blank (0 μg mL^{-1}), the two moderately hydrophobic strains recorded significant reductions in autoaggregation ability (*E. coli*, 44.44%; *S. aureus*, 25.88%; and *A. niger*, 59.11%) than the strongly hydrophobic strain and similar reduction in hydrophobicity of all strains (*E. coli*, 32.90%; *S. aureus*, 24.09%; and *A. niger*, 19.64%). Such reductions made the strains less hydrophobic and less autoaggregating. These observed decreases are hard to explain as little is known about the effect of metabolic inhibitor compound (like DEP) on microbial cell surface hydrophobicity; however, Teo et al. (1998) proposed that disappearance of cell clusters can cause inhibition of proton translocation across the microbial cell surface, resulting in reduced

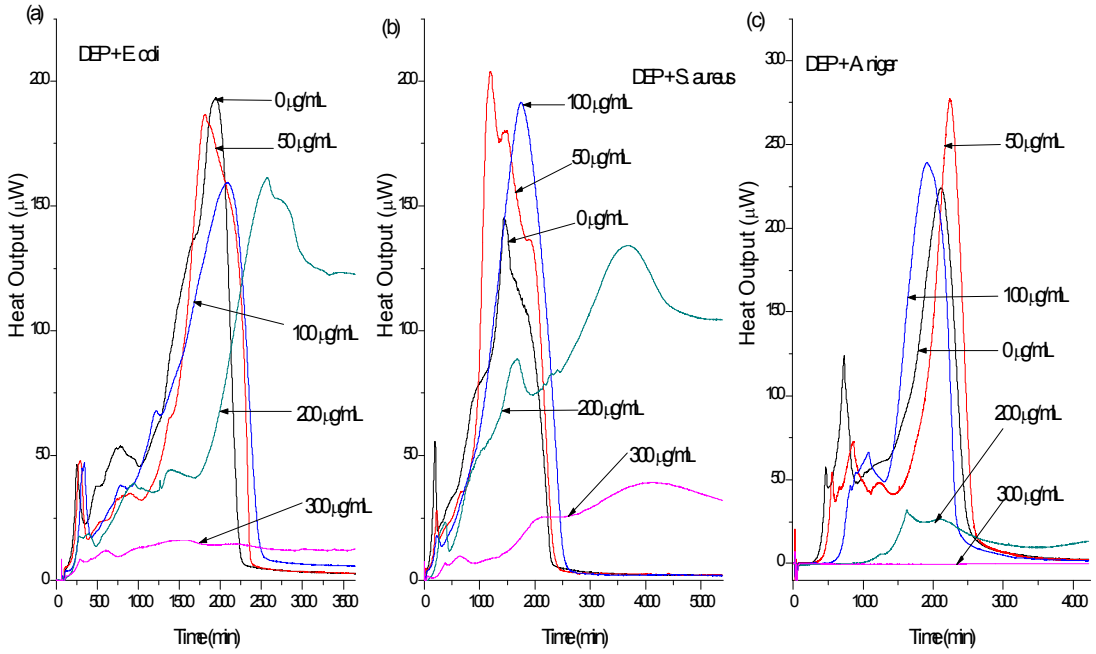

Figure 1. The growth thermogenic (power-time, P-T) curves of (a) *E. coli* in Luria Broth (LB) medium, (b) *S. aureus* in LB medium and (c) *A. niger* in potato sucrose medium (PSM) affected by varied doses of DEP at 28 ^{o}C.

dehydration of cell surface and subsequently leading to decreased hydrophobicity. This may be the likely explanation for the observed decreased in the hydrophobicity and/or adherence, thus decreasing the autoaggregation ability of the three strains. Furthermore, a possible reason for such differences could be attributed to the different compositions and origins of strains studied and the different compositions of nutrient medium; and that the surface physico-chemical characteristics of the strains are species-specific and probably decided by differences in chemical composition in the cell membrane (Christophe et al., 1997). A thorough understanding of all the significant factors, which influence the whole process, is of immense desire. Different methods to determine hydrophobicity may lead to differences to some extent. Figure 3 (b) shows the kinetics of autoaggregation followed by changes in the absorbance of the cultured medium with/without DEP. No significant decrease in absorbance was observed in all the strains. The distributions of CSH and autoaggregation values (Figures 2 and 3) shared much similarity. Regression analysis showed a significant positive linear correlation between hydrophobicity of microbial cultures and autoaggregation abilities of the strains [Figure 3 (a)], with correlation coefficient, R = 0.96826. This idea has been supported by other researchers including Jain et al. (2007). Generally, non parametric statistical analysis showed significant qualitative correlation between classes of hydrophobicity (i.e., high, moderate and low) and antibiotic resistance (IC_{50} values) at P = 0.74916, and from the regression analysis [Figure 4 (b)] we also found some kind of relationship, though a non-significant positive linear one (R = 0.3839), between CSH and the half inhibition dose (IC_{50}), which contradicted the finding of Tahmourespour et al. (2008) but supportive of those of Pan et al. (2006) and Kuntiya et al. (2005). The correlation between CSH and the DEP microbial degradation was also observed by Al-Tahhan et al. (2000) and Prabhu and Phale (2003), who observed that, as the cell surface becomes more hydrophobic, the association of the cell with the hydrophobic substrate becomes stronger, resulting in an increase in the degradation rate; but was contrary to Chao et al. (2006), who failed to observe any relationship between CSH and phthalate degradation potentials. This dichotomy, therefore, provides some information for further studies.

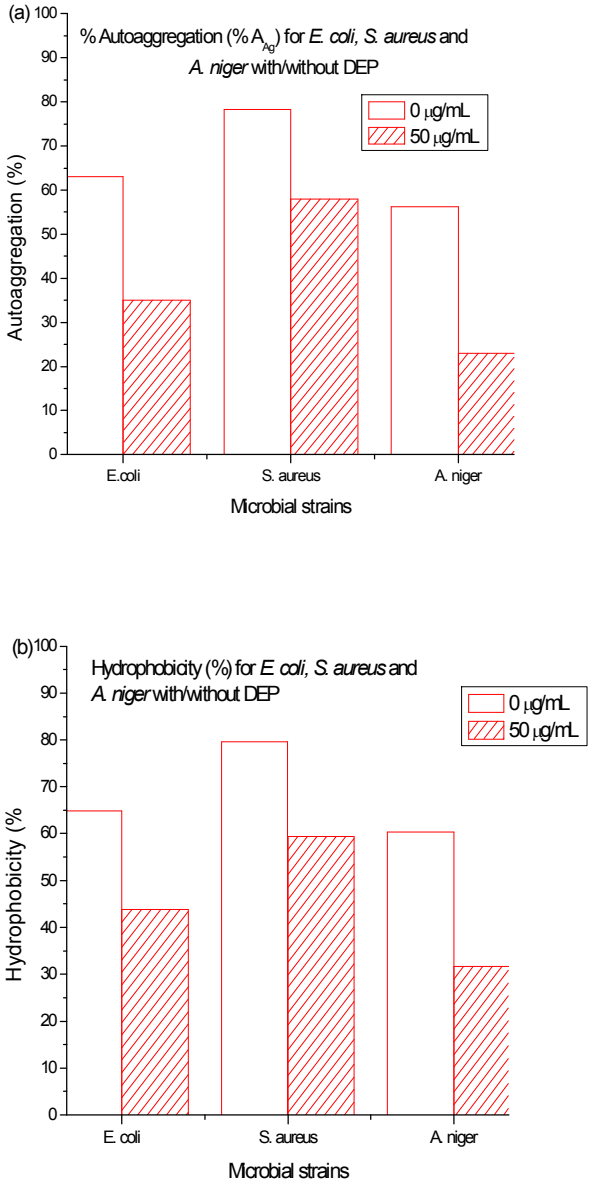

Figure 2. (a) Autoaggregation ability and (b) Surface Hydrophobicity of the three microbial strains grown in their respective medium only or a medium containing DEP.

The possible reasons for the observed trends in hydrophobicity and autoaggregation ability, as against DEP biodegradation, may include: (a) the occurrence of inhibitors enhances exopolysaccharide

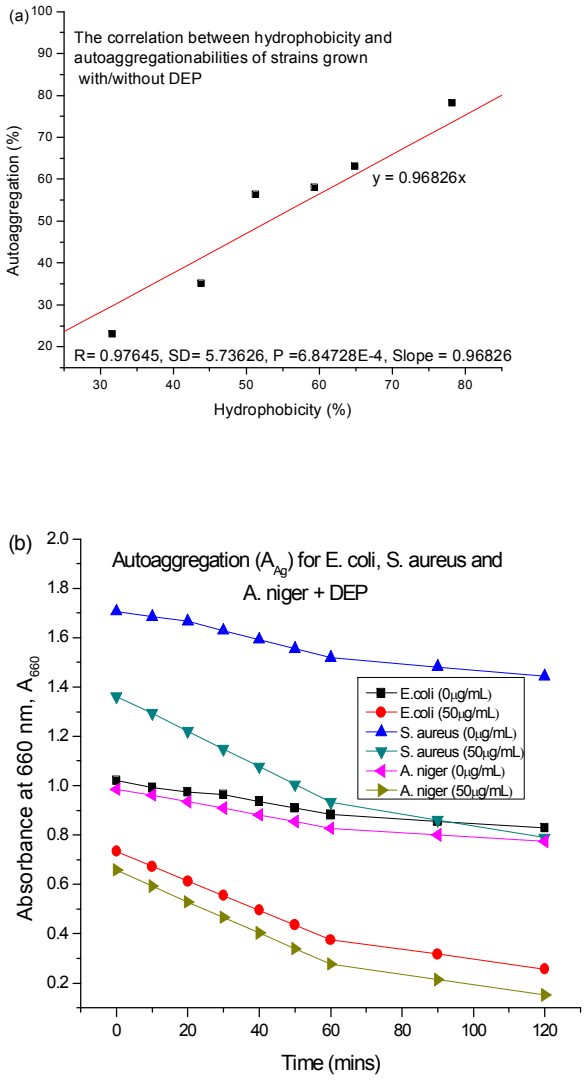

Figure 3. (a) The correlation between utoaggregation ability and the hydrophobicity and (b) autoaggregating kinetics of the three microbial strains to n-octane grown in their respective medium only or a medium containing DEP.

(EPS) production (Raihan et al., 1992; Singh and Fett, 1995) even though the mechanism hasn't been fully understood, which may, however, account for a decreased hydrophobicity (Caccavo et al., 1997), if the EPS are predominantly neutral or hydrophilic; (b) increase in the age of the cell leads to higher EPS production (Fattom and Shilo, 1984); and (c) nutrient starvation in the culture may also cause EPS production (Wrangstadh et al., 1986), thereby reducing the hydrophobicity. Additionally, Medrzycka (1991) and Busscher et al. (1995) reported that during surface hydrophobicity assay, the

hydrocarbons used are negatively charged, and this may cause repulsive (for Gram-negative cells) or attractive (for Gram-positive cells) electrostatic interactions and interfere with adherence of cells to hydrocarbons.

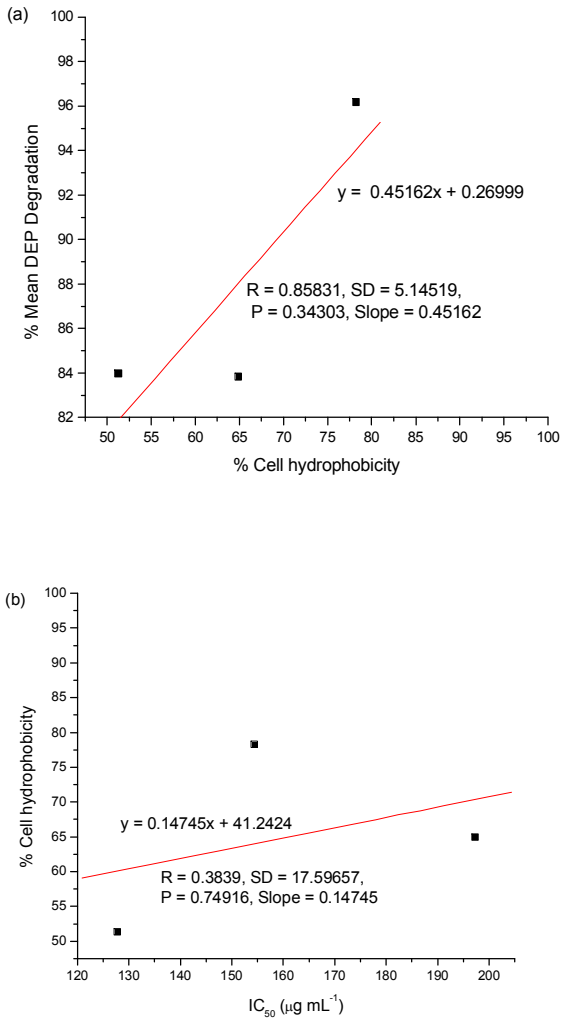

Figure 4. The correlation between the microbial cell surface hydrophobicity and (a) mean DEP degradation efficiency and, (b) inhibition (IC_{50}).

4. Conclusion:

Microcalorimetry can be a valuable supplement in the study of microbial inhibition (toxicity) and degradation of chemical compounds by determining valuable physico- and bio-chemical parameters including IC_{50}, used in this research to determine the sub-MIC value for the hydrophobicity and autoaggregation assays. There were significant positive correlations between microbial cell surface hydrophobicity and autoaggregation ability, biodegradability, IC_{50} values. This suggests the importance of hydrophobic interactions in the attachment of these cultures to chemical compounds. It was very clear that hydrophobicity had some kind of relation to autoaggregation ability [Figure 3 (a)], inhibitory effect [Figure 4 (b)] and thus DEP biodegradability [Figure 4 (a)] for the tested strains. So the substantiation of correlation between surface hydrophobicity and autoaggregation, vis-à-vis DEP biodegradation and inhibitory effect, could provide a means for characterizing these strains without complicated and protracted methods. This study also provided information to understand how these strains (*E. coli*, *S. aureus* and *A. niger*) work very well on the biodegradation of DEP, thereby, identifying these three strains as potential degraders of DEP, hence, their possible use in the DEP clean-up in the environment.

Acknowledgements:

This work was supported in parts by grants from National Outstanding Youth Research Foundation of China (40925010), International Joint Key Project from National Natural Science Foundation of China (40920134003), National Natural Science Foundation of China (40873060, 40673065), and International Joint Key Project from Chinese Ministry of Science and Technology, and the 111 Project (B08030).

Corresponding Author:
Alhaji Brima Gogra
State Key Laboratory of Biogeology and Environmental Geology of Chinese Ministry of Education, School of Environmental Studies and Sino-Hungarian Joint Laboratory of Environmental Science and Health, China University of Geosciences, 430074 Wuhan, PR China.
E-mail: abgogra@yahoo.co.uk

References

1. Al-Tahhan, R.A., Sandrin, T.R., Bodour, A.A., Maier, R.M., 2000. Rhamnolipid-induced removal of lipopolysaccharide from *Pseudomonas aeruginosa*: Effect on cell surface properties and interaction with hydrophobic substrates. Appl. Environ. Microbiol. 66:3262-3268.
2. Bouchez, M., Blanchet, D., Vandecasteele, J.P., 1995. Substrate availability in phenanthrene biodegradation: transfer mechanisms and influence on metabolism. Appl. Microbiol. Biotechnol 43:952–960.
3. Breslow, R., 1991. in Comprehensive Organic Synthesis, Volume 7 (Eds.: B. M.

Trost, I. Fleming), Pergamon Press, Oxford, p. 39.
4. Busscher, H.J., van de Belt-Gritter, B., van der Mei, H.C., 1995. Implications of microbial adhesion to hydrocarbons for evaluating cell surface hydrophobicity 1. Zeta potentials of hydrocarbon droplets. Colloid Surf B-Biointerf 5:111-6
5. Caccavo, F.Jr, Schamberger, P.C., Keiding, K., Neilson, P.H., 1997. Role of hydrophobicity in adhesion of the dissimilatory Fe (III) oxide. Appl. Environ. Microbiol. 63(10):3837-3843.
6. Chang, B.V., Yang, C.M., Cheng, C.H., Yuan, S.Y., 2004. Biodegradation of phthalate esters by two bacteria strains. Chemosphere 55:533-538.
7. Chao, W.L., Lin, C.M., Shiung, I.I., Kuo, Y.L., 2006. Degradation of di-butyl-phthalate by soil bacteria. Chemosphere 63:1377-1383
8. Chen, P., Pickard, M.A., Gray, M.R., 2000. Surfactant inhibition of bacterial growth on solid anthracene. Biodegradation 11:341-347.
9. Christophe, P., Christine, B., Chantal, C., et al., 1997. Cell surface characteristics of *Lactobacillus casci* subsp. casci. *Lactobacillus paracasci* subsp. Paracasei, and *Lactobacillus rhamnosus* strains. Appl. Environ. Microbiol. 63(5):1725-31
10. Churchill, S.A., Harper, J.P., Churchill, P.F., 1999. Isolation and characterization of a mycobacterium species capable of degrading three-and four-ring aromatic and aliphatic hydrocarbons. Appl. Environ. Microbiol. 65:549–552.
11. Critter, S.A.M., Freitas, S.S., Airoldi, C., 2001. Calorimetry versus respirometry for the monitoring of microbial activity in a tropical soil. Appl. Soil Ecol. 18:217.
12. Critter, S.A.M., Freitas, S.S., Airoldi, C., 2002. Microbial biomass and microcalorimetric methods in tropical soils. Thermochim. Acta 394:145
13. Doyle, R.J., 2000. Contribution of the hydrophobic effect to microbial infection, Microbes and infection/Institut Pasteur 2(4):391-400.
14. Duncan-Hewitt, W.C., 1990. Predicting the relative rate of wear of pharmaceutical compacts using the mechanical properties of their constituent crystals. Powder Technol. 60:265-272.
15. Edsall, J.T., 1992. Memories of early days in protein science, 1926-1940. Protein Sci.1(11):1526-1530
16. Efroymson, R.A., Alexander, M., 1995. Reduced mineralization of low concentrations of phenanthrene because of sequestering in nonaqueous-phase liquids. Environ. Sci. Technol 29:515–521.
17. Hashimoto, M., Takahashi, K., 1982. Calorimetric studies of microbial growth: quantitative relation between growth thermograms and inoculum size. Agricultural and Biological Chemistry 46:1559-1564.
18. Jain, A., Nishad, K.K., Bhosle, N.B., 2007. Effects of DNP on cell surface properties of marine bacteria and its implication for adhesion to surfaces. Biofouling. 23(3-4), 171-177.
19. Karplus, P.A., 1997. Hydrophobicity regained. Protein Sci. 6(6):1302-1307
20. Kauzmann, W., 1959. Some factors in the interpretation of protein denaturation. Adv. Protein Chem. 14:1-63.
21. Kimura, T., and Takahashi, K., 1985. Calorimetric studies of soil microbes: quantitative relation between heat evolution during microbial degradation of glucose and changes in microbial activity in soil. J. Gen. Microbiol. 131:3083-3089.
22. Kuntiya, A., Nicolella, C., Pyle, L., Poosaran, N., 2005. Effect of sodium chloride on cell surface hydrophobicity and formation of biofilm in membrane bioreactor. Songklanakarin J. Sci. Technol. 27(5):1073-1082.
23. Kurane, R., Suzuki, T., Takahara, Y., 1978. Microbial degradation of phthalate esters, *Agricultural and Biological Chemistry* 42:1469-1473.
24. Ljungh, Å., Hjertén, S., Wadström, T., 1985. High surface hydrophobicity of autoaggregating *Staphylococcus aureus* isolated from human infections studied with the salt aggregation test. American Society for Microbiology 47(2):522-526.
25. Ljungh, Å., Wadström, T., 1983. Fimbriation of Escherichia coli in urinary tract infections. Comparisons between bacteria in the urine and subcultured bacterial isolates. Current Microbiol. 8:263-8.
26. Marshall, K.C., 1991. The importance of studying microbial cell surfactants. In: Mozes N (ed) Microbial cell surface

analysis, 1st edn. Wiley-VCH Publishers, New York.
27. Medrzycka, K.B., 1991. The effect of particle concentration in extremely dilute solutions. Prog Colloid Polym Sci. 269:85 – 90
28. Miyoshi, M., 1895. Die durchbohrung von membranen durch pilzfäden. Jahrb Wiss Bot 28:269–289.
29. Nuñez, L., Barros, N., Barja, I., 1994. Thermochim. Acta 237:73-81.
30. Olivera, N.L., Commendatore, M.G., Delgado, O., Esteves, JL., 2003. Microbial characterization and hydrocarbon biodegradation potential of natural bilge waste microflora. J Ind Microbiol Biotechnol 30:542–548
31. Pan, W.-H., Li, P.-L., Liu, Z., 2006. The correlation between surface hydrophoicity and adherence of *Bifidobacterium* strains from centenarians' faeces. Food microbiology. Anaerobes 12:148-152.
32. Prabhu, Y., Phale, P.S., 2003. Biodegradation of phenanthrene by *Pseudomonas* sp. strain PP2: Novel metabolic pathway, role of biosurfactant and cell surface hydrophobicity in hydrocarbon assimilation. Appl. Microbiol. Biotechnol. 61:342-351.
33. Prado, A.G.S., Airoldi, C., 2000. Effects of the pesticide 2,4-D on microbial activity of the soil monitored by microcalorimetry. Thermochim. Acta 349:17-22.
34. Raihan, S., Ahmed, N., Ali, R., Khan, N., Eshaq, A., 1992. Production of exopolysaccharide by an indigenous soil isolates. JIAS. 5(4). http://www.medicaljournal-ias-org/5-4/Raihan.html
35. Rosenberg, E., Kaplan, N., Pines, O., Rosenberg, M., Gutnick, D., 1983. Capsular polysaccharides interfere with adherence of *Acinetobacter calcoaceticus* to hydrocarbon. FEMS Microbiol. Lett. 17(1-3):157-160.
36. Rosenberg, E., Legmann, R., Kushmaro, A., Taube, R., Adler, E., Ron, E.Z., 1992. Petroleum bioremediation – a multiphase problem. Biodegradation 3:337–350.
37. Singh, S., Fett, W.F. 1995. Stimulation of exopolysaccharide production by fluorescent pseudomonads in sucrose media due to dehydration and increased osmolarity. FEMS Microbiol. Lett. 130(2-3):301-306.
38. Tahmourespour, A., Kermanshahi, R.K., Salehi, R., Nabinejad., A., 2008. The relationship between cell surface hydrophobicity and antibiotic resistance of Streptococcal strains isolated from dental plaque and caries. Iranian Journal of basic medical sciences 10(4):251-255.
39. Teo, K.C., Xu H.L., Tay, J.H., 1998. Molecular mechanism of granulation. II: Proton translocation activity. J. Environ Eng 126:411 - 418
40. Tiehm, A., 1994. Degradation of polycyclic aromatic hydrocarbons in the presence of synthetic surfactants. Appl. Environ. Microbiol. 60:258-263.
41. Wadsö, I., 1997. Isothermal microcalorimetry near ambient temperature: An overview and discussion. Thermochim. Acta 294:1-11.
42. Wang, J, Liu, P., Qian, Y., 1995. Microbial degradation of di-n-butly phthalate. Chemosphere. 31(9):4051-4056.
43. Wessels, J.G.H., 1997. Hydrophobins: proteins that change the nature of a fungal surface. Adv Microb Physiol. 38:1-45.
44. Wrangstadh, M., Conway, P.L., Kjellberg, S., 1986. The production and release of an extracellular polysaccharide during starvation of a marine *Pseudomonas* sp. and the effect thereof on adhesion. Arch. Microbiol. 145(3):220-227.
45. Yao, J., Tian, L., Wang, Y., Djah, A., Wang, F., Chen, H.-L., Su, C.-L., Zhuang, R., Zhou, Y., Choi, M.M.F., Bramanti, E., 2008. Microcalorimetric study of the toxic effect of hexavalent chromium on microbial activity of Wuhan brown sandy soil: An in vitro approach. Ecotoxicology and Environmental safety 69:289-295.
46. Zeng, F., Cui, K., Li, X., Fu, J., Sheng, G., 2004. Biodegradation kinetics of phthalate esters by *Pseudomonas fluorescens* FS1. Process Biochemistry 39, 1125–1129

03/12/2010

Effect of planting dates and different levels of potassium fertilizer on growth, yield and chemical composition of sweet fennel cultivars under newly reclaimed sandy soil conditions

Abou El-Magd, M. M. *Zaki, M. F.* and Camilia Y. Eldewiny**
* Department of Vegetable Res., National Research Centre (NRC), Dokki, Cairo, Egypt
**Department of Soil and Water Use, National Research Centre (NRC), Dokki, Cairo, Egypt.

Abstract: Two field experiments were conducted at the Agricultural research Station, National Research Centre, El-Nobaria province, El Beheira Governorate, Egypt, during the two successive winter seasons of 2007/2008 and 2008/2009 on sweet in an area of newly reclaimed soil to study the effect of transplanting dates and different rates of potassium salphate fertilizer on vegetative growth, yield, quality and chemical content of six sweet fennel cultivars (cvs. Dolce, Zefa Fino, Selma, Fino, De Florance and Zwejahrig). Transplanting dates were early (15^{th} September) and late (1^{st} October) combined with four rates of potassium salphate,i.e. 0, 45, 60 and 75 kg K_2O/ fedd.(Feddan = 0.40 ha.). Results indicated that transplanting dates differed statistically in their effect on the vegetative growth of sweet fennel plants. The highest vegetative growth expressed as plant height, leaves number /plant, fresh and dry weight of the total plant and its organs, bulb dimensions (thickness, width and length); total green yield and macro-nutrients content in leaves and bulbs (N, P and K) were obtained by early plantation (15^{th} September). On the other hand, lower values of vegetative growth, green yield and quality of bulbs were obtained in the late plantation (1^{st} October). Results summarized that sweet fennel cultivars as mentioned previously differed statistically in their vegetative growth, bulb dimensions and total green yield as well as chemical content in leaves and bulbs of sweet fennel plants. Zwejahrig cultivar was superior in its vegetative growth expressed as plant height; leaves number; fresh and dry weight of the total plant and its organs; bulb dimensions (thickness, width and length); total green yield and macro-nutrients (N, P and K) content in leaves and bulbs compared with other cultivars. On the other hand, the lowest values were recorded by cvs. Dulce and Zefa Fino. With respect to potassium fertilizer rates, results reveal that sweet fennel plants treated with 75 kg K_2O/ fed. showed higher vegetative growth parameters (plant length, leaves number and bulb dimensions, thickness, width and length), fresh and dry weight of leaves, bulbs and total plant; total green yield; physical bulb quality (flatten, cylinder and elongated shape ratios) and macro-nutrients content (N, P and K) in tissues of sweet fennel leaves and bulbs than the lower rates of potassium. The results indicated that combined effect of transplanting dates and cultivars of sweet fennel caused significant increases in vegetative growth, green yield, bulb quality and chemical contents. The highest vegetative growth, yield and quality as well as chemical contents were obtained by cv. Zwejahrig combined with early date. The interaction effect between cultivars and rates of potassium fertilizer gave a significant increase in vegetative growth, bulb yield and chemical constituents. The highest values were obtained by adding the highest potassium rate (75 kg K_2O / fed.) to cv. Zwejahrig plants. The highest values were obtained by early date combined with the highest potassium rate (75 kg K_2O/ fed.). In addition, the highest vegetative growth with the maximum total green yield was obtained under the combination of cv. Zwejahrig in early date and the highest potassium rate. [Journal of American Science 2010;6(7):89-105]. (ISSN: 1545-1003).

Key words: Sweet fennel; Cultivars; Sowing dates; Potassium mineral fertilizer; N; P; K; Green yield and quality; Chemical content

1. Introduction

Sweet fennel (*Foeniculum vulgare* Mill.) is a plant belonging to the Umbelliferae (Apiaceae) family, which is an annual, biennial or perennial aromatic herb, depending on the variety **(Farrell, 1988, Wichtl and Bisset, 1994**). It is native to North Africa, Mediterranean Region, southern Europe and Asia **(Abd El- Wahab and Mehasen, 2009)**. It contains phytochemical hormones (saponins), flavonoids, lipids, proteins and essential oils. Medicinal and aromatic plants are important economic products which represent significant sources of economic revenue and foreign exchange and are among the most important agricultural export products **(Watt and Breyer, 1962)**. The Egyptian government in collaboration with the WHO seeks to protect fennel plants that serve as a source for pharmaceutical compounds and who might increase the export of these plants from Egypt to allover the world **(Egypt Magazine, 2000)**. Fennel is used in folk medicine as a stimulant, diuretic, carminative and sedative **(Charles *et al*. 1993)** and galactagogic, emmenagogic, expectorant and antispasmodic **(Chiej, 1984)**. It is also considered as a spice due to terpenoid compounds isolated from its fruits volatile oil **(Masada,**

1976). Also, fennel fruits are widely used in the preparation of various dishes like soups, sauces, pastries, confectioneries, pickles and meat dishes etc. **(Bhati *et al*. 1988)**. The leaf stalks and the tender shoots are also used in salads. Fennel is used in cooking for liqueurs **(Bhati *et al.* 1988)**. The essential oil of fennel is used to flavor different food preparations and in perfumery industries. There is a need to know which cultivar, sowing dates and K fertilizer rate are the most appropriate for a good quality. Therefore, it is important to increase its productivity through adoption of the proper agricultural practices among which is optimized fertilization. Sweet fennel develops an edible bulb, a thickened base of leaves, which is becoming increasingly popular as a specialty vegetable in the United States **(Simon, 1990)**.

Many investigators studied that effect of sowing dates on growth of sweet fennel plants **(Abdallah *et al*., 1978; Yadav *et al*., 2000**; **Sudeep *et al*., 2006**; **Abd El-Wahab *et al*., 2009). Baruah (2004)** on fennel found that fennel seeds should be sown from 15 September to 1 October for higher vegetative growth. Very little information is available on the specific requirements of sweet fennel fertilization in Egypt, especially in newly reclaimed land. So, this investigation carried out on potassium requirements for improving green yield and qualities of sweet fennel bulbs, grown in sandy soil are discussed. Potassium is necessary in young growing tissues for cell elongation and possibly for cell division. Potassium is very mobile in plants and therefore circulates freely and has vital role in maintenance of torpor pressure. It also helps in several physiological processes and uptake of other nutrient elements **(Sadananan *et al*., 2000)**. **Alt *et al*. 1999**; **Sadanandan *et al*., 2002** on fennel and **El-Bassiony, 2006** on onion confirmed that vegetative growth and yield tended to increase with increasing potassium levels. Some studies were conducted for evaluating sweet fennel cultivars (**Fawzy *et al*., 2006; Osman , 2009 and Zaki *et al*., 2009**). To successfully grow sweet fennel in the newly reclaimed soils, many factors have to be considered, such as using the right cultivars, suitable transplanting date, fertilization, compensating for the low amounts of available nutrients and low organic matter content as well as poor hydrophilic, chemical and biological properties. The best means of maintaining soil fertility and productivity could be done through periodic suitable rate of potassium fertilizer.

2. Material and Methods

Two field experiments were carried out on sweet fennel ***(Foeniculum vulgare Mill.*** Family: *Apiaceae*) in an area of newly reclaimed soil at El-Noberia, Beheira, Governorate, Egypt, during the two successive winter seasons of 2007/2008 and 2008/2009. The aim of this work was to study the effect of some agricultural practices such as transplanting dates and different levels of potassium mineral fertilizer on growth, vegetative yield, bulb quality and chemical content of sweet fennel. Soil samples were collected at random before planting from the top layer (0-30 cm depth) for physical and chemical analysis. Soil analysis is presented in Table (1) and was analyzed using the procedures described by **Page *et al*, 1982 and Klute, 1986.** Organic manure (poultry manure) contents of total available N, P and K are presented in Table (2) analyses followed the procedure of **Klute, 1986**. Seeds of sweet fennel were imported from Holland and Germany. Seeds were sown in foam trays filled with a mixture of peat moss and vermiculite (1:1 volume) and grown in nursery on the 1st and 15th of August in 2007 season and 3rd and 18th of September in 2008 season. Seedlings were transplanted in open field at 45 days age.

Table (1): Physical and chemical properties of the experimental soil during the two seasons of 2005/2006 and 2006/2007.

A. Physical properties															
Season			Sand %			Clay %			Silt %			Texture			
1st			58.75			5.56			35.69			Sandy			
2nd			57.72			5.81			36.47			Sandy			
B. Chemical properties															
Season	pH	E.C. (m mosh /cm	OM (%)	$CaCo_3$ (%)	Macro elements (ppm)			Cations (meq./L)				Anions (Meq./L)			
					N	P	K	Ca^{++}	Mg^{++}	Na^{+}	K^{+}	CO_3^{--}	HCO_3^{-}	Cl^{-}	SO_4^{--}
1st	7.83	2.24	0.60	19.7	20	65	168	11.00	4.20	4.80	1.39	Nil	1.40	1.80	18.19
2nd	7.78	2.18	0.58	19.6	18	56	161	11.20	3.26	3.82	1.43	Nil	1.42	1.70	16.59

Treatments were as follows:

1) - Transplanting dates: Included two treatments [Early cultivating date (15 September) and late cultivating date (1 October)].

2) - Cultivars: Seeds of seven sweet fennel cultivars (cvs. Dolce, Zefa Fino, Selma, Fino, De Florance and Zwejahrig) were sown in the nursery.

3) - Potassium levels: potassium was applied at four (0, 45, 60 and 75 K_2O units per feddan) using potassium sulphate (48 % K_2O).

The soil of the experiment was carefully prepared. Ditches 20 cm depth and 20 cm width were ditched at drip irrigation lines. Poultry manure was added through these ditches and covered with sand. Drip irrigation was practiced three days before transplanting and continued allover the growth season as requirements in every growth stage. Agricultural practices of growing sweet fennel were followed till harvest time. Potassium fertilizer treatments were added in three equal portions beginning 30 days after transplanting. The area of the experimental plot was 15.0 m^2 consisted of three rows, each row was 5 m length and 1m width and the planting distance was 50 cm apart. Seedlings were transplanted on two sides of each row.

Experimental design: A split-split plot design with four replicates was followed. Transplanting date's treatments were located in the main plots, whereas the cultivars of sweet fennel were assigned in the sub-plots and potassium levels located in the sub- sub plots.

Data recorded: A random sample of five plants was taken from each experimental treatment 90 days after transplanting and the following data were recorded during the two seasons**.**

I) Vegetative growth characters: Plant height (cm); leaf number per plant; bulb dimensions (length, width and thickness); leaves, bulbs and total plant fresh and dry weight (g/plant).

II) Total green yield and Physical bulb quality: All the plants of each plot were harvested at vegetative growth stage and the following data were recorded:

1) - Total green yield (ton/ fed).
2) - Flatten shape ratio = W / T
3) - Cylinder shape ratio = L / (WT) 0.05
4) - Elongated shape ratio = L / W

Where: W, width (cm); T, thickness (cm) and L, length (cm). Flatten shape, cylinder shape and elongated shape ratios were calculated according to **Pascale and Barbieri (1995)** equations.

III) Chemical composition; plant samples of leaves and bulbs were oven at 70 ^{0}C and digested. N, P and K were determined according to **Cottenie *et al*. (1982**).

Statistical analysis:- The data of the experiment was tabulated and subjected to statistical analysis according to **Snedecor and Cochran (1980)**.

3. Result Analysis

I) Vegetative growth characteristics:

A). Effect of transplanting dates: Table (2) shows clearly that sweet fennel vegetative growth expressed as plant height; leaves number /plant and bulb dimensions (thickness, length and width) as well as fresh and dry weight of leaves, bulbs and total plant were statistically influenced by transplanting dates. The highest values of these parameters were obtained with the early transplanting date (15 September) compared with the late date (1 October). These increases were statistically significant and similar in the two seasons. These increases in vegetative growth might be due to the suitable temperature and relative humidity appeared to be reflected on the vegetative growth and consequently yield and quality, since the obtained high yield of those characters was more pronounced in the early date **(Abd El-Wahab and Mehasen, 2009).** Also, this may be due to high temperature at maturity which resulted in forced maturity of the crop **(Sudeep *et al*., 2006). Abou El-Magd and El-Abagy (2003)** reported that the vegetative growth of the early sweet fennel plants was superior expressed as fresh weight of total plant and its organs. Many investigators reported that early sowing increased growth of sweet fennel plants (Abdallah *et al*., 1978; Yadav *et al*., 2000; Baruah (2004; Sudeep *et al*., 2006; Abd El-Wahab and Mehasen, 2009.

Table (2): Effect of transplanting dates on vegetative growth of sweet fennel during 2005/2006 and 2006/2007 seasons.

Transplanting dates	Plant Length (cm)	Leaves No./ plant	Bulb dimensions			Fresh weight (g/plant)			Dry weight (g/plant)		
			Thickness (cm)	Width (cm)	Length (cm)	Leaves	Bulb	Total	Leaves	Bulb	Total
First season (2005-2006)											
Early	73.39	11.10	7.90	12.15	10.95	509.09	406.52	915.60	59.00	45.64	104.64
Late	67.60	10.29	6.33	11.73	9.84	359.35	323.35	682.70	50.87	35.90	86.77
L.S.D. at 0.05	2.85	0.25	0.45	0.09	0.28	17.88	8.36	12.66	1.95	1.03	1.38
Second season (2006-2007)											
Early	71.88	10.19	6.69	10.95	10.45	478.95	387.54	866.50	54.64	43.05	97.70
Late	65.63	9.31	5.23	10.53	9.37	327.69	304.65	632.34	46.75	34.23	80.98

L.S.D. at 0.05	0.79	0.04	0.39	0.22	0.12	14.70	6.55	9.67	1.43	1.38	2.27

Table (3): Effect of varieties on vegetative growth of sweet fennel during 2005/2006 and 2006/2007 seasons.

Cultivars	Plant length (cm)	Leaves No./ plant	Bulb dimensions			Fresh weight (g/plant)			Dry weight (g/plant)		
			Thickness (cm)	Width (cm)	Length (cm)	Leaves	Bulb	Total	Leaves	Bulb	Total
First season (2005-2006)											
Dolce	69.67	10.17	6.42	11.19	9.22	429.77	295.92	725.69	55.14	41.26	96.40
Zefa fino	68.96	10.25	6.78	11.20	10.83	396.99	294.74	691.73	49.24	35.20	84.43
Selma	70.17	10.38	7.15	12.11	9.33	440.34	369.60	809.94	54.13	40.92	95.05
Fino	74.67	11.21	7.42	12.26	11.08	442.69	385.82	828.51	57.21	42.68	99.88
De Florance	70.63	10.88	7.38	12.18	10.85	393.76	379.69	773.45	50.08	38.28	88.36
Zwejahrig	68.88	11.29	7.56	12.71	11.10	501.76	463.82	965.59	63.83	46.28	110.11
L.S.D. at 0.05	1.32	0.30	0.20	0.28	0.29	10.90	9.17	15.06	1.86	1.87	2.86
Second season (2006-2007)											
Dolce	68.29	9.13	5.37	5.37	9.99	8.72	400.05	275.84	675.89	50.73	38.51
Zefa fino	67.04	9.50	5.62	10.00	10.33	362.27	278.40	640.68	45.78	33.95	79.72
Selma	68.33	9.42	6.04	10.91	8.83	409.79	349.10	758.89	50.04	38.42	88.47
Fino	72.83	10.21	6.19	11.06	10.58	413.39	365.32	778.71	52.71	40.18	92.88
De Florance	68.63	9.88	6.18	10.98	10.35	363.21	363.35	726.56	45.58	36.20	81.78
Zwejahrig	67.38	10.38	6.36	11.51	10.69	471.21	444.57	915.79	59.33	44.61	103.94
L.S.D. at 0.05	0.62	0.16	0.15	0.18	0.20	7.71	7.65	10.61	1.08	1.10	1.71

B). Effect of cultivars: Data in Table (3) show that cultivars were statistically differed in their vegetative growth. The highest values of vegetative growth expressed as leaves number and bulb dimensions (thickness, width and length) as well as fresh and dry weight of leaves, bulbs and total plant were obtained from cv. Zwejahrig compared with other cultivars. In comparison, the lowest values of plant growth were obtained by cvs. Dulce and Zefa Fino. The tallest plants were obtained by cv. Fino. The above mentioned findings were true in both seasons. Zwejahrig cv. recorded the highest vegetative growth copared with other caltivars.These results might be correlated with the gene action of the tested cultivars (**Fawzy *et al*., 2006).**

C). Effect of potassium levels: Data present in Table (4) reveal that vegetative growth of sweet fennel plants was enhanced by increasing potassium fertilizer levels up to 75 kg K_2O / fed. Moreover, The highest values of vegetative growth expressed as plant height; leaves number and bulb dimensions (thickness, width and length) as well as fresh and dry weight of leaves, bulbs and total plant were obtained from application of potassium at the rate of 75 kg K_2O / fed compared with other potassium treatments in both seasons. These results were in agreement with those obtained by **Alt *et al*. 1999** on fennel and **El-Bassiony, 2006** on onion.

Table (4): Effect of potassium levels on vegetative growth of sweet fennel during 2005/2006 and 2006/2007 seasons.

K levels	Plant length (cm)	Leaves No./ plant	Bulb dimensions			Fresh weight (g/plant)			Dry weight (g/plant)		
			T (cm)	W (cm)	L (cm)	Leaves	Bulb	Total	Leaves	Bulb	Total
First season (2005-2006)											
0	66.33	9.75	6.10	10.81	9.49	356.52	281.36	637.89	40.27	29.31	69.57
45	70.64	10.58	6.95	11.75	9.99	420.77	339.82	760.59	55.77	39.60	95.37
60	72.47	11.19	7.41	12.51	10.76	467.23	404.77	872.00	61.83	45.68	107.51
75	72.53	11.25	8.01	12.69	11.36	492.35	433.77	926.12	61.88	48.49	110.37
L.S.D.at.05	1.30	0.38	0.28	0.29	0.32	14.64	12.31	19.52	2.47	2.34	3.49
Second season (2006-2007)											
0	63.86	8.83	4.99	9.61	9.04	324.03	260.86	584.89	35.77	27.47	63.24
45	67.61	9.56	5.91	10.55	9.66	390.22	322.10	712.32	51.33	36.26	87.59
60	71.33	10.28	6.47	11.31	10.44	436.68	385.10	821.78	57.89	44.85	102.74
75	72.19	10.33	6.47	11.49	10.51	462.35	416.33	878.68	57.80	45.99	103.79
L.S.D.at.05	0.66	0.25	0.21	0.23	0.23	8.64	8.60	11.91	1.49	1.32	2.10

Where: T= Thickness W= Width L= Length

Potassium is necessary in young growing tissues for cell elongation and possibly for cell division. Potassium is very mobile in plants and therefore circulates freely and has vital role in maintenance of torpor pressure. It also, helps in several physiological processes and uptake of other nutrients. Potassium is known to play a vital role in photosynthesis and carbohydrate formation in fennel. It has also been shown that K plays a key role in the activation of more than 60 enzymes in plants. Contrast to other elements that are involved in the formation of cell structure, K functions in the cell sap. The high mobility of K permits it to move quickly from cell to cell or from older parts to newly developed tissues and storage organs. It has also, a role in stomata respiration, photosynthetic transfer; crop development studies on the removal of various nutrients during harvest of spice crops showed that all the spice remove more amount of K than any other element **(Sadanandan *et al*., 2002).**

D). Effect of interaction

Interaction between transplanting dates and cultivars: The obtained data revealed that the interaction treatments (Table, 5) significantly affected all growth parameters in the two seasons, except bulb width which failed to reach the 5% level of significance in the first season. In general, the highest values of vegetative growth of sweet fennel were obtained by cv. Zwejahrig grown in the early transplanting date. On the contrary, the lowest vegetative growth of sweet fennel was obtained by the combined effect of the late transplanting and cvs. De Florance, Selma, Fino, Dulce and Zefa Fino in a descending order in the two seasons.

Table (5): Effect of the interaction between transplanting dates and cultivars on vegetative growth of sweet fennel during 2005/2006 and 2006/2007 seasons.

Trans-Planting dates	Cultivars	Plant length (cm)	Leaves No./ plant	Bulb dimensions			Fresh weight (gm/plant)			Dry weight (gm/plant)		
				T (cm)	W (cm)	L (cm)	Leaves	Bulb	Total	Leaves	Bulb	Total
First season (2005-2006)												
Early	Dolce	73.08	10.33	7.20	11.21	9.78	505.12	328.22	833.34	56.04	49.25	105.29
	Zefa fino	69.25	10.58	7.39	11.02	12.05	506.86	303.83	810.69	56.82	35.17	91.99
	Selma	73.83	10.25	8.26	12.09	9.18	503.34	414.70	918.04	56.29	46.30	102.59
	Fino	76.25	11.75	7.81	12.53	11.81	486.54	368.33	854.87	59.18	39.26	98.44
	De Florance	74.42	12.17	7.89	12.78	11.30	484.47	436.01	920.48	58.00	45.61	103.61
	Zwejahrig	73.50	11.50	8.88	13.25	11.61	568.18	588.00	1156.18	67.70	58.22	125.92
Late	Dolce	66.25	10.00	5.63	11.17	8.66	354.41	263.62	618.04	54.25	33.27	87.52
	Zefa fino	68.67	9.92	6.17	11.38	9.61	287.12	285.65	572.77	41.65	35.23	76.87
	Selma	66.50	10.50	6.05	12.13	9.47	377.33	324.50	701.83	51.97	35.55	87.51
	Fino	73.08	10.67	7.03	11.99	10.34	398.85	403.30	802.15	55.23	46.09	101.32
	De Florance	66.83	9.58	6.88	11.57	10.39	303.05	323.36	626.41	42.17	30.95	73.12
	Zwejahrig	64.25	11.08	6.24	12.18	10.60	435.35	339.65	774.99	59.96	34.33	94.29
L.S.D.at.05		3.22	0.73	0.50	N.S.	0.71	26.70	22.46	36.88	4.55	4.58	7.01
Second season (2006-2007)												
Early	Dolce	70.50	9.25	6.06	10.01	9.28	474.57	308.56	783.13	51.54	46.25	97.79
	Zefa fino	69.75	10.08	6.28	9.82	11.55	476.31	291.66	767.97	53.16	34.34	87.49
	Selma	72.17	9.25	6.89	10.89	8.68	472.79	394.20	866.99	51.79	43.80	95.59
	Fino	74.58	10.75	6.55	11.33	11.31	458.49	347.83	806.32	54.68	36.76	91.44
	De Florance	72.58	11.17	6.69	11.58	10.80	453.92	415.51	869.43	53.50	41.44	94.94
	Zwejahrig	71.67	10.67	7.68	12.05	11.11	537.63	567.50	1105.13	63.20	55.72	118.92
Late	Dolce	66.08	9.00	4.68	9.97	8.16	325.53	243.12	568.65	49.92	30.77	80.68
	Zefa fino	64.33	8.92	4.97	10.18	9.11	248.24	265.15	513.38	38.40	33.56	71.96
	Selma	64.50	9.58	5.18	10.93	8.97	346.78	304.00	650.78	48.30	33.05	81.35
	Fino	71.08	9.67	5.83	10.79	9.84	368.30	382.80	751.10	50.73	43.59	94.32
	De Florance	64.67	8.58	5.68	10.37	9.89	272.50	311.20	583.70	37.67	30.95	68.62
	Zwejahrig	63.08	10.08	5.04	10.98	10.27	404.80	321.65	726.44	55.46	33.49	88.96
L.S.D.at.05		1.51	0.40	0.37	0.43	0.48	18.89	18.73	26.00	2.65	2.69	4.19

Where: T= Thickness W= Width L= Length

Interaction between transplanting dates and K levels: Results presented in Table (6) indicated that vegetative growth characters were significantly affected by the interaction between transplanting dates and mineral potassium fertilizer except bulb width in the first season. The highest values of vegetative growth characters expressed as leaves number and bulb thickness as well as fresh and dry weight of leaves, bulbs and total plant were obtained by early transplanting date combined with the high level of potassium fertilizer (75 kg K_2O / fed) compared with other treatments. In contrast, the lowest values of plant growth were obtained by late transplanting date combined with zero level of mineral potassium fertilizer (control). The above mentioned findings were true in both seasons.

Table (6): Effect of the interaction between transplanting dates and K levels on vegetative growth of sweet fennel during 2005/2006 and 2006/2007 seasons.

Trans-Planting dates	K levels	Plant Length (cm)	Leaves No./ plant	Bulb dimensions T (cm)	W (cm)	L (cm)	Fresh weight (g/plant) Leaves	Bulb	Total	Dry weight (g/plant) Leaves	Bulb	Total
First season (2005-2006)												
Early	0	69.56	10.00	6.72	10.97	10.10	428.82	303.73	732.55	45.08	31.23	76.31
	45	74.56	10.89	7.70	11.96	10.53	497.02	385.60	882.62	58.18	44.22	102.40
	60	74.39	11.61	8.17	12.86	11.22	550.64	461.09	1011.72	67.34	52.33	119.67
	75	75.06	12.06	9.03	12.79	11.99	553.20	475.65	1028.85	65.41	54.77	120.18
Late	0	63.11	9.50	5.49	10.66	8.97	284.23	258.99	543.22	35.45	27.38	62.83
	45	66.72	10.28	6.19	11.54	9.54	344.51	294.04	638.55	53.36	34.98	88.34
	60	70.56	10.78	6.65	12.15	10.21	379.94	348.45	728.39	56.33	39.03	95.36
	75	70.00	10.44	6.99	12.59	10.63	434.28	391.90	826.18	60.02	42.21	102.23
L.S.D.at.05		1.71	0.44	0.32	N.S.	N.S.	17.36	17.41	24.79	3.06	3.31	4.58
Second season (2006-2007)												
Early	0	67.22	9.17	5.52	9.77	9.38	399.93	283.23	683.17	40.58	29.51	70.09
	45	71.33	9.83	6.72	10.76	10.03	466.47	365.10	831.57	53.12	40.05	93.17
	60	73.94	10.72	7.44	11.66	10.97	523.98	440.59	964.56	63.95	50.94	114.89
	75	75.00	11.06	7.08	11.59	11.43	525.42	461.26	986.69	60.91	51.71	112.62
Late	0	60.50	8.50	4.46	9.46	8.71	248.12	238.49	486.62	30.95	25.44	56.39
	45	63.89	9.28	5.11	10.34	9.28	313.96	279.10	593.06	49.53	32.48	82.01
	60	68.72	9.83	5.49	10.95	9.91	349.39	329.62	679.01	51.83	38.75	90.58
	75	69.39	9.61	5.86	11.39	9.59	399.29	371.40	770.68	54.68	40.27	94.95
L.S.D.at.05		0.93	0.36	0.30	N.S.	0.30	12.21	12.16	16.85	2.11	1.87	2.98

Where: T= Thickness W= Width L= Length

Interaction between cultivars and K levels: Data in Table (7) reported that the highest values of most vegetative growth characters were obtained by cv. Zwejahrig combined with the high level of potassium fertilizer (60 and 75 kg K_2O / fed.) compared with other treatments. The lowest values of vegetative growth characters were obtained by cv. Zefa Fion which received zero level of potassium fertilizer. These results were similar in both seasons.

Interaction between transplanting dates, cultivars and K levels: Data in Table (8 and 9) reported that the highest values of most vegetative growth characters were obtained by the interaction between early transplanting date and cv. Zwejahrig combined with the high level of potassium fertilizer (75 kg K_2O / fed.) compared with other treatments. These results were similar in the two seasons.

Table (7): Effect of the interaction between cultivars and K levels on vegetative growth of sweet fennel during 2005/2006 and 2006/2007 seasons.

Cultivars	K levels	Plant Length (cm)	Leaves No./ plant	Bulb dimensions T (cm)	W (cm)	L (cm)	Fresh weight (g/plant) Leaves	Bulb	Total	Dry weight (g/plant) Leaves	Bulb	Total
First season (2005-2006)												

Dolce	0	62.83	9.17	5.48	10.57	8.75	368.84	241.94	610.78	40.10	26.39	66.49
	45	68.83	10.50	6.02	11.17	9.03	433.55	266.32	699.87	55.23	34.12	89.35
	60	72.33	10.67	6.47	11.92	9.28	491.30	345.58	836.87	71.45	52.00	123.45
	75	74.67	10.33	7.70	11.10	9.80	425.39	329.86	755.24	53.80	52.53	106.33
Zefa fino	0	68.33	9.33	6.20	10.67	9.80	337.98	245.88	583.86	34.83	31.40	66.22
	45	72.50	10.33	6.77	11.15	10.07	373.85	274.68	648.53	49.43	37.82	87.25
	60	67.00	10.67	7.05	11.48	10.77	396.50	303.54	700.04	52.75	33.90	86.65
	75	68.00	10.67	7.10	11.48	11.18	467.97	354.84	822.81	59.93	37.67	97.60
Selma	0	66.17	9.50	6.43	10.58	8.70	356.37	267.61	623.97	41.23	26.30	67.53
	45	71.33	10.00	6.77	12.23	9.13	443.22	373.41	816.63	55.74	40.71	96.45
	60	72.83	10.50	7.42	13.35	9.57	488.79	446.50	935.30	63.26	50.65	113.92
	75	70.33	11.50	8.00	12.27	9.90	472.97	390.88	863.85	56.28	46.03	102.31
Fino	0	71.67	10.33	6.48	11.07	9.80	372.91	303.65	676.55	43.33	33.99	77.32
	45	73.83	10.83	7.18	12.30	10.63	424.36	370.11	794.47	57.44	41.36	98.80
	60	78.00	11.50	7.82	12.62	11.68	457.84	413.59	871.42	62.00	42.71	104.71
	75	75.17	12.17	8.18	13.05	12.68	515.67	455.92	971.60	66.06	52.64	118.70
De Florence	0	64.83	9.50	6.17	10.87	9.68	310.21	285.37	595.58	38.42	25.61	64.03
	45	70.67	10.67	7.17	11.28	10.42	361.59	312.14	673.73	53.47	39.22	92.69
	60	73.50	11.17	7.68	12.20	11.27	418.55	360.25	778.80	48.79	33.37	82.16
	75	73.50	12.17	8.52	14.35	12.02	484.67	560.99	1045.66	59.64	54.93	114.57
Zwejahrig	0	64.17	10.67	5.85	11.12	10.47	392.84	343.73	736.57	43.68	32.16	75.84
	45	66.67	11.17	7.78	12.37	10.93	488.04	442.26	930.30	63.31	44.36	107.66
	60	71.17	12.67	8.02	13.47	11.72	538.76	559.15	1097.90	72.75	61.45	134.20
	75	73.50	10.67	8.58	13.90	12.30	595.76	510.16	1105.92	80.58	47.14	127.72
L.S.D.at.05		2.97	0.76	0.56	0.72	0.49	30.07	30.16	42.94	5.30	5.73	7.94
						Second season (2006-2007)						
Dolce	0	61.50	8.17	4.62	9.37	8.45	338.29	221.44	559.73	35.60	24.56	60.16
	45	66.33	9.17	5.05	9.97	8.73	403.00	245.82	648.82	51.06	31.62	82.68
	60	70.83	9.67	6.12	10.72	8.78	460.75	325.08	785.82	66.95	49.50	116.45
	75	74.50	9.50	5.70	9.90	8.90	398.17	311.02	709.19	49.30	48.36	97.66
Zefa fino	0	64.17	8.83	5.00	9.47	9.30	290.76	225.38	516.15	30.33	30.56	60.89
	45	66.33	9.50	5.63	9.95	10.07	343.30	254.18	597.48	48.27	31.99	80.25
	60	68.33	10.00	5.87	10.28	10.77	377.62	283.04	660.66	48.25	34.74	82.99
	75	69.33	9.67	5.98	10.28	11.18	437.42	351.01	788.42	56.27	38.50	94.77
Selma	0	64.17	8.50	5.40	9.38	8.20	325.82	247.11	572.92	36.73	23.80	60.53
	45	68.17	9.00	5.83	11.03	8.63	412.67	352.91	765.58	51.24	38.21	89.45
	60	71.17	9.67	6.35	12.15	9.23	458.24	426.00	884.25	58.76	48.15	106.92
	75	69.83	10.50	6.57	11.07	9.23	442.42	370.38	812.80	53.44	43.53	96.97
Fino	0	69.17	9.33	5.28	9.87	9.30	347.36	283.15	630.50	38.83	31.49	70.32
	45	71.83	9.83	6.33	11.10	9.63	393.81	349.61	743.42	52.94	38.86	91.80
	60	76.33	10.50	6.78	11.42	11.18	427.29	393.09	820.37	57.50	40.21	97.71
	75	74.00	11.17	6.35	11.85	12.18	485.12	435.42	920.55	61.56	50.14	111.70
De Florence	0	62.50	8.50	4.97	9.67	9.18	279.66	264.87	544.53	33.92	23.11	57.03
	45	67.83	9.67	5.97	10.08	10.33	331.04	308.30	639.35	45.64	33.39	79.03
	60	71.67	10.17	6.48	11.00	11.52	388.00	339.75	727.75	47.63	37.53	85.16
	75	72.50	11.17	7.32	13.15	10.35	454.12	540.49	994.61	55.14	50.76	105.90
Zwejahrig	0	61.67	9.67	4.65	9.92	9.83	362.29	323.23	685.52	39.18	31.32	70.51
	45	65.17	10.17	6.65	11.17	10.55	457.49	421.76	879.25	58.81	43.52	102.33
	60	69.67	11.67	7.22	12.27	11.15	508.21	543.65	1051.85	68.25	58.95	127.20
	75	73.00	10.00	6.92	12.70	11.22	556.88	489.66	1046.53	71.08	44.64	115.72
L.S.D.at.05		1.61	0.62	0.52	0.57	0.52	21.16	21.07	29.18	3.65	3.24	5.15

Where: T= Thickness W= Width L= Length

Table (8): Effect of the interaction between transplanting dates, cultivars and K levels on vegetative growth of sweet fennel during the first season of 2005/2006.

Trans-Planting dates	Cultivars	K	Plant Length (cm)	Leaves No./ plant	Bulb dimensions			Fresh weight (g/plant)			Dry weight (g/plant)		
					T (cm)	W (cm)	L (cm)	Leaves	Bulb	Total	Leaves	Bulb	Total
First season (2005-2006)													
Early	Dolce	0	67.00	9.33	6.33	10.47	9.27	418.90	247.37	666.27	32.54	24.85	57.38
		45	71.67	11.00	6.73	11.60	9.43	511.37	297.88	809.24	54.13	38.29	92.42
		60	73.67	10.67	7.07	12.77	9.83	616.00	414.78	1030.78	82.87	64.95	147.82
		75	80.00	10.33	8.67	10.00	10.57	474.21	352.87	827.08	54.62	68.91	123.53
	Zefa fino	0	67.33	9.33	6.60	10.13	10.40	403.02	239.14	642.16	36.70	29.03	65.73
		45	74.67	10.33	7.40	11.03	10.87	499.79	284.21	784.00	60.37	36.26	96.63
		60	67.00	10.67	7.70	11.33	11.70	533.76	313.97	847.73	62.06	30.77	92.84
		75	68.00	12.00	7.87	11.57	12.23	567.53	378.00	945.53	68.16	44.62	112.77
	Selma	0	69.67	9.67	7.47	10.60	9.10	470.15	316.67	786.81	54.49	32.57	87.06
		45	77.00	10.00	7.80	12.93	9.37	491.32	465.47	956.79	54.93	51.39	106.33
		60	78.00	10.33	8.43	13.67	9.53	568.20	509.13	1077.33	62.29	58.22	120.51
		75	70.67	12.00	9.33	11.17	9.87	483.70	367.54	851.24	53.43	43.03	96.46
	Fino	0	74.00	10.67	6.67	11.63	10.53	391.80	250.47	642.27	42.77	25.68	68.46
		45	76.00	11.33	7.57	12.43	11.00	468.31	359.96	828.27	55.13	37.01	92.14
		60	77.33	12.33	8.17	12.73	12.03	523.63	397.47	921.10	72.26	41.55	113.80
		75	77.67	12.67	8.83	13.30	13.67	562.41	465.44	1027.85	66.55	52.81	119.36
	De Florence	0	69.67	10.67	6.50	11.00	10.33	389.17	296.67	685.83	49.83	31.83	81.66
		45	74.67	11.67	7.43	11.43	10.83	471.79	343.80	815.59	64.51	45.50	110.01
		60	76.33	12.00	8.33	12.47	11.70	488.28	378.45	866.73	53.03	41.59	94.62
		75	77.00	14.33	9.30	16.23	12.33	588.63	725.13	1313.77	64.62	63.52	128.14
	Zwe-jahrig	0	69.67	10.33	6.73	11.97	10.97	499.87	472.09	971.96	54.17	43.43	97.60
		45	73.33	11.00	9.27	12.33	11.67	539.57	562.27	1101.83	60.00	56.85	116.85
		60	74.00	13.67	9.30	14.20	12.50	573.95	752.72	1326.67	71.53	76.90	148.44
		75	77.00	11.00	10.20	14.50	13.30	642.68	564.93	1207.61	85.10	55.72	140.81
Late	Dolce	0	58.67	9.00	4.63	10.67	8.23	318.78	236.51	555.29	47.66	27.94	75.60
		45	66.00	10.00	5.30	10.73	8.63	355.73	234.76	590.49	56.33	29.95	86.27
		60	71.00	10.67	5.87	11.07	8.73	366.59	276.37	642.96	60.02	39.05	99.07
		75	69.33	10.33	6.73	12.20	9.03	376.56	306.84	683.41	52.98	36.14	89.12
	Zefa fino	0	69.33	9.33	5.80	11.20	9.20	272.94	252.63	525.56	32.95	33.77	66.72
		45	70.33	10.33	6.13	11.27	9.27	247.91	265.15	513.06	38.49	39.38	77.88
		60	67.00	10.67	6.40	11.63	9.83	259.24	293.12	552.36	43.43	37.04	80.47
		75	68.00	9.33	6.33	11.40	10.13	368.40	331.68	700.08	51.71	30.72	82.43
	Selma	0	62.67	9.33	5.40	10.57	8.30	242.58	218.55	461.13	27.97	20.04	48.01
		45	65.67	10.00	5.73	11.53	8.90	395.12	281.35	676.47	56.54	30.03	86.57
		60	67.67	10.67	6.40	13.03	9.60	409.39	383.87	793.26	64.24	43.08	107.32
		75	70.00	11.00	6.67	13.37	9.93	462.23	414.22	876.45	59.12	49.04	108.15
	Fino	0	69.33	10.00	6.30	10.50	9.07	354.01	356.83	710.84	43.88	42.30	86.18
		45	71.67	10.33	6.80	12.17	10.27	380.40	380.26	760.66	59.75	45.71	105.46
		60	78.67	10.67	7.47	12.50	11.33	392.04	429.70	821.75	51.74	43.88	95.62
		75	72.67	11.67	7.53	12.80	11.70	468.93	446.41	915.34	65.56	52.47	118.03
	De Florence	0	60.00	8.33	5.83	10.73	9.03	231.25	274.08	505.33	27.01	19.38	46.40
		45	66.67	9.67	6.90	11.13	10.00	251.40	280.47	531.87	42.44	32.95	75.38
		60	70.67	10.33	7.03	11.93	10.83	348.83	342.05	690.88	44.56	25.14	69.70
		75	70.00	10.00	7.73	12.47	11.70	380.71	396.85	777.56	54.66	46.34	101.00
	Zwe-jahrig	0	58.67	11.00	4.97	10.27	9.97	285.80	215.37	501.17	33.20	20.88	54.09
		45	60.00	11.33	6.30	12.40	10.20	436.52	322.25	758.77	66.61	31.86	98.48
		60	68.33	11.67	6.73	12.73	10.93	503.56	365.58	869.14	73.96	46.00	119.96
		75	70.00	10.33	6.97	13.30	11.30	548.84	455.38	1004.22	76.07	38.57	114.64
L.S.D.at.05			N.S.	1.08	N.S.	1.02	N.S.	42.53	42.65	60.73	7.50	8.11	11.23

Where: T= Thickness W= Width L= Length

Table (9): Effect of the interaction between transplanting dates, cultivars and K levels on vegetative growth of sweet fennel during the second season of 2006/2007.

Trans-Planting dates	Cultivars	K	Plant Length (cm)	Leaves No./ plant	Bulb dimensions			Fresh weight (g/plant)			Dry weight (g/plant)		
					T (cm)	W (cm)	L (cm)	Leaves	Bulb	Total	Leaves	Bulb	Total
Second season (2006-2007)													
Early	Dolce	0	64.00	8.33	5.13	9.27	8.77	388.35	226.87	615.22	28.04	23.68	51.72
		45	69.00	9.33	5.77	10.40	8.93	480.82	277.38	758.19	49.63	35.79	85.42
		60	71.33	9.67	7.47	11.57	9.33	585.45	394.28	979.73	78.37	62.45	140.82
		75	77.67	9.67	5.87	8.80	10.07	443.66	335.70	779.36	50.12	63.08	113.20
	Zefa fino	0	66.00	9.33	5.40	8.93	9.90	372.47	218.64	591.11	32.20	29.86	62.06
		45	68.67	9.67	6.33	9.83	11.37	469.24	263.71	732.95	59.20	30.42	89.63
		60	71.67	10.33	6.53	10.13	12.20	526.54	293.47	820.01	57.56	34.94	92.50
		75	72.67	11.00	6.83	10.37	12.73	536.98	390.83	927.82	63.66	42.12	105.77
	Selma	0	68.00	8.67	6.27	9.40	7.80	439.60	296.17	735.76	49.99	30.07	80.06
		45	73.33	9.00	6.80	11.73	8.40	460.77	444.97	905.74	50.43	48.89	99.33
		60	76.00	9.33	7.23	12.47	9.43	537.65	488.63	1026.28	57.79	55.72	113.51
		75	71.33	10.00	7.27	9.97	9.10	453.15	347.04	800.19	48.93	40.53	89.46
	Fino	0	71.00	9.67	5.47	10.43	10.03	371.25	229.97	601.22	38.27	23.18	61.46
		45	74.00	10.33	7.07	11.23	10.50	437.76	339.46	777.22	50.63	34.51	85.14
		60	76.00	11.33	7.30	11.53	11.53	493.08	376.97	870.05	67.76	39.05	106.80
		75	77.33	11.67	6.37	12.10	13.17	531.86	444.94	976.80	62.05	50.31	112.36
	De Florence	0	67.33	9.67	5.30	9.80	9.83	358.62	276.17	634.78	45.33	29.33	74.66
		45	71.33	10.67	6.23	10.23	10.33	441.24	323.30	764.54	53.34	36.33	89.67
		60	75.33	11.00	7.13	11.27	11.83	457.73	357.95	815.68	55.19	39.09	94.28
		75	76.33	13.33	8.10	15.03	11.20	558.08	704.63	1262.72	60.12	61.02	121.14
	Zwe-jahrig	0	67.00	9.33	5.53	10.77	9.97	469.32	451.59	920.91	49.67	40.93	90.60
		45	71.67	10.00	8.10	11.13	10.67	509.02	541.77	1050.78	55.50	54.35	109.85
		60	73.33	12.67	9.00	13.00	11.50	543.40	732.22	1275.62	67.03	74.40	141.44
		75	74.67	10.67	8.07	13.30	12.30	628.80	544.43	1173.23	80.60	53.22	133.81
Late	Dolce	0	59.00	8.00	4.10	9.47	8.13	288.23	216.01	504.24	43.16	25.44	68.60
		45	63.67	9.00	4.33	9.53	8.53	325.18	214.26	539.44	52.49	27.45	79.94
		60	70.33	9.67	4.77	9.87	8.23	336.04	255.87	591.91	55.52	36.55	92.07
		75	71.33	9.33	5.53	11.00	7.73	352.68	286.34	639.02	48.48	33.64	82.12
	Zefa fino	0	62.33	8.33	4.60	10.00	8.70	209.05	232.13	441.18	28.45	31.27	59.72
		45	64.00	9.33	4.93	10.07	8.77	217.36	244.65	462.01	37.33	33.55	70.88
		60	65.00	9.67	5.20	10.43	9.33	228.69	272.62	501.31	38.93	34.54	73.47
		75	66.00	8.33	5.13	10.20	9.63	337.85	311.18	649.03	48.88	34.88	83.76
	Selma	0	60.33	8.33	4.53	9.37	8.60	212.03	198.05	410.08	23.47	17.54	41.01
		45	63.00	9.00	4.87	10.33	8.87	364.57	260.85	625.42	52.04	27.53	79.57
		60	66.33	10.00	5.47	11.83	9.03	378.84	363.37	742.21	59.74	40.58	100.32
		75	68.33	11.00	5.87	12.17	9.37	431.68	393.72	825.40	57.95	46.54	104.49
	Fino	0	67.33	9.00	5.10	9.30	8.57	323.46	336.33	659.79	39.38	39.80	79.18
		45	69.67	9.33	5.60	10.97	8.77	349.85	359.76	709.61	55.25	43.21	98.46
		60	76.67	9.67	6.27	11.30	10.83	361.49	409.20	770.70	47.24	41.38	88.62
		75	70.67	10.67	6.33	11.60	11.20	438.38	425.91	864.29	61.06	49.97	111.03
	De Florence	0	57.67	7.33	4.63	9.53	8.53	200.70	253.58	454.28	22.51	16.88	39.40
		45	64.33	8.67	5.70	9.93	10.33	220.85	293.31	514.16	37.94	30.45	68.38
		60	68.00	9.33	5.83	10.73	11.20	318.28	321.55	639.83	40.06	35.97	76.04
		75	68.67	9.00	6.53	11.27	9.50	350.16	376.35	726.51	50.16	40.50	90.66
	Zwe-jahrig	0	56.33	10.00	3.77	9.07	9.70	255.25	194.87	450.12	28.70	21.71	50.42
		45	58.67	10.33	5.20	11.20	10.43	405.97	301.75	707.72	62.11	32.70	94.81
		60	66.00	10.67	5.43	11.53	10.80	473.01	355.08	828.09	69.46	43.50	112.96
		75	71.33	9.33	5.77	12.10	10.13	484.95	434.88	919.84	61.57	36.07	97.64
L.S.D.at.05			2.28	0.88	N.S.	0.81	0.73	29.92	29.80	41.27	5.16	4.58	7.29

Where: T= Thickness W= Width L= Length

II) Total green yield and physical bulb quality:

A). Effect of transplanting dates: Results in Table (10) Show that total green yield and physical bulb quality (Flatten shape and Elongated shape ratios) of sweet fennel plants were influenced significantly by transplanting dates. The highest values of these parameters were obtained with the early transplanting date (15 September) compared with the late date (1 October). These increases were statistically significant and similar in the two seasons. This increase in the total green yield amounted to 3.861 and 3.934 ton/fed which equals 25.14 and 27.02 % in the two seasons, respectively. These increases might be due to the resulting increases in the vegetative growth and N, P and K content of leaves and bulbs as well as dry matter content by the early plantation. These findings were similar and true in both seasons of study. These increases in total green yield and good quality might be due to the suitable temperature and relative humidity appeared to be reflected on the vegetative growth and consequently yield and quality, since the obtained high yield of those characters was more pronounced in the early date **(Abd El-Wahab and Mehasen, 2009).** These results were in agreement with those obtained by **Abdallah *et al*., 1978; Yadav *et al*., 2000**; **Baruah, 2004**; **Sudeep *et al*., 2006** and **Abd El-Wahab *et al*., 2009.**

Table (10): Effect of transplanting dates on total green yield, Physical bulb quality and chemical content of N, P and K in leaves and bulbs of sweet fennel during the two successive seasons (2005/2006 and 2006/2007).

Trans-planting dates	Total yield (ton /fed.)	Bulb shape			Chemical content					
		Flatten ratio	Cylinder ratio	Elongated ratio	N (%)		P (%)		K (%)	
					Leaves	Bulbs	Leaves	Bulbs	Leaves	Bulbs
First season (2005-2006)										
Early	15.354	1.56	1.13	0.91	2.35	1.81	0.29	0.51	2.69	2.97
Late	11.493	1.87	1.15	0.84	2.16	1.51	0.25	0.47	2.49	2.93
L.S.D. at 0.05	0.117	0.03	N.S.	0.02	0.01	0.02	0.00	0.01	0.04	0.03
Second season (2006-2007)										
Early	14.557	1.65	1.24	0.97	2.38	1.86	0.34	0.49	2.71	2.97
Late	10.623	2.04	1.28	0.89	2.19	1.56	0.30	0.45	2.51	2.93
L.S.D. at 0.05	0.162	0.12	N.S.	0.00	0.02	0.02	0.00	0.01	0.04	0.03

B). Effect of cultivars: Data presented in Table (11) show that the differences between cultivars were significant. The highest values of total green yield and good physical bulb quality of sweet fennel plants were obtained from cv. Zwejahrig compared with other cultivars. On the contrary, the lowest values of green yield and quality were obtained by cvs. Dulce and Zefa Fino. The cultivar Zwejahrig resulted in statistical increases in the total green yield amounted to 4.685 and 4.065 ton/fed which equals 28.81 and 25.01 % of the cultivars of Zefa Fino and Dulce in the first and amounted to 4.622 and 4.030 ton/fed which equals 30.04 and 26.19 % in the second seasons, respectively. The above mentioned findings were true in both seasons. The superiority of cv. Zwejahrig might be due to the higher vegetative growth and its high content of N, P and K of bulbs which led to higher photo-synthetic activity and metabolic condensation. These results were completely similar in both seasons.

Table (11): Effect of cultivars on total green yield, Physical bulb quality and chemical content of N, P and K in leaves and bulbs of sweet fennel during 2005/2006 and 2006/2007.

Cultivars	Total yield (Ton /fed.)	Bulb shape			Chemical content					
		Flatten ratio	Cylinder ratio	Elongated ratio	N (%)		P (%)		K (%)	
					Leaves	Bulbs	Leaves	Leaves	Bulbs	Leaves
First season (2005-2006)										
Dolce	12.192	1.80	1.10	0.83	2.37	1.43	0.30	0.42	2.30	2.91
Zefa fino	11.572	1.68	1.20	0.94	2.53	1.54	0.25	0.45	2.45	2.96
Selma	13.607	1.74	1.02	0.78	2.15	1.39	0.30	0.43	2.70	2.76
Fino	13.919	1.67	1.17	0.91	2.09	1.88	0.29	0.56	2.62	2.97
De Florance	12.994	1.66	1.15	0.90	2.52	1.85	0.24	0.51	2.74	3.08
Zwejahrig	16.257	1.74	1.18	0.90	1.88	1.89	0.24	0.57	2.74	3.01
L.S.D. at 0.05	0.223	0.04	0.03	0.03	0.04	0.05	0.01	0.01	0.02	0.03
Second season (2006-2007)										
Dolce	11.355	1.91	1.21	0.88	2.41	1.48	0.35	0.40	2.32	2.91
Zefa fino	10.763	1.81	1.38	1.04	2.56	1.59	0.30	0.43	2.47	2.96
Selma	12.749	1.85	1.11	0.82	2.18	1.44	0.35	0.41	2.72	2.76
Fino	13.082	1.81	1.28	0.96	2.12	1.93	0.34	0.54	2.64	2.97
De Florance	12.206	1.79	1.27	0.96	2.55	1.90	0.29	0.49	2.76	3.08

Zwejahrig	15.385	1.92	1.29	0.94	1.91	1.94	0.29	0.55	2.76	3.01
L.S.D. at 0.05	0.178	0.04	0.03	0.03	0.04	0.05	0.01	0.01	0.02	0.03

C). Effect of potassium fertilizer levels: Data present in Table (12) reveal that total green yield and physical bulb quality of sweet fennel plants was enhanced by increasing potassium fertilizer levels up

to 75 kg K_2O / fed. Linear and gradual increases in total green yield were recorded by the increased levels of potassium fertilizer up to its highest level. Physical quality and N, P and K content followed the same trend of total green yield by the increases in potassium levels.

Table (12): Effect of potassium levels on total green yield, Physical bulb quality and chemical content of N, P and K in leaves and bulbs of sweet fennel during 2005/2006 and 2006/2007 seasons.

Potassium levels	Total yield (Ton/fed.)	Bulb shape			Chemical content					
		Flatten ratio	Cylinder ratio	Elongated ratio	N (%)		P (%)		K (%)	
					Leaves	Bulbs	Leaves	Leaves	Bulbs	Leaves
First season (2005-2006)										
0	10.716	1.80	1.18	0.88	1.87	1.33	0.20	0.36	2.36	2.70
45	12.778	1.73	1.12	0.86	2.28	1.53	0.26	0.49	2.59	2.93
60	14.617	1.71	1.12	0.86	2.44	1.90	0.32	0.60	2.73	3.11
75	15.582	1.61	1.13	0.90	2.44	1.88	0.31	0.50	2.69	3.05
L.S.D. at 0.05	0.295	0.06	0.03	0.03	0.05	0.07	0.01	0.01	0.03	0.04
Second season (2006-2007)										
0	9.826	1.97	1.32	0.95	1.90	1.38	0.25	0.34	2.38	2.70
45	11.967	1.83	1.24	0.92	2.31	1.58	0.31	0.47	2.61	2.93
60	13.806	1.79	1.24	0.93	2.47	1.95	0.37	0.58	2.75	3.11
75	14.762	1.80	1.23	0.93	2.47	1.93	0.36	0.48	2.71	3.05
L.S.D. at 0.05	0.200	0.06	0.05	N.S.	0.05	0.07	0.01	0.01	0.03	0.04

These results were in agreement with those obtained by **Alt *et al*. 1999** on fennel and **El-Bassiony, 2006** on onion. Data in Table (12) show that there were significant differences in flatten, cylinder and elongated shape ratios by using different levels of potassium fertilizer treatments in the two seasons of study. Appling of the high rate of potassium fertilizer (75 kg K_2O / fed.) caused a significant decreases in flatten shape ratio and increases in cylinder and elongated shape ratios of sweet fennel bulbs.

These results indicated that the high level of potassium fertilizer increased the exportable yield of sweet fennel crop. Higher values of flatten and cylinder shape ratios and lower values of elongated shape were recorded by zero potassium level (control). These results were similar in the two seasons. The depression in the flatten shape bulbs means that bulbs tended to be round in shape more than flattening, the decrease in cylinder shape ratio and increase in elongated shape bulbs means increases in the round bulbs, this is considered an improvement in quality of fennel bulbs **(El-Shakry, 2005)**.

D). Effect of interaction:

Interaction between transplanting dates and cultivars: The obtained data revealed that the interaction treatments significantly affected total green yield and bulb quality of sweet fennel is shown in Tables (13). Generally, it could be concluded that, the highest total green yield and good bulb quality of sweet fennel plants were recorded by the combined effect of early transplanting date and Zwejahrig cultivar. On the contrary, lower values of total green yield and bulb quality of sweet fennel were obtained by the combined effect of the late transplanting and cvs. De Florance, Selma, Fino, Dulce and Zefa Fino in a descending order in the two seasons.

Interaction between transplanting dates and K levels: Results presented in Table (14) indicated that total green yield was significantly affected by the interaction between transplanting dates and levels of potassium fertilizer in the two seasons. The highest values of total green yield was obtained by early transplanting date combined with the high level of potassium fertilizer at the rate of 75 kg K_2O / fed compared with other treatments. In contrast, the lowest values of total green yield were obtained by late transplanting date combined with zero level of potassium fertilizer (control). The above mentioned findings were true in both seasons.

Interaction between cultivars and K levels: Data in Table (15) reported that total green yield and physical bulb quality were significantly influenced by the interaction between cultivars and K levels in the two seasons except

bulb cylinder shape ratio did not reach to the level of significance in the first season. The highest values of green yield and bulbs good quality were obtained by cv. Zwejahrig combined with the high level of potassium fertilizer at the rate of 60 and 75 kg K_2O / fed compared with other treatments. These results were nearly similar in both seasons.

Interaction between transplanting dates, cultivars and K levels: Data in Table (16 and 17) demonstrated that, total green yield and physical bulb quality were significantly influenced by the interaction between transplanting dates**,** cultivars and K levels in the two seasons. The highest values of most vegetative growth characters were obtained by the interaction between early transplanting date and cv. Zwejahrig combined with the high level of mineral potassium fertilizer at the rate of 75 kg K_2O / fed compared with other treatments. These results were similar in the two seasons.

Table (13): Effect of the interaction between transplanting dates and potassium levels on total green yield, Physical bulb quality and chemical content of N, P and K in leaves and bulbs of sweet fennel during 2005/2006 and 2006/2007 seasons.

Trans-planting dates	Cultivars	Total yield (Ton/fed.)	Bulb shape			Chemical content					
			Flatten ratio	Cylinder ratio	Elongated ratio	N (%)		P (%)		K (%)	
						Leaves	Bulbs	Leaves	Leaves	Bulbs	Leaves
First season (2005-2006)											
Early	Dolce	14.000	1.58	1.10	0.89	2.46	1.58	0.33	0.45	2.41	2.95
	Zefa fino	13.522	1.50	1.26	1.03	2.63	1.69	0.27	0.47	2.57	2.98
	Selma	15.423	1.48	0.95	0.79	2.24	1.54	0.32	0.45	2.81	2.78
	Fino	14.362	1.62	1.20	0.94	2.19	2.01	0.32	0.58	2.71	2.99
	De Florance	15.464	1.62	1.14	0.90	2.62	1.99	0.26	0.53	2.82	3.10
	Zwejahrig	19.354	1.53	1.13	0.92	1.98	2.04	0.27	0.57	2.85	3.03
Late	Dolce	10.383	2.02	1.11	0.78	2.29	1.28	0.28	0.40	2.20	2.87
	Zefa fino	9.622	1.85	1.15	0.84	2.43	1.39	0.23	0.42	2.34	2.94
	Selma	11.791	2.01	1.08	0.76	2.06	1.24	0.28	0.41	2.59	2.74
	Fino	13.476	1.71	1.15	0.88	1.99	1.75	0.27	0.53	2.53	2.95
	De Florance	10.524	1.69	1.17	0.90	2.42	1.70	0.22	0.48	2.67	3.06
	Zwejahrig	13.160	1.96	1.23	0.88	1.78	1.73	0.22	0.57	2.63	2.99
L.S.D. at 0.05		0.546	0.10	0.08	0.06	N.S.	N.S.	N.S.	0.02	N.S.	N.S.
Second season (2006-2007)											
Early	Dolce	13.157	1.66	1.21	0.94	2.50	1.63	0.38	0.43	2.43	2.95
	Zefa fino	12.902	1.57	1.47	1.18	2.66	1.74	0.32	0.45	2.59	2.98
	Selma	14.566	1.58	1.01	0.81	2.27	1.59	0.37	0.43	2.83	2.78
	Fino	13.546	1.76	1.32	1.00	2.22	2.06	0.37	0.56	2.73	2.99
	De Florance	14.606	1.74	1.25	0.95	2.65	2.04	0.31	0.51	2.84	3.10
	Zwejahrig	18.566	1.62	1.17	0.93	2.01	2.09	0.32	0.55	2.87	3.03
Late	Dolce	9.553	2.16	1.22	0.83	2.32	1.33	0.33	0.38	2.22	2.87
	Zefa fino	8.625	2.05	1.28	0.90	2.46	1.44	0.28	0.40	2.36	2.94
	Selma	10.933	2.12	1.21	0.83	2.09	1.29	0.33	0.39	2.61	2.74
	Fino	12.618	1.86	1.24	0.91	2.02	1.80	0.32	0.51	2.55	2.95
	De Florance	9.806	1.85	1.30	0.96	2.45	1.75	0.27	0.46	2.69	3.06
	Zwejahrig	12.204	2.22	1.41	0.95	1.81	1.78	0.27	0.55	2.65	2.99
L.S.D. at 0.05		0.437	0.10	0.09	0.06	N.S.	N.S.	N.S.	0.02	N.S.	N.S.

Table (14): Effect of interaction between transplanting dates and K levels on total green yield, physical bulb quality and chemical content of N, P and K in leaves and bulbs of sweet fennel during 2005/2006 and 2006/2007 seasons.

Trans-planting dates	K levels	Total yield (Ton/fed.)	Bulb shape			Chemical content					
			Flatten ratio	Cylinder ratio	Elongated ratio	N (%)		P (%)		K (%)	
						Leaves	Bulbs	Leaves	Leaves	Bulbs	Leaves
First season (2005-2006)											
Early	0	12.307	1.65	1.18	0.92	1.97	1.45	0.23	0.38	2.46	2.71
	45	14.828	1.57	1.10	0.89	2.37	1.63	0.29	0.52	2.67	2.97
	60	16.997	1.59	1.10	0.88	2.54	2.12	0.34	0.62	2.84	3.13
	75	17.285	1.42	1.13	0.95	2.54	2.03	0.33	0.52	2.79	3.07
Late	0	9.126	1.96	1.18	0.84	1.77	1.21	0.18	0.35	2.26	2.69
	45	10.728	1.88	1.13	0.83	2.19	1.43	0.23	0.47	2.50	2.89
	60	12.237	1.84	1.14	0.84	2.35	1.68	0.30	0.58	2.62	3.09
	75	13.880	1.81	1.14	0.85	2.34	1.74	0.28	0.48	2.59	3.03
L.S.D. at 0.05		0.417	N.S.	N.S.	N.S.	N.S.	0.10	N.S.	N.S.	N.S.	N.S.
Second season (2006-2007)											
Early	0	11.477	1.79	1.29	0.96	2.00	1.50	0.28	0.36	2.48	2.71

	45	13.970	1.62	1.19	0.94	2.40	1.68	0.34	0.50	2.69	2.97
	60	16.205	1.57	1.19	0.95	2.57	2.17	0.39	0.60	2.86	3.13
	75	16.576	1.64	1.29	1.01	2.57	2.08	0.38	0.50	2.81	3.07
	0	8.175	2.14	1.36	0.93	1.80	1.26	0.23	0.33	2.28	2.69
Late	45	9.963	2.04	1.28	0.90	2.22	1.48	0.28	0.45	2.52	2.89
	60	11.407	2.01	1.28	0.91	2.38	1.73	0.35	0.56	2.64	3.09
	75	12.947	1.97	1.18	0.84	2.37	1.79	0.33	0.46	2.61	3.03
L.S.D. at 0.05		0.283	N.S.	0.07	0.05	N.S.	0.10	N.S.	N.S.	N.S.	N.S.

Table (15): Effect of interaction between cultivars and potassium levels on total green yield, physical bulb quality and chemical content of N, P and K in leaves and bulbs of sweet fennel during 2005/2006 and 2006/2007 seasons.

Cultivars	K levels	Total yield (Ton/fed.)	Bulb shape			Chemical content					
			Flatten ratio	Cylinder ratio	Elongated ratio	N (%)		P (%)		K (%)	
						Leaves	Bulbs	Leaves	Leaves	Bulbs	Leaves
First season (2005-2006)											
	0	10.261	1.98	1.16	0.83	2.06	1.21	0.25	0.37	1.90	2.69
Dolce	45	11.758	1.89	1.11	0.81	2.59	1.28	0.29	0.45	2.32	2.84
	60	14.059	1.85	1.07	0.79	2.64	1.39	0.36	0.54	2.47	3.00
	75	12.688	1.49	1.07	0.91	2.20	1.85	0.32	0.33	2.52	3.11
	0	9.809	1.74	1.21	0.93	2.17	1.19	0.21	0.32	2.39	2.89
Zefa fino	45	10.895	1.67	1.16	0.90	2.47	1.61	0.26	0.49	2.47	2.95
	60	11.761	1.65	1.20	0.94	2.59	1.41	0.27	0.60	2.54	3.16
	75	13.823	1.64	1.24	0.98	2.88	1.94	0.27	0.40	2.41	2.84
	0	10.483	1.69	1.06	0.82	1.67	1.01	0.21	0.31	2.37	2.32
Selma	45	13.719	1.84	1.01	0.75	2.21	1.23	0.28	0.45	2.78	2.91
	60	15.713	1.84	0.98	0.72	2.69	1.84	0.37	0.50	2.92	2.93
	75	14.513	1.61	1.01	0.82	2.05	1.48	0.36	0.48	2.74	2.87
	0	11.366	1.71	1.16	0.89	1.45	1.45	0.22	0.42	2.38	2.52
Fino	45	13.347	1.73	1.13	0.87	2.15	1.51	0.28	0.52	2.58	2.89
	60	14.640	1.62	1.18	0.93	2.34	2.53	0.35	0.72	2.72	3.49
	75	16.323	1.60	1.23	0.97	2.42	2.04	0.32	0.59	2.80	2.97
De Florance	0	10.006	1.77	1.18	0.89	2.10	1.62	0.17	0.29	2.62	2.88
	45	11.319	1.58	1.16	0.92	2.44	1.68	0.26	0.52	2.65	3.03
	60	13.084	1.60	1.17	0.93	2.48	1.90	0.28	0.54	2.86	3.11
	75	17.567	1.68	1.10	0.85	3.08	2.20	0.26	0.68	2.84	3.31
	0	12.374	1.93	1.32	0.95	1.75	1.52	0.17	0.48	2.50	2.91
Zwejahrig	45	15.629	1.65	1.13	0.89	1.82	1.89	0.20	0.55	2.72	2.95
	60	18.445	1.72	1.14	0.87	1.91	2.34	0.30	0.71	2.89	2.99
	75	18.579	1.67	1.14	0.89	2.03	1.80	0.31	0.54	2.84	3.19
L.S.D. at 0.05		0.721	0.15	N.S.	0.07	0.13	0.18	0.03	0.03	0.06	0.09
Second season (2006-2007)											
	0	9.403	2.06	1.29	0.90	2.09	1.26	0.30	0.35	1.92	2.69
Dolce	45	10.900	2.02	1.25	0.88	2.64	1.33	0.34	0.43	2.34	2.84
	60	13.202	1.81	1.11	0.82	2.67	1.44	0.41	0.52	2.49	3.00
	75	11.914	1.76	1.20	0.93	2.23	1.90	0.37	0.31	2.54	3.11
	0	8.671	1.92	1.36	0.99	2.20	1.24	0.26	0.30	2.41	2.89
Zefa fino	45	10.038	1.80	1.34	1.02	2.50	1.66	0.31	0.47	2.49	2.95
	60	11.099	1.78	1.38	1.05	2.62	1.46	0.32	0.58	2.56	3.16
	75	13.246	1.76	1.42	1.09	2.91	1.99	0.32	0.38	2.43	2.84
	0	9.625	1.79	1.18	0.88	1.70	1.06	0.26	0.29	2.39	2.32
Selma	45	12.862	1.93	1.10	0.79	2.24	1.28	0.33	0.43	2.80	2.91
	60	14.855	1.95	1.07	0.77	2.72	1.89	0.42	0.48	2.94	2.93
	75	13.655	1.73	1.09	0.85	2.08	1.53	0.41	0.46	2.76	2.87
	0	10.592	1.87	1.29	0.94	1.48	1.50	0.27	0.40	2.40	2.52
Fino	45	12.489	1.77	1.15	0.87	2.18	1.56	0.33	0.50	2.60	2.89
	60	13.782	1.69	1.27	0.98	2.37	2.58	0.40	0.70	2.74	3.49
	75	15.465	1.89	1.41	1.03	2.45	2.09	0.37	0.57	2.82	2.97
	0	9.148	1.96	1.33	0.95	2.13	1.67	0.22	0.27	2.64	2.88
De Florance	45	10.741	1.69	1.33	1.03	2.47	1.73	0.31	0.50	2.67	3.03
	60	12.226	1.71	1.37	1.05	2.51	1.95	0.33	0.52	2.88	3.11
	75	16.710	1.79	1.06	0.80	3.11	2.25	0.31	0.66	2.86	3.31
	0	11.517	2.20	1.49	1.00	1.78	1.57	0.22	0.46	2.52	2.91
Zwejahrig	45	14.771	1.78	1.26	0.95	1.85	1.94	0.25	0.53	2.74	2.95
	60	17.671	1.79	1.21	0.91	1.94	2.39	0.35	0.69	2.91	2.99
	75	17.582	1.90	1.21	0.88	2.06	1.85	0.36	0.52	2.86	3.19
L.S.D. at 0.05		0.490	0.15	0.12	0.08	0.13	0.18	0.03	0.03	0.06	0.09

Table (16): Effect of the interaction between cultivars, transplanting dates and K levels on total green yield, physical bulb quality and chemical content of N, P and K in leaves and bulbs of sweet fennel during the first season (2005/2006).

Trans-planting dates	Cultivars	K levels	Total yield (Ton/fed).	Bulb shape			Chemical content					
				Flatten ratio	Cylinder ratio	Elongated ratio	N (%)		P (%)		K (%)	
							Leaves	Bulbs	Leaves	Leaves	Bulbs	Leaves
First season (2005-2006)												
Early	Dolce	0	11.193	1.65	1.14	0.89	2.16	1.36	0.27	0.40	1.98	2.70
		45	13.595	1.73	1.07	0.81	2.68	1.43	0.31	0.48	2.43	2.98
		60	17.317	1.81	1.04	0.79	2.71	1.54	0.38	0.56	2.58	3.01
		75	13.895	1.15	1.14	1.06	2.30	2.00	0.34	0.35	2.63	3.12
	Zefa fino	0	10.788	1.55	1.28	1.03	2.27	1.14	0.21	0.34	2.50	2.89
		45	13.171	1.50	1.20	0.99	2.57	1.53	0.28	0.51	2.58	2.97
		60	14.242	1.48	1.26	1.03	2.69	1.99	0.29	0.63	2.65	3.19
		75	15.885	1.47	1.29	1.06	2.98	2.09	0.30	0.42	2.54	2.87
	Selma	0	13.218	1.42	1.02	0.86	1.77	1.16	0.23	0.31	2.48	2.34
		45	16.074	1.66	0.93	0.73	2.26	1.38	0.31	0.47	2.89	2.93
		60	18.099	1.62	0.89	0.70	2.79	1.99	0.38	0.52	3.03	2.95
		75	14.301	1.21	0.97	0.89	2.16	1.63	0.38	0.50	2.85	2.89
	Fino	0	10.790	1.75	1.20	0.91	1.55	1.60	0.25	0.44	2.49	2.53
		45	13.915	1.67	1.14	0.89	2.25	1.59	0.30	0.54	2.69	2.91
		60	15.474	1.56	1.18	0.94	2.44	2.68	0.37	0.74	2.83	3.51
		75	17.268	1.51	1.26	1.03	2.52	2.19	0.34	0.61	2.83	2.99
	De Florance	0	11.522	1.70	1.22	0.94	2.20	1.77	0.20	0.31	2.73	2.90
		45	13.702	1.54	1.18	0.95	2.54	1.83	0.28	0.54	2.63	3.05
		60	14.561	1.50	1.15	0.94	2.58	2.05	0.30	0.56	2.97	3.13
		75	22.071	1.75	1.01	0.76	3.18	2.33	0.28	0.70	2.95	3.33
	Zwejahrig	0	16.329	1.80	1.23	0.92	1.85	1.69	0.20	0.45	2.61	2.93
		45	18.511	1.33	1.10	0.95	1.92	2.04	0.22	0.57	2.83	2.97
		60	22.288	1.55	1.10	0.88	2.01	2.49	0.32	0.72	3.00	3.01
		75	20.288	1.42	1.10	0.92	2.13	1.95	0.32	0.53	2.95	3.21
Late	Dolce	0	9.329	2.30	1.17	0.77	1.96	1.06	0.22	0.35	1.83	2.68
		45	9.920	2.05	1.16	0.81	2.51	1.13	0.26	0.43	2.21	2.69
		60	10.802	1.89	1.09	0.79	2.58	1.24	0.33	0.51	2.35	2.99
		75	11.481	1.82	1.01	0.75	2.10	1.70	0.29	0.30	2.41	3.10
	Zefa fino	0	8.829	1.93	1.14	0.82	2.07	1.23	0.20	0.29	2.28	2.89
		45	8.619	1.84	1.12	0.82	2.37	1.69	0.23	0.46	2.36	2.93
		60	9.280	1.82	1.14	0.85	2.49	0.84	0.24	0.58	2.43	3.13
		75	11.761	1.80	1.19	0.89	2.78	1.79	0.25	0.37	2.29	2.81
	Selma	0	7.747	1.96	1.10	0.79	1.57	0.86	0.18	0.30	2.26	2.30
		45	11.365	2.02	1.09	0.77	2.16	1.08	0.26	0.42	2.67	2.89
		60	13.327	2.06	1.06	0.74	2.59	1.69	0.36	0.47	2.81	2.91
		75	14.724	2.01	1.06	0.75	1.93	1.33	0.33	0.45	2.63	2.85
	Fino	0	11.942	1.67	1.11	0.86	1.35	1.30	0.20	0.39	2.27	2.52
		45	12.779	1.79	1.13	0.85	2.05	1.42	0.25	0.49	2.47	2.87
		60	13.805	1.68	1.18	0.91	2.24	2.38	0.32	0.69	2.61	3.47
		75	15.378	1.70	1.19	0.91	2.32	1.89	0.29	0.56	2.77	2.95
	De Florance	0	8.490	1.85	1.15	0.84	2.00	1.47	0.15	0.26	2.51	2.86
		45	8.935	1.61	1.14	0.90	2.34	1.53	0.23	0.49	2.67	3.01
		60	11.607	1.70	1.19	0.91	2.38	1.75	0.25	0.51	2.75	3.09
		75	13.063	1.62	1.20	0.94	2.98	2.06	0.24	0.65	2.73	3.29
	Zwejahrig	0	8.420	2.07	1.40	0.98	1.65	1.35	0.15	0.50	2.39	2.89
		45	12.747	1.97	1.15	0.82	1.72	1.74	0.17	0.52	2.61	2.93
		60	14.601	1.89	1.18	0.86	1.82	2.19	0.27	0.70	2.78	2.97
		75	16.871	1.91	1.18	0.85	1.93	1.65	0.30	0.55	2.73	3.17
L.S.D. at 0.05			1.020	0.21	N.S.	0.10	N.S.	0.25	N.S.	N.S.	N.S.	N.S.

Table (17): Effect of the interaction between cultivars, transplanting dates and K levels on total green yield, Physical bulb quality and chemical content of N, P and K in leaves and bulbs of sweet fennel during the second season (2006/2007).

Trans-planting dates	Cultivars	K levels	Total yield (Ton/fed).	Bulb shape			Chemical content					
				Flatten ratio	Cylinder ratio	Elongated ratio	N (%)		P (%)		K (%)	
							Leaves	Bulbs	Leaves	Bulbs	Leaves	Bulbs
Scond season (2005-2006)												
Early	Dolce	0	10.336	1.81	1.27	0.95	2.19	1.41	0.32	0.38	2.00	2.70

		45	12.738	1.80	1.15	0.86	2.74	1.48	0.36	0.46	2.45	2.98
		60	16.460	1.55	1.00	0.81	2.74	1.59	0.43	0.54	2.60	3.01
		75	13.093	1.50	1.40	1.15	2.33	2.05	0.39	0.33	2.65	3.12
		0	9.931	1.66	1.43	1.11	2.30	1.19	0.26	0.32	2.52	2.89
	Zefa fino	45	12.314	1.55	1.44	1.16	2.60	1.58	0.33	0.49	2.60	2.97
		60	13.776	1.55	1.50	1.21	2.72	2.04	0.34	0.61	2.67	3.19
		75	15.587	1.52	1.51	1.23	3.01	2.14	0.35	0.40	2.56	2.87
		0	12.361	1.50	1.02	0.83	1.80	1.21	0.28	0.29	2.50	2.34
	Selma	45	15.216	1.73	0.95	0.72	2.29	1.43	0.36	0.45	2.91	2.93
		60	17.242	1.72	1.00	0.77	2.82	2.04	0.43	0.50	3.05	2.95
		75	13.443	1.38	1.08	0.92	2.19	1.68	0.43	0.48	2.87	2.89
		0	10.100	1.92	1.34	0.97	1.58	1.65	0.30	0.42	2.51	2.53
	Fino	45	13.057	1.59	1.18	0.94	2.28	1.64	0.35	0.52	2.71	2.91
		60	14.617	1.58	1.26	1.00	2.47	2.73	0.42	0.72	2.85	3.51
		75	16.410	1.94	1.51	1.09	2.55	2.24	0.39	0.59	2.85	2.99
	De Florance	0	10.664	1.86	1.37	1.00	2.23	1.82	0.25	0.29	2.75	2.90
		45	12.844	1.64	1.29	1.01	2.57	1.88	0.33	0.52	2.65	3.05
		60	13.703	1.58	1.32	1.05	2.61	2.10	0.35	0.54	2.99	3.13
		75	21.214	1.86	1.02	0.75	3.21	2.38	0.33	0.68	2.97	3.33
		0	15.471	1.98	1.30	0.93	1.88	1.74	0.25	0.43	2.63	2.93
	Zwejahrig	45	17.653	1.39	1.14	0.97	1.95	2.09	0.27	0.55	2.85	2.97
		60	21.430	1.45	1.07	0.89	2.04	2.54	0.37	0.70	3.02	3.01
		75	19.710	1.65	1.19	0.92	2.16	2.00	0.37	0.51	2.97	3.21
		0	8.471	2.31	1.31	0.86	1.99	1.11	0.27	0.33	1.85	2.68
	Dolce	45	9.063	2.23	1.35	0.90	2.54	1.18	0.31	0.41	2.23	2.69
		60	9.944	2.08	1.21	0.84	2.61	1.29	0.38	0.49	2.37	2.99
		75	10.736	2.01	1.00	0.71	2.13	1.75	0.34	0.28	2.43	3.10
		0	7.412	2.17	1.28	0.87	2.10	1.28	0.25	0.27	2.30	2.89
	Zefa fino	45	7.762	2.04	1.25	0.87	2.40	1.74	0.28	0.44	2.38	2.93
		60	8.422	2.01	1.27	0.89	2.52	0.89	0.29	0.56	2.45	3.13
		75	10.904	1.99	1.33	0.94	2.81	1.84	0.30	0.35	2.31	2.81
		0	6.889	2.07	1.33	0.92	1.60	0.91	0.23	0.28	2.28	2.30
	Selma	45	10.507	2.12	1.25	0.86	2.19	1.13	0.31	0.40	2.69	2.89
		60	12.469	2.18	1.13	0.76	2.62	1.74	0.41	0.45	2.83	2.91
		75	13.867	2.09	1.11	0.77	1.96	1.38	0.38	0.43	2.65	2.85
Late		0	11.084	1.82	1.24	0.92	1.38	1.35	0.25	0.37	2.29	2.52
	Fino	45	11.922	1.96	1.12	0.80	2.08	1.47	0.30	0.47	2.49	2.87
		60	12.948	1.81	1.29	0.96	2.27	2.43	0.37	0.67	2.63	3.47
		75	14.520	1.83	1.31	0.97	2.35	1.94	0.34	0.54	2.79	2.95
		0	7.632	2.07	1.29	0.90	2.03	1.52	0.20	0.24	2.53	2.86
	De Florance	45	8.638	1.74	1.37	1.04	2.37	1.58	0.28	0.47	2.69	3.01
		60	10.749	1.84	1.42	1.04	2.41	1.80	0.30	0.49	2.77	3.09
		75	12.205	1.73	1.11	0.84	3.01	2.11	0.29	0.63	2.75	3.29
		0	7.562	2.41	1.68	1.08	1.68	1.40	0.20	0.48	2.41	2.89
	Zwejahrig	45	11.890	2.17	1.37	0.93	1.75	1.79	0.22	0.50	2.63	2.93
		60	13.912	2.13	1.36	0.94	1.85	2.24	0.32	0.68	2.80	2.97
		75	15.453	2.15	1.23	0.84	1.96	1.70	0.35	0.53	2.75	3.17
L.S.D. at 0.05			0.693	N.S.	0.16	0.11	N.S.	0.25	N.S.	N.S.	N.S.	N.S.

III. Chemical composition

A). Effect of transplanting dates: Data presented in Table (10) demonstrated that, the N, P and K content in tissues of sweet fennel leaves and bulbs were significantly increased by early plantation compared with the late one. Increases in N, P and K content of leaves and bulbs with the late plantation were statistical and similar in the two seasons. These results were in accordance with those reported by **Yadav *et al.*, 2000**; **Sudeep *et al.*, 2006**; **Abd El-Wahab *et al.*, 2009** on fennel.

B). Effect of cultivars: Data presented in Table (11) indicated that cultivation of cv. Zwejahrig (German cultivar) increased N, P and K content in bulbs but decreased N and P content in leaves of sweet fennel plants. On the contrary, the lowest values of N, P and K content in bulbs were obtained with cv. Dulce. These findings were similar and true in both seasons of study. These results were in accordance with those reported by **Fawzy *et al.*, 2006 and Zaki *et al.*, 2009** on sweet fennel cultivars.

C). Effect of potassium fertilizer levels: Data present in Table (12) reveal that N, P and K content in leaves and bulbs of sweet fennel plants were enhanced by increasing potassium fertilizer levels up to 60 kg K_2O / fed. Linear and gradual increases in N, P and K content were recorded by the increased levels of potassium fertilizer up to 60 kg K_2O / fed. These findings were similar and true in both seasons of study. These results were in accordance with those

reported by **Alt *et al*. 1999**; **Sadanandan *et al*., 2002** on fennel and **El-Bassiony, 2006** on onion confirmed that N, P and K content tended to increase with increasing potassium levels. Furthermore, potassium plays a direct or indirect role in plant metabolism (**Kandil, 2002**) on fennel.

D). Effect of interaction:

Interaction between transplanting dates and cultivars: The obtained data revealed that the interaction treatments did not affect N, P and K content in leaves and bulbs except P in leaves of sweet fennel reached to the level of significance (Tables, 13). These results were similar in both seasons.

Interaction between transplanting dates and K levels: Results presented in Table (14) indicated that the interaction between transplanting dates and levels of potassium fertilizer in both seasons did not reach the level of significance for N, P and K content in leaves and bulbs except N content in bulbs was significantly affected by the interaction between sowing dates and K levels. The highest values of N content in bulbs was obtained by early cultivation combined with the high level of potassium fertilizer at the rate of 75 kg K_2O / fed compared with other treatments. In contrast, the lowest values of N content in bulbs were obtained by late cultivation combined with zero level of potassium fertilizer (control). The above mentioned findings were true in both seasons.

Interaction between cultivars and K levels: Data in Table (15) reported that N, P and K content in leaves and bulbs of sweet fennel were significantly influenced by the interaction between cultivars and K levels in the two seasons. The highest values of N, P and K content were obtained by cvs. Fino and Zwejahrig, respectively combined with the high level of potassium fertilizer at the rate of 60 and 75 kg K_2O / fed compared with other treatments. These results were nearly similar in both seasons.

Interaction between transplanting dates, cultivars and K levels: Data in Table (16 and 17) demonstrated that, N, P and K content in leaves and bulbs of sweet fennel did not significantly influenced by the interaction between transplanting dates**,** cultivars and K levels except N content in bulbs was significantly affected by the interaction in the two seasons. The highest values of N content in bulbs were obtained by the interaction between early cultivation for cv. Zwejahrig combined with the high level of mineral potassium fertilizer at the rate of 60 kg K_2O / fed compared with other treatments. These results were similar in the two seasons.

References

1. **Abd El- Wahab, M. A. and H. R. Mehasen (2009).** Effect of Locations and Sowing Date on (*Foeniculum Vulgare* Mill.) Indian Fennel Type under Upper Egypt Conditions. Journal of Applied Sciences Research, 5 (6): 677-685.
2. **Abdallah, N.; S. El-Gengaihi and E. Sedrak (1978).** The effect of fertilizer treatments on yield of seed and volatile oil of fennel (Foeniculum vulgare Mill.). Pharmazie, 33 (9): 607-608.
3. **Abou El - Magd, M.M. and H. M.H. El-Abagy (2003)** Vegetative growth and green yield of sweet fennel plants as affected by date of sowing, mineral and organic fertilization. Egypt. j. Appl. Sci.; 18(12B) 717-728.
4. **Alt, D.; H. Ladebusch and O. Melzer (1999).** Long-term trial with increasing amounts of phosphorus, potassium and magnesium applied to vegetable crops. Acta-Horticulturae, 506: 29-36.
5. **Baruah, G. K. S. (2001).** Effect of sowing dates and plant spacing on growth and seed yield of fennel in hills of Assam . Horticultural-Journal, 14 (1): 85-89.
6. **Bhati, D. S.; M. S. Shaktawat; L. L. Somani and H. R. Agarwal (1988).** Response of fennel (Foeniculum vulgare Mill.) to nitrogen and phosphorus. Transactions of Indian Society of Desert Technology, No. 2: 79-83.
7. **Charles, D.J.; M.R. Morales and J.E. Simon (1993).** Essential oil content and chemical composition of finocchio fennel. In: Janick, J. and J. E. Simon (eds.), New crops. Wiley New York, pp: 570-573.
8. **Chiej, R. (1984).** The Macdonald Encyclopedia of Medicinal Plants. Macdonald & Co., London.
9. **Cottenie, A.; M. Verloo; M. Velghe and R. Camerlynck (1982).** Chemical analysis of plants and soils, Lab, Anal Agrochem. State Univ., Ghent Belgium, pp: 63.
10. **Egypt Magazine (2000):** www.sis.gov.eg/public/magazine/iss023e/ht

ml/mag11.ht m.

11. **El-Bassiony, A. M. (2006).** Effect of potassium fertilization on growth, yield and quality of onion plants. Journal of Applied Sciences Research, 2(10): 780-785.
12. **El-Shakry, M. F. Z. (2005**). Effect of bio-fertilizers, nitrogen sources and levels on vegetative growth characters, yield and quality and oil yield of sweet fennel. Ph.D. Thesis, Fac. Agric. Cairo Univ., Egypt.
13. **Farrell, K.T. (1988)**. Spices, Condiments and Seasonings. AVI Publ. Westport, CT., pp: 106-109.
14. **Fawzy, Z.F., Hoda, A. Mohamed and M.M. Abou El Magd (2006).** Evaluation of some sweet fennel cultivars under organic fertilization. Egypt. J.of Appli., Sci., 21(1): 232-244.
15. **Kandil, M.A.M.H. (2002).** The effect of fertilizers for conventional and organic farming on yield and oil quality of fennel (*Foeniculum vulgare* Mill.) in Egypt. PhD. Thesis, Technischen Universitat Carolo-Wilhemina zu Braunschweig - Germany.
16. **Klute, A. A. (1986).** Methods of Soil Analysis. American Society of Agronomy, Part 1, Madison.
17. **Masada, Y. (1976)**. Analysis of essential oils by gas chromatography and mass spectrometry. Copyright by the Hirokawa Publishing company, INC printed in Japan.
18. **Osman, Y. A. H (2009).** Comparative study of some Agricultural treatments effects on plant growth, yield and chemical constituents of some fennel varieties under Sinai conditions. Research Journal of Agriculture and Biological Sciences, 5(4): 541-554.
19. **Page, A. L.; R. H. Miller and D. R. Keeny (1982).** Methods of soil Analysis Part II. Chemical and microbiological properties (2nd ed.) Amer. Soc. Agron. Monograph No. 9, Madison-Wisconsin. U.S.A.
20. **Pascale, S. D. and Barbieri (1995).** Effect of soil salinity from long term irrigation with saline sodic water on yield and quality of winter vegetable crops. Sci. Hort., 64:145-157.
21. **Sadanandan, A. K.; K. V. Peter and S. Hamza (2002).** Role of potassium nutrition in improving yield and quality of spice crops in India. Haryana and International Potash Institute, Switzerland, pp: 445-454.
22. **Simon, J. E. (1990).** Essential oils and culinary herbs, p. 472-483. In: J. Janick and J.E. Simon (eds.). Advances in new crops. Timber Press, Portland, OR.
23. **Snedecor, W. C. and W. G. Cochran. (1980).** Statistical Methods. 7 th ed., 2 nd printing. The Iowa State Univ. Press, Ames, Iowa, U.S.A.
24. **Sudeep, S.; G.S. Buttar and S. P. Singh (2006).** Growth, yield and heat unit requirement of fennel (*Foeniculum vulgare*) as influenced by date of sowing and row spacings under semi arid region of Punjab. Journal-of-Medicinal-and-Aromatic-Plant-Sciences. 2006; 28 (3): 363-365.
25. **Watt, A. and B. Breyer (1962)**. The medicinal and poisonous plants of southern and eastern Africa. Edinburgh: Livingstone.
26. **Wichtl, M. and N.G. Bisset (1994).** Herbal drugs and phytopharmaceuticals (ed), Med. Pharm scientific Publ Stuttgart, pp: 107-108.
27. **Yadav, B. D.; S. C. Khurana; K. K. Thakral and Y. S. Malik (2000).** Effect of sowing dates and planting methods on quality of seed produced by different order umbels in fennel . Haryana-Journal-of-Horticultural-Sciences, 29 (1/2): 108-110.
28. **Zaki, M. F.; Abou Hussein; Abou El-Magd, M. M.and H. M. H. El-Abagy (2009)**: Evaluation of some sweet fennel cultivars under saline irrigation water. European Journal of Scientific Research, Vol.30 No.1 (2009), pp: 67-78.

4/1/2010

An Expertise Recommender System for Web Cooperative Production

Muhammad Aslam[1], Ana Maria Martinez Enriquez[2], Muhammad Tariq Pervez[3], Zakia Saeed[4]

[1]Department of CS & E, U.E.T., Lahore, Pakistan
[2]Department of CS, CINVESTAV-IPN, Mexico
[3]Department of CS, Virtual University Shadman Campus, Lahore, Pakistan
[4]Faisalabad Institute of Cardiology(FIC), Faisalabad, Pakistan
tariq_cp@hotmail.com

Abstract: This paper focuses on providing dedicated expertise recommender system to enhance awareness among group members, working in a distributed cooperative environment. Normally, coauthors lack the information about the production capabilities of their colleagues. As a result of this lack, when they need assistance for the production of complex objects (formulae, figures, style sheets, etc.) they ask their colleagues for help, consequently the authoring process is disturbed. On the other hand, personal referrals may not be useful due to human biasing, liking, and disliking. The existing expertise recommender systems work on user profiles containing user qualification, experience, and history of solved problems. These systems require manual database updation which can be performed by only skilled person. We treat the issue by developing an expertise recommender system which is in-charge to seamlessly observe user activities and to auto detect a possible human expert of elaborated productions on the basis of a generic criterion. Whenever, a participant is deduced as a novice having some production problem, the developed system recommends him/her the presence of an expert with whom the novice can communicate. The entire goal is to enhance awareness coordination among collaborator activities and hence to generate a consistent shared production. [Journal of American Science 2010;6(7):106-112]. (ISSN: 1545-1003).

Keywords: Knowledge based systems, presence awareness, collaborative information filtering, recommender systems.

1. Introduction

In the term of Computer Supported Cooperative Work (CSCW), the CS interpretation deals with the design and development of suitable computer systems, including both hardware and software, to support the work produced by a group of people, distributed over local or wide area networks whereas, the CW interpretation concerns with the fundamental concepts of those disciplines that study the ways people work in groups. These fields are sociology, psychology, ergonomics, organizational theory, and management sciences. Thus, CS enforces technical requirements of such environment whereas CW emphasizes social factors of group users (Grudin, 1994) (Schmidt and Bannon, 1992).

In order to produce in groups, users are assigned roles and designated tasks. While assigning roles and tasks, knowledge and expertise level of each participant is taken into account. In a scenario, if a group member has to perform a task in which he has little or almost no experience he may frequently disturb his colleagues asking for assistance. This disturbance, not only affect the user efficiency but also affects the cooperative production process.

The assistance provided to users depends upon their familiarity with the system, the nature of problem, time constraints to complete the task, and so on. These factors give reasons to highlight four kinds of assistance like quick reference, task specific help, full explanation, and tutorial. All these supports require users to have some knowledge to put inquiries, their proper formats, syntax and semantics. These requirements may frustrate users loosing their interest in the actual task (Babin et al., 2009). Users are assisted by means of *wizards* that guide a user step by step to complete the task. The user can perform complex tasks safely, quickly, and accurately. However, wizards may constraint with some information that user may not have (Gutwin and Greenberg, 2002). An assistant is software tool which observes the sequence of user actions on the basis of which suggestions or hints are given to complete the task.

User can hide the assistant any time. But, this kind of help becomes irritating for its users as an assistant interrupts user work unnecessarily unless disabled.

On the other hand, the CSCW systems have no function integrated into them by means of which a user can be detected when he is in problem. Additionally, if a user faces a difficulty in common production, no information is provided to him/her about his/her participants who can assist in solving the problem. Thus, he/she leaves with no other means to use personal referrals to complete the tasks. Such references have their own limitations: human biasing, personality clashes, liking, and disliking.

Thus, it is needed to improve inter user assistance by automatically deduction of their expertise and the notification of available tools and human experts who help a beginner to reach their objectives. The investigated problem and the provided solution take place as part of the presence awareness. The developed system qualifies the user production on the basis of predefined criteria and deduces a user as possible expert. We validate our approach in designing and prototyping in a distributed coauthoring application that allows users to produce shared structured documents.

Expertise Recommender (ER) (McDonald and Ackerman, 2000) assists the user in trouble and makes a request by giving the area for expertise (e.g. technical support, programming development support), the choice from social network (e.g. students, professors, advisers) and the error code produced by the compiler. Users have the possibility to access the database of experts, and know their status. In this way, users can contact these experts, taking into account the topic area and "social network" level. The Expertise Finder (EF) (Hughes and Crowder, 2003) uses the record of the organization and the knowledge of the people to recommend the expertise. It provides a list of the documents and the experts with their contact numbers. Dynamic Expertise Modeling from Organizational Information Resources (DEMOIR) (Yiman and Kobsa, 2000) develops and tests expertise modeling algorithms. It recommends the documents and the experts that are locally or remotely available.

We present materials and methods of the expertise recommender system in Section 2. Section 3 presents results and discussions. Finally, we conclude our research (Section 4).

2. Materials and Methods

The developed system, Presence Awareness Recommender System (PARS) helps in finding experts and assists the beginners to complete their work. In the studied test bed application (Decouchant et al., 2001), the writing actions performed by authors on the produced document are captured in the form of events by means of a Distributed Event Management Service (DEMS) (Decouchant et al., 2002). An event represents a state change of a shared entity. A shared entity may be a document, hardware/ software, and participants. However, many actions not necessarily cause a change within a resource, such as select and copy or highlight any part of the document, and they are also perceived as events. DEMS acts as a communication mechanism between the producer and consumer applications of events. A producer generates events and can be configured for extending or restricting broadcasting of some events depending upon their scope. A Consumer subscribes to DEMS to receive events. There are some rules to filter events by category and their sources. When an author wants to stay intensively focused on his/her production, he/she may allow those events to be received which are resulted from coauthors who annotate the part of document he/she produces, whereas, other event notifications are restricted. Producers and consumers are uniquely identified by DEMS to control the event broadcasting, and different meta-data is associated to events:

- Entity user who produces events (login, his ID, the working site from where the user works, as well as the cooperative application).
- Entity resource within the cooperative environment (text, figure, formulae).
- Entity action is any performed action within the environment using cooperative application.

For example, in an event: galaxy_tito_ writing-editor_MathML_select, “tito” user works from the “galaxy” site, and selects a mathematical statement. Due to the “select” action DEMS identifies who is on line and his working site.

The developed system, an event consumer, uses rules written in the first order predicate logic. A rule is composed of the premise and the action part. The premise part consists of facts like performed action, user authoring role, nature of produced object. In the action part, the system deduces new knowledge or trigger actions to provide a dynamic user environment. When a user starts a session, the system is automatically

launched until session is closed. It follows these steps: a) information catching, b) the deduction of new facts, and c) the proposition of actions (Martinez et al., 2002).

Our authoring application uses MathML (Carlisle et al., 2003) to write, represent, and interpret mathematical statements. Specific events are generated during the production or selection of an expression. As a result of selecting, the author is notified about whether a formula is well-structured (wsf), implicit contextual functions related with (keyboard shortcuts), rewriting it as infix, prefix, or postfix form. In our approach, a criterion is established to evaluate the complexity of a formula that can be modified by editing the specific rule. A weight to the following steps is assigned (see Table 1):

- the way by which it is created: a sequence of symbols or by using the menu,
- steps taken to produce it: sequence of characters from the standard input (keyboard) or using menus dialog boxes or palette,
- elapsed time to complete it.

Weights assigned to a constant and a variable. These values are used to calculate the associated complexity of each MathML structure. Due to the different roles played by users within the cooperative environment, the evaluation of the collaborative production is necessary. Taking into account this evaluation, the developed system qualifies a user as an expert, so it is a dynamic evaluation.

3. Results and Discussions

3. 1. Evaluation of Mathematical Expressions

The evaluation refers to the analysis concerning: a) the kind of elements included in the shared document: text, tables, links, formulae, graphical. For instance, a figure is defined by the vertical and horizontal alignment, its appearance, etc. b) the number and the complexity of these elements, and c) the elapsed time to produce them. In the case of the mathematical production, the evaluation is based on: a) the number of well-formed formulas produced and their associated production complexity, b) the elapsed time to produce them, and c) the performed actions during their production (undo/redo, copy/cut/paste, etc.). Once a formula is concluded, the system verifies if it is well-structured formula (wsf). A MathML formula is said to be WSF if all components of MathML structure/pattern are filled a well-formed formula in mathematical context. Afterwards, its complexity is calculated.

a. The Complexity of a Formula

The complexity of a formula depends on the way by which a formula is created (either using "Type Menu" or "Math" icon), the steps taken, and the elapsed time to complete it: number of times the "type menus" are selected, as well as the math dialog box, and the math palette are used (see Table 1). A MathML pattern can be characterized by the number of components to be fulfilled:

- Single Component (e.g. square root). The complexity is equal to the complexity of the single component base expression, multiplied by 1.5. For instance, giving expression 1, and applying the rules #1, #2, #3, #4, #5, #9 and #10 from Table 1, the resultant complexity is 17.40.

$$\sqrt{x^2 - 2*x*y + y^2} \qquad \text{....1}$$

Table 1: Complexity of mathematical expressions

MathML Pattern	Rule No.	Complexity	MathML Pattern	Rule No.	Complexity
Constant	1	1.0	x_y	8	comp (x) + comp (y) + 0.8
Variable	2	1.5	x^y	9	comp (x)+comp (y) + 1.0
$x+y$	3	comp (x) + comp (y)	$\sqrt{x}$	10	comp (x) * 1.5
$x-y$	4	comp (x) + comp (y)	$\sqrt[y]{x}$	11	comp (x)+comp (y) * 1.8
$x*y$	5	comp (x) + comp (y) + 0.3	$\int_x^y z dz$	12	(comp (x)+comp (y)) * comp (z)
$x=y$	6	comp (x) + comp (y)	$\sum_x^y z$	13	((comp (x)+comp(y)) * comp (z)) + 1.5
$\frac{x}{y}$	7	comp (x)+comp (y) + 0.5	$\prod_x^y z$	14	Comp (x) * comp (y) * comp (z)

- Twofold component (e.g. fraction, under root). The complexity depends on the basic expression associated to the pattern as we see in Table 1, rules #7, #8, #9, and #11. The complexity of Expression 2 is 23.58.

$$\sqrt[x]{x^2 - 2*x*y + y^2} \qquad \ldots.2$$

- Threefold component (Sub-superscripts, and under-overscripts). The complexity of these patterns is related to the complexity of the "z" base component, (rules #12, #13, and #14 from Table). The computed complexity of Expression 3 is 10.00.

$$\int_1^4 3*x^2 dx \qquad \ldots..3$$

The complexity of a formula is calculated by the following rule:

```
Startrule "Computing complexity"
If author(fragment_1) = x
   role(x) = "Writer"
   nature(fragment_1) = "formula"
   update(fragment_1) = "true"
   evaluate_wff(fragment_1) = "true"
                              /* formula is wff */
Then
   announce(x)                <-
computed_complexity(fragment_1)
       /*Complexity of the formula is calculated */
Endrule
```

A user can ask the system explicitly to calculate the production complexity of a generated formula. Table 1 establishes the complexity of basic expressions, and these patterns are given as input data to the system, thus, it is possible to change these values without modifying the code of the system. We argue that this is dynamic criteria and can be updated as desired. In addition to complexity, other factors are also considered to evaluate the user's production.

b. Undo/Redo Actions

We performed an experiment with 10 users, 5 of them had knowledge how to write elaborated large documents (expert). We asked them to reproduce some formulas, like binomials, integrals, and quadratic ones. In our experiment, experts performed 20 actions and reverting 2 actions on the average to produce expression 4. While, beginners generated same expression with 38 actions while reverting 18 actions on the average. The counted actions are: starting of the formula (selection of "Math" button), insertion of each pattern (square root, superscript, etc.), positioning the cursor in the pattern, producing the greek letters from math palette, and insertion of each number, identifier, and operator from the standard input (keyboard).

$$\frac{-b \pm \sqrt{x^2 - 4*a*c}}{2*a} \qquad \ldots4$$

The following rule is applied to count do/undo/redo actions:

```
Startrule "Actions-time-size"
If action(x) = "start_formula"
   nature(fragment_1) = "formula"
Then
total_actions(x)<- start_count_total_actions(x)
                              /* actions are counted */
undo_actions(x)<-start_count_undo_actions(x)
                    /* reverted actions  are counted*/
init_time(fragment_1)<-reg_curr_time(fragment_1)
                     /* Starting time is recorded */
initial_size(doc)<-reg_init_size(doc)
                     /* doc initial size is recorded*/
Endrule
```

When a user starts a formula, the number of reverted actions, the current system time and the size of the document are registered. This information helps to evaluate the user production when he/she conclude the expression. When a user reverts more than half of his/her actions, he/she is notified of presence of experts with whom the former can communicate with.

When users produce a formula, their performed actions are observed, if they are in trouble, the system proposes them to contact experts using synchronous communication. The well-formed formulas produced within a shared document during a session are counted by another rule. Depending on the number of produced well-formed expressions and their complexity, the system can classify a user as a possible expert in writing expressions (see Section 5).

c. Elapsed Time

The time during which a user writes a well-formed expression in one session, without performing other activities is the "elapsed time". This time is calculated by taking the difference between the registered time (the "Actions-time-size" rule) when a user starts to produce a formula and when he/she completes it. The system memorizes the time when the formula is concluded. The following rule is applied:

```
Startrule "Final time-Final size"
If author(fragment_1) = x
   role(x) = "Writer"
   nature(fragment_1) = "formula"
   update(fragment_1) = "true"
Then
```

```
   final_time(x) <- register_current_time(x)
                              /* the time is recorded */
   final_size(fragment_1) <-
                          reg_final_size(fragment_1)
                                 */ size is recorded */
elapsed_time(x) <- final_time(x) - initial_time(x)
                       */elapsed time is computed */
calculate_change_size(fragment_1) <-
   final_size(fragment_1) –
                          finitial_size(fragment_1)
                    /* change in size is computed */
Endrule
```

From the group of 5 experts and 5 beginners, we studied that initially the beginners were spending more time to insert mathematical patterns (fractions, exponents, subscripts, etc.). The duration was decreased when the expertise was grown to insert data and produce elaborated expressions. The observed average spent time was:
Production time (seconds)= a*(no. of mathematical patterns)+ b*(no. of greek letters)+ c*(characters from standard input)+ (elapsed time for the selection of menus, math box, math palette, and position to insert characters), where, a=b=5, c=2.
These values were obtained according to the experimentation. We observed that experts take less than 5 minutes (average) to produce a formula containing mathematical patterns and greek letters (e.g. quadratic formula). Therefore, when a user spends more than 10 minutes to produce a formula, whose complexity is less than 16, he/she is informed about the existence of an expert. The following rule applies:

```
Startrule "Large elapsed time"
If  author(fragment_1) = x
    nature(fragment_1) = “formula"
    update(fragment_1) = "true"
    elapsed_time(x) > 10   /* time in minutes */
     computed_complexity(fragment_1) < 16
     status_open(authors_definition_db) = "true"
Then
    announce(x) <- MathML_expert_exists"
Endrule
```

The results obtained in the experimentation made for producing mathematical expressions is shown in Table 2. The produced formulas, their complexities, and the elapsed time by each expert and beginner are presented. The average spent time of experts and beginners is computed. For instance, to produce a quadratic formula (at serial 2), experts spent 97 seconds on average whereas beginners took 625 seconds.

Table 2: Time elapsed by experts and beginners

Expressions	Production Complexity	Time spent by Experts (sec) / Time spent by Beginners (sec)					Average time spent (E /N)
		E1/N1	E2/N2	E3/N3	E4/N4	E5 / N5	
$a^2 - b^2$	8.0	14/142	15/90	18/80	14/65	14/150	15/102
$\frac{-b \pm \sqrt{x^2 - 4*a*c}}{2*a}$	16.6	177/734	40/617	96/540	83/616	91/617	97/625
$\sum_{n=0}^{\infty} a_n * t^n$	16.2	118/526	70/430	80/152	91/420	86/223	89/350
$\int_{-\Pi}^{\Pi} f_N^2(x)dx$	26.0	135/425	70/356	104/183	109/265	99/225	103/290
$n! \sim \sqrt{2*\pi} * n^{\left(n+\frac{1}{2}\right)} e^{-n}$	21.7	93/360	65/282	73/125	79/124	89/221	80/222
$e^{-C*x} \frac{1}{x} * \prod_{n=1}^{+\infty} \frac{e^{\frac{x}{n}}}{1+\frac{x}{n}}$	50.6	100/585	102/425	121/747	113/494	111/280	109/506
$\int_a^b (1-t)^{x+y-1} \left(\frac{t}{1-t}\right)^x dt$	45.0	122/ 495	85/430	104/670	117/398	113/722	106/543

d. Evolution of the Production

The size of the shared document is registered when: 1) a user starts to produce a formula, and 2) he/she completes a well-formed version. The difference between registered sizes gives the variation in the size of the production in bytes. When an expert generate a formula, the document's size gradually increases, whereas, the change in size was very slow when a beginner produces it.

In our study, the average increased size is approximately 50 bytes per minute in case of expert's production whereas a beginner produces less than 15 bytes per minute. Thus, when the difference in size of the production is less than 10 bytes per minute, the user is asked if he/she is in trouble.

We emphasize again that knowledge/rule base of our PARS recommender system is entirely independent of its code. The weight/values like production weights in Table 1, related complexity, number of WSFs, the complexity of an expression used for bench mark, etc. can be seamlessly changed to any new value.

e. Expert Presence Awareness and Assistance

"*The information about the presence of collaborators, their attitudes during a communication session, when they are busy and how frequently they produce objects of a particular nature*" (Gutwin and Greenberg, 2002) is defined as presence/social awareness. The PARS system continuously observes the user actions. Whenever, it concludes based on irrelevant/undo actions, document evolution, errors, complexity that a user is in trouble, it notifies him/her about the presence of experts. The notification box offers three buttons: - "Information" to get data about expert like: login name, working site, and availability; - "Contact" to synchronously communicate with them; and - "Cancel" to close the notification box.

In a scenario, Stephan performs irrelevant and undo actions frequently while producing a mathematical formula. The PARS system informs him/her the expert existence, Paul who normally produces mathematical expressions. Stephan may start a communication session with him, and ask how to produce a quadratic expression, as we see in Figure 2. By means of the synchronous communication, offered by our PARS system, Paul explains Stephan step by step how to do it.

Once Stephan finishes the formula, he can send its position within the shared document, by selecting the formula. It means, a) the DEMS service captures the selection event and recovers the unique identifier(s) of the selected section(s): "focus of discussion"; b) using this unique identifier, the developed system displays the "focus of discussion" into all concerned coauthor's environments (Martinez et al., 2002). When the nature of the fragment that a user produces, does not match with his/her common production, he/she is also informed about the existence of experts. Following, we explain how to define experts.

A user who produces elaborated figures, well-formed formulas, and continuously adds different kind of elements, can be considered as an expert. He/she avoids loss of recent changes by saving the document after a gradual period of time By contrast, beginners take a lot of time to perform a simple task doing irrelevant and unnecessary actions because they do not know how to proceed. When a coauthor produces five well-formed formulas in the same session (dynamic evaluation) and the complexity of each one is greater than 16, he/she can be considered a writing mathematical expert. The following rule is applied:

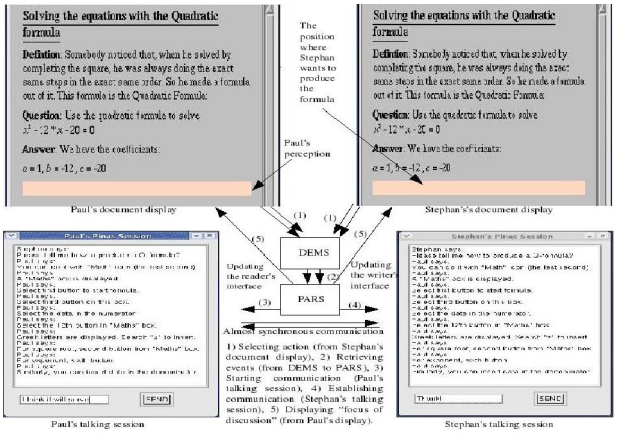

Fig: 2: The discussion between an expert and a beginner

```
Startrule "Defining expertise on writing formulas"
If author(fragment_1) = x
    role(x) = "Writer"
    nature(fragment_1) = "formula"
    update(fragment_1) = "true"
     complexity(fragment_1) > 16 /* from Table 1 */
    summary_wff(formula) > 5
                              /* formulas are counted */
    status_open(authors_def_data_base) = "true"
                               /* author's file is open */
Then
   author_definition(x) <==  "expert_Math"/*
                    'x' is an expert in writing formulae*/
Endrule
```

The expertise of a user is saved in the user definition database, as well as, his/her login, user name, working site, and the availability to communicate with. Precise information of an ad hoc expert is suitable information, in case of trouble.

4. Conclusion and Future Perspectives

In order to provide a friendly cooperative working environment to users, it is necessary to inform them the productiveness of their colleagues. The productivity of users on writing mathematical formulas can be determined on predefined criteria. By means of this evaluation, the developed expertise recommender system defines a user as a possible expert. The evaluation criteria can be modified at any time in the rule base interpreted by the system. It enhances presence awareness by notifying the presence of experts to users in trouble. Users can communicate with experts to ask for assistance and hence, they can coordinate their activities.

In future, we intend to establish criteria to evaluate the graphical production. For this purpose, the history of the different versions of the shared documents will be necessary, in order to determine the evolution of the graphical objects.

Acknowledgements:

Authors are grateful to the Department of CS & E, UET, Lahore, for financial support to carry out this work.

Corresponding Author:
Muhammad Tariq Pervez
Department of CS, Virtual University,
Shadman Campus, Lahore, Pakistan
E-mail: tariq_cp@hotmail.com

References

1. Babin L. M.,Tricot A., Mariné C., “Seeking and Providing Assistance While Learning to Use Information Systems”, Journal. of Computers & Education. 2009; 53: 1029–1039.
2. Carlisle, C., Ion, P., Miner, R., Poppelier, N., “Mathematical Markup Language MathML Version 2.0 (2nd Ed.)", W3C, 2003.
3. Decouchant, D., Favela, J., Martínez Enriquez A. M. “PIÑAS: A Middleware for Web Distributed Cooperative Authoring”, SAINT,2001;187-194.
4. Decouchant, D., Martínez, A. M., Favela, J., Morán, A. L., Mendoza, S., Jafar, S., “A Distributed Event Service for Adaptive Group Awareness”, MICAI’LNAI 2313, Mexico, Springer-Verlag, 2002;506–515.
5. Grudin, J., “Computer Supported Cooperative Work: History and Focus", IEEE Computer, 1994;7(5):19-26.
6. Gutwin, C., Greenberg, S., “A Descriptive Framework of Workspace Awareness for Real-Time Groupware", CSCW, 2002;11(3-4):411-446.
7. Hughes, G., Crowder, R., “Experiences in Designing Highly Adaptable Expertise Finder Systems", Proc. of DETC'03, USA, Sep. 2-6, 2003.
8. Martínez, A. M., Muhammad, A., Decouchant, D., Favela, J., “An Inference Engine for Web Adaptive Cooperative Work”. MICAI’2002;526–535.
9. McDonald D. W., Ackerman M. S., “Expertise Recommender: A Flexible Recommendation System and Architecture", ACM CSCW, P.A., 2000; 231-240.
10. Rizzi, C. B., Alonso, M. C., DE Seixas, L. M. J., Costa, J. S. Tamusiunas, F. R., DA Rosa Martins, A., “Collaborative Writing via Web - EquiText", Informatic Education, 2000.
11. Schmidt, K., Bannon, L., “Taking CSCW Seriously: Supporting Articulation Work", CSCW: An Int. J, 1992; 1(1):7-40.
12. Yiman, D., Kobsa, A., “DEMOIR: A Hybrid Architecture for Expertise Modeling and Recommender Systems", IEEE 9th International WET ICE'00, Mar. 14-16, 2000.

08/04/2010.

Impact Of Emission Uniformity On Nutrients Uptake And Water And Fertilizers Use Efficiency By Drip Irrigated 15 Years Old Washington Novel Orange Trees Grown On A Newly Reclaimed Sandy Area.

EL-Hady O.A[1]., S.M.Shaaban[2] and A.A.M., Mohamedin[3].
[1]Soils & Water use Dept. National Research Centre, Cairo, Egypt
[2]Water Relations and Field Irrigation Dept. National Research Centre, Cairo, Egypt
[3] Field Drainage Dept., Soils, Water and Environment Research Institute, Agriculture Research Center, Giza, Egypt
dr_mona_zaki@yahoo.co.uk

Abstract A two successive years (2008- 2009) completely randomized field experiment with four replications on ≈ 15 years old Washington novel orange trees was conducted in a drip irrigated newly reclaimed sandy area at Wadi El- Mollak, Ismailia governorate. Field emission uniformity (Eu) and absolute field emission uniformity (Eua) were determined for the area under study to be 85.6% for Eu and 86.8% for Eua. The irrigation system at the studied area could be considered as good. Although the uniformity of irrigation at the area under sandy has exceeded 85%, great differences were estimated between the discharge of the drippers that adversely affected the uniformity of growth, nutrients uptake, yield and both water and fertilizers use efficiency by the trees. With this respect, differences among the annual amounts of irrigation water received by the trees and consequently fertilizers dissolved in it have reached 43.1%. accordingly, significant variations were calculated to be 27.8% for leaf area, 26.7% for the dry weight of the leaves and 40.6% for obtained yield. Content of nutrients in the leaves of trees that received the maximum amount of irrigation water were higher than those of trees that received the minimum amounts by 18.3, 22.0, 25.8, 18.4 and 30.4% for N, P, K, Ca and Mg, respectively. Consequently, relative uptake of these nutrient took the same trend. Positive differences in this parameter were 45.3, 49.0, 51.8, 46.6 and 56.4% for the aforementioned nutrients, respectively. Values of water and fertilizers use efficiency by the trees were also greatly affected by the uniformity of irrigation. Higher amounts of irrigation water and applied fertilizers adversely affected both parameters. Improving the uniformity of emission of the trickle irrigation system to be more than 90% will lead to uniform fertigation. Uniform production (quantity and quality of fruits for each tree) is expected. [Journal of American Science 2010; 6(7):113-119]. (ISSN: 1545-1003).

Key Words: Trickle irrigation, Field emission uniformity, Sandy soil, novel orange, Water use efficiency, Nutrients uptake, Fertilizers use efficiency.

1. Introduction

For any irrigation system, the uniformity and efficiency of using both water and fertilizers by growing plants are of the major importance. Ideally, the application of water throughout the system should be absolutely uniform. With trickle irrigation, each dripper should deliver exactly a predetermined amount of water (Vermeiren and Jobling, 1980). Actually, drip irrigation system is not completely uniform. The variation or non –uniformity of emitter discharge in such irrigation system is the result of number of factors. The most important of these factors are the hydraulic variation and emitter discharge variation, (Bucks et.al., 1982). The hydraulic variation along the lateral line and sub main manifold is a function of land slope, length and diameter of the pipe and emitter discharge relationships. Emitter discharge variation at a given operating pressure is caused by manufacturing variability, and emitter plugging either complete or partial (Abou Khaled, 1982 & 1991; Bralts & Kesner, 1983 and Bralts et.al., 1985).

In Egypt, most of the newly reclaimed areas are planted with fruit trees under drip irrigation. Due to the variation in the amounts of irrigation water received by the growing trees in the same sub unit, growth, nutrients uptake, fruit yield and consequently both water and fertilizers use efficiency by the trees varied also from one tree to another (Ibrahim, 1993; El-Sonbaty & El-Hady, 1993; El-Hady et.al., 1994; El-Hady, 2002 and El-Hady and Abd El-Kader, 2003).

The present work aims at studying the effect of emission uniformity on ~ 15 years old novel orange trees grown in a newly reclaimed sandy area. In this study, the actual amounts of water and consequently fertilizers received by the trees through drip irrigation system were estimated. Nutrients uptake, fruit yield

and both water and fertilizers use efficiency by the trees were evaluated.

2. Material and Methods

A two consecutive years (2008 and 2009) completely randomized field experiment, with four replications for each treatment (Steel and Torrie, 1980) was conducted as follows:

Location: Station no 18, Wadi El- Mollak, Ismailia governorate.

Indicator plant: Fifteen years old Washington novel orange trees.

Soil:

A sandy soil (>80% sand). The main analytical data of the soil determined after Klute, 1986 and Page et.al., 1982 are presented in table 1.

Irrigation system:

Trickle irrigation, distance between laterals is 7m. distance between drippers is 3m. drippers discharge is ≈4 l/hr. number of drippers/ feddan (one fed.= 4200 m^2) are 400 i.e. 2 drippers for each tree.

Irrigation water:

El-Shabab canal water was used. Regarding its quality, it was classified as no problem water (Ayers and Westcot, 1976), Table 2.

Water requirements for the crop:

Water requirements for the crop determined after Doorenbos and Pruit (1977) and Vermeiren and Jobling (1980) are 6000 m^3/fed devided into 3750 hrs. table 3 presents the distribution of irrigation water during the growing season (National Campaign for improving Citrus productivity in Egypt, 2003).

Table 1: Analytical properties of Wadi El- Mollak soil.

1- Mechanical analysis											
Depth cm	Sand		Silt	Clay	Soil texture						
	Course 2000 - 200 µ %	Fine 200-20 µ %	20 – 2 µ %	‹2 µ %							
0-30	47.7	32.3	15.9	4.1	Loamy sand						
30-60	52.5	35.0	9.6	2.9	sand						
2- Chemical analysis											
Depth cm	pH 1:2.5	EC dSm^{-1}	$CaCO_3$ %	OM %	CEC Cmole kg^{-1}	Macro – nutrients (µg g^{-1})					
						Total			Available		
						N	P	K	N	P	K
0-30	7.95	0.65	6.12	0.35	7.9	520	435	770	36	6	65
30-60	8.30	0.40	7.35	0.19	7.3	415	312	546	32	6	58
3- Hydrophysical analysis											
Depth cm	Bulk density Mg m^{-3}	Total porosity %	Water holding capacity* %	Field capacity* %	Wilting percentage*	Hydraulic conductivity m day^{-1}			Mean diameter of soil pores µ		
0-30	1.51	43.0	19.6	6.45	2.55	4.65			13.3		
30-60	1.63	38.5	18.7	5.82	2.36	4.35			12.9		

*On dry weight basis.

Table 2: Analysis of irrigation water used

Source	pH	EC dSm^{-1}	Soluble cations (meq/l)				Soluble anions(meq/l)			
			Na^+	K^+	Mg^{++}	Ca^{++}	CO^{--}_3	HCO^{-}_3	Cl-	$SO^{=}_4$
El-Shabab canal	6.89	0.35	1.91	0.18	2.40	9.0	-	2.2	4.9	6.39

*Adj.SAR = 1.6.

** Fe = traces (<3 µg g^{-1})..

Uniformity of emission:

Irrigation uniformity was determined after Vermeirn and Jobling (1980). the lowest and the highest rate of discharge were 3.143 ± 0.029 and 4.663± 0.032 lh^{-1}, respectively with an average of 3.671± 0.132lh^{-1} (Fig.1). Calculated field emission uniformity (Eu) and absolute field emission uniformity (Eua) using Keller and Karmeli (1975) method were 85.6 and 86.8%, respectively. Talking into consideration that the general criteria for Eu values for systems which have been in operation for one or more seasons are greater than 90% excellent; between 80 and 90%, good; 70 to 80%, fair and less than 70%, poor (Merriam and Keller, 1978), the system could be considered good.

Table 3. Water requirements for 15 years old* trickle irrigated novel orange trees grown on a sandy soil at Wadi El- Mollak, Ismailia governorate.

Growth period	months	Average number of hours of daily irrigation	Gross irrigation requirements	
			l day^{-1}/tree	
management practices winter.	December January	6 6	48 48	≈ 30 m^3/tree /year
The beginning of vegetative growth (spring growth cycle), flowering and the beginning of fruit setting.	February March April	6 9 9	48 72 72	
growth of small fruits until the end of falling.	May June	12 15	96 120	
fruit growth.	July August	15 15	120 120	
Autumn growth cycle and the completion of fruit growth and maturity.	September October November	12 12 9	96 96 72	
Mean		10.5	84	

*Vegetative cover ≈ 70%.

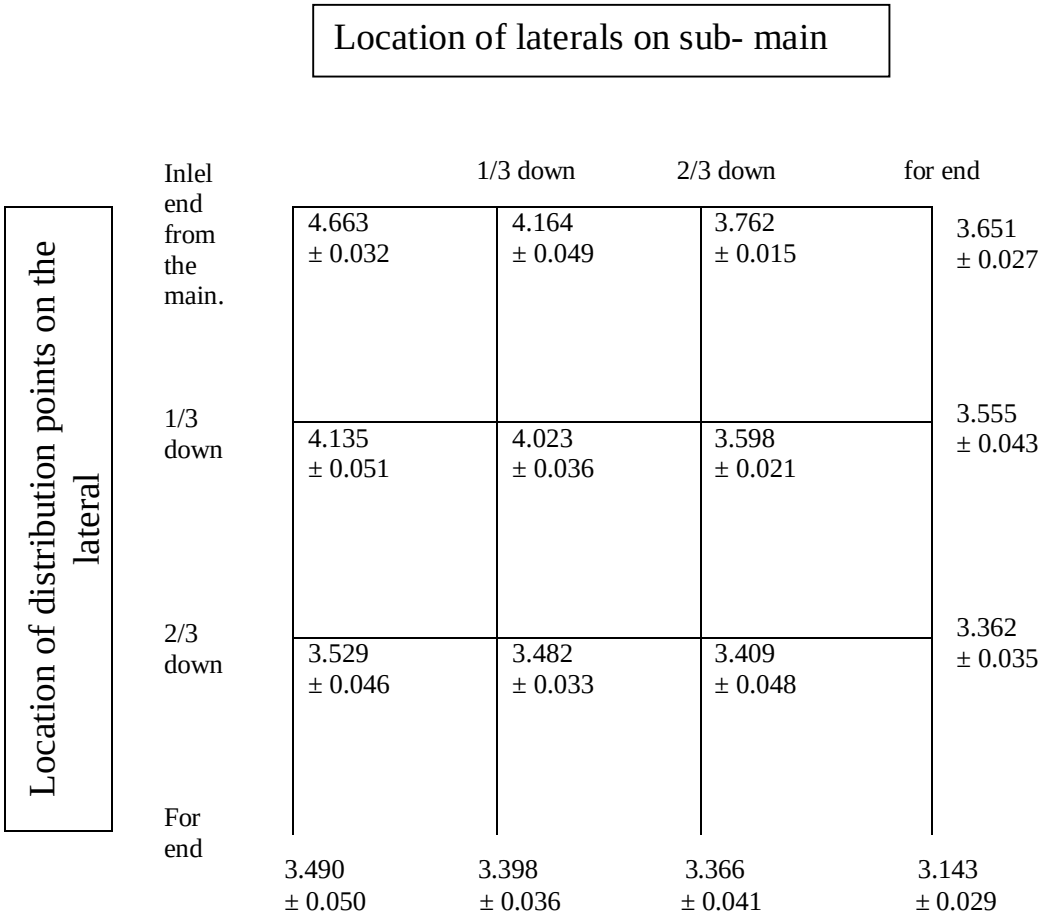

Fig.1. Discharge from selected distribution points (l/h) in the sub-main unit.
Field emission uniformity (Eu) = Minimum rate of discharge (l/hr) x 100/Average rate of discharge (l/h).
Absolute field emission uniformity (Eua) = 1/2[Average of lowest 1/4 of the field data emitter discharge (l/h) / Average of all the field data emitter discharge (l/h) + Average of all the field data emitter discharge (l/h) / Average of highest 1/8 of the field data emitter discharge (l/h)] x 100.

Fertilization:

1. Basal dose

Farmyard manure; superphosphate 15.5% P_2O_5, agricultural sulphur and potassium sulphate 48-52% K_2O at the rate of $20m^3$, 100kg, 100kg and 50kg /fed, respectively during January.

2. Fertigation

Ammonium nitrate 33.5% N, calcium nitrate 15.5% N, phosphoric acid 50% P_2O_5, potassium sulphate 48-52% K_2O and magnesium sulphate 33.3% MgO at the rate of 300, 150, 32, 200 and 20 kg/fed were distributed along the growing season beginning from 15th of February.

3. Foliar

Micro nutrients were sprayed thrice as chelates at the rate of 100, 100 and 200g of respectively, Mn (EDTA) 13% Mn, Zn (EDTA) 14% Zn and Fe (EDTHA) 6% Fe +1kg urea/600l just before flowering (February and March), after fruit setting (April) and during the period of fruit maturity (September), respectively.

Other agricultural practices:

The normal ones for novel orange

Choice of experimental units and treatments: Three sets of trees were chosen according to the amount of irrigation water received by the trees i.e. 6.286 ± 0.058, 7.342 ± 0.264 and 9.326± 0.064 l/h for sets no. 1, 2 and 3, respectively. These values correspond to the lowest, the average and the highest discharge of the emitters, in sequence. Each set consists of 24 trees divided into 4 replications. Accordingly, the annual amount of irrigation water received by the trees were 23.972, 28.259 and $36.142m^3$ for the three sets, respectively.

Studied parameters:

a) Some growth parameters that include: 1) Leaf area. 2) Average dry weight of leaves.

b) Content of N, P, K, Ca and Mg in the leaves (Cottenie et.al., 1982) and relative uptake of such nutrients. Leaf area and dry weight as well as leaf analyses were estimated for 6 months old leaves randomly sampled from each tree at the end of fertilization period i.e. 15th of October.

c) Number of fruits/ tree, average weight of fruit and obtained yield/ tree.

d) Water use efficiency by trees expressed as kg of the fruit yield produced by each m^3 of irrigation water used (Hillel, 1971).

e) Fertilizers use efficiency by trees expressed as kg of the fruit yield produced by each unit of fertilizers nutrient used (Barber, 1976).

Experimental design and statistical analysis:

The field experiment was designed in a completely randomized system. Results were statistically analyzed according to Snedecor and Cochran, (1980).

3. Results and Discussion

As the obtained results of both successive seasons were not significantly different, their average was taken into consideration.

Although the basal doses of fertilizers are the same for all trees of the studied area, variations in the amounts of irrigation water and consequently dissolved fertilizers received by trees greatly affect the nutrients uptake, yield and both water and fertilizers use efficiency by the trees. Table 4. presents the annual amounts of fertilizers received by trees through fertigation as affected by emission uniformity.

Table 4. Effect of irrigation uniformity on the amount of fertilizers received by the tree through fertigation (g/tree).

Set No.	N	P_2O_5	K_2O	CaO	MgO
Set 1	524.883	67.864	424.150	89.071	28.282
Set 2	618.750	80.000	500.000	105.000	33.340
Set 3	719.354	102.316	639.480	134.290	42.640

A. Emission uniformity and the nutrients uptake by the trees.

Content of N, P, K, Ca and Mg in the leaves as affected by the uniformity of irrigation are presented in table5. data show that the content of nutrients in the leaves of the trees of set 1 (that receive the minimum amounts of irrigation water) are lower than those of trees of set 2 (that receive the average amounts of irrigation water) by 8.2%% for N, 15.8% for P, 18.0% for K, 3.9% for Ca, and 21.1% for Mg. On the other hand, the content of nutrients in the leaves of trees of set 3 (that receive maximum amounts of irrigation water) are higher than those which receive the average amounts of irrigation water (trees of set 2) by 10.8, 8.4, 10.6, 14.6 and 13.0% for the aforementioned nutrients, respectively.

Taking the leaf area and the average of the dry weight of leaves as growth parameters, data in table 5 indicate that amounts of water delivered to the trees markedly affect such parameters. The higher amounts of irrigation water received by trees are the higher leaf area or average dry weight of leaf. Presented data show that the differences between the leaf area or average dry weight of leaves for set 1 and those of set 3 reached 30.8 or 32.6%.

Table 5. Effect of irrigation uniformity on the relative uptake of nutrients by the trees.

Set No	Average dry weight of leaf (mg)*	Leaf area (cm^2)**	Content %					Relative uptake				
			N	P	K	Ca	Mg	N	P	K	Ca	Mg
Set 1	221	18.01	2.320	0.165	1.670	2.300	0.380	0.513	0.036	0.369	0.508	0.084
Set 2	255	21.12	2.510	0.191	1.970	2.390	0.460	0.640	0.049	0.502	0.609	0.117
Set 3	289	23.89	2.780	0.207	2.178	2.740	0.520	0.803	0.060	0.629	0.792	0.150

* L.S.D. 0.05= 30 ** L.S.D. 0.05= 2.35.

According to the previous presentation of the data, relative uptake of nutrients are also shown in table 5. It is obvious that high quantities of irrigation water delivered to the trees coincide with high relative uptake of the nutrients under study. In other words, while the relative uptake of nutrients of set 1 was lower than those of set 2 by 24.8% for N, 36.1% for P, 36.0% for K, 19.9% for Ca and 39.3% for Mg, the relative uptake of nutrients by trees of set 3 that grown at the same sub- main unit was higher than those of trees of set 2 by 25.5, 22.4, 25.3, 30.0 and 28.2% for the aforementioned nutrients, in sequence.

B. Emission uniformity and yield.

Data of the fruit yield as affected by the uniformity of emission are presented in table 6. It is obvious that uniformity of emission markedly affected the number of fruits per tree and the average weight of the fruit. Consequently, the obtained fruit yields are significantly affected. The positive differences between the yield of the trees which receive the maximum amounts of irrigation water and that which receive the minimum amounts were 21.7, 24.4 and 51.5% for number of fruits per tree, the average weight of fruit and the fruit yield of the tree in kilograms, respectively.

Table 6. Effect of emission uniformity on the fruit yield and water use efficiency by the trees.

	Set 1	Set 2	Set 3	L.S.D 0.05
N	274.2	306.9	333.8	25.1
A	255	255	280	20.0
F	61.700	78.250	93.450	5.120
WUE	2.574	2.769	2.586	

N: Number of fruits/tree.
A: Average weight of fruit (g).
F: Fruit yield (kg/tree).
WUE: Water use efficiency by the tree (kgm^{-3}).

C. Emission uniformity and water use efficiency by the trees.

Values of water use efficiency by the trees expressed as kg of yield produced by each cubic meter of irrigation water used as affected by uniformity of emission are presented in table 6. Data show that the efficiency of water use by trees of set 1 (that received the minimum amounts of irrigation water) were the lowest. Values of water use efficiency by trees of set 1 are lower than those which receive the average amounts of irrigation water, i.e. trees of set 2 by 7.6%. on the other hand, water use efficiency by trees of set 3 (that received the maximum amounts of irrigation water) decreased. Value of water use efficiency by trees of this group (set 3) was 93.4% that of set 2. It seems that the amounts of water delivered to trees of set 3 are much more than that needed for growing the trees. Increments in the yield of this set is not correlated with the increment in delivered water to the trees.

D. Emission uniformity and fertilizers use efficiency by the trees.

Fertilizers use efficiency by the trees expressed as kg of yield produced by each one unit of N, P_2O_5, K_2O, CaO and MgO added through fertigation are presented in table 7. It is obvious that the amounts of water delivered to the trees and consequently fertilizers dissolved in it markedly affect the efficiency of using such fertilizers by the trees. The higher amounts of irrigation water received by trees are, the higher are the efficiency of using added fertilizers. This is true with only nitrogen fertilizers. Presented data (means of two subsequent seasons, 2008 and 2009) show that the negative difference between the value of N use efficiency by trees of set 1 and those of set 3 ≈ 10%. Regarding the other nutrients i.e. P, K, Ca and Mg and as previously mentioned with water use efficiency, high amounts of water delivered to trees of set 3 and consequently dissolved fertilizers in it negatively affected the efficiency of using these nutrients by the trees. With this respect, values of fertilizers use efficiency by trees of set 3 were lower than those of set 2 by ≈ 7%.

Table 7. Effect of emission uniformity on fertilizers use efficiency (g fruit yield/ g nutrient) by novel orange trees.

Fertilizer Nutrient	Set 1	Set 2	Set 3
Nitrogen	0.118	0.126	0.130
Phosphorus	0.909	0.978	0.913
Potassium	0.145	0.157	0.146
Calcium	0.693	0.745	0.696
Magnesium	2.182	2.347	2.192

Presented data indicate that uniformity of emission and consequently fertilizers application through trickle irrigation system greatly affect either the productivity or the nutritional status of the area. Although the uniformity of irrigation at the area under study has reached about 87%, great differences were estimated between the discharge of the drippers, that adversely affect the uniformity of growth, uptake of nutrients, obtained yield and water and fertilizers use efficiency by trees.

Various investigators have recommended that values of Eu of 94% or more are desirable and in no case should be below 90% (Abou Khaled, 1991, Vermeiren & Jobling, 1980, El- Sonbaty & El-Hady, 1993, El-Hady et.al., 1994, El-Hady, 2000 and El-Hady and Abd El- Kader, 2003). Therefore, care of irrigation system for raising the uniformity of emission to the aforementioned percentage is a must. This will lead to an uniform growth and uptake of nutrients during the growing season and at the same time will raise either the yield (quantity and quality) or both water and fertilizers use efficiency by growing trees.

4. References

Abou Khaled, A. (1982). Irrigation requiements of grapes under drip system in arid regions and performance of system. TF/REM/ 508 (MUL) Field document No. 29 Baghdad.

Abou Khaled, A. (1991). Fertigation and chemigation: An overview with emphasis on the Near East. FAO Consulatation on Fertigation/ Chemigation 8-11 Sept. Cairo, Egypt.

Ayers, R.S. and Westcot, D.W. (1976). Water quality for agriculture. FAO Irrigation and Drainage Paper No.29, 79 p., Rome.

Barber, S.A. (1976). Efficient fertilizer use. Agronomic Research for Food. Madison, WI. USA. Special Publication No 26. Amer. Sos. Agron. Patterson, E.I.ed.: 13-29.

Bralts, V.F. and Kesner, C.D. (1983). Drip irrigation field uniformity estimation. RANS. ASAE, 24 (5), 1369.

Bralts, V.F., Edwards, D.M. and Kesner, C.D. (1985). Field evaluation of drip/ trickle irrigation, sub main units. Proceeding of Third International Drip / Trickle Irrigation Congress. Vol. 1, 274-280.

Bucks, D.A., Nakayama, F.S., and Warrick, A.W. (1982). Principles, practices and potentialities of trickle / drip irrigation. Academic Press. Inc. New York. 1: 219-248. (C.F. Bralts et al., 1985).

Cottenie, A., Verloo, M., Kiekens, L., Velghe, G. and Camerlynck, R. (1982). Chemical Analysis of Plants and Soils. Lab. Agrochem. State Univ. Ghent, Belgium pp. 15-19.

Doorenbos, J., and Pruitt, W.O., (1977). Guidelines for predicting crop water requirements. Irrigation and Drainage Paper, 24, FAO, Rome. 144 p.

El-Hady, O.A., (2002). Water use efficiency by vine grapes grown on a newly reclaimed sandy area as affected by uniformity of emission. Egyptian Soil Science Society (ESSS) 6th Nat. Congress, Oct., 29-30, 2002 Cairo, paper no. O 6-a. and Egypt. J. Appl. Sci., 18(3): 286-296 (2003).

El-Hady, O.A. and A.A. Abd El- Kader (2003). Nutrients uptake and water and fertilizers use efficiency by vine grapes grown on a newly reclaimed sandy area as affected by uniformity of emission. Egypt.J.Soil Sci. 43(4): 577-588.

El-Hady, O.A., Bagdady, G.A. and Hammad, S.A. (1994). Effect of emission uniformity on novel orange trees grown in newly reclaimed sandy soils. Egypt. J. Appl. Sci., 9(4): 480-497.

El-Sonbaty, M.R. and El-Hady, O.A. (1993). Drip irrigation and fertilizers use for Le- Conte pear trees in newly reclaimed sandy soil. J. Agric. Sci. Mansoura Univ. 18 (7), 2128-2136.

Hillel, D. (1971). Soil and Water, Physical Principles and Processes. Academic Press, New York and London, 288 P.

Ibrahim, M.S. (1993). Fertigation and its evaluation in newly reclaimed soil. MSC. Thesis. Fac. Agric., Ain Shams Univ.

Keller, J. and Karmeli, D. (1975). Trickle irrigation design, Rain bird sprinkler Mag. Crop., Glen, (C.F. Vermeiren and Jobling, 1980).

Klute, A.A. (ed.), (1986). "Methods of soil analysis", part 1, 2nd ed. American Society of Agronomy. Inc., publisher, Madison, Wisconsin, U.S.A.

Merriam, J.L. and Keller, J. (1978). Farm irrigation system evaluation. A Guide for Management, 125-143.

National Compagne for improving Citrus Productivity in Egypt (2003). Ministry of Agriculture and Land Reclamation, Academy of Scientific Research and Technology and National Research Centre, Cairo, Egypt, pp.55.

Page, A.L., R.H. Miller and D. R. Keeny (eds.),(1982). Methods of soil Analysis. Part 2.chemical and biological properties. American Society of Agronomy. Inc., publisher, Madison, Wisconsin, U.S.A.

Snedecor, G. W. and Cochran, W. G. (1981). Statistical Methods, 7th ed., Iowa State Univ. Press., Iowa, USA.

Steel, R.G.D. and J.H. Torrie, 1980. Principles and Procedures of Statistics A Biomaterical Approach, 2nd ed. Mc. Grow – Hill Co. N.Y. USA.

Vermeiren, I. and Jobling, G.A. (1980). Localized irrigation: Design installation, operation, evaluation. Irrigation and Drainage paper 36. FAO Rome. 203 pages.

4/1/2010

Physiological Responses of Fennel (*Foeniculum Vulgare* Mill) Plants to Some Growth Substances. The Effect of Certain Amino Acids and a Pyrimidine Derivative

M. E. El-Awadi* and Esmat A. Hassan
Botany Department, Division of Agricultural and Biological Research National Research Centre, Dokki, 12311, Cairo, Egypt.
*el_awadi@yahoo.com

Abstract: In the Green house of the Botany Department (winter season 2007/08-2008/09) fennel seeds (*Foeniculum vulgare* Mill), from Department of Medicinal and Aromatic Plants, were cultivated after 3 hours soaking in the amino acids methionine and tryptophan and in the pyrimidine derivative material (SG93) provided by the Department of The Pharmaceutical Industry, each at 100 and 500mg/l. Growth measurements and chemical analyses of the plant were carried out at juvenile and fruiting stages, i.e. age of 84 and 119 days respectively. The pre-sowing seed treatment with the growth substances; methionine, tryptophan and the pyrimidine derivative (SG93) resulted in significant increases in plant height, number of leaves, number of branches, fresh and dry weight of shoots, number of umbels per plant, weight of seeds per umbel and per plant , in comparison to control. The pre-sowing seed treatments led to an elevation of leaf photosynthetic pigments` content, total protein, total phenolic compounds in the shoots and in the yielded seeds as well as in the percentage of fixed and essential oils as compared to the control. The highest content of the essential oil percentage was obtained as a result of seed-soaking treatment in methionine at 100mg/l concentration. In this connection, anethol represented the major component of such a percentage. [Journal of American Science 2010; 6(7):120-125]. (ISSN: 1545-1003).

Key words: Essential oil, *Foeniculum vulgare,* growth, growth substances, productivity

1. Introduction

Fennel (*Foeniculum vulgare* Mill. *Apiaceae*) is a perennial hemicryptophyte, inhabits the Mediterranean basin is known as a medicinal aromatic herb. Its fruit is used in the remedy against digestive disorders while bitter fennel is used as food flavor, in liqueurs and in the perfumery industry (Tanira, *et al*. 1996). The major volatile (essential) oil of the plant is anethole and fenchone (Simandi *et al*. 1999). Fennel extracts proved to have anti-inflammatory, antispasmodic, carminative, diuretic, expectorant, laxative, analgesic, stimulant of gastrointestinal mobility and are used in treatment of nervous disturbances (Choi and Hwang 2004). Anand *et al* (2008) reported the anticancer activity of fennel seed anthenol.

Growth regulating substances were shown to enhance the biosynthesis of certain chemical constituents in plants. In this respect the amino acids which have a high integrity with different metabolic pools in plants were used to promote plant growth (Coruzzi and Last, 2000). However, S-adenosyl - methionine play a role via the methyl group as a donor to produce estragole and t-anethole in cell-free extracts of the bitter fennel plant (Gross *et al*., 2002). Later, Maxwell and Kieber (2004) indicated the link of methionine to the biosynthesis of growth regulating substances, e.g cytokinins, auxins and brassinosteroids in plants. Whereas the link of tryptophan to the biosynthesis of auxins, the phytoalexin camalexin, phenylpropanoids and other related natural products in plants was recently reported (Tao *et al*. 2008).

Pyrimidine derivatives, which are the building blocks for nucleic acid synthesis, energy sources, precursors for synthesis of sucrose, polysaccharides, and phospholipids, were found to have a role in cellular regulation and biosynthesis of some amino acids and secondary products in plants (Stasolla *et al*., 2003).

This implicated the enhancement of vegetative growth and chemical constituents caused by amino acid treatments in *Pelargonium graveolens* L. (Talaat 2005) and in *Philodendron erubescens* (Abou -Dahab and Abd El-Aziz 2006) and in fennel in our present results.

In our previous investigations, the pyrimidine derivative (SG93) was found to modulate plant growth response of different plant spieces under certain abiotic stresses (Hassasn *et al*., 2006 and El-Awadi, 2007).

In the present study, we aimed to investigate the physiological responses to the amino acids methionine, tryptophan and to the pyrimidine derivative material (SG93) at different concentrations

on growth, productivity and chemical constituents of fennel plants.

2. Material and Methods

The present experiments were carried out using two successive winter seasons (2007/08-2008/09) in the green house of Botany Department, National Research Centre, Egypt.

The effect of the amino acids mthionine, tryptophan and the pyrimidine derivative compound (SG93 – Fig. 1) were investigated on growth, productivity and biochemical constituents of fennel plant *(Foeniculum vulgare* Mill.).

I-Cultivation .and treatments:

Fennel seeds were selected, sterilized in sodium hypochlorite solution (1%) for 15 minutes, washed thoroughly with distilled water, and then soaked in the following solutions for 3 hours:

1- Distilled water (control).
2- In methionine
3- In tryptophan and
4- In the pyrimidine derivative (SG93- Fig.1), provided by the Department of Pharmaceutical Industry of the National Research Centre.

All at 100 and 500mg/l. At 2cm depth, each 10 seeds were sown in pots (30-cm diameter filled with clay and sand; 2: 1 v/v) at the 17th of Nov. Standard agricultural practices were carried out as recommended. Each treatment included 5 replicates = 50 plant. The pots / treatments were distributed following a complete randomized design of distribution.

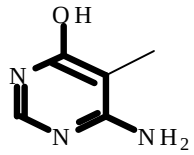

Figure 1: Chemical formula of SG93

II- Growth and yield measurements:

Plant samples were taken at the juvenile stage (age of 84 days) and at fruiting one (age of 119 days).Plant height, number of leaves, number of branches, fresh and dry weight of the shoots were recorded at both stages.

Yield of fennel plant was recorded as the number of umbels per plant, the number of seeds per umbel and per plant and weight of seeds per umbel and per plant.

III- Biochemical analyses:

Photosynthetic pigments were estimated in fresh tissues of fennel leaves according to **(**Wettstein 1957**)**. Protein percentage was determined according to A.O.A.C. (1990). Total Free amino acids were determined using the ninhydrin colorimetric method defined by Plummer (1978). Following the method reported by Snell and Snell (1952), total phenolic compounds were estimated.

Seed fixed oil content, was determined as reported in the (A.O.A.C., 1990) with Soxhelt apparatus using petroleum ether (40-60^{o}C).

The essential oil was extracted from the yielded dry seeds and estimated referring to the British Pharmacopoeia (1980), dehydrated over anhydrous sodium sulfate and then kept at refrigerators (-4^{o}c) till GLC analysis.

Essential oil of fennel seeds was analyzed by GC using a Agilent Technologies, (6890N Network GC system, U.S.A.) using capillary column HP 5% (30 m x 320 Um), 0.25um film thickness. Oven temperature was programmed at 70°C for 2 min. from 700°.190°C at rate of 4 ml/min. and finally 250°C (15 min) with N2: H2: Air at 30:30:300 ml/min. The temperature of the detector (FID) was maintained at 280°C. Identification of the oil components was based on the comparison of the Rts of the separated compounds with those of standard compounds that injected under the same conditions and confirmed for the major compounds by their relative retention indices.

IV- Statistical analysis:

A complete experimental randomized block design with 5 replicates was adopted. Combined results` analysis of the average values of the two seasons was carried out and the values of LSD were calculated as described by Snedecor and Cochran (1980).

3. Results and Discussion

1- Effect on growth and productivity

Data presented in Tables (1and 2) indicated that the pre-sowing seed soaking treatment in the amino acids methionine and tryptophan and in the pyrimidine derivative material (SG93) resulted in the promotion of growth and productivity of fennel plants. Both amino acids each at 100mg/l and the pyrimidine derivative at its high (500mg/l) concentrations caused significant increases in plant height, number of leaves, number of branches, fresh and dry weight of shoots as compared to the control (Table -1). The increases were remarkable at both the juvenile and fruiting growth stages. While observed at lower values, significant enhancement in growth was also obtained with other treatments. Therefore, the maximum effect was gained at the low concentration of each of the amino acids methionine and tryptophan followed by the high concentration

treatment of the pyrimidine derivative material (SG93).

From Table (2) significant increases were obtained in the number of umbels per plant, seed number per umbel and per plant and weight (gm) of seeds per umbel and per plant with methionine seed treatment at 100mg/l in comparison to the control. Similar results were obtained with the tryptophan at its low concentration (100 mg/l) and with the pyrimidine derivative material at its high concentration (500 mg/l).

These results are supported by those previously reported by of Talaat (2005) on *Pelargonium graveolens* L., and Abu-Dahab and Abd El-Aziz (2006) on *Philodendron erubescens.* In addition the pyrimidine derivative under test was found to enhance the growth and productivity of some monocots and dicot plants under certain abiotic stress conditions (Hassan *et al*., 2006) and El-Awadi, 2007).

Table 1: Effect of methionine, tryptophan and the pyrimidine derivative seed soaking on growth parameters of fennel plant at the age of 84 (A) and 119 (B) days.

	mg/l	Shoot length (cm)		No. of leaves		No. of branches		Shoot FW (g)		Shoot DW (g)	
		A	B	A	B	A	B	A	B	A	B
Control	**0**	52.48	67.80	7.56	20.33	4.19	7.84	35.36	16.90	1.30	3.20
Methionine	**100**	58.27	81.97	10.50	24.61	6.54	13.25	39.52	20.61	1.43	3.97
	500	57.04	79.93	10.18	21.73	5.03	11.49	39.41	20.32	1.37	3.85
Tryptophan	**100**	57.78	75.31	10.59	25.93	6.47	10.38	39.34	19.47	1.47	3.50
	500	54.79	75.10	9.28	21.42	5.23	11.83	32.41	18.12	1.30	3.59
Pyrimidine derivative	**100**	54.84	69.92	9.24	22.73	4.37	11.23	43.66	19.71	1.22	3.57
	500	54.99	75.31	10.87	23.41	5.20	12.40	39.36	17.74	1.35	3.24
L.S.D 5%		1.07	1.57	0.58	1.68	0.25	0.43	0.40	1.19	0.10	0.32

Table 2: Effect of methionine, tryptophan and the pyrimidine derivative (SG93) seed soaking on yield characteristics of fennel plant.

	mg/l	No. of umbels/ plant	No. of seeds/ umbel	Wt. of seeds/umbel	Wt. of seeds /plant
Cont	**0**	9.82	108.24	1.43	13.89
Methionine	**100**	10.80	134.21	1.85	19.28
	500	10.09	122.49	1.59	15.88
Tryptophan	**100**	10.61	128.53	1.68	17.05
	500	9.99	115.49	1.52	14.80
Pyrimidine derivative	**100**	10.17	113.88	1.56	15.47
	500	10.78	115.92	1.78	18.41
L.S.D 5%		0.92	5.39	0.15	1.16

In an implication, Tao *et al* (2008) pointed to the enhancement in plant growth as a result of amino acids` conversion to the growth promoter IAA.

2- Effect on chemical constituents:

Results in Table (3) indicated that the pre-sowing seed treatment of fennel in methionine and tryptophan both at 100 mg/l and in the SG93 at 500 mg/l caused significant increases in chlorophyll a, b and cartenoids contents as compared to the control. This was true at both the juvenile and fruiting growth stages. The influence of other treatments appeared to be insignificant.

At the juvenile stage, significant increases in total phenolic contents were recorded with the methionine and tryptophan treatments both at 100mg/l and with the pyrimidine material at 500mg/l. While at the fruiting stage the tryptophan at 100mg/l-seed treatment showed a sole effect (Table-3).

The amount of total protein at the juvenile stage was elevated as a result of all the treatments (Table 3). The significant promotion of protein biosynthesis was obtained at the fruiting stage with the pyrimidine material SG93 and with trypyophan both at100mg/l concentration-seed treatment.

In seeds produced by fennel plant, except with the pyrimidine material at 100mg/l, the total phenolic compounds increased in response to the pre-sowing seed treatments with all the growth factors under test in comparison to control (Table 4).

Table 3: Effect of the amino acids methionine and tryptophan and the pyrimidine derivative material (SG93) on leaf photosynthetic pigments, total phenols and protein content at the age of 84 (A) and 119 (B) days-old fennel pants.

		Ch. A (mg /g f. wt.)		Ch. B (mg /g f. wt.)		Cart. (mg /g f. wt.)		Total phenolic compounds (mg/g d. wt.)		Total protein (mg/g d. wt. equiv.)	
	mg/l	A	B	A	B	A	B	A	B	A	B
Cont	0	0.66	0.79	0.20	0.23	0.30	0.42	5.40	5.44	10.61	16.43
Methionine	100	0.71	0.79	0.24	0.26	0.34	0.45	5.90	4.71	14.56	16.64
	500	0.68	0.82	0.21	0.24	0.32	0.43	5.44	5.21	13.52	16.64
Tryptophan	100	0.70	0.84	0.23	0.25	0.33	0.44	5.48	5.65	12.90	18.72
	500	0.66	0.79	0.21	0.24	0.32	0.41	5.72	5.48	13.10	16.02
Pyrimidine derivative	100	0.67	0.82	0.20	0.24	0.32	0.42	4.61	5.01	15.60	18.10
	500	0.69	0.82	0.23	0.25	0.33	0.44	5.57	5.13	13.52	18.10
L.S.D 5%		0.02	0.04	0.01	0.02	0.02	0.02	0.14	0.09	1.40	1.00

Table 4: Effect of methionine, tryptophan and the pyrimidine derivative (SG93) material on some biochemical constituents of the yielded fennel seeds.

		Essential oil %	Fixed oil %	Total phenolic compounds (mg/g d. wt.)	Major essential oil constituents (%)							
	mg/l				αPinene	D Limonene	1,8 Cineol	Fenchone	Anethol	Estragol(Methyl chavicol)	Known	Unknown
Cont	0	0.79	5.82	1.17	0.37	0.07	5.09	4.13	86.11	0.05	4.18	95.82
Methionine	100	0.78	6.05	1.22	0.36	0.02	4.93	4.13	87.58	0.53	2.45	97.55
	500	1.01	6.49	1.24	0.39	0.11	4.50	4.12	85.61	0.84	4.43	95.57
Tryptophan	100	1.03	5.28	1.21	0.23	0.11	5.72	4.10	87.53	0.18	2.13	97.87
	500	1.06	6.68	1.31	0.33	0.13	6.22	3.70	87.14	0.23	2.25	97.75
Pyrimidine derivative	100	0.89	4.80	1.13	0.34	0.09	3.97	4.47	86.22	0.73	3.37	96.63
	500	0.95	5.46	1.20	0.48	0.17	4.38	3.80	86.77	0.67	3.73	96.27
L.S.D 5%		0.04	0.31	0.03	-	-	-	-	-	-	-	-

In this respect, the tryptophan and methionine were previously found to promote the biosynthesis of photosynthetic pigments in *Foeniculum vulgare* L, (Hassanein, 2003). This however, explained the present results (Table-3). El-Awadi (2007) reported similar observations in other plant spieces under abiotic stress condition, i.e. the increase in the photosynthetic pigments, total phenolic compounds and total amount of protein in other plants.

In addition Abu-Dahab and Abd El-Aziz (2006), proved the effect of tryptophan in increasing the total free amino acids and total phenolic compound in *Philodendron erubescens.*

The importance of the estimated phenolic contents of the fennel plant is referred to the observations mentioned by Oktay *et al* (2003) on their active role as strong antioxidant .This is coincided by the findings of Parejo *et al* (2004) who identified 42 phenolic compounds, 27 of which were confined to the fennel plant for the first time.

3- Effect on oil percentage and composition

The essential oil of the produced fennel seeds in all treatments were subjected to fractionation using gas liquid chromatography (GLC) and data are represented in Table (4).

The essential and fixed oil percentage in the produced fennel seeds were significantly influenced

in response to the pre-sowing seed soaking treatments in the methionine , tryptophan as well as in the pyrimidine material (Table 4). Methionine at its low and high concentrations had favored other treatments followed by tryptophan and the pyrimidine derivative material (SG93).

In comparison to the control, methionine seed treatment resulted in a significant increase in the fixed oil percentage at both its concentrations followed by tryptophan at its high concentration, whereas the effect of the pyrimidine derivative compound on the fixed oil percentage resulted in slightly values (Table 4).

From the same table, as compared to the control, anethol, 1,8 cineol and fenchone are recorded as the main components of the essential oil of the produced fennel seeds. Anethol percentage ranged from 85.61 to 87.58, while 1,8cineol and fenchone ranged from 3.70 to 5.72%. The highest percentage of anethol was obtained in the 100mg/l methionine-seed –treated plants. Whereas, a considerable increase in the percentage of 1.8cineol was obtained within response to the pyrimidine derivative material seed treatment (Table 4). On the contrary, the application of tryptophan and the pyrimidine compound (SG93) both at 500mg/l resulted in markable decreases in the percentage of fenchone (Table 4).

The findings of Tallat (2005) on *Pelargonium graveolens* L are in support to our present results on fennel.

According to Anand *et al* (2008) anethole, which is the principal active constituent of fennel seeds, showed an anticancer activity.

In earlier studies, El-keltawi and Croteau (1986) explained the influence of growth regulators on essential oil production to the alternation in levels and /or relevant enzymes. However, Gross *et al* (2002) referred the role of the S-adenosyl-L-methionine to the methyl group as a donor to produce estragole and t -anethole in cell-free extracts from bitter fennel.

From the present results, it is concluded that the treatments had affeced the metabolism of the important constituents of fennel plant. Therefore, the treatments could be concerned in elevating the productive value of the plant as a source for the use in medical research against certain diseases. Further experiments are currently taking place to learn more on such a subject.

Corresponding Author:

Dr. Mohamed. E. El-Awadi

Botany Department, National Research Centre, Dokki, 12311, Cairo, Egypt.

el_awadi@yahoo.com

5. References:

1. Anand P, Kunnumakara A, Sundaram C, Harikumar K, Tharakan S, Lai O, Sung B, Aggarwal B. Cancer is a preventable disease that requires major lifestyle changes. Pharmaceut. Res., 2008: 25: 2097–2116.
2. Abou Dahab T, Abd El-Aziz N. Physiological effect of diphenylamine and tryptophan on the growth and chemical constituents of *Philodenron erubescens* plants. World J. Agric. Sci., 2006: 2(1): 75-81.
3. A.O.A.C. Official Methods of Analysis of Association Agriculture Chemists. 15Ed. Washington, USA. 1990.
4. British Pharmacopoeia. Determination of volatile oil in drug. The Pharmacemical Press, London Uk. 1980 P. 87.
5. Choi E, Hwang J. Antiinflammatory, analgesic and antioxidant activities of the fruit of *Foeniculum vulgare*. Fitoterapia, 2004: 75 (6), 557–565.
6. Coruzzi G, Last R. Amino acids. In: Biochemistry and Molecular Biology of Plants. B. Buchanan, W. Gruissem, R. Jones (eds.). Amer. Soc. Plant Biol., Rockville, MD, USA. 2000:358-410.
7. El-Awadi M. The use of safeners to overcome physiological stress by dinitroaniline herbicides in some plants. Ph.D. Thesis, Fac. Sci., Ain Shams Univ. 2007.
8. El-keltawi N, Croteau R. Influence of phosphon D and cycocel on growth and essential oil of sage and peppermint. Phytochemistry, 1986b:25(7): 1603-1606.
9. Gross M, Friedman J, Dudai N, Larkov O. Cohen Y, Bar E. Ravid U. Putievsky E. Lewinsohn E. Biosynthesis of estragole and t-anethole in bitter fennel (*Foeniculum vulgare* Mill. var. vulgare) chemotypes. Changes in SAM: phenylpropene O-methyltransferase activities during development. Plant Science, 2002: 163:1047-1053.
10. Hassan E, Fedina I, El-Awadi M. New pyrimidine derivatives as modulators of plant response to salinity. Egypt. J. App. Physiol., 2006: 21(7): 21-29.
11. Hassanein R. Effect of some amino acids, traces elements and irradiation on fennel (*Foeniculum vulgare* L.). Ph.D. Thesis, Fac. Agric., Cairo Univ. 2003.

12. Maxwell B, Kieber J. Cytokinin signal transduction. In: Plant Hormones. Biosynthesis, Signal Transduction, Action. PJ Davies (ed.), Kluwer Academic Publishers, Dordrecht, the Netherland, 2004: 321-349.
13. Oktay M, Gul I, Kufrevio¢glu I. Determination of in vitro antioxidant activity of fennel (*Foeniculum vulgare*) seed extracts Lebensmittel-Wissenschaft und-Technologie, 2003: 36 (2): 263–271.
14. Parejo O, Jaregui F, S´anchez-Rabaneda F, Viladomat J, Bastida C, Codina C. Separation and Characterization of Phenolic Compounds in Fennel (*Foeniculum vulgare*) Using Liquid Chromatography−Negative Electrospray Ionization Tandem Mass Spectrometry. J. Agric. Food Chem., 2004: 52: 3679–3687.
15. Plummer D. An Introduction to Practical Biochemistry. 2nd Ed. McGraw-Hall Mook Company Limited, London, UK. 1978:144.
16. Simandi B, Deák A, Rónyai E, Yanxiang G, Veress T, Lemberkovics E, Then M, Sass-Kiss A, Vámos-Falusi Z. Supercritical carbon dioxide extraction and fractionation of fennel oil, J. Agric. Food Chem., 1999: 47: p. 1635.
17. Snedecore G, Cochran W. Statistical Methods. TBH Publishing Company, 6th edition. 1980.
18. Snell F, Snell C. Colorimetric Methods. Vol. III. Organic, D. Van Nostrand company, Inc. London. 1952: 606pp.
19. Stasolla C, Katahira R, Thorpe T, Ashihara H. Purine and pyrimidine nucleotide metabolism in higher plants. J. Plant Physiol., 2003: 160: 1271–1295.
20. Talaat I. Physiological effects of salicylic acid and tryptophan on *Pelargonium graveolens* L. Egypt. J. App. Sci., 2005: 20(5B): 751-760.
21. Tanira M, Shah A, Mohsin A, Ageel A, Quresehi S. Pharmacological and toxicological investigations on *Foeniculum vulgare* dried fruit extract in experimental animals. Phytother. Res., 1996: 10:33–36.
22. Tao Y, Ferrer J, Ljung K, Pojer F, Hong F, Long J, Li L, Moreno J, Bowman M, Ivans L, Cheng Y, Lim J, Zhao Y, Ballare C, Sandberg G, Noel J, Chory J. Rapid synthesis of auxin via a new tryptophan-dependent pathway is required for shade avoidance in plants. Cell, 2008: 133:164-178.
23. Wettstein D. Chlorophyll lethal und der submikro-skopiche formwechsel der plastiden. Expt. Cell Res., 1957: 12: 427-433.

3/9/2010

Vegetative Growth and Chemical Constituents of Croton Plants as Affected by Foliar Application of Benzyl adenine and Gibberellic Acid

Soad, M.M. Ibrahim, Lobna, S. Taha and M.M. Farahat

Department of Ornamental Plant and Woody Trees, National Research Centre, Dokki, Cairo, Egypt

Abstract A pot experiment was conducted during 2008 and 2009 seasons at National Research Centre, Dokki, Cairo, Egypt, Research and Production Station, Nubaria. The aim of this work is to study the effect of foliar application with benzyl adenine (BA) at (50, 100 and 150 ppm) and gibberellic acid (GA_3) at (100, 150 and 200 ppm) on the vegetative growth and some chemical constituents of croton plants. Most of the criteria of vegetative growth expressed as plant height, number of branches and leaves/plant, root length, leaf area and fresh and dry weights of stem, leaves and roots were significantly affected by application of the two factors which were used in this study.All foliar applications of BA and GA_3 separately promoted all the aforementioned characters in this study, as well as chemical constituents i.e. Chl. (a and b), carotenoids, total soluble sugars, total indoles ,total soluble phenols and N, P and K content compared with control plants. The highest recorded data were obtained in plants treated with GA_3 200 pm for all chemical constituents and growth parameters, except stem diameter and number of branches/plant, and N, P and K % while BA 150 ppm gave the highest stem diameter and number of branches and N, P and K % and content. [Journal of American Science 2010;6(7):126-130]. (ISSN: 1545-1003).

Keywords: croton plant, benzyl adenine (BA) , gibberellic acid (GA3) .

1. Introduction

Croton with their colorful, glossy foliage and variation of leaf types are one of the most popular plants in Egypt. It is a native of the tropics from Java to Australia and South Sea Islands. The agricultural strategy of Egypt gives much attention (interest) to ornamental plants production for local and exportation. Croton (*Codiaeum variegatum*) Family: Euphorbiaceae is one of the beautiful indoor and out door plants need extensive agriculture development. Cytokinins are important plant hormones that regulate various processes of plant growth and development, cytokinins appeared to play an important role in the regulation of cell division, differentiation and organogenesis in developing plants, enhancement of leaf expansion, nutrient mobilization an delayed senescence, Skoog and Armstrong (1970) and Hall (1973). Shudo (1994), reported that chemical structure of cytokinin active substances has determined two groups of adenine cytokinins and urea cytokinins with similar physiological effects, it has pronounced effect of cotyledon growth and expansion and other processes. The effect of cytokinins especially benzyl adenine on the plant growth and chemical constituents of different plants have mentioned by Eraki *et al*., (1993) on saliva plants, Mazrou (1992) on Datura, Mazrou *et al*.,(1994) on sweet basil, Mansour *et a.,l* (1994) on soybean plants and Vijakumari (2003) on *Andrographis panculata*. The stimulative response of gibberellic acid, which known to be one of the endogenous growth regulators, could be attributed to its unique roles in plant growth and development as reported by many investigators. Leopold and Kriedmann (1975) suggested that GA_3 has the capability of modifying the growth pattern of treated plants by affecting the DNA and RNA levels, cell division and expansion, biosynthesis of enzymes, protein, carbohydrates and photosynthetic pigments. The beneficial effects of gibberellic acid on different plants were recorded by Shedeed *et al*., (1991) on croton plant, Eraki (1994) on Queen Elizabeth rose plants, Bedour *et al*., (1994) on *Ocimum basillicum* and Soad (2005) on Jojoba plant, they concluded that gibberellic acid is used to regulation plant growth through increasing cell division and cell elongation.

The main object of the present work is to study the effect of benzyladenine and gibberellic acid on the growth and some chemical constituents of croton plants.

2. Material and Methods

The present work was conducted during the two successive seasons of 2008 and 2009 at greenhouse of National Research Centre (Research and Production Station, Nubaria). Plastic pots 30 cm in diameter were used for cultivation that were filled with media containing a mixture of sand and peat as 1:1 by volume. Seedlings of (*Codiaeum variegatum*)

pactum L. cv. Norma 23-25 cm height with 30-35 leaves were planted at the first week of March in both seasons. . The plants were fertilized with 20 g/pot kristalon in four doses after 4, 8, 16 and 20 weeks from transplanting.

The pots were arranged in complete randomize design with 6 treatments and 3 replicates (each replicate contained 5 plants) in addition to the control. Application of benzyladenine (50, 100 and 150 ppm) and gibberellic acid (100, 150 and 200 ppm) were carried out twice as foliar spray. The first was at the first week of April, the second was one month from the first at both seasons while the control was sprayed distilled water. An agricultural processes were performed according to normal practice.

At the first week of October 2008 and 2009, the following data were recorded: plant height (cm), stem diameter (mm), number of branches /plant, number of leaves/plant, leaf area (cm^2), root length (cm) fresh and dry weights of stem, leaves and roots (g). Total soluble sugars were determined in the methanolic extract by using the phenol-sulphoric method according to Dubois *et al.*, (1956), photosynthetic pigments including Chlorophyll (a and b) as well as carotenoids content were determined in fresh leaves as mg/gm fresh weight, according to the procedure achieved by Saric *et al*., (1976). The total indoles were determined in the methanolic extract, using P-dimethyl aminobenzaldhyed test " Erlic's reagent" according to Larsen *et al*., (1962). Total soluble phenols were determined calorimetrically by using Folin Ciocalte a reagent A.O.A.C. (1985). Nitrogen , phophorus and potassium were determined according to the method described by Cottenie *et al*., (1982) ., then the leaves contents of N, P and K were calculated. The data were statistically analyzed for each season and then a combined analysis of the two seasons was carried out according to the procedure outlined by Steel and Torrie (1980).

3. Results and Discussion

Growth parameters

Data presented in Table 1 and 2 show that, the foliar application of different concentrations of benzyl adenine (BA) and gibberellic acid (GA_3) had significantly stimulatory effect on growth parameters of croton plants in term of plant height, number of branches, and leaves/plant, root length and leaf area as well as fresh and dry weights of stem, leaves and roots (g)/plant compared with the untreated plants, in this respect Rawia and Bedour (2006) on croton mentioned that, benzyl adenine increased general growth compared with control plants. The most effective treatment which had the tallest plants, the largest leaf area and the highest number of leaves and fresh and dry weights of stems, leaves and roots /plant was (GA_3) when applied at concentration of 200 ppm. The results herein are in agreement with Shedeed *et al.*, (1991) and Rawia and Bedour (2006) on croton, Ibrahim *et al* .,(1992) on ment plant and Soad (2005) on Jojoba plant. However, (GA_3) is used to regulating plant growth through increased meristimatic activity due to enhance cell division and elongation Bhattuchajee *et al*., (2002) on *Corchourus olitorius* L. Treatment with BA at 150 ppm gave the highest value of the number of branches/plant and stem diameter compared with the other treatments and control.

Table 1: Effect of foliar application of benzyladenine (BA) and gibberellic acid (GA3) (on the growth of croton plants (average of the two seasons)

Treatments	Conc. (ppm)	Plant height	Stem diameter	Number / plant		Root length	Leaf area
		cm	mm	branches	leaves	cm	cm^2
Control		43..48	5.65	4.56	140.8	20.41	51.98
BA	50	49.02	7.49	6.56	195.1	23.69	67.91
	100	55.79	8.11	8.63	202.2	24.85	98.33
	150	61.48	8.47	9.57	210.8	27.29	117.82
GA_3	100	57.56	7.64	10.97	172.4	21.87	55.49
	150	68.33	7.41	9.49	228.9	24.25	84.08
	200	70.53	6.22	7.48	261.4	27.21	122.71
LSD 5%		6.69	NS	0.69	19.4	3.57	4.40

Table 2: Effect of foliar application of BA and GA3 on fresh and dry weights of stems, leaves and roots of croton plants (average of the two seasons)

Treatments	Conc. (ppm)	Fresh weights (g)			Dry weights (g)		
		Stem	Leaves	Roots	Stem	Leaves	Roots
Control		19.38	32.02	29.39	7.40	9.36	10.52
BA	50	26.24	45.22	32.50	10.41	11.32	11.53
	100	33.62	52.56	34.12	13.36	13.29	12.86
	150	35.97	65.39	36.55	14.25	16.37	12.96
GA_3	100	28.44	46.71	33.53	11.63	10.59	10.69
	150	36.24	67.35	35.85	14.57	16.50	11.47
	200	41.35	71.37	40.78	16.75	17.29	14.99
LSD 5%		3.28	4.16	3.75	1.65	2.27	0.17

Chemical constituents:

Pigments content

According to Table 3 it was found that the leaves content of three photosynthetic pigments chlorophyll (a and b) and carotenoids were gradually increased as the concentration of BA and GA_3 were increased. The highest value of Chl (a and b) and carotenoids was obtained at the highest concentration of GA_3 (200 ppm). The results herein are agreement with the finding of Mousa *et al*., (2001) on *Nigella sativa*, Shedeed *et al*., (1991) and Rawia and Bedour (2006) they mentioned that GA_3 treatments were more effective than kinetin in increasing photosynthetic pigments in croton leaves.

Table 3: Effect of foliar application of BA and GA3 on chemical constituents of croton plants (average of the two seasons) (mg/gm F.W.)

Treatments	Conc. (ppm)	Chlorophyll		Carotenoids	Total sugars	Total indoles	Total soluble phenoles
		(a)	(b)				
Control		2.29	1.74	0.23	0.94	0.63	1.35
BA	50	2.89	2.16	0.29	1.55	1.38	1.52
	100	3.82	2.27	0.33	1.97	1.75	1.64
	150	4.13	2.82	0.38	2.05	2.48	1.75
GA_3	100	3.31	2.22	0.35	1.56	0.82	1.62
	150	4.15	2.72	0.38	1.97	1.56	1.79
	200	4.64	2.95	0.42	2.22	2.07	2.28
LSD 5%		0.05	0.05	0.02	0.02	0.02	0.01

Total soluble sugars:

Data in Table 3 show that, the application of BA and GA_3 with different concentrations were favourable for accumulation of total soluble sugars in leaves of the tested plants compared with the control. The greatest content of total soluble sugars occurred in the leaves of plants treated with BA at 150 ppm and GA_3 at 200 ppm. In harmony with these results were those obtained by Rawia and Bedour (2006) and Nahed (2007) on croton and Sheren (2005) on flax plants recorded that GA_3 and BA application resulted in an increase of total soluble sugars content.

Total indoles and total soluble phenoles: Data in Table 3 reveal that, spraying croton plants with different concentration of BA and (GA_3) stimulated the content of total indoles and total soluble phynoles in croton plants compared with the control treatment. The greatest values of total indoles and total soluble phenols were obtained from plants sparyed with 150 ppm BA and 200 ppm (GA_3). These results are in line with those obtained by Lobna *et al*., (2008) on *Paulownia kowakamii*, who indicated that using BA at high concentration remarkably augmented the endogenous level of total indoles and total soluble phenols.

Table 4: Effect of foliar application of BA and GA3 on leaves percentage and content (mg) of Nitrogen, Phosphorus and Potassium of croton plants (average of the two seasons) .

Treatments	Conc. ppm	leaves DW %			leaves content (mg)		
		N	P	K	N	P	K

Control		1.73	0.252	2.851	159.1	23.4	266.7
BA	50	2.05	0.265	3.174	226.4	29.4	358.8
	100	2.21	0.283	3.305	292.3	37.2	438.5
	150	1.94	0.263	3.213	311.0	42.5	523.8
GA_3	100	1.63	0.244	2.726	169.4	25.4	288.0
	150	1.53	0.226	2.533	247.5	36.3	417.5
	200	1.42	0.205	2.456	242.1	34.5	423.6
LSD 5%		0.01	0.004	0.018	12.4	1.9	25.4

Leaves percentage of Nitrogen, Phosphorus and Potassium : Table (4) show a gradual reduction in the percentage of the three applied nutrients, nitrogen, phosphorus and potassium parallel to the increase in the concentration of GA_3 was sloping upward up to 200 ppm. The differences were statistically significant for N, P and K %. In harmony with the prementioned results were the findings of Mohammed (2003) on *Acacia saligna* and Soad (2005) on Jojoba plants. Table (4) also shows that the highest percentage of N, P and K were recorded in the plants sprayed with BA at concentration 100 ppm. However, increasing the concentration of BA from 100 ppm up to 150 ppm, decrease the percentage of N, P and K. These results pointed in the same direction of Nahed (2007) and Rawia and Bedour (2006) on croton plants.

Leaves content of Nitrogen , Phosphorus and Potassium : Data in Table (4) reveal that, spraying croton plants with different concentration of BA and GA_3 stimulated the leaves content of N, P and K in croton plants compared with the control treatment. The greatest leaves content of N, P and K were obtained from plants sprayed with 150 ppm BA. The increase in the leaves contents of such three nutrients due to GA_3 application is attributed to the influence of GA_3 in augmenting the leaves dry weights to a higher degree than its effect in reducing leaves percentages of each N, P and K. The role of increasing leaves contents of N, P and K by GA_3 application was emphasized by Sayed (2001) on *Khaya senegalensis* and Soad (2005) on jojoba.

5. References

1. .O.A.C., 1985. Official Methods of Analysis of The Association of Agriculture Chemist. 13th Ed., Benjamin Franklin Station, Washington, D.C., B.O. Box 450.
2. Bedour H. Abou-Leila, M.S. Aly and N.F. Abdel-Hady, 1994. Effect of foliar application of GA3 and Zn on *Ocimum basillicum* L. grow in different soil type. Egypt.J.Physiol. Sci., 18:365-380.
3. Bhattuchajee, A.K., B.W. Mittra and P.C. Miltra, 2002. Seed agronomy of Jute. III. Production and quality of *Corchorus oliforius* L. seed as influenced by growth regulators. Seed Sci. and Tech., 28:421-436.
4. Cottenie, A.,M.Verloo,L.Kiekens,G.Velghe and R.Camerlync, 1982. Chemical Analysis of Plant and Soil . Laboratory of Analytical and Agrochmistry . Sate Univ. Ghent , Belguin , pp: 100 – 129.
5. Dubois, M., F. Smisth, K.A. Gilles, J.K. Hamilton and P.A. Rebers, 1956. Colorimetric method for determination of sugars and related substances. Anal. Chem., 28: 350-356.
6. Eraki, M.A., 1994. The effect of gibberellic application and chelated iron nutrition on the growth and flowering of Queen Elizabeth rose plants. The first Conf. of Ornamental Hort., 2:436-444.
7. Eraki, M.A., M.M. Mazrou and M.M. Afify, 1993. Influence of kinetin and indole 3-acetic acid (IAA) on the growth, drug yield and essential oil content of *Salvia officinalis* L. plant. Zagazig J. Agric. Res., 20:1233-1239.
8. Hall, R.H. 1973. Cytokinins as a probe of development processes. Ann. Rev. Plant Physiology, 24:415-444.
9. Ibrahim, M.E., Sh.A.Tarraf, E.A. Omer and K.A. Turky, 1992. Response of growth, yield and essential oil of *Mentha piperita* L. to some growth regulators. Zagazig, J. Agric. Res., 19: 1855-1868.
10. Larsen, P., A. Harb, S. Klungsan and T.C. Asheim, 1962. On the biosynthesis of some indole compounds in the *Acetobacte xylinum* .Physio. Plant, 15: 552-562.
11. Leopold, A.C. and P.E. Kriedmann, 1975. Plant growth and development. Sec. Edit., McGraw ittil Book Co.
12. Lobna, S. Taha , M.M. Soad Ibrahim and M.M. Farahat (2008). A Micropropagation

Protocol of *Paulownia kowakamii* through in vitro culture technique. Australian J. basic and Appl. Sci., 2(3): 594-600.
13. Mansour, F.A., O.A. El-Shahaby, H.A.M. Mostafa, A.M. Gaber and A.A. Ramadan, 1994. Effect of Benzyl adenine on growth, pigments and productivity of soybean plant. Egypt.J. Physiol. Sci., 18:245-364.
14. Mazrou, M.M., 1992. The growth and tropane alkaloids distribution on the different organs of *Datura Innoxia* Mill. plant on relation to benzyl adenine (BA) application. Monofiya J. Agric. Res., 17:1971-1983.
15. Mazrou, M.M., M.M. Afify, S.A. El-Kholy and G.A. Morsy, 1994. Physiological studies on *Ocimum basillicum* plant. I. Influence of kinetin application on the growth and essential oil content. Menofiya J. Agric. Res., 19:421-434.
16. Mohammed, S.H., 2003. Evaluation and physiological studies on some woody plants. Ph.D. Thesis Dissertation, Fac. Of Agric., Minia Univ.
17. Mousa, G.T., I.H. El-Sallami and E.F. Ali, 2001. Response of *Nigella sativa* L. to foliar application of gibberellic acid, benzyl adenine, iron and zinc. Assiut J. Agric. Sci., 32: 141-156.
18. Nahed, G.Abd El-Aziz; 2007. Stimulatory effect of NPK fertilizer and benzyladenine on growth and chemical constituents of *Codiaeum variegatum* L. plant. American-Eurasian J.Agric. and Environ. Sci., 2(6): 00-00.
19. Rawia, A. Eid and Bedour, H. Abou-Leila, 2006. Response of croton plants to gibberellic acid, benzyl adenine and ascorbic acid application. World J.Agric. Sci., 2:174-179.
20. Saric, M.R., Kostrori, T. Gupina and I. Geris, 1967. Chlorophyll determination Univ. Sadu-Prakitikum is Kiziologize Bilijaka –Beagrad, Haucua Anjiga, pp: 215
21. Sayed, R.M., 2001. Effect of some agricultural treatments on the growth and chemical composition of some woody tree seedlings. Ph.D. Thesis Dissertation, Fac. Of Agric., Minia Univ.
22. Shedeed, M.R., K.M. El-Gamassy, M.E. Hashim and A.M.N. Almulla, 1991. Effect of fulifirtil fertilization and growth regulators on the vegetative growth of croton plants. Annals Agric.Sci., Ain Shams Univ. Cairo, Egypt, 36:209-216.
23. Shedeed, M.R., K.M. El-Gamassy, M.E. Hashim and A.M.N. Almulla, 1991. Effect of fulifertil fertilization and growth regulators on the chemical composition and photosynthesis pigments on croton vegetative growth of croton plants. Ph.D. Thesis, Fac. Agric. Cairo Univ, Egypt, 36:217-227.
24. Sheren, A. S. N., 2005. Some physiological studies on flax plant. Ph.D. Thesis Fac.Agric., Cairo Univ., Egypt.
25. Shudok, K., 1994. Chemistry of Phyenylurea Cytokinins. In Cytokinins: Chemistry, activity and function.
26. Skoog, F. and D.J. Armstrong, 1970. Cytokinins. Ann. Rev. Plant Physilogy, 21:359-384.
27. Soad, M.M. Ibrahim, 2005. Response of vegetative growth and chemical composition of jojoba seedlings to some agricultural treatments. Ph.D. Thesis, Fac. Of Agric. Minia Univ. Egypt.
28. Steel, R.G.D. and J.H. Torrie, 1980. Principles and Procedures of Statistics. Second Edition, McGraw-Hillbook Co.Inc. New York, Toronto, London.
29. Vijayakumari, B., 2003. Influence of foliar spray by GA3 and IAA on the growth attributes of *Andrographis paniculata* L. Journal of Phytological Research Physiological Society, Bharatpur, India, 12:161-163.

4/1/2010

Ability of Immobilized Starter Cells and Metabolites to Suppress the Growth Rate and Aflatoxins Production by *Aspergillus flavus* in Butter

Kawther El-Shafei; *Eman M. Hegazy and Zeinab I. Sadek*

Dairy Department and Food Toxicology and Contaminants Department, National Research Centre, Dokki, Egypt.
*E-mail address: zozok1@yahoo.com

Abstract: Antifungal activity of lactic acid bacteria (LAB)starter cultures, *Lactococcus lactis* ssp. *lactis* and *Leuconostoc mesenteroides* and their metabolites in single and mixed cultures were found to inhibit spoilage and aflatoxin production by *Aspergillus flavus* in butter ,and have potential as bio-preservative agents. Also, treating cream before churn with free cells culture proved to give the greatest antifungal control upon *A. flavus* growth and aflatoxin production; while the use of immobilized cells showed lower activity, then the immobilized metabolites of the mixed culture. In cream artificially contaminated with aflatoxin (B_1, B2, G_1andG_2) treated with immobilized cells or immobilized metabolites of the mixed cultures revealed a reduction of the concentration of aflatoxins recovered from butter made from this cream. The study indicated that the use of lactic acid bacteria and their metabolites in cream or butter have the potential to be as food-grade bio-preservatives for extending the shelf-life of butter and combating the problem of moulds and associated toxins. [Journal of American Science 2010;6(7):131-138]. (ISSN: 1545-1003).

1. Introduction

Contamination of milk and milk products particularly butter by undesirable moulds is a major problem in Egypt and many other countries having similar warm climat .Since the butter usually is unsalted, bulk-packed and repacked, the conditions allow the growth of these moulds. *Aspergillus spp.*the common spoilage moulds generally grow faster, resist low water activity and tend to dominate spoilage in warmer climates. Many of these commonly occurring moulds can not only cause off flavor and discoloration, but also may produce highly toxic and extremely carcinogenic mycotoxins such as aflatoxins, trichothecenes, fumonisin, ochratoxin A and patulin (Schnurer & Magnusson, 2005). Aflatoxins have implicated into hepato-cellular carcinoma and acute hepatitis (Devries et al., 1990).
Butter which is one of the popular varieties of dairy products with high nutritive value, and if moldy contaminated it might constitutes a public health hazard as well as economic losses throughout its deterioration (El-Diasty & Salem, 2007).The presence of moulds and yeasts in butter are objectionable, as they grow at a wide range of temperature and pH values and their count is used as an index of storability and sanitary quality of the product. Also, high lipid content and low water content make the butter more susceptible to spoilage by moulds than by bacteria (James and coulter, 1998). Moreover, many psychrotrophic strains of bacteria, yeasts and moulds have been implicated in spoilage of butter at temperatures below 5^{o}C and some even below 0^{o}C. (Rady and Badr, 2003). .Mycotoxigenic moulds were isolated from Egyptian butter samples (El-Diasty &Salem, 2007).Also,Aflatoxins has been detected in butter samples(Aycicek et al., 2001and Aycicek et al.,2005).

On the other hand, some strains of lactic acid bacteria (LAB) such as *Lactococcus* ssp. and *Leuconostoc mesenteroides* that are already proven to be suitable as LAB starter cultures, were also found to produce metabolites with high antimicrobial activity . The application of their metabolites as biopreservatives in both fermented and non-fermented dairy products has become one of the important trends in food preservation. Furthermore, the use of cell-free metabolites of LAB cells offer the advantage of minimizing texture and flavor changes especially in non -fermented dairy products (Ghita et al., 2004).

On the other side of LAB beneficial usage, investigations revealed that some strains of LAB have been shown to inhibit both growth of mold (Batish et al., 1991& Cabo et al., 2002) and the production of mycotoxins (Coallier-Ascah & Idziak, 1985).Also, they could remove aflatoxins from aqueous solution (El-Nezami et al., 1998; Haskard et al., 2001), and binding with aflatoxin in the animal or human gut that was suggested as a method for controlling aflatoxin levels (Bueno et al., 2007).

Cell immobilization is a method of retaining microorganisms in a discrete location of a fermentation system and also allows the potential to harness the advantages of free culture systems while minimizing the disadvantages. In this regard,

immobilization of LAB has been shown to offer many advantages for biomass and metabolite production compared with free-cell systems such as high cell density, reuse of biocatalysts, improved resistance to contamination or bacteriophage attack, and physical and chemical protection of cells (Champagne et al., 1994). A popular method for bacterial immobilization is entrapment in gel materials, especially in seaweed gel materials such as caraageenan or alginate (Willaert & Baron 1996). Also, microencapsulation of some metabolites such as nisin has proven to be a powerful microbial inhibitor (Benech et al., 2003).

Therefore, the purpose of this study was to investigate the potential antifungal activity of some mesophlic starter cultures, and their immobilized cells and metabolites as specific bio-preservatives in order to protect butter against the development of moulds. Thus, the ultimate aim is extending the shelf-life of fermented and non-fermented butter and avoids the danger of aflatoxins.

2. Material and Methods

2.1. Starter cultures

Reference test strains of *Lactococcus lactis spp. Lactis* CH-1 (culture A), *Lactococcus lactis spp .lactis biovar. diacetylactis* MB-1 (culture B) and *L. lactis spp. cremoris* CH-1 (culture C) were obtained from Chr. Hansens, Copenhagen, Denmark. *Leuconostoc mesenteroides spp. mesenteroides* B-1118 (D) was provided by Northern Regional Research laboratory (NRRL) IIIinois, USA.

2.2. Fungal test strains

Nine strains of moulds were obtained from Standard Association of Australia 80 Arthur st., North Sydney, NSW : *Aspergillus parasiticus* NRR*L* 2999, : *A. parasiticus* NRRL *2669,A. flavus* NRRL 3251, *A.flavus* NRRL 5906 ,*A.ochraceus NRRL* 3174, *Penicillium discolor* NRRL 1951, *Penicillium spp.*, *Fusarium manififorme* NRRL 6322, *F. manififorme* NRRL 2284

2.3. Reference aflatoxin and fungal inocula

Pure reference Aflatoxins (B_1, B_2, G_1 and G_2) (in acetonitrile:benzene 98:2 v/v) were purchased from Sigma, Chemical Company, St.Louis, USA.The spore suspension of fungal inocula was prepared according to the method of Arumsharma *et al*., (1980) by growing the mold on Potato Dextrose Agar (PDA) (Oxoid, Basingstoke, UK), for 7 days at 28 ^{o}C. The spores were harvested by adding 10 mL sterile distilled water and subsequently diluted to a turbidity gave a spore suspension of ~ 10^4 spores $mL^{-1}$by plating, previously experimented.

2.4. Antifungal activity assay

The agar overlay method of Magnusson & Schnauzer (2001) was used to detect antifungal activity. The four LAB strains separately were inoculated as 2 cm long lines on Elliker's agar plates (Oxoid) and incubated at 30 ^{o}C for 48h.The plates were then overlaid with 10 ml each of malt extract soft agar (2% malt extract and 0.7% agar) (Oxoid) containing the moulds to be tested (~10^4 fungal spores mL^{-1}). The plates were examined for the development of clear inhibition zones around the bacterial streak and the area of the zones was scored as follows : (-) no suppression; (+) no fungal growth on 0.1 to 3 % of the plate area per bacterial streak; (++) no fungal growth on 3 to 8 % of plate area per bacterial streak ; (+++) no fungal growth on > 8 % of plate area per bacterial streak.

2.5. Immobilization of the cells and metabolites:
Immobilization of the cells:

Cells were trapped in sodium alginate according to the procedure of Kilnkenberg et al., (2001). Elliker' s broth media (Gibson et al., 1965) (500 ml) was inoculated with 5% (v/v) active culture of *L.lactis ssp. lactis* and *lc. mesenteriodes* (1:1) and incubated at 35 ^{o}C for 48 h. Cells were harvested aseptically by centrifugation (8400 ×g, 20 min, 4 ^{o}C). The pellets were suspended in dilution buffer to a concentration of 4 g dry weight cells L^{-1}. Resuspended cells were mixed with an equal volume of 4 % (w/v) sodium alginate, yielding a final cell concentration of 2 g dry weight cells L^{-1}, which was used in the experiments. The mixture of alginate and cells was added drop wise into a sterile solution of sodium chloride (0.2 mol L^{-1}) and calcium chloride (0.05 mol L^{-1}). Sodium chloride was used in the gelling solution to ensure a homogeneous polysaccharide concentration throughout the beads. To ensure complete gelling, the beads were stirred for at least 40 min in this solution

Immobilization of the metabolites*:*

The same was carried using following mixed LABcultures (1:1) of A+D strains, A+B strains, C+ D strains and C+B strains.

After removing the cells by centrifugation as described above the supernatant was heat treated (80 ^{o}C for 10 min) to kill the remaining cells. The cell free supernatant (metabolites) was immobilized by mixing with equal volume of 4 % (w/v) sodium alginate solution and preceded as described for immobilization the cells (Kilnkenberg et al., 2001).

2.6. Effect of mesophilic starter culture on growth and toxin production by A flavus in broth

A previously tested spore suspension of ~10^4 spores ml^{-1} of *A. flavus* NRRL5906 was used to

inoculate 5 flasks, each containing 200 mL Elliker's medium. Four flasks were inoculated with 2 % (v/v) of one of the mixed (1:1) cultures: A+D, A+B, C+D and C+B. The fifth flask was kept as a control (without starter). All flasks were incubated at 25 ^{o}C for 21 days. Weights of myclia and aflatoxins production were determined at the end of incubation period.

Determinations of mycelial dry weights were obtained by drying filtered mycelium at 50^{o}C for 12 h. (Davis et al., 1986).

2.7. Effect of immobilized metabolites of the mixed cultures on the growth of A flavus on solid media

An agar overly method similar to that described above was used to determine the antifungal activity of immobilized metabolites. Immobilized metabolites of the mixed cultures: A+D cultures, A+B cultures, C+D cultures and C+B cultures, were laid separately on the middle line of the solid media containing ~10^4 cfu mL^{-1} of *A. flavus* (NRRL 5906) spores. The plates were incubated at 28 ^{o}C for 7 days and assessed as described before.

2.8. Effect of starter culture, immobilized cells of starter culture and their immobilized metabolite on the growth and aflatoxins production of A. flavus in butter

Fresh milk was separated to obtain 30% fat cream. The cream was pasteurized and divided into two portions, one for the sensory evaluation and the other was inoculated with *A. flavus* (NRRL 5906) suspension to give an initial count of ~10^4 cfu g^{-1}. Each portion of cream was divided into 4 equal portions and treated as follows: Treatment 1 = inoculated with 2 % mixed starter culture of A+D cultures, Treatment 2 = inoculated with 2 % beads of immobilized mixed starter culture of A+D cultures Treatment 3 = inoculated with 5 % beads of immobilized metabolite of the mixed starter culture of A+D cultures and Treatment 4 = kept as control.

All samples of creams were aged for 72h at 7-10 ^{o}C, and then churned (without removing of the inoculated beads).The resulting butters (unsalted) were then distributed into covered plastic cups and stored at 7-10 ^{o}C for 60 days and analyzed for counts of the fungi and aflatoxin production.

2.9. Effect of immobilized starter culture and their metabolites on aflatoxins

Pasteurized 30% fat cream was spiked (12 µ g ml^{-1}), with standard aflatoxins B_1, B_2, G_1 and G_2, each separately, and then divided into three portions. The first portion was inoculated with 2 % immobilized beads of the chosen mixed culture, the second with 5% immobilized metabolite of the mixed culture, the third kept as control. All treatments were churned and the resulting butters stored at 10 ^{o}C and analyzed for toxins on day 0, 15 30 45 and 60.

2.10. Microbiological analysis

Ten grams of the prepared samples were transferred into a sterile flask containing 90 ml of warm sterile peptone water 1% (40±1 ^{o}C) to prepare a dilution of 10^{-1} from which decimal dilutions up to 10^{-8} were prepared.

A. flavus (NRRL 5906) was counted on PDA (Oxoid) acidified to pH 3.5 with sterile lactic acid solution (10%). Plates were incubated at 25 ^{o}C for 4-5 days. Free cells of *L.lactis ssp. lactis* was counted on M17 agar (Oxoid). Plates were incubated at 30 ^{o}C for 48h. Free cells of *Lc.mesenteriodes* were counted on MRS agar (Oxoid) containing 30 µg mL^{-1} of vancomycin (Levata-Jovanovic & Sandine, 1997). Plates were incubated at 30 ^{o}C for 48-72 h.

2.11. Extraction and determination of aflatoxin

Aflatoxions (B_1, B_2, G_1 and G_2) were analyzed according to A.O.A.C (2000) method. Essentially,50 g test portion was weight into blender jar, then, 100 ml hexane and 250 ml methanol/water (55+45) were added and blended for 3 min at high speed. The blended sample was filtered and the filtrate transferred to a separating funnel. When the layers were separated, 20 ml of the lower layer was released into 150 ml beaker, heated on a hot plate at 60 ^{o}C till dryness, then cooled.

Toxins were detected qualitatively by thin layer chromatography (20×20 cm silica gel 60 aluminum sheets, Merck KGaA, Merck, Darmstadt, Germany) following the AOAC (2000) method. Quantitative detection of toxin was performed using high performance liquid chromatography (HPLC).The HPLC system comprised a Waters model 600 delivery system equipped with fluorescence detector model 470 and a Nova Pack (150×36 mm) C_{18}-column (Waters, Milford, MA, USA). A mobile phase of water/ methanol/acetonitrile (56:14:30, by vol.) was applied isocratically at used flow rate of 1 mL min^{-1}. Data were integrated and recorded using a Millennium Chromatography. Manger Software 2010 (Waters).

2.12. Sensory evaluation of butter

Sensory evaluation of butter as affected by immobilized starter, metabolites and free cells strains was carried out when fresh by trained 10 of panelist from the staff members of Dairy Science Departnent,National Research Centre, with score for flavor (50 points), body and texture (35 points) and appearance (15 points), according to Nelson and Trout (1956).

2.13. Statistical analysis

All experiments were repeated in triplicates and each analysis in duplicated and average results was tabulated. Data were statistically analyzed to calculate the least significant difference (LSD) at the 5% level of probability procedure according to Snedcor & Cochran (1980).

3. Results and Discussion

3.1. Screening for antifungal activity

Preliminary study for antifungal activity of the four strains of LAB, predominantly mesophilic starter strains against different nine strains of common butter spoilage moulds, as shown in Table, 1.The LAB strains tested showed a spectrum of activity against the majority of the tested moulds. Out of the tested cultures *Lc. mesenteroides* and *L. lactis spp. diacetylacts* had a broad antifungal inhibitory spectrum with activity against all of the tested moulds. The selection was for those showed strong antifungal activity against *A. flavus* and *A. parasiticus*, which were reported as two ubiquitous species frequently found to be contaminants of food and are major sources of aflatoxins (Rustom, 1997). These results are in complement to those found by Suzuki et al., (1991) who also recorded the antifungal activity of lactic acid bacteria and some *Leuconostoc* strains. Also, *L. lactis* ssp. *lactis* was able to exert antifungal activity especially against *A. flavus*. The obtained results were in agreement to those reported by Batish et al., (1997), Kumar et al., (2007) who recorded strong broad spectrum of antifungal activity of some Lactic acid bacteria especially *L. lactis* ssp. *lactis*.

3.2. Effect of immobilized metabolites of starter culture on the growth of A. flavus on solid media.

The immobilized metabolites in combinations pairs of the mixed starter cultures of *L. lactis* spp. *lactis* + *Lc. mesenteroides* (A+D) were found to be mostly active against the growth of *A. flavus*. Antifungal substances in the cell-free supernatants of some lactic acid bacteria have previously been reported (AbdAlla et al., 2005; Cabo et al., 2002; Kumer *et al.*, 2007). Generally, the combined metabolites in the current study enhanced the antifungal activity against the moulds tested compared with the individual strains. Trend may be concomitant with Effat (2000) who reported that combination between pairs of antifungal substances from LAB was found to be the most active against tested moulds.

It is noteworthy that the presence of immobilized metabolites from the mixed culture A+D (*L. lactis* ssp. *lactis* and *Lc. mesenteroides*) eliminated fungal growth and consequently prevented aflatoxin formation.

As *L. lactis* spp. *lactis* and *Lc. mesenteroides*, showed the highest antifungal activity,as they were selected for further application for producing lactic acid and aroma.

3.3. Effect of mixed cream starter cultures on the growth and toxin production of A. flavus in broth medium.

It is clear from the results in Table 2, that significant differences were found between the effects of the mixed cultures and the control on aflatoxin production by *A. flavus*. The highest values of aflatoxin production (8.03,6.48,4.04 and5.0µgL^{-1} for B1,B2,G1 and G2,respectively)and mycelium weight(16.94 g$L^{-1)}$ were recorded for the culture of *A. flavus*(NRRL 5906) with *L. lactis* ssp. *cremoris* + *Lc. mesenteroides* (C+D); as no significant difference was given between this mixed culture and the control (with respect to *A. flavus*). In contrast, results for co-culture of *A. flavus* with *L. lactis* ssp. *lactis* and *Lc. mesenteroides* showed that this LAB mixed culture prevented the production of aflatoxins (Fig.1, Table 2), and there was a more pronounced decrease in the mycelium weight of *A. flavus* than with the other cultures (as determined at the end of the incubation period for all treatments).

These results are in agreement with those obtained by El-Gendy & Marth (1981) who observed the arrested growth of *Aspergillus* spp. even after 2 weeks at 15 ^{o}C in the presence of *L. lactis spp. lactis* and *Lactobacillus casei*. Also, Coallier-Ascah & Idziak (1985) recorded that *L. lactis* produced inhibitors during the logarithmic phase of growth which reduced the amount of aflatoxin production by *A. flavus* .

3.4. Inhibition of growth of A. flavus and aflatoxins production in butter

Results in Table 3 reveal that mixed culture of *L. lactis* ssp. *lactis* and *Lc. mesenteroides* (treatment1)was effectively used in, preventing aflatoxin G_1 and G_2 production by *A. flavus* , and significantly reducing the levels of the aflatoxin B_1 and B_2 in all treatment. In contrast, in the inoculated control butter sample the mould grew and increased in counts to reach more than 10^7 cfu g^{-1} (Fig. 2). Also, aflatoxins B_1, B_2, G1 and G_2 were produced at concentrations between 4.42-2.76 µg kg^{-1} at day 30 with complete deterioration of the control butter (Table 3).Moreover,both immobilized cells and metabolites (treatments2&3)eliminated the growth of A. flavus (Fig.2, a) and retarded the aflatoxin production (Table 3). Immobilized cells were more effective than immobilized metabolites in inhibiting the growth of the fungi and consequently, the

production of aflatoxins. Therefore, immobilized metabolites can be used as biopreservation of sweet butter. The results obtained are also in accordance with that reported by Hegazy et al., (2006).

Counts of *Lactococcus* spp.and *Leuconostoc* spp.in butter (Treatment 1 and 2), as shown in Fig.2 b, c indicated that the counts of both strains increased slightly during the first month of storage ,possibly attributed to high fat content in butter samples and then these counts decreased gradually thereafter.

Concerning the sensory evaluation of the butter, the results showed that there were no difference in the flavor, body, texture and appearance of all butter samples and the panelist could not identify differences in mouth feel between butter with immobilized cultures and metabolites and control. Similar results were obtained by Hamayouni et al., (2008), and Ozer et al., (2009) who reported that addition of encapsulated culture had no significant effect on the sensory properties of some dairy products

3.5. Fate of Aflatoxins in the presence of immobilized starter cultures and their immobilized metabolites

Data regarding the percentage of the aflatoxins (B1, B2, G1and G2) bounded in butter samples that had been made from cream artificially contaminated with 12 µg mL-1 individually for each aflatoxin then stored for 60 days, are illustrated in Fig.3. The data indicate that butter made with cream treated with immobilized starter culture cells, all the aflatoxins tested were bound at 90% of the original concentration after storage for 60 days. In contrast, in butter made from cream treated with immobilized metabolites the levels of bounded aflatoxin were 45-56.3 % of the original concentration after 60 days storage. This is could be attributed to the removal of the toxin which involves physical binding to bacterial cell walls or cell wall components (Peltonen et al., 2001).The binding of the toxins by immobilized metabolites may be due to the dead cells of the culture (or possibly dead cell material) remaining in the supernatant after the heat treatment, since dead cells of bacteria still display binding ability (Bueno et al., 2007).

Treating butter with immobilized cells was more effective in binding or removing aflatoxins, in agreement with El-Nezami et al., (1998), and Haskad et al., (2001) who recorded that certain strains of lactic acid bacteria removed aflatoxins from liquid media by physical binding. Also, binding aflatoxin by LAB allowed the detoxification without the need for the removal of the bacterial-toxin complex from the food, so, this method renders the toxin unavailable for absorption in the intestine. Moreover, aflatoxin bound by bacteria showed no toxicity effect on rats liver tissues of rats fed on the toxin complex (Metwally,et al, 2008).

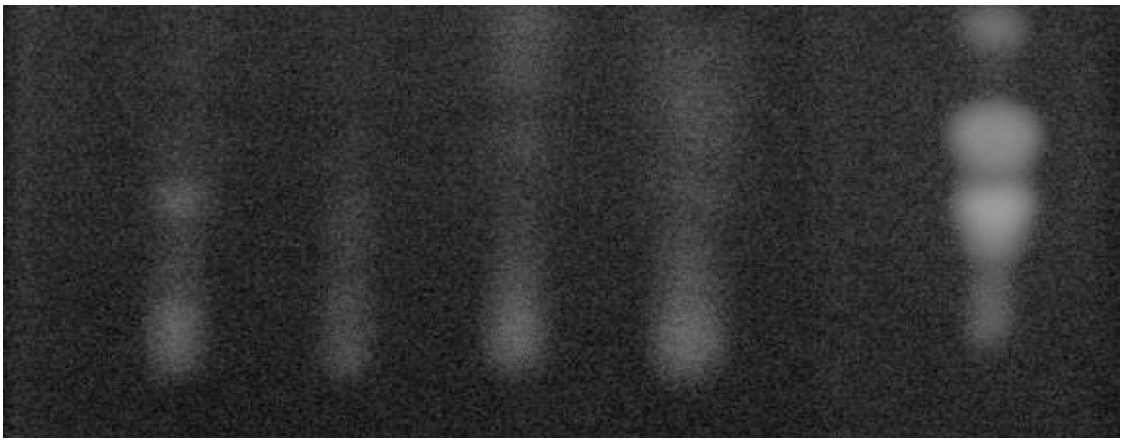

Control A+B A+D C+B C+D

Fig. 1 Effect of mixed mesophilic starter culture on toxin production by *A. flavus* in broth medium detected by thin layer chromatography. A, *Lactococcus lactis* ssp. *lactis*; B, *Lactococcus lactis* ssp. *diacetylactis*; C, *Lactococcus lactis* ssp. *cremoris*; D, *Leuconostoc mesenteroides* ssp. *mesenteroides*

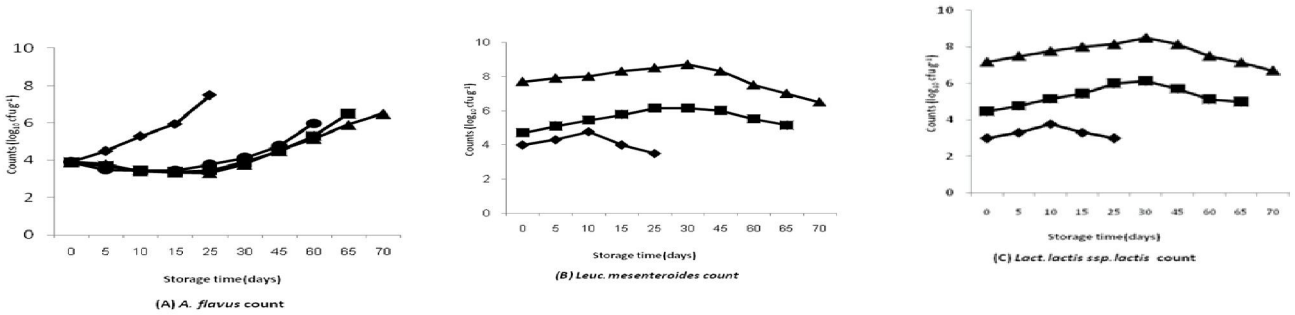

Fig.2. Changes in (A) *A.flavus*, (B) *Lc. mesenteroides* and *L. lactis ssp. Lactis* counts in treated butter during storage. (♦), Treatment 1: inoculation with 2 % mixed starter culture A+D; (■), Treatment 2: inoculation with 2 % beads of immobilized mixed starter culture A+D; (●), Treatment 3: inoculation with 5% beads of immobilized metabolite of the mixed starter culture A+D; (▲),Treatment 4: no inoculation (control).

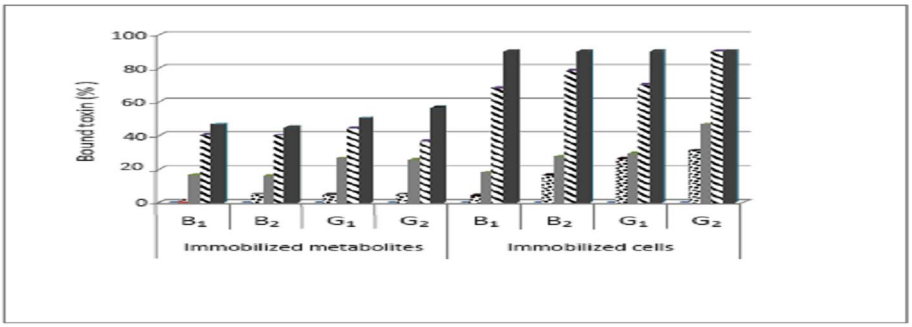

Fig. 3. Effect of immobilization of starter culture cells and their metabolites on aflatoxin binding in butter during storage: ( ), day 1; ( ), day 15; ( ) day 30; ( ) day 45; ( ), day 60. B_1, aflatoxin B_1; B_2, aflatoxin B_2; G_1, aflatoxin G_1; G_2, aflatoxin G_2.

Table 2.Effect of mixed starter culture on growth and toxin production by *A. flavus* in broth medium.

Cultures*	Aflatoxins (μg L^{-1})**				Mycelium weight of *A. flavus* (g L^{-1})**
	B_1	B_2	G_1	G_2	
Control (*A. flavus*)	10.69^{a}	7.99^{a}	6.70^{a}	5.00^{a}	17.00^{a}
(A + B)mixed culture	4.15^{c}	3.60^{b}	Traces	Traces	14.02^{bc}
(A + D)mixed culture	0.00^{d}	0.00^{c}	0.00^{c}	0.00^{c}	12.35^{c}
(C + B) mixed culture	5.34^{c}	4.98^{b}	5.14^{ab}	2.11^{b}	15.32^{b}
(C + D) mixed culture	8.03^{b}	6.48^{a}	4.04^{b}	5.00^{a}	16.94^{a}

*Cultures are: A, Lactococcus lactis ssp. lactis; B, Lactococcus lactis ssp. diacetylactis; C, Lactococcus lactis spp. Cremoris: D, Leuconostoc mesenteroides spp. mesenteroides.
**Values within columns followed by the same superscript letters are not significantly different at 0.05%.
***LSD, least squares difference.

Table 3.Deter the production of aflatoxins from *A. flavus* NRRL 5906 by inoculation with mixed cultures of *Lactococcus lactis* spp. *lactis* and *Leuconostoc mesenteroides* ssp. *mesenteroides* (A + D) and their immobilized cells and metabolites in butter stored at 10 °C.

Storage period (days)	Treatments[a,b]			
	Control	Treatment 1	Treatment 2	Treatment 3
	Aflatoxins (μg kg^{-1})	Aflatoxins (μg kg^{-1})	Aflatoxins (μg kg^{-1})	Aflatoxins (μg kg^{-1})

	B_1	B_2	G_1	G_2	B_1	B_2	G_1	G_2	B_1	B_2	G_1	G_2	B_1	B_2	G_1	G_2
5-25	nd	nd	nd	nd	nd	nd	nd	nd	nd	nd	nd	nd	nd	nd	nd	nd
30	4.15	3.08	4.42	2.76	nd	nd	nd	nd	nd	nd	nd	nd	nd	nd	nd	nd
35-55	-	-	-	-	nd	nd	nd	nd	nd	nd	nd	nd	nd	nd	nd	nd
60	-	-	-	-	nd	nd	nd	nd	nd	nd	nd	nd	3.86	2.94	2.05	traces
65	-	-	-	-	nd	nd	nd	nd	3.73	2.80	traces	traces	-	-	-	-
70	-	-	-	-	1.66	1.98	nd	nd	-	-	-	-	-	-	-	-

[t]reatments are: Control, mold, without LAB; Treatment 1, inoculation with 2 % mixed starter culture A+D; Treatment 2, inoculation with 2 % beads of immobilized mixed starter culture A+D; Treatment 3, inoculation with 5 % beads of immobilized metabolites of the mixed starter culture A+D.
[b]nd, not detected.
(-) not tested

4. Conclusion

From the foregoing results, it can be concluded that some LAB strains had antifungal activity and thus have the potential for being effective as food-grade bio-preservatives to combat the problem of mold growth and aflatoxins in butter. Though, immobilization technology is prospective field for food safety and effectively controls the risk of contamination by *A. flavus*. Moreover, immobilized metabolites of some mesophilic starter can be used to extend shelf-life, limiting fungal spoilage and toxin formation, but this requires further investigation. This approach could be used in reducing the risk of mycotoxins contamination without producing off-flavor in sweet butter as a novel strategy in preventing the formation of aflatoxins in foods.

5. References:

1. AOAC. (2000). Official Method of Analysis of AOAC International,25th ed. Maryland, USA: AOAC International.
2. AdbAlla, E.A.M., Aly, S., Saleh, E., Mary, S., & Hathout, A.S. (2005). The antimycotic effects of probiotic bacteria on the germination and ultra-structure of the aflatoxin fungi *Aspergillus parasiticus*. *Journal of Union Arab of Biologists, Cairo, 16B*, 33-48.
3. Arumsharma, A.G., Behere, S.R., & Padwal-Desal Nadharni, G.B. (1980). Influence of inoculums size of *Aspergillus parasiticus* spores of aflatoxin production. *Applied and Environmental Microbiology, 6*, 989-993.
4. Aycicek, H., Yarsan, E., Sarimehmetoglu, B., & Cakmak, O. (2002). Aflatoxin M1 in white cheese and butter consumed in Istanbul, Turkey. *Veterinary and Human Toxicology, 44*, 295-296.
5. Aycicek, H., Aksoy, A., & Saygi, S. (2005). Determination of aflatoxin levels in some dairy and food products which consumed in Ankara, Turkey. *Food Control,16*, 263-266.
6. Batish, V.K., Lat, R., & Grover, S. (1991). Interaction of *Streptococcus lactis* subsp. *diacetylactis* DRC-1 with *Aspergillus parasiticus* and *A. fumigatus* in milk. *Cultured Dairy Products Journal, 26*, 13-14.
7. Benech, R.O., Kheadr, E.E., Lacroix, C., & Fliss, I. (2003). Impact of nisin producing culture and liposome-encapsulated nisin on ripening of lactobacillus added-Cheddar cheese. *Journal of Dairy Science, 86*, 1895.
8. Bueno, D.J., Casale, C.H., Pizzolitto, R.P., Salvano, M.A., & Oliver, G. (2007). Physical adsorption of aflatoxin B_1 by lactic acid bacteria and *Saccharomyces cerevisiae*: A theoretical model. *Journal of food Protection, 70*, 2148-2154.
9. Cabo, M.L., Braber, A.F., & Koenraad, P.M.F. (2002). Apparent antifungal activity of several lactic acid bacteria against *Penicillium discolors* is due to acetic acid in the medium. *Journal of Food Protection, 65*, 1309-1316.
10. Champagne, C. P., Lacroix, C., & Sodini-Gallot, I. (1994). Immobilized cell technology for the dairy industry. *Critical Reviews in Biotechnology, 14*, 109–134.
11. Coallier-Ascah, J., & Idziak, E.S. (1985), Interaction between *Streptococcus lactis* and *Aspergillus flavus* on production of aflatoxin. *Applied and Environmental Microbiology, 49*,888-891..
12. Davis,N.D.,Clark,E.M.,Schrey,K.A.&Diener,U.L.(1986).In vitro growth of Acremonium coenophialum,an endophyte of toxic tall fescue grass. . *Applied and Environmental Microbiology, 52*,888-891.
13. Devries, H.R., Maxwell, S.M., & Hendrickse, R.G. (1990). Aflatoxin excretion in children with

Kwashiorkor or marasmic Kwashiorkor: a clinical investigation. *Mycopathology*, *110*, 1-9.
14. Effat,B.A(2000).Antifungal substances from some lactic acid bacteria and Propionibacteria for use as food preservatives. *Journal of Agriculture science Mansoura University,25,*6291-6304.
15. El-Diasty, E.M., & Salem, R.M., (2007). Incidence of lipolytic and proteolytic fungi in some milk products and their public health significance. *Journal of Applied Science Research*, *3*, 1684-1688.
16. El-Gendy, S.M., & Marth, E.H (1981). Growth and aflatoxin production by *Aspergillus parasiticus* in the presence of *Lactobacillus casei*. *Journal of Food Protection*, *44*, 211-212.
17. El-Nezami, H., Kankaanpaa, P., Salminen, S., & Ahokas, J. (1998). Ability of dairy strains of lactic acid bacteria to bind common food carcinogen aflatoxin $B_{1.}$.*Food Chemistry and Toxicology*, *36*, 321-326.
18. Ghita, E.I.,Girgis E., Abd El-Fattah, E.S., & Badran, S.M. (2004). Biopreservative effect of the metabolites of some Lactic acid bacteria on cream and low fat butter. *Egyptian Journal of Dairy Science, 31*, 221-236.
19. Gibson, C.A., Landerkin, G.B., & Morse, P.M. (1965). Survival of strains of lactic streptococci during frozen storage. *Journal of Dairy Research*, *32*,151-155
20. Homayouni ,A.,Azizi ,A.,. Ehsani M.R,. Yarmand M.S, Razavi S.H. (2008).Effect of microencapsulation and resistant starch on the probiotic survival and sensory properties of synbiotic ice cream. *Food Chemistry 111*,50–55
21. Haskard, C.A., El-Nezami, H.S., Kankaanbaa, P.S., Salminen, S., & Ahokas, J.T. (2001). Surface binding of aflatoxin B_1 by lactic acid bacteria. *Applied and Environmental Microbiology*, *67*, 3086-3091.
22. Hegazy, E.M., Sadek, Z.I., & El-Shafei, K. (2006). Elimination the risk of aflatoxins production by *Aspergillus parasiticus* NRRL2999 by using some starter cultures. *Journal Union Arab Biology, Cairo, Microbiology and Viruses*, *15B*, 15-40.
23. Klinkenberg, G., Lystad, K.Q., Levine, W., & Dyrset, N. (2001). pH-controlled cell release and biomass distribution of alginate-immobilized *Lactococcus lactis* subsp. *lactis. Journal of Applied Microbiology*, *91*, 705-714.
24. Kumar, C.N., Narayanan, R., Kavitha, N., & Dhanalakshmi, B. (2007). Antifungal property of lactic acid bacteria. *Egyptian Journal of Dairy Science, 35*, 141-145.
25. Ozer,B.,Kimaci,H.A.,Senel,I.,Atamer,A.,Hayaloglu,A.(2009). Improving the viability of Bifidobacterium bifidum BB-12 and Lactobacillus acidophilus LA-5 in white-brined cheese by microencapsulation. *International Dairy Journal 19*,22–29
26. Levata-Jovnnovic, M., & Sandine, W.E. (1997). A method to use *Leuconostoc mesenteroides* ssp. *cremoris* 9140 to improve milk fermentations. *Journal of Dairy Science*, *11*, 11-19.
27. Magnusson, J., & Schnurer, J. (2001). *Lactobacillus coryniformis* subsp. *coryniformis* strain Si3 produces a broad-spectrum proteinaceous antifungal compound. *Applied and Environmental Microbiology*, *67*, 1-5.
28. Metwally, M.;. Abd Allah,EL S., Farag A. H., Sanaa M.A. B., & Nouh, A. (2008). Factors affecting lactic acid bacteria adsorption of aflatoxin and the effect of adsorbed toxin on rats' liver tissues. *Journal of.Agriculture. Scince. Mansoura University*, 33 ,5187-5201.
29. Nelson, J.A. and Trout, G.M. (1956). Judging dairy products.4th Ed.The Olsen publishing Co., Milwaukee Wis. 53212.
30. Peltonen, K., El-Nezami, H., Haskard, C., Ahokas, J., & Salminen, S. (2001). Aflatoxin B1 binding by dairy strains of lactic acid bacteria and bifidobacteria. *Journal of Dairy Science*, *84*, 2152-2156.
31. Rustom, I.Y.S. (1997). Aflatoxin in food and feed: Occurrence, legislation and inactivation by physical methods. *Food Chemistry*, *59*, 57-67.
32. Rady, A.H & Bader,H.M.(2003).Keeping the quality of cows' butter by irradiation
33. *Grasasy Aceites, 54*, 410-418.
34. Schnurer, J., & Magnusson, J. (2005). Antifungal lactic acid bacteria as bio-preservations. *Trends in Food Science and Technology*, *16*, 70-78.
35. Snedcor, G.W., & Cochran, G.W. (1980). Statistical methods 6th edn. Iowa, USA: *University Press.*
36. Suzuki, I., Nomura, M., & Morichi, T. (1991). Isolation of lactic acid bacteria which suppress mould growth and show antifungal action. *Milchwissenschaft*, *46*, 635-639.
37. Willaert, R., & Baron, G. (1996). Gel entrapment and micro-encapsulation: Methods, applications and engineering principles. *Review of Chemistry Engineering, 12 N*, 1-2.

3/9/2010

Development of Doubled Haploid Wheat Genotypes Using Chromosome Eliminating Technique and Assessment under Salt Stress

*A. Y. Amin[1] and G. Safwat[2,3] and G., El-Emary[4]

1 Department of Plant Physiology, Faculty of Agriculture, Cairo University, Giza, Egypt
2 Horticulture Research Institute, Agriculture research Centre, Doki, Giza, Egypt
3 Faculty of Biotechnology, October University of Modern Sciences and Art, Egypt
4 Institute of Efficient Productivity, Zagazig University.

Abstract: The chromosome elimination technique is an efficient method by which beneficial characters for salt tolerance can be combined within a short time and a large number of doubled haploid (DH) genotypes with desirable variability can be produced. In the present study 120 spring wheat DH genotypes has been developed using the wheat (*Triticum aestivum L.*) x millet (*Pennisetum glaucum*) crosspollination method with the F1 cross between Kharchia (Indian cultivar) one of the most cultivar recorded as salt tolerance worldwide and Sakha 93 (Egyptian breeding cultivar) cultivated in saline soil and recommended for newly reclaim lands, north area of Egypt. Under normal conditions the DHs agronomical traits (i.e. flowering time, number of spikelets per spike (NSPS), plant height, spike length and 1000 grain weight) distribution was normal and significant transgressive segregation was observed. ANOVA analysis showed significant differences among DH genotypes for all agronomical traits, and the DH 11, 22, 57, 98, 106, 111 and 118 lines found to have better yield characters SNPS, spike length and 1000 grain weight than the parents under non-saline condition. The 120 DHs and both parents were grown in hydroponics culture medium, with the concentration of NaCl : $CaCl_2$ 4:1 being 150mM. Some of those DHs showed much high in responses to growth under salinity than both parents. The variances between DH lines were significant for Na^+ and Cl^- ions, leaf Fresh weight (lfw), leaf dry weight (ldw), leaf 2 extension rate before salt additions (LE-b), leaf 4 extension rate after salt additions (LE-a), number of spikes per plant (SNPP), number of spikelets per spike (NSPS), number of grains per plant (GN) and grain weight per plant (GW), and non-significant for K^+ ion and water percentage (W%). Overall the mean values for the DHs were higher than the parents values under salt stress, for the DH 3, 12, 38, 57 and 96 genotypes mid-values of LE-a were close to the average of LE-b under non-saline conditions. A significant negative correlation was determined between Na content and yield parameters i.e. SNPP, NSPS, GN and GW. In contrast it was positively correlation with W%, which might indicates that better yield characters of DH lines i.e. 10, 25, 42, 57, 68, 96, and 114 than parents under salt conditions may be due mainly to better exclusion of Na from the shoots. [Journal of American Science 2010;6(7):139-148]. (ISSN: 1545-1003).

Keywords:- *doubled haploid , chromosome elimination, salinity, Triticum aestivum L, breeding*

1. Introduction

Changing climatic conditions and misuse of agricultural lands over the last few years have lead to a rapid increase in the area of soil under salinity. There is, therefore, an urgent need for more salt tolerant varieties of various crops, in particular wheat. By using the utilization of conventional plant breeding techniques, the selection intensity and number of selection cycles necessary to improve tolerance effectively needs years. Obviously, any method that can accelerate and increase the efficiency of a programme to produce salt tolerant crop plants will be beneficial. The use of chromosome elimination in wheat DH production is one technique which can contribute to this development. By simplifying and accelerating breeding programmes, this is the quickest possible way of achieving homozygosity. From a breeding point of view, in self pollinated species, such as the small grained cereals, doubled haploids can be used directly for the production of varieties, since each DH has the potential to become a new variety.

In Wheat, the production of uniform homozygous lines enhances selection efficiency, allowing a better discrimination between genotypes in breeding nurseries within only one generation, making it a useful technique for both wheat breeding and genetical studies. Plant anther culture is one of the plant breeding techniques that have been developed to produce new homozygous cultivars within a relatively short time (Flavell, 1981). Progress has been made in the anther culture technique through modifying the culture medium (Ghaemi et al., 1994). Nevertheless, this method may cause unpredictable genetic alterations due to

gametoclonal variation (Huang 1996; Raina 1997). These factors could affect the means and genetic variances of a breeding population, thus affecting selection (Ma et al., 1999).

Moreover, wheat DHs can be produced by inter-specific crosses. In this technique, haploid embryos appear as a result of selective elimination of the alien chromosomes during embryogenesis. The first use was by barely (*Hordeum bulbosum*) as the pollen parent for this purpose (Barcley 1975). However, most wheat varieties show no crossability with *Hordeum bulbosum* due to the presence of the Kr1 locus on chromosome 5B and/or Kr2 locus on chromosome 5A (Snape et al., 1979). The dominant alleles of these genes, Kr1 and Kr2, are responsible for the poor crossability.

In contrast, wheat x maize cross-pollination has been used for producing wheat haploid plants, and no recalcitrant genotypes have been reported because the maize chromosomes are eliminated at early embryonic stages (Laurie and Bennett, 1988a), and the efficiency of haploid production is not affected by *Kr* genes (Laurie and Bennett 1988b).
Several studies have been proven that different species such as sorghum (*Sorghum bicolor*) and pearl millet (*Pennisetum qlaucum*) are also possible pollinators for wheat haploid production (Ahmad and Comeau 1990; Inagaki and Mujeeb-Kazi 1995).

In Egypt, wheat is the most important daily food cereal, however, only 40% of its annual domestic demand can be produced (Salam, 2002). In present, cultivated land, comprises only 3% of total land area in Egypt, is already salinized. The government strategic plain is to increase the total agriculture land by adding newly reclamation land irrigation with saline underground water, due to limitation of other water resource from Nile river and low precipitation (less than 25mM annual rainfall) (Ghassemi et al., 1995). Therefore, it is necessary to disseminate newly released cultivars with more salt tolerance to be introduced for the newly recrimination land irrigated by underground water, which affected by access salt from Mediterranean and Red Seas (Shannon, 1997; Pervaiz et al., 2002). According to results by Kingsbury and Epstein, (1984) it was found that among spring wheat (*Triticum aestivum*) cultivars, Kharchia showed relatively high salt tolerance in respect of growth and grain yield. However, as compared to other relatively salt tolerant varieties it accumulated more Na^+ in the shoot when grown under salt conditions (Mahmood 1991). Similarly, the spring wheat breeding genotypes Sakha 93 was obtained from Agricultural Research Centre, Giza, Egypt is usually cultivated in saline areas in Egypt for restricted Na^+ accumulation in the shoot, and salt tolerance in respect of growth and grain yield (El-Hendawy et al., 2005), indicating that the two parents might contain a different set of genes with different strategy to survive under salt stress conditions.

Due to observed differences in the negative effect of salinity on growth processes among and within species, many of the traits like plant height (Chauhan and Singh, 1993), fresh and dry weight of shoots and roots (Ashraf and Noor, 1993), leaf area (Romero and Maranon, 1996), and number of leaves per plant (Yang et al., 1990) are now widely used as measures of the degree of plant salt tolerance. In wheat, the total grain yield from a plant is a combination of number of spikes per plant, weight per grain, and grain number per spike. Often, salinity affects the traits contributing to yield structure. Thus, total grain yield in wheat was reduced under irrigation with water with an EC 16 dSm^{-1}, to about 60% (Chauhan and Singh, 1993).

Disturbances in grain yield under salinity are caused by a ranges of factors, e.g., a decrease in spikelet numbers per spike (Grieve et al., 1993), disturbed pollen viability (Sacher et al., 1983), and a reduction in the number of fertile tillers per plant (Khatun and Flowers, 1995). The aim of this research was to develop of doubled haploid lines that might contain individuals having a better performance under salt stress, due mainly to recombination of desirable characters from both parents Sakha 93 and Karchia. Because of the importance of biomass and grain yield indices for assessing plant response to salinity, this paper describes work done to assess and establish the relationship between some characteristics during early and later stages of growth including yield components under non-saline and salin conditions, which will help in deciding the optimal genotype for more studies on wheat.

2. Material and Methods

Development DHs Genotypes

Two spring wheat were chosen as parents on the basis of highly response to salinity. The parent varieties were Kharchia (Indian cultivar; relatively salt tolerant) and Sakha 93 (Egyptian genotype; salt tolerance and high exclusion of Na^+). A cross between these two genotypes was made and the resulting F_1s were crossed to produce a haploid wheat using pearl millet (*Pennisetum glaucum*) pollen as the male parent, which were doubled by following the procedure described by Amin (2002). Wheat spikes were emasculated 1-2 day(s) before anthesis and pollinated 1 day later with fresh pearl millet pollen. Twenty-four hours after pollination the florets were injected with a drop of 50 ppm Dicamba. In total 75 spikes were pollinated with fresh millet pollen and covered with polyethylene bags. Haploid embryos

were excised and cultured on Gamborg's medium with B5 vitamin following the procedure described by Amin (2002). When seedlings had developed an adequate shoot and root, they were gently pulled out of the culture tube and potted into very wet seedling compost in 6 cm pots. When the seedlings were about 15-20 cm high, one-third of the roots and shoots were cut. Root haploids were then immersed into colchicine solution (12ml distilled 0.5% colchicine, with 2% dimethyl sulfoxide and few drop of tween-20), and left for 5.5 h at room temperature. After treatment the roots of the plants were washed in running tap water to remove chemicals before being re-potted into 15 cm pots of compost. The setting of seed on the colchicine-treated plants was the indicator of the success of chromosome doubling. Ten replicates of each DH line and the two parents Kharchia and Sakha 93 were grown to maturity. Five parameters were measured i.e. flowering time, NSPS, spike length, 1000 grain weight and plant height.

Hydroponics Culture Medium

Four seedlings of each DH line were planted one per pot, with three replicates; these pots were placed randomly. The hydroponics was set up as described by Amin (2002). For the first week, plants were irrigated with only water, after that solution with half strength Hoagland nutrient medium was replaced the water. When leaf 2 was half emerged, NaCl and $CaCl_2$ (4:1) were added gradually by 50mM a day to give a final concentration of 150mM. The nutrient solution was added daily to the initial level in the tank, and replaced twice weekly. The experiment was performed in a greenhouse conditions, at about 20^{o}C with 16/8 day/night natural daylight supplemented with lamps.

Measurements of Inorganic Ions

Two weeks after the addition of salt, the leaf 3 was collected. Leaf samples were ashed in porcelain crucibles in an oven at 500 ^{o}C for 5 h. After cooling down, 2ml of concentrated nitric acid was added to each crucible to dissolve the ash. The solution was transferred into 50 ml plastic tubes and made up to 50 ml with ddH_2O. Na^+ and K^+ ions were measured using a flame photometer (Corning 410). Cl^- was determined using a Russell combination Cl^- ion selective electrode directly in the tubes after the determination of cations.

Growth Characteristics

Fresh weight (lfw), dry weight (ldw) and percentage of water (W%) traits were measured in the leaf 3 for determination of ions under salt stress. For determining leaf extension rate before salt additions (LE-b), the length of leaf 2 was measured from its tip to the sand surface and to the ligule of leaf 1. Same thing after salt addition, the length of leaf 4 was scored (LE-a) day by day from the moment it protruded from the subtending leaf sheath, until no increase in length could be detected. At maturity, plants were harvested and the following traits were measured: number of spikes per plant (SNPP), number of spikelets per spike (NSPS), total number of grains per plant (GN) and grain weight per plant (GW).

3. Results

In total, of 150 haploid embryos (Figure 1) that were rescued and cultured, only 125 haploid seedlings have survived. Finally, 120 doubled haploid plants reached the flowering stage and developed seeds. A combined analysis of variance of DHs under normal conditions showed significant differences between DH lines for flowering time, NSPS, plant height, spike length and 1000 grain weight (Table 1). The range of expression of differences amongst the DH lines under normal conditions was determined in the form of frequency distributions, shown in Figures (2). The DH 11, 22, 57, 98, 106, 111 and 118 lines were found to have better yield characters than the parents under normal conditions. These also showed that Sakha 93 has a better performance comparing with Kharchia over all parameters. The normality was tested using the MINITAPE soft wear. Overall, the distribution of above traits was normal and significant transgressive segregation was observed. A comparison for various parameters between DH means and parental means values is shown in Table (2). Under non-saline conditions, DH means were higher than Kharchia and Sakha 93 means.

Hydroponics culture

Some of the data for yield parameters under salt conditions were skewed from the normal distribution, as 25 DHs did not developed seed under salt stress. Such data were transformed by natural logarithms prior to statistical analyses (i.e. SNPP, NSPS, GN, and GW). Normality of frequency distributions was tested using the normality test in MINITAB software.

Ion contents

Kharchia accumulated 1.5 times more sodium than Sakha 93 and its Na and K concentrations were very close to the population means (14.59 mg gDW^{-1} and 9.12 mg gDW^{-1} respectively) (Table 3). The parents contrasted with respect to Cl concentrations. Sakha 93, on average,

Fig. 1 Wheat haploid embryo from wheat x millet cross pollination

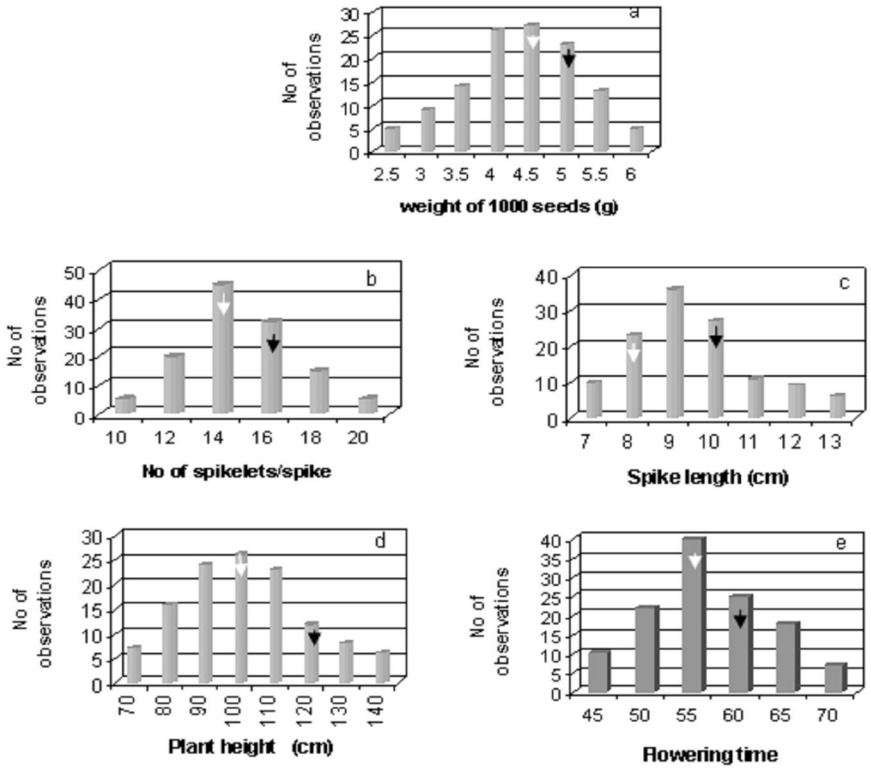

Fig. 2 Distribution of the doubled haploid lines and the two parents Kharchia (whit arrow) and Sakha 93 (black arrow) for five characters (a)1000 grain weight (b)number of spikelets per spike (c) spike length (d) plant height (e) flowering time

Table 1 Analysis of variance of agronomics traits under non-saline conditions

Trait	Source of variation between DHs		F-test	*P*
	df	MS		
weight of 1000 seeds (g)	119	1925	3.79	<0.001**
plant height	119	704	1.04	0.207
No. of spikelets/spike	119	1590	2.39	0.003**
Spike length	119	867	1.4	<0.001**
flowering time	119	2384	4.67	<0.001**
grain number / ear	119	1590	2.4	<0.001**

Table 2 Mean values for agronomics traits under non-saline conditions

Trait	N	Mean	Min.	Max.	Kharchia	Sakha 93	Std. Deviation
weight of 1000 seed (g)	120	4.6	2.8	6.2	3.7	5.0	0.60
Plant height (cm)	120	107	75	152	92	115	10.18
No of spikelets/spike	120	15.7	11.2	21.9	12.7	18.0	2.36
Length of spike (cm)	120	10	7.4	14.2	8.6	11.2	1.15
Flowering time	120	62	48	83	52	63	5.51
No of grain/ear	120	40	7	70	28	45	7.77

Table 3 Analysis of variance and means values for all characteristics of doubled haploid population described in the hydroponics culture

Trait	Means	Minimum	Maximum	Kharchia	Sakha 93	Sdve.	Source of Variance Between DHs			
							D.F.	M.S.	F-test	***P***
Leaf Na content (mg/g DW)	15.49	2.68	35.81	14.59	9.12	4.144	119	164.07	3.99	<0.001***
Leaf K content (mg/g DW)	1.24	0.41	2.4	1.15	1.10	0.442	119	0.91	1.45	0.076
Leaf Cl content (mg/g DW)	8.11	0.77	37.80	4.26	6.98	3.992	119	2.312	3.88	<0.001***
leaf 2 extension rate (cm/day)	4.34	3.06	5.608	3.550	5.34	1.464	119	0.196	2.57	0.033*
leaf 4 extension rate (cm/day)	2.06	0.87	4.344	2.436	1.08	0.131	119	0.204	3.60	0.014*
Water content	79.14	68.17	83.243	81.354	74.4	4.003	119	0.018	1.91	0.094
Leaf fresh weight FW (gm)	0.145	0.056	0.269	0.189	0.082	0.017	119	0.8061	4.99	<0.001***
Leaf dry weight (gm)	0.042	0.018	0.073	0.054	0.026	0.005	119	0.593	4.47	<0.001***
No. of ears per plant	0.174	0.283	0.991	0.850	0.765	0.435	99	0.592	3.09	0.0012**
No. of spikelets per spike	1.004	0.425	6.232	4.532	4.079	2.268	99	0.156	1.67	0.043*
No. of grains per plant	0.361	0.283	2.974	1.133	1.020	0.496	84	1.557	2.80	0.024*
Grain weight per plant (g)	0.026	0.059	0.016	0.032	0.029	0.011	84	2.981	3.42	0.017*
Total dry weight (g)	0.228	0.068	0.589	0.269	0.197	0.026	119	3.316	2.12	0.04*

**:p < 0.01 *:p <0.05

accumulated almost 1.6 as much chloride as Kharchia though still less than the mean value of Cl for the DHs (8.11 mg gDW^{-1}). Large variations in the concentrations of Na, K, and Cl were observed among the doubled haploid population (Table 3) with genotypic values ranging from 2.68 to 35.81 mg gDW^{-1} for Na, 0.41 to 2.4 mg gDW^{-1} for K, and 0.77 to 12.8 mg gDW^{-1} for Cl. Analysis of variance among DH lines for the Na, K and Cl under salt conditions is presented in Table 3. The differences between DH lines were significant for sodium, chlorine, and non-significant for potassium content.

Growth Characters

In saline conditions, lfw, ldw and water percent (W%) were affected by the transgressive segregation of beneficial traits coming from both parents for salt tolerance (Table 3). Among the parents, Kharchia had a higher W% average than Sakha 93 (81.354% and 74.4%, respectively) as well as almost twice as much lfw and ldw (Table 3). The lfw of doubled haploids ranged from 0.056 to 0.269 per plant (average 0.145), ldw varied from 0.018 to 0.073 per plant (average 0.042), and W% from 68.17 % to 83.243 % (average 77.14 %) (Table 3). Leaf extension rate is expected to be correlated with traits determining plant growth under normal or saline conditions. Under salt stress, Kharchia had a better extension rate (2.436 cm/day) than Sakha 93 (1.08 cm/day) and than the average of DH lines (2.06 cm/day), in contrast with normal conditions, when Sakha 93 (5.34 cm/day) had a better performance than Kharchia (3.55 cm/day). Among the DH lines there were differences in Leaf extension rate between contrasting conditions reflect the transgressive segregation (Table 3). Under salt stress the leaf extension rate ranged from 0.87 to 4.344 cm per day (Table 3), whereas with the non-stressed condition the value of this trait ranged between 3.06 to 5.608 cm per day. The leaf extension rate of DH line 3, 12, 38, 57 and 96 under salinity was close to the average for plants under non-saline conditions. Analysis of variance showed the differences between genotypes were significant for all growth characteristics except for W% (Table 3).

Yield Characters

The distribution for all yield parameters values are shown in table 3. Overall, Kharchia was found to be more tolerant than Sakha 93 under salt stress. Moreover, the distributions indicate that about 20% of the DH lines performed better than the parents under salt conditions. The traits such SNPS, NSPS, GN, and GW were examined; there was a skewed distribution toward zero values. As Eighteen DHs affected by salinity and did not produce any spike, add to that 7 DHs produced ears were completely sterile. These zero values were eliminated from the datasets for analyses of variance. A separate analysis of variance of DHs and parents for each character was carried out, and showed that DHs differed significantly for all yield characters.

Correlations between all characters

A simple correlation between the all parameters for DHs under salt conditions were calculated on a genotype mean basis. As we expected, the SNPP, NSPS, GN, and GW had significantly negative correlation with Na and Cl content (e.g. Figure 3), and were non-significant with K content.

As expected the W% was positively correlated with lfw, however, it was unexpected to be as well positively correlated with Na and Cl contents (e.g Fig 4). Other significant correlations are presented in figure (5a and 5b) between the leaf size with leaf extension rate, which showed opposite direction under normal (positive correlation) and saline condition (Negative correlation).

4. Discussion

Although DH production for wheat has been available for over two decades, there is a few reports in the literature (Amin., 2002; Mahmood and Baenziger, 2008) where this technique has been used for the production of progenies differing in salt tolerance. Nevertheless, many reports exist where the DH system has proven better than other breeding methods in respect of efficiency and for the production of genotypes with improved agronomic characters. In the present work the better performance of some DH lines (11, 22, 57, 98, 106, 111 and 118) compared with that of the parents in normal conditions may be due to the recombination of desirable characters in DH lines.

In agreement with this, Laurie and Snape (1990) and Snape et al. (1988) reported that a large number of DH lines with varying degrees of ariation in agronomic characters may be the result of gametoclonal variation. They also observed that within a population of DH lines derived using chromosome eliminating technique, there was significant genetic variation for biomass production and grain yield. Similar results were found and presented in Table 1 and 2, with the differences between DH lines being significant for all the characters studied under normal conditions except plant height. In barley, Bozorgipour and Snape (1991) observed that DH progenies of the haploid plantlets which had bigger embryo size and faster

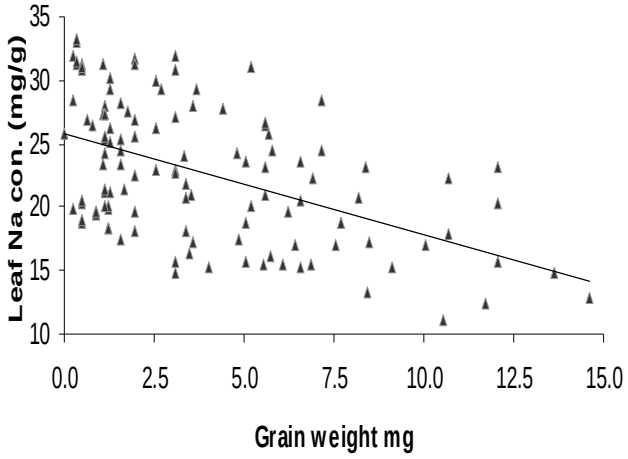

Fig 3 Relationships between leaf Na content and grain weight per plant

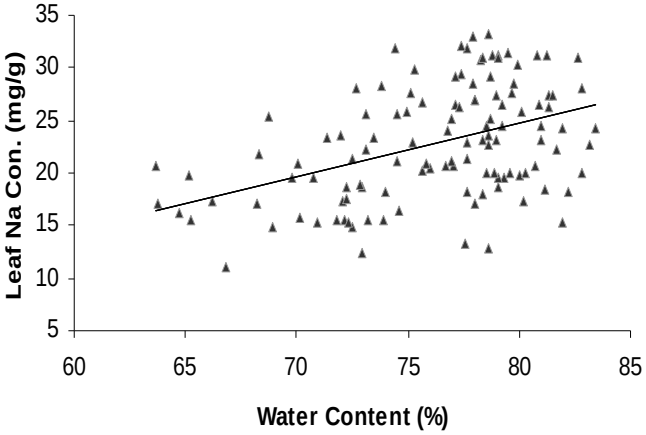

Fig 4 Relationships between leaf Na content and water content (%)

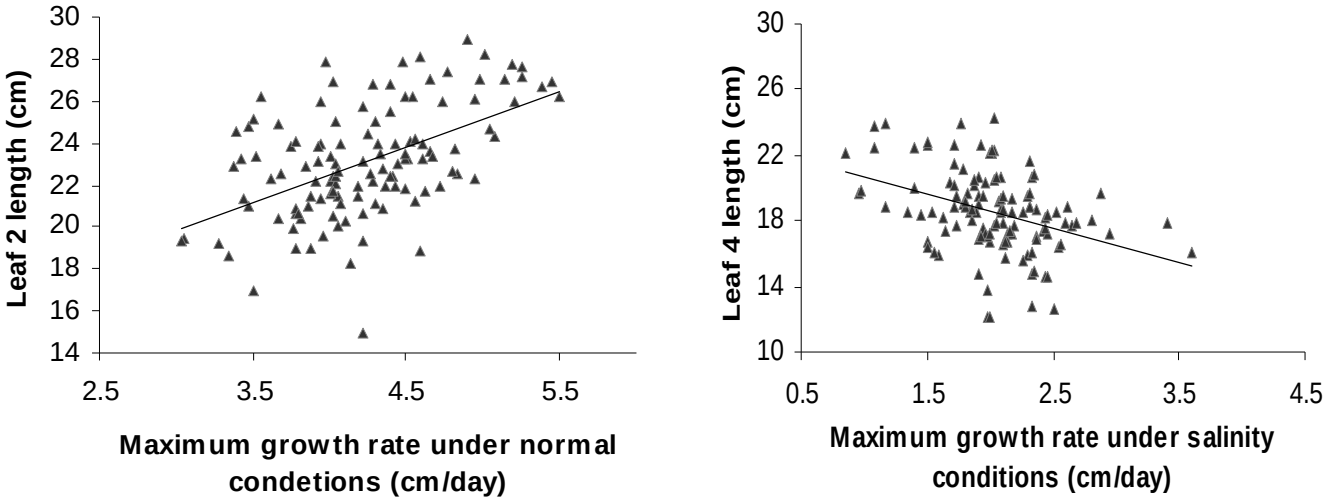

Fig. 5 Relationships between leaf length and maximum growth rate under normal condition (a), and under salinity conditions (b).

growth rate at germination, were superior to the other lines with respect to a number of agronomic characters including plant biomass, plant height and grain yield. According to that DHs DH 11, 22, 57, 98, 106, 111 and 118 may have developed from the vigorous embryos, which ultimately produced more vigorous DH lines.

This experiment was designed to improve salt tolerance of the existing wheat cultivars by the appropriate combination of desirable characters from a good background parents i.e. Sakha 93 and Kharchia for salt tolerance within a short time and a large number of homozygous genotypes. In this research work, the 120 DH genotypes exhibited large variation in all the traits described in Table 3 under saline conditions. Forster et al. (1990) mentioned, in terms of growth, that higher salt tolerance of some of the DH lines than either of the parents can occur through transgressive segregation over the better parents for growth. Absence of the typical bimodal distribution indicates that single major genes with large effects controlled none of the traits studied. The transgressive segregation observed in almost all the traits (Table 3) strongly supports this deduction. Evidently, these traits were controlled not by a single gene with a large effect but rather by a combination of several genes with smaller effects.

On the basis of previous research by Amin (2002), the better performance of some DH lines compared with the mid performance of the parents (similar to the result obtained in Table 3) more likely to be due its ability of use different mechanisms for salt tolerant, which is provided by both parents Sakha 93 and Kharchia. As the mechanisms of salt tolerance are still not fully understood, all the sources of these variations detected between the DH lines for all the characters studied in this work remain unclear. It is also difficult to identify which processes had the greater effect on growth under salt conditions or which of them worked together to increase the plant salt tolerance.

Sodium affects, mostly negatively, on plant physiological and biochemical systems (Murthy et al., 1979). Similar to the result presented in Figure 3, wheat grain yield was found to decrease with increased Na concentrations in leaves. On anther study, salt tolerance of wheat plants, defined as relative grain yield, was found to be negatively correlated with the concentration of Na in leaf 5 (Schachtman et al., 1992). Out of 120 DHs only 95 DHs eventually produced one or more ears with a highly significant variation among DHs (Table 3) seven of them were not developed any grain. In many cases under salt stress, this was attributed to a decrease in pollen viability and pollen fertilization (Khatun and Flowers, 1995), was considered to be sufficient to retard the germination of a pollen grain and growth of the pollen tube (Sacher et al., 1983). This might indicates that better growth performance of DH lines i.e. 10, 25, 42, 57, 68, 96, and 114 than parents under salt conditions may be due mainly to better exclusion of Na from the shoots. For Cl measurements under salt stress, a significant variation in the amount of Cl absorbed was detected within the DHs (Table 3). However, non-significant negative correlation was found between this trait and grain yield characters. It might be related to some kind of gene, who can restrict Cl influx into cells, thus avoiding its negative effects. So far, only a soybean gene, Ncl, involved in chlorine uptake has been described (Abel, 1969).

According to the difference between both results for the correlation between leaf length and plant growth rate under normal and salt conditions (Fig 5), it seems that under salt stress, phenological escape is one of the strategies employed by plants to survive such environmental conditions, when plants decrease leaf size as well as the life cycle smaller leaves maintain higher growth rates. In agreement with this, the reduction in leaf area reduces the evaporative surface and by doing so inhibits gas exchange (Gale et al., 1967), the rate of transpiration and ultimately the efficiency of photosynthesis (Cramer et al., 1990), which is one of the mechanisms plants use to tolerate the reduced ion uptake effects of the soil salinity (Flowers and Yeo, 1989).

The water percent showed significant differences amongst doubled haploids (Table 3). Surprisingly, the relationship between percentage of water and Na accumulation in the leaf was significantly positive (Fig. 4). This result contrasts with findings by Hoffman and Jobes, (1978). In their experiment, the severe reductions in growth of the plant in salt conditions were thought to be at least partly due to the negative correlation with water content. For these unexpected results the obvious explanations, it may have happened because the older leaf, still green, that was sampled for the ion measurements, was accumulating ions in that leaf to protect the youngest leaf from the effects of toxicity. This is one of the mechanisms plants employ to survive the adverse effects of the salt stress.

5. References:

1. Ahmad, F., and Comeau, A., 1990. Wheat x pearl millet hybridization: consequence and potential. Euphytica 50:181–190
2. Amin, A. 2002. Markers for quantitative trait analysis and bulk segregant analysis of salt tolerance in wheat (Triticum aestivum L.), PhD.

Dissertation, submitted to University of East Anglia, England.
3. Abel, G. H., 1969. Inheritance of the capacity for chloride inclusion and chloride exclusion by soybean. Crop Sci. 9: 697-698.
4. Ashraf, M. and Noor, R. 1993. Growth and pattern of ion uptake in *Eruca sativa* Mill. under salt stress. Angewandte Botanik. 67:17-21.
5. Barclay, I. R., 1975. High frequencies of haploid production in wheat (*Triticum aestivum*) by chromosome elimination. Nature, Lond, 256, 410411.
6. Bozorgipour, R. and Snape, J.W. 1991. The relationship between in vitro performance of haploid embryos and the agronomic performance of the derived doubled haploid lines in barley. Theor Appl genet. 23:321-332.
7. Chauhan, C.P.S. and Singh, S.P. 1993. Wheat cultivation under saline irrigation. *Wheat Inf. Serv*. 77:33-38.
8. Cramer G.R., Epstein, E. and Läuchli A. 1990. Effects of sodium potassium and calcium on salt stressed barley. I. Growth analysis. Physiol. Plant. 80. 83-88.
9. El-Hendawy, S.E., Hu, Y., and Schmidhalter, U., 2005. Growth, ion content, gas exchange, and water relations of wheat genotypes differing in salt tolerances. Aust. J. Agric. Res. 56:123–134.
10. Flavell, R.B. 1981. An overview of plant genetic engineering in crop improvement. A Rockefeller Foundation conference, USA. 3-11.
11. Flowers, T.J and Yeo A.R. 1989. Effect of salinity on plant growth and crop yield. In: Environmental stress in Plants. Springer-Verlag, Berlin, Heidelberg. 101-119.
12. Forster, B.P., Phillips, MS., Miller, T.E., Baird, E. and Powell, W. 1990. Chromosome location of genes controlling tolerance to salt (NaCl) and vigour in *Hordeum vulgare* and *H. chilense*. Heredity, 65:99-107.
13. Gale, J., Kohi, H.C. and Hagon, R.M. 1967. Changes in the water balance and photosynthesis of onion, bean, and cotton plants under saline conditions. Physiol. Plant. 20. 408-420.
14. Ghassemi, F., Jakeman A. J., and Nix. H. A. 1995. Salinization of land and water resources:
15. human causes, extent, management and case studies. Canberra, Australia: The Australian
16. National University. Wallingford, Oxon, UK: CAB International.
17. Grieve, C.M., Lesch, S. M., Maas, E.V. and Francois, L. E. 1993. Leaf and spikelet primordia initiation in salt- stressed wheat. Crop Sci. 33:1286-1292.
18. Hoffman, G.J. and Jobes, J.A. 1978. Growth and water relations of cereal crops as influenced by salinity and relative humidity. Agron. J. 20:765-769.
19. Huang, B. 1996. Gametoclonal variation in crop improvement. In: Jain SM, Sopory SK, Veilleux RE (eds) In Vitro Haploid Production In Higher Plants, vol 2: application. Kluwer Academic Publ, Dordrecht, 73-91.
Inagaki, M.N., and Mujeeb-Kazi A., 1995**.** Comparison of polyhaploid production frequencies in crosses of hexaploid wheat with maize, pearl millet and sorghum. Breed Sci 45:157–161.
20. Khatun, S. and Flowers, T.J. 1995. The estimation of pollen viability in rice. J. Exp. Bot. 46:151-154.
21. Laurie, D.A. and Bennett, M.D. 1988a. The production of haploid plants from wheat x maize crosses. Theor Apply Genet 76:393-397.
22. Laurie, D.A. and Bennett, M.D. 1988b. chromosome behaviour in wheat x maize, wheat x sorghum crosses. Proceeding of Kew chromosome Conference 3:167-177.
23. Laurie, D.A. and Snape J.W. 1990. The agronomic performance of wheat doubled haploid lines derived from wheat x maize cross-es.Theor Appl Genet 79:813-816.
24. Ma, H., Busch, R.H., Riera-Lizarazu, O. and Rines, H.W. 1999. Agronomic performance of lines derived from anther culture, maize pollination and single-seed descent in a spring wheat cross. Theor. Appl. Genet. 99. 432-436.
25. Mahmood, A. 1991. Genetic, physiological and biochemical studies of salt tolerance in wheat and its related species, PhD. Dissertation, submitted to Cambridge University, England.
26. Mahmood, P. S. Baenziger 2008. Creation of salt tolerant wheat doubled haploid lines from wheat × maize crosses Cereal Research Communications Volume 36, Number 3/September 2008
27. Murthy, A.S.P., Venkataraman, M.N. and Yadav, J.S.P. 1979. Effect of saline water irrigation on sodium and potassium uptake in UP301 wheat (*Triticum aestivum L.*). Ann Arid Zone, 18:62-67.
28. Pervaiz, Z., Afzal, M., Xiaoe Y., and Ancheng, L. 2002. Selection criteria for salt tolerance in wheat cultivars at seedling stage. Asian J. Plant Sci.,1: 85–7.
29. Raina, S.K. 1997. Doubled haploid breeding in cereals. In: Janick J (ed) Plant breeding reviews, vol 15. John Wiley and Sons, New York, 141–186.

30. Romero, J.M. and Maranon, T. 1996. Allocation of biomass and mineral elements in *Melilotus segetalis* (annual sweetclover): effects of NaCl salinity and plant age. New-Phytologist. 132:565-573.
Sacher, R.F., Mulcahy, D.L., Staples, R..C., Mulcahy, D.L. and Ottaviano, E. 1983. Developmental selection during self pollination of *Lycopersico*n X *Solanum* F1 for salt tolerance of F2 Pollen: biology and implications for plant breeding. Proceedings of the symposium, Villa Feltrinelli, Lake Garda, Italy, 23-26 June, pp. 329-334.
31. Salam, A.G. 2002. Current status of durum wheat in Egypt and Future prospects. http://www.Fineprint.com.
32. Schachtman, D.P., Lagudah, E.S. and Munns, R. 1992. The expression of salt from Triticum tauschii in hexaploid wheat. Theor Appl Genet 84:714-719.
33. Shannon, M.C. 1997. Genetic of salt tolerance in higher plants. In: Strategies for improving Salt Tolerance in Higher Plants (P. K. Jaaiwal, R. P. Singh, and A. Gulati, Eds.). 265-289.
34. Shannon, M.C. 1997. Adaptation of plants to salinity. Advances in Agronomy, 60:75-120.
35. Snape, J.W., Henry, Y., Buyser, J.D., Agache, S. and Parker, B.B. 1988. Comparisons of methods of haploid production and perfor-mance of wheat lines produced by doubled haploid and single seed descent. In: Miller TE, Koebner RMD (eds) Proc 7th Int Wheat Genet Symp. Bath Press, Bath, UK, 1087–1092.
36. Snape, j.W., Chapman, V., Moss, J., Blanchard, C.E. and Miller, T.E. 1979b. the crossibility of wheat varieties with Hordeum bulbosum. Heredity, 42:291-298.
37. Yang, Y.W., Newton, R.J. and Miller, F.R. 1990. Salinity tolerance in Sorghum. I. Whole plant response to sodium chloride in *S. bicolor and S. halepense*. Crop-Science. 30:775-781.

4/2/2010

A New Method for Fabrication and Laser Treatment of Nano-Composites

Hebatalrahman. A
Housing & Building National Research Centre (HBRC), Egypt.
Hebatalrahman@naseej.com

Abstract: A new method for manufacturing of nano-composites was invented; a new technique calls Composite material machine with four strokes was established. Composite material machine is a machine for manufacturing of both plastic and metals matrix composites independent on size, type, and volume fraction of fillers. The machine works in four strokes, each of which worked separately. It depends on the material. The four stokes can be controlled to work in schedule controlled by the main control unit connected to the computer, the machine also work manually. The final products were treated by laser irradiation to improve mechanical properties without any significant change in composition. The new technique is cheap, qualified and simple design. The technique was full automated and has been transferred to industry successfully. [Journal of American Science 2010;6(7):149-154]. (ISSN: 1545-1003).

Keywords: Fabrication, parameters, nanocomposite, laser irradiation, nanoparticles, reinforcement

1. Introduction

Nanocomposites are materials that are created by introducing nanoparticulates (often referred to as filler) into a macroscopic sample material (often referred to as *the matrix*). This is part of the growing field of nanotechnology [1, 2]. After adding nanoparticulates to the matrix material, the resulting nanocomposite may exhibit drastically enhanced properties. For example, adding carbon nanotubes tends to drastically add to the electrical and thermal conductivity. Other kinds of nanoparticulates may result in enhanced optical properties, dielectric properties or mechanical properties such as stiffness and strength [3]. In general, the nano-substance is dispersed into the matrix during processing [3]. The percentage by weight (called *mass fraction*) of the nano-particulates introduced is able to remain very low (on the order of 0.5% to 5%) due to the incredibly high surface area to volume ratio of nanoparticulates. Much research is going into developing more efficient combinations of matrix and filler materials and into better controlling the production process [4, 5].

Historical Background

A. Applications of Nano-composite materials

An important use of nano-particles and nano-tubes is in composites, materials that combine one or more separate components and which are designed to exhibit overall the best properties of each component. This multi-functionality applies not only to mechanical properties, but extends to optical, electrical and magnetic ones [6, 7]. Currently, carbon fibres and bundles of multi-walled CNTs are used in polymers to control or enhance conductivity, with applications such as antistatic packaging. The use of individual CNTs in composites is a potential long-term application. A particular type of nano-composite is where nano-particles act as fillers in a matrix; for example, carbon black used as a filler to reinforce car tyres. However, particles of carbon black can range from tens to hundreds of nanometres in size, so not all carbon black falls within our definition of nano-particles [8-10].

b. Laser Method

In 1996 CNTs were first synthesized using a dual-pulsed laser and achieved yields of >70wt% purity. Samples were prepared by laser vaporization of graphite rods with a 50:50 catalyst mixture of Cobalt and Nickel at 1200°C in flowing argon, followed by heat treatment in a vacuum at 1000°C to remove the C60 and other fullerenes. The initial laser vaporization pulse was followed by a second pulse to vaporize the target more uniformly [11]. The use of two successive laser pulses minimizes the amount of carbon deposited as soot. The second laser pulse breaks up the larger particles ablated by the first one, and feeds them into the growing nano-tube structure. The material produced by this method appears as a mat of “ropes”, 10-20nm in diameter and up to 100μm or more in length. Each rope is found to consist primarily of a bundle of single walled nano-tubes, aligned along a common axis. By varying the growth temperature, the catalyst composition, and other process parameters, the average nano-tube diameter and size distribution can be varied. Arc-discharge and laser vaporization are currently the principal methods for obtaining small quantities of high quality CNTs. However, both methods suffer

from drawbacks. The first is that both methods involve evaporating the carbon source, so it has been unclear how to scale up production to the industrial level using these approaches. The second issue relates to the fact that vaporization methods grow CNTs in highly tangled forms, mixed with unwanted forms of carbon and/or metal species. The CNTs thus produced are difficult to purify, manipulate, and assemble for building nanotube-device architectures for practical applications[12-14]

2. Material and Methods

Experimental study

a) The System Descriptions

When the four stroke composite material machine is describe, it is not only machine for manufacturing of composites but it is a complete system for manufacturing include grinding of raw materials, addition of additive, mixing and manufacturing in four steps. The manufacturing parameters are indicated as temperature, Pressure, cooling rate, and time of application of force. Fig (1) shows the main steps of manufacturing.

The unit Dimensions =Height 4.5m-* width 5m *length 7m

The machine operations follow the following steps:-

1-Grinding to prepare raw materials in nano-size

2-The nano-size particles moves on the belt to add additive and other reinforcement

3-All components was mixed in a multi-speed mixer

4-The powder mixture was added to the iron mold

5-The mold was heated and treated with lubrication before mixture added

6-The manufacturing cycle work in four steps heating, Pressing, cooling and extraction of final products

7-The electronic arm moves mold and mixture away from heaters to the cooling path and vise verse

8- The control unit was adjusted to control both manufacturing parameters and movement of the electronic arm.

Fig (2) shows the workshop design and Fig (3) shows the main parts of the four stroke composite material system. The system design was simple and abundant to be suitable for small investment and youth projects. The system is suitable for plastic matrix composite, metal matrix composite, powder metallurgy, recycling of powder waste and fabrication of thermoplastics and thermosets.

b) Fabrication of composite

To prove the quality of the system, it was used to prepare FRP (plastic matrix composite) PMMA reinforced by fiber glass.

PMMA (poly methyl metha acrylate) are Considered as the material which have the best biocompatibility to be used in medical applications, but have a lot of disadvantages such as low hardness, low strength, high shrinkage, high water absorption and low thermal conductivity. These disadvantages have already overcome by making composite material consists of PMMA (poly methyl metha acrylate) as matrix and use fibre glass type E as reinforcement. Type E fibre glass has a lot of characteristics because it is cheap, abundant and effective to overcome the disadvantages. Fibre glass was used in Volume fractions (zero %, 17 %, 35%, 50%, 65%) and the length to diameter ratio were (L/D = 1) (L/D=50). The manufacturing quality parameters are indicated as temperature, pressure, time of application of force and cooling rate. The material is treated using two different types of lasers such as Argon — ion laser with wavelength 514. 5nm and Nd — YAG with 355nmwavelength(third harmonic generation).

C) Material Preparation

The material prepared by grinding and mixing for PMMA in the powder form which have diameter less than 100μm with short fibre type E-fibre glass which is mechanically cut to certain sizes. The fibre size which is recorded by length to diameter ratio L/d=50 Ownes Corning Co, 731ED 1/32" was chosen. The mixing of fibre with PMMA is done with certain volume fractions as mentioned above.

d) Determination of Manufacturing Parameters

The manufacturing parameters were adjusted and the effect of temperature, pressure and cooling rates were recorded. Design and test of the new system were evaluated. The nano- composite material consists of poly methyl metha acrylate as matrix reinforced with fibre glasses as filler The manufacturing steps may be summarized in the following steps:-

1-Grinding of PMMA by electrical blinder-and control the grinding time to be less than 1.5 min to avoid temperature rise and agglomeration of particles after that use mesh < 300μm diameter for sieving.

2-Short fibre have used in powder form.

3- Mixing of the two powders.

4- Heating the mold.

5- Compress the mixture with (5:10 ton) hydraulic system.

6- Cooling the mold with water JET.

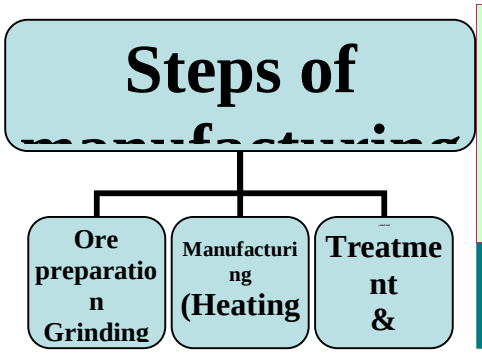

Fig (1) Steps of Manufacturing

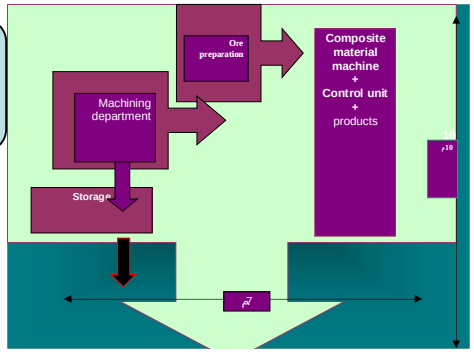

Fig (2) The workshop design

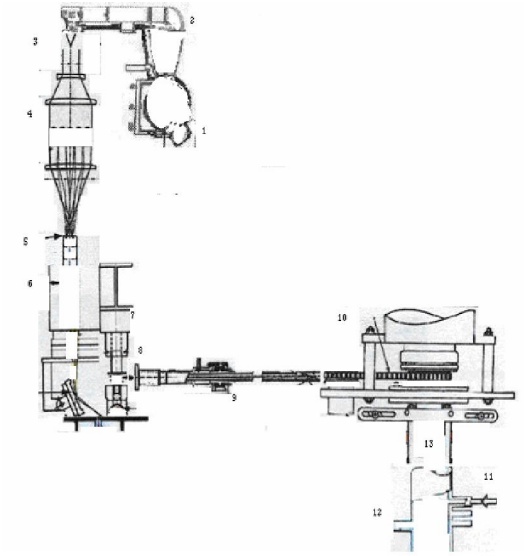

(Four Stroke Composite Material Machine)

1-Grinding machine
2-belts
3-addition of raw materials
4-multi speed mixer
5-Cones for mold feeding
6- Shaping mold
7-press 100ton
8-Heaters 220volt,3000watt, 500C
9- electronic arms
10-control of automatic arm
11- water inlet
12-water outlet
13- fans

Fig (3) Main parts of the four stroke composite material system

e) Laser Irradiation

Samples used in this investigation were in a shape of disk of 25mm diameter and 7mm length. The irradiation is done on both sides of the samples and in different positions to cover all the area of the sample and achieve homogeneous surface suitable for testing .The different lasers irradiated samples at different conditions were examined before and after laser irradiation and the effect of laser was determined.

The type of laser used is Nd-YAG I used in the third harmonic (wavelength =355nm) which lies in the ultra violet (UV) region with power of bout 10milli watt, duration time 7nsec,repetition rate 17HZ and energy (40mmj/pulse) [6]

F) Microscopic Examination

All specimens were prepared metallographically first by grinding on different grades of silicon carbide "SiC" paper coarse grinding and then fine grinding. The process had to be repeated several times to obtain best results and to produce uniform level of matrix. All of these pictures were carried out in several areas in each specimen by making negative at 500x by Olympus optical microscope

g) Raman Spectroscopy

The behaviour of the material was studied by variation of the modes obtained from FT (IR) Raman spectrum. The results were obtained using Brucker FTIR Raman spectrometer using Nd-YAG laser power of 500MW as source of excitation. After irradiation the thin film of sample with different lasers, the spectra were obtained in the range 400 to 4000 cm-1. The samples to be measured was fixed to holder and placed in front of the beam [7].

3. Results and Discussion

Fabrication Procedures

The fabrication quality parameters are indicated as follow: -

1. Maximum fibre percentages to achieve success fabrication were (65%) increasing the fibre percentage up on this value will produce less qualified fabricated material.

2- Temperature is the most significant parameter in Fabrication. Over heating temperatures at all fibre percentage leads to dissociation of PMMA to monomers and different gases. As a result of low fabrication temperatures, viscosity becomes insufficient for deformation so the optimal deformation temperature is required to get viscous matrix suitable for addition of reinforcement.

3- The pressure required for deformation and time of force act were strong functions of both volume fraction and fibre percentages.

5- The fast cooling rate (water cool) may be recommended as the suitable Cooling rate regardless of fibre percentage and volume fraction.

6- The density of nano-composites will not be affected by laser irradiation.

7- Laser irradiation is used to improve the surface properties of the material as follow:

A - The hardness will improved from (43 to 63) barcoul about (50%) when the exposure time increase from 21 nano second to 70 nano second and after that the hardness remain constant with increasing time.

B — the hardness improved with increasing fibre percentages and the maximum value was (60 Barcoul) at L/D = 1 and volume fraction 50%. This improvement increase with laser irradiation and reach its maximum at (80 Barcoul) with argon - ion laser at L/D =50 and volume fraction 50%.

C — the wear rate is improved with fibre percentage to reach (3.8m/m) at L/D = 50 and volume fraction 50%.

8 – The wear rate and coefficient of friction were improved more with laser irradiation to reach 0.4m/m wear rate and 0.75 coefficient of fraction at argon irradiation (L/D =50 and volume fraction 50%)

9- Alkali resistance is excellent before and after laser irradiation and weight loss is less than 0.01% at exposure time more than 30000 hours.

All of the above tests were done according to standard methods ASTM [3-7]

b) Microstructure Analysis

The reinforcement strength to weight ratio and volume fraction have a significant effect on the manufacturing conditions and mechanical properties. Fig (4-a) and fig (4-b) show the microstructure of nano-composites when the length to diameter ratio equal 50, the fiber volume fraction is 17% and 50% respectively, fibers were distributed in random manner in the structure and cross linked together in different positions, this distribution prevents the crack propagation. In other words, the crack does not reach the critical size. Cross linking of reinforcement in the matrix is the main reason of improvement in the mechanical properties. When the volume fraction of fibers increased to 50%, the cross linking of fibers were increased, the crack propagation became very limited. The mechanical properties were improved as a result of increase in fiber volume fraction. In fig (4-c) and fig (4-d) show the microstructure of nano-composites when the length to diameter ratio equal 1, the fiber volume fraction is 17% and 50% respectively. When the fiber shape was circular the cross linking was relatively limited, when compared with the fibers in fig (4-a), that is the main reason for extra improvement in mechanical properties when the fiber size (length to diameter ratio) increased at the same volume fraction. When comparing fig (4-d) with both figure (4-a) and (4-b), the random distribution of particles with high volume fraction 50% improves the mechanical properties and crack propagation theme better than fig (4-c). The amount of cross linking was still lower than both fig (4-a) and fig (4-b). The qualitative analysis of the microstructure of nano-composite explains the improvement in mechanical properties in terms of fiber shape, size and volume fraction. The laser irradiation effect was not detected by optical microscope so spectroscopic analyses of the samples were done.

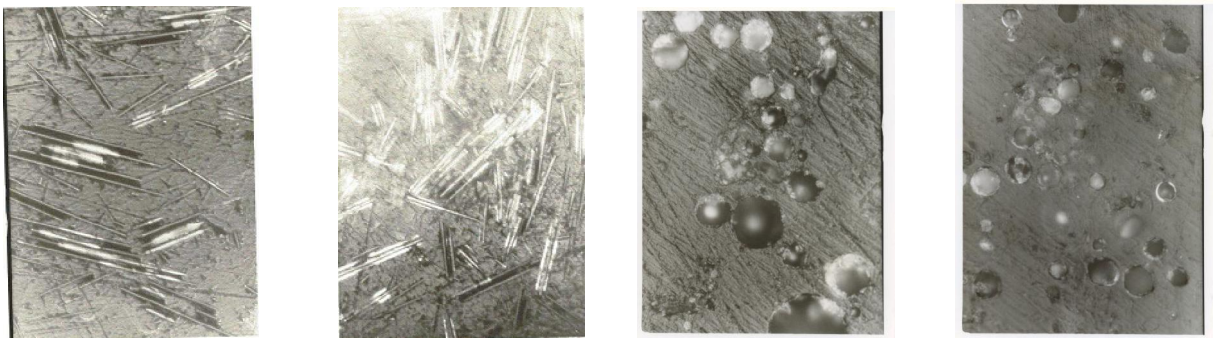

A) 17% fibre, L/D=50, 500x b) 50 % fibre, L/D=50, 500x C) 17% fibre, L/D=1, 500x D) 50 % fibre, L/D=1, 500x

Fig (4) the fibre impeded into the matrix before laser irradiation at 500x and at different percentages of fibres.

c) Raman Spectroscopy

Laser irradiation was a very good method for treatment of nano-composite without any change in morphology of the samples surface. Fig (5) Raman spectrum of the nano-composite at different length to diameter ratio and different volume fractions before and after laser irradiation by Nd-YAG and Argon lasers. The spectrum was affect by laser type volume fraction of fiber, fiber shape and length to diameter ratio (fiber size). In quantitative analysis of the IR spectrum of the material each absorption band is characterized by four parameters

1-band shape F(x)

2-Intensity of the band (integral intensity rather than peak depth)

3-Half band width of the band (the width of the band at its half depth)

4-The centre of mass of the band.

The complex behaviour reflecting two regions of dependence on the characteristics of lasers, which might be related to the structure changes and introduce the parameters characterizing the vibration motion of the vibrating groups such as the vibration activation energy in certain vibration energy levels.

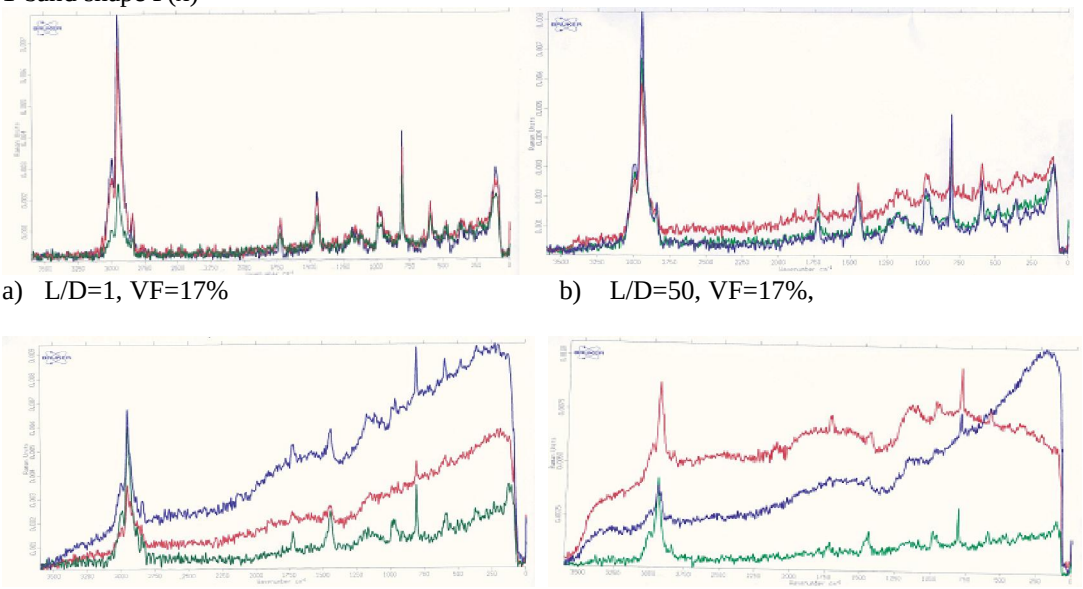

a) L/D=1, VF=17% b) L/D=50, VF=17%, VF=50% ,L/D=50 d) % VF=50 c) L/D=1,

Fig (5) Raman spectrum of the nano-composite at different length to diameter ratio and different volume fractions before and after laser irradiation by Nd-YAG and Argon lasers.

Fiber is considered as the element that more affected by laser in the structure, the change in fibre shape leads to increase in the area exposed to lasers. Argon laser treated samples recorded higher peak values almost at all curves. The results were relatively compatible with the mechanical properties. The ability of material to absorb a certain laser wavelength is a property of the material as a function of laser type, wavelength, power and repetition rate.

4. Conclusions and Recommendations

Four strokes composite material machine is considered as economic and qualified method in production of nano-composites. The system is a multifunction system in compact design.

The initiative produces scientific contribution in a very specific field. The production of thermoplastic based composite material is a new trend all over the world, with these patents Egypt is one of the countries all over the world build and transfer new technology, the initiative produces 40 compounds contribute in more than 120 industries. Now shafts, gears, rods, chairs, tables, and electrical equipment are made from composites. Very small units for production of the parts mentioned above is established, this small unit works full automatic

The following Recommendation may be considered for future research:

1- Irradiation of fiber glass before manufacturing
2- Using laser in cutting of fiberglass and study how the fiber properties changes.
3- Using different types of lasers with different wavelength and study the differences.
4- Study the effect of laser irradiation on other types of fiber and matrix to reach the optimum properties and best treatment method.
5- Study the different manufacturing parameters to increase the economical value.

Acknowledgements

This work was supported by the design and research centre and Shoubra Company for engineering (patent number 20841, 23021 and 399/2004). I also thank all stuff of N.I.L.E.S in Cairo University for their helpful advice guidance and stimulating discussions.

5. References

1. Bogomolov V N, Feoktistov N A, Golubev V G, Hutchison J L, Kurdyukov D. A, Pevtsov A B, Sloan J and Sorokin L M 1999 Proc. 7th Int. Symp. `Nanostructures: Physics and Technology', (St Petersburg, Russia) p 52
2. Bogomolov V N, Feoktistov N A, Golubev V G, Hutchison J L, Kurdyukov D A, Pevtsov A B, Schwarz R, Sloan J and Sorokin L M 2000 J. Non-Cryst. Solids 266 1081
3. Cardona M 1982 Light Scattering in Solids II ed M Cardona and G Guntherodt, Topic in Applied Physics vol 50 (Berlin: Springer) p 117
4. Davydov V Yu, Kitaev Yu E, Goncharuk I N, Smirnov A N, Graul J, Semchinova O, Uffmann D, Smirnov M B, Mirgorodsky A P and Evarestov R A 1998 Phys. Rev. B 58 12 899
5. Filip Van den Abeele, Joris Degrieck, Wim Van Paepegem, Experimental characterization and numerical modelling of impact damage in fibre-reinforced composites; Proceedings of the 12th European Conference on Composite Materials, Biarritz, France (ECCM 2006)
6. Patricia Verleysen, Joost Van Slycken, Filip Van den Abeele, Joris Degrieck, Advances in High Strain Rate Material Testing; Proceedings of the Ninth International Conference on Structures Under Schock and Impact, Wessex Institute of Technology, New Forest, UK (SUSI 2006)
7. Filip Van den Abeele, Joris Degrieck, Wim Van Paepegem, Impact Damage Model for Fibre-Reinforced Composite Materials; Proceedings of the 7th Congress on Theoretical and Applied Mechanics, FPMs-Faculty of Engineering, Mons, Belgium (NCTAM 2006)
8. C. Suryanarayana, Progr. Mater. Sci. 46, 1-184 (2001).
9. L. Takacs, Progr. Mater. Sci. 47, 355-414 (2002).
10. F.Kh. Urakaev, L. Takacs, V. Soika, et al., Russian J. Phys. Chem. 75, 1997-2002 (2001).
11. K. Tkácová, N. Stevulová, J. Lipka, V. Sepelák, Powder Technology. 83, 163-171 (1995).
12. J.Z. Jiang, R.K. Larsen, R. Lin, at al., J. Solid State Chem. 138, 114-125 (1998).
13. P.P. Chattopadhyay, S. Talapatra, S.K. Pabi, Mater. Chem. Phys. 68, 85-94 (2001).
14. P. Balaz, E. Boldizarova, S. Jelen, Hydrometallurgy. 67, 37-43 (2002).

4/5/2010

Optimized Conditions for Increasing *Escherichia coli* Resistance to p-Hydroxybenzoic Acid

Mohamed M. Aboulwafa[1], *Ramadan A. El Domany[2], Riham M. Shawky[2] and Shima M. A. Ibrahim[2]

Microbiology & Immunology Department, Faculty of Pharmacy, Ain Shams University[1], and Microbiology & Immunology Department, Faculty of Pharmacy, Helwan University[2]

*E-mail: Rdomanii@yahoo.com

Abstract: The present study aimed at increasing resistance of *Escherichia coli* to p-hydroxybenzoic acid (pHBA) through manipulation of different environmental and physiological factors. According to the study, different incubation temperatures, pHs, agitation rates and medium components were tested to characterize *E. coli* resistance to pHBA in shake flask and a laboratory fermentor. Genetic analysis using PCR of four representative *E. coli* isolates showed that *yhcP* gene was detected in both sensitive and resistant wild isolates of natural sources, a finding that stressed the importance of studying different environmental, physiological and genetic factors affecting the regulation of *yhcP* gene. MIC of pHBA against *E. coli* strain BW25113 that has the YhcP efflux pump showed a 64 fold increase by changing the growth medium from nutrient broth to basal medium containing 2% peptone and 2.6% glucose and keeping the pH constant at 8. Increased resistance of *E. coli* to pHBA could provide an effective solution to the toxicity of acid to the producing host bacterial cell which in turn will help to increase production of this molecule for commercial use. [Journal of American Science 2010;6(7):155-169]. (ISSN: 1545-1003).

Keyword: *Escherichia coli*, p-hydroxybenzoic acid, environmental, physiological factors, *yhcP* gene

1. Introduction

E. coli resistance to pHBA is mediated through an efflux pump (Van Dyk *et al*., 2004). Efflux systems export toxic metabolites from the cells, and consequently are capable of conferring resistance to different chemotherapeutic agents. Transport proteins taking part in the extrusion of noxious agents may be specific for one or for a range of structurally different substrates (Kern et al., 2000). Five families of bacterial efflux systems have been identified (Putman *et al*., 2000). These include: i) the small multidrug resistance family SMR (a member of the much larger drug⁄metabolite transporter (DMT) superfamily (Poole, 2004); ii) the resistance nodulation division (RND) family (Zgurskaya and Nikaido, 2000), which is part of the larger RND permease superfamily (Tseng et al., 1999); iii) the major facilitator superfamily MF (Pao et al., 1998); iv) the ATP binding cassette family (ABC) (van Veen and Konings, 1998); and v) the multidrug and toxic compound extrusion family MATE (Brown *et al*.,1999).

Treatment of *E. coli* with pHBA resulted in upregulation of *yhcP*, encoding a protein of the putative efflux protein family & the adjacent genes *yhcQ*, encoding a protein of the membrane fusion protein family, and *yhcR*, encoding a small protein without a known or suggested function. The function of the upstream, divergently transcribed gene *yhcS*, encoding a regulatory protein of the LysR family, in regulating expression of *yhcRQP* was shown. The efflux function encoded by *yhcP* was proven by the hypersensitivity to pHBA of a *yhcP* mutant strain. A *yhcS* mutant strain was also hypersensitive to pHBA. Expression of *yhcQ* and *yhcP* was necessary and sufficient for suppression of the pHBA hypersensitivity of the *yhcS* mutant. Only a few aromatic carboxylic acids of hundreds of diverse compounds tested were defined as substrates of the YhcQP efflux pump. Thus, a proposal for renaming yhcS, yhcR, yhcQ, and yhcP, was made to reflect their role in aromatic carboxylic acid efflux, to aaeR, aaeX, aaeA, and aaeB, respectively. The role of pHBA in normal *E. coli* metabolism and the highly regulated expression of the AaeAB efflux system suggest that the physiological role may be as a "metabolic relief valve" to alleviate toxic effects of imbalanced metabolism (Van Dyk et al., 2004).

pHBA is a key monomer used in the production of liquid crystalline polymers (LCPs) and its cost is a major portion of the high cost of LCPs, and limits the commercial applications for which they can be used. A large proportion of the cost of pHBA, and consequently LCPs, is related to the cost of its chemical synthesis (Amaratunga *et al*., 2000). pHBA has an additional utility as a chemical intermediate for the manufacture of paraben preservatives and other products (Johnson *et al*., 2000).

Earlier reports (Amaratunga *et al*., 2000); (Johnson *et al*., 2000) of improved biosynthesis of pHBA relied on plasmid localization of *ubiC* to achieve significant overexpression of chorismate lyase. The use of ion-exchange resin to remove product during fermentation runs had a particularly pronounced impact in the earlier report (Johnson *et al*., 2000) on microbial production of pHBA. In the absence of product removal using ion-exchange resin during the course of a fermentation run, 6.2 g/L of pHBA was synthesized by the construct (Amaratunga *et al*., 2000)

that resulted from two rounds of selection for resistance to antimetabolites and over-expression of plasmid-localized *ubiC*. However, a total of 22.9 g/L of pHBA was synthesized when anion exchange resin was used to remove product during the course of the fermentation (Johnson *et al*., 2000).

By repeatedly passing culture medium through the anion-exchange resin during the fermentation, the concentration of pHBA in the culture medium was likely kept at a level that reduced its toxicity towards the producing microbe. This is not to suggest that pHBA toxicity was completely avoided. It was observed that a substantial reduction in cell biomass and product concentration at concentrations of pHBA of 10 g/L. More effective solutions to the toxicity of pHBA have to be found given that pHBA negatively impacts *E. coli* metabolism even at 10 g/L concentrations under fed-batch fermentor conditions. Several methods of producing aromatic carboxylic acids from recombinant microorganisms are described in the literature, however it will be advantageous to optimize production of these molecules for commercial use, route to optimized production is increased yield, as many of these aromatic carboxylic acids are toxic to the producing host cell, another route may be to minimize the toxic effect the end product has on the host cell. A family of ubiquitous the proteins that may be able to address both of these issues are the efflux proteins (Sariaslani and Van Dyk, 2007).

This proposed study aimed at optimizing a simple fermentation method for increasing resistance of *E. coli* BW25113 which has *yhcP* gene that codes the efflux pump of pHBA. The study was conducted on flasks level and in a laboratory fermentor.

2. Materials and methods

Microorganisms

E. coli standard strains*: E. coli* BW25113 which has *yhcP* gene that codes the efflux pump of pHBA & *E. coli* BW25113Δ*yhcP* which lacks such gene.

E. coli isolates: a total number of 38 isolates were isolated from different sources and identified biochemically according to Bartelt,1999 then categorized according to the isolation source into clinical isolates coded (1,2,3,9,10,11,17, 18, 19, 23, 24, 25, 26, 27, 28, 29, 20, 21, 22, 30) & isolates from food handlers coded (12, 13, 14, 15, 31, 32, 33, 34, 35, 36, 37, 38) & isolates from veterinary source coded (39, 40) & isolates from miscellaneous sources (4, 5, 6, 16).

Media and chemicals

All reagents and materials used for the growth and maintenance of bacterial cells were obtained from Merck (Germany), Biolife (Italy), Britania (Argentine), Oxoid (England), or Difco laboratories (Detroit, USA). The basal medium used is composed of: Ammonium sulphate (0.500 gm), Calcium chloride.$2H_2O$ (0.001 gm), Magnesium sulphate.$7H_2O$ (0.05gm), Di-Potassium hyderogen orthophosphate (1.740gm), Potassiom dihydrogen orthophosorthophosphate (1.360 gm), distilled H_2O to 100 ml, peptone or beef extract were used as protein source & glucose was incorporated to the required concentration by adding a specified volume from sterilized glucose stock solution after autoclaving.

Determination of susceptibility of *E. coli* isolates/strains to pHBA

The susceptibility of the tested *E. coli* isolates/strains to pHBA was assessed by determining the MIC against it. The MIC was determined by microdilution technique according to Van Dyk et al., 2004 with some modifications. The inoculum was 10 µL prepared by suspending a fresh slant of the tested *E. coli* isolate/strain in 3 ml 0.9% physiological saline solution. The turbidity of the suspension was adjusted to 0.5 McFarland standards ($1\text{-}2x10^8$ cfu/ml). The suspension was further diluted one thousand fold to yield $1\text{-}2x10^5$ cfu/ml. The plates were incubated at 37^oC for 24 hours. The MIC of the resulting diluted suspension was determined in nutrient broth against pHBA. For each tested isolates/strains, duplicate measurements were conducted.

Studying the different environmental factors affecting the susceptibility of some *E. coli* isolates/strains to pHBA in shake flasks

The effect of different environmental factors on susceptibility of the two standard *E. coli* strains (BW25113 and BW25113Δ*yhcP*) and eight selected *E. coli* isolates to pHBA was studied. Five of the ten tested isolates/strains were of high MIC values (7, 9, 15, 20, and 37) and the other five were of low MIC values (3, 8, 24, 25 and 34). The different factors studied included; agitation rate, incubation temperature and initial pH. The experiment was carried out in 100 ml Erlenmeyer flasks, each containing 25 ml nutrient broth. The flasks were inoculated with the bacterial suspension (10^5 cfu/ml) of the test strain at 2% v/v inoculum size. The inoculum of the test strain was prepared as described in the determination of susceptibility of *E. coli* isolates/strains to pHBA. The stock solution of pHBA (500 mM) was incorporated in the culture flasks to the final concentration of 2.5 mM. Control flasks were similarly prepared but contained no pHBA. The flasks were incubated in an incubator shaker (ROMO Company, local supply) at the specified temperature and agitation rate. In case of studying the effect of initial pH only, the initial pH of the culture medium was adjusted before autoclaving to the required value. In all cases, aliquots were removed at different time intervals for determination of O. D at 600 nm.

Effect of different culture medium components on the MIC of pHBA against the tested *E. coli* isolates/strains

The MIC values of pHBA against the two standard *E. coli* strains (BW25113 and BW25113Δ*yhcP*) and the eight selected *E. coli* isolates to pHBA were determined in microtitre plate principally as described in the determination of susceptibility of *E. coli* isolates/strains to pHBA. The inoculum was prepared in shake flasks using a culture medium similar to the corresponding medium used for MIC determination in each case. The flasks (100 ml) contained 25 ml culture medium were inoculated with 0.5 ml aliquots of 10^8 cfu/ml of fresh bacterial suspension prepared as described in the determination of susceptibility of *E. coli* isolates/strains to pHBA and incubated overnight at 37^{o}C and 320 rpm.

The optical density of the growth obtained was determined and the count was then adjusted to10^8 cfu/ml using the equation 1 O. D_{600} = 1x10^9 cfu/ml. The 1 O. D_{600} = 10^9 cfu/ml /ml expressed the average value of 1 O. D_{600} = 8x10^8 cfu/ml (Becker *et al*., 1996) and 1 O. D_{600} = 1.7x10^9 cfu/ml (determined experimentally), and then serially diluted with physiological saline to 10^5 cfu/ml. The adjusted bacterial suspension obtained was used as inoculums for MIC determination in microtitre plate. The different factors studied included variable concentrations of sodium and potassium chloride salts (0.5, 1 and 2%), tween 80 (1 and 2%), 1.5% (glucose and sucrose) and 1% starch, and different protein/glucose combinations. All factors were studied in nutrient broth except the different protein/glucose combinations the used protein source was added to the basal medium (described in materials and methods) containing either 2.6% or 5 % glucose. The protein source was added at 2% final concentration. In addition the two protein sources (beef extract and peptone) were separately tested at 4% final concentration in basal medium containing only 2.6% glucose.

Genetic analysis of some selected *E. coli* isolates for their acquisition of the pHBA efflux pump gene, *yhcP*

Four isolates were subjected to PCR amplification for screening of the *yhcP* gene as two isolates of high MIC values (isolates 9 and 37) and the other two were of low MIC values (isolates 3 and 34) against pHBA. *E. coli* strains BW25113 (strain 7) and BW25113Δ*yhcP* (strain 8) were used as positive and negative controls, respectively.

The extraction of the chromosomal DNA was carried out according to Wu, *et al*., 2004. The DNA primers used in the PCR reaction were: Left primer: GCGTCAGCGATAGCGTATTG and right primer: GTGGATCGAGAGCTGGAAAG.

The PCR reaction mixture: Buffer (2.5 ml), $MgCl_2$ (1µL), (20 pico) primer R (2 µL), (20 pico) primer left (2 µL), (10 mM) dNTP's (0.5 µL), template DNA (2 µL), Taq (0.25 µL), PCR H_2O (14.75 µL). Total volume (25 µL).

The PCR reaction conditions were: initial denaturation at 94^{o}C for 3 minutes and then 40 cycles, each consisted of (1) denaturation at 94^{o}C for 1 minute, (2) annealing at 56^{o}C for 1 minute, (3) extension at 72^{o}C for 1 minute. A post-extension period at 72^{o}C for 7 minutes was allowed. The PCR product was approximately 200 bP.

Fermentor experiments

Fermentation process. Vessel preparation with culture medium

The culture medium applied was basal medium containing 2% peptone to which glucose was added after sterilization to the final concentration of 2.6%. Sterile glucose solution was incorporated from 5% glucose solution (500 ml plastic bottles) which was obtained from a local commercial source and their labeled concentration was checked experimentally using glucose quantization kits. The culture medium was dispensed in BioFlo 110 advanced fermentation kit equipped with a heat blanketed 5 L glass fermentation vessel and the different fermentation processes were carried out using 3 liters working volume. The vessel containing the culture medium and the liquid addition bottles of acid, base and antifoam were sterilized batch wise in an autoclave at 121^{o}C for 15 minutes. Aeration was conducted by admission of compressed air after its passage through two types of filters, the first filter was located in the front of the air exit from the compressor and it was used for the removal of dust and graze while the second one (resterilizable cartridge bacterial filter, 0.2 µm) was located just above the vessel head plate and was connected to the sparger by an autoclavable silicon tube.

The cartridge filter was sterilized by autoclaving while connected to the vessel. The aeration was controlled at 3 vvm for the different fermentation cycles. The dissolved oxygen was monitored during the fermentation cycles by the aid of dissolved oxygen probe which was calibrated after sterilization and before inoculation to the scale zero and 100. The readings were recorded during the fermentation cycles manually. Temperature was detected by a thermowell and controlled automatically through the fermentor microprocessor at 37^{o}C by the use of heat blanket and internal cooling coils installed inside the vessel. The agitation was conducted by a motor (Magmotor Corporation a

SatCon Co.) connected to the agitator shaft above the vessel head plate and operated at a fixed rate of 200 rpm for the different fermentation cycles. The pH was controlled automatically to the tested values (6, 7, 8) using 5 M NaOH and 1 N HCL and by the aid of sterilizable pH probe which was calibrated before use. NaOH and HCl bottles were connected to the acid and base ports by autoclavable silicon rubber tubes passed through peristaltic pumps. Foaming was monitored visually and suppressed by the addition of soybean oil (Agriculture research center, soybean research institute) using the manual mode of the primary control unit.

Inoculum build up

The inoculum was prepared in shake flasks using a culture medium similar to that used for cell growth in the fermentor. The flasks (250 ml) contained 60 ml culture medium were seeded with 2% V/V of 10^8 cfu/ml fresh bacterial suspension prepared as described in the determination of susceptibility of *E. coli* isolates/strains to pHBA and incubated overnight at 37^{o}C and 320 rpm. The inoculum was added to the vessel manually through the inoculation port at an inoculums size of 2% V/V after establishment of different operating parameters (temperature, pH and dissolved oxygen).

Effect of pH on growth profile and susceptibility to pHBA of the tested *E. coli* strains grown in the fermentor

A number of fermentation cycles for the two *E. coli* strains BW25113 and BW25113Δ*yhc*P were carried out at constant pH values of (6, 7 and 8) in laboratory fermentor (New Brunswick Scientific's BioFlo® 110 fermentor).

At the different tested pHs, samples were withdrawn at the time intervals of 0, 2, 4, 6, 8, 10, and 11 hour and at the end of the fermentation cycle (about 24 hours), appropriately diluted with physiological saline and their optical densities were determined with spectrophotometer at 600 nm to obtain the growth profile.

The growth obtained was tested for susceptibility to pHBA using two approaches (MIC determination and Killing Kinetics); both were carried out on a sample collected after 6 hours growth in the fermentor. The stock pHBA solutions used for MIC determination and killing kinetics studies were prepared at the tested pHs of 6, 7 and 8.

1- Determination of MIC using cells grown in the fermentor as inocula

MIC was determined in microtitre plates using a culture medium similar to that used for cell growth in the fermentor and of the same pH (6, 7 or 8). The pH of the medium used for MIC determination in the microtitre plate was adjusted before autoclaving then rechecked and corrected to the required pH after sterilization using sterile NaOH (4M) or HCl (1M).The cells collected after 6 hours growth in the fermentor were harvested by centrifugation (6000 rpm for 5 minutes) in a cooling centrifuge. Then, the cell pellets were washed twice with physiological saline then resuspended in physiological saline with the same pH of the fermentor medium used in each run (6, 7 or 8). The resulting bacterial suspension was adjusted to a viable count of 1-2x10^8 cfu/ml using 0.5 McFarland standard then serially diluted with physiological saline of the same pH to 10^5 cfu/ml. The adjusted bacterial suspension obtained was used as inoculums for MIC determination in the microtitre plate.

Stock solution of pHBA adjusted to the same pH of the growth medium was serially diluted in the wells of the microtitre plate. The wells of the microtitre plates were inoculated by 10 µL aliquots of the bacterial suspension under test. The plates were incubated at 37^{o}C for 24 hours and the MICs were determined by visually assessing turbidity after 24 hours. For each tested strain, triplet measurements were conducted.

2- Killing Kinetics determination

The bacterial cell suspension was prepared as described above then standardized by viable count. The killing kinetics experiment was carried out using stock pHBA solution of the same pH of the fermentor medium used in each run (6, 7 or 8). The bacterial suspension (2 ml) was mixed with (20, 251, 666µL) of the stock pHBA solution (2048, 1430, 1280 mM) in a Wassermann tube to give (20, 160, 320 mM) final concentration respectively. Aliquots (100 µL) were withdrawn at different time intervals (0, 2,5,50 minutes) for pH 6 and (0, 18, 103, 230 minutes) for pH 7 and 8. Aliquots were serially diluted in test tubes containing 10 ml physiological saline solution of the same pH. Then, the count of the residual surviving cells was determined by surface viable count by spreading method (Brown *et al.*, 1989) using nutrient agar as growth medium. Then, a death curve between the number of survivors and time intervals was constructed.

3. Results

Susceptibility of *E. coli* isolates and other *E. coli* reference strains to pHBA

The MIC values of pHBA against the collected *E. coli* isolates/strains were determined by microdilution technique in microtitre plates and the results are shown in Table 1.

Environmental factors affecting the susceptibility of some *E. coli* isolates/strains to pHBA in shake flasks

The effect of agitation rate

It was studied by varying the RPM (0, 140, 240 and 320) of the incubator shaker. The results displayed in Figures 1 & 2 as representatives of the ten isolates showed that the isolates of the code numbers 3 & 8 didn't exhibit growth in the presence of pHBA in comparison to control isolates (without pHBA). The same happened with isolates 24, 25 and 34 (data not shown).

However, the isolates coded 7 & 9 showed an increase in growth in the presence of pHBA by increasing the rpm in most cases. The same happened with isolates 15, 20 and 37 (data not shown). For most isolates their growth was comparable to that of the controls (without pHBA). The agitation rate of 320 rpm showed maximum growth with most isolates and it was applied in the subsequent experiments conducted in shake flasks.

Effect of incubation temperature

It was studied at two temperature degrees (37^oC and 40^oC) and at 320 rpm in shake flasks. The isolates having the code numbers of 3 & 8 showed no appreciable growth in the presence of pHBA for the two tested temperature degrees in comparison to control isolates (without pHBA) Figures 3 &4. The same happened with isolates 24, 25 and 34 (data not shown). However, for isolates of code numbers 7 & 9 the results showed that their growth in the presence of pHBA increased at both the tested temperature degrees (in most cases) becoming nearly equal to these of controls (without pHBA). The same happened with isolates 15, 20 and 37 (data not shown).

Effect of initial pH

Before studying the effect of initial pH on susceptibility of the ten selected *E. coli* isolates to pHBA, both growth and pH profiles of the tested isolates/strains were monitored for cells grown in nutrient broth and at different initial pH values. The results are shown in Figures 5 & 6. Both *E. coli* strains 7 and 8 behaved alike at the different tested initial pHs regarding growth and pH profiles. The two isolates 3 and 9 also behaved alike regarding pH profile although they showed different growth values at some data points. The resistant isolate 9 showed higher growth after 5 hours of incubation than the sensitive isolate 3 at the different tested pHs. Both isolates 3 and 9 showed similar maximum growth values at the different tested pHs. The susceptibility of the selected isolates/strains to 2.5 mM pHBA at three different initial pH values (5.3, 5.7 and 6.8) was studied. At the initial pH 5.3 both sensitive and resistant isolates/strains showed no growth at all data points. For the sensitive isolates, the effect of pHBA was aggravated at the initial pH 5.7 where nearly no growth was observed with the different isolates (Figures 7 & 8). In contrast, the resistant isolates showed high growth values except for the strain 7. At the initial pH 6.8, still high growth was obtained with the resistant isolates compared to the corresponding sensitive isolates in most cases. The pH profiles for resistant isolates showed differences compared to those of the sensitive isolates at some data points.

Effect of different culture medium components on the MIC of pHBA against the tested *E. coli* isolates/strains:

Effect of variable concentrations of sodium and potassium chloride salts

Results in Figure 9 showed that for isolates 8, 3, 24, 25 and 34 which have low MIC values for pHBA, their MIC increased from 2.5 mM (Table 1) to 5 mM (became equal to those of isolates 7, 9, 15, 20 and 37) with the addition of sodium chloride to nutrient broth at all concentrations tested (0.5, 1 and 2%). The same pattern was obtained with the addition of potassium chloride to nutrient broth at concentrations of 0.5 and 2% but not at 1% where the isolate 34 showed even higher increase in MIC to be equal to 10 mM. However, for isolates 7, 9, 15, 20 and 37 which have high MIC values for pHBA, the results displayed in the same Figure showed that the susceptibility of the isolates to pHBA was not affected by addition of any concentration (0.5, 1, 2%) of KCl or NaCl to nutrient broth except for the isolate 37, the MIC increased to 10 mM at 1% KCl concentration, compared to 5 mM in absence of KCl.

Effect of variable concentrations of tween 80

Results in Figure 10 showed that for isolates which have low MIC values for pHBA (Table 1), their MIC values increased from 2.5 mM to 5 mM with the addition of tween 80 to nutrient broth at both concentrations tested (1 and 2%) while isolate 34 showing even higher increase in MIC to be 10 mM with 2% tween 80. However, for isolates 7, 9, 15, 20 and 37 which have high MIC values for pHBA (Table 1), the results displayed in the same Figure showed that the susceptibility of these isolates to pHBA was not affected by addition of tween 80 to nutrient broth at concentration of 1% where their MIC values remained unchanged (5 Mm). While the addition of 2% tween 80 to nutrient broth increased the MIC values of isolates 7, 9, and 37 to be 10 mM.

Effect of some carbohydrate sources

For isolates 8, 3, 24, 25 and 34, the following results were displayed in Figure 11: the

Table 1. Summarization of *E. coli* isolates/strains from various sources according to their MIC values against pHBA

	MIC (mM)	Number of isolates/strains (their code numbers) from various sources according to their MIC values				
		Reference strains	Clinical isolates	Isolates from food handlers	Isolates from veterinary source	Miscellaneous isolates
pHBA	5	2 (BW25113)	13 (1,2,9-11, 17-23, 29)	5 (12-15, 37)		2 (4,6, 16)
	2.5	1 (BW25113Δ*yhcP*)	7 (3, 24-28, 30)	7 (31-36, 38)	2 (39, 40)	1 (5)

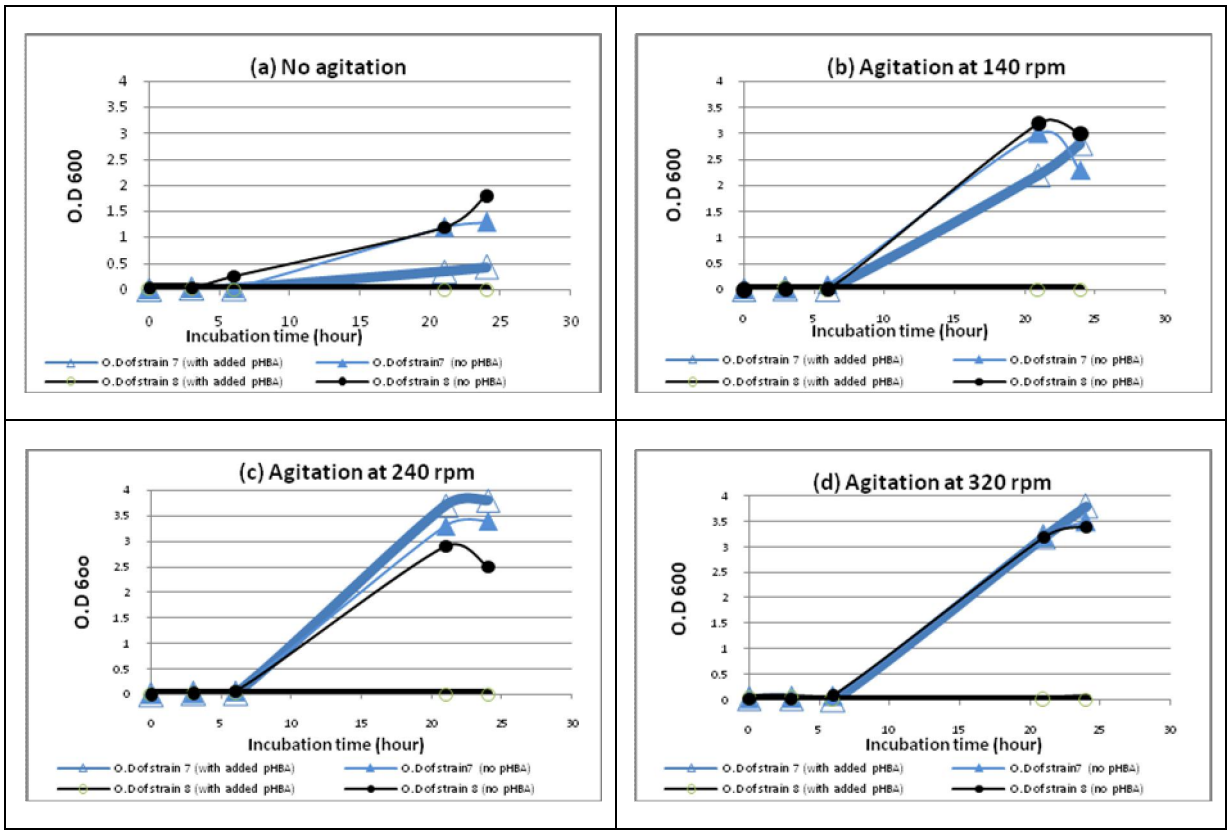

Figure 1. Effect of agitation rate on susceptibility of *E. coli* strains BW25113 (strain 7) & BW25113Δ*yhcP* (strain 8) to 2.5 mM pHBA in shake flasks

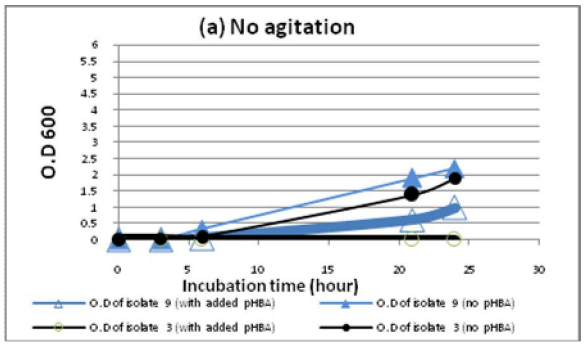

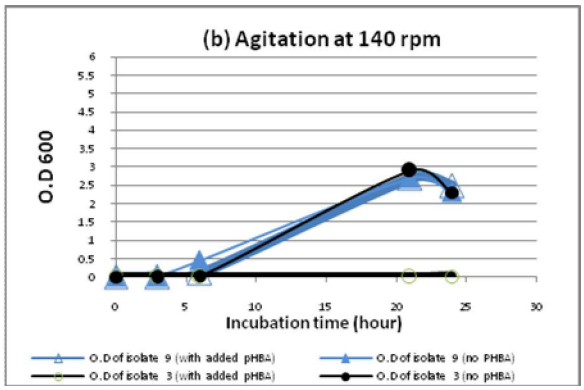

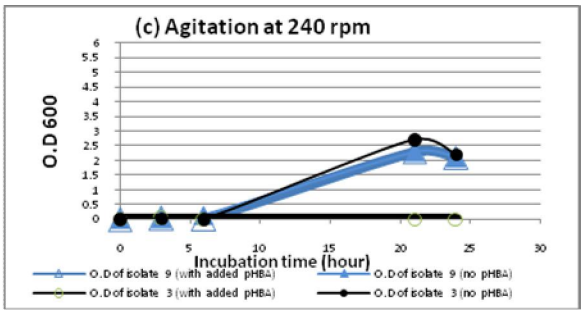

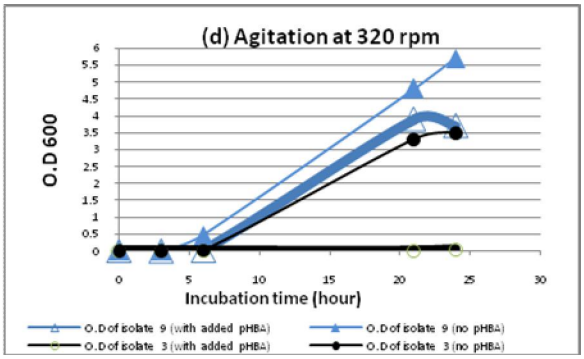

Figure 2. Effect of agitation rate on susceptibility of *E. coli* isolates 9 and 3 to 2.5 mM pHBA in shake flasks

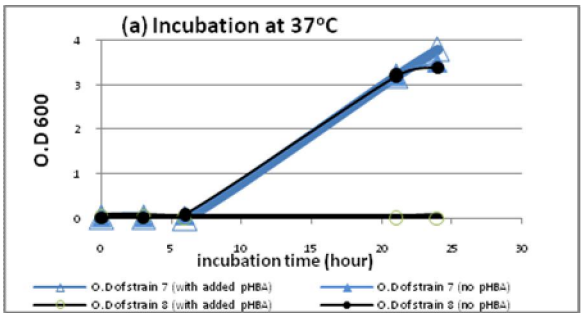

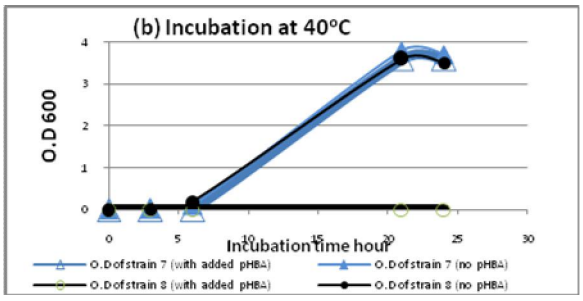

Figure 3. Effect of incubation temperature on susceptibility of *E. coli* strains BW25113 (strain 7) and BW25113Δ*yhcP* (strain 8) to 2.5 mM pHBA in shake flasks.

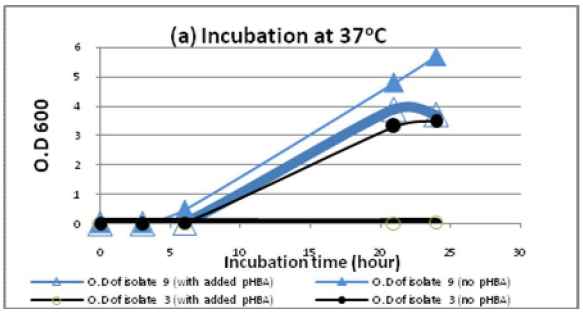

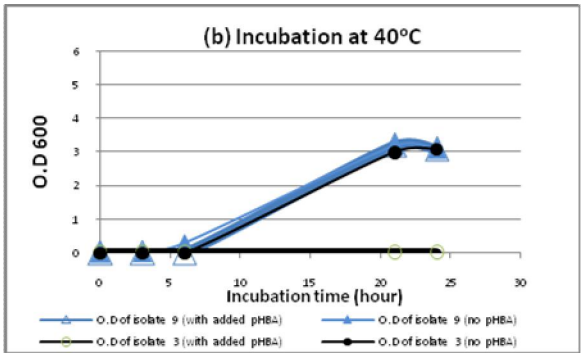

Figure 4. Effect of incubation temperature on susceptibility of *E. coli* isolates 9 and 3 to 2.5 mM pHBA in shake flasks

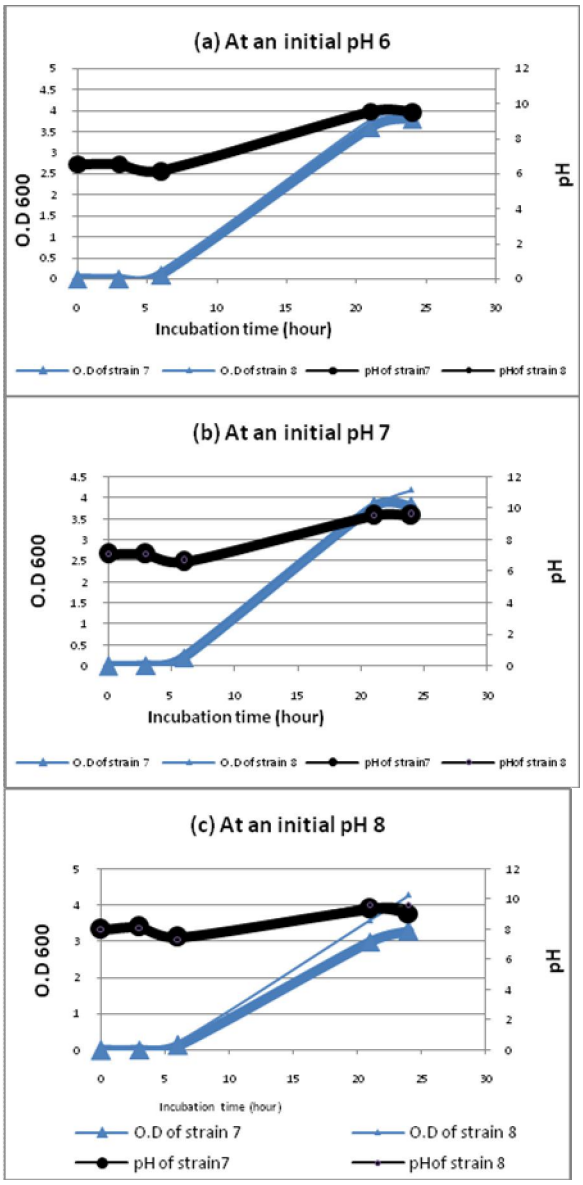

Figure 5. Growth and pH profiles of *E. coli* strains BW25113 (strain 7) and BW25113Δ*yhcp* (strain 8) grown in nutrient broth at initial pHs of 6, 7 and 8 in absence of pHBA

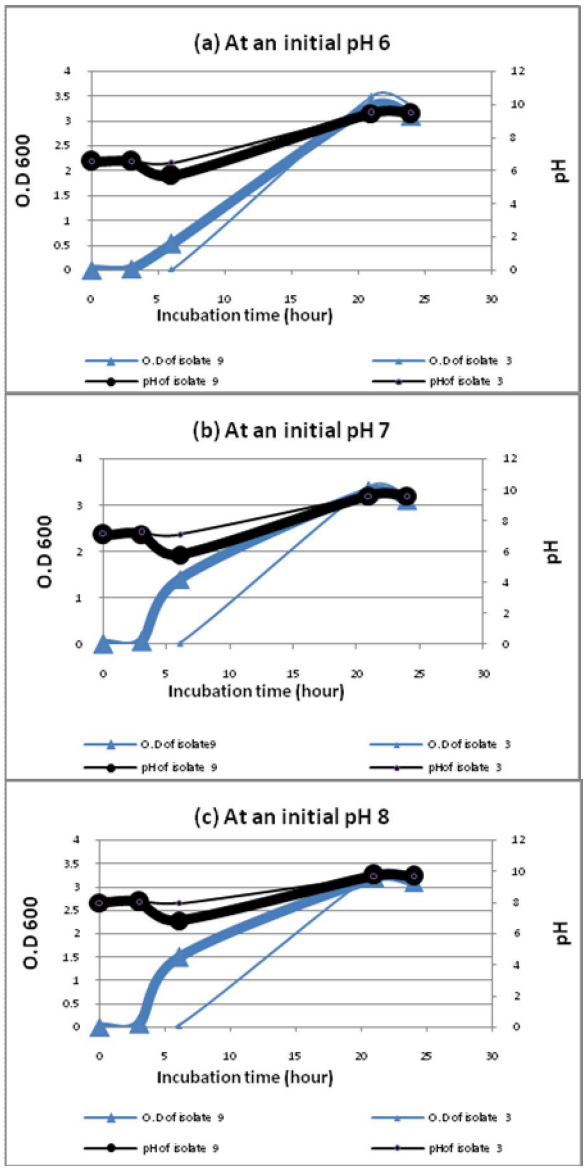

Figure 6. Growth and pH profiles of *E. coli* isolates 9 and 3 grown in nutrient broth at initial pHs of 6, 7 and 8 in absence of pHBA

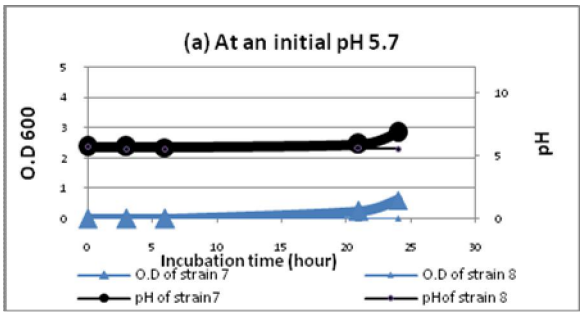

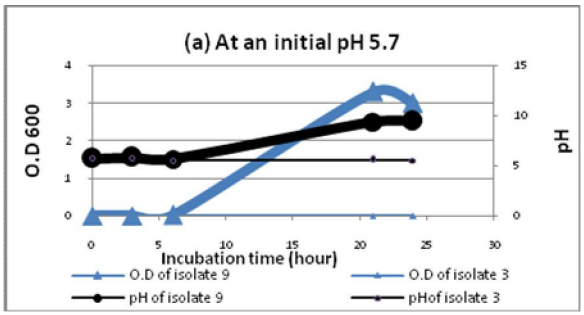

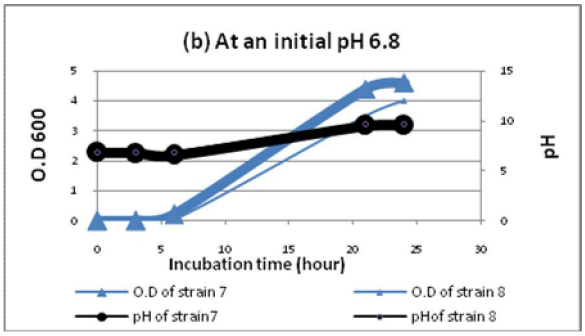

Figure 7. Growth and pH profiles of *E. coli* strains 7 and 8 grown in nutrient broth at initial pHs of 5.7 and 6.8 in presence of 2.5 mM pHBA

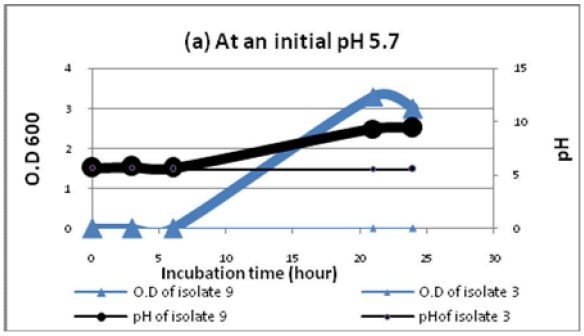

Figure 8. Growth and pH profiles of *E. coli* isolates 9 and 3 grown in nutrient broth at initial pHs of 5.7 and 6.8 in presence of 2.5 mM pHBA

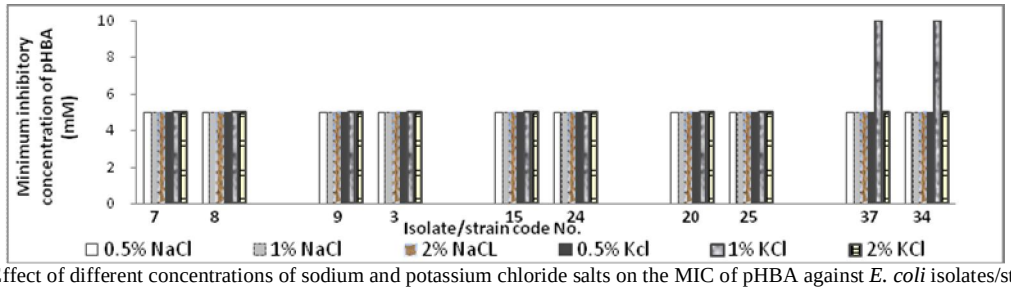

Figure 9. Effect of different concentrations of sodium and potassium chloride salts on the MIC of pHBA against *E. coli* isolates/strains as determined by microdilution technique. The tested agent was added to nutrient broth.

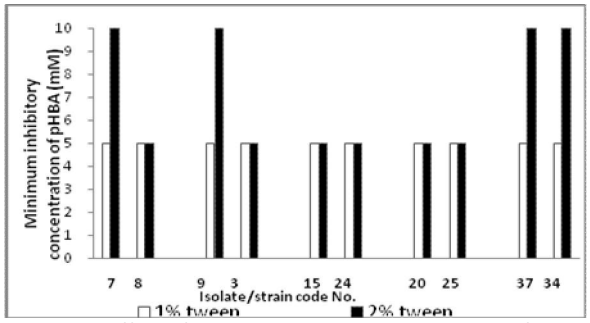

Figure 10. Effect of tween 80 (1and 2%) on the MIC of pHBA against *E. coli* isolates/strains as determined by microdilution technique. The tested agent was added to nutrient broth.

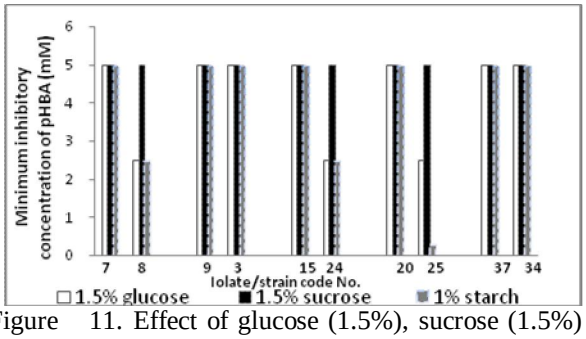

Figure 11. Effect of glucose (1.5%), sucrose (1.5%) and starch (1%) on the MIC of pHBA against *E. coli* isolates/strains as determined by microdilution technique. The tested agent was added to nutrient broth

addition of glucose (1.5%) caused no change in the MIC values (2.5 mM) of isolates 8, 24 and 25 while such addition caused two fold increase in the MIC values of isolates 3 and 34. The addition of sucrose (1.5%) to nutrient broth increased the MIC values from 2.5 mM to 5 mM for all these five isolates. The addition of starch (1%) increased the MIC values from 2.5 mM to 5 mM of isolates 3 and 34 while the MIC of isolate 25 sharply decreased to 0.3125 mM (8 fold reduction). However, for isolates 7, 9, 15, 20 and 37 the susceptibility to pHBA was not affected by addition of glucose (1.5%) , sucrose (1.5%) or starch (1%) to nutrient broth to (the MIC remained 5 mM).

Effect of different protein/glucose combinations

At peptone/glucose ratios of 2/2.6 and 2/5 and for the same test isolate no change in MIC values was observed except for isolate 9 where its MIC value decreased at high glucose concentration (Figure 12). At peptone/glucose ratios 2/2.6 and 4/2.6 and for the same test isolate, increasing protein concentration caused a decrease in MIC values of isolate 9, an increase in MIC values of isolates 24 and 37 and no change in MIC values of other isolates (Figure 12).

Comparison of the MIC values of the pHBA resistant isolates with those of their corresponding sensitive isolates, revealed that: the overall pattern showed a difference in MIC values with one condition or more for strain 7 versus strain 8 which reached 4 fold, isolate 9 versus 3, isolate 15 versus 24 and isolate 37 versus 34.

However, no such difference in MIC values was observed with isolate 20 versus 25 (Figure 12).

For beef extract/glucose combinations the following was observed: At beef extract/glucose ratios of 2/2.6 and 2/5 and for the same test isolate no change in MIC values was observed except for isolate 8 where high MIC value was obtained at high glucose concentration (Figure 13). At beef extract /glucose ratios 2/2.6 and 4/2.6 and for the same test isolate, increasing protein concentration caused no change in MIC values except for isolate 8 where high MIC value was obtained at high protein concentration (Figure 13).

Comparing the MIC values of the pHBA resistant isolates with those of their corresponding sensitive isolates, the following was observed: the overall pattern revealed a difference in MIC values for only strain 7 versus strain 8. While such difference in MIC values became nearly absent with other isolates (Figure 13).

PCR detection of the pHBA efflux pump gene, *yhcP* in four *E. coli* isolates

Results in Figure 14 showed a clear intensive band exhibited by each tested isolate and of size corresponds to that of the positive control.

Fermentor experiments

The cell growth and dissolved oxygen profiles of the two strains under the different tested pH values are shown in Figure 15. Both strains showed similar dissolved oxygen profiles at the different tested pHs (6, 7 and 8) while some differences between the two strains were noted in the growth profiles especially at pH 6 and 8. The results of killing kinetics for both strains are presented in Figure 16; they clearly exhibited different killing patterns. Almost in all cases, the killing kinetics rate of strain BW25113Δ*yhcP* was greater than that of strain BW25113 especially in the early periods of exposure to pHBA. The results of MIC determination of pHBA against the two tested strains at the different tested pH values are represented in Table 2.

4. Discussion

A better understanding of medium components and environmental factors affecting the susceptibility of some *E. coli* strains to pHBA on flasks level can be used to improve their resistance to pHBA.

The results displayed in Figures 1 & 2 showed that the susceptibilities of isolates of code numbers 3&8 to pHBA weren't affected at any rpm (140, 240, 320) or in absence of agitation.

However, the susceptibility to pHBA of the isolates coded 7& 9 was affected for agitated cultures in comparison to non agitated ones. In comparison to control, agitation supported growth in the presence of pHBA. Higher agitation rates (240 & 320 rpm) showed nearly similar growth for the tested isolate in the presence and absence of pHBA. In addition, in most cases higher agitation rate (320 rpm) produced more growth than lower agitation rates either in the presence or absence of pHBA. The agitation rate of 320 rpm was used by Amaratunga *et al*.,2000 in shake flask for increasing production of pHBA from *E. coli*. This may be attributed to the fact that stirring accomplishes two things: It mixes the gas bubbles through the liquid and it mixes the organism through the liquid, thus ensuring uniform access of microbial cells to the nutrients (Madigan *et al*., 2003).

The temperature in a vessel or pipe is one of the most important parameters to monitor and control in any process (Stanbury *et al*., 1995). The results displayed in Figures 3 & 4 showed that that the susceptibilities of isolates of code numbers 3&8 to pHBA weren't affected at any tested temperature in the presence of pHBA. However, the susceptibility to pHBA of the isolates coded 7& 9 was affected as they showed similar growth in the presence and in absence of pHBA in most cases at both the two tested temperature degrees (37, 40°C). However, in a number of cases the growth attained at 37◦C was higher than that attained at 40◦C. The temperature 37◦C is the incubation temperature used for pHBA MIC determination and

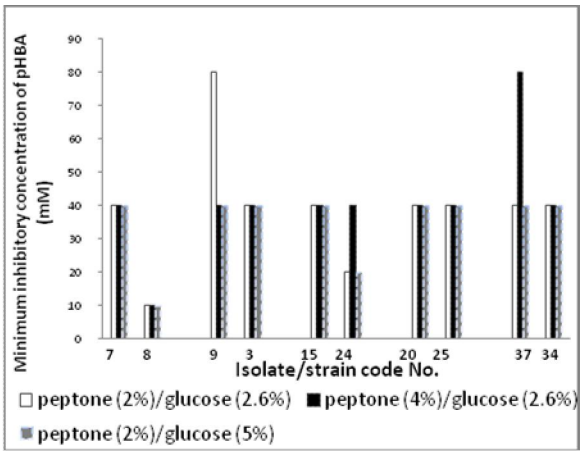

Figure 12. Effect of different peptone/glucose combinations on the MIC of pHBA against *E. coli* isolates/strains as determined by microdilution technique. Peptone/glucose combinations were added to the basal medium

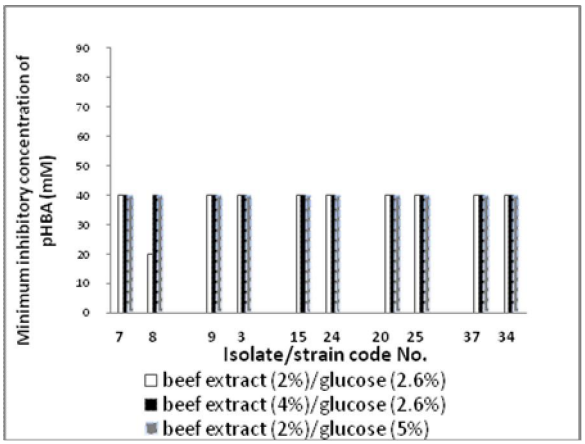

Figure 13. Effect of different beef extract/glucose combinations on the MIC of pHBA against *E. coli* isolates/strains as determined by microdilution technique. Beef extract/glucose combinations were added to the basal medium .

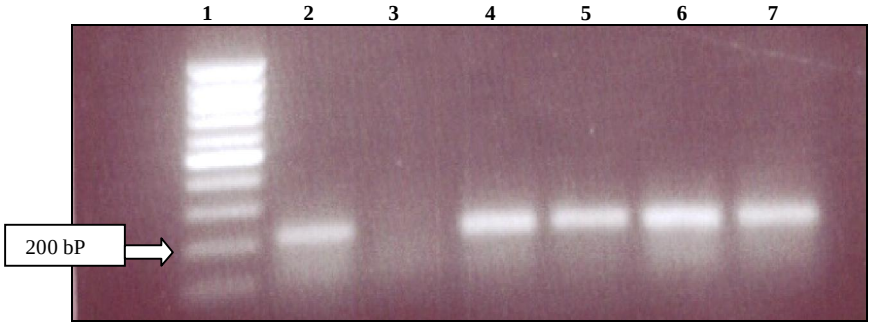

Figure 14. Agarose gel electrophoresis of PCR product of some selected *E. coli* isolates.
Lane 1, Marker; lane 2, positive control (*E. coli* strain BW25113); lane 3, negative control (*E. coli* strain BW25113Δ*yhcP*); lane 4, isolate 9; lane 5, isolate coded 3; lane 6, isolate coded 37; lane 7, isolate code

Table 2. Susceptibilities of the two *E. coli* strains BW 25113 and BW 25113Δ*yhcp* grown at different pHs in a laboratory fermentor (BioFlo 110)* to pHBA as determined by MIC.

pH	MIC (mM) of pHBA against:		Fold difference
	BW25113	BW25113Δ*yhcp*	
6	20	5	4
7	160	20	8
8	320	80	4

*) the produced cells were withdrawn after 6 hours for inoculation of microtitre plates for determination of MIC under similar conditions to that used for cell growth in the fermentor whenever possible

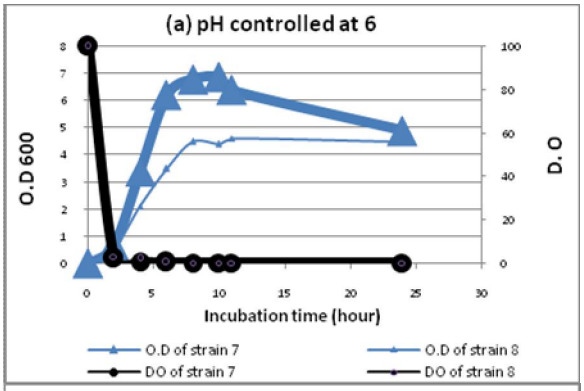

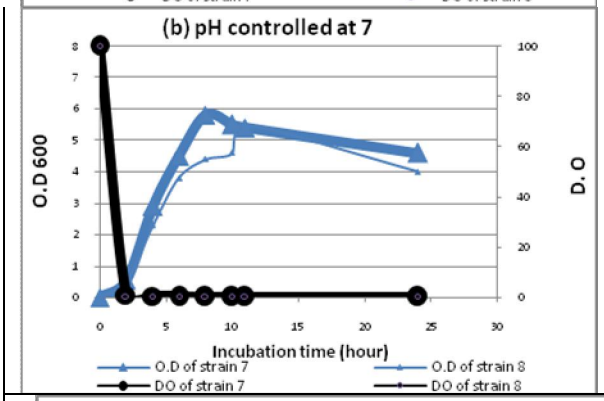

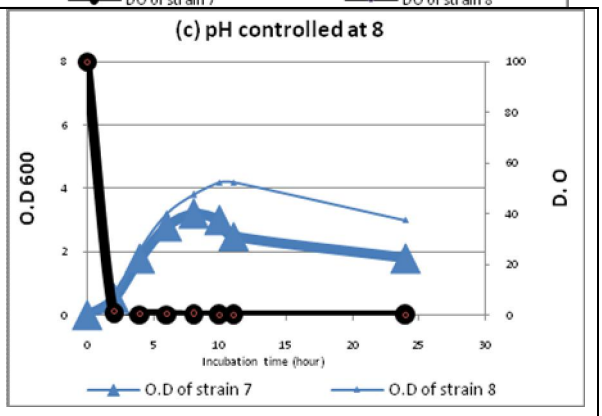

Figure 15. Growth and dissolved O_2 profiles of *E. coli* strains BW25113 and BW25113Δ*yhcP* grown in a laboratory fermentor under controlled pH of 6, 7 and 8. The basal medium containing 2% peptone and 2.6% glucose was used as a growth medium

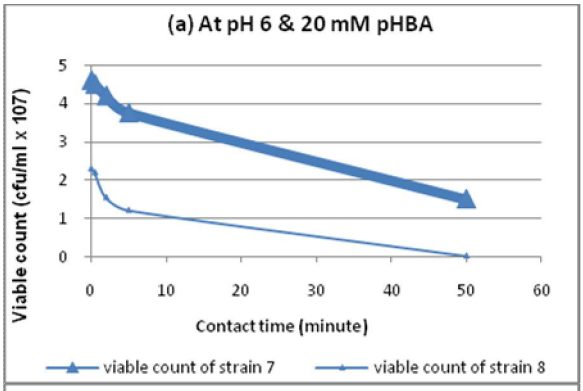

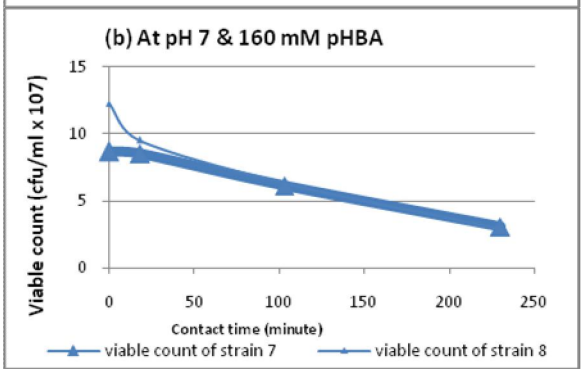

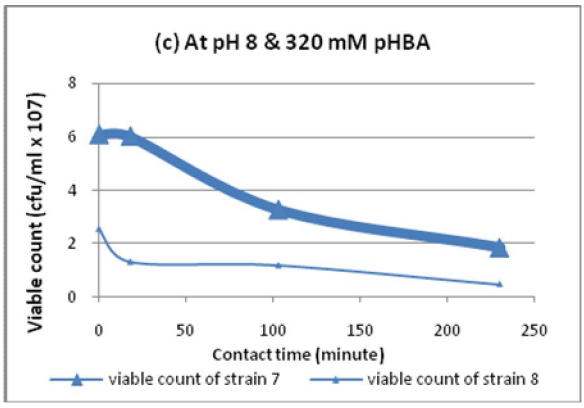

Figure 16**.** Killing Kinetics of *E. coli* strains BW25113 and BW25113Δ*yhcP* by pHBA at different pHs using cells grown in a laboratory fermentor. The cells were grown in a basal medium containing 2% peptone and 2.6% glucose at different pHs. Killing Kinetics was conducted at the same pH used for the cell growth.

production by Sariaslani and Van Dyk, 2007; Amaratunga *et al*., 2000 and Van Dyk *et al*., 2004.

Several variables must be controlled to obtain accurate reproducible results as with any assay system, among these variables that was mentioned by Amsterdam,1996 is pH. The results in Figures 5 & 6 showed that for *E. coli* strains BW25113 and BW25113Δ*yhcp* there was no difference in both growth and pH profiles at the different tested initial pHs in absence of pHBA. The resistant isolate 9 showed similar pH profile but different growth profile to its corresponding sensitive isolate 3.

The susceptibility of the selected isolates/strains to 2.5 mM pHBA at three different initial pH values (5.3, 5.7 and 6.8) was studied. At the initial pH 5.3 both sensitive and resistant isolates/strains showed very high susceptibility. At the initial pH 5.7 there was a clear difference in both the growth and pH profiles between the resistant isolates and their corresponding sensitive isolates as shown in Figures 7 & 8. The susceptibility of the sensitive isolates to pHBA was high at all data points in contrast to the resistant isolates that showed higher growth profiles. At the initial pH 6.8, susceptibility of the resistant isolates was still lower than the corresponding sensitive isolates in most cases however, a considerable increase in the growth profiles was obtained for the sensitive isolates in comparison to their own profiles at the lower initial pH 5.7. The pH profiles for resistant isolates showed differences compared to those of the sensitive isolates at some data points. Increasing the initial pH caused an increase in the resistance of both sensitive and resistant isolates/strains to pHBA. Results showed that pH 6.8 was the best to increase resistance of the isolates/strains to pHBA.

Van Dyk et al., 2004 recorded that the pHBA sensitivity of *E. coli* strain MG1655 (MIC, 100 mM) as compared to the *tolC* mutant (MIC, 56 mM) showed hypersensitivity conferred by the *tolC* mutation. They suggest the presence of one or more pHBA efflux pumps in *E. coli* that utilize the TolC channel. The opening and closing of TolC was shown to be a pH-dependent process, with wild-type TolC closing at low pH (Andersen *et al*., 2002)then the efflux of pHBA is diminished at the low pHs leading to increased effect on the *E. coli* isolates/strains.

At the end of the study of the effect of different environmental fermentation conditions, it can be concluded that, the optimum fermentation conditions for increasing the growth and/or resistance of the *E. coli* isolates to pHBA in shake flasks included: incubation at 37◦C, 320 rpm, agitation and growth at Initial pH 7 or 8.

Several variables must be controlled to obtain accurate reproducible results as with any assay system; among these variables that were mentioned by Amsterdam, 1996 was medium composition and cation concentration.

Treatment of *E. coli* with pHBA resulted in upregulation of *yhcP*, encoding a protein of the putative efflux protein family that contains highly conserved regions or motifs that are indicative of proteins in the Major Facilitator Superfamily (Sariaslani and Van Dyk, 2007) which functions as secondary transporters, catalysing drug–ion (H+ or Na+) antiport (Poole, 2004). That is why Na and K were tested. Results in Figure 9 showed that for isolates number 3, 8, 24, 25 and 34 their susceptibility to pHBA decreased (MIC became 5 mM instead of 2.5 mM) with the addition of sodium chloride to nutrient broth at all concentrations tested (0.5, 1 and 2%). Sodium chloride concentrations change the osmolarity of medium and have a marked effect on the activity of the aminoglycosides and also the ß-lactams shown as decrease in activity and increase in MICs. This effect of osmolarity varies from strain to strain of bacterium (Amsterdam, 1996) this could help understanding the increase in MIC of isolates 3, 8, 24, 25, 34. The same happened with the addition of potassium chloride to nutrient broth at concentrations of 0.5 and 2 while at 1% concentration, isolate no.34 showed even higher resistance. However, the susceptibility of the isolates 7, 9, 15, 20 and 37, which are of a high MIC for pHBA, their susceptibility to pHBA was not affected by addition of any concentration (0.5, 1, 2%) of KCl or NaCl to nutrient broth as shown in Figure 9.

Potentiation by low concentrations of several nonionic macromolecules does not occur (Coates and Richardson, 1973). Moreover, according to Evans, 1964, polysorbate 20 inactivates phenols, phenol derivatives, benzoic acid, pHBA and their esters. Results in Figure 10 showed that for isolates 3, 8, 24, 25 and 34, their resistance to pHBA increased with the addition of tween 80 to nutrient broth at both concentrations tested (1 and 2%) with isolate 34 showing even higher increase in the resistance with 2% tween 80, the MIC values of pHBA increased two fold by the presence of tween 80 and for the isolate 34, such MIC increased 5 fold. However, for isolates 7, 9, 15, 20 and 37 which are of high MIC values for pHBA, the results displayed in the same Figure showed that the susceptibility of these isolates to pHBA was not affected by addition of tween 80 to nutrient broth at concentration of 1%. While the addition of 2% tween 80 to nutrient broth increased the resistance of isolates 7, 9 and 37, their MIC values increased two fold by the presence of tween 80.

Results shown in Figure 11 demonstrate that for isolates 8, 3, 24, 25 and 34: the addition of glucose (1.5%) decreased susceptibility to pHBA of only isolates 3 and 34 while such addition didn't affect the susceptibility of the other isolates. The addition of sucrose (1.5%) to nutrient broth increased the resistance of all these five isolates. The addition of starch (1%) increased the resistance of isolates 3 and 34 while the resistance of isolate 25 sharply decreased (8 fold reduction in MIC). However, for isolates 7, 9, 15, 20 and 37, the results displayed in the same Figure showed that the susceptibility of these isolates to pHBA was not affected by addition glucose (1.5%) or sucrose (1.5%) or starch (1%) to nutrient broth (the MIC remained 5 mM).

Results shown in Figure 12 demonstrate that resistance of all the isolates showed an increase which could be attributed to the fact that in many instances growth will be faster with a supply of organic nitrogen (Stanbury *et al*., 1995). Comparing the MIC values of the pHBA resistant isolates with those of their corresponding sensitive isolates, the following was observed: the overall pattern revealed that a difference in susceptibility to pHBA could be attained with one condition or more for strain 7 versus strain 8 which reached 4 fold, isolate 9 versus 3, isolate 15 versus 24 and isolate 37 versus 34. While such difference in susceptibility became nearly absent with isolate 20 versus 25 (Figure 12).

Results shown in Figure 13 demonstrate that the addition of beef extract to the basal medium in all concentrations tested resulted in an increase in resistance of all the ten tested isolates. They became all of equal MIC of 40 mM except for strain no.8 (BW25113Δ*yhcP*) which showed MIC value of 20 mM with 2 fold difference from strain no.7 (BW25113) with the combination of 2% beef extract and 2.6% glucose.

Results shown in Figure 14 revealed that the *yhcP* gene was detected in both sensitive and resistant wild isolates of natural sources. This may indicate that the resistance wasn't solely dependent on gene acquisition but the regulation of expression is crucial for the development of resistance. Accordingly, the different environmental, physiological and genetic factors affecting the regulation of *yhcP* gene should be studied and controlled for the purpose of increasing bacterial production of pHBA.

In batch culture the pH of an actively growing culture will not remain constant for very long time (Stanbury *et al*., 1995).The results in Figure 15 show that the two strains had similar dissolved oxygen profiles at the different tested pHs (6, 7 and 8) but different growth profiles. Both strains showed higher growth rates at pH 6 and 7 than that at pH 8. The results in Figure 16 showed that the killing kinetics rate of strain BW25113 was less than that of strain BW25113Δ*yhcP* especially in the early periods of exposure to pHBA. This could be due to the fact that *E. coli yhcP* encodes an efflux pump for which pHBA is a substrate. Hence, the absence of this efflux pump results in increased intracellular concentrations of pHBA, which in turn is manifested as the hypersensitive phenotype (Van Dyk et al., 2004) and of course a higher killing kinetics rate. The killing kinetics rates of the two strains were higher at pH 6 than those at pH 7 and 8 showing a remarkable decrease in the number of survivor cells by 50 minutes while at pH 7 and 8 it took a much longer time about 4 hours to give such a decrease. pHBA is a weak acid and the undissociated form, HA, is the active antimicrobial form (Hugo & Russell, 1998) then the low pH (pH 6) caused an increase in the active form of the pHBA and consequently increased effect on both strains noticed by the high kinetics rates but of course the presence of the pump helped strain 7 which showed a relatively lower killing rate in comparison to strain 8. Increasing the pH will cause the weak acid to dissociate thus decreasing the active or diffusible form leading to a slower rate of killing kinetics for both strains, yet a difference between strain 7 and 8 is present due to the presence of the pump in the former strain. The same can be applied for the MIC values of pHBA against the two tested strains at the different tested pH values (Table 2). The MIC against the two tested strains increased by increasing the pH as the acid effect decreased but the obvious difference between the 2 strains (4 and 8 fold) is attributed to the efflux pump. The highest difference in MIC values between the two strains was observed at pH 7 (8 fold differences). This could be attributed to the fact that the uncharged acid form, which is the moiety that diffuses into the cell, is a minor component at neutral pH (Van Dyk et al., 2004).

From this study it can be concluded that the optimum fermentation conditions for increasing the growth and/or resistance of *E. coli* BW25113 to pHBA in a laboratory fermentor include: incubation at 37◦C, 200 rpm agitation, growth in basal medium containing 2% peptone and 2.6% glucose under controlled pH 8.

Further work applying these optimized fermentation conditions on genetically improved *E. coli* strains with active efflux pump may lead to striking results in terms of increased production of pHBA and could provide an effective solution of its toxicity to the producing host bacterial cell which in turn will help to increase production of this molecule for commercial use.

5. References:

1. Amaratunga, M., Lobos, J. H., Johnson, B. F., Williams, E. D., 2000. Genetically engineered microorganisms and method for producing 4-hydroxybenzoic acid. United States Patent. 6030819.
2. Amsterdam D (1996) Susceptibility testing of antimicrobials in liquid media. In: Lorian V (ed) Antibiotics in laboratory medicine. Williams &Wilkins, London, pp 52-111.
3. Andersen C, Koronakis E, Hughes C, Koronakis V (2002) An aspartate ring at the TolC tunnel entrance determines ion selectivity and presents a target for blocking by large cations. Mol Microbiol 44:1131–1139.
4. Bartelt, M., 1999. Diagnostic Bacteriology: A Study Guide. F.A. Davis Company, Philadelphia, pp 133-147.
5. Becker JM, Caldwell GA, Zachgo EA (1996) Biotechnology: A laboratory course. 2nd .Ed. Academic press, London, pp 219.
6. Brown R, Poxton IR, Wilkinson JF (1989) Centrifuges, colorimeters and bacterial counts. In: Collee JG, Duguid JP, Fraser AG, Marmion BP (ed) Practical medical microbiology. Churchill Livingstone Edinburgh, London, pp 246.
7. Brown, M. H., Paulsen, I. T., Skurray, R. A., 1999. The multidrug efflux protein NorM is a prototype of a new family of transporters. Mol. Microbiol., 31, 393-395.
8. Coates D, Richardson G (1973) Relationships between estimates of binding of antimicrobial agents by macromolecules, based on physiochemical and microbiological data: Benzoic acid and a nonionic surfactant. J appl Microbiol 36 (2): 257 – 262.
9. Evans WP (1964) The solubilisation and inactivation of preservatives by nonionic detergents. J Pharm Pharmacol 16: 323-331.
10. Hugo WB, Russel AD (1998) Pharmaceutical microbiology. 6th. Ed. Blackwell Science, pp 212.

11. Johnson, B. F., Amaratunga, M., Lobos, J. H., 2000. Method for increasing total production of 4-hydroxybenzoic acid by biofermentation. United States Patent. 6114157.
12. Kern, W. V., Oethinger, M., Jellen-Ritter, A. S., Levy, S. B., 2000. Non-target gene mutations in the development of fluoroquinolone resistance in *Eshcerichia coli*. Antimicrob. Agents Chemother., 44, 814-820.
13. Madigan MT, Martinko JM, Parker J (2003) Brock biology of microorganisms. 10th. Ed. Prentice Hall, pp 969.
14. Pao, S. S., Paulsen, I. T., Jr., M. H., 1998. Major facilitator superfamily. Microbiol. Mol. Biol. Rev., 62, 1-34.
15. Poole, K., 2004. Review Efflux-mediated multiresistance in Gram-negative bacteria. Clin. Microbiol. Infect., 10, 12–26.
16. Putman, M., van Veen, H. W., Konings, W. N., 2000. Molecular properties of bacterial multidrug transporters. Microbiol. Mol. Biol. Rev., 64, 672-693.
17. Sariaslani, F. S., Van Dyk, T. K., 2007. Methods for increasing the resistance of a host cell to aromatic carboxylic acids. United States Patent. 7279321 B2.
18. Stanbury PF, Whitaker A, Hall SJ (1995) Principles of fermentation technology. 2nd. Ed. Pergamon, UK, pp 1-9,101, 216,225.
19. Tseng, T.-T., Gratwick, K. S., Kollman, J., Park, D., Nies, D. H., *et al*., 1999. The RND permease superfamily: an ancient, ubiquitous and diverse family that includes human disease and development proteins. J. Mol. Microbiol. Biotechnol., 1, 107-125.
20. Van Dyk, T. K., Templeton, L. J., Cantera, K. A., Sharpe, P. L., Sariaslani, F. S., 2004. Characterization of the Escherichia coli AaeAB Efflux Pump: a Metabolic Relief Valve?. J. Bacteriol. , 186 (21), 7196–7204.
21. van Veen, H. W., Konings, W. N., 1998. The ABC family of multidrug transporters in microorganisms. Biochim. Biophys. Acta., 1365, 31-36.
22. Wu, C., Sun, S., Nimmakayala, P., Santos, F.A., Springman, R., *et al*., 2004. A BAC and BIBAC-based physical map of the soybean genome. Genome research , 22, 221-229.
23. Zgurskaya, H. L., Nikaido, H., 2000. Multidrug resistance mechanisms: drug efflux across two membranes. Mol. Microbiol. , 37, 219-225.

4/2/2010

Immunomodulation of Hepatic Morbidity in Murine *Schistosomiasis mansoni* Using Fatty Acid Binding Protein

Ibrahim Rabia[1]; Eman El-Ahwany[2]; Wafaa El-Komy [1] and Faten Nagy[2]

[1]Parasitology [2]Immunology Department,Theodor Bilharz Research Institute,Giza, Egypt.
dr_mona_zaki@yahoo.co.uk

Abstract: Hepatic fibrosis and portal hypertension are responsible for morbidity in schistosomiasis *mansoni*.The objective of this study was to evaluate the possible anti-morbidity effect of fatty acid binding protein (FABP) of *Schistoma mansoni* when given to mice before infection. Multiple small doses of FABP were injected intra-peritoneally into experimental animals (100 µg of purified FABP followed 2 weeks later by two booster doses of 50 µg each at weekly intervals) and the experimental design included 3 groups of 15 mice each; the first group received FABP (immunized group), the second group was injected with the 3 doses of FABP one week prior to infection with 100 *S.mansoni* cercariae (immunized-infected group) and the third group served as infected control. Data revealed reduction in CD4+ cells and increase in CD8+ cells of hepatic granuloma in FABP-immunized infected group, resulting in significant decrease in CD4+/CD8+ ratio, in comparison to infected control group; the serum cytokine levels of both TNF-alpha and IFN-gamma were also significantly decreased. Histopathological examination of liver revealed remarkable increase in percent of degenerated ova within hepatic granuloma which decreased in diameter (12%). In this study, significant reductions in worm burden (46%) and tissue egg loads (42.8% and 50% for hepatic and intestinal ova respectively) were observed in addition to decreased percent of immature stages with increase in percent of dead ova in Oogram pattern .This work could present a trial contributing to shaping the severity of hepatic morbidity. [Journal of American Science 2010;6(7):170-176]. (ISSN: 1545-1003).

Key words: Schistosomiasis. – fatty acid binding protein – immunization. – histopathology.

1. Introduction

In schistosomiasis, the manifestations of immunopathology are mainly acute granulomatous inflammation and late fibrosis. The mechanisms driving fibrogenesis are distinct from those regulating inflammation (Wynn, 2008) .

Fibrosis is the end result of chronic inflammatory reactions induced by a variety of stimuli including infections, allergic responses, tissue injury and others. The key to fibrosis lies in the control of extracellular matrix (ECM) deposition in response to cytokines (Wang et al., 2009). In a previous study, Boros (1989) presumed that the diminished granulomatous response could be advantageous to host in a way that, if granuloma is retained in smaller size and less activated cell populations it could lessen the possibility of tissue damage. Stadecker (1992) added that, regulation of the host reaction to *Schistosome* egg antigen (SEA) by induction of specific T-cell unresponsiveness could be potent prophylactic measure to prevent excessive destruction of host tissues by the granulomatous inflammation characteristic of acute schistosomiasis.

Recently, a variety of secretory-excretory products, from different stages of *S.mansoni*, have been identified to induce a level of host-protective immune responses with amelioration of morbidity (Maher *et al*., 2003; El-Ahwany *et al*., 2006).

In infection with *S. mansoni*, hepatic granuloma formation is mediated by CD4+ T lymphocytes sensitized to egg antigens (Singh *et al.*, 2004).The systematic identification of immunogenic egg components is important to understand the specific basis of egg-induced immuno-pathology in schistosomiasis. To gain further insight into the specific immune response against parasite eggs, Asahi *et al.* (2003), characterized several egg antigens with a molecular weight of 25 kDa (Sm-p25). They added that a recombinant Sm-p25 protein elicited significant proliferative and cytokine responses in addition to induced antibody responses, and the highest levels of antibody were detected in infection sera obtained after parasite oviposition. Doenhoff *et al,*(2003), reported that a 27kDa enzyme secreted by *S. mansoni* eggs is presumed to be responsible for the *Schistosome* egg fibrinolytic activity.

The intracellular fatty acid-binding protein (FABP) Sm14 is essential for schistosomes in the

uptake, transport and compartmentalization of host derived fatty acids (*Esteves et al., 1997*). Lipids are necessary for schistosomes to synthesize and maintain their complex membrane systems; fatty acids act as precursor for lipid and phospholipids synthesis and have significant contribution in the parasite life cycle including membrane formation, functioning as lipid anchors for proteins, sexual maturation, and regulation of egg production (*Furlong, 1991*). These parasites lack the oxygen dependent pathways required for the synthesis of sterols and fatty acids, thus they must acquire host lipids. Sm14 was localized in *S. mansoni* by anti-Sm14 specific antibodies in the basal lamella of the gut and underlying the tegument (*Brito et al., 2002*). Experimental models of protective immunity in schistosomiasis have identified several promising trials (Pearce *et al.,* 1988 and Wolwezuk *et al.,* 1989) by using intraperitoneal injection of different doses of SEA (Botros et al., 1995, Hassanein *et al.,* 1997 and Hassanein *et al* 1999). Mountford and Harrop (1998) focused attention on an approach that aims to identify proteins from *Schistosoma mansoni* that are capable of stimulating protective Th1 cell–mediated immune responses.

The present study was designed to investigate different parasitological and immunological parameters in response to injection of purified fatty acid binding protein (FABP) of *S. mansoni* into mice prior to infection with *S. mansoni* cercariae as an experimental trial to decreasing or modulating severe hepatic morbidity.

2. Material and Methods

1- Animals

Laboratory bred male albino mice of *Mus musculus* strain, weighing 18-20 grams were used. Experimental animals were kept for 8 w responsible for animal ethics.

Schistosoma mansoni cercariae were obtained from (SBSP) at (TBRI) and infection was performed by subcutaneous injection of 100 *S. mansoni* cercariae to each mouse (Liang *et al.,* 1987).

2- Preparation of fatty acid binding protein.

Adult *S. mansoni* worms were homogenized in 2 vol. of 20 mM Tris-HCL buffer (BDH Chemicals, England) containing 5 mM Phenylmethylsulfonyl fluoride (PMSF) as a protease inhibitor (Sigma–Aldrich, Louis, USA) at 20.000 rpm using IKA T20 homogenizer (IKA, Staufen, Germany). The homogenate was centrifuged at 30.000 rpm for 30 min. The entire process of homogenization and centrifugation was performed at 4˚C. The supernatant fractions were decanted and assayed for protein content and stored at -20˚C until used as crude extracts.

Thirty milligrams of crude extracts were loaded on a G-200 Sephadex column, and then eluted with 0.1 M PBS, pH 7.4. Four milliliters of fractions were collected and their absorbances were measured at 280 nm. Fractions from peak II and III were pooled and dialyzed against TBS (Tris-Buffered Saline) at 4°C and their protein contents were measured and stored at –20°C until used (Timanova *et al.,* 1999).

3- Experimental design:

The mice were divided into 3 groups of 15 animals each; all groups were sacrificed 8 weeks following the beginning of experiment:

Group (1): FABP immunized group:

Each mouse was injected intra-peritoneally with 100 µg/ml of FABP antigen emulsified with complete Freunds' adjuvant. Then, the animals were boosted two weeks later with 50ug/ml of FABP emulsified with incomplete Freund's adjuvant and boosted again one week apart. the mice were sacrificed 8 weeks following last dose of FABP.

Group II: - Each mouse was injected intraperitoneally with 100 µg/ml of FABP antigen emulsified with complete Freunds' adjuvant. Then, the animals were boosted two times at three weeks intervals with 50µg of FABP emulsified with incomplete Freund's adjuvant. Mice were infected with 100 *S. mansoni* cecariae, one week after last immunization by sub-cutaneous injection the mice were sacrificed 8 weeks post –infection.

Group III: *Shistosoma mansoni* infected control group, animals were infected sub-cutaneously with 100 cercariae and sacrificed 8 weeks later.

4- Parasitological parameters:

a- Worm recovery: Perfusion of adult worms from liver and porto-mesenteric system was performed 8 weeks after infection according to Duvall and Dewitt (1967).

b- Tissue egg load: The number of eggs per gram tissue (liver and intestine) was studied according to the procedure by Cheever (1968).

c- Oogram pattern: The percentages of immature, mature and dead ova in the small intestines were computed from a total of 100 eggs per intestinal segment and classified according to the categories previously defined by Pellegrino *et al.* (1963).

5- Histopathological Study:

Granuloma measurement:

Livers of mice were fixed in 10% buffered formalin, processed into paraffin blocks, serially cut at 4µm thickness, and stained with hematoxylin and eosin. Hepatic granuloma measurements were done according to Von Lichtenberg (1962) using an ocular

micrometer for those containing a central ovum only. The percent reduction in granuloma diameter relative to the infected controls was calculated as follows:

$$\% \text{ reduction of granuloma diameter} = \frac{\text{Mean diameter of control s - mean diameter of test s}}{\text{Mean diameter of control group}} \times 100$$

Counting was carried out in five successive microscopic fields (10x10) in serial tissue sections of more than 250 µm apart.

6- Immunological Parameters:

a- Detection of serum TNF-alpha and IFN-gamma by sandwich ELISA:

Serum murine TNF-α and IFN-γ levels were measured with an ELISA kit (Quantikine M, R&D systems, Minneapolis, MN, USA). The detection limit of the assay was consistently ~20 pg/ml. The concentration was calculated from the standard curve that was performed in the same assay.

b- Enumeration of T-cell subsets:

Fluorescein isothiocyanate (FITC)-conjugated monoclonal antibodies for L3T4+ and Lyt2+ T-lymphocytes were used to determine the number of intralesional T-cells in formalin fixed tissues,embedded in paraffin using a modified method of Swoveland and Ghonson (1979). Sections were treated according to histological procedures to remove paraffin and taken through several washes in graded alchohol to rehydrate the tissues. Slides were washed in 0.05 M Tris buffer (pH 7.4), and incubated for 10 min in a humidified chamber after immersion in a solution of freshly prepared 1% trypsin. Slides were washed in 0.05 M Tris buffer and distilled water. FITC-labeled L3T4+ (CD4+) and Lyt2+ (CD8+) antibodies diluted 1:1 in Tris buffer, pH 7.6, were used to stain two slides per mouse. Slides were incubated overnight with the monoclonal antibodies in a humidified chamber at 4°C, washed in Tris buffer and mounted with entellan (Sigma) to enhance fluorescence prior to quantification. T-cells of each type were counted in two 50 mm wide bands perpendicular to each other in a single granuloma containing a single centrally positioned egg. The mean count per 50 mm band was obtained by dividing the sum of the two bands by two. A disaster Reichertjung fluorescent research microscope (Cambridge Instruments) objective 20X was used.

Statistical analysis:

Comparison was performed between the treated groups and untreated control. The percentage change between each two groups to be compared was assessed using the formula: Differences between the mean scores of any of the two groups to be compared were tested for significance, using an unpaired 2-tailed Student's t-test. The data were considered significant if *p* values were less than 0.05.

3. Results

The results in (Table 1) are showing significant reduction (49.3%) in the mean number of *S. mansoni* adult worms in the group of infected mice immunized with purified FABP antigen compared to the infected controls (P< 0.001). Moreover, significant reduction in the mean number of ova / gram tissue (liver and intestine) was detected in the group immunized with purified FABP antigen compared to infected controls (P< 0.01). The percent of immature ova was less in the immunized group than the infected one while the percent of dead ova was higher (16.2) in the immunized group than the infected control (P<0.05).

Table-1: Different parasitological parameters detected 8 weeks post- infection in animal groups.

Animal groups	**Worm Load**	**Hepatic Ova**	**Intestinal Ova**	**Oogram pattern**		
				Immature stage	**Mature stage**	**Dead ova**
Control infected group	30.0±0.28	8600.0±87.0	17909±81.0	63.2±0.31	34.2±11	2.6±0.1
FABP-Immunized group	15.21±0.33*	5100.0±29.2*	8610.0±57.0*	32.1±0.24*	51.7±0.22	16.2±1.0*
% Reduction	49.3 %	41.7%	52.9%	Reduced 49.2%	Increased 23.7 %	Increased 78.54%

* Significant difference from infected control (P < 0.01).

Table 2: Number of granuloma T cell phenotypes per 50 µm band (Mean ± SEM) in the different studied groups.

Animal groups (n=10)	CD4+ Mean±SEM	CD8+ Mean±SEM	CD4+/CD8+ Mean±SEM
Uninfected Control	10.4 ±2.3	12.3 ±2.0	1.3 ±1.3
Immunized Group	12.6±1.1	14.4 ±2.2	1.4 ±2.0
Infected Control Group	25.3±2.1	9.2±1.4	2.75±2.1
FABP-Immunized infected Group	14.2±1.9*	18.9±1.9*	0.75±1.8*

* p<0.001 significant vs infected control group.

Immunological Parameters: -

a- Enumeration of T cell phenotypes in hepatic granuloma:

In the FABP-Immunized infected group, the L3T4+ (CD4+) T cells significantly decreased (p<0.001) compared to the infected control group. However, Lyt2+ (CD8+) T cells were significantly increased (p<0.001) in the FABP -immunized group compared to infected control group. Also, there was a significant decrease in the ratio of (CD4+/CD8+) T-cells in the immunized infected group.

b- Detection of serum TNF-alpha and IFN-gamma by sandwich ELISA:

In the FABP -immunized infected group, the serum cytokine levels of both TNF-α and IFN-γ were significantly decreased (p<0.05) compared to the infected control groups.

Table 3: Serum TNF-α and IFN-γ levels against FABP antigen in different studied groups.

Animal Groups (n=10)	TNF-α Mean Pg/ml±SEM	IFN-γ Mean Pg/ml±SEM
Uninfected Control	166±5.11	299.8±4.55
Immunized Group	292±5.3	613±10.1
Infected Control Group	612±19.6	1312±31.1
FABP-Immunized Group	300±24.3*	989±53.7*

*****p<0.05 significant vs infected control groups.

Histopathological Parameters:

The mean granuloma diameter in infected control group was 390.34±0.49 while in FABP -immunized infected group, it was 340.22±0.22, and the reduction in granuloma diameter was 12.84%.

4. Discussion

The morbidity in Schistosome infection is primarily due to fibrosis resulting in large part from healing of the inflammatory granulomatous focal damage around deposited eggs. This granulomatous reaction is most vigorous at the acute stage of infection (8-10 weeks post-infection), when T helper lymphocytes produce high levels of inflammatory lymphokines (Stadecker, 1992) and induces activation of granuloma macrophages (El-Ahwany *et al.*, 2000). Some investigators indicated that, early in infection, probably even prior to egg production, schistosomes induce an immunologic environment that is highly conductive to the establishment of strong immunoregulatory mechanisms.

A lot of trials have been conducted to find a possible way for amelioration of the disease severity or morbidity by inhibition of host reaction around *S.mansoni* eggs. Schistosomal granuloma is mediated by class II MHC CD4+ T helper (Th) lymphocytes and is specifically directed to egg antigens (Zouain *et al.*, 2002). The magnitude of schistosome granuloma depends upon the type of activated Th cell population in response to the quality and quantity of inducing antigen (Stadecker *et al.*, 2001; Hanallah *et al.*, 2003).

In the murine model, cells displaying different functions can be partially differentiated by cell surface phenotype markers such as CD4+ and CD8+ (Smith *et al.*, 2004). In this work, phenotypic T cell subsets showed decrease in CD4+/CD8+ T cell ratio, in the SEP-immunized infected group compared to the corresponding infected control group. This finding was mainly due to an increase in

the percentage of CD8+ subset in the SEP-immunized infected group. A shift in CD4+/CD8+ T cell ratio in favor of CD8+ lymphocytes in the circulation of chronically *S. mansoni* infected patients was reported by other investigators (Lukacs and Boros, 1993). The differences in T cell subset profile within the hepatic granuloma might be reflected by the functional activity of T cells. Thus, the reduction in granuloma diameter was concurrently associated with reduction in CD4+ cells and increase in CD8+ cells in SEP-immunized infected group. Although the decrease in granuloma diameter was not high, yet a marked increase in percent of degenerated ova was observed in SEP-treated infected group. In a study by Hassanein *et al. (*1997), they attributed hypo-responsiveness and decreased granuloma diameter to T-cell anergy following intravenous injection of SEA.

In this study, administration of SEP prior to infection resulted in decreased worm load, hepatic and intestinal ova together with change in Oogram pattern. This could be due to enhancement of immune response or would be acting as assort of primary infection that somewhat hinders the challenge one. Similarly, immunization with SEP of lung stage schistosomula prior to infection induced protective effect, manifested by reduction in parasitological parameters, increased levels of specific immunoglobulins as well as raised hepatic m-RNA expression of TNF-alpha and TGF-beta (Maher *et al.*, 2003). In the present work, at 8 weeks post infection the serum levels of IFN-γ and TNF-α were significantly reduced compared to the infected controls, showing the most pronounced reduction of granuloma diameter. The cytokines play an important role in regulation of the inflammatory granulomatous response in schistosomiasis (Garraud and Nutman, 1996). IFN-γ and TNF-α appears to play an important role in the generation and maintenance of egg-induced granuloma (Chensue *et al.*, 1993 and Hoffman *et al.*, 1998). The diminished focal and systemic production of IFN-γ and TNF-α may be implicated in the downmodulation of the granulomatous response (Joseph and Boros, 1993 and Hassanein *et al.*, 1999). In a studt by Singh *et al.*, (2004), they reported that the decrease of the gene expression of TNF alpha and TGF-beta few months following successful treatment *of S. mansoni* infected mice, was correlated with resorption of liver fibrous tissue.

The development of hepatic fibrosis and portal hypertension is the principal cause of morbidity and mortality in schistosomiasis *mansoni.* Nevertheless, relatively little is known about the mechanisms that lead to excessive collagen deposition during infection with *Schistosoma mansoni*.

Our findings revealed that immunization with FABP of *Schistosoma mansoni* antigen induced some sort of protective effect manifested by, reduction in worm burden, egg load and granuloma size 8 weeks post-infection; the miracidia inside granulomas were mostly degenerated. This was accompanied by decreased ratio of T cell subsets (CD4+/CD8+) and decreased serum levels of both IFN-γ and TNF-α.

Further achievement trials concerned with immunization protocols against schistosomiasis are recommended and are ongoing to helpfully show more promise.

5. References:

1. Asahi H, Oke T, Lopes da Rosa J, Williams DL, Stadecker MJ. (2003): sm-p25: A new egg component stimulating T-cell and antibody responses in murine schistosome infection. *Am J Trop Med Hyg, 52nd Annual meeting, suppl.* 69(3): 346.
2. Boros, D.L. (1989): Immunopathology of *Schistosoma mansoni* infection. *Clin. Microbiol. Rev*., 2:250-269.
3. Botros S., Hassanein H., Hassan S., Akl M., Sakr S., Shaker Z., Hafez G., Ghorab N. and Dean D. (1995). Immunoregulatory potential of exogenous *S. mansoni* soluble egg antigen in a model of experimental in Schistosomiasis 1- regulation of granuloma formation in *vitro*. *Int.J. Immunopharmac*, 12:707-718.
4. Brito CFA, Oliveira GC, Oliveira SC, Street M, Riengrojpitak S, Wilson RA, Simpson AJG, Oliveira RC (2002). Sm 14 gene expression in different stages of the *Schistosoma mansoni* life cycle and immunolocalization of the Sm 14 protein within the adult worm. *Braz J Med Biol Res 35*: 377-381.
5. Bradford M.M. (1976). A rapid sensitive method for the quantization of microgram quantities of protein utilizing the principle of protein dye binding. *Anal. Biochem* .72: 248-254.
6. Cheever A.W. (1968). Condition affecting the accuracy of potassium hydroxide digestion technique for counting *S.mansoni* eggs in tissues. *Bull wld Hlth Org*, 39: 328-331.
7. Chensue S.W., Warmington K.S., Hershey S.D., Terebuh P.D., Othman M. and Kunkle L. (1993). Evolving T cell-response in

murine schistosomiasis. *J Immunol*, 151: 1391-400.
8. Doenhoff M, Stanley RG, Curtis RHC and Pryce D (2003).A fibrinolytic enzyme in *Schistosoma mansoni* eggs. *Am J Trop Med Hyg, 52nd Annual meeting, suppl.* 69(3): 347.
9. Duvall R.H. and Dewitt W.B. (1967). An improved perfusion technique for recovering adult *Schistosoma* from laboratory animals. *Am. J. Trop. Med. Hyg.* 16: 483- 4.
10. El- Ahwany E.G, Hanallah SB, Zada S,El-Ghorab N M,Badir B,Badawy A,Sharmy R,and Hassanein HI (2000). Immunolocalization of macrophage adhesion molecule-1 and macrophage inflammatory protein-1 in schistosomal soluble egg-induced granulomatous hyporesponsiveness. *Int J Parasitol*, 30:837-84.
11. El- Ahwany E.G., Nosseir M.M. and Aly I.R. (2006). Immunompulmonary and hepatic granulomatous response in mice immunized with purified lung- stage schistosomulae antigen. *J. Egypt. Soc. Parasitol.* 36(1): 335-350.
12. Esteves A, Joseph L, Paulinos M, Ehrlich R (1997). Remarks on the phylogeny and structure of fatty acid binding proteins from parasitic platyhelminths. *Int J Parasitol 27*: 1013-1023.
13. Furlong ST. (1991). Unique roles for lipids in *Schistosoma mansoni. Parasitology today*, 2: 59 - 62
14. Garraud O., Nutman T.B. (1996). The role of cytokines in human B –cell differentiation into immunoglobulin –secreting cells. *Bull. Pasteur*. 94: 285-309.
15. Hanallah SB,El-Lakkany N,Mahmoud S,Mousa m and Botros S (2003).Altered immunoglobulin isotype profile and anti-immature worm surface immunoglobulins in mice harboring a praziquantel resistant *Schistosoma mansoni* isolate.*APMIS*,111:1125-1132.
16. Hassanein H., Akl. M., Shaker Z., El-Baz H., Abo- Elala I., Rabia I., Sharmy R. and Doughty B. (1997). Induction of hepatic egg granuloma hypo responsiveness in murine schistosomtasis *mansoni* by intravenous injection of small doses of soluble egg antigen. *APMIS.* 105:77-83.
17. Hassanein, H., Kamel, M., Badawy , A., El-Gorab, N., Abdeen , H., Zada, S., El-Ahwany , E. and Doughty, B. (1999). Anti-miracidial effect of recombinant glutathione S- transferase 26 and soluble egg antigen on immune response in murine schistosomtasis *mansoni. AMPIS*, 107: 723-736.
18. Hoffmann K.F., Caspar P, Cheever A.W. and Wynn T.A. (1998). IFN-gamma, Il-2 and TNF-alpha are required to maintain reduced liver pathology in mice vaccinated with *Shistosoma mansoni* eggs and IL-2. *J Immunol*, 15: 4201-4210.
19. Jaton J., Brandt D.C. and Vassalli P. (1979). The isolation and characterization of immunoglobulins, antibodies and their constituent polypeptide chain. *J. Immunol. Meth.* 2: 43- 67.
20. Joseph A.L., and Boros D.L. (1993). Tumor necrosis factor plays a role in *Schistosoma mansoni* egg induced granulomatous inflammation. *J. Immunol.*, 151: 5461-5471.
21. Maher, K. M., El- Shennawy, A. M.; Ibrahim, R. B.; Aly, E. and Mahmoud, S. (2003): Protective and antipatholy potential of immunization with *Schistosoma mansoni*-secretory/ excretory product. *New Egypt J Med* , 28: 173-182.
22. Mountfourd,A.P and Harrop, R. (1998). Vaccination against schistosomtasis: The case for lung –stage antigens. *Parasitol. Today*, 14: 109- 114.
23. Liang U.S., Bruce J.I. and Boyd D.A. (1987). Laboratory cultivation of *Schistosoma* vector snails and maintenance of schistosome life cycle. Proceedings of the 1st Sino-*Amercian Symposium*, 1: 34-48.
24. Lightowlers, M.W. and Rickard, M D. (1988). Excretory secretory products of helminthes parasites: Effects on the host immune responses. *Parasitol.* 96: 5123- 66.
25. Pearce E.J., James S.L., Hieny S., Lanar D.E. and Sher A. (1988). Induction of protective immunity against S. mansoni by vaccination with *S. mansoni* paramyosin (SM97), a non-surface parasite antigen. *Proceedings of the National Academy of Science, USA.* 74:5463-5467.
26. Pellegrino J., Oliveira C.A., Faria J. and Cumha A.S. (1962). New approach to the screening of drugs in experimental *Schistosoma mansoni* in mice. *Am. J. Trop. Med. Hyg.*, 11: 201-215.
27. Singh KP, Gerard HC, Hudson AP, Boros DL. (2004): Expression of matrix metalloproteinases and their inhibitors during the resorption of schistosome egg-induced fibrosis in praziquantel-treated mice. *Immunology*. 111(30:343-52.

28. Smith, P.; Walsh, C. M.; Mangan, N. E; Fallon, R.E.; Sayers, J.R.; Mckenzie, A.N. and Fallon, P.G. (2004): *Schistosoma mansoni* worms induce anergy of T-cells via selective up-regulation of programmed death ligand 1 on macrophages. *J.Immunol*., 173: 1240-1248.
29. Stadecker, M.J. (1992): The role of T-cell anergy in immunomodulation of schistosomiasis. *Parasitol. Today*, 8: 199-204.
30. Stadecker, M.J.; Hernandez, H.j. and Asahi, H. (2001): The identification and characterization of new immunogenic egg components: implications for evaluation and control of the immunopathologic T-cell response in schistosomiasis. *Mem. Inst. Oswaldo. Cruz.*, 96:29-33.
31. Swoveland, p. and Ghonson, K. (1979): Enhancement of florescent antibody staining of viral antigens in formalin fixed tissue by trypsin digestion, *J. Infect. Dis.*, 140:458-462.
32. Von Lichtenberg, E.V. (1962). Host response to eggs of *Schistosoma mansoni* .Granuloma formation in the unsensitized laboratory mouse. *Am. J. Pathol.,* 41: 711.
33. Wolwezuk C., Auriault H., Gras-Mass G., Vendeville J., Balloul, M., Tartar A. and Capron, A. (1989). Protective immunity in mice vaccinated with *Schistosoma mansoni. J Immunol*, 142: 1342-1350.
34. Wynn A. (1999). Immune deviation as a strategy for schistosomtasis vaccines designated to prevent infection and egg induced immunopathology. *Microbes and infection,* 1: 525-534.
35. Zouain C.S., Gustavson S., Silva-Teixeira D.N., Contigli C., Rodrigues V., Leite M.F. and Goes A. M. (2002). Human immune response in schistosomtasis: The role of P24 in the modulation of cellular reactivity to *S. mansoni* antigens. *Hum Immunol.,* 63: 647-656.

3/1/2010

Fault Determination Using One Dimensional Wavelet Analysis

S. Morris Cooper, Liu Tianyou, Innocent Ndoh Mbue
Institute of Geophysics and Geomatics, China University of Geosciences, Wuhan 430074, China;
smorriscpr@gmail.com

Abstract: Faults play an important role in mineral exploration and volcanic activities. Their identification, a major problem in the world of geosciences, is significant to both geologists and geophysicists. Multiscale wavelet analysis, a powerful tool for filtering and denoising, has been applied to solve many problems in geophysics. Wavelet transforms have advantages to traditional Fourier methods in analyzing physical situations where the signal contains discontinued and sharp spikes. In this paper we advance the use of one dimensional multiscale wavelet for the identification of faults from potential field data. The method is based on the power of the discrete wavelet utilizing the concept of breakline and discontinuity (edge detection) and uses the Daubachies wavelet. The method is applied to synthetic data and real potential field data from Dagang, southern China yielding very good results. [Journal of American Science 2010;6(7):177-182]. (ISSN: 1545-1003).

Keywords: Wavelet decomposition, Fault, Potential field, Dagang Oilfield

1. Introduction

Faults and fractures are essential in the interpretation of potential field data. The identification and mapping of shallow and deep faults are necessary in the petroleum industry, earthquake detection and ground water displacement.

Exploration for a wide range of mineral deposits is critically dependent on knowledge of the location and age of fractures and faults. Oil and gas fields in many sedimentary basins are distributed along fault-controlled linear trends (Lyatsky, H. 2004), and fault identification is often used effectively for target-area selection in hydrocarbon exploration. Similarly, mineral deposits in various geologic settings are commonly associated with fluid-conducting faults.

Generally, the main features used to discriminate faults according to gravity or magnetic anomalies are linear gradient trends, boundaries of anomalies, an anomalous linear transitional belt, a linear anomaly belt, and so forth. Therefore, linear trends and their parametric information play an important role in gravity and magnetic-data interpretation. However, owing to geologic- or geophysical conditions, these linear features are not always apparent in images. Thus, we sometimes need to apply methods of enhancing lineaments to aid geologic interpretation. The commonly used methods are anomaly separation (continuation or filtering), correlative analysis, and directional derivatives.

Traditional methods, upward continuation and derivatives, of fault inference rely on the experience of the interpreter, the different nature of the anomaly, dramatic changes with the positive and negative anomaly; abnormal intensity of the adjacent line mutation, abnormalities with the level of dislocation axis and so forth.

These methods are prone to uncertainties and are often unreliable. In downward continuation abnormality is often flatten, information greatly reduced, and there is blurriness in characteristics resulting to inference difficulty.

To mitigate these uncertainties and making it simple for both the experience and inexperience interpreters, we are proposing the use of one dimensional discrete wavelet analysis for the inference of faults based on potential field data.

2.0 Method

2.1 Multiscale Wavelet

Wavelets are mathematical functions which split data into different frequency components and then each component is studied with a resolution to match its scale. Wavelet transforms have advantages to traditional Fourier methods in analyzing physical situations where the signal contains discontinued and sharp spikes. Wavelets were developed independently in the fields of mathematics, physics, electrica1 engineering and geophysics. Interchanges between these fields during the last ten years have led to many new wavelet application such as image compression, turbulence, human vision, radar and earthquake prediction,. The application of wavelet to potential field (gravity and magnetic) over the years have gained favorable results where exploration is concern.

We consider the space $L^2(R)$ of measurable functions $f(x)$, defined on the real line R that satisfies

$$f(x) \in L^2(R) \Rightarrow \int_{-\infty}^{\infty} |f(x)|^2 dx < \infty \quad (1)$$

The continuous wavelet transform *(cwt)* of $f(x)$ is given as,

$$cwt_{(a,b)} = \frac{1}{\sqrt{a}} \int_{-\infty}^{\infty} f(x) \psi\left(\frac{a-b}{a}\right) dx \quad (2)$$

Where ψ is called the mother wavelet. The variables a and b are integers that scale and dilate the mother wavelet (ψ). The scale index a indicates the wavelet's width, and the location index b gives its position. Setting $a = 2^{-j}$ and $b = a.k$ in Eq.(2), the discrete wavelet transform *(DWT)* is written as,

$$DWT_{j,k}(a,b) = \Sigma\Sigma f(x) 2^{-j/2} \psi(2^{-j} x - k) \quad (3)$$

The dilations and translations are chosen based on power two, so-called dyadic scales and positions, which make the analysis efficient and accurate.

Mallat (1989) introduced an efficient algorithm to the DWT known as the Multi-Resolution Analysis (MRA). Multi-scale representation of signal $f(x)$ may be achieved in different scales of the frequency domain by means of an orthogonal family of functions $\phi(x)$. In MRA, $L^2(R)$ is nested subspaces:

$$A_j \ldots \subset A_{-2} \subset A_{-1} \subset A_0 \subset A_1 \subset A_2 \subset \ldots \quad (4)$$

such that the closure of their union is $L^2(R)$,

$$\overline{\bigcup_{j=-\infty}^{\infty}} A_j = L^2(R) \quad (5)$$

and their intersection contains only the zero function

$$\bigcap_{j=-\infty}^{\infty} A_j = \{0\} \quad (6)$$

Considering the dyadic case, when each subspace A_j is twice as large as A_{j+1}, a function $f(x)$ that belongs to one of the subspaces A_j has the following properties:

$f(x)$ member of $A_j \Leftrightarrow$ dilation $f(2x)$ member of A_{j+1} (7)

$f(x)$ member of $A_0 \Leftrightarrow$ translation $f(x + 1)$ member of A_0 (8)

If we can find a function $\phi(x) \in Ao$ such that the set of functions consisting of $\phi(x)$ and its integer translates then,

$$\{\phi(x-k)\}_{k \text{ member of } z} \quad (9)$$

form a basis for the space *Ao*, we call it a scaling function. For the other subspaces A_j (with $j \neq 0$) we define

$$\phi(x) = 2^{-j/2} \phi(2^{-j} x - k);\ j, k \text{ member of } z \quad (10)$$

We can express $\phi(x)$ and $\psi(x)$ in terms of basis functions of *Aj*

$$\phi(x) = 2 \sum_{k=0}^{n=1} h_k \phi(2x - k) \quad (11)$$

$$\psi(x) = 2 \sum_{k}^{n=1} g_k \phi(2x - k) \quad (12)$$

Due to the multi-resolution analysis, these relations are also valid between *Aj+1, Aj* and *Dj* for arbitrary *j*. h_k and g_k are called filter coefficients that uniquely define the scaling function $\phi(x)$ and the wavelet $\psi(x)$.

2.2 Multiscale Edge Detection via Wavelet Transform

Potential field theory is suitable for multiscale wavelet analysis. In both gravity and magnetic data most of the information is contained in irregularities in the analytical signal which in turn, map the boundaries of contrasting properties of subsurface rocks (contacts, faults, etc).. Multiscale edge mapping is an automatic process of picking edges in potential field data at a variety of different scales (Hornby. P., Boschetti, F. and Horowitz, G. F., 1999., Archibald, N. J., Gow, P. and Boschetti, F., 1999).

Many traditional potential field operations have an elegant and compact expression in wavelet domain, the most obvious being the equivalence between the concept of change of scale and upward continuation. This results in a mathematically common and rigorous framework for different potential field applications. The following authors have dealt extensively with multiscale and its application to edge diction; Blakely and Simpson (1986) for modeling. Hornby *et a*l (1999) for a formal presentation of the underlying theory, to Archibald *et al.* (1999) for the application of multiscale edges to the enhanced visual interpretation of potential field data, to Boschetti, F., Moresi, L. and Covil, K., (1999) for applications to feature-based signal processing, Boschetti, F., Hornby, P. and Horowitz, F., (2000) for application to mathematical inversion, and Martelet. G., Sailhac. P., Moreau., F. and Diament. M., (2001) for application of 1D DWT to boundaries characterization.

2.3 Spectral Analysis

Spectral analysis of potential field data has been used extensively over the years to derive depth to certain geological features, such as magnetic basement (Spector &

Grant 1970, Hahn & Mishra 1976, Connard *et al*, 1983, Garcia and Ness 1994) or the curie-temperature isotherm (Shuey *et al.* 1997, Blakely 1998, Okubo and Matsunaga 1994). Spector and Grant (1970) provided a foundation for these techniques. A matched filter seeks to deconvolve the signal from one such source using parameters determined from the observations. Matched filtering is a Fourier transform filtering method which uses model parameters determined from the natural log of the power spectrum in designing the appropriate filters. This method uses the power spectrum graph of a magnetic grid in the spectral domain. Magnetic and gravity sources at similar depths show straight-line segments.

This method assumes that you can summarize the power spectrum in terms of two straight line segments, characterizing the regional and shallow sources. The slope (fig. 1) of a line segment indicates the depth of the sources that it characterizes. The intercept with the vertical axis is an indication of the intensity of the source at that depth.

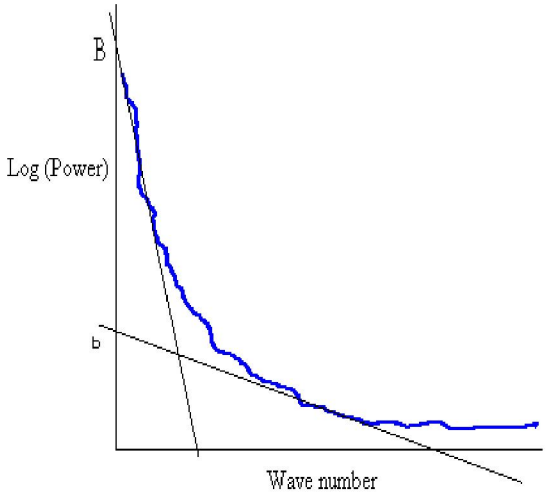

Figure 1: Spectral analysis separation filter

Where B is the Y intercept of the line segment representing the regional sources; b is the Y intercept of the line segment representing the shallow sources; H is the slope of the line segment representing the regional sources; h is the slope of the line segment representing the shallow sources.

3.0 Results

This research is directed at locating deep faults from potential field data employing the discrete wavelet to model faults and actual fiend data obtaining great result as seen below.

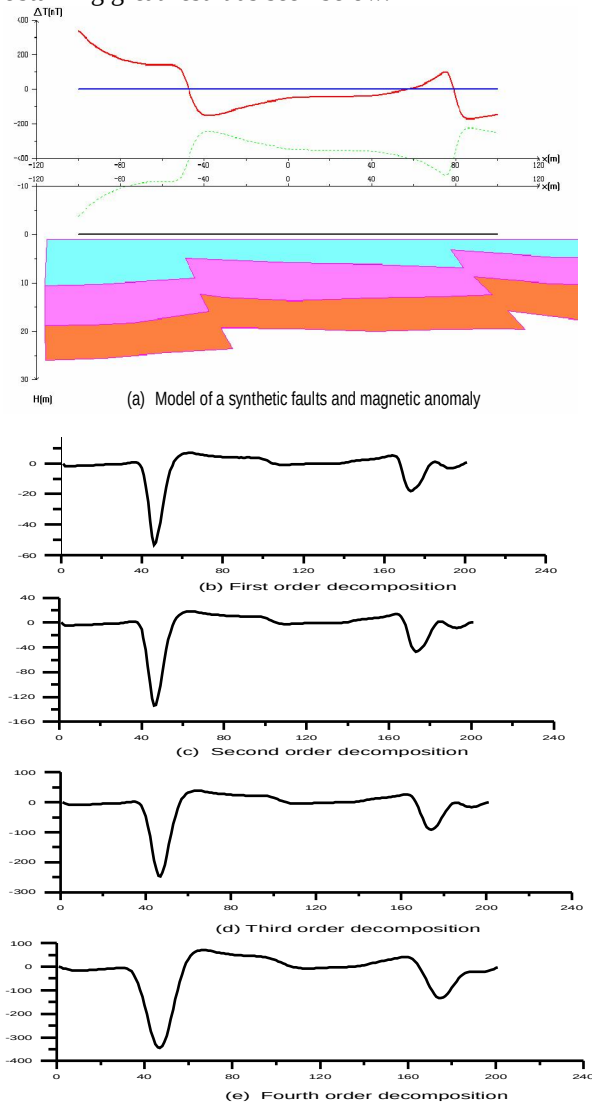

Figure 2: Model fault and decomposition result (a) model showing three strata with magnetic anomaly (b) first order detail (C) second order detail (d) third order detail (e) fourth order detail

From the decomposition of the model one clearly sees where faults are located as shown in the four details (fig. 2). However, it is very sharp in the first and second levels pointing out exact positions but the third and fourth do not. Points of relative inflection or change in the trend are also noticed in the first detail. Power spectral analysis shows depths estimate of the details be to be 0.1km, 0.17km, 0.25km, 0.4km and 0.6km for the fist to the fourth details respectively.

Multiscale edge analysis indicates that the location and amplitude of edges contain the same information as the original profile. Accordingly, information about causative sources can be obtained by analysing the multiscale edge.

The total magnetic and bourger gravity maps show Dagang oilfield indicated with black lines and the research area is denoted by white lines as shown in figure 3. The oil field is replete with complex fault system that varies from north to south. Our research area, around the Qikou depression is characterized with diabase related reservoir overflow volcanic rocks.

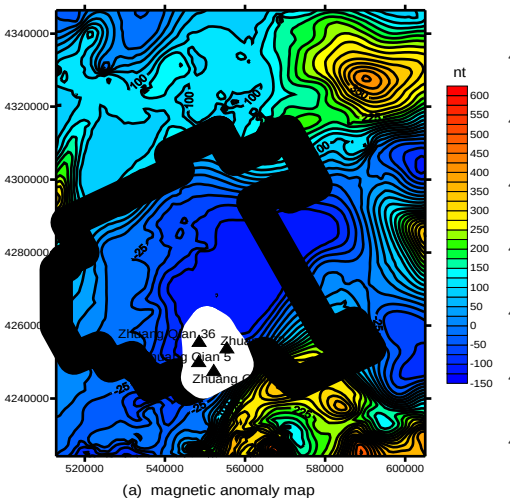

(a) magnetic anomaly map

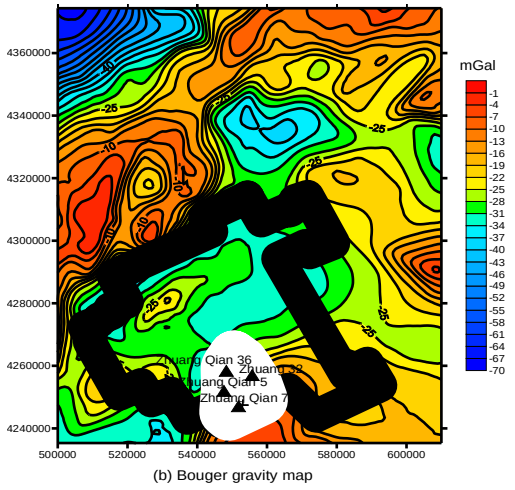

(b) Bouger gravity map

Figure 3: Magnetic anomaly (top) and bourger gravity (bottom) maps of the Dagang area with area of research marked white and few well positions

A profile (fig. 4) across our area of interest is taken and decomposed via daubachies wavelet (db2) at level 4 and compared to a seismic line of the same area.

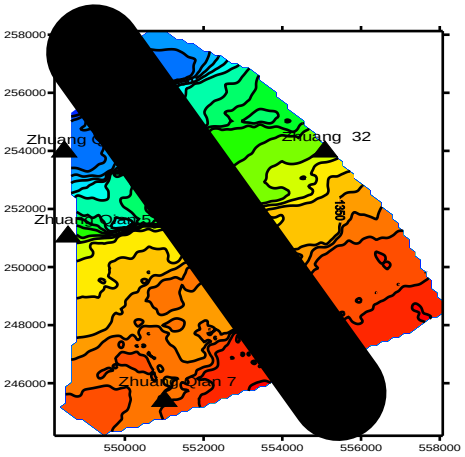

(a) Selected area with profile

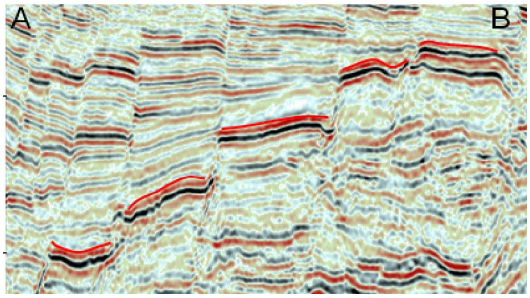

(b) Seismic cross section of the profile

Figure 4: (a) Selected area of interest and (b) seismic line matching the location indication location of faults along the profile AB. A whole body of igneous rock is separated by four faults.

The results of the decomposition (fig.5 and 6) on both gravity and magnetic data respectively show the location of breakpoints indicating faults as depicted in the seismic section. The troughs indicate a brought change in the density of the strata while the peaks signify the midpoint of a given finite mass. The higher the level of decomposition , the less apparent the break point or fault position since faults are associated with high frequency, thus a good result may be obtain at lower levels. The apparent depths of the faults using spectral analysis range from 200m to 1km.

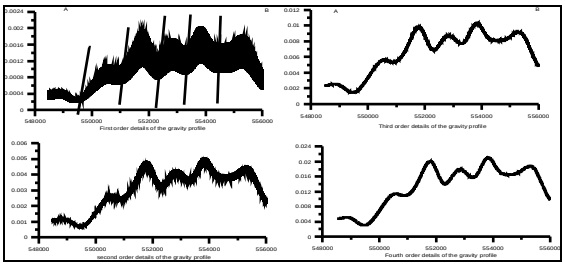

Figure 5: Decomposition of gravity profile of our area of interest (a) first order details with position of faults (b)second order details (c)third order details and (d) fourth order details. Note: the vertical lines are drawn to indicate positions of the faults.

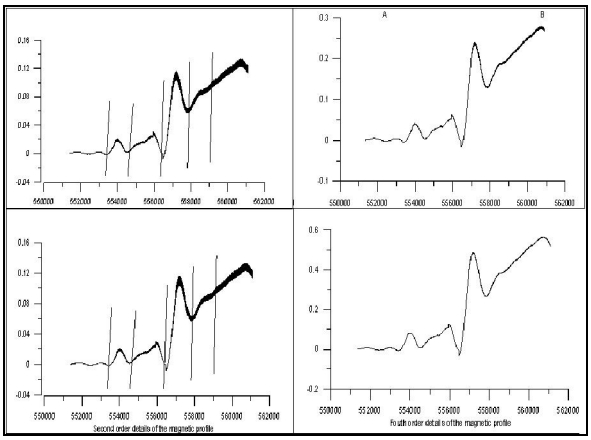

Figure 6: Magnetic profile decomposition (a) first order details with faults locations (b) second order details with faults locations(c) third order details (d) fourth order details. Note: The vertical lines indicate the positions of the faults.

The second, third and fourth levels of the magnetic decomposition clearly indicate points of interest showing changes in susceptibility and break points or edges. The positions of the faults are indicated by troughs/minima as with those of the gravity decomposition. Source discontinuity or dis-homogeneity are marked by minima or decay in the coefficient of the details (Moreau, F. Gilbert, M. Holschneider and Saracco, G. 1999) However, the first order detail is not too distinct due in part to the very small difference in magnetic susceptibility and noise. The amplitudes and change in the gravity decomposition is an indication of sharp density contrast between each section and their separation in terms of depth difference

4.0 Discussion

The multiresolution analysis is obtained by applying the inverse wavelet transform to the coefficients of each level. Note that the multiresolution is not translation invariant; a shifted version of the same signal can give different multiresolution representations. The choice of the type of wavelet is very important in the processing of data. We use the Haar or the Daubachies wavelets in this research. This particular family of wavelet is suitable for the processing and detection of break points and edges, as the processing scales are linked to the speed of the change.

The deterministic part of the signal may undergo abrupt changes such as a jump, or a sharp change in the first or second derivative. In image processing, one of the major problems is edge detection, which also involves detecting abrupt changes. Also in this category, we find signals with very rapid evolutions such as transient signals in dynamic systems. The main characteristic of these phenomena is that the change is localized in time or in space. This is shown in the decomposition of the potential field data. The first and second order details localized points of discontinuity as expected when dealing with discrete wavelet. The results indicate that faults and edges can easily be identified and localized. Where potential field is concerned the density contrast is evident in the amplitudes generated as a consequence of the decomposition.

Noise reduction (Leblanc and Morris, 2001, J.C.S. de Oliveira Lyrio, L. Tenorio and Y. Li, 2004) which is an important attribute of the DWT is also shown in the decomposed signals. The first two details in both the gravity and magnetic results (fig 5 & 6) clearly manifest same. There are marked differences and noise is greatly reduced from first to fourth orders..

It should be noted that short wavelets are often more effective than long ones in detecting a signal rupture. The shapes of discontinuities that can be identified by the smallest wavelets are simpler than those that can be identified by the longest wavelets. The presence of noise, which is after all a fairly common situation in signal processing, makes identification of discontinuities more complicated. If the first levels of the decomposition can be used to eliminate a large part of the noise, the rupture is sometimes visible at deeper levels in the decomposition.

5.0 Conclusion

We have shown that one dimensional discrete wavelet analysis can be effectively applied to infer faults from potential field data. This was demonstrated using synthetic fault models and actual field data with very good results obtained. The method is easy to use, pointing out hidden faults and reducing the propensity for errors in potential field interpretation. Their depth estimates using power spectral range from 200m to 1km from the shallowest to the deepest. We are of the strong conviction that this method will be useful at all levels of interpretations. However, one should be careful when selecting the levels of decomposition and the type of wavelet family and note that the multiresolution analysis is obtained by applying the inverse wavelet transform to the coefficients of each level.

Acknowledgements:
The Corresponding author is grateful to Feng Jie and Wu Xia Yang for their meaningful suggestions and constructive criticisms that helped to improve this work.

Corresponding Author:
Mr. S Morris Cooper
China University of Geosciences
Wuhan, Hubei
China.
Email: smorriscpr@gmail.com

References

1. Archibald, N. J., Gow, P. and Boschetti, F., 1999, Multiscale edge analysis of potential field data: *Expl. Geophys.***,** 30, 38-44.
2. Blakely, R.J., 1988. Curie temperature isotherm analysis and tectonic implications of aeromagnetic data from Nevada, J. Geophys. Res., 93, 11817-11832.
3. Blakely. J. R. and Simpson. R. W., 1986, "Approximating edges of source bodies from magnetic or gravity anomalies", Geophysics, 51, 7, pp. 1494-1498.
4. Boschetti, F., Hornby, P. and Horowitz, F., 2000, Developments in the analysis of potential field data via multi-scale edge representation. In press Expl. Geophys.
5. Boschetti, F., Moresi, L. and Covil, K., 1999, Interactive Inversion in Geological Applications: KES99, International Conference on Knowledge-based Intelligent Information Engineering Systems, Adelaide, 1999.
6. Connard, G., Couch, R. and Gemperle, M., 1983, analysis of aeromagnetic measurements from the Cascade Range in central Oregon, *Geophysics*, 48, 376-390.
7. de Oliveira Lyrio, J.C.S.. Tenorio, L. and Li, Y. 2004. Efficient automatic denoising of gravity gradiometry data, *Geophysics* (69), pp. 772–782.
8. G.E. Leblanc and W.A. Morris, Denoising of aeromagnetic data via the wavelet transform, *Geophysics* (66), pp. 1793–1804.
9. Garcia-Abdeslem, J. and Ness, G. E., 1994. Inversion of power spectrum from magnetic anomalies, *Geophysics*, 59, 381-401.
10. Hahn, A., Kind, E.G. and Mishra, D.C., 1976. Depth Estimation of magnetic sources by means of Fourier amplitude spectra, Goephys. Prospect., 24, 287-308
11. Hornby. P., Boschetti. F., and Horowitz. G. F., 1999, "Analysis of potential field data in the wavelet domain",. Geophysical Journal International, 137, pp. 175-196.
12. Lyatey, Henry. 2004. Detection of subtle basement faults with gravity and magnetic data in the Alberta Basin, Canada: A data-use tutorial, The Leading Edge , December 2004
13. Mallat, S., 1989. Multiresolution approximation and wavelet orthonormal bases of L2(R), *Trans. Amer. Math. Soc.*, 315**,** 69–87.
14. Martelet. G., Sailhac. P., Moreau. F., and Diament. M., 2001, "Characterization of geological boundaries using 1-D wavelet transform on gravity data; theory and application to the Himalayas", Geophysics Geophysics Online (SEG), http://www.geoonline.org/eman/emanlist.html
15. Maus, S. & Dimri, V.P., 1994. Scaling properties of potential fields due to scaling sources, Goephys. Res. Lett, 21, 891 -894
16. Moreau, F., Gilbert, D., Holschneider, M. and Saracco, G. 1999. Identification of potential fields with the continuous wavelet transform: basic theory, *Journal of Geophysical Research* (104), pp. 5003–5013
17. Okubo, Y. and matsunaga, T., 1994. Curie point depth in northeast Japan and its correlation with regional thermal structure and seismicity, *J. geophys. Res.*, 99, 22363-22371
18. Shuey, R.T., Schellinger, D.K., Tripp, A.C. and Alley, L.B., 1977. Curie depth determination from aeromagnetic spectra, Goephys. J. R. Astr. Soc., 50. 75-101
19. Spector, A. and Grant, F. S., 1970. Statistical modes for the interpreting aeromagnetic data, Geophysics, 35, 293-302.

62/7/2010

The Empirical Mode Decomposition (EMD), a new tool for Potential Field Separation

S. Morris Cooper[1], Liu Tianyou[2], Innocent Ndoh Mbue[3]
[1, 2] Institude of Geophysucs and geomatics, China University of Geosciences, Wuhan
[3] Faculty of Earth Sciences, State Key Laboratory for Geological Processes and Mineral Resources, China University of Geosciences, Wuhan
E-mail: smorriscpr@gmail.com

Abstract: In this paper we are proposing the use of the Empirical Mode decomposition method as a tool for potential field data separation. The empirical mode decomposition (EMD) is a new data analysis method suitable to process non-stationary and nonlinear data. Its power to filter and decompose data has earned it a high reputation in signal processing. Its decomposition results in what is called "Residual", which is similar to the regional anomaly of a potential field data. This residual does not require any preset parameters unlike contemporary field separation methods. The method is applied to a magnetic data from the Jianshandian mine in Hubei, China enabling us to construct a 2.5D inverse model inferring the existence of deep ore deposits. The method is effective at separating both local and regional data from magnetic data. [Journal of American Science 2010;6(7):183-187]. (ISSN: 1545-1003).

.

Keywords: Empirical Mode decomposition (EMD), Intrinsic Mode Functions (IMF), potential field separation, Jianshandian Mine

1.0 Introduction

Geophysical potential field separation is a process in which the regional and the local anomalies are separated. Generally, regional anomaly is associated with a larger amplitude and scope but smaller horizontal gradient caused by the widely distributed mid-deep sources; while the local anomaly is vice versa. There are several field separation methods in use today based on Fourier or wavelet transforms. The Fourier transform (FFT) is designed to work with linear and stationary signals. The wavelet transform, on the other hand, is well-suited to handle non-stationary data, but it is poor at processing nonlinear data (Hassan and Pierce, 2008). Prominent among these methods are Polynomial fitting, moving average, upward and downward continuation and wavelength filtering. The regional anomalies obtain via these methods depend largely on preset parameters. Moreover, geophysical data are nonlinear and non stationary.

The combination of the well-known Hilbert spectral analysis (HAS) and the recently developed empirical mode decomposition (EMD) [Huang *et al.*, 1996, 1998, 1999], designated as the Hilbert-Huang transform (HHT) by NASA, indeed, represents a paradigm shift of data analysis methodology. The key part of HHT is EMD with which any complicated data set can be decomposed into a finite and often small number of intrinsic mode functions (IMFs). This decomposition method is adaptive and therefore highly efficient. As the decomposition is based on the local characteristics of the data, it is applicable to nonlinear and nonstationary processes. Contrary to almost all the previous decomposition methods, EMD is empirical, intuitive, direct, and adaptive, without pre-determined basis functions (Huang & Wu., 2008). It has been applied in severals fields such as meteorology (Iyengar and. Kanth,2005), signal processing (Linderhed, .2004),and geosciences (Hassan and Pierce, 2008) The decomposition is designed to seek the different simple intrinsic modes of oscillations in any data based on local time scales. A simple oscillatory mode is called intrinsic mode function (IMF) which satisfies: (a) in the whole data set, the number of extrema and the number of zero-crossings must either equal or differ at most by one; and (b) at any point, the mean value of the envelope defined by the local maxima and the envelope defined by the local minima is zero. The residual value obtained by removal of a series of IMFs is the trend component that represents the average trend, which is similar to the geophysical regional anomaly. In light of the power of the EMD as a decomposer, we are proposing its use as a potential field separator.

2.0 Material and methods

2.1 Study Area

Our area of study is Jinshandian ore mine in located in Hubei, China and characterized as a typical

contact metasomatic deposit bed. It is distributed in or around the contact zone of the monzonite granite and Triassic sandstone and shale (fold in the carbonate rocks), with a north-west (NW) strike direction and a length of 3km approximately (Fu *et al*, 2008) It contains several cluster of deposits. It is an open mine and extraction of mineral has been ongoing reaching a depth of 400m. Based on the geological background, ore geology, gravity and magnetic abnormities and coupled with a large scale residual gravity and magnetic anomaly, it is predicted that concealed ore bodies could be at greater depth than those already known. Profile AA' is taken in the southern portion away from the main ore body to deduce the presence of magnetite at this part (fig.1).

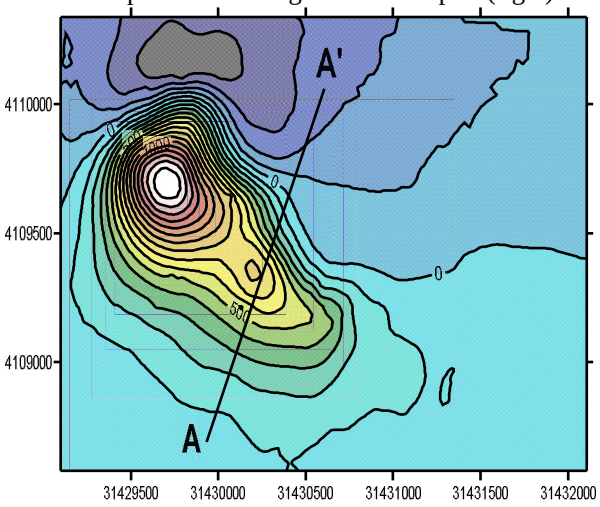

Figure 1: Aeromagnetic map of Jianshandian showing profile AA'

2.2 Principle of the EMD

The EMD is an adaptive decomposition technique with which any complicated signal can be decomposed into a definite number of high-frequency and low frequency components by means of a process called "sifting". The sifting process decomposes the original signal, *S(x)*, into a number of intrinsic mode functions (IMFs) according to the following formula:

$$S(x) = \sum_{i=1}^{n} c_i(x) + r_n(x) \qquad (1)$$

Where $r_n(x)$ is the residual after n IMFs and $c_i(x)$ the IMFs.

These IMFs have well-behaved Hilbert transforms and are defined as functions that:

(a) have the same number of zero- crossings and extrema, and

(b) the mean value of the upper and the lower envelopes is equal to zero.

A sifting process extracts IMFs from the signal iteratively sequentially to obtain a component that satisfies conditions mentioned above. The sifting process separates the IMFs with decreasing order of frequency, i.e., it separates high frequency component first and the low frequency component at the end. The IMFs obtained by sifting processes constitute an adaptive basis. This basis usually satisfies empirically all the major mathematical requirements for a time series decomposition method, including convergence, completeness, orthogonality, and uniqueness, as discussed by Huang et al. [1998]. The EMD technique (Huang et al., 1998) is illustrated in Figure 2 for a simple signal consisting of chirp. The technique happens to naturally cope with superimposed smooth trends (Flandrin, P., Rilling, G., and Gonçalvés, P., 2004). The decomposition of the signal into IMFs is performed as follows:

1. Identify the positive peaks (maxima) and negative peaks (minima) of the original signal.
2. Construct the lower and the upper envelopes of the signal by the cubic spline method. *(U(t), L(t))*
3. Calculate the mean values by averaging the upper envelope and the lower envelope. *m(t)= (U(t) + L(t))/2*
4. Subtract the mean from the original signal to produce the first intrinsic mode function *IMF1* component. *S(t) – m(t) = h(t) note h(t) =IMF1*
5. Calculate the first residual component by subtracting *IMF1* from the original signal. This *IMF1* component is treated as a new data and subjected to the same process described above to calculate the next IMF. *S(t) – h(t) = r(t)*
6. Repeat the steps above until the final residual component becomes a monotonic function and no more IMFs can be extracted.

The sifting process produces a set of *IMF*s that represent the original data vector broken down into frequency components from highest to lowest frequency. This process is subject to a symmetry condition called the stoppage (of sifting criteria) which is a normalized squared difference between two successive sifting operations. In this paper we use the one by Huang *et al* (1998) giving as:

$$SD_k = \frac{\sum_{t=0}^{T} |h_{k-1}(t) - h_k(t)|^2}{\sum_{t=0}^{T} h_{k-1}^2(t)} \qquad (2)$$

A value of 0.2 ~ 0.3 for SD is considered acceptable for a calculated IMF, that is *h(t)*. If all of the IMFs for a given signal are added together, the resulting "summation" signal is a near perfect match for the original signal (i.e., with little or no leftover), yielding a high level of confidence in the EMD results.

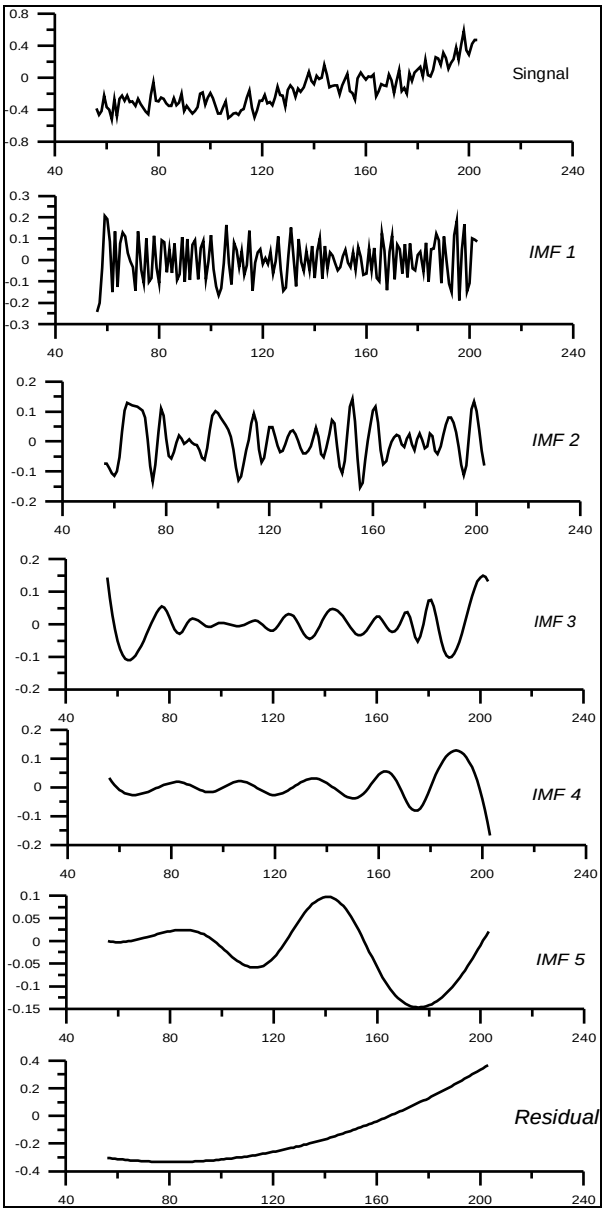

Figure 2: An empirical mode decomposition (EMD) of a signal producing five IMFs and a residual. The first curve is the plot of a chirp

3.0 Result and Discussion

To separate the regional and the local anomalies from the superinposed total magnetic anomaly profile , we use the Empirical Mode Decoposition resulting into seven IMFs and a residual(fig. 3), which is equivallent to the regional anomaly when applying conventional mehtods. The same profile was seperated using trend analysis and the result showed that the lacal and the original anomalies are almost the same signifiyingthat the complexity of the anomaly was due largely to shalow sources.

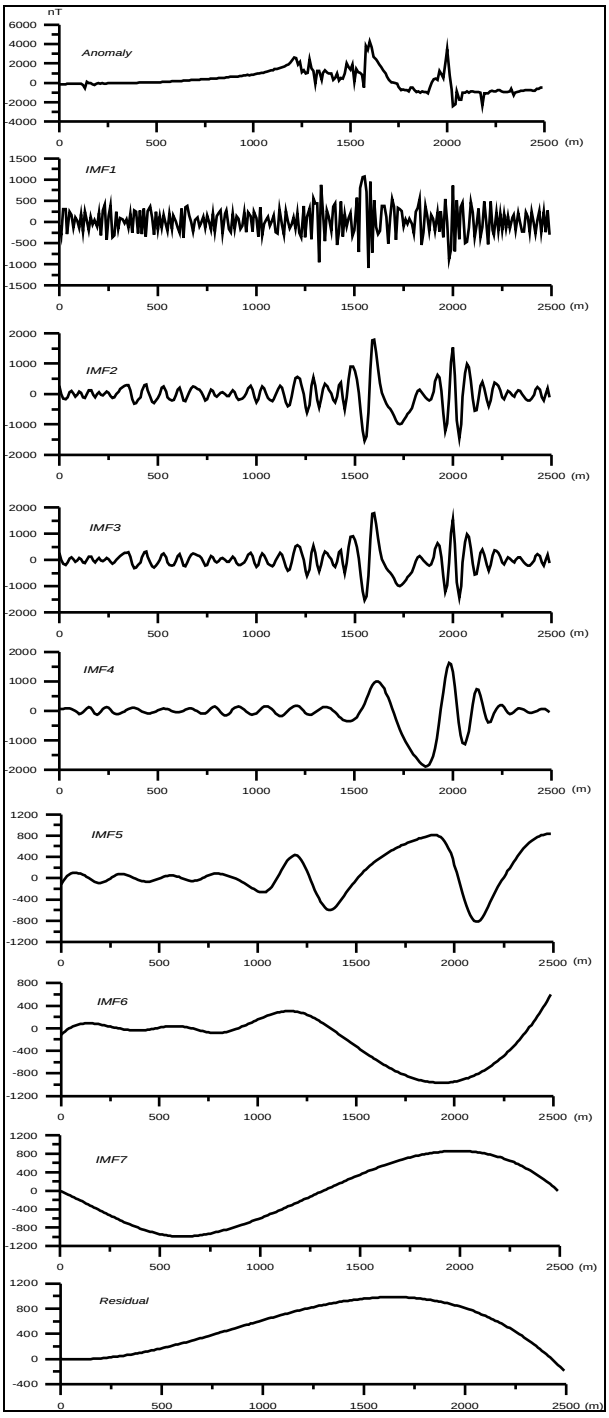

Figure 3: An Empirical mode decomposition of

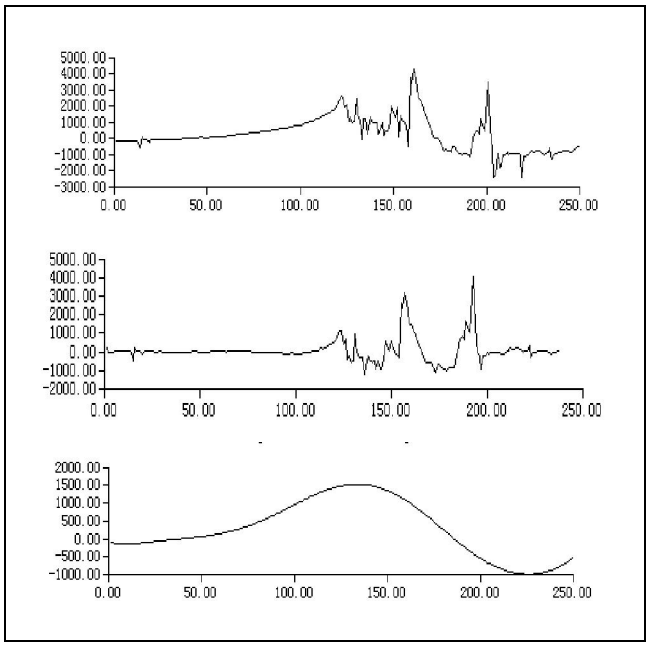

profile AA' showing seven IMfs and a residual. The topmost graph is the anomaly of the magnetic profile.

Figure 4: A trend analysis field seperation of profile AA'. The top is the total anomaly, the middle is the local anomaly and the bottom is the reginal anomaly.

The anomaly(fig.4) produced as a result of profile AA' clearly shows serious suprficial interferences and the presence of shallow bodies thus resulting to an abnormal complex form. Fitting such curves to the theoritical values and infering deep sources can sometimes be difficult. However, from magnetic survey and the drilled core, blastopsammite, hornfels, skarn (with thin magnetite) as well as some other rocks, such as diorite, diorite porphyrite and diabase are known to be interbeded in the sandstone at the south edge of this area. They possess some degree of magnetism, which is the main factor of influence.

Magnetic parameters were based on the above analysis and in consideration of the drill core results in constructing the 2.5D forward and inverse models (fig. 5 & 6). Since the local anomaly is similar to the total anomaly, this indicates that the local anomaly mainly reflects the anomaly of the rocks and deposits at shallow depth. From 2.5D inverse model based on the EMD residual, which is similar to the regional anomaly obtained via trend analysis, we deduce that there may be 2 unknown iron deposits at greater depths. The deposits colored red and yellow have different magnetizations. The one marked yellow was partially penetrated during drilling and found to be iron III. We believe that a thick section of magnetite lie beneath this low grade. ore below the level of -400m (Fig.6), which is in conformity with assumptions based on potential field data analysis in the area (Fu Qunhe,Li Langtian, Kuang Qingguo, Zhao Zhixiang 2008).

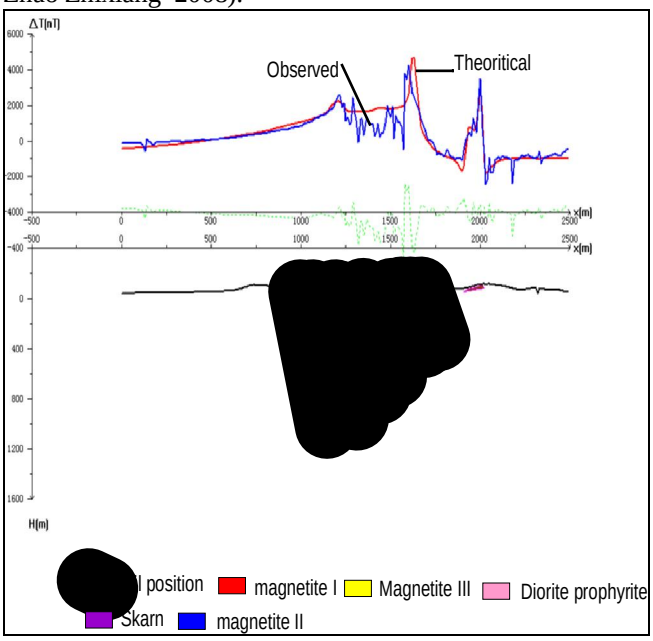

Figure 5: 2.5D forward model of the profile AA'. The black lines indicate drill positions

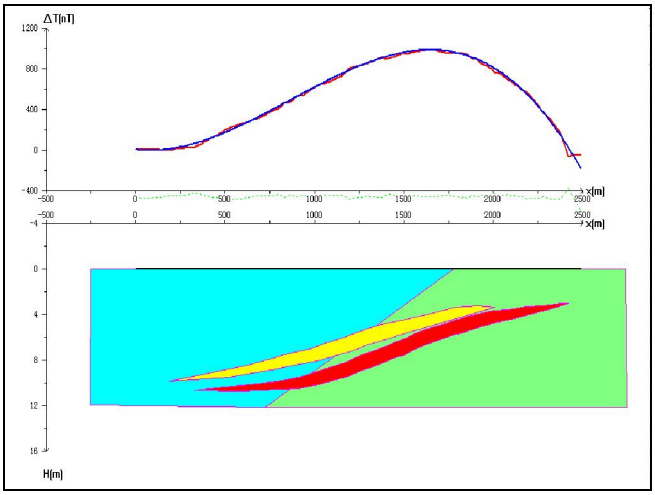

Figure 6: 2.5d inverse model based on the the residual of the EMD

4.0 Conclusion

In this paper, the EMD is proposed and applied in the separation of geophysical potential field superimposed anomalies caused by several anomalous sources. The EMD is a new and powerful technique use to analyze nonlinear and non-stationary

signals such as potential field data. It decomposes the signal to a summation of zero-mean AM-FM components, called Intrinsic Mode Functions (IMF). These IMFs show the main components of the analyzed signal The EMD was applied to a magnetic data from Jianshandian iron deposit in Hubei, China and found to be effective at separating the local and regional from magnetic data and the result was compared to that of trend analysis and found to be similar. The separation was carried out without any pre-set parameters as done in traditional separation methods. A 2.5D inverse model was realized from the residual of the EMD resulting into an inference of ore bodies at greater depth below 400m.

Corresponding Author:
Mr. S. Morris Cooper
China University of gepsciences
Wuhan, Hubei, china
E-mail: smorriscpr@gmail.com

References

1. Flandrin, P., G. Rilling, and P. Gonc¸alves (2004), Empirical mode decomposition as a filter bank, IEEE Signal Process. Lett., 11, 112–114, doi:10.1109/LSP.2003.821662
2. Hassan H. H. and Pierce J.W. 2008, Empirical Mode Decomposition (EMD) of potential field data: airborne gravity data as an example. CSEG RECORDER, Focus Article 25, pp 26-30
3. Huang, N. E., S. R. Long, and Z. Shen (1996), The mechanism for frequency downshift in nonlinear wave evolution, Adv. Appl.Mech., 32, 59–111
4. Huang, N. E., Shen, Z., and Long, S. R.: A new view of Nonlinear water waves: the Hilbert Spectrum, Ann. Rev. Fluid Mech., 31, 417–457, 1999.
5. Huang, N. E., Z. Shen, S. R. Long, M. C.Wu, H. H. Shih, Q. Zheng, N.-C. Yen, C. C. Tung, and H. H. Liu (1998), The empirical mode decomposition and the Hilbert spectrum for nonlinear and nonstationary time series analysis, Proc. R. Soc. London, Ser. A, 454, 903–993
6. Huang, N.E., Wu,M.L.., Long, S.K., shen, S.S.P., Qu, W.D. Glooersen, P. and Fan, K.L. . “A confidence limit for the empirical mode decompositi-on and the Hilbert spectral analysis”, Proc. of Roy. Soc. London, A459, 2003: pp.2317-2345.
7. Iyengar, R. N., and S. T. G. R. Kanth (2005), Intrinsic mode functions and a strategy for forecasting Indian monsoon rainfall, Meteorol. Atmos. Phys., 90, 17 –36, doi:10.1007/s00703-004-0089-4.
8. Liu Hongguang, Luo Ying, Zhao Guoqi, Li Zhongfang,. “A new concrete damage AE signal analysis method that based on HHT”, Journal of Disaster Prevention and Mitigation Engineering, Vol.27 No.2 2007, pp.187-191.
9. Norden E.Huang, “An adaptive data analysis method for nonlinear and nonstationary time series:the empirical mode decomposition and Hilbert spectral analysis”, Applied and numerical harmonic analysis, Brikhauser Verlag Basel/Switzerland, 2006,pp363-373.
10. Qunhe, F., Langtian, L.,Qungguo, K. and Zhixiang, Z. (2008). Gravity and magnetic Abnormalityand Resource Potential Prediction in the jian shan dian iron Mine, Eastern Hubei, Geology and prospecting Vol 44, 3, 2008pp6-10

3/1/2010

Remote Sensing Data Dissemination and Management: Potential of Replication and Provenance Techniques

Tauqir Ahmad [1], Abad Ali Shah [2]

Department of Computer Science
University of Engineering and Technology, Lahore

tauqir_ahmad@hotmail.com abad_shah@uet.edu.pk

Abstract: With the proliferation of computer technology in almost every sphere of life such as e-government, health care and services sector, there is an increased reliance on digital data. More recently, satellite and remote sensing data has gained importance owning to its applications in real time decisions for GIS, military and strategic needs, and, surveillance and security systems. However, real time access to the digital repositories most of which are web based is plagued by various management and dissemination issues. In data intensive domains such as scientific computations, bioinformatics and e-commerce, replication and provenance have been used successfully for improved performance of data sources by handling the issues of availability, discovery, reliability, authenticity and consistency. In this paper we argue that remote sensing data dissemination and management share common issues and problems with the data intensive domains mentioned above. We also suggest that replication and provenance techniques offer a promising solution to remove the bottleneck of data dissemination and management for real time decision making based on remote sensing data. [Journal of American Science 2010;6(7):188-198]. (ISSN: 1545-1003).

Keywords: Remote sensing data, data dissemination, data management, replication, provenance

1. Introduction

Remote Sensing (RS) is the science of using electromagnetic radiations to identify earth surface features and estimation of their geo-bio physical properties through analysis and interpretation of its spectral, spatial, temporal and polarization signatures using electromagnetic radiations [1]. With the gradual and increased shift of critical and important systems in both private and government sectors towards computerization, remote-sensing data and GIS's are being seen as critical contributor for both short-term and long-term planning in many domains such as social sciences, agriculture, disaster management, security and surveillance, and, military [2]. However, success and reliability of systems based upon remote sensing data and GIS's depends upon its accessibility level and its successful integration with non-spatial data such as socio-economic and population data [2].

The accessibility issues in a remote sensing application consist of remote sensing data acquisition, its maintenance and archiving, and, its dissemination and distribution [3]. The data accessed is then analyzed and interpreted to with other spatial and non spatial data to address various needs. Although, much research is being done on the various stages towards the realization of remote sensing application, the area of remote sensing data dissemination and distribution has not attracted much attention. Although remote sensing data is acquired in real time, its dissemination and distribution constitutes the bottle neck, owning to the various hops over the network in a distributed environment [4]. As remote sensing applications are distributed and real-time, data dissemination and distribution issues form the weakest link in the chain. Interrelated and interdependent to data dissemination and distribution bottlenecks are the issues of remote sensing web service discovery and data provenance. Meaningful and efficient analysis and interpretation of remote sensing data may be significantly facilitated by

annotating it with semantic and provenance meta-data [5].

In literature, replication has been used successfully to handle the problems of data dissemination and distribution in data intensive domains such as scientific computations, bioinformatics and e-commerce [4]. Also in [5] authors have proposed a set of factors that may be used as provenance meta-data to enhance the semantic understanding of both web services and web-based data source [6]. However, these techniques have not been widely adapted by remote sensing community to solve the problems of remote sensing data dissemination and management. The reason for this can be traced back to early remote sensing systems that were mostly government owned and centralized [7]. However with the ubiquitous use of remote sensing data in myriad of applications, there has been a gradual shift towards distribution of remote sensing data. This has increased the need for better dissemination and management mechanisms. In this paper we explore the potential of replication and provenance meta-data to enhance the capability of existing remote sensing applications with enhanced data accessibility, service discovery and trust.

The rest of the paper is organized as follows: Section 2 consists of literature survey in which the importance of remote sensing data and its applications is discussed. Also included in this section are the accessibility and dissemination issues of web based data resources and how replication techniques are being used to handle them. Existing work on provenance is also included in this section. In Section 3 we argue the need of replication and provenance techniques for remote sensing data dissemination and management. We end this research paper with conclusions and suggested future work in Section 4.

2. Literature Survey

In the last two decades, increasingly powerful computing and communication technologies have revolutionized the world through the realization of e-systems such as e-governments, e-commerce, and e-sciences [8]. These e-systems are data-driven and data-intensive, collecting myriad of information for both short-term and long-term decision making [8]. The information collected varies from business transactions, medical and personal information to scientific, satellite and surveillance information [9]. The data describing this information may itself be spatial, multimedia or hypertext documents. This diversity of information and data adds an element of complexity to the management and successful execution of e-systems [10]. Conventional database technologies have been deficient and unsuitable to handle this huge amount of data and information stores owning to its diversity in content and format [11]. E-systems have peculiar needs such as effective, efficient and real-time information retrieval [12]. This information further needs to be enriched with semantic information for discovery of patterns. Over the last two decades, most of the data and information resources covering a broad variety of topics have been made available through World Wide Web (WWW) making it the most important repository of data. However, with the unstructured, dynamic and heterogeneous nature of its contents that are inter-connected with hyper-links, WWW adds yet another layer of complexity [13]. In addition to the conventional problems of redundancy and inconsistency, various other issues such as of data provenance, data dissemination, interoperability, and heterogeneity need to be addressed for the successful management of Web-based data and information resources[5],[14].

2.1 Role of Remote Sensing Applications in E-Systems

Amongst the resources that enable the e-systems, remote sensing applications (RSAs) based on spatial and non-spatial data resources have attracted much attention more recently[15]. RSAs are being extensively used for critical applications in various domains such as social sciences, agriculture, disaster management, security and surveillance and, military [16]. In social sciences RSAs are used to monitor environmental conditions, resource management, epidemiology, archaeology and anthropology, international relations, human health conditions, law, and demographic and urban studies [17]. Agriculture benefits from RSAs for example through identification of cultural wastelands,

marginal lands and monitoring of temporal behavior of vegetation [18]. Inland wetlands mitigate the harmful effect of pollutants, help control floods, and are used by fish and wild life as breeding, nursery, and feeding grounds. Other direct and indirect benefits include increased yield, improvement of soil fertility, site specific management of agriculture, preservation of eco-diversity and creation of supportive infrastructure such as irrigation [19]. RSAs play key role in effective disaster management. They provide, analyze and interpret data for mapping fire fuels, accessing fire effects, monitoring fire danger, and measuring progress in implementing any fire rescue and control plan [20]. In a similar manner they help design contingency and mitigation plans for electrical outages, floods, tornadoes, earth quacks, volcanic eruption, tsunami, hurricanes, landslides and human caused disaster (e.g. terrorism)[21]. Remote sensing data is also critical to help make timely and intelligent decisions in military operations. Accurate spatial information is critical to the concept of command, control, communication and coordination in military operations. GIS is used by military in a variety of applications that include cartography, intelligence gathering, battle field management, terrain analysis and remote sensing of objects [22].

2.2 Remote Sensing Data: Issues and Problems

In Section 2.1, we discussed the role and importance of remotes sensing data which is used by remote sensing applications for decision making in many E-Systems. However, issues of data dissemination and data provenance need to be addressed if these E-Systems are to make any reliable real time decisions based on remotely sensed data.

2.2.1 Data Dissemination Issues

Remote Sensing Data is difficult to manage and disseminate because of its peculiar characteristics as shown in Table 1 and explained below.

	Remote Sensing Data	**Conventional Data**
i)	Distributed- Temporally and Spatially categorized	Centralized- Static and Stable
ii)	Critical Response time	Not critical;
iii)	Temporal in nature: volatile	Stable: non volatile
iv)	Have validity constraints	Validity is permanent
v)	Evolutionary	Static
vi)	Uncertain, imprecise	Precise, Exact
vii)	Heterogeneous	Homogeneous
viii)	Voluminous	Medium to small scale
ix)	Broad context	Limited Context

Table 1: Comparison of Remote Sensing and Conventional Data

i) Remotely sensed data is either constantly acquired or may be acquired on request for specific purposes. In both the cases, it is organized in some host primary machine using a conventional DBMS [3], [23]. However, fetching fresh data directly from primary site is not efficient. This is because datasets of remotely sensed data may be organized into multiple files containing a subset of data elements categorized temporally and spatially [23].

ii) The response time of such data sets may be adversely affected as multiple queries access these datasets for the same temporal or spatial information [24]. The effect of write operations may even be more adverse as consistency is compromised resulting in conflicting results. Moreover, many real-time applications need to share data that are distributed from a primary site among multiple sites [25].

iii) Remotely sensed data can be categorized into temporal data and non-temporal data. Real time sensor data representing the physical world is temporal in nature [26]. Temporal data objects are difficult to manage and analyze as they have validity intervals and are updated periodically. For example, temperature zones, its spread, location is example of temporal data in a fire management application [27, 28].

iv) As compared to temporal data, non-temporal data do not change dynamically with time. Thus they do not have validity intervals and they do not need to be updated by periodic system updates. However, as most of these data and applications are hosted in a distributed environment, the issues of data dissemination relating, availability, consistency and response time affect non-temporal data also [29].

v) Remote Sensing Data is highly evolutionary, uncertain and incomplete. The latest findings, weather conditions, natural and human activities may invalidates the previous information and data.

vi) Remote sensing data is heterogeneous consisting of sequence data, graphs, high-dimensional data, geometric information, scalar and vector fields, patterns, constraints, images, spatial information, models, prose and declarative knowledge such as hypotheses and evidence

vii) High volume of remote sensing data must be gathered and then disseminated Remote sensing data must have i) ***Factor comprehensiveness***, which reflects the numbers of objects that can be measured at once ii) ***Time-line comprehensiveness***, which represents the time frame within which measurements are made (i.e., the importance of high-level temporal resolution), and iii) ***Item comprehensiveness***—the simultaneous measurement of multiple items, All of these considerations suggest that in addition to being highly heterogeneous, remote sensing data must be voluminous if they are to support comprehensive investigation and interpretation.

viii) The usage of remote sensing data is very broad, with different perceptions, contexts and objectives.

Conventional databases and information technologies have many limitations to overcome the problems mentioned above. As discussed in Section 1, other data-intensive domains such as

bioinformatics share the above mentioned issues and problems. In Section 3, we will describe how replication techniques, which have been used to solve similar problems in scientific domains such as bioinformatics, can be applied for remote sensing data dissemination and management.

2.1.2 Data Provenance Issues

With the increased capability and usage of the Internet, various research groups with common interests have moved towards collaborative research [30]. Due to heterogeneity and distribution of data resources, the usability of data resource for a particular domain depends upon the provenance information attached to the data resource. More generally, Data Provenance is the information about data, describing its origin and sequence of tasks (workflows/processes) that were responsible for its transformation; structurally, logically, physically and/or geographically. It provides a qualitative and quantitative metric to analyze the quality and dependability of the data based on consumer trust of the source of creation and the sources that were responsible for modification. Therefore, data provenance has a significant role to play for remote sensing domain in addressing the concerns of trust, quality and copyright [5].

In Geographical Information Systems (GIS), Provenance information includes description of the lineage of the data product including description of the data source, the transformations used to derive it, references to the control information and mathematical transformations of the coordinates used [5]. Recording lineage helps the user of the data product to decide if the data meets the requirements of their application [31]. Spatial Data Transfer Standard (STDS) is one such lineage recording system that helps in using the data product by deciding whether the data meets the requirements of the domain or not. Lineage Information Program (LIP) is for GIS and is used for informational purposes, update stale data, regenerate and compare data. [31] LIP follows a data-oriented provenance technique [31]. Provenance data relates to spatial layers, the basic dataset of GIS, the transformation algorithm and intended use of the data [5], [31]. Semantic Information is not included. To be useful, the data to be transferred must also be meaningful in terms of data content and data quality We feel that if this lineage information is stored and recorded in the machine readable from using Resource Description Framework (RDF) and Ontologies, an efficient automated validation of results is possible with the potential for increased access to and sharing of spatial data, the reduction of information loss in data exchange, the elimination of the duplication of data acquisition, and the increase in the quality and integrity of spatial data. Annotating data from one organization with enough metadata will enable other organizations to use the purposefully and in more meaningful ways [5]. However, there are only a few data provenance systems catering for remote sensing domain which primarily focus data provenance as an issue [5]. In Section 3, we discuss the potential of replication and provenance techniques to solve the problems of remote sensing data dissemination and management.

3 .Potential of Replication and Provenance Techniques

E-Systems are real-time distributed applications and they need real-time data accessibility for prompt and timely decision making. Providing such real-time data accessibility is, however, a challenging task is due to long remote data accessing delays, network hops and inflexible temporal requirements of real-time transactions. Replication is a technique that has been used to ensure the availability of data in a distributed environment to improve the performance and meet the stringent response time requirements of real-time applications [5]. As discussed in Section 2, a real-time data intensive application should be supported by provenance data to establish its authenticity, trust and reliability [5, 13]. More importantly, the provenance data can also be used to avoid duplication of the data replication efforts [5]. As early remote sensing applications were primarily government owned and centralized, the need for replication and provenance techniques was not realized and needed. Examples of such systems are those systems which were used by military for defense, intelligence and reconnaissance purposes [7]. However, with the ubiquitous use of remote sensing (RS) data in myriad of applications such as fire fighting, control surveys, environmental

studies, ecology, social sciences etc., there has been a gradual shift towards distribution of RS data [7]. This has increased the need of better dissemination and management mechanisms. We feel that real-time data intensive remote sensing applications can get benefit from the existing replication and provenance techniques. Based on this argument, we advocate the need of applying replication and provenance techniques in remote sensing applications. In our opinion, by applying the replication and provenance techniques, we can address the issues of dissemination of RS data, and achieve the following objectives:

i) Data availability enhancement of data during disk-failure in a multi-disk system,

ii) Speed up I/O performance of read-intensive applications,

iii) Maintain consistency of temporal data,

iv) Maintain reliability of transactions accessing temporal data,

v) Efficient execution of batch-shared I/O oriented data-intensive tasks in web based distributed environment.

RS data is usually "write-once" and "read-many" type of the data and the read performance of an application becomes an important factor [32]. This type of stored data is generally is accessed through range type of queries which retrieve a range of key values from a distributed high dimensional data set [6, 13]. To minimize the disk retrieval time for range queries various non-replication based schemes have been used that distribute data blocks among parallel disks [17, 33]. In these schemes, data files are de-clustered into fragments and spread across multiple disks so that the application can exploit the I/O bandwidth reading and writing the disks in parallel [33]. However, to achieve objectives i) and ii) using the data replication technique, two problems need to be addressed [6, 13, 28 and 29]. These two problems are listed below.

a) The data placement problem of determining the optimal scheme for storing copies of each data block on a particular disk, and

b) the scheduling problem, i.e., to minimize the retrieval time from the disk for a data block.

The replication technique is classified into two categories, i.e., *eager* and *lazy* [6, 11]. In the eager replication approach, all copies of a data item are updated by a single transaction, and his makes it relatively easy to guarantee the consistency as in one-copy serializability for the replicated data, the eager protocols are unsuitable if all replicas are not available [28, 34]. Moreover, it performs poorly if a large number of replicas need to be updated [28]. In the lazy replicated approach, separate transactions are used to update replicas while primary copy is updated through a separate update transaction resulting in a faster response time but compromised consistency [13, 28 and 33]. In case of remote sensing applications and data, most of the transactions are read-only. For a set of requested data blocks, scheduling is better achieved through the lazy approach by retrieving data blocks from the earliest updated replica thus minimizing the retrieval time (better response time) [33, 34].

The objectives iii) and iv) may be achieved by hosting both temporal data objects and non-temporal data objects at a primary site which also keeps record of replicas of the temporal data objects hosted within the application [6]. Any recent changes to the temporal data objects, then, may be periodically recorded at the primary site and then updated in the replicas [21]. We are actively working on a hybrid replication model using both the lazy and eager approaches. A lazy approach is a better approach for those applications where most requests are *read-only* over temporal data with critical response time requirements [28]. For critical static data, the eager replication approach guarantees consistency [34]. The transactions may be divided into two types: *system update transactions* and *user transactions* [28]. In the case of remote sensing applications, temporal data update transactions should get priority over replica update transactions to keep consistency [21]. All transactions are validated before accessing fresh data. If the accessed data is stale, then the transaction is restarted. A transaction commits only if it has been validated. We are suggesting that the same validation procedure can be adopted for transactions accessing copies of data available at replicas [11, 12].

Data-Intensive Remote Sensing Applications usually store datasets in collections of files. Such applications may require access to large numbers of files and huge data volume [6, 8]. When mapping tasks to compute nodes, I/O overheads can be minimized by co-coordinating staging of the files because in a batch-shared I/O the same file may be required by multiple tasks in a batch. The objective v) can be achieved by accomplishing the following tasks:

a) to find a mapping of tasks to nodes,

b) to decide which files need to be remotely transferred and their corresponding destination nodes,

c) to determine which files need to be replicated and their corresponding source and destination nodes, so as to minimize the batch execution time.

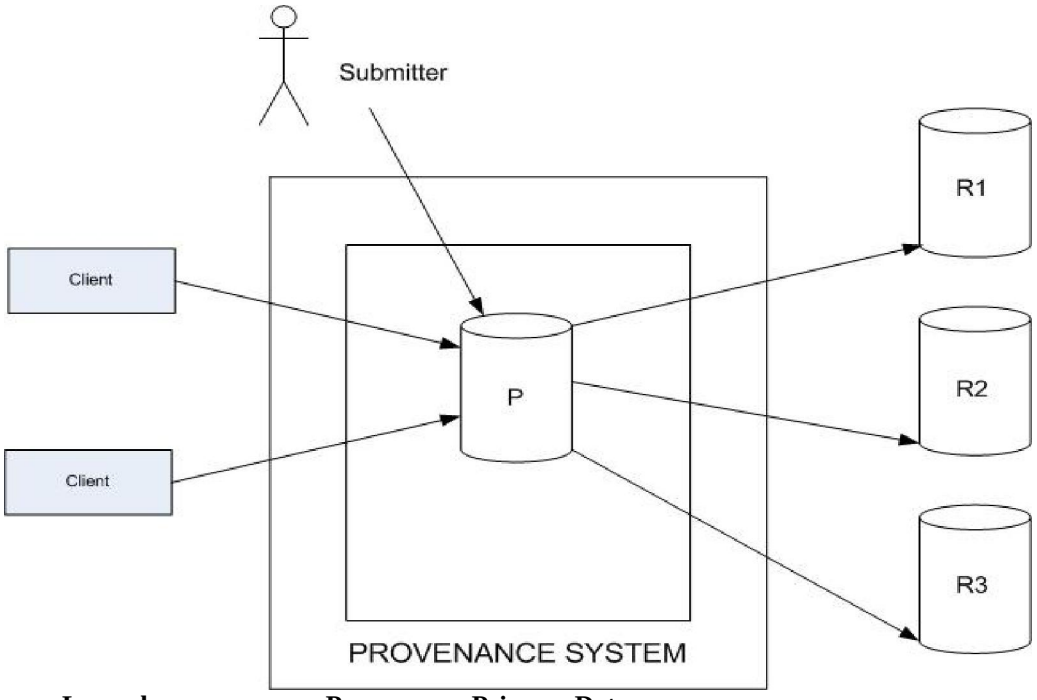

Legend: **P : Primary Data**
R1, R2, R3: Replicas

Figure 1: Use of replication and provenance for RS data dissemination

In a submarine control system, example of temporal data is its position, speed and depth needed for ship maneuvering. Different combat ships and submarines share this remotely sensed data through real-time distributed database systems. Compared to stand alone local systems, data access is slow in such distributed real-time database systems owning to multi-hop network operations that take substantially more time than the local data accesses. This results in slow response time. Also as a result of delayed transaction completion time, some of the relevant data items used in transaction processing may already have become stale. In a military and defense domain such as a submarine control system, where real time decisions are needed, stale and invalid data may result in disastrous consequences. In this case replication can be used to ensure the availability of data and meet the real time response time requirements. This data needs to be supported by provenance data to establish its authenticity, trust and reliability.

Provenance of data and its replicas enhance the trust, authenticity, and credibility of remote sensing applications [35, 36 and 37]. We suggest that RS data should be annotated with the following provenance meta-data to facilitate its dissemination.

i) **Granularity**: RS data is only useful if it is collected at a required level by the domain and the application. It is for the user to decide the acceptable level of granularity for a particular domain and also recording of replication history.

ii) **Format:** Annotations written in Resource Description Framework (RDF) and Web Ontology Language (OWL) are automatically recorded as they have the advantage of being machine readable.

iii) **Data Core-Elements**: The core elements are: title, description, subject, data and unique identifier which must be recorded.

iv) **Authority**: This parameter determines the trust a user places in a particular data source and its origin.

The provenance data can facilitate the following tasks [39]:

i) Ranking of a data resource,
The user of a web resource may assign a comparative value to it tools reflecting the relevance of the web resource based on its experience.

ii) Updating data resources and its replicas.
Meta-data relating representing the last update to a replica or a resource may be annotated by meta-data relating to its most recent usage

iii) Recommending a data resource
To establish the relevance of a web resource to a user based on usage patterns and user profiles.

iv) Measuring the usefulness of data resources
Calculating how useful a web resource has been to a certain community.

v) Standardizing selection based on a minimum acceptable standard,
A quality analysis using the provenance information can be carried out to determine whether the record complies with a minimum standard to be accepted. This could be especially important for automatic generators of provenance information.

vi) Selection of the most appropriate replication instance [40].
A web resource can have several provenance instances that describe it. The quality could be taken in account when selecting the most appropriate record for each situation (search, evaluation, assembly, etc).

v) **Timeliness**: This parameter determines how current information is as determined by its current status of usefulness, the age of provenance data (old data tend to be more obsolete) and how often the data source is used.

In Figure 1, the submitter which may be a RS data generation /collection entity submits data to a primary site. The submitted data is annotated with provenance meta-data such as submitter authority, data-core elements, format etc., as mentioned above. The data is replicated to R1, R2 and R3 with necessary information. The clients accessing the primary site or its replicas also record necessary information relating to their usage patterns, accessibility and recommendation etc. In this way all transactions are annotated with the necessary meta-data relating to a particular transaction. This annotated meta-data also helps avoid duplication of replication efforts for RS data, remote sensing services and workflows [38].

4 Conclusion and Future Work

Replication and provenance techniques have been used successfully to handle the problems of data dissemination in Web-based data intensive domains such as e-commerce and bioinformatics. However, these techniques have not been adapted by mainstream remote sensing community. With the increasing reliance of E-systems on remote sensing data and remote sensing applications, we feel that replication and provenance techniques must be adapted by remote sensing community if it is to handle the data dissemination issues and problems. In this paper we have proposed that usage of existing replication and provenance techniques to provide a basis for remote sensing data and applications. Although our work is in preliminary stage, we are working on a hybrid model consisting of lazy and eager replication techniques which can cater for peculiar problems of remote sensing data and applications such as its hyper-rectangular nature, spatiality and temporal volatility. We are also extending the list of necessary meta-data categories presented in this paper and working on a provenance system that records and

annotates semantic information relating to a data resource and its replica. In our opinion, existing replication and provenance systems in other scientific domains such as bioinformatics will provide us the necessary impetus to realize a functional model of using these techniques for remote sensing applications.

ACKNOWLEDGEMENT
We acknowledge the support extended by Higher Education Commission (HEC), Pakistan and University of Engineering and Technology, Lahore.

REFERENCES

[1] Ranganath, R., Navalgund, V., Jayaraman, and Roy, P. S., "Remote sensing applications: An overview", Current Science, VOL. 93, NO. 12, pp. 1747-1766, Space Applications Centre, Ambawadi, India,2007.

[2] Charles, G., David, K, "Land Use Planning and Security in Terrains of Terror", Conference on "the Science and Education of Land Use: A transatlantic, multidisciplinary and comparative approach" in Washington, DC, USA. Sep, 24-26, 2007.

[3] Rajitha, K. , Mukherjee, C.K., and Vinu Chandran, R., "Applications of remote sensing and GIS for sustainable management of shrimp culture in India", Aquacultural Engineering, ScienceDirect, www.elsevier.com/locate/aqua-online, volume 36,No.1, pp. 1–17,USA, 2007

[4] NICHOLAS, M.S., "The Remote Sensing Tutorial". 2007 http://rst.gsfc.nasa.gov/Front/tofc.html

[5] Ahsan, S., Shah, A , "Designing software-intensive systems: methods and principles", Quality Metrics for data provenance, chap. 25.. Published by Idea Group Inc (IGI),USA, pp. 455-473.

[6] Baker, M., Buyya, R. and Laforenza, D.," Grids and Grid technologies for wide-area distributed computing", Software- Practice And Experience (DOI: 10.1002/spe.488) Copyright 2002 JohnWiley& Sons, Ltd. 2002.

[7] John, R., Jensen, "Remote Sensing of the Environment, An Earth Resource Perspective", Pearson Education Singapore, 2000, Ch-3, pp.53-80

[8] Bagchi, S., Kar, G., Hellerstein, J.," Dependency Analysis in Distributed Systems using Fault Injection: Application to Problem Determination in an e-commerce Environment", 12th international workshop on distributed systems: operations and management DSO '2001 Nancy France, 2001.

[9] Fang, Z., "E-Government in Digital Era: Concept, Practice, and Development School of Public Administration", National Institute of Development Administration (NIDA),Thailand, International Journal of The Computer, The Internet and Management, Vol. 10, No.2, , pp. 1-22, Thailand, 2002.

[10] Longley, P., Michael F., David, J.M., David, W. R.," Geographical Information Systems and Science", 2nd edition, Published by JohnWiley and Sons, USA , pp. 3-7, 2005.

[11] PATRICK, V., "Parallel database systems: Open problems and new issues", Distributed and Parallel Databases, Springer. Volume 1, No. 2, pp. 137-165, Netherlands, 1993.

[12] Brown, P. J., Jones, G. J. F., "Context-aware Retrieval: Exploring a New Environment for Information Retrieval and Information Filtering, Personal and Ubiquitous Computing", Publisher, Springer, Volume 5, No. 4, pp. 253-263, London, 2001.

[13] Cooley, R., Mobasher, B. and Srivastava, J.,"WebMining: Information and Pattern Discovery on the WorldWideWeb" Proceedings, Ninth IEEE International Conference on, Tools with Artificial Intelligence, Location: Newport Beach, CA, USA, References Cited: 56, pp. 558-567, 2002.

[14] Goble, C., David, D R.," The Grid: An Application of the Semantic Web" Volume 31, No. 4, Pages: 65 – 70, ACM SIGMOD Record, USA, , 2002.

[15] Anselin, L., Kim, Y.W., and Syabri, I.,"Web-based analytical tools for the exploration of spatial data", Journal of Geographical Systems, 6 : pp. 197–218 ,USA, 2004.

[16] Sherbinin, A.D., Deborah, B., Karina, Y., Malanding, J., Francesca, P., Chandra, G. and Antroinette, W," A CIESIN Thematic Guide to Social Science Applications of Remote Sensing". Chapter 3 updated January 2006 Center for International Earth Science Information Network (CIESIN) Columbia University, 2002.

[17] Ronald, R., Paul, C., stern, R.," Linking remote sensing and social science: the need and the challenges", People and pixels, By Diana M. L., Published by National Academies Press, National Research Council (U.S.), 1998.

[18] Srinivasa, S R., Murthey, K., Adiga, S. and Emmineedu, E.," Performance Index for Watershed development", J.Ind. Geophys, Union, Vol, No.4, pp. 239-247, India, 2003.

[19] Bambaradeniya, C., "Freshwater Wetlands in Sri Lanka: Their Conservation Significance and Current Status In: IUCN Sri Lanka", Proceedings of the National Symposium on Wetland Conservation and Management, pp. 19-24, 2004.

[20] Emilio, C., Pilar, M., and Chris, J.," Innovative Concepts and Methods in Fire Danger Estimation", 4th International Workshop on Remote Sensing and GIS Applications to Forest Fire Management, Ghent – Belgium, 5-7 June 2003.

[21] Haddi, A. A. El, Lee, V., Banks, J., Sustman, P.," Using File replication for business continuance and content distribution", Accessed on: 2007, Constant Data Inc (www.constantdata.com), (2003).

[22] Stanley, D. Brunn, Susan, L. Cutter, James, W. Harrington, Geography and technology. Published by Springer, USA, ch-18, pp. 401-430, 2004.

[23] Gary, L. G., Cort, J.W.," Geography in America at the dawn of the 21st century", Published by Oxford University Press, Ch, 29. PP. 376-418, 2006.

[24] Buetow 1, T., Chaboya, L., Christopher, O.T., Cushna, T., Daspit, D. Petersen, T., Atabakhsh, H., and Chen, H.," A Spatio Temporal Visualizer for Law Enforcement", Lecture Notes in Computer Science, Springer-Verlag Berlin Heidelberg, volume: 2665/2003 pp. 181–194, 2003.

[25] Hoschek, W., Javier, JM., Samar, A. Stockinger, H., and Stockinge, K., "Data Management in an International Data Grid Project", Lecture Notes in computer science, Volume 1971/2000, pp. 333-361,. Springer-Verlag Berlin Heidelberg, 2000.

[26] Birant, D., Kut, A.," ST-DBSCAN: An algorithm for clustering spatial–temporal data", Data & Knowledge Engineering, Volume 60 ,pp. 208–221, Holand, 2007.

[27] Kao, B., Kam, Y. L., Cheng, R.," Maintaining Temporal Consistency of Discrete Objects in Soft Real-Time Database Systems", IEEE TRANSACTIONS ON COMPUTERS, ACM USA, VOL. 52, NO. 3, MARCH 2003

[28] Yuan, W., Andrew A. Aslinger, S.H. John, S., Stankovic, A.," ORDER: A Dynamic Replication Algorithm for Periodic Transactions in Distributed Real-Time Databases", In Proceedings of Real-time and Embedded Computing Systems and Applications (RTCSA 04) U.S.A. pp. 152-169, 2004.

[29] Vestal, S., "Real-Time Sampled Signal Flows through Asynchronous Distributed Systems", Proceedings of the 11th IEEE Real Time and Embedded Technology and Applications Symposium (RTAS'05), ISSN: 1080-1812, pp. 170-179, USA, 2005.

[30] Foster, I., Kesselman, C., Tuecke, S., "The Anatomy of the Grid: Enabling Scalable Virtual Organizations", International Journal of High Performance Computing Applications, 15 (3). pp. 200-222, SA, 2001.

[31] Yogesh, L., Simmhan, Plale, B. and Dennis, G.," A Survey of Data Provenance in e-Science", ACM SIGMOD Record, Volume 34, No.3 pp. 31–36, USA, 2005.

[32] J. Gray, P. Helland, P. E. O., Neil, and D. Shasha," The dangers of replication and a solution. In *Proc. SIGMOD*, USA, pages 173– 182, 1996.

[33] Li Jianzhong, S. Jaideep and Srivastava Doron Rotem, "CMD: A Multidimensional Declustering Method" In Proceedings of the Int. Conf. on Very Large Data Bases, 3– 14, 1992.

[34] Sang H. S., and Fengjie, Z.,"Real-Time Replication Control for Distributed Database Systems: Algorithms and Their Performance", Proceedings of the Fourth International Conference on Database Systems for Advanced Applications (DASFAA '95) Ed., Tok Wang Ling and Yoshifumi Masunaga, Singapore, April 10-13, 1995.

[35] Zhao, J., Wroe, C., Carole, G., Stevens, R., Quan, D., and Greenwood, M., "Using Semantic Web Technologies for Representing E-science Provenance", Lecture notes in computer science., Volume 3298/2004 pp. 92–106, 2004. ISSN: 0302-9743 (Print) 1611-3349 (Online), Publisher: Springer Berlin / Heidelberg DOI 10.1007/b102467.

[36] C. Goble. (2002). Position Statement: Musings on Provenance, Workflow and (Semantic Web) Annotations for Bioinformatics,. Workshop on Data Derivation and Provenance, Chicago

[37] D. P. Lanter.(1990). Lineage in GIS: The Problem and a Solution.Technical Report: National Center for Geographic Information and Analysis,.

[38] D. P. Lanter.(1993). A Lineage Meta-Database Approach Towards Spatial Analytic Database Optimization. Cartography and Geographic Information Systems, vol. 20, pp. 112-121.

[39] H.~Veregin and D. P. Lanter.(1995). Data-quality enhancement techniques in layer-based geographic information systems. Computers, Environment and Urban Systems, vol. 19, pp. 23-36

[40] J. Zhao, C. A. Goble, R. Stevens, and S. Bechhofer.(2004). Semantically Linking and Browsing Provenance Logs for E-science. ICSNW, pp. 158-176.

4/1/2010

Potential field Investigation of the Liberia Basin, West Africa

S. Morris Cooper
Institute of Geophysics and Geomatics
China University of geosciences

Email: smcooper2002@yahoo.com

Abstract: Euler deconvolution is a useful tool for providing estimates of the localities and depth of magnetic and gravity sources. Wavelet analysis is an interesting tool for filtering and improving geophysical data. The application of these two methods to gravity and magnetic data of the Liberia basin enable the definition of the geometry and depth of the subsurface geologic structures. The study reveals the basin is sub-divided and the depth to basement of the basin structure ranging from 5km at its Northwest end to 10km at its broadest section eastward. [Journal of American Science 2010;6(7):199-207]. (ISSN: 1545-1003).

Keywords: Wavelet transform, Euler deconvolution, Potential field, Liberia basin

1. Introduction

The Liberia basin is the larger of two basins found along the continental shelf offshore Liberia. It runs parallel to the margin bordering on the west by the Sierra Leone basin and to the east with the Harper basin and the so-called Liberia high (See figure 2).

The basin including the continental shelf and margin of the Liberian coast has been of great interest both in the past and present prompting several geological and geophysical investigations culminating into the drilling of several wells offshore along the coast. . Simultaneous block faulting occurred with deposition of Cretaceous or younger sediments (White, 1972; Thorman, 1972). The faults extend across the continental shelf with northwest and west- northwest trends. Inferred basement relief associated with faulted basins is up to 5km (Behrendt and Wortoson(1970)).

Three fracture zones (St. Paul, Cape Palmas, and Grand Cess) (figure 1) are located on the basis of magnetic and gravity data supported by bathymetric and seimic reflection data (Behrendt et al, (1974). The fracture zones appear as separate lineament near the cost of Liberia and maybe part of the same transform fault crossing the Atlantic (St Paul Fracture Zone). They also indicated that a thick section of sedimentary rock, possibly as great as 8km and could be associated with basins beneath the shelf.

In the advent of recent study revealing two distinct hydrocarbon basins (Kara and Don, 2002) off the coast of Liberia, the Liberia Basin being the larger of the two and coupled with the growing quest for mineral exploration, the need to understand the geometry and stratigraphy of said basin is of some importance.

Our investigation is aimed at helping to understand the distribution of shallow intrusives, intrasedimentary faulting, and basement geometry, all of which are integral to unraveling the structural development of the basin and reducing exploration risk. The wavelet decomposition and euler's methods are being applied to achieve these goals.

2.0 Geological Setting

Liberia is on the edge of the West African Shield, dated 2.7 to 3.4 Ga. comprising mainly of granite, schist, and gneiss. In Liberia this shield has been intensely folded and faulted and is interspersed with iron-bearing formations known as itabirites. Beds of sandstone are common along the coast, with occasional crystalline-rock outcrops. Monrovia, a coastal city in Liberia, is a ridge of diabase (a dark-colored, fine-grained rock). It is a typical example of such an outcropping. Most of the crystalline rocks are of Precambrian age. The western half of country is typically of Archean age. In the eastern half of the country, lenses of Proterozoic greenstone belts occur surrounded by rocks of probable Archean age. Rocks of Pan African age extend northwesterly along most of the Liberian coastline from the Cestos shear zone.

R. W. White (1969) has discussed the geology of the sedimentary rocks of coastal Liberia in considerable detail; his work is briefly summarized here. Unmetamorphosed sedimentary rocks are known onshore mainly in the area between Buchanan and Monrovia. The sedimentary sequence along the coast is underlain by a northwest-trending belt of Precambrian crystalline basement rocks comprising granulite, granitic rock, quartzo-feldspathic gneiss, schist, amphibolite, and iron-bearing rocks. A strong gravity gradient is associated with the transition from granulite-facies to amphibolite-facies rocks along the coast. Overlying the crystalline basement near Monrovia is the Paynesville Sandstone which is

assigned an early Paleozoic age considering similar rocks in other parts of West Africa. The thickness of this unit is not known, but geologic comparisons in West Africa and field evidence suggests a maximum of about 1 km. The Monrovia Diabase intrudes the Paynesville Sandstone and has been K/A dated at two locations as 176 and 192 m.y. (Early Jurassic) (White and Leo, 1969). This intrusive rock is quite magnetic and is the source of a number of magnetic anomalies in the area east of Monrovia.

Seven drill wells were realized on the continental shelf between 1970 and 1984 along the Liberian coast. Four of these wells were realized in 1971 off the shore of Monrovia and one was about 150km southeast of Monrovia, with depth ranged from 1.67km to 3.12km. They reached on volcanic rock of Jurassic age, or sedimentary rock of early cretaceous age, or sand stone inferred to be of Paleozoic age (Schlee *et al*, 1974).

The oldest sedimentary rock drilled at that time includes limestone, orthoquarztite, shale, and sand stone of early Devonian age based on spores analysis (Ayme 1965). Sheridan *et al.* (1969) and Lehner and Deruiter (1976) suggested that Paleozoic rocks extends as far as to the continental shelf-slope break which seems to fit well with the Mesozoic era continental breakup. The Paleozoic rocks have been intruded by dikes and sills, and are overlain by basalt flow of early Cretaceous and Jurassic age.

2.1 Liberia Basin

The origin of the basin (fig.1) is poorly known due to the limited number of studies in the area. The basins developed in two phases (Kara and Don 2002), a syn-rift phase followed by a phase of usual passive margin. They were both significantly overprinted by wrenching due to Atlantic Transform Fault Systems. The main rift phase, accompanied by continental to marginally marine sedimentation, took place during Lower Cretaceous Aptian to Middle Albian times.

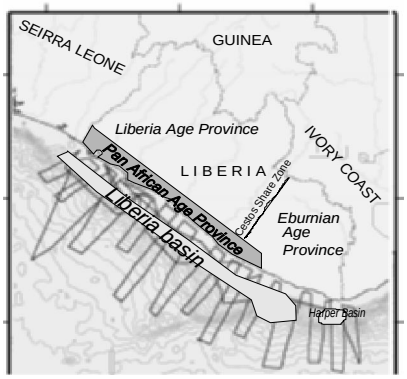

Figure 1: A diagram of the Liberia Basin (not to scale). The lines are the survey lines as conducted along the cost.

The passive margin coeval with wrenching, initiated with seafloor spreading, began in Late Albian time and continues to the present. The Liberia Basin is a long-standing depo-center, defined by faulting and basement highs to the northwest and southeast. From west to east, the Liberia Basin is affected by three distinct fault zones – Monrovia fault zone, Buchanan and Greenville fault zones. The Monrovia fault zone forms the boundary between the Sierra Leone and the Liberia. A fourth fault zone, the Liberia hinge fault zone, is present in the eastern part of the Liberia basin and forms the western border of the Liberia High, a basement-cored structural divide between the deep sedimentary Liberia Basin to the west and the Harper Basin to southeast.

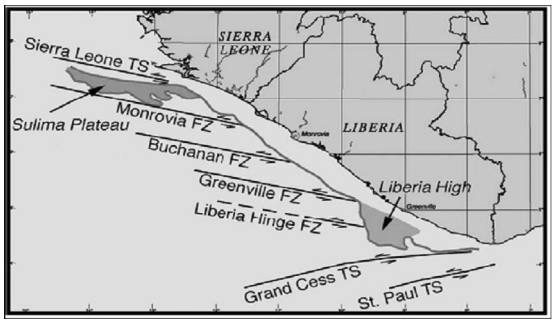

Figure 2: Fault zones (FZ) and transforms systems (TS) adopted from Kara and Don, (2002).

The Monrovia fault zone, associated with the Sierra Leone Transform (Fig. 2), is a complex series of strike-slip associated faults trending NW, which intersects the coast forming an angle of about 30°. The fault zone consists predominantly of low-angle faulting which has produced large rotation blocks. It is dominantly transtensional, with locally large transpressional accommodation zones (Kara and Don, 2002). The Buchanan fault zone, a narrow transpressional zone expressed as a positive flower structure, intersects the coast at about 32^0 trending NW. The Greenville fault zone is a wide diffuse band of low-angle faults forming a bowl-shaped extensional flower structure that intersects the Liberia coast in the area of Greenville.

3.0 Data sources and analysis

3.1 Gravity data

The gravity data, used in this study were collected using a Lacoste-Romberg gravimeter, during the USGS cruise (Leg 5 – IDOE) conducted along the coast of Liberia. Gravity maps (Figures 3 & 6), derived from these data, reflect anomalies that may arise from contrasts in density due to contacts between different rock units, partial melting, or phase transitions. It clearly delineated the basinal region

and structural highs, with gravity low of -100mgal and a high of -5mgal and interval of 5mgal (fig.3). Generally, long-wavelength anomalies with smooth gradients originate from sources at depths greater than sources of short-wavelength anomalies that display steep gradients. While short-wavelength anomalies must arise from sources at shallow depths, long-wavelength anomalies could arise from shallow, thin sources that have gently sloping sides.

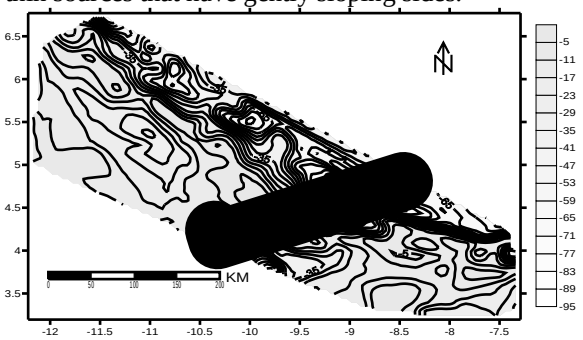

Figure 3: Bourger gravity map of the Liberia Basin grid using triangulation method with a contour interval of 5mgal. Vertical and horizontal axes are in degrees. AA' is a profile across the basin

In order to produce a gravity map reflecting lateral variations in density in the crust, raw gravity measurements were reduced using standard gravity reduction methods (Dobrin and Savit, 1988; Blakely, 1995). These reductions remove the effects of elevation, topography, total mass, rotation, and ellipsoidal shape of the Earth and yield the complete Bouguer gravity anomaly (CBA).

3.2 Magnetic data

The magnetic data, from the same source as the gravity data, was obtained using a Variam magnetometer with a profile spacing of about 15 miles. The magnetic anomaly (fig.4) shows that magnetic high is sporadic and marked around the southern end of the basin separating it from the Harper basin. These may be probably cause by magnetic substances within shallow depth due to their high frequencies and amplitudes. This area is observed to have the presence of sub marine canyon and steepened eroded slope as well as crumpling and faulting strata. The field inclination is horizontal since Liberia virtually lies on the magnetic equator. Generally, magnetic highs arise from mafic igneous and crystalline basement rocks, whereas lows arise from felsic igneous, sedimentary, or altered basement rocks. Igneous outcrops not associated with high-amplitude magnetic anomalies might be thin or contain low concentrations of primary magnetic minerals, or lost them due to alteration.

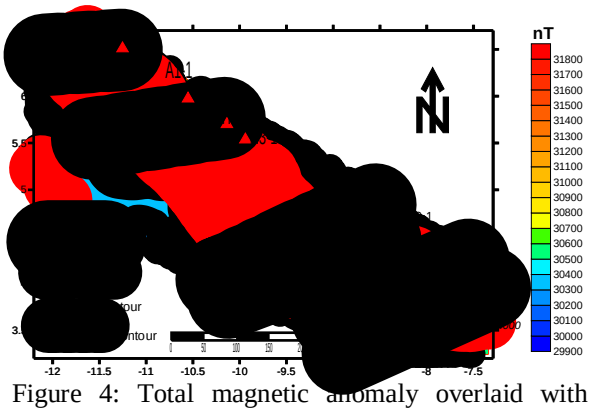

Figure 4: Total magnetic anomaly overlaid with bathymetry contour lines (with depths) and fault zones. Monrovia fault zone (Mon), Buchanan fault zone (BC), Grand Cess fault zone (GS), Cape Palmas Fault (CP) and St. Paul transform zone (SP). The axes are in degrees and the distance in kilometers. The triangles represent locations of experimental drill holes.

3.3 Wavelet Analysis

Wavelets are mathematical functions which split data into different frequency components and then each component is studied with a resolution to match its scale. Wavelet transforms have advantages to traditional Fourier methods in analyzing physical situations where the signal contains discontinued and sharp spikes. Wavelets were developed independently in the fields of mathematics, physics, electrica1 engineering and geophysics. Interchanges between these fields during the last ten years have led to many new wavelet applications such as image compression, turbulence, human vision, radar, earthquake prediction, and separation of gravity and magnetic anomalies. Some of the recent applications in geophysics are processing of potentia1 data (Davis *et al*, 1994; Li and Oldenburg, 1997; Fedi and Quarta, 1998; Ridsdill-Smith and Dentith, 1999) and processing of seismic data (Charraborty and Okaya, 1995; Grubb and Walden, 1997).

The wavelets, first mentioned by Haar in 1909 are not continuously differentiable. In the 1930s, representation of functions using scale-varying basis functions that can vary in scale and conserve energy has been researched by several researchers. Grossman and Marlet (1985) defined wavelets within the context of physics. Mallat (1989) elevated to digital processing by discovering pyramidal algorithms, and orthonormal wavelet basis. Daubechies (1990) applied Mallat's work to construct a set of wavelet orthonormal basis functions that are the cornerstone of wavelet application today. The schematic of this process is shown below in figure (5).

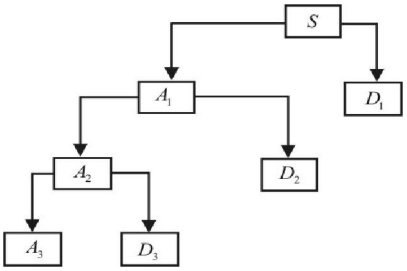

Figure 5: Structure of the multiscale wavelet analysis. S is the input signal, details are D1, D2, and D3 and approximations are A1, A2, and A3.

3.4 Euler Deconvolution

Euler deconvolution method is traceable to Hood (1965) who first formulated Euler's homogeneity equation relative to the magnetic case and defined the rate of change of the field now known as the structural index. Thompson (1982) showed the first semi-automated method exploiting Euler's differential homogeneity equation. It is essentially a statement of scaling relationships (controlled by the Structural Index (SI) and requires measured or calculated field gradients. He applied it to profiles, but also gave the equivalent equation for grids. Reid *et al* (1990) implemented the grid version, extended the theory to handle steps, and named the process Euler deconvolution by analogy with Werner deconvolution. The 3D Euler's equation can be defined (Reid *et al.*, 1990) as:

$$(x - x_o)\frac{\partial F}{\partial x} + (y - y_o)\frac{\partial F}{\partial y} + (z - z_o)\frac{\partial F}{\partial z} = -NF$$

Where the homogeneous function F is the observed potential field at location (x, y, z) caused by a source at location (x_0, y_0, z_0) and N, denoted as the structural index, is a measure of the rate of change of the potential field with distance. The Euler deconvolution method is a constituent of techniques referred to as 'automatic' depth estimation methods. Two important parameters of Euler deconvolution are the choice of window and structural index. Other researchers (Williams *et. al.*, 2005) and (Li and Morozov, 2006) suggested a structural index of 0.5 to obtain suitable results.

In our study, we seek to locate the magnetic contacts that may delineate sedimentary basins. Theoretically, a structural index of 0 is an appropriate value for contact models. However, this value usually gives unstable results. We found that a structural index of 0.5 was suitable to locate the possible magnetic contacts from the observed magnetic data. Reid *et a1* (1990) and Ravat (1996) discussed adequately the effect of the size of the operated window on the estimation of source location using the Euler technique. Generally, selection of the window size is a function of the grid cell and should be selected to be large enough to incorporate substantial variation of the total field and their gradients (Ravat, 1996). Solutions calculated from larger windows would contain fewer artifacts due to the effects of noise.

Because the Euler method relies on the gradients of the magnetic field, the resulting depth readings relate primarily to the areas of basement heterogeneities identified as distinct sources of the field. These depth values from adjacent spatial windows are further interpolated to produce maps (fig. 10) showing the positions of magnetic sources and sources of high density contrast. Thus, by the nature of this interpolation favoring high depth values, only the local maxima in the resulting maps should be taken into consideration. Estimation of the absolute depth proved to be unreliable, and our model relies mainly on the constraints from well log within the proximity of the basin and seismic data.

4.0 Results and discussion

To determine the geometry of the Liberia basin, the bounding faults and lithology of the basement we derived derivatives of the total magnetic anomaly several and the gravity bouger anomaly maps. The horizontal and vertical derivatives as well as their functions are the most important tool for determining structure element boundary and revealing possible faults. A variety of derivatives and filtering techniques were employed in order to enhance the data sets. The horizontal derivative and the first vertical derivative are often used for definition of major element boundaries.

Wavelet decomposition is performed on both maps and correlated to determine the shape and orientation of the subsurface. A profile of the Basin is taken along the its broadest section(Fig. 3) to determine possible faults, high and low amplitudes and to construct a model of the subsurface using available well data and seismic profiles. Second, third and fourth order wavelet decomposition is carried out to infer the substructure orientation.

From the wavelet decomposition, one sees that there are several magnetic substances at shallow depth along the continental shelf and margin which maybe a direct consequence of rifting and volcanic activities due to their high frequencies/amplitudes. The date of intrusion (176 to 192 m.y.) is approximately that of the initial rifting associated with the separation of Africa from South and North America in this area; this date has been obtained from several lines of evidence (Dickson *et al*, 1968; Bullard *et al*, 1965; Gough *et al*, 1964; and Creer, 1965), although the active phase of drift possibly did not begin until 120 to 130 m.y. ago, at which time large-scale sedimentary deposition began *(*Allard and Hurst,

1969). Their depths range from 0.09km to 0.42km with an average depth estimated at 0.25km. The average depths of substances reflected in the third order wavelet decomposition of the magnetic data is put at 0.6km while the average depth of the fourth order decomposition is 1.7km. From the second and third order decomposition of the magnetic data, there seems to be a fault running northwest and southeast. This is probably reflected in the seismic line (fig. 11) as a deep hidden fault.

The wavelet decomposition (fig. 6) of the gravity data reveals the substructure of the basin suggesting it contains several smaller basins from east to west. These separations could possibly be attributed to basement uplift and fault systems interesting the basin. Basins are separated by basement ridges, or elevations inherited from geological evolution preceding rifting of Gondwanaland, and consisting of Precambrian, Pan-African or Paleozoic material. Some times basins are subdivided longitudinally by basement ridges, for example the Gabon basin. In the intermediate equatorial regions, basins are separated by ridges marking out fracture zones. These ridges serve as sedimentation dams by obstructing mass sedimentary transport. One may also infer that a larger portion of the basin may be in deep waters but overlaid as reflected by the wavelet decomposition during gravity analysis.

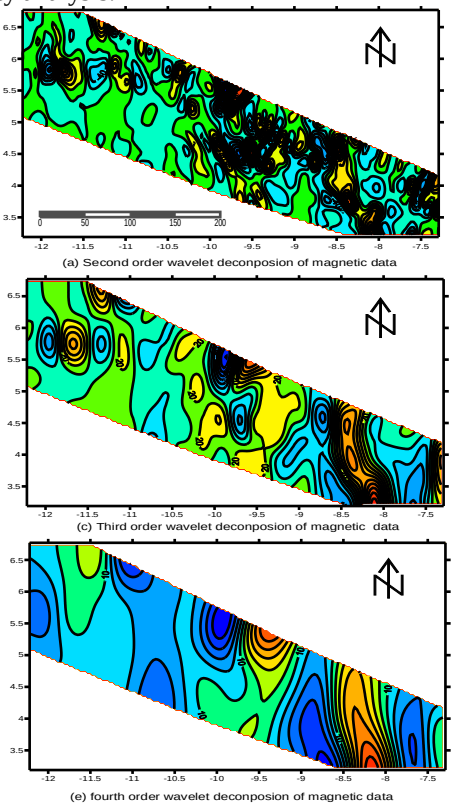

Figure 6: Wavelet decomposition of the magnetic data. Second, third and fourth orders from top to bottom respectively

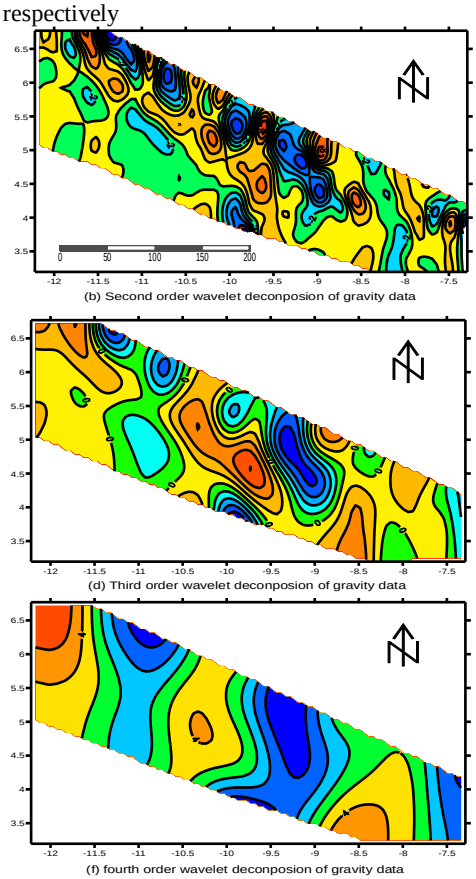

Figure 6b: Euler deconvolution of gravity data. They are second, third and fourth orders respectively from top to bottom.

. Figures 6a,6c and 6d are second ,third and fourth orders wavelet magnetic decompositions respectively while 6b 6d and 6f are those of gravity data wavelet decompositions in the same order.

To determine the depth of the basin Euler deconvolution is carried out on both the gravity and magnetic data using a structural index of 0.5 and a window size of 10 grid cells on the magnetic data while a window size of 15 grid cells was selected for the gravity data and grids (Fig. 9) created using a software. The structural index was chosen by inspecting the maps deduced from each structural index and the best depth estimates with tightest clustering considered. The choice of the window sizes depended on the wavelength of the studied anomalies.

To reduce the noise factor due to shallow structures and to increase the accuracy of depth estimate, a low pass filter is carried out on the data to enhance deeper structures before realizing the deconvolution. The Euler deconvolution results are

given as figure (7) of the gravity and magnetic respectively.

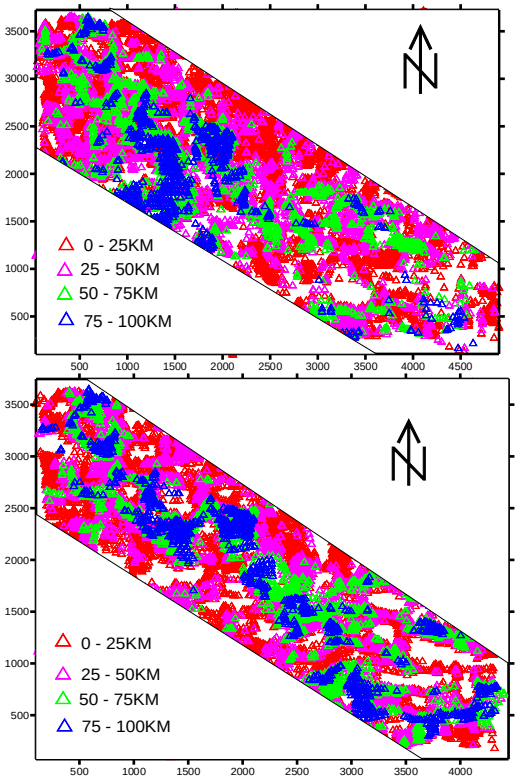

Figure 7: An Euler deconvolution of the (a) gravity and (b) magnetic maps showing various depths.

The high identified during magnetic deconvolution also correspond to high on the gravity map. These may be possible crustal intrusives with high density or crustal thickening/variations. The gravity grid of the decomposition delimits where the sediments thicken and their depth extent above the basement.

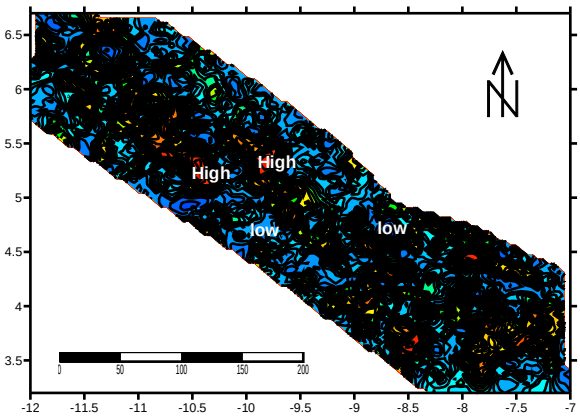

(a) A grid of the euler deconvolution of the bouger gravity

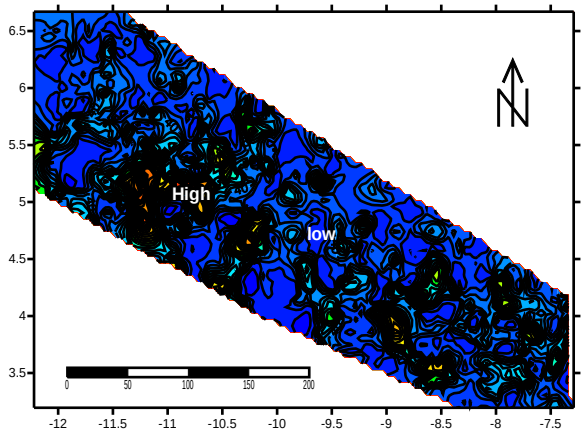

(b) A grid of the euler deconvolution of the total magnetic data

Figure 9: (a) grid of the euler deconvolution of the observer bouger gravity data and (b) the observed magnetic data contour intervals of 5 and 10 respectively.

Behrendt and Wortorson. (1970) and Behrendt *et all* (1974) showed magnetic basement maps of the continental shelf based on depth estimate from aeromagnetic profiles using the method of Vacquier *et al* (1951), which assumes semi-dike flat-topped bodies. In this investigation we use the Parker's method (1974) to determine the depth to basement which shows some difference in terms of depth. The sedimentary rock seems too thickened on the slope and rise between Buchanan and Greenville. The depth to basement of the broadest section of the basin (figure 10) shows the structure of the basin with a depth estimated at over 10 km which is in agreement with previous studies (Behrendt and Wortorson, 1971 and Kara and Don, 2002). Two wells drilled within the proximity of the broadest portion of the basin in 1972 and 1986 by Frontier and AMOCO respectively reached a depth of a little over 3km even though they did not reach the basement. The deposition of sediment and the depth extent of the basin at this location could be attributed to the St. Paul Transform Zone and its subsequent fault system.

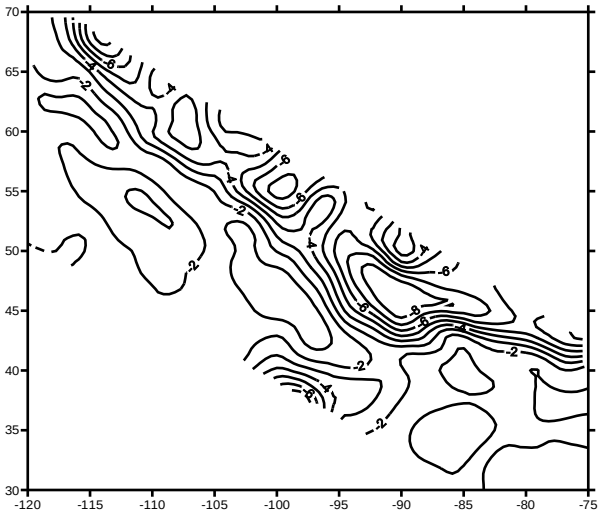

Figure 10: A depth to basement anomaly of the Liberia basin based on Parker's method

A profile through the basin using one of the wells (S3-1) as a reference point and matching same to a seismic section along the direction of the profile shows some degree of disparity between the gravity and magnetic anomaly. The difference could be attributed to the low density of the upper strata due to deposition of sediments in the basin and the presence of shallow intrusive of high magnetic susceptibility (Fig. 11).

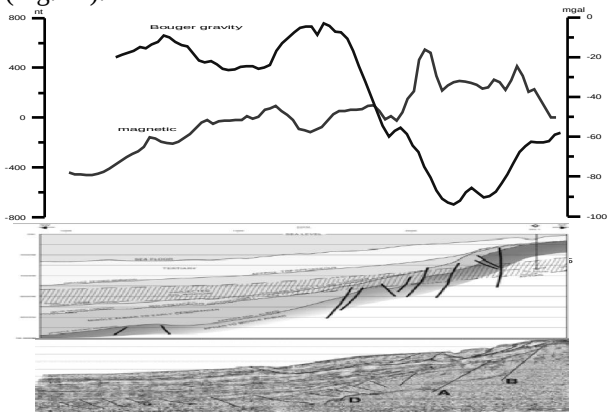

Figure 11: A profile across the basin intersecting one of the wells along its shoulder is compared to seismic section along the same line showing deep structure fault and entrapment of sediments and stratigraphy of the shelf.

5.0 Conclusion

The Liberia basin can be to be subdivided into three basins separated by uplifts and complex fault systems with the broadest and deepest section located at its eastern end. The depth to basement of the basin is estimated at over 10km at its broadest section. Analysis of the magnetic data indicates shallow intrusives ranging from a depth of 0.09km to 0.42 km with an average depth of 0.25km. Other intrusives can be found at average depths of 0.6km and 1.7km respectively within the confines of the basin. A Euler deconvolution showed that magnetic contacts were to a depth of 10km.

Acknowledgements:

Authors are grateful to the USCS for providing the data use in this research.

Corresponding Author:
S. Morris Cooper
China University of Geosciences
Wuhan. China
E-mail: smorriscpr@gmail.com

References

1. Allard, G. O., and Hurst, V. J**.,** 1969, Brazil Gabon geologic link supports continental drift: Science, v. 163, p. 528-532.
2. Ayme, J. M.., 1965, The Senegal salt basin (Kennedy, W. Q., Salt Basins around Africa) London Institute of Petroleum, p. 83-90.
3. Behrendt, J. C., and Wotorson, C. S., (1970)., Aeromagnetic and gravity investigations of the coastal and continental shelf of Liberia, West Africa, and their relation to continental drift :Geological Society American Bulletin , v 81, p 3563 - 3574
4. Behrendt, J. C., and Wotorson, C. S., 1974, Geophysical survey of Liberia with tectonic and geological interpretations: U.S. Geological Survey Prof. Paper 810.
5. Blakely, R.J., 1995, Potential Theory in Gravity and Magnetic Applications: New York, Cambridge University Press.
6. Bullard, E. C., Everett, J. E., and Smith, A. G., 1965, The fit of the continents around the Atlantic, in a symposium on continental drift Royal society London Philos. Trans , ser. A, no.1088, p41-51
7. Chakraborty, A. and Okaya, D. (1995), *Frequency-time Decomposition of Seismic Data Using the Wavelet Transform-based Methods*, Geophysics *60*, 1906-1916.
8. Creer, K. M**.,** 1965, Paleomagnetic data from the Gondwanic continents, *in* Symposium on continental drift: Royal Soc.

London. Phil. Trans., ser. A, no. 1088, p. 27-40.
9. Daubechies, (1990), *The Wavelet Transform Time-Frequency Localization and Signal Analysis,* IEEE Trans. on Information Theory 36.
10. Davis, A., Murshak, A., and Wiscombe, W. *Wavelet-base multi-Iractal analysis ofnon-stationary and/or intermittent geophysical signals.* In *Wavelets in Geophysical* (eds. E. Foufoula Georgiou and P. Kumar). (Academic Press, Ine. 1994) pp. 249-298.
11. Dickson, G. O., Pitman, W. C., Ill, and Heirtzler, J. R., 1968, Magnetic anomalies in the South Atlantic and ocean floor spreading: Jour. Geophys. Research, v. 73, p. 2087-2100.
12. Dobrin, M., and Savit, C. H., 1988, Introduction to geophysical prospecting: Mc- Graw Hill Book Co.
13. Fedi, M. and Quarta, T. (1998), *Wavelet Analysis for the regional-residual and Local Separation at Potential Field Anomalies.* Geophys. Prosp. 46, 507-525.
14. Gough, D. I., Opdyke, N. D., and McElhinny, M. W., 1964, The significance of paleomagnetic results from Africa: Jour. Geophys. Research, v. 69, p. 2509-2519.
15. Gromme, S., and Dalrymple, G. B., K Ar ages and paleomagnetism of dikes in Liberia [abs]: EOS (Am. Geophys. Union Trans), v. 53, no. 11, p 1130.
16. Grossman, A. and Marlet J. *Mathematics and Physics* 2, (ed. L. Streit) (World Scientific Publishing, Singapore (1985)).
17. Grubb, H. and Walden, A. (1997), *Characterizing Seismic Time Series Using the Discrete Wavelet Transform,* Geophys. Prosp. 45, 2, 183-205.
18. Hood, P. J., Gradient measurement in aeromagnetic surveying. Geophysics 30 (5) 891-902.
19. Hurley, P. M., Leo , G. W., white , R. W., and Fairbairn, H. W., 1871, The Liberian age province (ca. 2700m.y.) and adjacent provincesin Liberia and Seirra Leone: Geol. Soc. America, v. 82, p 3483 – 3490.
20. Kara C. Bennet and Don Rusk (2002), 2D seismic interpretation and exploration potential deepwater Sierra Leone and Liberia, West Africa;, The Leading Edge.
21. Lehner, P., and DeRuiter, P.A. D., 1976, Africa Alantic margin typified by string of basins: Oil nad Gas journal, v. 76, p. 252-266.
22. Li, J. and Morozov, I.B. (2006): Structural styles of the Precambrian basement underlying the Williston Basin and adjacent regions – an interpretation from geophysical mapping; *in* Summary of Investigations 2006, Volume 1, Saskatchewan Geological Survey, Sask. Industry Resources, Misc. Rep. 2006-4.1, CD-ROM, Paper A-2, 18p.
23. Li, Y. and Oldenburg, D. (1997), *Fast Inversion of Large-scale Magnetic Data Using Wavelets, 67th* Ann. Internat. Mtg., Soc. Exp. Geophysics., Expanded Abstract, 490-493.
24. Mallat, S. (1989), *A Theory for Multi-resolution Signal Decomposition the Wavelet Representation,* IEEE Trans. Pattem Ana L. And Machine Intelligence 31, 679-693.
25. Parker, R.L. (1974) Best bounds on density and depth from gravity data, *Geophysics,* 39**:** 644-649.
26. Ravat, D., 1996, Analysis of the Euler method and its applicability in environmental magnetic investigations: J. Environ. Eng. Geophys., **1**, 229–238.
27. Reid, A.B., Allsop, J.M., Granser, H., Millett, A.J., Somerton, I.W., 1990. Magnetic interpretation in three dimensions using Euler deconvolution. Geophysics 55, 80–91.
28. Ridsdill-Smith, T. A. and Dentith, M. C. (1999), *The Wavelet Transform in Aeromagnetic Processing,* Geophysics 64, 1003-1013.
29. Schlee, J., Behrendt, J. C., and Robb, J.M., 1974, Shallow stratighaphy of the Liberian Continental margin: American Association of Petroleum Geologist Bulletin, v. 58, pp. 708 -728.
30. Sheridan , R. E., Houtz, R. E., Drake, C. L., and Ewing , M., 1969, Structure of the continenetal margin off Seirra Leone, West Africa: Journal of Geophysicsl Reseach, v. 74, p . 2512 – 2530.
31. Thompson, D.T., 1982. EULDPH: a new technique for making computer-assisted depth estimates from magnetic data. Geophysics 47, 31–37.
32. Thorman, C. H., 1972, the boundary between the Pan African and Liberian age provinces, Liberia, West Africa: Geological society of America, Abs. with Programs (ann. Mrg), v.4 no. 7, p.690:
33. White, R. W., and Leo, G. W., 1969, Geological reconnaissance in western Liberia: Liberian Geol. Survey Spec.

34. White, Richard W. 1972. Stratigraphy and structure of basins on the coast of Liberia. Monrovia: Republic of Liberia, Ministry of Lands and Mines, Liberian Geological Survey, Special Papers - Liberia, Geological Survey.
35. Williams, S. E., Fairhead, J. D., and Flanagan G., 2005, Comparison of grid Euler deconvolution with and without 2D constraints using a realistic 3D magnetic basement model: Geophysics, 70, 13–21.

2/24/10

Joint magnetic and seismic interpretation; Determining Depth and Orientation of Volcanic Rock in the Qikou Depression, China

S. Morris Cooper, Liu Tianyou
[1] Institute of Geo physics and Geomatics, China University of Geosciences
Wuhan, China
smorriscpr@gmail.com

Abstract: Identification of volcanic rocks is important in both the oil and gas industry since they may serve as either hindrance or source rocks. Their exploration in deep layer, especially when judging their geological properties, is usually difficult, even for 3-D seismic method. However, these special geological bodies vary distinctly in density, susceptibility and resistivity, which laid a foundation for adopting comprehensive geophysical prospecting techniques to solving this kind of problems. In this paper we use integrated geophysics method to construct a 2.5d inverse model of an igneous rock in the Qikou depresson, eastern China. The model was constrained by a seismic straitigraphic model based on reflection coefficient and well data. The combination of seismic and magnetic data for the inversion of volcanic rocks produces a much clearer understanding as to the orientation of said rocks as demonstrated in this paper. [Journal of American Science 2010;6(7):208-212]. (ISSN: 1545-1003).

Keywords: Reflection coefficient, seismic data, magnetic data, modeling**,** Qikou depression

1. Introduction

The earth and its content have long been concerns to mankind. Man has tried to unravel its complexity and delve into its origin via various methods. The subsurface has been of a particular concern to earth scientists, who seek to x-ray it using diverse means, some for the purpose of simply having adequate knowledge and prevent disaster while others do it for exploration purpose.

With advances in technology and the need to have a clearer picture of the subsurface and its contents, earth scientists have deemed it necessary to utilize the properties associated with its interior. These geophysical properties which vary from one substance to another include resistivity, conductivity, susceptibility, and density.

Existing geophysics exploration methods (magnetic, gravity, seismic and electromagnetic) are based on the geophysical properties of the subsurface. However, these methods are limited in scope since each one of them is only applicable to one of these properties at a time. For example, the seismic method is related to the thickness and density of a substance since it deals with the velocity of waves in a given material. The exploration of special geological bodies in deep layer, especially when judging their geological properties, is usually difficult, even for 3-D seismic method. However, these special geological bodies vary distinctly in density, susceptibility and resistivity, which laid a foundation for adopting comprehensive geophysical prospecting techniques to solve this kind of problems (Yang *et al*. 2005).

Integration of seismic and non-seismic methods in the exploration for hydrocarbons is not a new concept. Potential field information has, for several decades, been successfully used to address the problem of defining the salt/sediment boundary, where even the best quality 3-D seismic data task does not meet the challenges (Nafe & Drake 1957, Gardner 1974). Similarly, the combination of gravity and magnetic information, have complimented seismic data in the interpretation of basin basement character and structure. Data from these two methods have been used in a wide range of tasks; from definition of the tectonic setting of the sedimentary basin, to detailed mapping of the character of the basement in conjunction with information from seismic data.

The combination of two or more geophysics methods in studying the subsurface was first introduced in earlier 70s and continues today. These combinations eliminate unnecessary models and reduce ambiguity thereby narrowing down to specifics based on the properties exhibited. There is an ever present need to reduce risk and save time, resources and energy where exploration is concerned. With the advent of new technologies and improvements in existing methods, integrated geophysics methods remain the way forward for the industries and comprehensive study of the substructures.

In this paper, using the concept of velocity and density coefficient, we combine seismic and aeromagnetic data to model volcanic rock and the

strata of the subsurface in the Qikou area of the Dagang oilfield.

1.1 Study Area

Qikou depression is located in the south of Tianjin, Huanghua, north of Changzhou City, east to the Bohai Bay area. Qikou depression is the largest of the Huanghua depressions with a regional tertiary sediment thickness of about 9km and a tick, big and wide source rooks (Anon, 1987). It covers an area characteristic of resource exploration of about 3900km^2. It is a petroliferous Cenozoic basin and has apparent geometrical and kinematic similarities with the other Meso-Cenozoic extensional basins located along the eastern margin of the Eurasian Plate (Nabelek *et al*, 1987 and Xu, 1997). Previous studies have suggested that the Bohai Basin of which Qikou is a part is a typical extensional basin and has two tectonic evolution phases, rifting during the Paleogene period and thermal subsiding since Neogene's (Allen *et al*, 1997, Ye *et al*, 1985) This area is replete with complex fault system and plutonic rocks as a result of tectonic activities characteristic of eastern china (Liu *et al*, 2004). Several of the well drilled bottomed on such rock with a thickness of about 200m. Because the Cenozoic sediments above the basalt do not contain hydrocarbon reserve, the exploration in this area focuses mainly on identifying sediments below basalt and evaluating its thickness. As seismic alone fail to adequately image the basalt structure due to its complex lithology, facies and content, the present work is an attempt to address the problem using a joint seismic magnetic inversion constrained by well data.

2.0 Material and Method

2.1 Seismic data

A 3d seismic data was acquired from the qikou depression along with well two logs. A cross section (taken between two wells) of the data revealed faults and complex strata (fig 1).

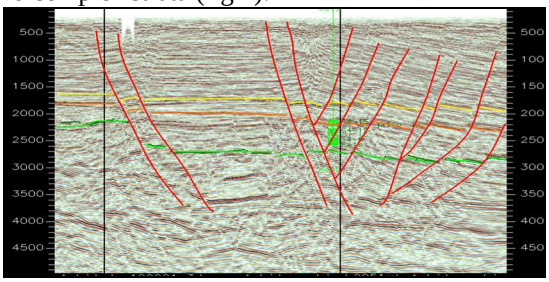

Figure 1: Seismic line of the of he Qikou depression including the positions of two wells. The red vertical lines are inferred faults and the horizontal color lines are horizons or strata

.2 Magnetic data

An aeromagnetic map (fig. 2) of the area indicates regions of high and low amplitudes. The high amplitudes are caused probably by igneous rocks of various susceptibilities. The low amplitudes are most likely due to sedimentary rocks and other nonmagnetic sources. Generally, magnetic highs arise from igneous and crystalline basement rocks, whereas lows arise from felsic igneous, sedimentary, or altered basement rocks. Igneous outcrops not associated with high-amplitude magnetic anomalies might be thin or contain low concentrations of primary magnetic minerals, or lost them due to alteration.

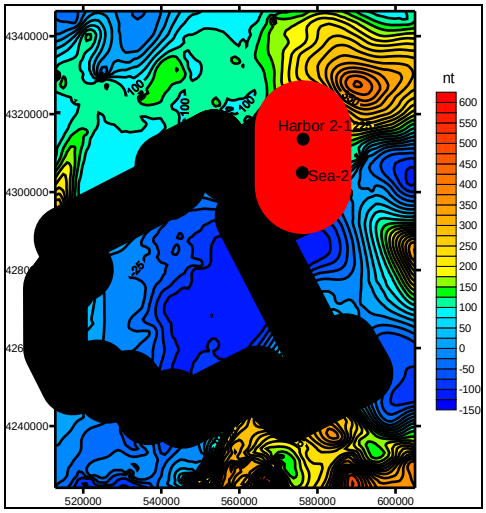

Figure 2: Aeromagnetic map of Dagang and it surrounding. The red vertical line is the position of the profile passing through the wells Harbor2-1 and Sea -2.

2.3 Logging constrained layer velocity inversion

This is generally based on the change in the rate in lithology; therefore, the speed parameter in seismic exploration is very important. The use of the reflection coefficient sequence stratigraphic interval in seismic lithologic inversion is an important means and methods. The basic principle is: Consider two distinct homogeneous layers with one lying on top of the other. The speed of waves in the first is V_n and its density is ρ_n, the next layer has speed V_{n+1} and density ρ_{n+1} respectively. The reflection coefficient (Aki and Richards) between the two layers is givens as:

$$R_n = (v_{n+1}\rho_{n+1} - v_n\rho_n)/(v_{n+1}\rho_{n+1} + v_n\rho_n) \qquad (1)$$

In practice due to inadequate information or very small change in the density for a given region, the density is ignored and equation (1) reduces to:

$$R_n = (v_{n+1} - v_n)/(v_{n+1} + v_n) \quad (2)$$

The above equation (2) can be expressed in terms of V_{n+1} as:

$$v_{n+1} = v_0 \prod [(1+R_i)/(1-R_i)] \quad (3)$$

Where R_i is for the first i_{th} layer interface coefficient and V_0 is the initial velocity. From (3) we see that the reflection coefficient (R_1, R_2, R_3…R_n) is recursive changing with change in velocity of successive layers. From equation (3) we were able to with the availability of sonic log data construct an initial velocity model considering all seismic signatures.

The seismic signature of a geological interface represents lateral variations in the vertical positioning of a reflection (event) across a seismic profile. These variations are due to "real" subsurface structure and/or velocity-generated, time-structural relief or both. "Real" subsurface structure can be the result of primary depositional patterns, postdepositional deformation (faulting, folding, uplift, diapirism), erosion, salt dissolution, ifferential compaction, etc. Velocity-generated time-structural relief is due to lateral variations in the average velocity of the sedimentary section overlying the reflector of interest, and can be caused by lateral facies variations and lateral variation in the thickness of individual sedimentary layers (Anderson *et al*, 1995). These are taken into consideration when modeling is carried out.

The modeling is assisted by visualization technology which plays an important role in displaying, describing and understanding the surface and subsurface geological phenomena. The process is such that a stratigraphic structural interpretation of a seismic line is use as reasonable initial model followed by a 2.5d computer-human interaction model based on well logged data. The third set of 2.5d model is based on potential field data constrained by well log and the seismic models. In our case we used a magnetic data to model volcanic rock in the Qikou depression.

3.0 Result and discussion

3.1 Velocity inversion

Due to the apparent velocity difference between different rock layers, it is possible to use velocity calculation for analysis of igneous rock. From the acoustic logging the velocity of different rocks in the area of study is as follows: Qikou Sag Tertiary basalt is generally 4500-5500m/s, Low porosity basalt is 4000m/s, diabase has a velocity between 5500-6500m/s, for tuff it is 2500-3500m/s, sand and shale ranges from 3000-3500m/s. This velocity difference provides favorable conditions for the application layer identification technology for volcanic rocks. An initial model of the subsurface strata as inferred from the seismic profile based on velocity analysis is shown below (fig.3).

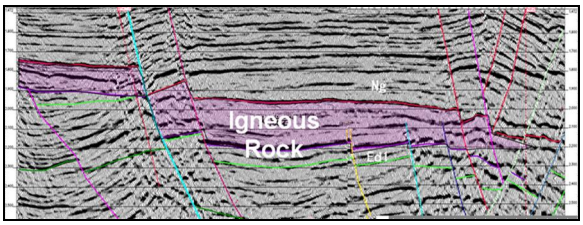

Figure 3: interpretation of the seismic line showing three strata and igneous rockwith locations of faults.

The purple shaded area shows a layer of igneous rock and horizontal color lines or marks indicate horizons while vertical lines show fault pattern. In this initial reasoning, we assume three distinct strata with an igneous rock as the center of the three. This is similar to the inverse forward 2.5D model (fig 4) constrained by sonic log data and the use of reflection coefficient. The reflection seismic signature of a subsurface body includes all features in recorded reflection seismic data that can be confidently attributed to the presence of that body. Geophysical signatures in reflection seismic sections have two basic components: time-structural relief and character variations. The seismic signature of a subsurface body is usually best defined through forward modeling.

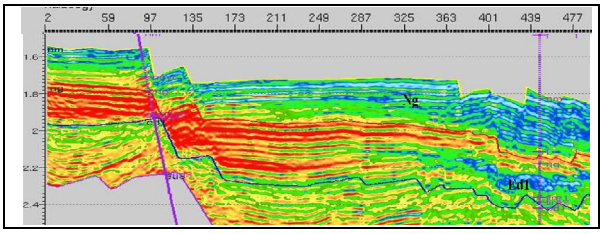

Figure 4: A model of the seismic profile showing regions of low and high densities. The positions of welss are indicated by purple vertical lines. On the left is Harbor 2-1 and on the right is sea2.

The vertical purple lines are positions of well while the deep red horizontal lines indicate region with high speed and density. The upper strata based on this model composed mainly deposits of Miocene era and that below the volcanic rock is mostly those of Oligocene. This model based on reflection coefficient does not fully give us the orientation (size and shape) of the igneous rock but one can clearly demarcate the various strata or horizons.

3.2 Magnetic Inversion

To visualize the approximate position of the volcanic rock magnetic data is use taking a profile of the area of interest. The profile is then use to construct model (fig. 5).

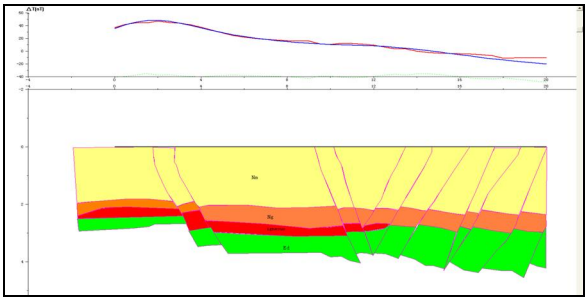

Figure 5: An inverse model of the magnetic profile. The blue curve is the observed anomaly and the red is the calculated. The red potion is the shape of the inferred igneous rock. The first strata is Pliocene (Mn), second Ng is Miocene and Ed is Oligocene all of which are Cenozoic. The vertical lines are faults as inferred from the seismic profile.

The inverse model is constrained by well log and seismic data as well as initial model based on seismic interpretation and reflection coefficient respectively. The model shows three different strata and a slap of igneous rock. The three strata contain material of the Cenozoic era namely Pliocene, Miocene and Oligocene from top to bottom respectively. Tertiary sedimentary strata magnetic susceptibility is approximately (0-50) × 10-5SI; magnetic susceptibility of igneous rocks is about 1500 × 10^{-5}SI. The average thickness of the igneous rock is about 500m.

4.0 Conclusion

We have shown that a joint seismic –magnetic inversion constrained with well log produces a clearer understanding (size and depth) of volcanic rocks in a hydrocarbon prone region where the source rocks are found below such mass volcanic rocks. The thickness of the rock is calculated at 500m and it susceptibility is 1500x10^{-5}SI. The straitigraphy was also distantly demarcated with the aid of well data. This reduces exploration risk and help to identify areas for possible drilling and locating source rocks.

Acknowledgement:
The corresponding author is thankful to Dr. Ndoh for his suggestion and Sinoepec for providing the data use in this study.

Corresponding Author:
S. Morris Cooper
Institute of Geophysics and Geomatics
China University of Geosciences
430074, Wuhan
Hubei, China
E-mail: smorriscpr@gmail.com

References

1. Allen, M., Macdonald, D., Zhao, X. *et al.*, 1997. Early Cenozoic two-phase extension and late Cenozoic thermal subsidence and inversion of the Bohai Basin, northern China, Marine and Petroleum Geology, 1997, 14(7-8): 951—972.
2. Aki, K., Richards, P.G., 1980. Quantitative Seismology, Freeman and Co., New York
3. Anderson, N. L., D. E. Hedke, and R. W. Knapp, 1995. Forward seismic modeling - applications and utility: Geophysical atlas of selected oil and gas fields in Kansas, Kansas Geological Survey Bulletin 237, 28-33.
4. Anon., 1987. Dagang Oilfield. In: Petroleum Geology of China, volume 4. Petroleum Industry Press, 1987. Beijing.
5. Gardner, G. H. E, Gardner, L. W & Gregory, A. R. (1974): Formation velocity and density - the diagnostic basis for stratigraphic traps. - Geophysics, 39, 770-780.
6. Liu, M., Cui, X., Liu, F., 2004. Cenozoic rifting and volcanism in eastern China: a mantle dynamic link to the Indo-Asian collision? Tectonophysics, 2004, 393(1-4): 29—42.
7. Nabelek, J., Chen, W., Ye, H., 1987. The Tangshan earthquake sequence and its implications for the evolution of the North China Basin, Journal of Geophysical Research 1987,92(12):12615 - 12628
8. Nafe, J. E. & Drake, C. L. (1957): Variation with depth in shallow and deep water marine sediments of porosity, density, and the velocities of compression and shear waves. - Geophysics, 22, 523-552.
9. Xu, J., 1997. Similarities between Cenozoic basins of different magnitudes in East Asia continental margin, Experimenal Petroleum Geology (in Chinese), 1997, 19(4): 297—304.
10. Yang Zhanjun and Wei Yan, 2005. The gravity & seismic data jointed formation separation technique for deep structure

study, 75th meeting of Society of Exploration Geophysicists
11. Ye, H., Shedlock, K., Hellinger, S. *et al.*, 1985. The North China Basin: an example of a Cenozoic Rifted interaplate basin, Tectonics, 1985, 4(2): 153－169.

2/25/2010

Non-insect benthic phytomacrofauna and organism-water quality relations in a tropical coastal Ecosystem: impact of land based pollutants.

C.A. EDOKPAYI, R.E.UWADIAE and C. E.NJAR (In memoriam)
Benthic Ecology Unit, Department of Marine Sciences, University of Lagos, Akoka, Lagos, Nigeria.
Email: eferoland@yahoo.com. **Tel:** +2347059497190.

Abstract. The impact of land based pollutants on the non-insect benthic phytomacrofauna and water quality in Epe lagoon was investigated between September, 2004 and February, 2005. Five study stations impacted by land based pollutants were selected upstream along the course of the Lagoon. The study showed that land based pollutants caused a decrease in dissolved oxygen and pH and an increase in biochemical oxygen demand (BOD) and phosphates. Significant differences in these parameters were established among the stations sampled. A post hoc test indicated that stations 2, 3, and 4 were mostly impacted by pollutants. A generally low taxa population and diversity were recorded in this study. Eight taxa were identified from a total of 65 individuals collected from the five stations along the lagoon. No organism was recorded in station 3.The analyses showed that the overall abundance of fauna differed significantly among the stations. Analysis of variance showed that the abundance of Lymnaeidae was significantly higher ($P<0.05$) than those of the other families. The dominance of the taxa Lymnaeidae was a clear indication of pollution which resulted in a decline and total elimination of other benthic macroinvertebrates, which are intolerant of the effects of polluting effluents. This study suggests that the response of benthic phytomacrofauna is important in the study of impacted aquatic systems. [Journal of American Science 2010;6(7):213-220]. (ISSN: 1545-1003).

Keywords: phytomacrofauna, water quality, tropical coastal ecosystem.

Introduction

Water demands in Nigerian coastal urban areas coupled with increased human populations and the concomitant changes in land use have made aquatic systems vulnerable to pollution. Human population levels have been increasing at a high rate in the metropolitan city of Lagos and the neighboring cities like Epe (OFFICIAL GAZATTE: FGP, 2006 Census) with potentially negative effects on water quality due to typical stressors associated with urbanization. In addition, historical expansion of agriculture in most of the cities have not only put strains on local water supplies but have led to present day regional changes in ecosystem dynamics, such as the transport of pollutants from the inland waters and adjourning lands. Runoff from urban areas can be extensive, contain numerous chemicals and cause increased sediment loads in receiving water bodies (Edokpayi *et al*., 2000; Rueda *et al*., 2002).

Relative to agricultural lands, urban areas can have similar land applications of some chemicals (e.g., phosphorus and herbicides) and the runoff from urban areas can contain a much greater variety of pollutants (Walsh *et al*., 2002). Untreated storm water runoff from urban areas can contain levels of some parameters (e.g., total solids) that exceed those found in untreated wastewater (Walsh *et al*., 2002). These pollutants entering water bodies as a result of urbanization can be harmful to aquatic organisms.

Numerous industrial and domestic wastes find their way into the Nigerian coastal aquatic systems. According to Singh *et al* (1995), an estimated 10,000m^3 of industrial effluents are discharged into the Lagos lagoon systems per day. In addition, owing to seasonal distribution of rainfall, the lagoon system and creeks experience seasonal flooding which introduces a lot of detritus, nutrients as well as pollutants from land. Such pollutants arising from land based activities include domestic and industrial effluents, urban storm run-off, agricultural land run-off, sediment and contaminants from garbage and waste dump (Portmann *et al.*, 1989). The most notable point source arises from the dumping of untreated or partially treated sewage (Nwankwo and Amuda; Ogbuogu and Akinya, 2002; Adakole and Anunne, 2003), and discharge of bio-degradable wood wastes from sawmill located along the stretch of the lagoons (Nwankwo, 1998). Wood shavings and leachates are sources of inert solids as well as toxic pollutants that directly clog gills of aquatic animals

(Nwankwo, 1998) and indirectly reduce light penetration (Nwankwo, 1998) which limits productivity.

Contamination of the aquatic environment, makes aquatic organisms vulnerable (Uwadiae, 2009). Aquatic fauna are impacted by pollutants primarily as a result of changes in primary production and in the chemistry of water column and sediment. These changes potentially lead to reduced diversity and abundance (Ofojekwu *et al.*, 1996; Zabbey and Hart, 2006), shifts in community composition, physiological changes and mass mortality. The sensitivity of aquatic fauna to conditions of pollution varies with individual organisms due to differences in feeding habits, mobility, and life cycle (Rueda *et al.*, 2002). As a result, measures of the structure of faunal communities can be used to assess the impacts of pollution on aquatic ecosystems (Rosenberg and Resh, 1993). Benthic macroinvertebrates, in particular, are widely accepted as useful biomonitoring tools for assessing impacts of pollution in aquatic ecosystems.

Although, a number of publications on benthic macroinvertebrate communities of the lagoon systems of southern Nigeria have demonstrated relationships between macroinvertebrate community structure and water quality, not much have investigated the impact of pollutants on benthic phytomacrofauna.

The overall objective of this work was to examine the impacts of land based pollutants on Epe lagoon using non-insect benthic phytomacrofauna community as bioindicators. Phytomacrofauna composition and community structure were assessed to identify possible influences of pollutants. The specific hypothesis being tested was that the structure of benthic phytomacrofauna communities is a reflection of water quality.

Materials and Methods

Description of study area

The study was conducted in a stretch of Epe lagoon (Figure 1), Nigeria, located between longitudes 5°30' – 5°40'E and latitudes 3°50' – 4°10'N. The lagoon receives river Oshun (which drains a number of cities and agricultural lands) in the North -West end. The study area is bordered on the west by a number of cultivated lands and receives wood wastes from local wood processing outfits located at the bank of the lagoon. The lagoon is used for transportation of timber logs (possible source of wood particles and leachates) from the villages to the city of Lagos. The lagoon houses a major jetty at Epe (Station 2), where different forms of wastes from human activities in and around the jetty are deposited indiscriminately. The absence of toilet and other sanitary facilities in most of the villages along the bank of the lagoon, result in the deposition of untreated sewage into the lagoon. Washing of clothes is a common practices in all the stations used for this study.

Large amounts of terrigenous particulate matter, nutrients and sediments are introduced into the lagoon from adjourning forested and agricultural lands which could strongly influence the physical, chemical and geological features of the lagoon. Thick mat of aquatic macrophytes covers a large part of the lagoon inhibiting boat traffic. Notable among these plants are water hyacinth (*Eichornia crassipes*), water letus (*Pistia stratiotes, Ipomea aquatica, Salvinia nymphellula, Lemna sp. and Hydrocharis marsus-renae.* The wide spread distribution and luxuriant growth of these aquatic macrophytes in the study area was reported as an indication of pollution (Uwadiae, 2009). Brief descriptions of the stations used for this investigation are presented in Table 1.

Table 1. Description of the study stations

Station	Dept (m)	Coordinates	Major land based Human activities
1	2.6	(06^{O}34.729'N and 004^{O}03.710'E)	Domestic washing, bathing
2	2.0	06^{O}34.658' N and 003^{O}58. 719'E)	Domestic washing, bathing, Jetty operations, defecation, domestic wastes disposal
3	4.7	(06^{O}36.564'N and 003^{O}58.799'E)	Domestic washing, bathing, defecation, agricultural activities, domestic wastes disposal, deposition of organic debris
4	1.7	06^{O}36.929'N and 003^{O}44.800'E)	Domestic washing, bathing, domestic wastes disposal
5	0.7	(06^{O}36.799'N and 003^{O}42. 568'E)	Domestic washing, bathing, Jetty operations, domestic wastes disposal

Figure 1: Map of Epe Lagoon Showing the Sampling Stations.

Sampling Protocol

Sampling for water quality parameters and benthic fauna was carried out in five study stations at monthly intervals between September, 2004 and February, 2005 covering parts of the rainy and dry seasons.

In situ measurements and collection of samples

In situ measurements of surface water temperature (^{0}C), pH, dissolved oxygen (mg/l) and electrical conductivity (mScm-1) were was carried out using battery operated Horiba U10 water quality checker model.

Water samples for physico-chemical analysis were collected using 1 litter plastic sampling bottles at approximately 0.5m below the water surface and 3.0m from the shoreline in each sampling station. Collection of phytomacrofauna samples was carried out as reported in Edokpayi *et al* (2008).

Sample Analyses

Total dissolved solids (TDS) and nutrient elements were determined according to the methods described in APHA (1985).The methods used by Edokpayi *et al* (2008) was adopted in the laboratory processing of phytomacrofauna samples.

Results

Water quality conditions

A summary of some of the water quality parameters investigated at the study stations is given in Table 2. Of all parameters BOD, DO and phosphate were significantly different ($P<0.05$) among the study stations. The BOD of stations 1 and 5 were significantly lower ($P<0.05$) than those of stations 2, 3 and 4, which were not different from each other. The dissolved oxygen of stations 4 and 5 were significantly lower ($P<0.05$) than those of stations 1, 2 and 3, which were not different from each other.

The values of phosphate in water of stations 1, 2, 3 and 5, were similar and significantly lower

(P<0.05) than that of station 4. The pH of stations 2 and 4 were relatively lower than those of stations 1, 3 and 5.

Faunal composition, abundance and distribution

Figure 2 shows the taxa composition, abundance and distribution of non insect phytomacrofauna in the study area. Eight taxa were identified from a total of 65 individuals collected. Station 1 had one taxon, while stations 2, 4 and 5 had 3, 2 and 3 taxa respectively. No fauna was collected in station 3. Of l the total number of individuals collected, stations 1 and 2 accounted for 1.54 and 50.7% respectively while stations 4 and 5 contributed 21.54 and 10.77% respectively. A summary of the relative contribution of the major groups in the study area is presented in Figure3.

Lymnaeidae was most important at stations 1 and 4 where it contributed 72.72 and 78.54% of the total abundance in these stations respectively. At station 5, it made no contribution. *Lymnaea auriculata* was the representative of the Lymnaeidae group. The family Eleotridae occurred in stations 1 and 4 where it accounted for 27.27 and 14.29 % respectively. It was represented by one taxa; *Eleotris* sp. In station 5, three groups were represented; Eulimidae, Neritidae, and Hydrobiidae. They accounted for 14.29, 28.57 and 57.14% respectively of the total non – insect phytomacrofauna population in these stations. Analysis of variance showed that the abundance of Lymnaeidae was significantly higher (P<0.05) than those of the other groups.

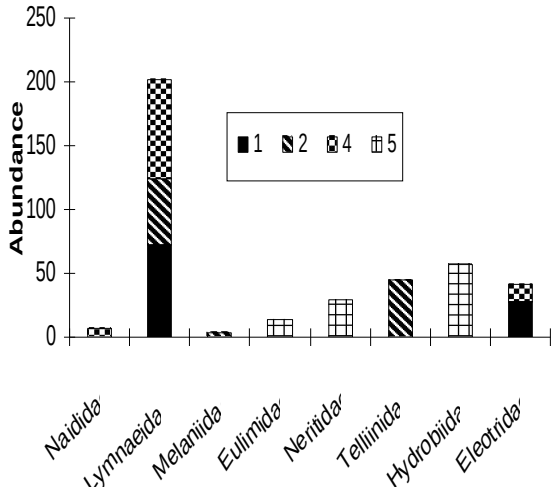

Figure 2. Relative contribution of major non insect phytomacrofauna families to the overall faunal abundance at study stations

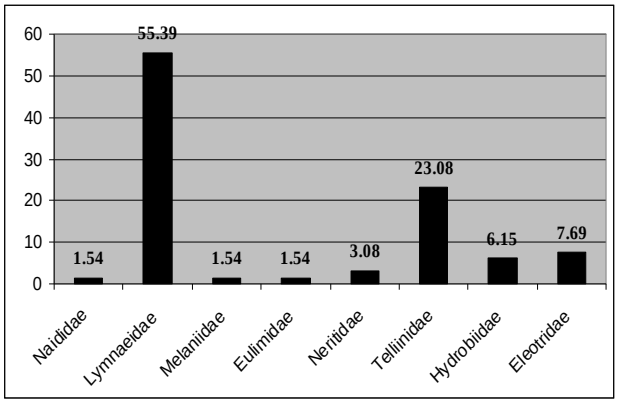

Figure 3. Relative contribution of major groups of phytomacrofauna in the study area.

Diversity and dominance

Diversity and dominance indices calculated for the five stations are summarized in Tables 3 and 4. The taxon richness (d) was highest in station 5 and the lowest in station 3. Station 4 had higher taxon richness than station 1. Shannon diversity (H) was significantly higher in station 5 than in the other stations (P<0.05), which were not different from one another. Evenness index (E) followed the same trend.

Lymaeidae recorded the highest dominance values in stations 1, 2 and 4. Hydrobiidae whose occurrence was restricted to station 5 recorded the highest dominance value in that station. Melaniidae, Eulimidae, and Naididae recorded 3.03, 14.29 and 7.14 respectively as dominance values in their different single station representation at stations 2, 4 and 5 respectively.

Faunal similarity of sampling stations

Table 5 summarizes the fauna similarities of the study stations. Renkonen similarity indicated that the faunal at station 1 was significantly similar (>50%) to those of stations 2 and 4. The faunal of station 2 was also significantly similar (>50%) to the faunal of station 4.

Table 2: Summary of the physico – chemical properties of the study stations in Epe lagoon.

* Indicates significant difference

Parameter	Station 1			Station 2			Station 3			Station 4			Station 5			
	Max	Min	Mean ± SE	Max	Min	Mean ± SE	Max	Min	Mean ± SE	Max	Min	Mean ± SE	Max	Min	Mean ± SE	Probability
Ph	7.3	6.9		7.0	6.7		7.4	6.9		7.2	6.5		7.4	7.1		
TDS (mg/L)	218	70	142.3 ± 26.76	220	110	174. ± 15.98	1860	50	506 ± 81.81	583	100	273. ± 72.64	955	100	365 ± 50.77	> 0.05
Conductivity (mg/L)	555	185	347 ± 53.49	700	310	550.5 ± 8.06	462	230	368.6 ± 32.8	1013	150	560.3 ± 144.4	1089	318	650 ± 161.8	> 0.05
(DO (mg/L)	5.4	4.0	4.9 ± 0.24	5.9	3.7	4.8 ± 0.30	6.1	4.3	5.3 ± 0.28	5.9	3.2	4.6 ± 0.42	4.9	2.4	3.6 ± 0.45	< 0.05*
BOD_5 (mg/L)	29.6	9.6	16.08 ± 3.15	66.4	11.1	32.3 ± 8.26	40.7	14.6	25.8 ± 3.73	42.4	10.8	24.3 ± 4.73	27.0	8.9	14.8 ±2.77	< 0.05*
COD (mg/L)	432	214	313.8 ± 37.72	547	69.6	253 ± 66.23	382	109.3	184.4 ± 41.0	405	111.6	249.1 ± 47.14	514	167	340.5 ± 54.6	> 0.05
PO_4-P (mg/L)	1.20	0.25	0.8 ± 0.13	1.0	0.42	0.64 ± .02	1.6	0.33	1.02 ± 0.21	4.88	0.38	1.59 ± 0.67	2.4	0.08	0 8 ± 0.35	< 0.05*
NO_3-N (mg/L)	5.00	0.6	2.67 ±0.69	4.15	0.8	2.6 ±0.51	6.50	0.4	3.4 ±1.06	12.20	0.9	3.8 ± 1.75	1.65	0.56	1.38 ± 0.10	>0.05

Table 3 Diversity of non-insect benthic phytomacrofauna in Epe lagoon.

	Stations				
	1	2	3	4	5
Number of sample	6	6	6	6	6
Number of Taxa	2	3	-	3	3
Number of individuals	11	33	-	14	7
Margalefs index (d)	0.96	1.31	-	1.74	2.36
Shannon Wieners Index (H')	0.2545	0.3501	-	0.2849	0.4150
Evenness (E)	0.8455	0.7338	-	0.5971	0.8698

Table 4: Dominance of non – insect benthic phytomacrofauna major groups in the study stations. xx = Dominant; x = Subdominant

	Station				
Taxa	1	2	3	4	5
Naididae	-	-	-	7.14*	-
Lymaeidae	72.72^{xx}	51.56^{xx}	-	78.57**	-
Melaniidae	-	3.03*	-	-	-
Eulimidae	-	-	-	-	14.29*
Telliinidae	-	45.45^{xx}	-	-	-
Neritidae	-	-	-	-	28.57**
Hydrobiidae	-	-	-		57.14^{xx}
Eleotridae	27.27**	-	-	14.28*	-

Table 5. Renkonen similarity faunal comparison of non-insect benthic phytomacrofauna in the study stations of Epe lagoon. *Significant similarity ≥50%.

	1	2	3	4	5
1	100	51.51*	-	87.02*	-
2		100	-	51.51*	-
3			100	-	-
4				100	-
5					100

Discussion

The values of water quality parameters reported in this study are obvious reflection of a degraded aquatic system, and these have direct influence on the structure of the benthic phytomacrofauna. Addition of land based pollutants to aquatic systems changes the hydrological, chemical, physical and biological characteristics of an aquatic ecosystem. Siltation resulting from the inflow of sediment from cultivated lands increases the amount of suspended solids in water, which in turn reduces light penetration and water transparency. Siltation also results in alteration of the depth and general characteristics of the bottom sediment. Decrease in depth and the absence or reduction of water current resulting from siltation could lead to poor oxygen circulation, which could affect the growth and development of aquatic macrophytes. The generally low level of dissolve oxygen and high BOD recorded at the sampling stations indicated deteriorating water quality and probably resulted from the deposition and decomposition of organic waste from domestic sources at the study stations.

The overall community composition of the study area is poor when compared to records of similar studies in the lagoon systems of southern Nigeria. The taxa recorded in this study is lower than that reported by Edokpayi *et al.* (2008; 2009) for phytomacrofauna arthropod community in the same lagoon and for phytomacrofauna communities in a non – tidal creek in south-western Nigeria, respectively, and that recorded by Saliu (1989).

The non-insect benthic phytomacrofauna community composition structure, abundance and diversity were greatly affected by water quality. Pollutants create uncondusive environment for plant growth and general development. Poor growth of aquatic macrophytes diminishes the amount of space available for attachment of phytomacrofauna groups and this subsequently reduces the number of colonizing taxa (Cyr and Downing, 1988a; 1988b). No taxon was recorded in station 3; this observation is similar to that reported by Uwadiae *et al.* (2009). This is not unusual since reduction or complete decimation of benthic population has been observed as a response of benthic communities to pollution and habitat alteration (Uwadiae, 2009). Station 3 is a deposition site for organic wastes from a number of domestic and agricultural operations.

The distribution and abundance of specific taxa could be used in assessing the levels of impact in the study stations. Lymnaeidae gastropod molluscs respond to polluted environment by increase in abundance (Bouchard, 2004). Their significantly higher overall abundance in this study could be attributed to opportunistic condition created by pollution. Naidid oligochaetes respond to organic pollution by increase in abundance. Their wide spread distribution in the study area could be an indication of organic enrichment. They can live in extremely polluted waters with very low oxygen levels (Bouchard, 2004).

The taxa richness (d), general diversity (H') and evenness (E) all revealed the decimating impact of land based pollutants on non-insect benthic phytomacrofauna communities. The absence of any taxa in station 3 and the generally low taxa recorded in the other

study stations are similar to the typical response of benthic communities to pollutants. Two theories have been propounded to explain this response; theory of habitat reduction and theory of habitat change (Lenat *et al*., 1981; Ogbeibu and Oribhabor, 2004). If habitat reduction were most important in this instance; one would expect all groups to have been equally affected (Ogbeibu and Oribhabor, 2004). In this study all the groups were not equally affected, there was a significant reduction in the abundance of all groups except molluscs and oligochaetes which had relatively higher populations in station 2. The overall change displayed in this study is a demonstration of a typical response of a community to environmental alteration.

The overall diversity of benthic community is the product of all spatial and temporal changes affecting the community. The absence of taxa in station 3 and the generally low taxa metrics in all the stations are reflections of community instability in these stations. Renkonen similarity indicated that the faunal of study stations (except stations 3 and 5) were similar and showed close affinity and shared pollutant tolerant taxa.

A more elaborate study with more stations across the length of the lagoon involving a comprehensive analysis of water quality parameters is imperative to fully understand and establish the impact of pollutants on the water quality and community structure of benthic macro-invertebrates of the coastal lagoon.

Corresponding Author
Roland Efe Uwadiae PhD
Benthic Ecology Unit,
Department of Marine Sciences,
University of Lagos, Akoka, Lagos, Nigeria.
Email:eferoland@yahoo.com.
Tel: +2347059497190.

References

Adakole JA, Annue PA. Benthic Macroinverteberates as indicators of Environmental quality of an urban stream, Zaria, Northern Nigeria. J. Aquat. Sci. 2003; 18(2): 85-92

American Public Health Association (APHA) (1985). Standard Methods for the Examination of Water and Wastewater. 16th edn. American Public Health Association, Washington, DC.

Arimoro FO, Osakwe EI. The influence of sawmill wood wastes on the distribution and population of macroinvertebrates at Benin River, Niger Delta Area, Nigeria. Chemistry and Biodiversity. 2006; 3: 578–592.

Arimoro FO, Ikomi RB. Iwegbue CMA. Ecology and abundance of oligochaetes as indicators of organic pollution in an urban stream in southern Nigeria. Pakistan Journal of biological Science. 2007; 10 (3): 446–453.

Bouchard RW.Jr. Guide to aquatic macroinvertebrates of the Upper Midwest. Water Resources Center, University of Minnesota, St. Paul, MN. 2004; 208pp.

Biochino AA, Biochino GI. Quantitative estimation of phytophilous invertebrates. Hydrobiologia. 1980 ; 15: 74–76.

Brown CL, Poe JR, French III, Schloesser, DW. Relationships of phytomacrofauna to surface area in naturally occurring macrophyte stands. Journal of the North American Benthological Society. 1988; 7:129–139.

Cyr H, Downing, JA. Empirical relationships of phytomacrofaunal abundance to plant biomass and macrophyte bed characteristics. Canadian Journal of Fisheries and Aquatic Sciences. 1988a; 45: 976-984.

Cyr H, Downing JA. The abundance of phytophilous invertebrates on different species of submerged macrophytes. Freshwater Biology. 1988b; 20: 365-374.

Edokpayi CA, Okenyi JC, Ogbeibu AE, Osimen EC. The effect of human activities on the macrobenthic invertebrates of Ibiekuma stream,Ekpoma, Nigeria. Bioscience Research Communications. 2000; 12 (1): 79–87.

Edokpayi CA, Uwadiae RE, Asoro AO, Badru AE. Phytomacroinvertebrates arthropods associated with the roots of *Eichorrnia crassipes* (water hyacinth) in a tropical West African Lagoon. *Ecology, Environment and* Conservation. 2008; 14(2-3): 241-247.

Krecker FH. A comparative study of the animal population of certain submerged aquatic plants. Ecology. 1939; 20: 553–562.

Krull JN. Aquatic plant-macroinvertebrate associations and waterfowl. Journal of Wildlife Management. 1970; 34: 707–718.

Lenat DR, Penrose DL, Englson KW. Variable effects of sediment addition on stream benthos. Hydrobiologia. 1981; 79**:**187 - 194

Mallo YII. Nature of suspension sediment transport in an urbanized tropical stream, Northern Nigeria. Acad J. Sci & Tech. 2001; 2: 103-108

Nwankwo DI, Amuda SA. Periphyton Diatoms on three floating Aquatic Macrophytes in a polluted South-Western Nigerian Creek. International Journal of Ecology and Environmental Sciences. 1993; 19: 1 – 10.

OFFICIAL GAZATTE (FGP 71/52007/2,500(OL24). Legal Notice on Publication of the Details of the Breakdown of the National and State Provisional Totals. 2006 Census.

Ogbeibu AE, Oribhabor BJ. Ecological impact of river impoundment using benthic macroinvertebrates as indicator. Water Research. 2002; *36*: 2427–2436.

Ofojekwu PC, Umar DN, Onyeka JOA. Pollution status of Industrial wastes and their effects on

macroinvertebrate distribution along Anglo – Jos water channel Jos, Nigeria. J. Aquat. Sci.1996; 11:1-6.

Ogbogu SS, Hassan AI. Effects of sewage on the physico-chemical variables and Ephemeroptera. (Mayfly) larvae of a stream-Reservoir system. J. Aquat. Sci. 1996; 11: 43-55.

Portman J, Biney C, Childilbe A, Zabi S. State of the marine environment West and Central African region. UNEP Regional seas. Rep. and stud. 1989; No 108.

Rosenberg DM, Resh VH. Freshwater biomonitoring and macrobenthic invertebrates. Chapman and Hall, London. 1993; 488pp.

Rueda J, Camacho, A, Mezquita, F, Hernanadez, R, Roca, JR. Effect of episodic and regular sewage discharge on water chemistry and macroinvertebrate fauna of a Mediteranean stream. Water, air and soil pollution. 2002; 140: 425 – 444.

Saliu JK. Aquatic insects associated with plant in two reservoirs at Ibadan, Nigeria. Communications.1989; 7(2):217 – 219.

Singh J, Hewawassam H, Moffat D. Nigeria: Strategic options for redressing industrial pollution. Vol. 1. Industry and Energy division, West Central Africa Department. 1995; 45pp.

Uwadiae RE. An ecological study on the macrobenthic invertebrate community of Epe lagoon, Lagos. Ph.D Thesis University of Lagos. 2009; 253pp.

Uwadiae RE, Edokpayi CA, Adegbite O, Abimbola O. Impact of sediment characteristics on the macrobenthic invertebrates community of a perturbed tropical lagoon. Ecology, Environment and Conservation. 2009; 15(3): 441-448

Walsh C, Gooderham JP, Grace MR, Sdraulig S, Rosyidi MI, Lelono A. The relative influence of diffuse and point-source disturbances on a small upland stream in East Java Indonesia: a preliminary investigation. Hydrobiologia. 2002; 487: 183–192.

Zabbey N. and Hart AZ. Influence of some physicochemical parameters on the composition and distribution of benthic fauna in Woji Creek, Niger Delta, Nigeria. Global Journal of Pure and Applied Sciences. 2006; 12 (1): 1–5

.

15/03/2010

Rare Plants Protection Importance and Implementation of Measures to Avoid, Minimize or Mitigate Impacts on their Survival in Longhushan Nature Reserve, Guangxi Autonomous Region, China

Dado Toure*, J. Ellis Burnet*, Zhou Jianwei*
*China University of Geosciences (Wuhan), School of Environmental Studies
Wuhan, Hubei. 430074. Lumo Lu. P.R.China
touredado@yahoo.fr , cactais@gmail.com

Abstract: Longhushan reserve is a karst forest of very high geological and biological quality. Located in South of China, Guangxi Region, the area reflects the high diversity of Guangxi, whose biological resources are among the first in China, and which ranks first among the Chinese provinces in terms of rare plant species. The present research was undertaken to examine the ecosystems within the forest, and thus generate an awareness of the importance of rare plant species in order to stimulate the conservation role of Authorities and population. A field survey was conducted, plant species were recorded from 17 quadrats, geological and soil samples were collected to examine some of their chemical and physical characteristics significance on the vegetation formation. During the survey, 152 plant species were recorded, 35 species were found as dominant canopy and substrata species, and 12 species were identified as endangered. Within those endangered species, 6 are included in the International Union for Conservation of Nature and Natural Resources (IUCN) red list for endangered species and 3 are endemic. Analysis of geological and soil samples revealed that dolomite appears to be the factor that impacted species distribution, while rare plants and dominant species responded differently to soil type, PH, moisture and organic matter (OM) content. Which lead to say that in the reserve each karst environment is unique due to its localized conditions, geological and soil properties, land use practices, climatic conditions, hydrological and geomorphologic status. The results also pointed out the evidence of karst ecosystem fragility which makes the vegetation formation or restoration a slow and difficult process. Therefore, plant species protection especially endangered species is fundamental in the area because their conservation is central not only to biodiversity conservation but also to the preservation of karst ecosystems. [Journal of American Science 2010;6(7):221-238]. (ISSN: 1545-1003).

Key words: Rare plants protection; Longhushan; avoidance, minimization/mitigation measures; Impact.

1– Introduction

The main focus in the protection of natural areas across the globe has been in the context of preserving landscape beauty, natural heritage, unique biological habitat or recreation. China, despite of the importance of natural reserves creation, has its endangered species faced with an onslaught of threats. China contains some of the world's richest troves of biodiversity, yet the surveys of plants and animals reveal a bleak picture that has grown bleaker during the past decade. According to scientists, for plants the situation is worse: nearly 70% of all nonflowering plant species and 86% of flowering species are considered threatened (Yardley, 2007). For centuries, Chinese leaders emphasized dominance over nature rather than coexistence with it. Animals and plants are still often regarded as commodities valued for use as medicine or food, rather than as essential aspects of a natural order. The whole idea of ecology and ecosystems is a new thing in the culture. China's status as a leading center of biodiversity makes the threatened state of wildlife a global concern. Being the third largest country in the world, with the greatest population, the diversity of its topography and climate is reflected in its animals and plants species. China is one of a small handful of countries, maybe a dozen, that has a remarkably high numbers of species, and a remarkably high number of species that are not found anywhere else (Yardley, 2007). The biodiversity ranks eighth in the world, first in the northern hemisphere and an estimated 10% of the world's plant species are found within its vast expanse (Watters, et. al 2002). In large part, this high diversity is due to the variety of habitats and landscapes. But the effectiveness of provincial parks and conservation authorities in protecting endangered species varies considerably. Many places have greater emphasis on exploiting the natural environment for human enjoyment than on protecting habitats or rare plants. Longhushan Reserve is a tangible example of this type of situation. The area belongs to Guangxi which is one of the key forest areas in southern China, ranking first among the Chinese provinces in homing to the rare species of plants. About 8,354 wild plants have been found in the region, including 122 kinds which are near extinction and need special protection (Chinese Business World).

The question we are about to ask our self is why do we have to protect plants from extinction? why not let the nature take its course and allow plants to die out? There are many reasons for that. Our planet is

experiencing species extinction rates unprecedented in the history (US National Academy of Science, 1995). Scientific work over recent decades has given a good understanding of the risks these extinctions pose for the planet and its human inhabitants. Science has also provided us with an understanding of the basic requirements for effective conservation of biological diversity. The main reason that many species are endangered or threatened today is because people have changed the habitats upon which these species depend. Extinction is a natural process that has occurred throughout world history, but in recent times humans have become the major threat to the survival of many plants. Technological developments and increasing pressure for agricultural land combined with the exploitation of timber, minerals and other natural resources, are causing rapid environmental changes. These threaten whole ecosystems, such as the rain forest in tropical countries. As a result, the survival of thousands of plant species is threatened (Morton, Canadian Encyclopedia).

The initial data and observation collection resulting in preliminary mapping of Longhushan reserve showed that a large proportion of the "secondary" forest on the lower mountain slope is, in fact, a plantation forest with a simple canopy structure or complex sub-strata. The transitional stage to an analog forest has not yet been reached, although there are indications that in some forest stands there is sufficient regeneration and the forest is dynamically robust to evolve in the future (Ellis Burnet, Mbue et. al 2008).

In fact, the karst mountains in Southwestern China are usually bare rock with little or no vegetation due to their low soil forming capability and their relative shortage in nutritive elements. This explains the fragility of these areas and the difficulty of restoring vegetation once destroyed. For the specific case of Longhushan, after the massive cutting of part of the natural forest for the benefit of medicinal plantation in the 1960s, the area is now almost completely covered by vegetation with plants growing through the rocks' fissures to the summit (*Figure 1*, *Figure 2*). This is the peculiarity of the area and raises our interest for the understanding of this rare ecological system and the necessity of controlling human activities for the maintenance of its ecosystems and so its endangered species. Because currently, the development of tourism activities with an uncontrolled number of primates, in addition to the continuing fragmentation of habitat through construction of small roads to facilitate tourists access to different parts of the forest, are threatening the ecological stability of Longhushan reserve which although small, but no less rich, may represent an important resource in Guangxi in terms of vegetation formation in a karst ecosystem.

Figure 1*: Longhushan reserve view from a summit/ Peak cluster depression landform*

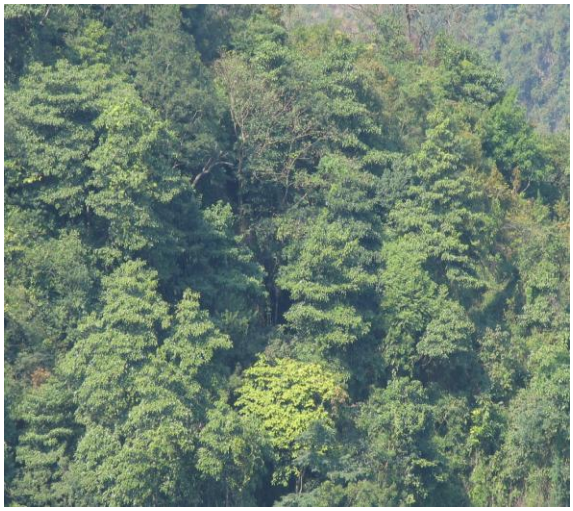

Figure 2*: Longhushan middle elevation forest*

Since the 1990's, there have been illegal activities recorded in the reserve and it is the responsibility of the protected area's administration to prevent these activities. The following illegal activities have been significant: cutting firewood 20%; poaching 30%; digging up rare or valuable plants 45%; and illegal cattle grazing (Ellis Burnet et. al 2008). Due to the various species which characterize the study area, the influence of local inhabitants who live around the reserve, the development of tourism activities, and

increasing of primate population over the last 20 years (estimated to be a thousand), the site become an interesting spot and open natural laboratory to study karst forest sustainable management, botanical species, karst ecological system and the geomorphological interaction with vegetation formation.

The reserve is small but its floral biodiversity and the lack of wildlife information has lead to the belief that some aspects of its ecology are not well known, therefore need to be studied in detail, consequently, the species can be identified and protected. This study was initiated to draw attention to this small reserve with its rich biodiversity so as to greater public awareness about the importance of rare plants species in order to stimulate the conservation role of Governments, administrators and population, with the hope that publicity could prevent further habitat destruction leading to possible extinctions.

The main purposes of this study are to: (i) identify endangered or endemic plant species and their importance for biodiversity conservation, the dominant canopy and substrata species within the reserve; (ii) examine soil characteristics and their significance for the vegetation formation; and (iii) suggest avoidance, minimization, and/or mitigation measures for sensitive areas as wilderness and ecological reserves in which effective protection can be provided to any rare plants growing in them.

We hope this study will generate more scientific interest in the local area and further research will be undertaken to investigate habitat, fauna and flora of the reserve so as to generate a sustainable conservation perspective.

2. Materials and Methods

2.1. Site location and description:

The present study was conducted in Longhushan nature reserve located in South of China, Guangxi Zhuang Autonomous Region, Nanning city, Long'an County (*Figure 3*). It is approximately 36 kilometers away from the county headquarters and 90 kilometers away from Nanning city, the provincial capital. The reserve covers an area of 2255.7 hectares and is bounded between latitudes 22°56′-23°00′N and longitudes 107°27′-107°41′E. Longhushan has a monsoon climate characteristic of the subtropical zone and is influenced by the regulation of a maritime climate. It has abundant sunshine combined with high rainfall, but with little frost and no snowfall. The annual average temperature is 21.8Cº, with the annual average precipitation of 1500 mm which is mostly centralized in summer.

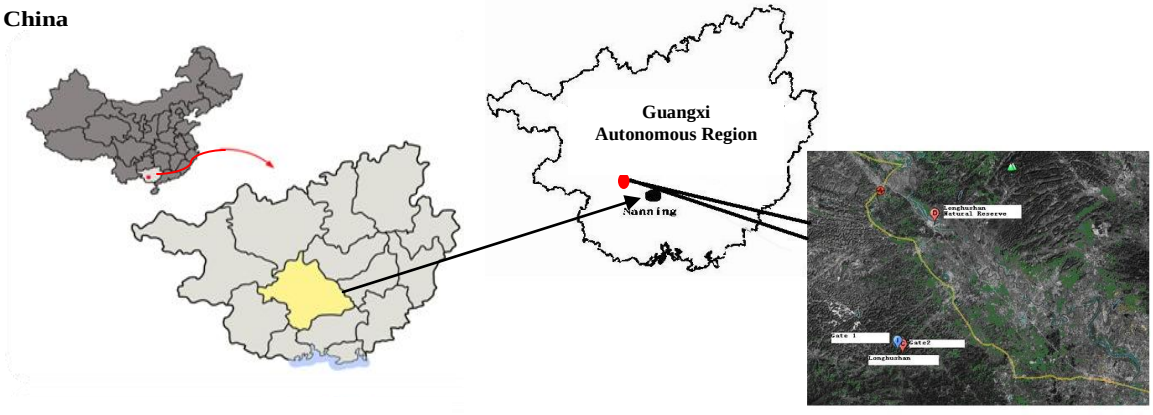

Figure 3*: Longhushan reserve location*

The reserve was established in 1980, under the administration of the Ministry of Health. Because of the significance of its medicinal herbs, it became a reserve with its present name in 1982. The Ministry of Forestry took over the administration of the reserve in 1987 in order to strengthen its protection and in November 1991 the status changed to forest and wild animal protected area.

In the reserve there is an altogether different world, with green hills, the Green River channel, karst caves, and stone forests. The protected area is a typical peak cluster depression landform and is divided into three sectors by two landscape barriers: the highway from Nanning to Daxin and the Green River (*Figure 4 and Figure 5*). There is an underpass beneath the highway linking the northern sector of the reserve

which also allows the passage of precipitation run-off during intense rain events. Several bridges span the Green River linking the southern sector to the central sector. The protected area is small but the public road Nanning-Daxin running through it and dividing the park into two parts makes environmental protection difficult. The floral biodiversity is rich, about thousand plant species with different types of canopy cover and substrata species: small trees, shrubs, high trees, vines, and invasive weed species. However, it is in a karst area easily exposed to rock desertification. The fragility of the karst ecological system in tropical and subtropical regions is the basis of rock desertification, but the desertification sequences are triggered by anthropogenic impacts including population pressure, inappropriate land use policies, planning and practice.

Figure 4: ***View from a summit/*****Green river** ***passing through the reserve***

Figure 5: ***View from a summit/Highway Nanning-Daxin passing through the reserve***

2.2 Field survey and sampling methods:

In order to achieve the objectives of this study, two field surveys were conducted in Longhushan reserve, during August and November 2008. The survey was carried out using 30 meters square quadrats randomly located along north-south transects lines equidistant apart. In order to ascertain the forest stand structure, dynamic and condition in relationship to the parent geology, soils, human and primate impact on the synecology of the forests. Data was collected from 17 quadrats refer to as X1, X2,……X17 along 4 transect lines: geological samples (surface rocks) and soil samples were collected from each quadrat for chemical analysis. Dominant canopy and sub-strata species were recorded and botanical samples also were collected for identification. All samples were recorded on the day of collection in a Field Register and all data recorded were logged into a computer base using Excel and SPSS programs. The geological samples were collected from the surface of each quadrat, while the soil samples were collected from the topsoil layer (0–10 cm) after removal of leaf litter. A total of 17 surface soil and geological samples were collected for analysis and both geological and soil samples were bagged separately in clean zip-lock plastic bags and labeled.

In addition to the systematic sampling, the opportunity was also taken throughout the survey for empirical observation and talk to local people in order to get their thoughts about the area, obtain more information about the Reserve's management, human activities and their impact on the reserve, the reserve's environmental protection and sustainable use.

2.3 Analysis

The botanical specimens were identified within two weeks of collection in the South China Herbarium, Nanning-Guangxi and were preserved for future reference. The botanical nomenclature of the South China Institute of Botany (1987, 1991, and 1995) was adopted. All botanical samples were identified in Guangxi Botanic Garden. The status of rare plant species were established by illustrated handbooks of Guangxi vegetation and China high vegetation, as well as the Red Book. The endangered species list published by Chinese Government was also referenced. In order to know the nature of parent rock and its relation with vegetation, geological samples were analyzed for the percentage of calcite and dolomite while the soil samples were tested for their texture, moisture, PH, and OM content so as to examine the soil properties and their significance on vegetation formation. To

determine dolomite and calcite content in the geological samples, HCl was used on the samples to define dolomite and calcite by the naked eye and alizarin-red used to determine them using microscopic observation. Soil moisture content was obtained using the standard oven-dry method calculated from soil sample weights before and after drying and expressed as a percentage of the mass of the oven-dried soil. Soil-water suspension method was used to test soil PH. For OM content, the classic dichromate wet oxidation method for the determination of organic carbon in soils was used. To examine soil type for its physical characteristic, the United State Department of Agriculture (USDA) method was used to determine soil textural classes based on percentage content of sand, silt, and clay.

3. Results

During the survey, from the 17 quadrats studied, 152 plant species were identified, among them 35 species were found as dominant canopy and substrata species, and 12 species were identified as endangered in 8 quadrats (X1, X2, X3, X4, X6, X14, X16, and X17).

3.1. Rare plant species

Within the 12 endangered species recorded, 6 are included in the IUCN Red List for endangered species, 3 are endemic. The following table (*Table1*) shows the list of rare plant species recorded with their botanical taxonomy.

Table 1: Rare plant species identified in Longhushan Reserve

N°	Location	Scientific name	Status	Phylum	Class	Order	Familly
1	T1 QIV	***Burretiodendron tonkinense* (Gagnep.)Kosterm**	Endangered (IUCN red list)	Tracheophyta	Magnoliopsida	Malvales	Tiliaceae
2	T1 QII; T1 QIII	***Camellia pubipetala* Y.Wan & S.Z.Huang**	vulnerable (IUCN red list)/ ***Endemic***	Magnoliophyta	Magnoliopsida	Malpighiales	Theaceae
3	T4 QIII	***Canthium dicoccum* (Gaertn.) Teijsm. & Binn**	Vulnerable (IUCN red list)	Tracheophyta	Magnoliopsida	Rubiales	Rubiaceae
4	T1 QI	***Desmos chinensis* Lour**	Locally endangered	Magnoliophyta	Magnoliopsida	Magnoliales	Annonaceae
5	T1 QII; T1 QIII	***Garcinia paucinervis* Chun & How**	Endangered (IUCN red list)	Tracheophyta	Magnoliopsida	Hypericales	Clusiaceae
6	T2 QII	***Habenaria ciliolaris* Kraenzl**	Locally endangered	Magnoliophyta	Liliopsida	Asparagales	Orchidaceae
7	T4 QIV	***Hainania trichosperma* Merrill**	***Endemic***	Tracheophyta	Magnoliopsida	Malvales	Tiliaceae
8	T4 QIII	***Hartia sinensis* Dunn**	Locally endangered	Magnoliophyta	Magnoliopsida	Theales	Theaceae
9	T1 QII; T1 QIII	***Machilus salicina* Hance**	Locally endangered	Magnoliophyta	Magnoliopsida	Laurales	Lauraceae
10	T4 QI	***Malania oleifera* Chun et S.Lee**	Vulnerable (IUCN red list)/ ***Endemic***	Tracheophyta	Magnoliopsida	Santalales	Olacaceae
11	T2 QII	***Mallotus philippinensis* Mull.-Arg**	Locally endangered	Magnoliophyta	Magnoliopsida	Euphorbiales	Euphorbiaceae
12	T2 QII	***Zenia insignis* Chun**	Near threatened (IUCN red list)	Tracheophyta	Magnoliopsida	Fabales	Fabaceae

Burretiodendron tonkinense (Gagnep.) Kosterm*:* is a species of flowering plant native in China (Guangxi, Yunnan) and Vietnam extending from southern China to northern Vietnam. The species is confined to forest in limestone areas and considerable population declines have been observed. It is *endangered A1d ver 2.3* (IUCN red list) threatened by habitat loss, overexploitation of the timber and lack of sufficient regeneration.

Camellia pubipetala Y.Wan & S.Z.Huang: species of shrub or small tree, known from two locations, Long'an and Daxin in China (Guangxi), *endemic* to China. This species occurs in evergreen broadleaved forest at the base of limestone mountains,

between 190 and 230 m. It is *vulnerable B1+2c, D2 ver 2.3* (IUCN red list), threatened by constant threats of cutting and habitat clearance.

Canthium dicoccum (Gaertn.) Teijsm. & Binn*:* also called "Ceylon box wood" in English, is a species of plant native in Sri Lanka. It is also found in tropical South Asia and Southeast Asia. This is a species of shrubs or trees restricted to lowland wet evergreen forest. It is *vulnerable A1c ver 2.3* (IUCN red list).

Desmos chinensis Lour*:* called "Dwarf Ylang Ylang Shrub" is a climbing shrub with straggling branches, up to 5 m tall. Its distribution is throughout Nepal, Eastern India, Burma (Myanmar), Indo-China, southern China, Thailand, Peninsular Malaysia, Sumatra, Java, Borneo and the Philippines. It occurs in open locations and borders of lowland forest. It is also found in living fences and brushwood, up to 600 m altitude. The plant is used as a folk medicine in China for the treatment of malaria and of dysentery, parturition and vertigo.

Garcinia paucinervis Chun & How*:* is a species of flowering plant native in China (Guangxi, Yunnan) and Viet Nam. The populations are confined to central Guangxi and to Malipo in south-east Yunnan, extending into northern Viet Nam, distributed in forest on limestone, rarely above 600 m. This is a valuable timber species but is *Endangered B1+2e ver 2.3* (IUCN red list) threatened by habitat loss, cutting of large trees; very few remain and regeneration also appears to be insufficient. This species is vulnerable to extirpation because of its restricted and scattered distribution, overcutting, and poor seed germination and natural reproduction. The wood is hard, heavy, and extremely water-tolerant. It is used for shipbuilding, construction, quality furniture, and in the military industry.

Habenaria ciliolaris Kraenzl : is a terrestrial plant 30 to 50 cm tall on forest floor with rich humus, shaded places in forests or along valleys with forest trails at low to mid elevations; it is distributed from South East China to Vietnam and Taiwan.

Hainania trichosperma Merrill: is a species of tropical plant, up to 15m tall; native in Hainan, Guangxi and Yunnan in China. It is *endemic* to China and is light-demanding and drought resistant, adapts to limestone soil and acid soil. It is also a fairly good tree species for afforestation on limestone hill area or barren hills in Hainan and southern Guangxi.

Hartia sinensis Dunn*:* species of tree or shrub, 6–15 m tall, evergreen found in China (Sichuan, Yunnan, Guizhou, Guangxi, Guangdong, Hunan, and Jiangxi). It is located in woodland rich clay soil, must have high humidity and semi shade.

Machilus salicina Hance*:* is a medicinal plant species, usually 3-5 m tall located in stream sides and riversides of low elevations; it grows well on river banks and can be used to protect the bank from flooding. It is found in China (Guangdong, Guangxi, S Guizhou, Hainan, S Yunnan), Cambodia, Laos, and Vietnam.

Malania oleifera Chun et S.Lee*:* is a species of plant, native in China (Guangxi, Yunnan), scattered in western Guangxi and eastern Yunnan. It is *endemic* to China and the genus is monotypic. It is found in tropical and warm-temperate regions, confined to limestone mountains up to 1,640 m. It is *Vulnerable B1+2c ver 2.3* (IUCN red list 2006) threatened by habitat loss. Wild populations are much reduced as a result of continued logging and habitat clearance.

Mallotus philippinensis Mull.-Arg*:* or "Kamala" tree in English is a species of tree locally common in shrub land and young secondary forest. It is found throughout tropical regions: China (Sichuan, Yunnan, Guizhou, Hubei, Hunan, Jiangxi, Anhui, Jiangsu, Zhejiang, Fujian, Taiwan, Guangxi, Guangdong, Hainan), S & SE Asia, and tropical Australia. It is used for industrial oil, dyeing silk and wool, also for medicine. In India, the increasing demand of natural dyes has attracted the attention of herb traders towards this common but useful herb. This demand can create the pressure on natural population.

Zenia insignis Chun: is a species of plant native from China (Guangdong, Guangxi, Guizhou, Hunan, Yunnan) and Viet Nam, concentrated in limestone areas at low elevation. The subpopulations are widespread throughout southern China and in several of the northern provinces of Viet Nam. It is the only member of the genus. This species is classed *lower Risk/near threatened ver 2.3* (IUCN red list) but it is threatened by habitat loss. In China constant overcutting of the tree and its habitat has resulted in the species becoming scarce.

3.2. Dominant canopy and sub-strata species

Among the 35 dominant species identified, 19 were dominant canopy and the rest were found as dominant substrata species (*Table2*).

Table 2: Identified dominant canopy and sub-strata species in Longhushan Reserve

N°	Scientific Name	dominant	Location
1	***Aesculus chinensis***	canopy	T4 QI
2	***Albizia chinensis***	can: s-st	T2 QIV; T3 QIII; T3 QIV; T3 QII
3	***Ardisia brunnescens***	sub-strata	T1 QI; T2 QIII; T1 QIII; T1 QIV; Qca
4	***Ardisia depressa***	sub-strata	T2 QII; T3 QI; T3 QIV; T4 QIV
5	***Ardisia virens***	sub-strata	T3 QII; T4 QII OOL
6	***Bischofia javanica***	canopy	T3 QIII; T2 QI; T2 QII; T3 QI
7	***Breynia fruticosa***	sub-strata	T1 QII
8	***Boehmeria Macrophylla***	sub-strata	T2 QIV
9	***Castanopsis indica***	canopy	T1 QI
10	***Clausena excavata***	sub-strata	T1 QII; T1 QIII; T1 QIV; T2 QII;
11	***Cleistocalyx operculatus***	can; s-st	T1 QII; T1 QIII
12	***Croton cavaleriei***	can: s-st	T2 QIII; T1 QII
13	***Eurya groffii***	sub-strata	T4 QIII
14	***Hainania trichosperma***	canopy	T4 QIV
15	***Laportea violacea***	sub-strata	T1 QII
16	***Ligustrum lucidum***	sub-strata	T4 QII
17	***Liquidamber formosana***	canopy	T4 QI; T2 QI
18	***Machilus salinina***	can: s-st	T1 QII; T1 QIII
19	***Maesa balansae***	sub-strata	T2 QI; T3 QI
20	***Maesa japonica***	sub-strata	T3 QI; T4 QI; T4 QII
21	***Millettia walkei***	sub-strata	T1 QI
22	***Phlogancanthus curviflorus***	canopy	T4 QII
23	***Pithecellobium clypearia***	canopy	T1 QI; T2 QIII
24	***Pomocarpus tumatus***	canopy	Qca
25	***Psychotria rubra***	sub-strata	T1 QI; T2 QIV; T4 QI; T4 QII; out of line
26	***Pyrus calleryana***	sub-strata	T2 QII; T2 QIII; Qca
27	***Rubus leucanthus***	sub-strata	T2 QI
28	***Saraca chinensis***	canopy	T1 QIII
29	***Sterculia euosma***	canopy	T4 QIII
30	***Sterculia lanceolata***	canopy	T2 QIV; T2 QIII; Qca
31	***Sterculia nobilis***	canopy	T4 QII; T3 QII; T1 QI; T2 QIII; T1 QIII; T1 QIV; T3 QI; T3 QIV
32	***Syzgium jambus***	canopy	T1 QIV
33	***Teonongia tonkinensis***	can: s-st	T3 QIV; T4 QIII; out of line
34	***Wendlandia uvarifolia***	canopy	T1 QIII
35	***Zanthoxylum dissitum***	sub-strata	T3 QIII

Of the 19 dominant canopy trees recorded in Longhushan Reserve, *Sterculia nobilis* (Noble Bottle Tree) was the highest occurring species being dominant in eight quadrats. It has medicinal properties and the wood is hard making is suitable for furniture products. The tree is rich in resin which is used as an industrial material. *Sterculia nobilis* is shade tolerant, easily grown from branch cuttings and fast growing. It

develops a broad crown of beautiful shape. For these reasons it is apparent that it was a preferred plantation species used in the rehabilitation of cultivation terraces.

The second most prevalent canopy species was *Bischofia javanica*, which was recorded in four quadrats. It is commonly called the java cedar or Bishop Wood and can be found naturally in temperate and tropical regions of Asia and the Pacific Islands. *Bischofia javanica* is an evergreen tree commonly growing to between 12 – 18 meters in height. It is fast-growing from seed or cuttings, thriving best in moist soil. The leaves can be deciduous in times of drought. It also suckers from the roots making it an invasive species.

Albizia chinensis commonly known as the silk tree, occurred as the dominant canopy tree in three quadrats surrounding the Tourist Square area. It is a useful shade tree and reforestation species and also has a timber value. It is native to the temperate regions of southern China and tropical areas of the Indian sub-continent and South-east Asia. It is a deciduous species, can grow in the forest and in the field, but grows best near streams and in the valley. Its bark can be used as a traditional Chinese herb.

Sterculia lanceolata, Liquidamber formosana, Pithercellobium clypearia, Cleistocalyx operculatus, Machilus salinina, Croton cavaleriei, and *Teonongia tonkinensis* were found as dominant canopy in two quadrats. Although these species occurred as dominant in two quadrats, the most prevalent among them were the first four species. *Sterculia lanceolata* usually grows near streams and is native to southern China. It is considered the most widely distributed member of the genus *Sterculia*, the leaves have medicinal properties, but also can used as fiber and the seed can be eaten and extracted oil used to produce soap. *Liquidamber formosana* is a deciduous cone-shaped tree with star shaped leaves which can reach 40 m in height. It is dark green during summer but becomes ornamental in a blaze of orange and red during autumn. The wood is used for furniture, interior finish, paper pulp, veneers and baskets of all kinds. *Pithercellobium clypearia* also known as *Archidendron clypearia* is a species known for its medicinal properties. It has also been widely used in forest rehabilitation schemes to provide structure as a nitrogen fixing legume. Its bark contains tannin which can be extracted. It can be used as a host plant for the lac insect to produce lac and has a timber value. *Cleistocalyx operculatus* is a species of herb commonly used as an ingredient for tonic drinks in southern China. It is reported that cleistocalyx operculatus extracts can improve cardiac contraction through inhibiting the activity of Na+/K+-ATPase, and decrease rate of contraction.

Syzgium jambus, Aesculus chinensis, Castanopsis indica, Hainania trichosperma, Phlogancanthus curviflorus, Saraca chinensis, Sterculia euosma, and *Wendlandia uvarifolia* occurred in one quadrat as dominant canopy. *Syzygium jambus* was predominant and is a fast growing tree which grows and crops abundantly in most subtropics conditions. Various parts of the tree are used in traditional medicine, and some have in fact been shown to possess antibiotic activity. The wood is reddish, hard and grows to dimensions large enough for construction purposes. This plant is attractive to bees, butterflies and/or birds. This plant can be quite invasive in areas where it has been introduced and is a threat to several ecosystems.

Twenty one dominant sub-strata species were recorded and the most prevalent were four species: *Psychotria rubra, Clausena excavate, Ardisia brunnescens,* and *Ardisia depressa*. The first three species have all medicinal properties and were found as dominant substrata in four quadrats.

Ardisia virens, and *Maesa japonica* occurred as dominant substrata species in three quadrats. *Ardisia virens* is a species of dense evergreen broad-leaved forests, hillsides, dark damp places, valleys, humus-rich soils; 300-2700 m. *Maesa japonica* is a species of plant 1 to 5 m height. The newborn leaves can be taken as tea and the leaves are employed in traditional Chinese medicine to cure seven-year itch.

Maesa balansae, and *Pyrus calleryana* were recorded in two quadrats as dominant substrata. *Pyrus calleryana* is a tree which can reach 30-50 ft (9-15.2 m) in height and *Maesa balansae* is an important medicinal plant in the treatment of tropical disease.
The remaining species were recorded only once as a dominant sub-strata species.

3.3. Geological and soil properties

3.3.1. Geological characteristics:

Dolomite and calcite content of surface rocks collected in each quadrats are presented in *table 3*. It appears that dolomite was dominant in 9 samples ranging from 70 to 98% and representing 60% of the samples plots.

So, according to the obtained results 60% of the surveyed area has high dolomite content and 53.33% has dolomite content ≥90%, which lead us to say that dolomite is prevalent in the area. This could mean that considering the surveyed plots, the bedrock although carbonate is more dolomitic than calcitic.

Table 3: Calcite and dolomite rate of geological samples

Quadrat	Location	Calcite	Dolomite
X1	T1 QI	<2%	>98%
X2	T1 QII	n/d	n/d
X3	T1 QIII	>90%	<10%
X4	T1 QIV	>90%	<10%
X5	T2 QI	>85%	<15%
X6	T2 QII	30%	70%
X7	T2 QIII	<5%	>95%
X8	T2 QIV	<5%	>95%
X9	T2 QV	>90%	<10%
X10	T3 QI	2%	98%
X11	T3 QII	70%	30%
X12	T3 QIII	<2%	>98%
X13	T3 QIV	10%	90%
X14	T4QI	n/d	n/d
X15	T4 QII	<2%	>98%
X16	T4 QIII	10%	90%
X17	T4 QIV	90%	10%

3.3.2. Soil characteristics:

a. Soil type

Soil types for the 17 samples collected in Longhushan are presented in *Table 4*. Considering the USDA soil texture classification system and the results revealed by the analysis, the soil texture obtained in the area could be classified as: ***coarse*** in 1 quadrat, ***moderately coarse*** in 3 quadrats, ***medium*** in 5 quadrats and ***fine*** in 7 quadrats. So, the soil appears to be fine textured in 43.75% of the surveyed plots, medium textured in 31.25%, moderately coarse textured in 18.75% and coarse textured in 6.25%. Which means in most of the investigated site the soil tends to be from fine to medium textured although the percentage of coarse and moderately coarse texture is not negligible.

Table 4: Soil texture

Quadrat	Location	Sand (%)	Silt (%)	Clay (%)	Soil type
X1	T1QI	66.67	20.00	13.33	Sandy loams
X2	T1QII	39.29	39.29	21.42	Loam
X3	T1QIII	65.38	26.92	7.69	Loamy sand
X4	T1QIV	28.00	32.00	40.00	Clay/clay loam
X5	T2QI	23.33	40.00	36.67	Clay loam
X6	T2QII	36.36	36.36	27.27	Clay loam
X7	T2QIII				
X8	T2QIV	25	53.12	21.88	Silt loam
X9	T2QV	57.14	21.43	21.43	Sandy clay loam
X10	T3QI	33	56	11	Silt loam
X11	T3QII	50.00	42.86	7.14	Sandy loam
X12	T3QIII	35.29	29.42	35.29	Clay loam
X13	T3QIV	20.69	34.48	44.83	Clay
	Qca ①	71.43	25.51	3.06	Loamy sands
	Qca ②	45.16	38.71	16.13	Loam
X14	T4QI	28.12	46.87	25.01	Clay loam
X15	T4QII	48.39	32.26	19.35	Loam
X16	T4QIII	48.00	32.00	20.00	Loam
X17	T4QIV	55.28	35.52	12.20	Sandy loams

b. Soil chemical characteristics

Some chemical properties of the surface soils at the sample sites are presented in *Table 5*. The analysis shows that the soil PH values in the surveyed plots tend to be from *near neutral* in 5 quadrats (ranging from 6.66 to 7.46) representing 29.41% of the studied plots, to *moderately alkaline* in 10 quadrats (ranging from 7.57 to 7.91) representing 58.82% of the surveyed plots. Except for 2 quadrats representing 11.76% of the studied area and which have the PH *moderately acidic* (ranging from 5.25 to 5.71). The moisture and OM content also varied from quadrat to quadrat. The variation of these 3 characteristics per quadrat is presented in *Figure 6*. The OM content varied from 2.35% to 12.51%. Unlike PH and moisture content, there is no simple interpretation for soil OM levels as the necessary amount for plant varies depending on other factors like soil texture. But according to Hartz, (2007) who considered as high OM, soil with OM content >5%, we could say that of the surveyed plots 52.94% have high OM content (more than 5%) and 47.06% have low organic matter content (less than 5%). The moisture content varied from 14.14% to 57.49%. Despite of the fact that the soils in the quadrats are mostly fine or medium textured and the samples were taken in the very raining season, the moisture content of most of the samples was less than 50%; except for 2 quadrats which also appears to have 2 of the 3 highest OM content. So, according to the obtained data and using the soil moisture interpretation chart adapted from Harris and Coppock (1991), 88.23% of the sampled plots have *not enough available moisture* (50% or less) and 11.76% of the plots have *enough available moisture* (50 to 75%). The results also revealed that mostly high values of OM content corresponded with high values of moisture content and low values of OM corresponded with low values of moisture. In addition, coarse textured soil (ex. loamy sand) corresponded with lowest moisture and OM content. This means the moisture content and soil texture are correlated with the OM content and have impact on it; but its quantity could depend on other factors including the available dead material and the intensity of microbial activity.

Table 5: Soil moisture, PH, and organic matters content

Quadrat	Location	%Moisture content	PH	%Organic Matters
X1	T1QI	29.82	6.66	9.88
X2	T1QII	23.53	7.21	4.14
X3	T1QIII	14.14	6.67	2.84
X4	T1QIV	42.44	7.46	8.02
X5	T2QI	45.03	7.58	8.77
X6	T2QII	47.57	7.80	8.95
X7	T2QIII	23.65	5.25	4.45
X8	T2QIV	29.21	7.80	2.35
X9	T2QV	49.65	7.83	12.51
X10	T3QI	57.49	7.67	11.82
X11	T3QII	42.64	7.91	4.81
X12	T3QIII	35.32	7.41	6.80
X13	T3QIV	41.45	7.91	4.75
X14	T4QI	54.65	7.57	11.77
X15	T4QII	40.11	5.71	4.67
X16	T4QIII	30.70	7.87	4.36
X17	T4QIV	40.80	7.70	9.91

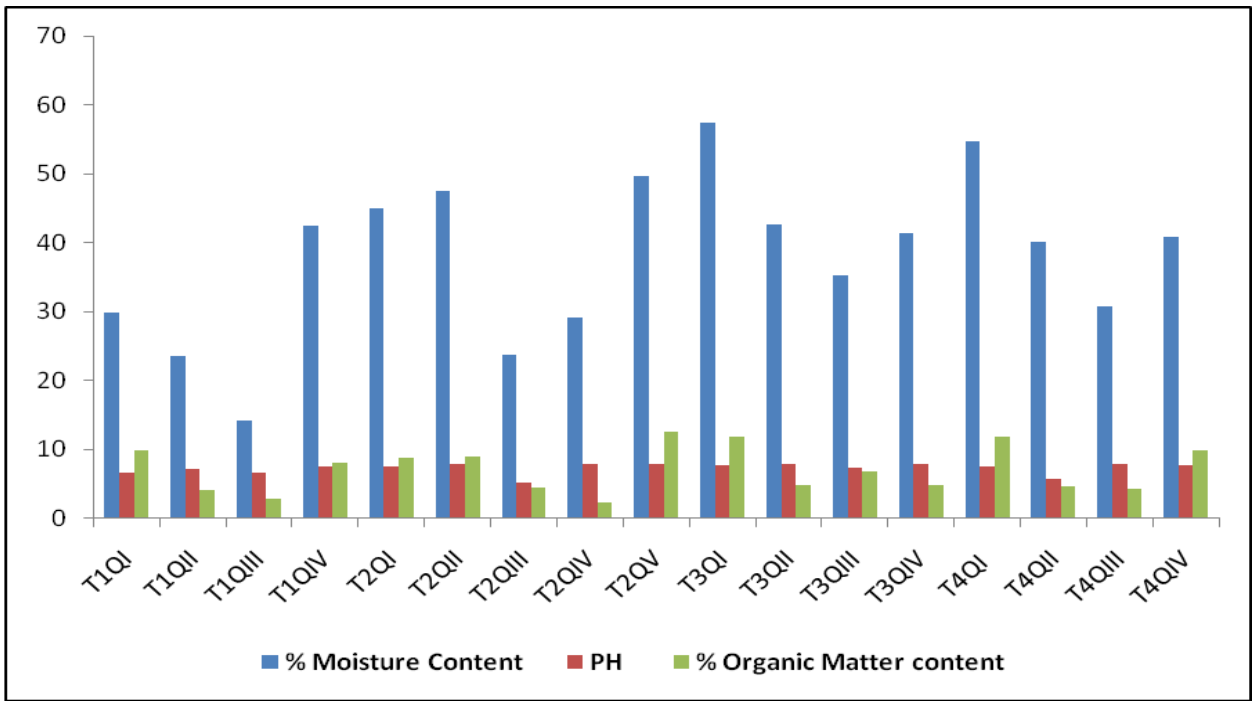

Figure 6: Three (3) chemical properties of surface soil from each quadrat

4. Discussion

4.1 Geological and soil characteristics significance for vegetation

The physical and chemical characteristics of karst geology and soil are of importance for plants species from the viewpoint of the karst ecosystem changeability. Analysis of 5 factors related to dolomite and calcite content, soil texture, moisture, OM content and PH, revealed some qualities of Longhushan soils upon which plants species depend. Maintaining these soil qualities in good conditions are important in the conservation of habitats and rare plants, because it was proved that soils have taken important role in karst processes and karst ecosystem (Li et al. 2004). According to the botanical species studied and the properties examined, it appears that the habitats in the quadrats are different depending on several factors including geological and ecological factors. Dolomite seems to be the factor that has some effect on species distribution. Because from the dominant canopy species identified, *Castanopsis indica*, *Pithecellobium clypearia*, *Sterculia lanceolata*, *Teonongia tonkinensis*, *Phlogancanthus curviflorus*, and *Sterculia euosma* were apt to live only in a high dolomite percentage; while *Cleistocalyx operculatus*, *Machilus salinina*, *Saraca chinensis*, *Wendlandia uvarifolia*, *Aesculus chinensis*, *Syzgium jambus*, *Liquidamber formosana* and *Hainania trichosperma* were apt to grow in a low dolomite percentage; although *Sterculia nobilis*, *Croton cavaleriei*, *Bischofia javanica*, *Albizia chinensis* were adapted in both situation (*table 3, table 6*). Also from the rare plant species collected, *Desmos chinensis*, *Habenaria ciliolaris*, *Mallotus philippinensis*, *Zenia insignis*, *Canthium dicoccum* and *Hartia sinensis* were found in a high dolomite percentage while *Camellia pubipetala*, *Garcinia paucinervis*, *Machilus salicina*, *Burretiodendron tonkinense*, *Malania oleifera* and *Hainania trichosperma* were collected in a low dolomite area.

On the other hand, dominant species and rare plants seem to have different response to the soil type, PH, moisture and OM content. But the suitability for plants of one characteristic in a quadrat may depend on other factors because all characteristics have correlation at some levels and impact plants' nutrients uptake. *Fine* and *medium* textured soil represent 75% of the studied area and *near neutral* to *moderately alkaline* PH represent 88.23%. The PH values classified as *near neutral* (for 5 quadrats) could be considered as the best conditions because in general, it is suitable for most plant and microbial species. While the quadrats with soil PH values *moderately acidic* (2quadrats) and *moderately alkaline* (10 quadrats) which represent both 70.58% of the surveyed plots may be subject to some nutrient deficiencies. In fact the significance of soil PH lies in its influence on nutrient availability for plants, cation exchange capacity, biological activities and on the solubility of toxic nutrient elements in soil. In extreme cases (strongly acidic or alkaline) toxic materials normally not available to plants become uptakeable. Also at high PH values, Phosphorus and most micronutrients tend to be

less available in soil while at low PH values it is the macronutrients which tend to be less available.

Soil varied in texture from fine to coarse but fine and medium textured soil being dominant could be considered as good up to a point. Because as the relative percentages of silt and/or clay particles become greater, properties of soils are increasingly affected. From *Table4 and Table5*, mostly finer-textured soils contain more OM, and have higher moisture content while sandy soils tend to be low in ability to retain moisture and OM content; which confirms the claims of Rasmussen and Collins (1991). However, when soils are so fine-textured as to be classified as clayey (which is the case for 6 quadrats), they are likely to exhibit properties which are somewhat difficult for plant to endure or overcome. Such soils have usually drainage problem and could be often too moist when wet or too dry when not for nutrient availability for plants; OM could play an important role in this kind of situation.

Despite of the high percentage of fine and medium textured soil and the sampling season, the moisture content was not very important in most of the quadrats which may be due to several other factors not examined in this study including canopy cover, ground cover, temperature, soil structure, elevation, slope… This means in the dry season, most of these species with the related microorganisms could suffer from a high water shortage. In *Table 5* and *figure 6*, mostly high moisture content corresponding with high OM content could mean that moisture has some effect on soil microorganism's activity, so on the amount of OM. Also from the 8 quadrats where rare plants were recorded, only 1 quadrat X14 had moisture content more than 50% (*enough available water*) and in this quadrat is located 1 rare plant (*Malania oleifera).* All the other 11 endangered species were collected in 7 quadrats which have *not enough available water* (*table5 and table6*). From the dominant canopy species, only 3 species were collected in plots with *enough available water*, the remaining dominant species were all located in *not enough available water* condition (*table5 and table6*). However, soil moisture is of primary importance because it impacts in general the distribution and growth of vegetation, soil aeration, soil microbial activity, soil erosion, the concentration of toxic substances, and the movement of nutrients in the soil to the roots.

The OM content varied from coarse to fine textured soils and was somewhat important according to the results. It appears that more than 50% of the studied area has a high level of OM, although the 47.06% which has a low level is not negligible. Because as the level of OM is reduced below 5 percent, many of the soil's natural and beneficial functions begin to diminish. Soils with very low OM cannot support the populations of beneficial organisms needed for very important functions that both feed and protect plants. The amount could be influenced by all soil forming factors like climate, vegetation, parent material, topography, age (Jenny, 1941). Soil OM also increases with increasing precipitation and decreases with increasing temperature; the benefits of higher soil OM and associated soil fauna are often mentioned in association with good soil: increased soil aggregation, improved drainage in fine textured soils, better water-holding capacity in sandy soils, higher cation exchange capacity, increased nutrient reserves, etc. This is an important soil characteristic in karst ecosystem as it appears to be the factor that could improve other properties like texture, moisture and PH for a good quality of soil or nutrient availability for plants growth. It is necessary to improve or protect conditions to maintain high levels of OM in the reserve because soil organic matter is a huge reserve of plants and microorganisms nutrients. Plant residues that cover the soil surface also protect the soil from sealing and crusting by raindrop impact, thereby enhancing rainwater infiltration and reducing runoff. The less the soil is covered with vegetation, mulches, crop residues, etc., the more the soil is exposed to the impact of raindrops; and increased soil cover reduces the impact of rain drops to the soil which results in reduced soil erosion rates very important in South China Karst areas. This is generally due to human encroachment (i.e. tourism), inappropriate land management, forest clearance, digging up plants, etc resulting in vegetation and soil loss. In fact in the reserve, anthropogenic impact was most important in 5 quadrats: X1, X5, X7, X14 and X15 and the OM content especially in X7 and X15 was among the low values. Quadrats X1, X5 and X7 were disturbed by primate behavior and tourist pressure, X15 was only disturbed by tourist behavior while X14 was disturbed by former plantation activities. These plots were located at low elevation and near the highway under passway and 2 of them (X1, X14) contain 2 endangered species respectively *Desmos chinensis* and *Malania oleifera* which is endemic and figures in the Red List. From the empirical observation based on former and recent studies, the greatest percentage of karst tropical secondary forest species in the reserve was at the advanced regrowth stage (Zang, 2008). But karst geochemical background is known to impact the release of some mineral nutrient elements in soil, so it is suggested that some mineral elements are deficient or less available in limestone soils for plant growth (Jianhua et. al 2004). Considering this fact in addition to the soil properties, we could say that vegetation formation or restoration may be a slow process in the area. The plant communities in general look evergreen with delimitation between arbor layers, shrubs and grasses. But anthropogenic and natural forces have

influenced the severity of disturbance events and the rate and mode of recovery processes within the forests. This was confirmed by Jianhua et. al (2004) in a study on karst ecosystem of Guangxi region who stated that: "without anthropogenic disturbance, the vegetation evolution is commonly from grass community, grass-bush community to arbor community. Therefore, it is suggested that the vegetation development constrained by the karst geological setting in Guangxi Zhuang Autonomous Region. i.e. it implies the plant growth and community evolution is slower in karst area than that in non-karst area".

Table 6: Dominant canopy species for the location of the rare plant species

Quadrat	Location	Rare plant species	Dominant canopy species
X1	T1QI	*Desmos chinensis*	*Castanopsis indica* *Pithecellobium clypearia* *Sterculia nobilis*
X2	T1QII	*Camellia pubipetala* *Garcinia paucinervis* *Machilus salicina*	*Cleistocalyx operculatus* *Croton cavaleriei* *Machilus salinina*
X3	T1QIII	*Camellia pubipetala* *Garcinia paucinervis* *Machilus salicina*	*Cleistocalyx operculatus* *Machilus salinina* *Saraca chinensis* *Sterculia nobilis* *Wendlandia uvarifolia*
X4	T1QIV	*Burretiodendron tonkinense*	*Aesculus chinensis* *Sterculia nobilis* *Syzgium jambus*
X5	T2QI	-	*Bischofia javanica* *Liquidamber formosana*
X6	T2QII	*Habenaria ciliolaris* *Mallotus philippinensis* *Zenia insignis*	*Bischofia javanica*
X7	T2QIII	-	*Croton cavaleriei* *Pithecellobium clypearia* *Sterculia lanceolata* *Sterculia nobilis*
X8	T2QIV	-	*Albizia chinensis* *Sterculia lanceolata*
X9	T2QV	-	
X10	T3QI	-	*Bischofia javanica* *Sterculia nobilis*
X11	T3QII	-	*Albizia chinensis* *Sterculia nobilis*
X12	T3QIII	-	*Albizia chinensis* *Bischofia javanica*
X13	T3QIV	-	*Albizia chinensis* *Sterculia nobilis* *Teonongia tonkinensis*
X14	T4QI	*Malania oleifera*	*Liquidamber formosana*
X15	T4QII	-	*Phlogancanthus curviflorus* *Sterculia nobilis*
X16	T4QIII	*Canthium dicoccum* *Hartia sinensis*	*Sterculia euosma* *Teonongia tonkinensis*
X17	T4QIV	*Hainania trichosperma*	*Hainania trichosperma*

4.2 Importance of rare plant species protection in Longhushan reserve:

To talk about rare plant species importance in Longhushan, it is relevant to insist on the benefit of plants in general in this area because these endangered plants are important not only as species at risk of being lost but also as plant species in an environmental fragile system. In general, in covered karst the vegetation covers the limestone. This has two important effects on the geology: vegetation produces CO_2 in the earth, which fastens the corrosion (dissolution) of limestone. The growth of caves is faster than in bare karst. On the other hand, the vegetation covers the limestone from the air, so there is much less erosion depending on weather.

Plants are also essential to wildlife because all living species, including people, depend on other species for survival. Other than the plant species in Longhushan, faunal assemblage was dominated by the primate, Rhesus macaque or *Macaca mulatta* a near threatened species whose home range is determined by the quality of vegetation and the rhesus population density (Jiang et. al 1991). But also several different species of snail, snake, butterflies, spiders, worms, birds, insects,… were observed. Through mutual adaptation, plants meet the exact food and shelter needs of wildlife and wildlife-plant relationships are often extremely specialized.

Plants are essential to ecosystem function in the reserve because they build soil which is deficient in karst areas, then soil stores water and mediate floods (Daily et. al 1997). Soil produces the foods we eat and the commodities we use (Mueller et. al 1974), as karst soils are known with a low productivity and the local population in the area very poor. Plants help ecosystems reduce flooding by facilitating water infiltration into soil, reducing runoff, and through absorbing and transpiring water (Wilson et. al 2001). Plant roots, shoots, and foliage also reduce erosion by holding soil in place and softening raindrop impact (Myers, 1997) which also might be a very important factor in karst area for the prevention of rock desertification.

Plants produce valuable commodities; they are reservoirs of genes that may be useful for the production of medicines and other commodities, for the maintenance of food supplies, or for ecosystem survival. South China is known for its richness in medicinal plants and besides, several plant species including some endangered plants recorded in the reserve have medicinal properties. The United Nations Environmental Program (UNEP, 1995), in its Global Biodiversity Assessment based on contributions by more than 1500 scientists stated that: it is clear that the loss of biodiversity has serious economic and social costs. The genes, species, ecosystems and human knowledge that are being lost represent a living library of options available for adapting to local and global change. Therefore, all life as well as the quality of life depends on plants.

Plants provide invaluable aesthetic and recreational benefits, they afford pleasure and relaxation to many people, and provide a source of inspiration in most art forms; they are the most visible elements of ecosystems. Longhushan reserve is all valleys and mountains, the area view from the summits gives a green peak cluster land form around a valley crossed by a green river (*Figure 1 and Figure 4*). The entire tourism activities in the reserve depend on the landscape view and its biodiversity. Tourism is also the most important activity in the locality and supports most of the local people jobs.

Rare species conservation is central to biodiversity conservation; Longhushan is located in Guangxi, one of the key tropical forest areas of southern China. Guangxi has more species of rare plants than any other province of China and Longhushan reserve, as a microcosm of Guangxi, reflects this rich diversity. In this study, from the plant species recorded, 12 were identified as endangered among which six are included in the IUCN red list for endangered species and three are endemic to China. The importance of these biological resources cannot be overestimated not only for China which is a leading center of biodiversity, but also for the global biodiversity conservation. As three of the endangered species are not found anywhere else but China and one of these three (*Camellia pubipetala*) is known only from Long'an (the study site county) and Daxin county, just next to Long'an. Moreover, with the presence of rare and endemic plant species, the fragility of the karst ecosystem, human and tourism impact including: primate damage, facilities, habitat fragmentation by small roads (*Figure 7, Figure 8*) there is a tendency of habitats destruction which leads to species extinction. Whereas these endangered species can only survive if their habitat is protected. Efficient conservation planning for the protection of rare plants is often overlooked as a result of lack of understanding of their ecological and biological importance. This is often the case where threatened tropical and subtropical species are concerned. As Raven, 1993 stated: Of all the global problems that confront us, this is the one that is moving the most rapidly and the one that will have the most serious consequences. And, unlike other global ecological problems, it is completely irreversible. Many question the importance of maintaining biodiversity in today's world, where conservation efforts prove costly and time consuming. The fact is that the preservation of all species is necessary for human survival and diversity of life and living systems are a necessary condition for human development

(Ishwaran et. al 2005). Species should be saved for aesthetic and moral justifications, the importance of wild species as providers of products and services essential to human welfare, the value of particular species as indicators of environmental health or as keystone species crucial to the functioning of ecosystems, and the scientific breakthroughs that have come from the study of wild organisms (Wilcove et. al 2008). In other words, species serve as a source of art and entertainment, provide products such as medicine for human well-being, indicate the welfare of the overall environment and ecosystem, and provide research that results in scientific discoveries. So, endangered species could prove to be useful to human development, maintenance of biodiversity and preservation of ecosystems.

Rare species are also indicators of endangered ecosystems; species are rare because the ecosystems they inhabit are unusual or degraded. In fact, in the reserve most of the rare plant species are endangered because of cutting and habitat clearance, overexploitation and lack of sufficient regeneration, logging and habitat loss. Rare species, therefore, are not isolated entities, but indicators of larger problems. Rare species help us determine which habitats require special conservation attention if a native biological diversity is to survive.

Rare species may perform valuable functions; with their habitats, they must also be conserved because more often than not, we do not know what critical functions they may perform, now or in the future. They may provide essential ecosystem services. They may be reservoirs of genetic diversity that will maintain sustainable food and commodity production. They may be required for other species or ecosystems to survive climate change or disturbances such as flood, fire or disease. A U.S. Forest Service fact sheet on biological diversity stated: the extinction of even a single plant species may result in the disappearance of up to 30 other species of plants and wildlife (USDA, 1993).

So Longhushan reserve, despite of its smallness could also be an interesting spot and open natural laboratory for researchers, students or other scientists to study botanical species including rare plant species, biological diversity, karst forest sustainable management, karst ecological system and the geomorphological interaction with vegetation formation.

Figure 7: Small roads through the forest

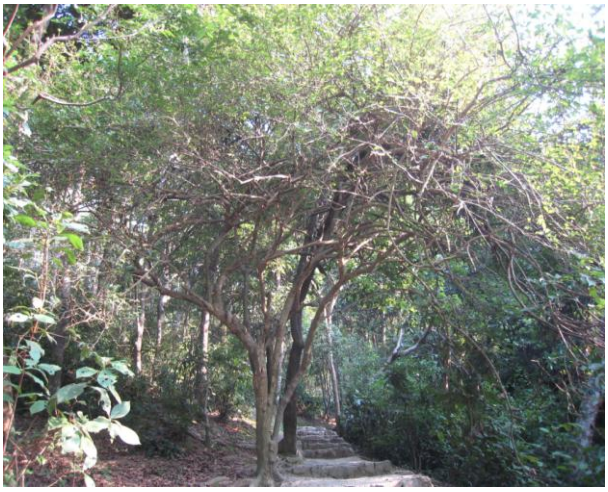

Figure 8: Primate Damage to the plants

5. Measures to avoid, minimize, and/or mitigate impact on rare plants survival:

Longhushan reserve, despite of its status as a natural reserve, might be not well known in term of wild and endangered species because there is very little record from previews studies. The field survey carried out for this research did not cover all the reserve, yet 12 endangered plants species were collected, which means there could be more. So before any measure can be taken, there is a need to implement a general survey of the reserve in order to record its faunal and floral species and identify all the species that are threatened or endangered of extinction. Then those species could be added to the Guangxi list of threatened and endangered species for its global monitoring and sustainable management strategies. Some of the main factors that cause species to become endangered in the area are habitat destruction and overexploitation. Habitat destruction is also known as the single greatest threat to species around the globe. Because destruction

of habitat is now the principal cause of endangerment, habitat protection is the only effective way to save plants from extinction. The consequence of habitat protection is also a reduction in flooding with a corresponding reduction in soil erosion, ensuring survival of viable forests. It was noted in fact in the reserve that 2 quadrats X2 and X3 located on the banks of the Green River where vegetation has been cut to facilitate tourists' activities, were flooded every monsoon season. Soil, microorganisms and plants live together in a natural system with interdependence; conditions for improved functioning of this system must be facilitated and protected. In Longhushan this system is already fragile as shown by the results because of the karst geological and ecological background. So reducing human impact including deforestation, forest fragmentation, tourists' access to the forest or any other practices that can also influence the long-term buildup or depletions of soil OM, must be priority in order to maintain or improve habitats, geological and soil properties, vegetation cover. A crucial measure for the success of habitat conservation plan is the choice and implementation of measures to avoid, minimize, and mitigate impacts on the species. Therefore, the first step in Longhushan could be to conserve significant habitat areas within the reserve which means identifying which species are in danger of extinction throughout all or part of their range and adding them to the endangered species list. Species must be placed on the endangered species list if one or more factors put it at risk, including habitat destruction or degradation, overutilization. The reasons for rarity or scarcity must then be identified and controlled or eliminated. Key plant populations must be protected. This can require fencing, Invasive plant control, Planting native plants, ongoing research, propagation and reintroduction, biological monitoring/documentation, and educational meetings with the local people. A research and monitoring program for rare and threatened plant can also be elaborated upon, so once the extent of a plant species' distribution and population numbers are determined, a recovery plan can be developed to ensure the plant's survival. But protecting only one population is not a viable option as it could be destroyed by a catastrophe such as a cyclone or fire. Protecting several populations of a species is essential. Without genetic variation, a species becomes weak and more susceptible to other threats. Reforestation of deforested parts of the reserve for example the river side and former plantations is also necessary for soil erosion control. Other important factors can be also considered directly or indirectly as cause of plant species endangerment in the reserve: an important primate population with their damaging activities to the environment, important tourism activities, insufficient law enforcement of protected areas, and lack of monitoring and management plan for sustainability. In order to preserve habitat without endangering rare and vulnerable plant species, the following measures can also be undertaken:

- Ascertain and correct any inconsistency in the primate population data;
- Improve skills in primate censoring and monitoring by the reserve's staff;
- Understand the rate of high human impact through encroachment and tourism;
- Sufficient law enforcement of the protected areas;
- Monitoring and management for sustainability;
- Ascertain forest status for various habitat areas.

The plant species recorded in surveyed quadrats as endangered and endemic species require already special protection. More attention should be paid to maintaining their habitats at a high level of conservation as required; in order to keeping them from tourist access, habitat fragmentation by construction of roads for example or any other land use planning perspective, so as to protect those species. The primate population overloads vegetative community carrying capacity and tourism development also beyond the current environmental carrying capacity. So the primate population overloaded with the tourism development need to be addressed in relation to the vegetative community and the current environmental carrying capacity. Both problems should be under control in order to limit these impacts on the forest. Forbidding further felling and plantation activities in the reserve, the training of local people in the knowledge of keeping an ecological balance and further public awareness in order to encourage tourists to protect the existing forest is essential.

Note that Plant conservation is a long-term task especially in karst environment, with strategic significance. It is important for conservation of biodiversity and maintenance of a balanced ecosystem. In addition to the above measures, there still could be other research work to be carried out in the reserve. For instance, the ecology and reproductive biology of certain rare plant species could be further studied whereas advanced techniques on propagation of rare plants could be explored. These important tasks to succeed need the support of reserve managers, local academics and scientific researchers.

4 - Conclusion

Many research have been conducted in southern China concerning protected areas, karst ecosystem and biodiversity, but not much attention has been paid to small Nature Reserves like Longhushan. This study is significant not only because it contributes to the literature of the importance of plant protection including rare plant species in Longhushan karst

environment, but also because it provides some evidence of karst ecosystem's fragility and the reserve's soil characteristics significance on the vegetation. Considering these characteristics per quadrat and the diversity of species, we could say that in Longhushan each karst environment is unique due to its localized conditions, geological and soil properties, former and current land use practices, climatic and micro-climatic conditions, hydrological and geomorphologic status. Soil erosion extremely faster than soil formation, soil moisture-short and mineral elements deficient or les available are the main factors impacting plants growth in karst area; so to avoid or minimize any practices that could trigger these factors must be a priority. Dolomite content appears to be the factor which played a part in the species distribution although other factors like elevation, aspect,... not analyzed in this study could also be significant environmental factors determining plant community and dominant species distribution. While the rare plants and dominant species responded differently to soil type, PH, moisture and OM content. All these characteristics of the karst environments create significant ecological niche differences across elevation gradients which need special attention for a better conservation of biodiversity, especially for endangered species for which habitat protection is fundamental for their survival. So, considering the sensitivity of the karst ecosystem and all the geological and soil properties, the vegetation formation or restoration once destroyed must be a slow and difficult process; because karst areas have a typical thin soil and vegetation deficient in nutritive elements, very sensitive to anthropogenic disturbance**s.** The vegetation cover is considerable in the reserve which makes it even more special and deserves close attention for their protection knowing that many plant species are endangered in the reserve and several southern China karst areas are now threatened by rock desertification.

Therefore, rare plant species must be conserved so that Longhushan ecosystems can continue to provide the ecosystem services that drive the Guangxi economy and enhance the quality of life. We all depend upon plants and wildlife. From studying them, we have learned new ways of growing foods, making clothing, and building houses. If we fail to protect threatened or endangered species, we will never know how they might have improved our lives. The potential for economic and material benefit is unlimited and we have barely begun to exploit the wealth of useful products contained in wild plants. At this early stage, we cannot afford to let plants become extinct - once lost, a species can never be recreated. Plants are a part of our natural heritage - a heritage that we have an obligation to preserve for the benefit of future generations of mankind.

Acknowledgments

This research was made possible by a grant and logistical support of the "Green Research" project lead by Prof. J. Ellis Burnet who provided valuable advice over the course of the research, and reviews that greatly improved the manuscript. I would like to particularly acknowledge her generous help and support to conduct this study. I am also grateful to Liang Ming Zhong (John) in Guangxi Normal Education University, Nanning, who shared his views on the environmental issues in Longhushan during the study for his help with the field work, data collection and his great care all along the survey.

Correspondence to:

Dado Toure

China University of Geosciences (Wuhan)

School of Environmental Studies

Lumo Lu, Wuhan, Hubei 430074, China

Cell phone: 0086-27-62521159; 0086-15972993853

Email: touredado@yahoo.fr

References

1. CBW (ChineseBusinessworld.com), Guangxi Province. Available on: http://www.cbw.com/general/gintro/guangxi.html
2. Daily GC, Matson PA, Vitousek PM. *Ecosystem Services Supplied by Soil*. In: Daily GC, Ed. Societal Dependence on Natural Ecosystems. Nature's Services. Washington DC: Island Press. 1997.
3. Ellis Burnet J, L Shen, Mbue I. *The Impact of Plantation Species on a Karst Neo-tropical Restoration Forest, Guangxi Zhuang Minorities Autonomous Region, China*. A field report on the Formation and Evolution of Karst Secondary Forests in Guangxi. 2008. School of Environmental Studies, China University of Geosciences (Wuhan) & Institute of Karst Geology, Guilin.
4. Ellis Burnet J, Lina S, Mingzhong L, Jing M, Chen C, Yang A, Liao X, Zheng F, Xu P. *An Overview of the Synecology of Longhushan and Nongla Forests*. A field report on the Formation and Evolution of Karst Secondary Forests in Guangxi. Green Search 2008; China University of Geosciences (Wuhan) and Institute of Karst Geology, Guangxi Normal Education University.
5. Harris RW, Coppock RH (eds.). *Saving water in landscape irrigation*. Oakland, CA University of California. Division of Agriculture and Natural Resources. Publication University of California (System); 2976. 1991.

6. Hartz TK. *Soil Testing for Nutrient Availability. Procedures and Interpretation for California Vegetable Crop Production*. University of California. Vegetable Research and Information Center, 2007; 1-7.
7. Ishwaran N, Erdelen W. *Biodiversity Futures.* Frontiers in Ecology and the Environment 2005; 3(4):179.
8. Jiang H, Liu Z, Zhang Y, Southwick C. *Population ecology of rhesus monkeys* (*Macaca mulatta*) *at Nanwan Nature Reserve, Hainan*. China.Am. J. Primatol 1991; 25: 207–217.
9. Jianhua C, Daoxian Y, Cheng Z, Zhongcheng J. *Karst ecosystem constrained by geological conditions in Southwest China: Relationship between carbonate rock exposure and vegetation coverage*. Earth and Environment, 2004; 32(1):212-218.
10. Jenny, H. 1941. Factors of soil formation. McGraw-Hill, New York, NY.
11. Li W, Yu LJ, Yuan DX, Xu HB, Yang Y. *Bacteria biomass and carbonic andhydrase activity in some karst areas of Southwestern China*. Journal of Asian Earth Sciences 2004; 24 (2):145-152.
12. Montagnini F, Sancho F. *Impacts of native trees on tropical soils*: *a study in the Atlantic Lowlands of Costa Rica*. Ambio, 1990; 19: 386-390.
13. Morton J. *Endangered Plants*. The Canadian Encyclopedia. Historica Foundation of Canada. Available on: http://www.thecanadianencyclopedia.com/index.cfm
14. Mueller DR, Ellenberg H. *Aims and methods of vegetation ecology*. New York. John Wiley and Sons. 1974.
15. Myers N. *The World's forests and their ecosystem services.* In: Daily GC, Ed. Societal Dependence on Natural Ecosystems. Nature's Services. Washington DC: Island Press. 1997.
16. Rasmussen PE, Collins HP. Long-term impacts of tillage, fertilizer, and crop residue on soil organic matter in temperate semiarid regions. Advances in Agronomy, 1991; 45:93-134.
17. Raven P. Missouri Botanical Gardens. Former Home Secretary of the National Academy of Sciences (USA). Former President of the American Association for the Advancement of Science. 1993.
18. United Nations Environment Program (UNEP). *Global Biodiversity Assessment*. New York, NY. Cambridge University Press. 1995.
19. USDA Forest Service. *Every Species Counts: Conserving Biological Diversity*. Program Aid 1499. Washington DC. USDA Forest Service. 1993.
20. US National Academy of Science (US NAS). *Science and the Endangered Species Act*. Washington, DC. National Academy of Science. 1995.
21. Watters, Lawrence, Xi, Wang. *The Protection of Wildlife and Endangered Species in China*. Spring 2002; 14(3): 489-524.
22. Wilcove DS, Master LL. *How Many Endangered Species are there in the United States?* Frontiers in Ecology and the Environment 2008; 3(8):418.
23. Wilson EO, Perlman DL. *Conserving Earth.s Biodiversity CD ROM*. Washington, DC. Island Press. 2001.
24. Yardley J. *China's Turtles, Emblems of a Crisis*. New York Times 2007; Choking on Growth Part VI. Available on: http://www.nytimes.com/2007/12/05/world/asia
25. Zang RG, Ding Y. *Ecological restoration of tropical forest vegetation*. Acta Ecologica Sinica 2008; 28 (12):6292-6304.
26. International Union for Conservation of Nature and Natural Resources (IUCN). 2006. 2007. 2008. *IUCN Red List of threatened species*. www.iucnredlist.org.
27. USDA Natural Resources Conservation Service 2003. http://plants.usda.gov/java/profile?symbol=CICA
28. Kadoorie Farm and Botanic Garden. 2002. *Report of a Rapid Biodiversity Assessment at Mulun National Nature Reserve, North Guangxi, China*. South China Forest Biodiversity Survey Report Series: No. 13
29. Kadoorie Farm and Botanic Garden. 2002. *Report of a Rapid Biodiversity Assessment at Fusui Rare Animal Nature Reserve, Southwest Guangxi, China*. South China Forest Biodiversity Survey Report Series: No. 12.
30. Kadoorie Farm and Botanic Garden. 2002. *Report of a Rapid Biodiversity Assessment at Heweishan Forest Farm, Southwest Guangdong, China*. South China Forest Biodiversity Survey Report Series: No. 6.
31. Wikispecies.2007. *Free species dictionary*. http://species.wikimedia.org/wiki
32. Zipcodezoo, http://zipcodezoo.com/Plants/
33. NLBIF Biodiversity Data Portal http://www.nlbif.nl/species_details.php?tab
34. Flora of China, http://www.efloras.org/florataxon.aspx?flora http://flora.huh.harvard.edu/china/mss/alphabetical_families.htm#T

3/20/2010

BIOMIMETIC SYNTHESIS OF GUIDED-TISSUE REGENERATION HYDROXYAPATITE/POLYVINL ALCOHOL NANOCOMPOSITE SCAFFOLDS: INFLUENCE OF ALIGNATE ON MECHANICAL AND BIOLOGICAL PROPERTIES.

E. TOLBA[1], B. M. ABD-ELHADY[1], B. ELKHOLY[1], H.ELKADY[2],M. ELTONSI[3]

[1.] Biomaterial Department, National Research Center, Cairo, Egypt.
[2.] Civil Engineering Department, National Research Center, Cairo, Egypt.
[3.] Physics Department, Faculty of science, El-Mansoura University, El-Mansoura, Egypt
hala.elkady@gmail.com

Abstract: This paper presents a part of a major research, in which HA/PVA/alginate scaffolds -with different alginate compositions -up to 20wt% were fabricated by a modified freeze-extraction method. This method includes the physical cross-linking of PVA and chemical cross-linking of the alginate. Characterization of the prepared scaffolds was performed by morphology observations using scanning electron microscopy (SEM). Different physical properties – as porosity and density-were measured. It was noticed that by increasing alginate composition scaffolds exhibited highly porous, open-cellular pore structures with almost porosity about 90%, regardless of alginate composition and the pore sizes from about 150 to about 300μm.The In Vitro bioactivity and biodegradability of nano-composite scaffolds were investigated by incubation in simulated body fluid (SBF) and water under osteoclastic resorption conditions, respectively. The in-vitro bioactivity test indicating the higher bone-bonding ability of the biomimetically synthesized a scaffold that is awarded by the fast formation of bonelike apatite on their surfaces within one day. Also The addition of alginate to HA/PVA scaffolds increased the biodegradability compared with that one without alginate. Mechanical behavior of scaffolds was investigated under axial loading. Scaffolds stress strain behavior, maximum true stress, and elastic moduli, were calculated. It was found that increasing alginate content from 0 to 20% by weight, decreased the compressive modulus from 85.3 to 44.7 MPa, whereas the maximum compressive strength decreased from 6 to 5 MPa. Finally, it was concluded that the proposed scaffolds expressed promising performance, despite of the resulting degradation in their mechanical behavior. The obtained compressive strength and modulus of elasticity were still within satisfactory limits. [Journal of American Science 2010;6(7):239-249]. (ISSN: 1545-1003).

Keywords: Tissue re-generation, Poly(vinyl), composites, scaffolds

1. Introduction

One of the main goals in bone tissue engineering is to develop biodegradable materials as bone graft substitutes, especially for filling large defects [1-3]. Besides bone forming cells and growth factors, synthetic biomaterials served as scaffolds play a critical role in bone tissue engineering and osteogenesis. They provide a three dimensional (3-D) space for cell growth and extracellular matrix (ECM) formation, and structural support for the newly formed bone tissue. The ideal synthetic scaffolds for osteogenesis should meet certain criteria to serve this function, including good biocompatibility, sufficient mechanical properties, and adequate biodegradability at a controlled rate commensurate with remodeling [4, 5]. Being the major mineral component of natural bone and structurally similar to the bone, hydroxyapatite (HA) is the prospective one of inorganic biomaterials for bone regeneration[6,7]. HA ceramics were high biocompatible in bone tissue and had a high osteogenic potential (osteo-conduction and osteo-integration), but the brittleness and fatigue failure in the body limit their clinical applications only for unloading bearing repair and substitute [8, 9]. This fact restricts the use of these materials in a wide range of applications. One alternative that is being considered and studied is the production of composites and hybrid systems. Hence, the development of composite materials is regarded as a promising approach for preparing bioactive scaffolds [10]. Composites, which include synthetic and biological polymers with HA, have the potential capability of combining bioactive behavior with adequate mechanical properties.

Among several choices of polymers, poly(vinyl alcohol) (PVA), a water-soluble polyhydroxy

polymer, has been frequently explored as an implant material in biomedical applications such as drug delivery systems, dialysis membranes, wound dressing, artificial skin, cardiovascular devices and surgical repairs because of its excellent mechanical strength, biocompatibility and non-toxicity [11,12]. PVA is considered as a biologically friendly material but with some reduced integration to living tissues due to its relative limited biodegradability and bioactivity, compared to poly(ethylene oxide) (PEO), poly(lactic-co-glycolic acid) (PLGA) and others. Therefore, it is promising to blend PVA with biopolymers such as alginate to produce a new polymeric system applicable for a variety of purposes [13]. In order to overcome the limited biological performance of synthetic polymers and to enhance the mechanical characteristics of biopolymers, a new class of specially designed materials, 'bioartificial polymeric materials', has been introduced [14]. These materials based on blends of both synthetic and natural polymers such as alginate could be usefully employed as biomaterials. Alginate, a polysaccharide derived from brown seaweed, has been widely utilized as cell carriers since the 1970s [15] due to the simplicity for fabricating cell-immobilized beads or 3D porous scaffolds, low price compared to proteins or other natural polymers and non-toxicity to cells. It is also approved by the Food and Drug Administration (FDA) for human use as wound dressing material and food additive. The alginate, the monovalent salt form of alginic acid is a linear block copolymer composed of *β*-D-mannuronate (M-block) and *α*-L-guluronate (G-block) linked by 1,4-glycoside linkage [16]. The G-block of alginate has correspondingly high affinities for divalent ions such as calcium (Ca2+), strontium (Sr2+) and barium (Ba2+) at room temperature and thus in an aqueous solution of divalent ions, the alginate chains are rapidly cross-linked *via* the stacking of G-blocks to form an egg-box structure and subsequently become gel [17].

In our previous work, HA/PVA nanocomposite was synthesized by using biomimetic method and subject to freeze extraction technique in conjugation with liquid descant drying regime to obtain the three dimensional HA/PVA scaffolds[18]. The resultant scaffolds exhibit a high interconnectivity and maximum pore size of 150 µm, indicating preferred morphology for tissue engineering application.

In the presented study, a series of HA/PVA/Alginate scaffolds with 0, 5, 10 and 20% alginate were fabricated by freeze extraction method followed by chemical cross-linking of alginate. The porosity, pore size, mechanical property of the scaffolds was investigated as functions of alginate content. In addition, the in vitro bioactivity and biodegradability of nano-composite scaffolds were investigated by incubation in simulated body fluid (SBF) and water under osteoclastic resorption conditions, respectively. The emphasis of this study was placed on the development of a novel scaffold suitable for hepatic tissue-engineering application.

Mechanical properties of a scaffold are important both for integrity during handling and implantation, and for support of tissue subject to load during healing. Measures to improve mechanical properties without sacrificing other properties (biocompatibility, osteoconductivity) are thus highly desirable. There are numerous reports in literature describing the improvement of the mechanical properties of polymers by adding bioactive inorganic materials, such as hydroxyapatite (HA). As with the modulus, it is natural for the strength of the scaffold to increase with increasing volume fraction of the filler content, especially if there is strong interaction between the matrix and the filler. A careful literature survey has shown that polymer/HA composites are complex systems [27-29].

2. Experimental procedure for scaffolds manufacturing.

2.1. Materials

Through out the entire preparation part of the work, double distilled water as well as the following reagent-grade chemicals were used calcium hydroxide [$Ca(OH)_2$],BDH-Laboratory,England; ammonium dihydrogen phosphate($NH_4H_2PO_4$), MERCK, Germany; PVA with an average molecular weight of 124,000 and degree of hydrolysis 98 - 99%, Loba Chemie, India. Sodium alginate (also called algin or alginic acid sodium salt) from Sigma (USA). Ammonia solution (NH_4OH) (33%), absolute Ethanol and pure Acetone, El Nasr Pharmaceuticals and Chemicals Co. Egypt.

2.2. Samples preparation

2.2.1. Synthesis of HA/PVA/ alginate gels

HA/PVA/alginate gels with different alginate compositions (0, 5, 10, and 20 wt %) were fabricated by using the freeze extraction method. Making a deviation from our early employed post precipitation technique, including freeze extraction method (18), the present study involves chemical cross-linking of alginate extracted gels. In brief, Sodium alginate was easily soluble in cold water. Then, the solution was added to the synthesized HA/PVA mix solution. The mixture was then left under stirring for approximately 4 h at room temperature until a completely homogenous solution was obtained. After each the mixture solutions were poured in cylindrical Teflon vials. The freeze extraction step was used necessary to obtain the

physically coherent gels having the ability to keep their original shape (mold shape) before alginate cross-linking. The obtained gels were then immersed in 5 wt% $CaCl_2$ solution for 12 h to chemical cross-linking of alginate with calcium ions. The resultant gels with 0, 5, 10 and 20% alginate were designated by the abbreviations AHP, 5AHPG, 10AHPG and 20AHPG, respectively.

3. Samples characterization

3.1. Bulk density and apparent porosity measurement

The bulk density and apparent porosity of the porous scaffolds were measured by using the Archimedes' principle [19]. This method is based on soaking the samples under kerosene for 2hrs in a vacuum desiccator to saturate their open-pore structure with the latter. The weight of saturated sample suspended in kerosene (Wi) and its saturated weight in air after removal of kerosene film from outer surface (Ws) were recorded. Triplicate measurements were carried out to obtain their mean values. Bulk density (D) and apparent porosity (P) were calculated according to the following equations (1):

$$D=\frac{W}{(Ws-Wi)}x\rho$$

$$P=\frac{(Ws-W)}{(Ws-Wi)}x100\% \qquad (1)$$

ρ= specific gravity of kerosene (0.78).

3.2. Morphological observations

Morphological observation of the resultant scaffolds was preformed by Philips XL 30 Scanning Electron Microscope (SEM) with an acceleration voltage of 30 kV. Whereby specimens were cut from liquid nitrogen-treated (frozen) scaffold to avoid disturbing of the pore structure. Specimens were placed on a stub using a carbon sticker and were examined under the microscope after the samples were sputtered with a thin coat of gold.

3.3- Axial Compression Mechanical test

3.3.1-Instrumentation and test setup

A universal (SHUMADZU) testing machine was utilized to conduct the compression mechanical test. A computer-controlled module monitored and controlled the entire testing. Input and output data were recorded related to compression test using the machine acquisition system. Three specimens were cast for each of the investigated scaffolds: $AHP_{10\text{-}6}$, and $20AHPG_{10\text{-}6.}$ Dimensions of each sample were measured prior to testing. Averages of measured dimensions are 16 and 14 mm (diameter and height respectively.) Tests were conducted in room temperature. The crosshead speed was set at 0.5 mm/min.

3.4 (In-Vitro Test):

3.4.1- Water-binding capacity testing

The dry scaffolds ($AHP_{10\text{-}6}$, $5AHPG_{10\text{-}6}$, $10AHPG_{10\text{-}6}$ and $20AHPG_{10\text{-}6}$) were immersed were placed in a small bottle containing 20 ml water (pH 7.4) and incubated at 37°C for 24h. The water binding capacity (expressed as a percentage) was calculated by comparing the initial weight (W_0) with the wet weight after swelling (W_1), as shown in Equation (2). Three individual experiments were performed, and then the average value was gained.

$$\text{Water - binding capacity} = \frac{W1-Wo}{Wo}x100 \qquad (2)$$

3.4.2- Biodegradation testing

The in-vitro biodegradation study of the resultant scaffolds ($AHP_{10\text{-}6}$, $5AHPG_{10\text{-}6}$, $10AHPG_{10\text{-}6}$ and $20AHPG_{10\text{-}6}$) was carried out under the conditions of osteoclastic bone resorption, i.e. at a pH of about 4.5 in order to simulate the general remodelling of the skeletal system (20). Samples were immersed into water (100 ml each) at pH 4.5 and temperature 37 °C. The pH was checked and adjusted at regular intervals (2 h). If the pH was increased due to neutralization of the basic calcium phosphate, 0.001 N HNO_3 was added in order to maintain an average pH of 4.5. The samples were taken out after 72 h and weighed after being dried. The biodegradation was monitored as the change in sample weight over time. Weight loss was calculated by comparing the initial weight (W_0) with the mass measured at a given time point (W_2), as shown in Equation 2. Three individual experiments were performed, and then the average value was gained:

$$\text{Weight loss} = \frac{W2-Wo}{Wo}x100 \qquad (3)$$

3.4.3- Bioactivity testing

Standard in vitro bioactivity test was carried out to evaluate the formation of an apatite layer onto the surface of the samples. In order to study the bioactivity, the samples were soaked in simulated body fluid (SBF) which was proposed by Kokubo et al. [21] at 37 ºC and pH 7.4 for several periods of times (1, 2, 4 and 8 days**).** The specimens were removed from the SBF solution and were abundantly rinsed with water in order to remove the soluble inorganic salts and to stop the reaction.The formation and elemental composition of the bioactive layer were characterized using Philips XL 30 Scanning Electron Microscope (SEM) with an acceleration

voltage of 30 kV coupled with energy dispersive X-ray analysis (EDXA) detector with an accelerating voltage of 20 kV.

4. Results

4.1.Morphological observations

The extracted gels were dried via liquid desiccant method. The result indicating that there was a great improvement in the shrinkage values with the chemical cross-linking of alginate with Ca^{2+} ions (Figure 1). As experimentally found the alginate gels attained a level of 62% and 51% for 5 and $10AHPG_{10\text{-}6}$ gels, respectively, much more than $20AHPG_{10\text{-}6}$ one, which shrunk by an amount of 38% as shown in Table (1). The density and porosity of the obtained scaffolds are presented in the same table. Results revealed that the porosity of the alginate scaffolds varied
from 69.9% to 89.7% depending on the percentage addition of alginate. This indicates that the rigid structure of alginate formed by chemical cross-linking tends to regulate the overall pore size as well as the interconnectivity of the HA/PVA scaffolds. On the other hand, the density of the scaffold exhibited a downward trend with alginate addition. Regarding the physical property values quoted in Table (1), it goes without saying that there is a complete agreement between them. Saying in practical terms, as the shrinkage decreases the porosity and pore size substantially increase, meanwhile the density decreases greatly.

The alginate-containing scaffolds were prepared by freeze extraction method followed by chemical cross-linking in $CaCl_2$ solution, displayed different pore morphology, as judged by SEM examination. Figure (2) depicts the SEM images of alginate scaffolds taken at two different magnifications (50× and 800×). This may be due to The G-block of alginate has correspondingly high affinities for divalent calcium ions. The resultant porous structure was found to be comprised of directionally organized pores and the pore size increases with alginate addition. The pores appear to have an elongated shape. The alginate chains appear to be orderly mineralized with HA nano-particles that cover the flat area of the polymeric ribbons which are organized in a network. A further increase of alginate causes the formation of a typical egg-box structure which is the result of anisotropic growth of isomorphological molecular units [13]. It can be seen that, the alginate-containing scaffolds have tubule-like oriented pore structure, whereas their diameter, wall thickness, and structure regularity are different. With increase in alginate content, the regularity of the oriented pore structure of the scaffold was improved. For the $20AHPG_{10\text{-}6}$, the diameters of the tubule-like macropores reached 300 μm, formed well shape conjugations by regular arrayed organization, as shown in Figure (2). There was a systematic increase in the number and size of these egg-box structures with increasing the alginate contents.

4.2. Mechanical characteristics

Figure (3) presents one of the samples during the compression test, and samples shape after compression test was conducted. Some differences in failure patterns were noticed. The barrel shape resulting from friction is clear in sample 3. As for sample 1 and 2 homogenous compression is noticed, and slight compressive instability at the edges due to work-softening of material

Using engineering stress- strain relationship did not seem convenient for such highly deformable material. So load versus displacement were captured from the output acquisition system, to be interpreted into true stress- strain curve for each tested sample. The following equations were applied to obtain true stresses and strains, taking in consideration the actual dimensions of the sample at each captured result:

Compressive true stress=load × $(h_0\text{-}h)$ /vol of sample,
Compressive true strain=lnh_0 /h

Where: h_0=initial thickness, and h=instantaneous thickness during compression.
Figure (4) presents the average true stress =strain curves for investigated scaffolds.

Straightening out (re-arrangement) in material is noticed at the first non-linear zone of all the curves. The next part is the elastic portion of the curve to be used in calculating the Young's modulus of the material (Table 2). This Linear zone located between 0.02 to 0.09 strains. Non-linear plastic zone extended from 0.07 strains till end of test, indicating matrix degradation towards failure. Maximum average true stress for sample $AHP_{10\text{-}6}$ was 6 MPa, while that for sample $20AHPG_{10\text{-}6}$ was 5Mpa.

4.3- (In-Vitro Test):

4.3.1 Water-binding capacity

Figure 5 shows the water binding capacity of the AHPG scaffolds with different alginate content. It can be observed that after 1 day of immersion, compared with HA/PVA scaffold, the water content of all the alginate scaffolds increased with the introduction of alginate, which contains negatively charged carboxylic and hydroxyl groups that can form hydrogen bonds with water. A mass increase of 320% is observed for $AHP_{10\text{-}6}$ scaffolds, while for $AHPG_{10\text{-}6}$ scaffolds, this increase ranges

from 356% to 443%. In additions, the water binding ability of the scaffolds gradually increases with further increase of alginate contents due to the increase in porosity. This result agrees with the results of the porosity analysis (Table 1).

4.3.2 Biodegradation test

Figure (6) shows the relative weights of the obtained scaffolds after 72 h in osteoclastic resorption conditions (pH=4.5) [20]. It can be observed that the rate of weight loss of the scaffolds increased with alginate additions. Among the four scaffolds, it can be seen that the scaffold with a 0 wt% alginate had a lowest weight loss rate, while the scaffolds with 20% alginate had a highest rate owing to the highest porosity and also the water binding capacity.

4.3.3 Bioactivity behavior

The $AHP_{10\text{-}6}$ and $20AHPG_{10\text{-}6}$ scaffolds were subjected to the in vitro bioactivity test. The two types of scaffolds showed same biomineralization behaviors in SBF. Figure (7) shows the SEM micrographs of the porous HA/PVA composite scaffolds after 1, 2, 4 and 8 days of immersion in SBF. After 1day immersion, a lot of tiny apatite crystals deposited on the surface of the specimens, as shown in Figure 7-b. The particles formed in vitro have a near-spherical shape. Except some large particles with a diameter of about 1–2μm, reflecting the nucleation of new mineral particles. After a longer immersion (e.g. 8 days), a more compact mineral layer was found on the samples surfaces (Figure 7-d). As reported in other study [22], the Ca–P nucleus formed on the surface of biomaterials increased both in number and coalesced with an increase in immersion time and as a consequence of particle growth from the nuclei formed at different times, there was a wide size distribution. The average particle diameter, density (number of particles per unit surface area), and total apatite mass increased with incubation time. They attributed the nucleation and growth of mineral layer on the surface to the enhanced water-uptake capability of the HA induced by the presence of polymer in the nanocomposite[23].

The presence of Ca and P was confirmed by the EDX analysis of the newly formed crystals on the AHP (Figure 8). The Ca/P peak intensity ratio was 1.5, which might be indicative of the presence of a Ca-deficient apatite. This Ca–P deposition is of greater biological interest than stoichiometric HA since the Ca/P ratio in natural bone is lower than 1.67 [24].

5. Discussion

In this study, 3D porous HA/PVA/alginate scaffolds with different alginate compositions (up to 20 wt %) were prepared from the HA/PVA/alginate mixture solutions by freeze extraction and the following chemical cross-linking of alginate. The ultimate porous morphology of a scaffold, including pore size, pore shape, porosity, mechanical and biological properties was affected by alginate addition. The mixture solutions did not show any phase separation for the mixing ratios used in this study owing to their good compatibility. The freeze-extraction step before alginate cross-linking was necessary to keep the original shape of the mixture gel disk, where the freeze-extraction process induces the physical cross-linking of polymer chains by the hydrogen bonding [13]. Hydrogen bonding is thought to be the directional interaction that causes a physical cross-link to form in the gel. The latter was then chemically cross-linked in $CaCl_2$ solution to form interpenetrating networks, as demonstrated in Figure (9).

From SEM observations, it can be seen that the scaffolds dried via liquid desiccant method exhibit the interconnected macroporous network with interconnected pore diameter of 150–300 μm. Generally, for the ideal scaffolds for bone tissue regeneration, the macropore diameter and the macropore interconnections should be larger than 100 μm [25]. If the diameters of these interconnected macropores are not large enough, tissue in-growth and vascularization will not occur efficiently In Vivo and the damaged tissue cannot be fully regenerated [26]. Most of the researchers have found that the pores between 100 μm determine osteoid growth and the pores larger than 100 lm facilitate proliferation of cells, vascular in-growth, and internal mineralized bone formation. Therefore, here these $AHP_{10\text{-}6}$ and $AHPG_{10\text{-}6}$ scaffolds have suitable macroporous structure to allow cell migration, bone ingrowth and vascularization.

The difference in the processing technique, the degree of porosity and interconnectivity of the pores in the scaffolds are some of the factors which may have contributed to the variations in the mechanical properties of the scaffolds. In the present study, the decreased compressive strength values can be attributed to presence of macropores within the scaffold; it is well known that it is difficult to achieve high compressive strength for porous materials because of the negative effects of the porous structure. So it is reasonable in this case that the compressive strength and modulus decreased with the growth of scaffold's porosity.

The degradation of the prepared scaffolds at osteoclastic resorption conditions, increased with decrease in alginate content due to the increase in

obtained porosity. These in-vitro results suggested the possibility of preparing scaffolds with different degrees of solubility for the needs for different applications. The scaffold with higher alginate composition have higher water uptake. This event may be attributed to the hydrophilicity of alginate. The scaffold with more alginate composition suffered from greater weight loss because the higher water uptake causes faster degradation of the scaffold. In this context, When the HA/PVA and alginate containing composites implanted in body using as tissue scaffold, the degradation of the composite makes room for the growth of new bone and then is substituted by new bone completely. Moreover, the surface of composite is hydrophilic; this was also confirmed by the rate of water binding capacity, which can facilitate cell adhesion, proliferation and differentiation [25]. So the obtained scaffolds, used as bone substitutes, are hopeful to activate the regeneration and remodeling of bone tissue.

The formation of HA is regarded as the essential requirement for implanted materials to bond to bone in the living body. It has been widely accepted that SBF can well reproduce the in vivo surface changes of certain biomaterials. Many factors affect the nucleation and growth of Ca–P in the SBF solution. The results imply HA particles were rapidly formed on the surface of the scaffolds during SBF soaking. This may be due to the enhanced water-uptake capability (increasing of hydroxyls groups) of the composite induced by the addition of PVA and alginate. This kinetics difference of surface structural change indicating the higher bone-bonding ability of the biomimetically synthesized HA/PVA and alginate containing scaffolds that is awarded by the fast formation of bone-like apatite on their surfaces within one day.

The obtained compressive strength of $AHP_{10\text{-}6}$ (contain 70wt% HA) was 6 MPa. Whereas the alginate-containing ($20AHPG_{10\text{-}6}$) possessed a compressive strength of 5MPa Comparing the obtained results with Sinha et al. [30] who conducted a study on the fabrication of HA/PVA scaffolds for tissue engineering applications using the freeze thawing technique, though their attempts to improve the mechanical properties of the porous scaffolds by incorporating HA. The obtained results show an enhancement in the compressive strength from 2.5MPa to 21.0MPa, for samples comprising 25wt, 40wt and 50wt% HA.

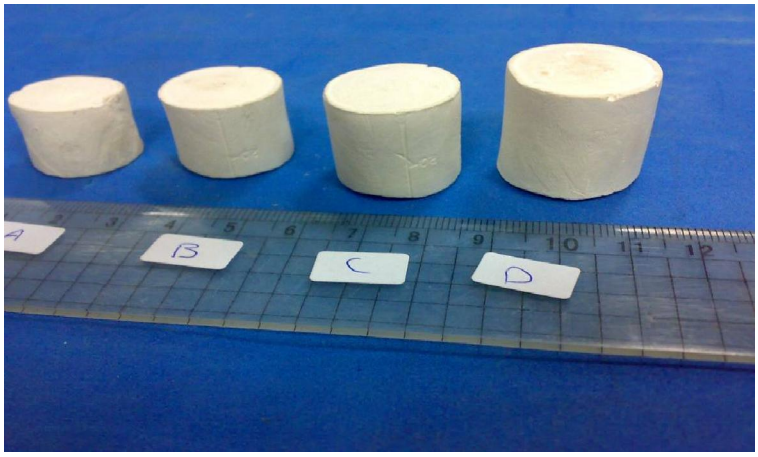

Figure (1). Photographs of scaffolds (a) AHP (b) 5AHPG (c) 10AHPG (d) 20AHPG.

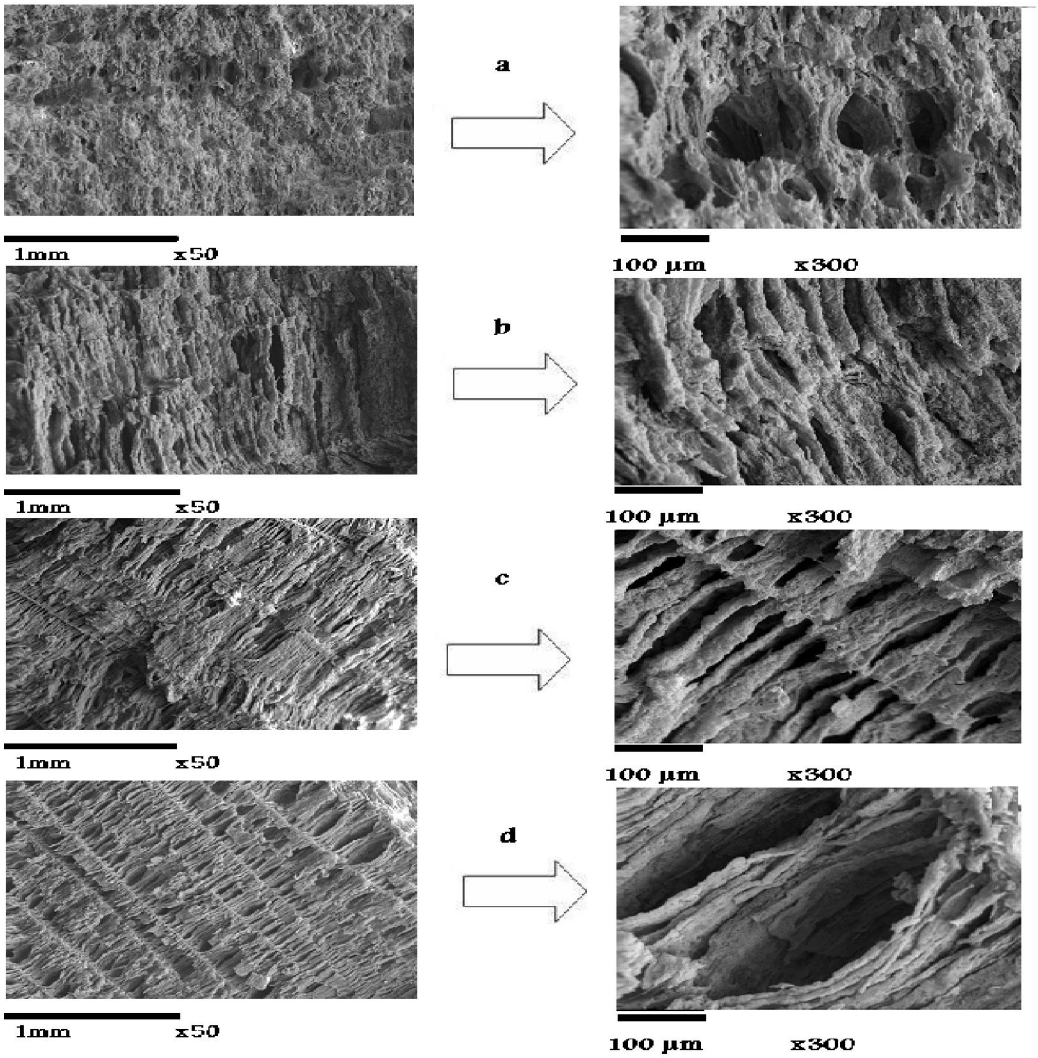

Figure (2). SEM micrographs of resultant scaffolds (a) AHP (b) 5AHPG (c) 10AHPG (d) 20AHPG.

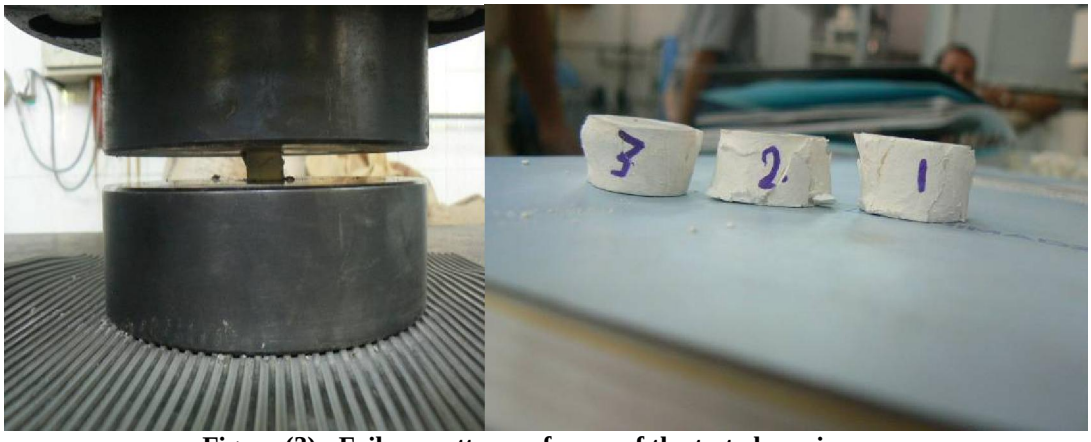

Figure (3): Failure patterns of some of the tested specimens.

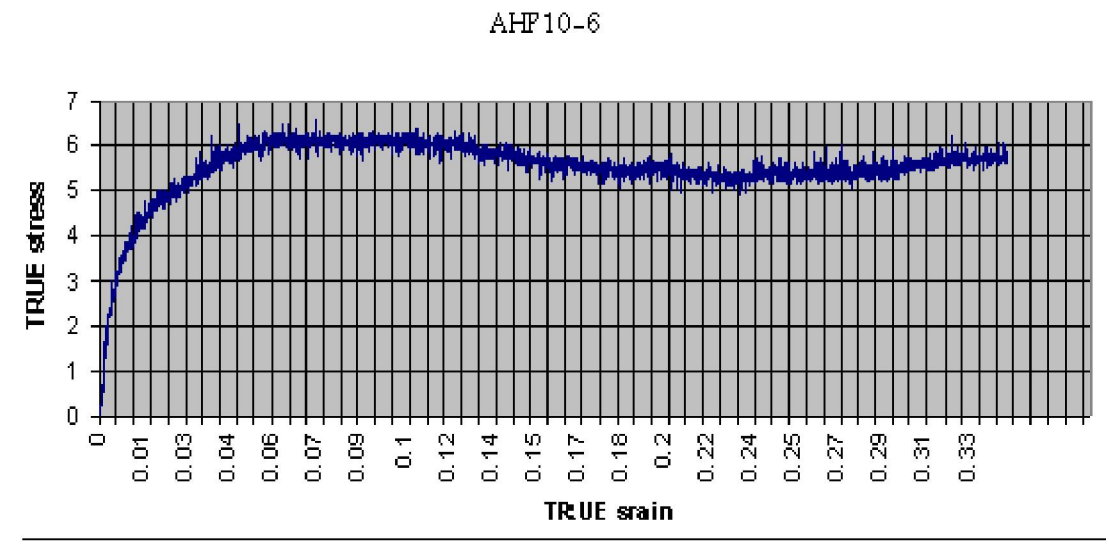

Figure (4): True stress- strain curves of tested scaffolds.

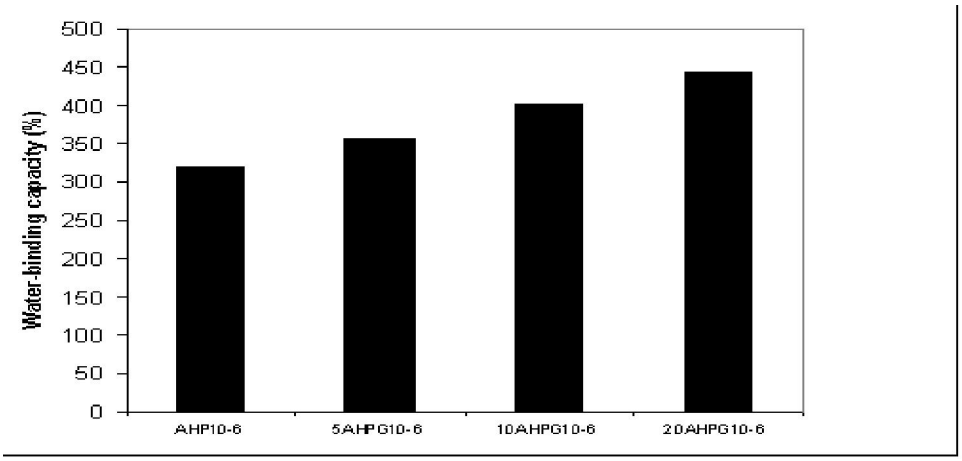

Figure (5). Water binding capacity of resultant scaffolds after one day of immersion in water.

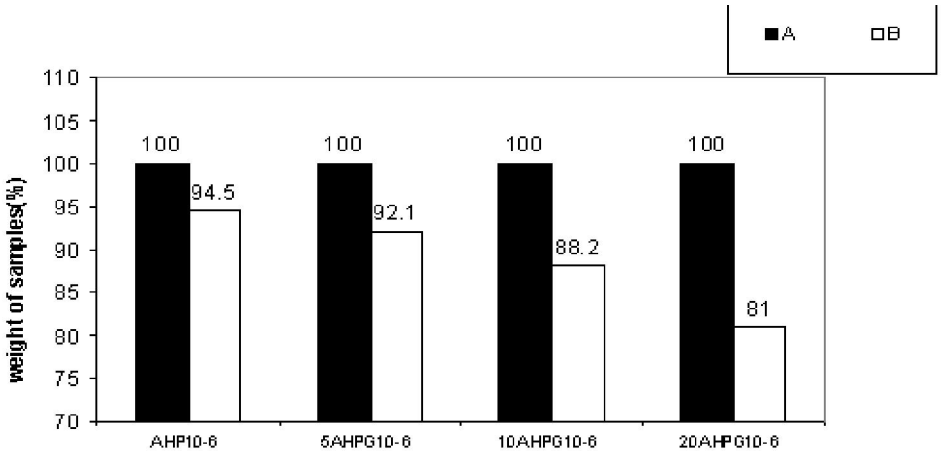

Figure (6). Biodegradation of scaffolds in water pH = 4.5 (simulation of osteoclastic resorption). A, 0 h. B,72 h.

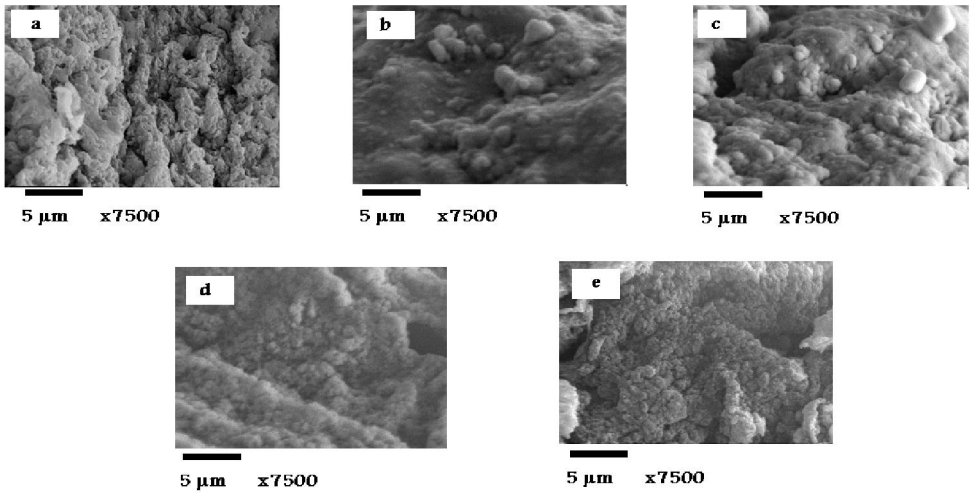

Figure (7). Morphology of the porous AHP_{10-6} scaffolds after immersion in SBF for different periods, observed by SEM: (a) 0, (b) 1, (c) 2 (d) 4 and (e) 8 days.

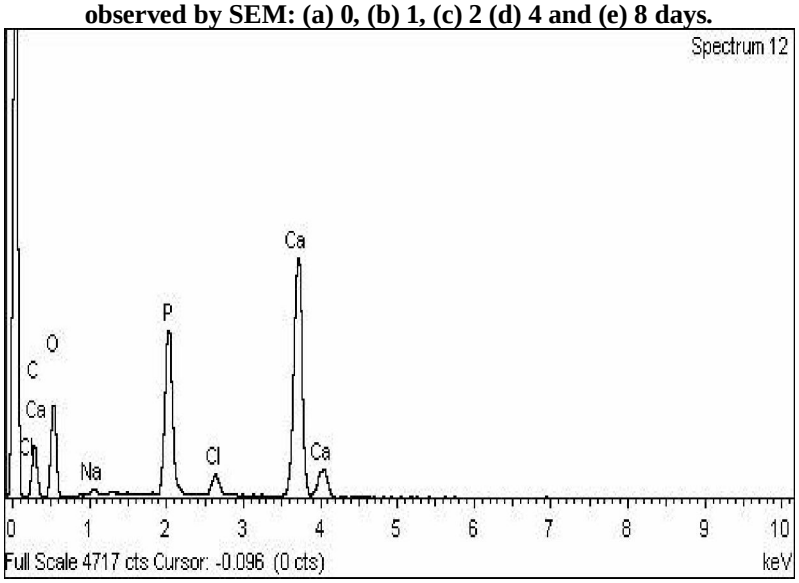

Figure (8). EDX analysis of the AHP_{10-6} scaffold after immersion in SBF for 4 days.

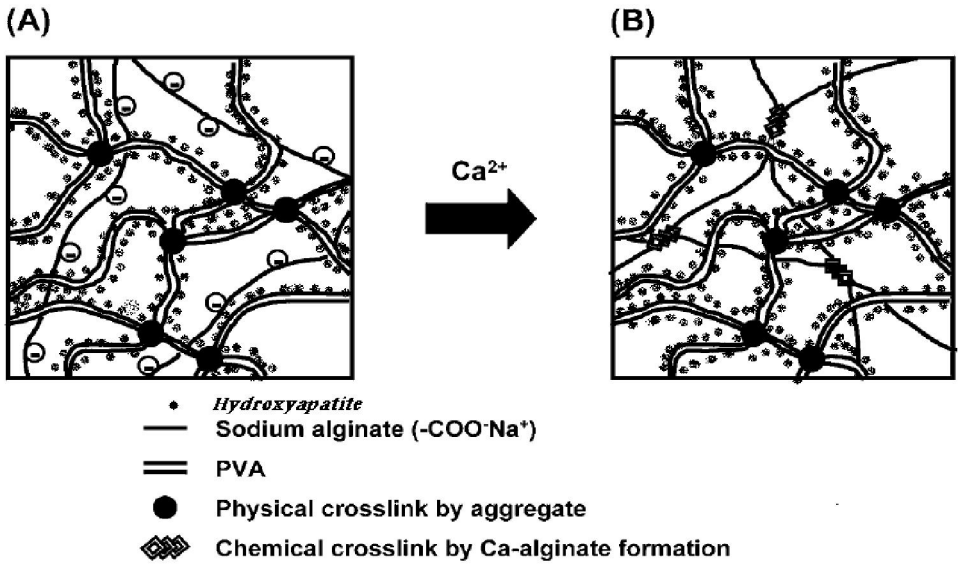

Figure (9): (a) physical cross-links of PVA chains by freeze extraction and (b) the following chemical cross-links of sodium alginate chains by $CaCl_2$.

Table (1). Density, Porosity and Related properties of the fabricated HA/PVA and alginate scaffolds.

Samples designation	Density (g/cm^3)	Porosity (%)	Maximum pore size (µm)	Degree of pores interconnectivity	Shrinkage (%)
AHP_{10-6}	0.89	62.3	150	medium	70
$5AHPG_{10-6}$	0.75	69.6	150	High	62
$10AHPG_{10-6}$	0.61	75.1	200	High	51
$20AHPG_{10-6}$	0.48	89.7	300	High	38

Table (2). Maximum compressive strength and elastic modulus of the resultant scaffolds along with cancellous bone.

Samples designation	Maximum compression strength (MPa)	Elasticity modules (MPa)
AHP_{10-6}	6	85.3
$20AHPG_{10-6}$	5	44.7
Cancellous bone	2 - 12	50 - 500

6. Conclusions

- A series of characteristic interconnected open pore microstructures with pore sizes ranging from 150 to 300 microns were fabricated by a modified freeze-extraction method including the physical cross-linking of PVA and the following chemical cross-linking of alginate.
- The porosity of the scaffolds was found to vary from 62.9% to 89.7% depending on the percentage addition of alginate. This indicates that the rigid structure of alginate formed by chemical cross-linking tends to regulate the overall pore size as well as the interconnectivity of the scaffolds. On the other hand, the density of the scaffold exhibited a downward trend with alginate addition.
- The compressive strength of spongy bone is in the range of *2–12MPa*. Hence, the measured compressive strength *(5-6 MPa)* of the present scaffolds falls in this range.
- In-vitro water binding capacity and biodegradation studies, clearly demonstrates that

it is possible to fine-tune the biodegradation and correspondingly the biological lifetime of the scaffolds by varying the alginate contents ratios. The characteristics of the resultant nanocomposite scaffolds indicating that the addition of alginate provided a more promising scaffold for tissue engineering applications.

- A biologically active apatite layer forms within a short period on composite scaffolds after its immersion in SBF, demonstrating high *in vitro* bioactivity of the composite.
- The goal of an ideal scaffold that provides good mechanical support temporarily while maintaining bioactivity and that can biodegrade at later stages at a tailorable rate is achievable with the developed alginate containing scaffolds.

7- Acknowledgement

The authors wish to thank The National Research Center of Egypt, for facilitating this fruitful co-operation between both departments, which facilitated the investigation of the proposed scaffoldings from different aspects.

8- References

[1] B.D. Ratner, S.J.Bryant., Annu Rev Biomed Eng (2004); 6:41-75.
[2] A. Atala , Exp Opin Biol Ther (2005); 5(7):879-92.
[3] J.M Pachence, J. Ln Kohn, RP Lanza, R. Langer, J. Vacanti, Principles of tissue engineering. San Diego: Academic Press; (2000).
[4] E.L.Chaikof, et al, Academic Science (2002); 961:96-105.
[5] D.W. Hutmacher, Biomaterials Jr. (2000); 21:2529–43.
[6] W. Suchanek, M. Yoshimura, J Mater Res (1998); 13:94–117.
[7] R.Z. LeGeros, P.W.Brown, B. Constantz, editors. Biological and synthetic apatites. Boca Raton: CRC Press; (1994).
[8] M. Jarcho,. Clinical Orthop Relat Res (1981); 157:259–78.
[9] T. Kitsugi, T. Yamamuro, T. Nagamura, S. Kotani, T. Kokubo, H.Takeuchi,., Biomaterials Journal (1993); 14:216–24.
[10] S. Yang, K.-F. Leong, Z. Du, C.-K. Chua, The design of scaffolds for use in tissue engineering. Part I. Traditional factors, Tissue Eng. 7 (6) (2001) 679–689.
[11] T. Yamaoka, Y. Tabata, Y. Ikada, Comparison of body distribution of poly(vinyl alcohol) with other water-soluble polymers after intravenous administration, J. Pharmaceut. Pharmacol. 47 (1995) 479–4
[12] A.P.V. Pereira, L.V. Wander, R.L. Orefice, Novel multicomponent silicate–poly(vinyl alcohol) hybrids with controlled reactivity, J. Non-Cryst. Solids 273 (2000) 180–185.
[13] S S. H. Cho et al. J. Biomater. Sci. Polymer Edn, (2005) Vol. 16, No. 8, pp. 933–947.
[14] M.G. Cascone, N. Barbani, C. Cristallini, P. Giusti, G. Ciardelli, L. Lazzeri, Bioartificial polymeric materials based on polysaccharides, J. Biomater. Sci. Polym. Edn. 12 (3) (2001) 267–281.
[15] M. Kierstan and C. Bucke, Biotechnol. Bioeng. **19**, 387 (1977).
[16] K. Nilsson, W. Scheirer, O. W. Merten, L. Ostberg, E. Liehl and H. W. D. Katinger, Nature **302**, 629 (1983).
[17] L. Shapiro and S. Cohen, Biomaterials 18, 583 (1997).
[18] E. Tolba.; B. Abd El-Hady; M. El-Tonsy, and B. El-Kholi, Egypt. J. of Appl. Sci., 24(12B) 2009.
[19] ASTM Designation: (2000). C 20-92.
[20] N. Rameshbabu, K.P. Rao., Current Applied Physics 9 (2009) S29–S31
[21] T. Kokubo., H.Kim., M. Kawashita, H. Takadama.,T. Miyazaki, M. Uchida,. And T. Nakamure, Glastech. Ber. Glass Sci. Tech. (2001); 73: 247-254.
[22] I.B.Lonor, A. Ito, K.Onuma, Kanzaki N, R.L.Reis,Biomaterials 2003; 24:579–85.
[23] D.Z. Chen et al, .Composites Science and Technology 67 (2007) 1617–1626.
[24] T. Kobayashi, S. Nakamura, K. Yamashita, J Biomed Mater Res 2001; 57:477–84.
[25] K. J. Burg, S. Porter, J. F. Kellam, Biomaterials 2000, 21, 2347.
[26] S.F. Hulbert, F.A. Young, R.S. Mathews, J.J. Klawitter, C.D. Talbert, F.H. Stelling, Potential ceramic materials as permanently implantable skeletal prostheses, J. Biomed. Mater. Res. 4 (3) (1970) 433–456.
[27] S. Rammelt, T. Illert, S. Bierbaum, Biomaterials 27 (2006) 5561.
[28] J. Zhao et al, . Colloids and Surfaces B: Biointerfaces 74 (2009) 159–166.
[29] QI. Xiaopeng, YE. Jiandong,W. Yingjun,. JR. Biomed Mater Res (2009) 89A: 980–987.
[30] A. Sinha et al, Materials Science and Engineering C. (2007), 27, 70–74.

Chlorpyrifos (from different sources): Effect on Testicular Biochemistry of Male Albino Rats.

Afaf, A. El-Kashoury* and Hanan, A. Tag El-Din**
* Department of Mammalian and Aquatic Toxicology, Central Agricultura Pesticides Laboratory, Agricultural Research Center, Giza, Egypt.
** Chemistry Department, Hormonal Lab., Animal Health Research Institute, Dokki, Giza, Egypt.
drofscience@ymail.com

Abstract

Organophosphates are known primarily as neutrotoxins. However, reactive oxygen species (ROS) caused by organophosphates may be involved in the toxicity of various pesticides. Therefore, in this study we aimed to investigate the toxic effects of three trade names of chlorpyrifos (CPF) pesticide, from different local manufactures [chlorozan (K) pestpan (W) and pyriban (H)] on testicular weight , testicular oxidative stress and some testicular biochemical parameters in male albino rats. **Methods:** Three compounds (K, W and H) were administrated orally to rats at dose of 23.43, 21.40 and 17.43 mg/kg b.w., respectively (which represent the 1/4 LD_{50}) with 5 doses per week for 28 days. Twenty-four hours after the last treatment the rats were sacrificed using anesthetic ether. Testes were collected , cleaned and weighed. Right testes were fractionated and supernatant of testicular homogenate was obtained by centrifugation, lipid peroxidation (LPO), total glutathione, activities of alkaline and acid phosphatases, lactate dehydrogenase and total protein were measured. Moreover, the left tests were histologically examined. **Results:** The testes weights were significantly decreased in (W) group only. Chlorpyrifos treatments (K, W and H) alter markedly the testicular lipid peroxidation (LPO) levels, while, the decline in the total glutathione (GSH) was occurred only in (W and H) groups, in comparing with the control group. Also, there was significant decrease in the activities of alkaline and acid phosphatase (ALP and ACP) and lactate dehydrohenase (LDH) in all treated groups. Total protein (TP) level exhibited an elevation in testicular tissue in comparison with the control group. Treatment-dependent histopathological changes were seen in testes of CPF-W group only. **Conclusion:** Chlorpyrifos (CPF) alters testicular functions possibly by induction of testicular oxidative stress and inhibition of the activities of marker enzymes, thereby disrupting male reproduction. [Journal of American Science 2010;6(7):252-261]. (ISSN: 1545-1003).

Keywords: Chlorpyrifos; rats; lipid peroxidation; total glutathione; acid and alkaline phosphatase; lactate dehydrogenase; total protein ; tests.

1- Introduction

The widespread use of organophosphorus insecticides (OPIs) has long been shown to exert deleterious effects on living organisms. For instance, the exposure of laboratory animals to OPIs, in particular to chlorpyrifos [O, O-diethyl – O -(3, 5, 6-trichloro- 2- pyridyl) phosphorothionate], elicits a number of effects including hepatic dysfunction **(Gomes *et al.*, 1999 and El-Kashoury and El-Said, 2007)**, ciliotoxicity **(Swann *et al.*, 1996)**, immunological abnormalities **(Blakley *et al.* , 1999)**, genotoxicity **(Song *et al.* , 1998)** and testicular damage **(Joshi *et al.* , 2007)**.

Chlorpyrifos was introduced to the Egyptian market, since thirty years at least recently over ten trade names are available in the market but the most common used are the previous mentioned trade names (K, W & H), commonly used to control cotton pests.

Organophosphorus pesticides exert their biological effects mainly through electrophilic attack of cellular constituents with simulataneous generation of reactive oxygen species (ROS). ROS may be involved in the toxicity of various pesticides **(Dwivedi *et al.* , 1998)**.

Malondialdehyde (MDA) is a marker of membrane lipid peroxidation resulting from the interaction of ROS and the cellular membrane **(Aslan *et al.*, 1997)**. The final membrane damage can lead to a loss of cellular homeostasis by changing the membrane characteristics **(Swann *et al.*, 1991)**. ROS are produced by univalent reduction of dioxygen to superoxide anion (O^-_2), which in turn disproportionates to H_2O_2 and O_2 spontaneously or through a reaction catalyzed by superoxide dismutase (SOD). Endogenous H_2O_2 may be converted to H_2O either by catalase or glutathione peroxidase

(GSH-Px). Otherwise, it may generate a highly reactive free hydroxyl radical (-OH) via a Fenton reaction, which is responsible for oxidative damage. GSH-Px converts H_2O_2 or other lipid peroxides to water or hydroxy lipids, and during this process glutathione (GSH) is converted to oxidized glutathione **(Bachowshi *et al.*, 1997)**.

Virtually, no available literatures concerning the comparison of the toxic effects of the three trade products of chlorpyrifos (K, W and H) on the testicular toxicity, therefore, the present study is an effort aimed:

1- To investigate the adverse effects of three trade names of chlorpyrifos on oxidative status.
2- To verify the effect of subacute exposure to chlorpyrifos on the activity of specific enzymes that responsible of spermatogenesis (ALP, ACP and LDH), TP level in testicular tissue of male rats and the histopathology of the testes.

2-1- Materials

Three trade names of chlorpyrifos active ingredient, 48 % EC., (an organophosphorus group), locally formulated in Egypt and were used in this study:
First: Trade name chlorzan (K), obtained from Kafr El-Zyat Co.
Second: Trade name pestban (W), obtained from El-Watania Co.
Third: Trade name pyripan (H), obtained from El-Helb Co.

2-2- Preparation of the dose:

Each emulsifiable concentrate (EC) was emulsified in water immediately before use and orally administrated to animals by esophageal intubation (per os).

The calculated median lethal dose (LD_{50}) of the three trade names of chlorpyrifos (K, W and H) were 93.75, 85.58 and 71.13 mg/kg b.w., respectively, according to Weil's method **(Weil, 1952)**.

Sub-acute dose, represents 1/4 LD_{50} for each emulsifiable concentrate was diluted in water and used for dosing through experimental priod.

2-3- Animals:

Male albino rats weighting 150 $\pm$ 10 g obtained from the farm of General Organization of Serum and Vaccine (Helwan Farm), Egypt, were used for the study. The animals were housed in plastic cages and allowed to adjust to the new environment for a week before starting the experiment. Rats were fed standard food pellets and tap water ad *libitum*. The rats were housed at 23 $\pm$ 2ºC and in daily dark/light cycle.

2-4- Experimental design:

Animals were randomly divided into four groups of twenty animals each as the following: Group-C: animals served as control group and given tap water instead of pesticide in parallel to the treated group. Group-K: animals were given CPF-K at 23.43 mg/kg b.w. Group-W: animals were given CPF-W at 21.40 mg/kg b.w. Group-H: animals were given CDF-H at 17.83 mg/kg b.w.

Each rat was given orally repeated dose of chlorpyrifos over period of 28 days (5 doses / week). Clinical signs were monitored daily and animals were weighed twice weekly throughout the experiment and the dose was adjusted accordingly.

2-5- Sampling

After completion of treatment period (28 days), five animals from each group were anaesthetized with ether and sacrified. The testes were removed immediately, cleaned of adhering tissues and weighed. The right testes were kept in a deep freezer (-40ºC) for biochemical estimations. Left testes were removed and fixed in 10 % formaline for routine histopathology.

2-6- Biochemical estimations:

Frozen testes were washed with saline solution, then minced and homogenized (10 % w/v) in ice-cold saline, using a chilled glass-teflon porter-Elvehjem tissue grinder tube. Te homogenate was centrifuged at 10,000 Xg for 20 min. at 4ºC and the resultant supernatant used for determination of lipid peroxidation (LPO) which is represented by malondialdehyde (MDA), total glutathione (GSH), alkaline phosphatase (ALP), acid phosphatase (ACP) and total protein (TP). Also, a 10 % homogenate of testes was prepared in ice-cold 0.1 M phosphate buffer, the homogenate was centrifuged at 12,000 Xg for 30 min. at 4ºC, the supernatant used for determination of lactate dehydrogenase (LDH). The different assays were carried out using diagnostic kits (Table 1).

Table (1): Procedures adopted for biochemical parameters in the testicular tissues.

Parameters	Reference
Lipid peroxidation (LPO)	**Ohkawa *et al.* (1979)**
Total glutathione (GSH)	**Akerboom and Sies (1981)**
Alkaline phosphatase (ALP)	**Babson (1965)**
Acid phosphatase (ACP)	**Babson and Read (1959)**
Lactate dehydrogenase (LDH)	**Moss and Handerson (1994)**
Total protein (TP)	**Bradford (1976)**

2-7- Histopathological studies

For histopathological observations at light microscopic level, fresh testes were immersed in 10 % formalin saline.

Following an overnight fixation, the specimens were dehydrated in ascending grades of alcohol, cleared in benzene and embedded in paraffin wax. Blocks were made and 5 µm thick sections were double stained with hematoxylin and eosin and observed under microscope **(Banchraft *et al.* , 1996)**.

2-8- Statistical analysis

Data analysis and evaluation of statistical significance among different values was done using Student's-test **(Snedecor and Cochran, 1980)**.

3- Results

3-1- Testes weights

The variations in the testes weights of rats subjected to chlorpyrifos (CPF) for 28 days are shown in Table (2).

There was significant decrease ($P < 0.05$) in the testes weights of the group W only as compared to control group.

Table (2): Effect of oral administration of chlorpyrifose (K, W and H) on testicular weights of rats after sub-acute exposure (28 days).

Parameter	Control group	Chlorpyrifos		
		K-group	W-group	H-group
Testes weight (g)	**2.713 ± 0.074**	**2.845 ± 0.073**	**2.479 ± 0.036***	**2.605 ± 0.105**

The data expressed as mean ± SE , n = 5., * $P < 0.05$ (Student's test).

3-2- Testicular oxidative stress:

The influence of sub-acute toxicity of three trade names of chlorpyrifos (K, W and H) administration on testicular lipid peroxidation (LPO) and total glutathione (GSH) levels are shown in Table (3). The results showed significant increase ($P < 0.001$, $P < 0.01$ and $P < 0.01$) in LPO as measured by the amount of MDA formed after treatment with chlorpyrifos (K, W and H, respectively) in comparing with the control group.

In addition, chlorpyrifos treatment (W and H) caused a significant decrease ($P < 0.01$) in the levels of testicular total glutathione (GSH), compared with the control group.

Table (3): Effect of oral administration of chlorpyrifos (K, W and H) on testicular oxidative status in rats after sub-acute exposure (28 days)

Treatment / Parameters	Control group	Chlorpyrifos		
		K-group	W-group	H-group
Malondialdehyde (MDA) n mol/g wet w	78.86 ± 2.185	126.44 ± 4.963***	103.57 ± 4.304**	103.57 ± 6.164**
Total glutathione (GSH) µ mol/g wet w	31.44 ± 2.786	28.57 ± 0.698	17.98 ± 1.399**	18.48 ± 1.416**

The data expressed as mean ± SE , n = 5. ** P < 0.01, *** P < 0.001 (Student's test).

3-3- Biochemical assays

Testicular biochemistry have been recorded in Table (4). Decline in alkaline phosphatase activity (P < 0.01) in the three chlorpyrifos-treated groups was recorded as compared to control group. Also, acid phosphatase activity was decreased (P < 0.05, P < 0.01 and P < 0.05) in the chlorpyrifos-treated groups (K, W and H, respectively) when compared with the control group. Moreover, the results showed significant decrease (P < 0.01, P < 0.05 and P < 0.01) in the levels of lactate dehydrogenase (LDH) after sub-acute exposure to chlorpyrifos (K, W and H, respectively).

In addition, total protein levels were found to be significantly raised (P < 0.001, P < 0.05 and P < 0.01) in chlorpyrifos-treated animals (K, W and H groups, respectively) in comparing with the control group.

Table (4): Effect of oral administration of chlorpyrifos (K, W and H) on some testicular biochemical parameters in rats after sub-acute exposure (28 days)

Treatment / Parameters	Control group	Chlorpyrifos		
		K-group	W-group	H-group
Alkaline phosphatase (U/mg protein)	0.096 ± 0.006	0.052 ± 0.005**	0.066 ± 0.003**	0.072 ± 0.001**
Acid phosphatase (U/mg protein)	0.110 ± 0.011	0.065 ± 0.006*	0.062 ± 0.004**	0.071 ± 0.007*
Lactate dehydrogenase (U/mg protein)	1.650 ± 0.080	1.090 ± 0.059**	1.280 ± 0.061*	1.120 ± 0.051**
Total protein (mg/g tissue)	16.870 ± 0.876	23.080 ± 0.252***	20.110 ± 0.668*	23.380 ± 0.961**

The data expressed as mean ± SE, n = 5. * P < 0.05, ** P < 0.01, *** P < 0.001 (Student's test).

3-4- Testicular histopathology:

In addition to the findings listed above, we have observed many microscopic changes in the testes of male albino rats after sub-acute exposure to chlorpyrifos.

Histological findings of testes from control and treated groups (K, W and W) are presented in Figures 1, 2, 3 & 4 respectively.

Control and CPF-treated groups (K and H) testes revealed normal mature semineiferous tubules with complete series of spermatogenesis and high spermatozoal concentration in the lumen (Fig. 1, 2 and 4). Meanwhile, the testes of chlorpyrifos-treated group (W) showed degeneration and atrophy of non functioning seminifrous tubules with few numbers of sperm cells in the lumen of the seminiferous tubules (Fig. 3).

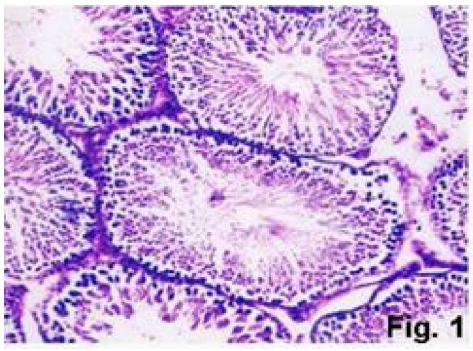

Fig..(1):Testis of rat in control group showing the normal histological structure of mature seminiferous tubules with complete spermatogenic series. (H&E X40)

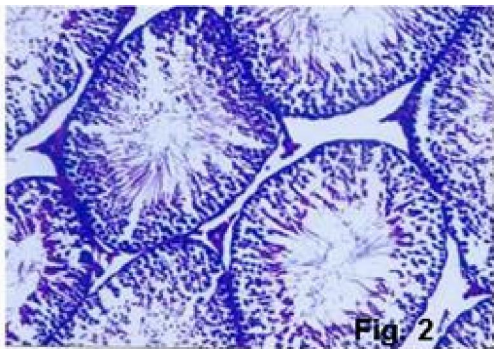

Fig.(2):Testis of rat administrated chlorpyrifos(K) showing mature testicular tissue with full spermatogenesis in the seminiferous tubules . (H&E X40).

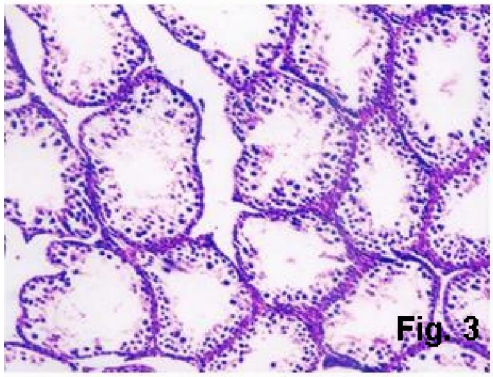

Fig.(3): Testis of rat administrated chlorpyrifos (W) showing degeneration and atrophy of non-functioning seminiferous tubules.(H&E X40).

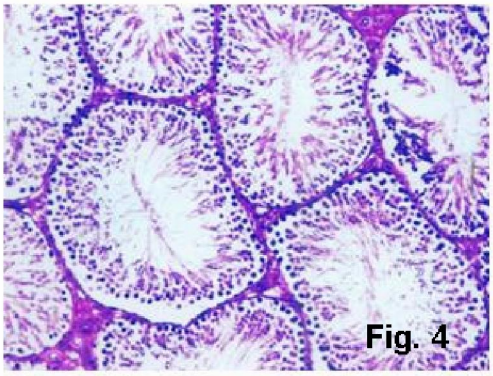

Fig.(4):Testis of rat administrated chlorpyrifos (H) showing normal functioning mature seminiferous tubules .(H&E X40).

4- Discussion

Organophosphates (OPIs) are among the most widely used synthetic pesticides. The wide spread use of OPIs has stimulated research into the possible extence of effects related with their reproductive toxic activity **(Joshi *et al.* , 2007)**.

Our results showed that the weights of testes were significantly decreased in chlorpyrifos-treated group (W) only, as compared to the control group. The decrease in testicular weight in the treated rats may be due to reduced tubular size as confirmed by the histopathological findings of the testes which show degeneration and atrophy of non functioning seminiferous tubules (Fig. 3). This was in accordance with **Joshi *et al.* (2007)** who found mild to sever degenerative changes in seminiferous tubules at various dose levels (7.5, 12.5 & 17.5 mg/kg b.w./day) for 30 days and decreased testes weight.

Also, spermatogenic arrest and inhibition of steroid biosynthesis of leydig cells , a site of steroid biosynthesis may contribute to the decline of testes weight **(Sujatha *et al.* , 2001)**. Another, explanation was reported by **Chitra *et al.* (1999)** which indicate that the decrease in testicular weight may be a result of impairment at testicular, pituitary, or hypothalamic level.

Similar results were recorded by **Choudhary and Joshi (2003)** who reported significant reduction in the testes weight after exposure of rats to endosulfan (organo-chlorine pesticide) at the dose levels of 5, 10

and 15 mg/kg b.w./day for 15 and 30 days. In addition, **El-Kashoury (2009)** showed that the weight of testes was significantly lowered in male rats exposed to profenofos (OPIs) at the dose of 23.14 mg/kg b. w. for 60 days.

The present results confirm the previous reports of **El-Kashoury and El-Far (2004)** who mentioned that administration of rats with profenofos at 23.14 and 46.30 mg/kg b.w. for 28 and 60 days, respectively, induced significant decrease in thyroid hormone levels. There is ample evidence that thyroid hormone is essential to the normal development of testes **(Cook *et al.* , 1994 and Hardy *et al.* , 1996)**.

Links between oxidative stress and adverse health effects have been suggested for several diseases such as cardiovascular, respiratory and neurological as well as for the general aging process. Several drugs, xenobiotics and environmental pollutants are known to cause this inbalance between formation and removal of free radicles. Testes is the main organ of male reproduction. So, the principle objective of the present study was to assess the oxidative damage sustained by testes following sub-acute exposure to three trade names of chlorpyrifos. The present study revealed an elevation in malondialdehyde levels (an indicator of LPO) in three of CPF-treated groups (Table, 3).

Lipid peroxidation, is an oxidative deteriorative process of unsaturated fatty acids, due to excess generation of free radical. Our results suggest but don't prove that free-radical mediated lipid peroxidation, may be involved in toxic manifestation of chlorpyrifos. Similar results were reported by **Gultekin *et al.* (2000) and Gultekin *et al.* (2001)** who indicated that increasing chlorpyrifos concentration caused asignificant reduction in the activities of superoxide dismutase (SOD) and catalase (CAT) and asignificant increase in the level of malondialdehyde and glutathione peroxidase. SOD catalyses the conversion of superoxide radical (O^{-}_{2}) to hydrogen peroxide (H_2O_2), while CAT converts H_2O_2 to H_2O. So, these enzymatic antioxidants may counteract oxidative stress and can alleviate the toxic effects of reactive oxygen species, ROS **(Bagchi *et al.* , 1995)**. Also, **Joshi *et al.* (2007)** reported that sub-acute exposure to chlorpyrifos induce oxidative stress in testes of rats. Furthermore, OPIs such as phosphomidon, trichlorfon and chlorvos have been reported to induce oxidative stress as shown by enhanced MDA production **(Naqvi and Hasan, 1992)**.

The most important non-protein thiol in the cells, the tripeptide glutathione (GSH), which is not only partner in the recycling of oxidized α-tocopherol and ascorbic acid but it is an important water-phase antioxidant and essential cofactor of antioxidant enzymes.

Oxidants such as hydrogen peroxide (H_2O_2) activate specific gene expression through the antioxidant responsive elements. Also, elevation of glutathione level in the testes, may help to preserve physiological integrity of the testes **(Rushmore *et al.*, 1991)**.

In the present study, a significant decrease in the total GSH level was observed following treatment with CPF (W and H) compared with the control group (Table, 3). This result go hand-to-hand with **Gultekin *et al.* (2000)** who found that GSH-Px was indirectly activated by chlorpyrifos inducing ROS. Therefore, the decreased level of total GSH in the testicular tissue after sub-acute exposure to chlorpyrifos may be due to activation of GSH-Px. This enzyme converts H_2O_2 or other lipid peroxides to water or hydroxy lipids, and during this process glutathione (GSH) is converted to oxidized glutathione **(Bachowshi *et al.*, 1997)**.

Meanwhile, it has been reported that OPIs, such as phosphomidone, trichlorfom and dichlorvos caused a decrease in glutathione peroxidase (GSH-Px) activity **(Naqvi and Hasan, 1992)**. Also, administration of mixture of pesticide including chlorpyrifos reduced the activities of GSH-Px in rat testes **(Mattson *et al.*, 1996)**.

In addition, **Latchoumycandane *et al.* (2002)** indicated that methoxychlor (O'ch), a widely used pesticide, has been shown to induce reproductive abnormalities in male rats causing reduced fertility by inducing oxidative stress in the epididymis and epididymal sperm due to decreased antioxidants enzymes (superoxide dismutase, catalase and glutathione reductase) and increased levels of hydrogen peroxide and lipid peroxidation after 4 or 7 days of treatment.

The present results suggest that chlorpyrifos treatment caused a marked decrease in the activities of alkaline, acid phosphatase and lactate dehydrogenase in all treated groups (Table, 4), which reflect suppression in testicular function. Activities of these marker enzymes are considered to

be functional indicators of spermatogenesis **(Johnson *et al.*, 1970)**.

The results in this study go hand-to-hand with the finding of **Salem *et al.* (1989)** who investigated the influence of methamidophos (OPIs) on rats at a dose of 100 ppm in drinking water for 9 and 45 days. They found that acid, alkaline phosphatase and lactate dehydrogenase were reduced significantly in the testicular tissue.

Also, **Moustafa *et al.* (2007)** reported that profenofos is considered as one of the male reproductive toxicants. Moreover, **El-Kashoury (2009)** found significant decrease in the activities of ALP, ACP and LDH in testicular tissues of rats exposed to profenofos for 60 days at a dose of 23.14 mg/kg b.w. per day.

ALP is primary of testicular and epididymal origin and, therefore suitable for differentiation of oligo-and azoospermia **(Turner and McDonell, 2003)**. Decline in ALP activity indicated that chlorpyrifos treatment produced a state of decreased steroidogenesis where the intercellular transport was reduced as the metabolic reactions to channelize the necessary inputs for steroidogenesis slowed down **(Latchoumycandane *et al.* 1997)**.

Acid phosphatase is an enzyme capable of hydrolyzing orthophosphoric acid esters in an acid medium. The testicular acid phosphatase gene is up-regulated by androgens and down-regulated by estrogens **(Yousef *et al.* , 2001)**.

LDH is associated with the maturation of germinal epithelial layer of seminiferous tubules and associated with post meiotic spermatogenic cells **(Sinha *et al.* , 1997)**. An inhibition in the activity of LDH in testes of chlorpyrifos-treated rats points to the interference of chlorpyrifos with the energy metabolism in testicular tissues **(Mollenhauer *et al.* , 1990)**.

Concerning the testicular protein level, results of the present study exhibit an increase in its level in all chlorpyrifos-treated groups (K, W and H). The testicular fluid contains both stimulatory factors as well as inhibitory factors that selectivity alter the protein secretions **(Brooks, 1983)**. Thus the changes in protein suggested that there is a reduction in the synthetic activity in testes.

The elevation in testicular protein level in the present study confirms the previous results by **Choudhary and Joshi (2003), Joshi *et al.* (2007) and El-Kashoury (2009)** who mentioned that the protein content of the testes was raised at significant levels in endosulfan (O'ch), chlorpyrifos and profenofos-treated rats, respectively.

Gupta *et al.* (1981) ; Singh and Pandey (1989) found that an elevation in testicular protein may be due to the hepatic detoxification activities caused by endosulfan which results in inhibitory effect on the activities of enzyme involved in the androgen biotransformation.

In accordance with the findings of the present study, **Rao and Chinoy (1983)** suggested that the accumulation of protein occurred in testes and epididymus due to androgen deprivation to target organs. This deprivation effect led to a reduction in testicular and cauda epididymus sperm population, loss of motility in the latter and an increase in number of abnormal spermatozoa, thereby manifesting 100 % failure in treated animals.

From the afore-mentioned results, it could be concluded that chlorpyrifos (W) decreased the testes weight in comparing with chlorpyrifos (K and H). Meanwhile, chlorpyrifos (K, W and H) had induced a distinct oxidative stress in testicular tissues except (K) for total glutathione. Moreover, chlorpyrifos (K, W and H) induced adverse effects on testicular function by altering biomarker enzymes. In general, CPF-W had a pronounced effect on testicular function more than the other two emulsifiable concentrate (CPF-K and CPF-H). Thus care should be taken and more studies should be done to increase the validity of those information.

Abbreviation used

OPIs, organophosphorous insecticides; O'ch, organochlorine, LPO, lipid peroxidation; GSH, glutathione; CPF, chlorpyrifos; ROS, reactive oxygen species; SOD, superoxide dismutase; CAT, catalase,; GSH-Px, glutathione peroxidase; K, chlorzan; W, pestban; H, pyripan; ALP, alkaline phosphatase; ACP, acid phosphatase; LDH, lactate dehydrogenase, TP, total protein; EC, emulsifiable concentrate.

Achnowledgment:

Authors are thankful to Dr. Adel Bakeer Kholoussy (Pathology Depart., Fac. Vet. Med., Cairo Univ.) for accomplishing the histopathological examination .Also, thanks to the Central Agricultural Pesticides Laboratory and Animal Health Research Institute for helpful and support .

Corresponding author:
Hanan, A. Tag El-Din, Animal Health Research Institute, Dokki, Giza, Egypt.
drofscience@ymail.com

REFERENCES

Akerboom, T. M. P. and Sies, H. (1981). Assay of glutathione, glutathione disulfide and glutathione mixed disulfides in biological samples. Met. Enzymol., 77 : 373 – 782 .

Aslan, R.; Sekeroglu, M. R. ; Gultekin, F. and Bayiroglu, F. (1997). Blood lipoperoxidation and antioxidant enzymes in healthy individuals : relation to age, sex, habits, life style and environment. J. Environ. Sci. Health A., 32 (8) : 2102 – 2109 .

Babson, L.A. (1965). Phenolphalein monophosphate methods for the determination of alkaline phosphatase. Clin. Chem., 11 : 789.

Babson, A.L. and Read, A.P. (1959). Colourimetric method for the determination of total and prostatic acid phosphatase. Am. J. Clin. Path., 32 : 89-91.

Bachowshi, S.; Kolaja, K. L.; Xu, Y.; Ketcham, C. A.; Stevenson, D. E.; Walburg, E. F. and Klaunig, J. (1997). Role of oxidative stress in the mechanism of dieldrin's hepatotoxicity. Ann. Clin. Lab. Sci., 27 (3) : 196 – 209 .

Bagchi, D.; Bagchi, M.; Hassoun, E. A. and Stohs, S. J. (1995). In vitro and in vivo generation of reactive oxygen species, DNA damage and lactate dehydrogenase leakage by selected pesticides. Toxicol., 104 : 129 – 140 .

Banchraft, J. D.; Stevens, A. and Turner, D. R. (1996). Theory and practice of histological techniques. 4th Ed., Churchill Livingstone, New York, London, San Francisco, Tokyo.

Blakley, B. R.; Yole, M. J.; Brousseau, P. ; Boermans, H. and Fournier, M. (1999). Effect of chlorpyrifos on immune function in rats. Vet. Hum. Toxicol., 41 : 140 – 144 .

Bradford, M. M. (1976). A rapid and sensitive method for the quantitation of microgram quantities of protein utilizing the principle of protein-dye binding. Analyt. Biochem., 72 : 248-254.

Brooks, D. E. (1983). Effect of androgen on protein synthesis and secretion in various regions of the rat epididymis, as analysed by two dimensional gel electrophoresis. Mol. Cell Endocrinol., 29 : 255-270.

Chitra, K. C.; Latchoumycandane, C. and Mathur, P. P. (1999). Chronic effect of endosulfan on the testicular functions of rat. Asian J. Andrology, 1 : 203-206.

Choudhary, N. and Joshi, S. C. (2003). Reproductive toxicity of endosulfan in male albino rats. Bull. Environ. Contam. Toxicol., 70 : 285 – 289 .

Cooke, P. S.; Zhao, Y. D. and Bunick, D. (1994). Triiodothyronine inhibits proliferation and stimulates differentiation of cultured sertoli cell: Possible mechanism for increase adult testis weight and sperm production induced by neonatal goitrogen treatment. Biol. Reprod., 51 : 1000 – 1005 .

Dwivedi, P. D.; Das, M. and Khanna, S. K. (1998). Role of cytochrome P_{450} in quinalphos toxicity: effect on hepatic and brain antioxidant enzymes in rats. Food Chem. Toxicol, 36: 437 – 444.

El-Kashoury, A. A. (2009). Influence of sub-chronic exposure of profenofos on biochemical markers and microelements in testicular tissue of rats. Nat. Sci., 7 (2) : 16 – 29 .

El-Kashoury, A. A. and El-Far, F. A. (2004). Effect of two products of profenofos on thyroid gland, lipid profile and plasma APO-1/FAS in adult male albino rats. Egypt. J. Basic Appl. Physiol., 3: 213 – 226.

El-Kashoury, A. A. and El-Said, M. M. (2007). Toxicological impact of certain emulsifiable concentrates of chlorpyrifos on male albino rats with regard to therapeutic role of selenium. J. Egypt. Soc. Toxicol., 37 : 27 – 37 .

Gomes, J.; Dawodu, A. H.; Liyod, O.; Revitt, D. M. and Anilal, S. V. (1999). Hepatic injury and disturbed amino acid metabolism in mice following prolonged exposure to organophosphorus pesticides. Hum. Exp. Toxicol., 18 : 33 – 37 .

Gultekin, F. ; Delibas, N.; Yasar, S. and Kilinc, I. (2001). In vivo changes in antioxidant systems and protective role of melatonin and a combination of vitamin C and vitamin E on oxidative damage in erythrocytes induced by chlorpyrifos-ethyl in rats. Arch. Toxicol., 75 : 88 – 96 .

Gultekin, F.; Ozturk, M. and Akdogan, M. (2000). The effect of organophosphate insecticide chlorpyrifos-ethyl on lipid peroxidation and antioxidant enzymes (in vitro). Arch. Toxicol., 74 : 533 – 538 .

Gupta, P. K.; Shrivastava, S. C. and Ansari, R. A. (1981). Toxic effects of endosulfan on male reproductive organs in rats. Indian J. Biochem. Biophys., 18 : 159-163.

Hardy, M. P.; Sharma, R. S.; Arambepola, N. K. ; Sottas, C. M.; Russel, L. D.; Bunick, D.; Hess, R. A. and Cooke, P. S. (1996). Increased proliferation of ledig cells induced by neonatal bypothyroidism in the rat. J. Androl., 17 : 231 – 238 .

Johnson, A. D.; Gomes, M. and Vandemark, N. L. (1970). The testis. 1st Ed., Academic Press, New York and London.

Joshi. S. C.; Mathur, R. and Gilati, N. T. (2007). Testicular toxcity of chlorpyrifos (an organophosphate pesticide) in albino rat. Toxicol. Ind. Health., 23 : 439-444.

Latchoumycandane, C.; Gupta, S. K. and Mathur, P. P. (1997). Inhibitory effects of hypothyrodism on the testicular functions of postnatal rats. Biomed. Lett., 56 : 171-177.

Latchoumycandane, C.; Chitra, K. C.; and Mathur, P. P. (2002). The effect of methoxychlor on the epididymal antioxidant system of adult rats. Reprod. Toxicol., 16 (2) : 161 – 172 .

Mattson, J. P.; Wilmer, J. W.; Shankar, M. R.; Berdasco, N. M.; Crissman, J. W.; Maurissen, J. P. and Bond, D. M. (1996). Single-dose and 13-week repeated-dose neurotoxicity screening studies of chlorpyrifos. Food Chem. Toxicol., 34: 393 – 405 .

Mollenhauer, H. H.; Morre, D. J. and Rowe, L. D. (1990). Alteration of intracellular traffic by monensin : mechanism, specificity and relationship to toxicity. Biochem. Biophys. Acta, 1031 : 225-246.

Moss, D. W. and Handerson, A. R. (1994). Lactate dehydrogenase 2nd Ed., Textbook of clinical chemistry, chapter 20, Enzymes, pp. 812-818

Moustafa, G. G.; Ibrahim, Z. S.; Hashimoto Y.; Alkelch A. M.; Sakamoto K. Q.; Ishizuka M. and Fujita S. (2007). Testicular toxicity of profenofos in matured male rats. Arch Toxicol., 81 (12) : 875 – 881 .

Naqvi, S. M. and Hasan, M. (1992). Acetylhomocysteine thiolactone protection against phosphoamidon-induced alteration of regional suproxide dismutase activity in central nervous system and its correlation with altered lipid peroxidation. Ind. J. Exp. Biol., 30: 850 – 852 .

Ohkawa, H.; Ohishi, N. and Yagi, K. (1979). Assay for lipid peroxides in animal tissues by thiobarbituric acid reaction. Anal. Biochem., 95 : 351 – 358 .

Rao, M. V. and Chinoy, N. J. (1983). Effect of estradiol benzoate on reproductive organs and fertility in the male rat. Eur. J. Obstet. Gynecol. Reprod. Biol., 15 (3) : 189-198.

Rushmore, T. H.; Morton, M. R. and Pickett, C. B. (1991). The antioxidation responsive element: Activation of oxidative stress and identification of the DNA consequence required

for functional activity. J. Biol. Chem., 226 : 11632 – 11639 .

Salem, H. A.; Younis, M.; El-Tohamy, M.; El-Herrawie, M.; Soliman, M. and Khalaf, A. (1989). Thyrotrophic and thyroid hormones concentration and some testicular biochemical parameters as affected by oral administration of methamidophs (Organophosphorus) into adult male rats. J. Egypt. Vet. Med. Ass. 49: 667-675.

Singh, S. K. and Pandey, R. S. (1989). Differential effects of chronic endosulfan exposure to male rats in relation to hepatic drug metabolism and androgen biotransformation. Indian J. Biochem. Biophys., 26 : 262-267.

Sinha, N.; Narayan, R. and Saxena, D.K. (1997). Effect of endosulfan on the testes of growing rats. Bull. Environ. Contam. Toxicol., 58 : 79-86.

Snedecor, G. W. and Cochran, W. G. (1980). Statistical methods (7th ed). Lowa State University Press. Ames.

Song, X.; Violin, J. D.; Seidler, F. J. and Slotkin, T. A. (1998). Modeling the developmental neurotoxicity of chlorpyrifos in vitro : macromolecule synthesis in PC12 cells. Toxicol. Appl. Pharmacol., 151 : 182 – 191 .

Sujatha, R.; Chitra, K. C.; Latchoumycandane, C. and Mathur, P. P. (2001). Effect of lindane on testicular antioxidant system and steroidogenic enzymes in adult rats. Asian J. Androl., 3 : 135-138.

Swann, J. M.; Schultz, T. W. and Kennedy, J. R. (1996). The effect of organophosphorous insecticides dursban and lorsban on the ciliated epithelium of the frog palate in vtro. Arch. Environ. Contam. Toxicol., 30 : 188 – 194 .

Swann, J. D.; Smith, M. W. ; Phelps, P. C. ; Maki, A.; Berezesky, I. K. and Trump, B. F. (1991). Oxidative injury induces influx dependent changes in intracellular calcium homeostasis. Toxicol. Pathol., 19 : 128 – 137 .

Turner, R. M. and McDonell, S. M. (2003). Alkaline phosphatase in stallion semen : characterization and clinical applications. Theriogenology, 60 : 1-10.

Weil, C. S. (1952). Tables for convenient calculation of medium effective dose (LD_{50} or ED_{50}) and instruction in their use. Biometrics., 8 : 249 – 263 .

Yousef, G. M.; Diamandis, M.; Jung, K. and Eleftherios, P. (2001). Molecular cloning of a novel human acid phoshatase gene that is highly expressed in the testes. Genomics, 74 (3): 385-395.

2010/4/4

Issues In Interacting With GIS In Hydrocarbon Exploration Industry

Muhammad Shaheen [1], Muhammad Shahbaz [2], Zahoor ur Rehman [3], M. Sarshar Aurangzeb[4]

[1,2,3.] University of Engineering & Technology Lahore, Punjab Pakistan
[4] Pakistan Accumulators Pvt. Ltd. Pakistan
[1] shaheen@uet.edu.pk, [2] m.shahbaz@uet.edu.pk, [3] xahoor@gmail.com, [4] sarshar_zeb@yahoo.com

Abstract: Technology changed the scenarios in past few decades. Recent developments in the processing power and storage capacity revolutionized the industrial development and even troubleshooting. There was a time when basic computational tools were very slow or even unavailable in industry but now state of the art tools and technologies can envisage exploring virtual reality. In energy sector, world is desperately looking for large reserves of fossil fuels along with other reserves. The efforts in hydrocarbon discovery phase deplete lots of resources resulting in either a very small sized reservoir or in failure. Geographic information system (GIS) along with related technology of remotely sensed satellite images, information system skeleton, graphical user interfaces (GUIs) and analytical tools can also be used for automated hydrocarbon explorations. GIS is operated by GIS analysts who have specialized skills in geo-spatial technologies. Therefore the exploration companies especially in the developing countries of the world do not rely on the capabilities of GIS and remote sensing. The reasons are concluded to be. (1). Interface of GIS is not friendly for non-specialist and/or novice user. (2). Accuracy of spatial data is not convincing for accuracy-critical tasks. (3). Unavailability of standards of spatial / non-spatial data display. The paper addresses the issues in interacting with GIS for hydrocarbon exploration and proposes enhanced model of Geographic Information System (GIS) for making it a reliable technology in any part of the world in hydrocarbon discovery phase. [Journal of American Science 2010;6(7):262-271]. (ISSN: 1545-1003).

Keywords: Geographic Information System (GIS), Usability, Interactivity, Human-GIS Interaction, Positional Accuracy, Hydrocarbon Exploration, Backpropogation Neural Network

1. Introduction

Technology has allowed an incredible increase in the success rate of discovering various sources of energy. Oil and natural gas are and will remain major energy sources in most part of this century. There are some big reserves of natural gas in Asian region which made the countries to sustain balance between exploration rate and consumed resources. Beneath earth's surface the accumulation of this treasure is a gift of nature and over the surface, experts are the source to detect and explore it. A lot of resources are consumed in exploration phase resulting in either a big reservoir or inadequate prediction.

Hydrocarbon exploration passes through subsequent phases starting from lead identification to discovery and finally feeding the reserve to production plant (McLay et.al. 2003). Remote sensing and GIS can contribute with all its potentials not only in geological mapping but also for analytical purposes and interpretation of geological data for making hydrocarbon explorations accurate and cost-effective (Everett et.al. 2002). Geographical Information Systems do also have significant contributions in developing risk simulation models on spatial data for diverse class of systems (Thumerer et.al. 2000; Fuest et.al. 1998; Chang et.al. 1997; Lovett and Parfitt, 1996; Emmi and Horton, 1995; De silva et.al. 1993; Goodchild et.al. 1993; Vanvoris et.al. 1993). These systems can help making reconnaissance maps, spud date maps, operator maps, geological structure map and production maps etc to support hydrocarbon exploration. The systems are also effective for spatial correlations, statistical analysis, identification of changes in features marked at remotely sensed image due to the presence of hydrocarbons and spatial analysis (Barrel, 2000). The launch of IKONOS satellite in 1999 enabled the world to get updated, small and compact satellite images every day. Steve Adam (Adam, 2000) recommended the use of IRS-1 satellite imagery for positioning and classification of structures in low/moderate density environments and IKONOS's imagery to take digital ortho-photos in high density environments. The advances in Global Positioning Systems (GPS) contributed a lot in accuracy-critical tasks. A GIS data collection project can now be completed with the help of PDAs and assistant software (Wadwani, 2000).

Geo-technology made geo-spatial data mapping a powerful tool and geo-analysis more intelligent. In oil and gas exploration scenario it is used to characterize and analyze reservoirs (Walters et.al. 1996), characterize isotopic data (Neilson et.al.

1995), seismic and geological data (Neilson and Nash, 1997) and Lineament data (Warner, 2000). Nash and Adams (2001) used GIS to enhance tracer analysis by incorporating GIS functions in different sort of interfaces. The use of GIS in natural resource industry is discussed by various researchers including Ramdan et.al (2009; 1999), Williams (2000), Porter et.al (2000), Shah (2003) and Iqbal (2004). Implementation of GIS is beneficial not only in exploration monitoring but also in generating self-revenue by utilizing the services of petroleum exploration data management (Shah, 2006).

In spite of the above stated facts, the use of GIS and remote sensing imagery is rare especially in developing countries. The planning departments of these countries are interested in increasing the usage of GIS and its applications in natural resource exploration but unfortunately, it is not well practiced in various explorations and planning departments.

Robert L.Labarbera (2006) in Fort Bend County US realized that GIS is not in public access as it is rarely articulated in newspaper and television. Internet, periodicals and conferences are the only sources of information of GIS. Unfortunately all the three are not regularly interacted by planning departments in third world countries. Robert also identified that Fort Bend County individuals were not knowledgeable of new technologies and trends in GIS. The company was lacking in GIS personal resources and products and there was no GIS feedback from clientele. Dutch market research reflected that municipalities have low confidence on geographic data (Kroode, 1994). This market research was made in Netherland when they were infant users of GIS. The growth level of GIS in various parts of the world (especially developing countries) is still very low. Onsrud et.al (Onsrud and Masser, 1993) argued that the initial rate of adoption of technology is slower until the volume of users increase. The increase in number of users gives rapid boom to the technology. Masser (1998) concluded that the unavailability of digital data is one of the factors for which GIS is not used commonly. Rhind (1995) pointed out the role of government in improving the diffusion of GIS. Governments in most of the countries are primary sponsor of national geodetic framework hence stands at prominent position to ensure spatial accuracy. R.Colijin (2000) surveyed about the rate of GIS adoption, GIS policies, and expectations and goals of GIS adoption.

The use of GIS in developing country is much greater than its use in developing countries of Asia (Yeh, 2004). Ibrahim Elbeltagi et.al (2005) studied the factors influencing the usage of information systems in less developed countries. He concluded from the results that Perceived Ease of Use (PEU) and Perceived Usefulness (PU) affect the use of information system. The arguments by Goodman & Green (Goodman and Green, 1992), Krovi (1993), and Lu et.al (1989) revealed that poverty, trade barriers and lack of infrastructure affect the usage of information technology. Technology Adoption Model (TAM) is one of the stronger tools applied in developed world for measuring the acceptance of technology by finding user perceptions (Boudreau et.al. 2001). An organization's culture also contributes a lot in adoption and use of GIS. W.H.Erik et.al (De Man, 2002) underlined the importance of social conditions and cultural desirability in the adoption of GIS. Ian Muehlenaus (2007) identified the extents of GIS ubiquity and diffusion in various states. He concluded that considerable growth with potential in developed countries has been observed in industrial as well as non-industrial sector.

The variability and distribution of natural resources can help decision-makers to keep predicted values in mind while making decisions about future. In spite of the mentioned fact the use of GIS in which this industry is disappointing (Huizing et.al. 2002). In spite of the incorporation of geo-spatial information and presence of digital maps, managers tend to use paper maps (Kevany, 2003; Zerger and Smith, 2003; Cahan and Ball, 2002). There are certain cases when the interest of decision-maker considering various factors for an unchallengeable decision is constrained by non-integration of information, inaccessibility, incomprehensibility, lake of expertise etc (Dalal-Clayton et.al. 1993). Amira Sobeih (2005) stated that the use of GIS has neither penetrated in business community nor in user community in Egypt. The penetration is not expected until communication and participation channels are built at all levels i.e. local, regional, national and international. Only after that natural resource exploration in all its activities can exploit GIS (Sobieh, 2005).

Hydrocarbon exploration if combined with GIS utilization required analysis of satellite imagery, digital imagery, GPS surveys, surface interpretations, geological studies and infrastructure evaluation. GIS today can help to find and derive spatial relationships among environmental factors, well logs, sedimentary rock analysis and equipment installed on pipelines. The GIS is in infancy stages whereas the applications for which GIS can be utilized are mature in industry. Following this demand, the paper identified the reasons for non-exploitation of GIS and proposed model to overcome the dilemma. Guoray Cai et.al (2006) worked on effective GIS interfaces to support crisis management in the terms of immediacy, relevancy and sharing.

The hydrocarbon exploration companies do not much rely on the capabilities of GIS. This paper

identifies the reasons that why GIS is not used inspite of its potential and what are the reasons prevailing behind it for not using this state of the art technology. The paper proposed a model for making certain modifications in existing GIS framework so that it becomes more usable in industry. The reasons for non-exploitation of GIS in hydrocarbon exploration are found to be:

1. The graphical interface of GIS is not friendly for non-specialist user.
2. Accuracy of spatial data is not relied in accuracy-critical tasks.
3. The standards of spatial/non-spatial attributes in GIS do not exist.

These points are elaborated one by one in the succeeding sections.

Non-Friendly GUIs

Mark et.al (1992) gave some generic design guidelines for GIS interface design. These include degree of agreement, smart menus, conceptual structure of program, easy to learn interfaces, direct computation and spatial data presentation. Anselin (1999) focused on visualization of spatial distribution where as Trevor et.al (Trevor and Gaterell, 1995) suggested a design which is easy and appropriate for analytical operations. Dykes (1997) suggested including dynamic graphics and brushing for spatial exploration. He worked on making the interface design simpler so that the user working on MS-Office would be able to use it.

Technologically backward industries of developing countries find it hard to use graphical user interface of GIS. In our study, an investigative survey has been accomplished in energy companies including MOL (Marine Online), SNGPL (Sui Northern Gas Pipelines Ltd), SSGCL (Sui Southern Gas Companies Ltd), MOL and LMKR (Landmark Resources) to extract the factors causing limited or no usage of GIS in hydrocarbon exploration activities. The survey along with field visits to different companies enabled us to conclude on following enhancements in design of graphical user interface of GIS.

- The companies had been using management information systems, transaction processing systems and other decision support systems for a long time. They are well aware of its operational and analytical capabilities hence working on it regularly or at least periodically. The interface of GIS is quite different. The diffusion of other information systems was quick because of its compatibility with manual system in execution but GIS is not an alternate to some existing file system. For example national survey sheets are used for cartographic mapping in SNGPL. The cartography is overlaid on these sheets by using AUTOCAD. The use of AUTOCAD is still popular for such cartographic mapping whereas GIS has the capability to digitize existing networks on satellite imagery.
- The annotations used in the GIS for hydrocarbon exploration are not similar with commonly used terminologies in the company. It is very difficult for an experienced manager to work on new terminologies especially when the work is time bound and need faster performance.
- Various functions which are used for statistical analysis are facilitated in GIS but are not easy to use. These functions need specialized skills of GIS professional whereas the human mediator skills become bottleneck when quick information transfer is needed (Egenhofer, 1995). Most of the managers are not even aware of handling basic interface options so they have to depend on GIS technical persons. Technical training of GIS that is designed within the company is insufficient for exploiting esteemed capabilities of GIS.
- The companies are working on paper maps. The managers feel operational hurdles while working on satellite imagery. The configuration of both of these differs in spatial identification of points as well as in layout.

1.1.1. In the light of above discussion, a model for designing graphical user interface of GIS is designed which is presented in Figure 1. The model includes such flexibilities so that non-specialist GIS user would equally be able to use the application. *Base Map Options:* The Interface should be equipped with options to select base map. The developer can rectify the image on different base maps. When one selects the base map for GIS, the corresponding rectification would automatically be applied and the layers got adjusted.

1.1.2. *Expertise-Wise Usage:* There should be an option for the users to define its expertise. Whether the user is expert, mediator or beginner etc (The expertise will be classified according to the available human resources). Each user will be offered the interface options according to his expertise. For example an experienced user will be able to use analytical tools and play with the incorporated spatial database whereas a beginner will only be able to utilize the facilities like searching a location, printing data and displaying attributes.

1.1.3. *Wizards for GUI:* The GIS in the above mentioned companies do have graphical user interfaces on which the attribute information of various features is displayed. For example, in pipeline industry the GUIs of Town Border Stations, Cathodic Protection (CP) Stations and Sales Metering Stations (SMS) have been incorporated. These GUIs contain the attributes of above mentioned pipeline network

assets like No of CP Bond Box in CP Station or no of pre-fabricated insulating joints in CP station etc. The GIS interface (ESRI's ArcGIS is most commonly used) should contain wizards to create new GUIs by selecting the fields to be included into GUI from the list provided. The user should have the option to name the fields of GUI according to his own understandings.

1.1.4. *Annotation Libraries:* The features of GUIs are annotated just like the labelling of a biological diagram. There should be an inclusion of various categories of annotation libraries including hydrocarbon exploration annotations, pipeline annotations, hazard management annotations, geological annotations, refinery annotations etc. These annotations and symbols should be finalized after consulting international organizations. For example it is necessary to consult ASME (American Standards for Mechanical Engineers) in order to finalize the annotation libraries related to oil and gas engineering. The user does have the option to select the desired annotation library before presenting GIS to the concerned manager.

1.1.5. *Division of Interface:* The interface of GIS may possibly be separated in three different frames.

(1). Information retrieval window.
(2). Information analysis window
(3). Information querying window

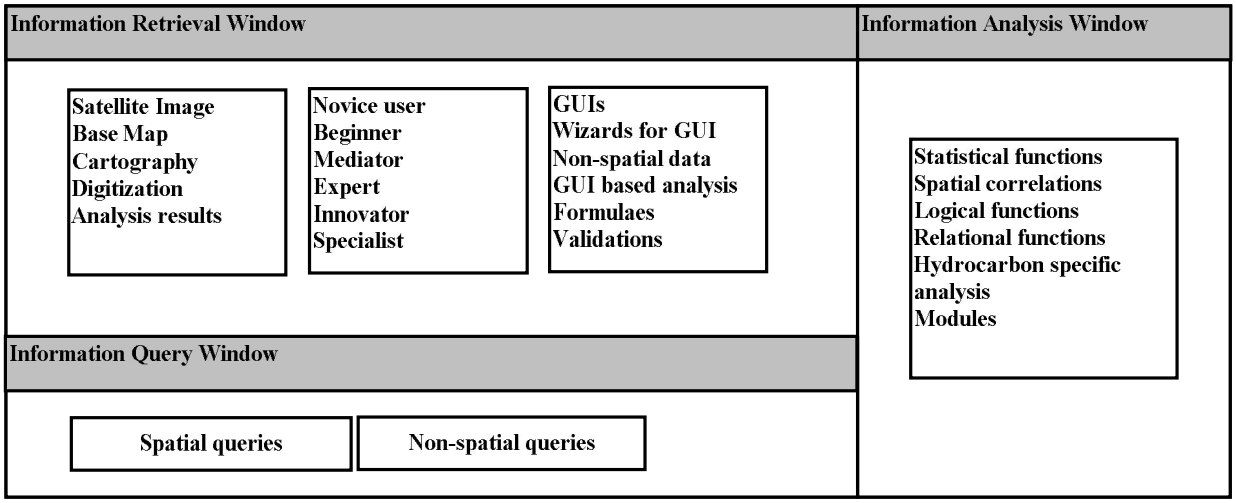

Figure 1 – Components of GIS Interface

Unreliable accuracy in accuracy critical tasks

The concepts of precision and accuracy in geomatic engineering are usually exemplified by standard deviations and root mean square errors (Li and Yuan, 2002). Error handling in spatial information is major research focus, which is the evidence of discrepancies, caused of inaccurate spatial information. In the applications where the accuracy is evaluated at a broader scale are excluded from the list. Li and Gao (1997) proposed quantitative analysis of error propagation in information retrieval from remotely sensed image through GIS. Spatial data is mostly obtained by three different methods. (1), Field Survey (2), Digitizing maps and (3), Remote Sensing. Xiaosheng (2005) classified errors in spatial data which is obtained by above methods. The errors which are produced in accuracy critical tasks especially in energy sector i.e. in exploration industry, pipeline industry etc.

field survey are because of error in centering, reading, errors of instruments and impact of environmental elements including atmospheric pressure, temperature and lateral refraction and climate etc (Ying, 2002). The errors in digitization are caused because of errors in maps, distortion errors and vectoring errors (Litao, 2003). Errors in remote sensing data can be isolated at each step of remote sensing procedure i.e. data collection, data processing, data analysis, data transition and artificial interpretation. The described errors are common in nature and exist in all data. The most prominent error which is specific and annoying to the companies of third world countries is positional accuracy error. The error is not affordable in

ZENG Yanwai (2007) identified paper map distortion, scanning error, image processing or geometry adjustment error, map orientation error,

data acquisition error and editing error. Above all, a default error of 2-10 meters is included in GPS coordinate readings.

To avoid map positional error in particular and scanning, geometry adjustment and map distortion error in general, the interface is equipped with a back propagation artificial neural network. ZENG tested positional accuracy from coordinate difference using the formula.

$$\sigma_x = \pm\sqrt{\sum_1^n \Delta x_i^2 / n}\ ,\quad \sigma_y = \pm\sqrt{\sum_1^n \Delta y_i^2 / n}\ ,\quad \sigma_z = \pm\sqrt{\sum_1^n \Delta z_i^2 / n}$$

x,y are representing coordinate positions and h is for elevation. Δx, Δy, Δh represent coordinates differences. σ_x, σ_y and σ_z represent positional accuracy.

In proposed system, a backpropogation neural network (BPNN) is trained on positional accuracy values extracted by above equations. The BPNN will validate the positions which lie within the range of acceptable values. Similarly the same network is trained on map distortion acceptable range and geometry adjustment error. BPNN is multi layered network with number of hidden layers. The learning stages contain two phases. (1). Forward Pass (2). Backward Pass shown in equation 3 and 4 (Trappey et.al. 2005)

In Equation 1 W_{ij} is the weight connected with input layer. X_i is the positional accuracy. NI represents net input. In Equation 2 W_{jk} is the weight connected with different hidden layers and H_j represents particular hidden layer number.

The forward pass calculates net input of every node to generate output using activation function. The net input from input layer to the hidden layer and output at output layer is calculated in the Equation 1 and 2 respectively.

$$(\mathrm{NI}) = \sum_{i,j=1}^{n} W_{ij} X_i \qquad (1)$$

$$\mathrm{Out_k} = f\left(\sum_{j=1}^{n} W_{jk} H_j\right) = f\left(\sum_{j=1}^{n} W_{jk}\, f\left(\sum_{i=1}^{n} W_{ij} X_i\right)\right) \qquad (2)$$

In backward pass, the output is passed back to previous hidden layer by adjusting weights on the basis of error. The weight adjustment is determined by Equation 3.

$$\Delta W_{jk} = -\xi \frac{dE}{d W_{jk}} \qquad (3)$$

Where ξ the constant adjustment value and E is the amount of error.

In our study, Backpropogation learning technique is used for learning of accurate or near optimal positional values and acceptable values geometric image distortion. A training sample is presented to the neural network. The desired output of the sample is calculated by calculating the value of OUT_k . The desired output is compared by the actual output and the value of error is computed. Scaling factor is measured to determine whether an adjustment is required or not. The local error (scaling factor) is evaluated on the previous layer by specially considering the neurons with higher weights. The procedure is repeated until the amount of error become negligible.

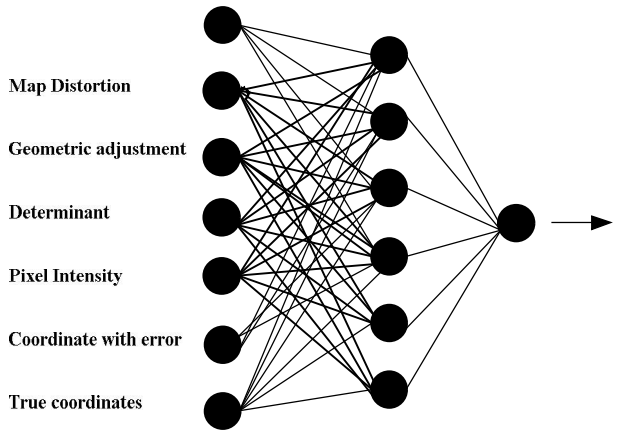

Figure 2 – Backpropogation neural network for ensuring accurate data acquisition

Standardization of Symbology/ Spatial Data

GIS Engineers spent good amount of time for selecting symbology and representing different attributes on GIS maps. A part of spatial data can suit user requirements if it is represented in the most common format which is already in practice. Every GIS owning company use symbology set to represent its assets. Symbols can represent the category of the data being mapped by adopting certain characteristics. These characteristics include symbol size, shape, orientation, texture, hue, brightness and lightness or simply they can be said as visual variables (Supermap Vector Map Symbol Library Exchange Format 2.0, 1999). The GIS which is built for proper man-

agement of information during hydrocarbon exploration also need to represent symbols which are specific to hydrocarbon industry.

In GIS interface for non-specialist user, it would be better to incorporate the same symbology. The user is well aware of that symbology and can easily browse through the maps. The standards of symbology and attribute data representation have not yet been developed in developing countries. SU Kehua et.al (2008) proposed virtual machine for cross-platform symbolization. Virtual machine technology is adopted to share symbols between various GIS applications. In the first step we proposed standardization in symbology while in the second virtual machine technology is proposed which have not been adopted yet.

The interface of GIS is equipped with a library which contains standard symbols for various domains of hydrocarbon exploration industry including (1). Geology (2). Geochemical (3). Pipeline (4). Environment (5). Natural Objects (6). Soil (7). Microbial prospects

These symbols are selected and finalized after coordinating with various companies through online questionnaire and later through a coordination meeting. Standardization is explained in Figure 3.

2. Material and Methods

A system namely GINU (Geographical Interface for Novice Users) has been implemented after the completion of study. The purpose of development was to provide flexibility in interface of ArcGIS to incorporate above mentioned innovations. The interface addressed the issues of (1). Friendly GUIs (2). Data accuracy and symbology in an integrated manner. The goal of GINU is to increase diffusion of GIS by improving the interface of GIS application. The use of GIS is limited in developing countries because of the above mentioned reasons. Especially, the managers of hydrocarbon exploration industry were reluctant to use GIS inspite of the fact that GIS is beneficial for going through various steps of hydrocarbon exploration. GINU integrated the concepts of multiple domains including Human-Computer Interaction, artificial neural networks and social sciences.

GINU is composed of two types of databases. One is to store spatial and non-spatial database just like normal database management in GIS software. An instance of spatial database is proposed (not actually embedded yet) to incorporate virtual machine technology which was proposed by SU Kehua et.al (2008). The second type of database is the one which handles attribute data. The interface is divided into information retrieval window, information querying window and information analysis window. Raw input by user is directed towards the appropriate module and will be retrieved by either spatial or non-spatial database as per requirements of the user. For Information analysis, the user is given with the option to perform three types of analysis.

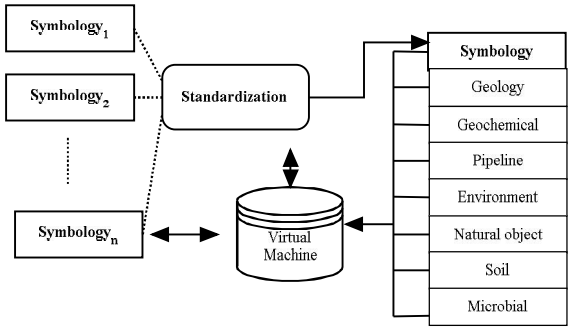

Figure 3 – Standardization of symbology through incorporation of virtual machine

Statistical analysis: The user will perform normal statistical analysis which is most common in industries. Normal statistical analysis can use methods of correlation, sum if, average if etc.

Non-Statistical analysis: Every analysis other than statistical analysis is placed in the category of non-statistical analysis. For example the user is interested to find terrains with large number of obstacles in reconnaissance survey etc.

Validation analysis: Validation analysis is performed to validate the accuracy of data incorporated in GIS. As stated earlier that positional accuracy or image geometric accuracy can be validated by using back-propogation neural network (BPNN).

The architecture of GINU is illustrated in the Figure 5. Validation analysis is quite innovative and incorporated in the system for testing purposes. So the results of backpropogation neural network for validation analysis are described in Table1.

Table 1. Results Summary of BPNN

	Training Set	**Test Set**
Iterations trained	2478	N/A
No of Rows	486	115
Tolerance	0.2	0.3
No of good forecasts	288	96
No. of bad forecasts	96	19
Average MSE	0.1724	13.254

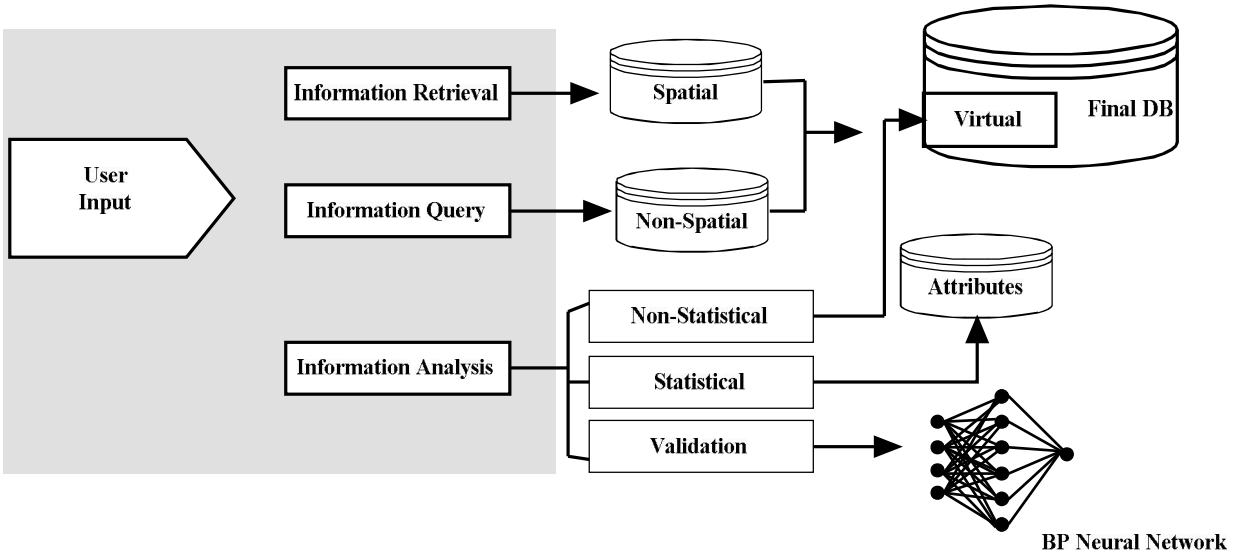

Figure 4 – GINU's Architecture

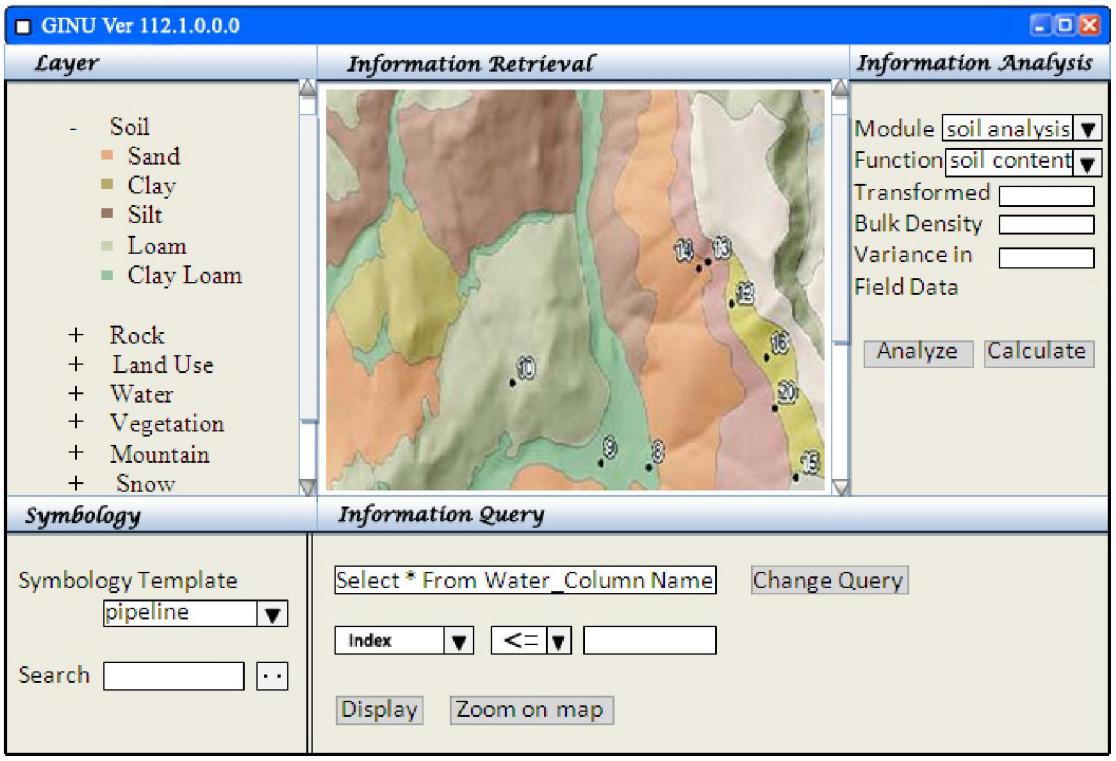

Figure 5 – Proposed GINU's Interface Design

3. Conclusion and Future Work

We have presented an overview of the reasons for non-diffusion of GIS in hydrocarbon and other industries of developing countries. We identified three reasons for non-diffusion. (1). Non-friendly GUIs (2). Unreliable accuracy of spatial data (3). Non-standardization of GIS symbology. For the first one we proposed few enhancements in existing GIS interfaces so that the interfaces become usable and easy for novice users. To deal with positional and imagery inaccuracy, backpropogation neural network is introduced which is trained on different ranges and new data is validated on the basis of those ranges. New data can also define certain change in previous range. For standardization of GIS symbology, all the organizations are motivated to follow standard symbologies. Virtual machine is incorporated to ensure standardization of symbology. A system GINU is developed to support novice users in GIS usage hence increasing the diffusion of GIS in hydrocarbon industry.

The work can be extended to actually include virtual symbology storage in the system. The validation of data for ensuring accuracy can also be enhanced by identifying patterns, trends and distribution of data in the existing database and to enforce new input to follow the same pattern and trend.

Corresponding Author:
Muhammad Shaheen, Ph.D (Computer Science)
Department of Computer Science
University of Engineering & Technology Lahore
Punjab, Pakistan. Tel: (92)331-4525045
E-mail: shaheen@uet.edu.pk,
shaheentanoli@gmail.com

References

1. Adam S. High Resolution Satellite Imagery: From Spies to Pipeline Management. Proceedings of GIS for Oil and Gas Conference 2000.
2. Anselin L. Interactive techniques and Exploratory Spatial Data Analysis. In: 1999 Geographical Information Systems: principles, techniques, management and applications. Cambridge: Geoinformation International.
3. Barrel K.A. GIS: The Exploration and Exploitation Tool: Geographic information systems in petroleum exploration and development. AAPG Computer Applications in Geology. 2000; 4, 237–248.
4. Boudreau M.C, Gefen D, Straub D. Validation in IS Research: A State-of the-Art Assessment. MIS Quarterly. 2001; 25, 1-24.
5. Cahan B, Ball M. GIS at Ground Zero: Spatial technology bolsters World Trade Center response and recovery. 2002; GEOWorld, 26–29.
6. Cai G, Sharma R, MacEachern A.M, Brewer I. Human-GIS Interaction Issues in Crisis Response. International Journal of Risk Assessment and Management. 2006; 6(4), 388-407.
7. Chang N.B, Wei Y.L, Tseng C.C, Kao C.Y.J. The design of a GIS-based decision support system for chemical emergency preparedness and response in an urban environment. Computer, Environment, and Urban System. 1997; 21(1), 67-94.
8. Colijn R. The Diffusion of GIS at Municipalities in the Netharlands. 2000; M.Sc Thesis. Vrije University Amsterdam.
9. Dalal-Clayton B, Dent D. Surveys, plans and people. A review of Land Resource Information and its use in developing countries. IIED, Environmental Planning. 1999; Issues No. 2. FAO and UNEP.
10. De Man W.H.E, Toorn W.H.D. Culture and the adoption and use of GIS within Organizations. International Journal of Applied Earth Observation and Geo Information. 2002; 4(1), 51-63.
11. De Silva F, Pidd M, Eglese R. Spatial decision support systems for emergency planning: an operational research/geographic information systems approach to evacuation planning. In International emergency management and engineering conference: Society for Computer Simulation, 1993; 130–133.
12. Dykes J. Exploring Spatial Data Representation with Dynamic Graphics. Computers and Geosciences. 1997; 23(4), 364-378.
13. Egenhofer M. User interfaces. In Cognitive Aspects of Human-Computer Interaction for Geographic Information Systems. Kluwer Academic Publishers: Dordrecht. 1995; 143-145.
14. Emmi P.C, Horton C.A. A Monte Carlo simulation of error propagation in a GIS-based assessment of seismic risk. International Journal of Geographical Information Systems. 1995; 9(4), 447- 461.
15. Everett J. R., Jengo C., Staskowski R. J., 2002. Remote sensing and GIS enable future exploration success. *World Oil.* 223(11), 59-65.
16. Fuest S, Berlekamp J, Klein M, Matthies M. Risk hazard mapping of groundwater contamination using long-term monitoring data of shallow drinking water wells. Journal of Hazardous Materials. 1998; 61(1-3), 197-202.
17. Goodchild M.F, Parks B.O, Steyaert L.T. Environmental Modelling with GIS. 1993; Oxford Univ. Press.

18. Goodman S, Green J. D. Computing in the Middle East. Communications of the ACM. 1992; 35(8), 21-25.
19. Huizing H, Toxopeus A.G, Dopheide E, Kariaga B.M. 2002. GIS and natural resource management : prospect and problems Kanyati Communal Lands, Zimbabwe. 2002; In Proceedings GISDECO.
20. Iqbal M. Integration of Satellite Data and Field Observations in Pishin Basin, Baluchistan. Pakistan Journal of Hydrocarbon Research. 2004; 14, 1-17.
21. Kevany M.J. GIS in the World Trade Center attack--trial by fire. Computers, Environment and Urban Systems. 2003; 27(6), 571-583.
22. Kroode T. Veel voeten in de aarde, Stand van zaken op het terrein van de gemeentelijke vastgoedinformatievoorziening. 1994; Gravenhage: VNG-uitgeverij.
23. Krovi R. Identifying the causes of resistance to IS implementation: A change theory perspective. Information & Management. 1993; 25, 327-335.
24. LaBarbera R.R. Strategically planning Fort Bend County's GIS: An Enterprise GIS User's Guide – Case Study. 2006; Future Graduate Internship Class, University of Houston Clear Lake.
25. Li D, Yuan X. Error processing and reliability theory. 2002; Wuhan University Press.
26. Li X, Gao F. Uncertainty and sensitivity matrices in parameter inversion by remote sensing. Journal of Remote Sensing. 1997; 1(1), 5-14.
27. Litao H. Approach to related problems regarding the spatial date quality. Northeast Surveying and Mapping. 2003; 26(1), 11-14.
28. Lovett B.J, Parfitt J. Assessing hazardous waste transport risks using a GIS. International Journal of Geographical Information Systems. 1996; 10(7), 831-849.
29. Lu M.T, Hsieh C, Pan C. Implementing Decision Support Systems in Developing Countries. 1989; IMDS (7), 21-26.
30. Mark David M, Andrew U. F. User Interfaces for Geographic Information Systems: Report On The Specialist Meeting. 1992; National Center for Geographic Information and Analysis NCGIA Report 92-3.
31. Masser I. Governments and Geographic Information. 1998; Taylor & Francis, London.
32. McBride N.K, Elbeltagi I, Hardaker G. Evaluating the Factors Affecting DSS usage by Senior Managers in Local Authorities in Egypt. Journal of Global Information Management. 2005; 13(2), 42-65.
33. McLay K, Muggli R, Mazrui S. ArcGIS in the Oil and Gas Exploration Workflow. 2003; 23rd Annual ESRI International User Conference San Diego.
34. Muehlenhaus I. Beyond Mapping? GIS Diffusion and the Deterritorialization of Geopolitics. 2007; Conference Proceeding, Association of American Geographers.
35. Nash G.D, Adams M.C. Cost Effective use of GIS for Tracer Test data mapping and Visualization. Geothermal Resources Council Transactions. 2001; 25.
36. Nielson D. L, Nash G.D. Structural fabric of the Geysers. Geothermal Resources Council Transactions. 1997; 21, 643-649.
37. Nielson D.L, Nash G.D, White W.S. Reservoir characterization using image analysis of core examples from The Geysers geothermal field: E. Barbier, G. Frye, E. Iglesias,G. Pàlmason. Proceedings of the World Geothermal Congress, 1995, Florence, Italy, 3017-3021.
38. Onsrud H.J, Masser I. Diffusion and use of geographic information technologies, Proceedings of the NATO Advanced Research Workshop on Modelling the Diffusion and Use of Geographic Information Technologies. 1993; Kluwer academic Publishers.
39. Porter T. R, Isaac M. R, Martin M. R. Seismic Metadata Management: Optimization with GIS. Leading Edge. 2000; 19, 204-206.
40. Ramadan T. M, El Mongy S. A, El Dein S. S. Exploration for Uranium and Thorium Mineralizations at Wadi Um Laseifa Area, Central Eastern Desert, Egypt Using Remote Sensing Technique. Australian Journal of Basic and Applied Sciences. 2009; 3(2), 689-697.
41. Ramadan T.M, El-Lithy B.S, Nada A, Hassaan M. M. Application of Remote Sensing and GIS in Prospecting for Radioactive Minerals in the Central Eastern Desert of Egypt. Journal of Remote Sensing and Space Sciences. 1999; 2, 141-151.
42. Rhind D. Spatial data from government. The 1995 AGI Source Book for Geographic Information Systems. 1995; Chicester Wiley.
43. Shah Z.U.H. Geographic Information System – An ultimate tool for Hydrocarbon exploration and Exploitation. Journal of the Virtual Explorer. 2006; 23, paper 2.
44. Shah Z. U. H. Implementation of GIS for the Petroleum Sector - A Case Study. 2003; Proceedings of a National Conference on Information & Communication Technology (ICT) for Development, Bridging the Digital Divide, Remote Sensing and GIS Technology, Islamabad.
45. Sobeih A. Geographic Information System in Egypt, A developing connection: Bridging the

policy gap between the information society and sustainable development. 2005; IISD Publishers Canada.
46. Su K, Zhu X, Kong F. Cross platform Adaptive GIS symbolization. The International Archives of the Photogrammetric, Remote Sensing and Spatial Information Sciences. 2008; 37(B2), 751-754.
47. SuperMap Vector Map Symbol Library Exchange Format 2.0. Beijing Super Map GIS Lit. 1999,12. http://www.gischina.com/maindoc/simchin/gisforum/format/vector006.htm, (Chinese).
48. Thumerer T, Jones A.P, Brown D. A GIS based coastal management system for climate change associated flood risk assessment on the east coast of England. International Journal of Geographical Information Science. 2000; 14(3), 265-281.
49. Trappey A.J.C, Lin S.C.I, Wang A.C.L. Using Neural Network Categorization Method to Develop an Innovative Knowledge Management Technology for Patent Document Classification. 2005; 9th International Conference on Computer Supported Cooperative Work in Design Proceedings. 830-835.
50. Trevor B, Gatrell A.C. Interactive spatial data analysis. 1995; Harlow, Longman Scientific and Technical.
51. Vanvoris P, Millard W.D, Thomas J, Urban D. Terra-Vision - the Integration of Scientific Analysis into the Decision-Making Process. International Journal of Geographical Information Systems. 1993; 7(2), 143-164.
52. Wadwani A. Recent Advances in GPS/GIS Data Collection. 2000; Proceedings of GIS for Oil and Gas Conference.
53. Walters M. A, Moore J. N, Nash G. D, Renner J. L. Oxygen isotope systematic and reservoir evolution of the Northwest Geysers, Ca. Geothermal Resources Council Transactions. 1996; V. 20.
54. Warner T.A. Geobotanical and Lineament analysis of LandSat Satellite Imagery for hydrocarbon microseep. 2000; Information Bridge, DOE scientific and technical information.
55. Williams A. K. The Role of Satellite Exploration in the Search for New Petroleum Reserves in South Asia. NPA Paper. 2000; Proceedings of SPE-PAPG Annual Technical Conference, Islamabad Pakistan.
56. Xiaosheng L, Weibo W.B, Xiaoli Z. A Study on Methods for Quality Control of Spatial Data in Poyang Lake Area. ISPRS Workshop on Service and Application of Spatial Data Infrastructure China. 2005; 36, 221-224.
57. Yeh A. Development and Applications of GIS in Asia. 2004; Proceedings of GISDECO.
58. Ying W. Discuss about sources of errors of GIS data and methods to correct them. Hydrographical Surveying and Charting. 2002; 22(1), 18-20.
59. Zeng Y. Spatial Data positional accuracy analyzing and testing. ISPRS Workshop on Updating Geo-spatial Databases with Imagery & the 5th ISPRS Workshop on DMGISs. 2007; 257-262.

3/18/2010

Surgical Site Infections and Associated Risk Factors in Egyptian Orthopedic Patients

[1]Khaleid M. Abdel-Haleim, [2]Zeinab Abdel-Khalek Ibraheim, [3]Eman M. El-Tahlawy

Departments of [1]Orthopedic Surgery, [2] Medical Microbiology and Immunology, Cairo University, [3]Departement of environmental health, National Research Center, Egypt
we.za.2007@hotmail.com

Abstract: Background:Surgical site infections (SSIs) were identified on inpatient surgical wards, and most were associated with cardiac, abdominal, and orthopedic surgery. SSIs surveillance data are the foundation of effective infection control programs. **Aim of the work**:This study was conducted to estimate the risk factors and major pathogens involved in SSIs in orthopedic ward in a public hospital in Cairo, Egypt. **Materials and Methods**:During a 9-months period; a total of 93 consecutive orthopedic surgery patients were followed prospectively for 30 days after surgery. Risk factors for SSIs development were assessed for each patient. Swabs from infected surgical wounds were inoculated into routine culture media. Isolates were identified to the species level, and antimicrobial resistance patterns were determined. **Results:**The present study detected an overall SSIs rate of 25.8% (from 4.1% in clean wound to 66.7% in dirty contaminated wounds). Surveillance of risk factors of SSI, defined age**,** obesity (Body mass index "BMI" > 25), smoking, length of stay in hospital, class of wound, number of persons in the operating room, duration of operation and National Nosocomial infections surveillance (NNIS) index as independent risk factors for SSIs development. Microbiological study of infected surgical sites detected 47 pathogens. *S. aureus* was isolated most frequently 42.6%, Coagulase negative staphylococci "CoNS" and Enterococci were detected in 10.6% and 6.4% of isolates respectively. *K. pneumonia, P. aeruginosa, K. oxytoca, E. coli and A. baumannii* were detected in percentages of 14.9%, 10.6%, 4.3%, 4.3% and 2.1% of isolates respectively. *Candida albicans* was also detected in 4.3% of isolates. Antimicrobial susceptibility testing of isolates detected Oxacillin resistant S.aureus (ORSA) in 65% of *S. aureus* isolates. Enterococcus species resistance to vancomycin (VA) was 33.4%, and that to ampicillin (AMP) was 66.7%. Fluoroquinolones (FQs) resistance was detected in 20% of *P. aeruginosa* isolates. Extended-spectrum cephalosporin resistance (ESBLs) was detected in 50% of *K. oxytoca* isolates, 40% of *P. aeruginosa* and 28.6% of *K. pneumonia* isolates. Carbapenem resistance was detected only in *K. pneumonia* isolates (14.2%). **Conclusion:**We concluded that incidence of SSIs in orthopedic patients in Egypt is higher than that reported in some developing countries. *S. aureus* is the most common pathogens associated with orthopedic SSIs. ORSA, VA-resistant Enterococcus species, ESBLs producing *Klebsiellae* species and *P. aeruginosa*, as well as FQs resistant *P. aeruginosa and* carbapenem resistance *K. pneumonia* pose an ongoing and increasing challenge to the antimicrobial policy in our hospital. In orthopedic surgery unit risk factors for SSIs that may represent points of intervention including; limiting the number of personnel entering the operating room, improving NNIS risk index of patients and reduction of duration of surgery. In the era of restricted hospital budgets and increased bacterial resistance, long-term surveillance of SSIs rates and follow-up of compliance may provide a way to improve performance at low costs. [Journal of American Science 2010;6(7):272-280]. (ISSN: 1545-1003).

Key words; Surgical site infections (SSIs); Risk factors of SSIs; *S. aureus*, Oxacillin resistant S. aureus (ORSA); Extended-spectrum cephalosporin resistance (ESBLs); Carbapenem resistance**.**

1-Introduction

Surgical site infections (SSIs) were the most common procedure-associated Health care associated infections (HAIs) CDC(2007). SSIs were identified on inpatient surgical wards, and most were associated with cardiac, abdominal, orthopedic surgery and neurosurgery, Alicia et al.,(2008). SSIs increase morbidity and mortality and can bring considerable costs to an already overwhelmed health care system, Green and Wenzel(1977) and Taylor et al.,(1990).

Antimicrobial-resistant pathogens that cause healthcare-associated infections (HAIs) pose an ongoing and increasing challenge to hospitals, both in the clinical treatment of patients and in the prevention of the cross-transmission of these problematic pathogens, Esposito and Leone(2007); Schwaber and Carmeli (2007). Surveillance for SSI is a standard procedure in many hospitals, CDC(1996) has stated that United States has a countrywide surveillance system . Surgical site infection rates are an established measure of quality of clinical care,Wenzel(1985); Haley(1985), and reliable surveillance data are the foundation of effective infection control programs,CDC(1996).

Unfortunately, Surveillance of SSIs is a persistent problem in orthopedic surgery, M'-Irrazi(2005). Despite the fact that, infection control program has been introduced to every hospital in Egypt few years ago, yet its implementation was questionable. In Egypt, Surveillance of SSIs -particularly in orthopedic surgery- has not been well known and was thus investigated in this study aiming to define

the level of risk for our patients, and to recognize a trend within our department that may allow for targeted prevention measures.

Aim of the work

This study was conducted to estimate the risk factors and major pathogens involved in surgical site infections in orthopedic ward in a public hospital in Cairo, Egypt

2-Materials and Methods

2.1.Materials:

This single institution study was conducted at the department of orthopedic surgery, Mobarak hospital (which is a public hospital (< 200 beds) in Cairo, Egypt). During the 9-months period from March through December 2009. Operating rooms in the hospital were built in new modern way maintained at positive pressure with respect to corridors and adjacent areas. All ventilation and air conditioning systems in operating rooms have two filter beds in series. Surgical instruments were sterilized by autoclaving (monitoring of steam autoclave performance is satisfactory). Surgical attire and drapes –scrub suits, caps/hoods, shoe covers, masks, gloves, and gowns were used properly. Adherence to the principles of asepsis by all scrubbed personnel, excellent surgical technique, post-operative incision care, and discharge planning with optimum protocols for home incision care have been perfectly implemented.

2**.1.1.Subjects**:

-A total of 93 consecutive orthopedic surgery procedures were performed. Those patients were followed prospectively for 30 days after surgery,according to (Mangram et al., (1999). Wounds were inspected for signs of sepsis at the 3rd, 5th, 7th, and 14th postoperative day or whenever there was clinical suspicious of wound infection. Patients were taught to return to the hospital for reexamination whenever any signs or symptoms of woundinfections,pain,tenderness,localized swelling, or fever- were developed afterdischarging from the hospital.

- Pretested questionnaire was collected included: social data (Age, Gender, Body mass index (BMI), Diabetes, Nicotine abuse, Chronic diseases) , and surgical details (Type of operation "elective or emergency", Duration of operation, Wound class**,** Surgical drains, Number of persons attending the operation, length of stay in hospital (LOS), and Preoperative skin preparation including shaving with razor) , according to Mangram et al., (1999).

-Each patient was classified according to American Society of Anesthesiologists (ASA) score , and National Nosocomial infections surveillance (NNIS) risk index which was calculated by assigning one point for a contaminated wound, an ASA score >3, and surgical procedures lasting longer than NNIS-derived 75th percentile for the duration of procedure, Edwards etal.,(2008) .

2.2. Methods:

2.2.1.Bacteriological study

Swabs from infected surgical wound were transported to the Microbiology laboratory, Faculty of medicine, Cairo University to be inoculated (within 2 h of collection) and inoculated onto sheep blood (5 %), chocolate and MacConkey agar plates (Oxoid, Basingstoke, United Kingdom). Plates were incubated at 37°C aerobically (MacConkey & blood) and in 5% carbon dioxide (chocolate).Plates were examined after 24 and/or 48 h. Isolates were identified to genus level by conventional methods, Murrayet al., (1995).

Staphulococcusaureus(S.aureus) identification was based upon colony morphologies , Gram stain and positive catalase reaction. Tube coagulase test for the detection of free coagulase activity on rabbit plasma (bio-Me´rieux, Marcy l'Etoile, France), and rapid slide latex agglutination tests (Slidex Staph Plus; bioMe´rieux) were performed for definitive identification of *S.aureus*. Slidex Staph Plus (bioMe´rieux); is a slide agglutination test based on latex particles sensitized with human fibrinogen and monoclonal antibodies for the simultaneous detection of clumping factor, staphylococcal protein A, and group-specific antigens on the *S.aureus* cell surface. The test was performed according to the manufacturers' instructions. positive tube coagulase test and latex agglutination test indicated *S.aureus*.

Gram negative isolates were identified to the species level by API 20E kit (bio-Me´rieux, Marcy l'Etoile, France).

Antimicrobial susceptibility testing (agar disk diffusion methods) using Mueller-Hinton BBL II agar (Becton Dickinson, Heidelberg, Germany), and antibiotic disks (Oxoid, Basingstoke, United Kingdom) were performed. The choice of antibiotic and interpretation of inhibition zones were done according to guidelines of CLSI (M100-S18) **(**Clinical and Laboratory Standards Institute,2008) Multidrug resistant, including Oxacillin resistant *S.aureus* (ORSA), vancomycin-resisant VA)Enterococcus(,extendedspectrumcephalospori-resistant (ESBLs) *Klesiella pneumonia*(*K.pneumonia),Pseudomonas aeruginosa (P. aeruginosa)* and *Escherichia coli (E. coli)*, as well as carbapenem-resistant *P. aeruginosa,Acinetobacterbaumanni(A. baumannii), K. pneumoniae, K. oxytoca, and E. coli* were investigated among studied isolates. This classification was based on the recognition that the mechanisms of resistance in these phenotypes confered resistance to multiple classes of antimicrobial agents, Alicia et al.,(2008).

Oxacillin resistant *S.aureus* (ORSA) was identified as specified in M100-S15, Clinical and Laboratory Standards Institute(2005) using 30µg cefoxitin disks. *S. aureus* with a zone diameter of ≤ 19mm

were scored as resistant and those with a zone diameter of ≥ 20mm were reported as susceptible. *S. aureus* strains ATCC 29213 and ATCC 25923 were included for quality control.

Double-disk diffusion test was done to confirm ESBLs activity; 30µg antibiotic disks of cefotaxime, ceftazidime, cefpodoxime and cefepime (Oxoid, Basingstoke, United Kingdom) were placed around an amoxicillin/clavulanic acid disk (20µg/10µg, respectively) at a distance of 25 mm. A clear extension of the edge of the inhibition zone of any of these disks toward the disk containing clavulanate (Keyhole effect) was interpreted as synergy, indicating the presence of an ESBLs, Tzelepi et al., (2000).

2.2.2.Statistically analysis:

Analysis was conducted for qualitative data using number, percent and Chi-square test, for numeric data using mean, standard deviation and analysis of variance test, and for ASA and NNSI scores using proportional trend test with significant level at P-value < 0.05

a; NNIS (National Nosocomial infections surveillance) risk index score was calculated for each patient by assigning one point each for a contaminated wound, an ASA (American Society of Anesthesiologists) score >3, and surgical procedures lasting longer than the NNIS-derived 75th percentile for the duration of the procedure, Edwards etal.,(2008) .

3-Results

Table1: Characteristics of operated patients

Characteristics of patient	**No. (%)**
Gender:	
Males	66 (71%)
Females	27 (29%)
Age group (years):	
16 - 40	20 (21.5%)
>40 - 60	41 (44.1%)
>60ys	32 (34.4%)
Nicotine abuse	
Smoker	68 (73.1%)
Non smoker	25 (26.9%)
Body mass index (BMI)	43 (46.2%)
BMI < 25	50 (53.8%)
BMI > 25	
Diabetes mellitus	
Diabetics	13 (14%)
Non Diabetics	80 (86%)
ASA score[a]:	
< 3	64 (68.9%)
≥ 3	29 (31.1%)
Class of wound	
Clean	49 (52.7%)
Contaminated	35 (37.6%)
Dirty/infected	9 (9.7%)
Type of operation	
Emergency procedures	52 (55.9%)
Open reduction and internal fixation	41 (44.1%)

a; American Society of Anesthesiologists, Mangram et al., (1999)

Table (2): Incidences of surgical site infections (SSI)

	No. of SSI	**No. of operated patients**	**Incidence rate**	***P* value**
Total SSI	24	93	25.8%	
SSI rate stratified by NNIS risk index[a] score:				0.000
0	2	42	4.7%	
1	7	26	26.9%	
2	13	23	56.5%	
3	2	2	100%	
SSI rate stratified by Class of wound:				0.000
Clean	2	49	4.08%	
Contaminated	16	35	45.7%	
Infected/dirty	6	9	66.6%	

Table (3): Association between investigated risk factors and surgical site infections

Variable	No. of patients with SSI	without SSI	P value[d]
Incidence of SSI	24	69	
Age group: 16 - 60ys	9	52	**0.000**
>60ys	15	17	
Gender Males	16	50	**0.58**
Females	8	19	
BMI[a] >25	23	27	**0.000**
Nicotine abuse Smoker	21	47	**0.02**
Non smoker	3	28	
Diabetes mellitus	5	8	**0.48**
ASA score[b]<3	14	64	**0.33**
ASA score ≥3	10	29	
NNIS risk index[c] > 2	15	10	0.000
Class of wound Clean	2	49	
Contaminated	16	35	**0.000**
Dirty/infected	6	9	
Length of stay in hospital (Mean ± SD)	13±1.6	7±1.4	**0.000**
Type of operation Emergency	16	42	**0.61**
procedures	8	27	
Open reduction fracture			
Duration of surgery >75th percentile for the duration of the procedure	13	20	**0.02**
Presence of drain tube	14	37	**0.4**
No. of persons in the operating room (mean ± DS)	6.6±1.5	5±1.5	**0.000**
Preoperative shaving with razor	8	20	**0.44**

a; Body mass index
b; American Society of Anesthesiologists score[13]
c; NNIS (National Nosocomial infections surveillance) risk index score was calculated for each patient by assigning one point each for a contaminated wound, an ASA (American Society of Anesthesiologists) score >3, and surgical procedures lasting longer than the NNIS-derived 75th percentile for the duration of procedure[18].
d; Significant level at P-value < 0.05

Table4: Frequency of different isolated organisms

Organism	Frequency No (%)
Gram positive cocci	**28 (59.6)**
- *S.aureus*	20 (42.6)
- *Coagulase negative staphylococci*	5 (10.6)
- *Enterococcus spp.*	3 (6.4)
Gram negative bacilli	**17 (36.1)**
- *Klebsiella pneumonia*	7 (14.9)
- *Klebsiella oxytoca*	2 (4.2)
- *Pseudomonas aeruginosa*	5 (10.6)
- *E. coli*	2 (4.3)
- *Acinetobacter baumannii*	1 (2.1)
Candida albicans	**2 (4.3)**

Table5: Resistance patterns of isolated organisms

Type of resistant organism	Total number of isolates	% of Resistant isolates
S.aureus	20	
ORSA[a]		65%
Enterococci	3	
VA resistant		33.4%
AMP resistant		66.7%
Pseudomonas aeruginosa	5	
FQs resistant		20%
PIP resistant		20%
ESBLs[b] "CTR, TAZ, or CPM" resistant		40%
Carbapenem "IMI or MERO" resistant		NR[c]
Klebsiella pneumoniae	7	
ESBLs "CTR or TAZ" resistant		28.6%
Carbapenem"IMI, or MERO"resistant		14.2%
Klebsiella oxytoca	2	
ESBLs "CTR or TAZ" resistant		50%
Carbapenem"IMI, or MER resistant		NR

a; Oxacillin resistant S.aureus, b; Extended-spectrum cephalosporin-resistant, c; Not reported
AMP, ampicillin; CPM, cefepime; CTR, ceftriaxone; FQs, fluoroquinolones (ciprofloxacin, levofloxacin, moxifloxacin, or ofloxacin); IMI, imipenem; MERO, meropenem;; PIP, piperacillin; TAZ, ceftazidime; VN, vancomycin.

4-Discussion:

Surveillance of SSIs detected an overall SSIs incidence rate of 25.8% (from 4.1% in clean wound to 66.7% in dirty contaminated wounds). Maksimovic et al.,(2008) and Graf et al.,(2009), detected an overall SSIs incidence of 22.7% and 22.5% respectively. SSIs rates from 13.2% in clean wound to 70% in dirty contaminated wounds were also reported by Maksimovic et al.,(2008)which are comparable results to ours. Meanwhile, lower incidence rates were detected in some developing countries, Kasatpibal et al.,(2004);Thu et al.,(2005); Gastmeier et al.,(2005);Alicia et al.,(2008).

The present study defined age older than 60 years as significant risk factors for SSIs development (P value= 0.000), and no specific gender was significantly associated with SSIs. A recent study reported that age older than median age of 68 years was significant risk factor for SSI development Eli et al.,(2003); Maksimovic et al.,(2008) and Graf et al., (2009) reported that no significant differences in age or gender between case-patients and matched controls were noted.

The present study pointed to obesity **(**BMI > 25**)** as a significant risk factor for SSIs (P value = 0.000). Similar results have been reported by many researchers,He et al.,(1994)and Barber et al.,(1995)· Maksimovic et al.,(2008) defined obesity as a non significant factor in SSIs development

The contribution of diabetes to SSI risk is controversial· Nagachinta et al.,(1987);Lilienfeld et al.,(1988). While our study found that Diabetes was not associated with increased SSI risk.Recent studies defined diabetes and high intraoperative blood glucose level as significant risk factors for SSI development, Estrada et al.,(2003)and Graf et al.,(2009). More studies are needed to assess the efficacy of pri-operative blood glucose control as a prevention measure for SSIs, Mangram et al.,(1999).

As reported by many researchers, Jones and Triplett(1992)and Holley et al.,(1995) and results of our study; smoking was corroborated as significant SSI risk factor, nevertheless. In addition, Maksimovic et al.,(2008), denied that association.

As reported by Graf et al., (2009) and Maksimovic et al.,(2008)and the present study;it was found that length of stay in hospital was significantly longer for SSIs case patients (P value = 0.000). Prolonged preoperative hospital stay was frequently suggested as a patient characteristic associated with increased SSI risk, Mangram et al.,(1999) . Taylor et al.,(2003)and Graf et al., (2009) , could not get significance in this respect because they

cannot show clearly if a longer stay is due to an infection or if the infection causes a longer stay. In our hospital, there was increasing tendency towards short-stay hospitalization policy due to lake of resources, and thus the majority of SSIs in the present study occurred after discharging from hospital .

The results of our study supported the previously published data that the duration of surgery was significantly longer for SSI patients, Eli et al.,(2003). Maksimovic et al.,(2008) and Graf et al.,(2009) reported that duration of operation ($\geq 75^{th}$ percentiles) was not significantly associated with SSIs.

As reported by Eli et al.,(2003), no significant differences in surgery type between case-patients and matched controls were noted in our study. On the other hand, Maksimovic (2008) reported that open reduction fracture is a risk factor associated with SSIs, while emergency procedures were not significantly associated with SSIs.

As reported by others, Scherrer(2003); Devaney and Rowell(2004)and Maksimovic et al.,(2008); our study showed that the number of persons in operating room had a significant risk factor for SSIs (p value = 0.000). In our hospital a lot of house officers and residents tended to attend orthopedic operations because the orthopedic unit invited a lot of famous Egyptian and foreign orthopedic surgeons and the operation rooms were not designed as a teaching setting. Reduction of number of persons in the operating room, may reduce the incidence of SSIs, Scherrer (2003).

Although the ASA score predicts surgical site infection, Cullen et al.,(1994);Soleto et al., (2003)and Maksimovic et al.,(2008) noted that length of hospital stay, and risk for death was limited as a risk adjustment measure because of its subjectivity and poor inter-rater reliability. Our results showed that ASA score was not significantly associated with SSIs. Because of the fact that a good percentage of our patients were HCV positive with no or mild symptoms, that might affect the significance of ASA as predictor of SSIs in this study.

The present study confirmed the well known fact that the NNIS index was found to be a good predictor of SSIs ,Thu et al.,(2005); Hernandez et al.,(2005)and Maksimovic et al.,(2008) (P value = 0.000).

Although the usefulness of wound classification is doubtful, Ferrraz et al.,(1992), the present study supported the previously published data of Mangram et al.,(1999);Soleto et al.,(2003) and Maksimovic et al.,(2009) that contaminated or dirty wounds were independent risk factor of SSIs (P value = 0.000).

It was well known that shaving with razor Mangram et al.,(1999) and Maksimovic et al., (2008) or hair removal by any means Winston (1992)and Moro et al., (1996) increases the risk of SSIs. The present study detected no significant association between shaving with razor and SSIs.Probably due to the fact that most of the patients involved in the present study underwent emergency procedures (55.9%) without proper preoperative preparations including shaving and if shaving is a must it is done immediately before surgery.

The present study showed no significant association between the presence of drain tube and SSIs. Results that fit in between data reported by Maksimovic et al.,(2009), and Graf et al.,(2009).

Bacteriological study of infected surgical sites detected 47 pathogens out of 24 SSIs cases cultured. Polymicrobial infections were detected in some cases .

As reported by others, Madsen et al.,(1996);Thu et al.,(2005);Maksimovic et al.,(2008)and Markovic et al.,(2009). The present study showed that *S. aureus*; Coagulase-negative *staphylococci* (CoNS); Gram negative bacilli were the most common pathogens associated with cases of surgical site infection in orthopedic surgery units. *S. aureus* were isolated most frequently (42.6%), Coagulase negative staphylococci (CoNS) and Enterococci were detected in 10.6% and 6.4% of isolates respectively. *K. pneumoniae, P. aeruginosa , K. oxytoca, , E. coli and A. baumannii* were detected in percentages of 14.9%, 10.6%, 4.3%, 4.3% and 2.1% of isolates respectively. *Candida albicans* were detected in 4.3% of isolates. Alicia et al.,(2008), reported that the most common pathogens associated with cases of surgical site infection in orthopedic surgery units were as follows; *S. aureus* (48.6%), CoNS (15.3%), Enterococcus species (3 – 5 %), *P. aeruginosa* (3.4%), *K. pneumoniae* (1.2%), *A. baumannii* (0.9%), *K. oxytoca* (0.4%), and *Candida albicans* (0.2%). *S. aureus* is the most common pathogen causing SSIs in orthopedic surgery Maksimovic et al.,(2008); Saadatian-Elahi et al.,(2008)and Markovic et al.,(2009).

Antimicrobial-resistant pathogens that cause healthcare-associated infections included ORSA, VA-resistant Enterococcus species, ESBLs producing *E. coli* and *Klebsiella* species, as well as fluoroquinolone- or carbapenem-resistant Enterobacteriaceae or *P. aeruginosa* Chambers (2005)and Deshpande et al.,(2007). Describing the magnitude of the problem with respect to these antimicrobial-resistant pathogens is challenging, because the levels of antimicrobial resistance vary for different types of healthcare facilities and for different geographic areas, and some resistance phenotypes were difficult for laboratories to detect, Alicia et al.,(2008). In the present study, the most common resistance patterns associated with isolated organisms were as follows; ORSA was reported in (65%) of isolated *S. aureus*. *Enterococcus* species resistance to VA was

(33.4%), and that of AMP was (66.7%). Alicia et al.(2008) reported ORSA in (49.2%) of *S. aureus* isolates. Enterococcus species resistance to VA was up to (33%), and that of AMP was up to (71.0%). Graf et al.,(2009) reported ORSA in 52% of S. aureus isolates. Markovic et al.,(2009) reported that 79.2% of *S.aureus* isolates were ORSA. ORSA isolates have been detected in percentages as low as 20% -reported from Canada,Jones et al.,(2004) and as high as 80% reported from southern European countries, Vincent et al., (1995)

In the present study FQs resistance were detected in 20% of *P. aeruginosa* isolates. ESBLs was detected in 50% of *K. oxytoca* isolates, 40% of *P. aeruginosa* isolates and 28.6% of *K. pneumonia* isolates. Carbapenem resistance were detected only in *K. pneumonia* (14.2% of *klebsiellae* isolates). Alicia et al.,(2008) reported that FQs resistance were detected in 15.9% of *P. aeruginosa* isolates while ESBLs, and PIP resistant *P. aeruginosa* were detected in 5.7 – 7.3%, and 7.9% of *P. aeruginosa isolates* respectively. The percentage of ESBLs resistance among *K. pneumonia* was 29% of pathogenic isolates and that of *K. oxytoca* was 15% and no carbapenem-resistant *K. oxytoca* pathogenic isolates were reported by Jones et al.,(2004).The first reports of carbapenem resistance among *Klebsiella* species (21% of pathogenic isolates) started to appear from New York hospitals around 2004(Bradford et al., (2004)and Streit et al., (2004). In Europe the prevalence of ESBLs in *klebsiellae* ranged from as low as 3% in Sweden to as high as 34% in Portugal, Hanberger et al.,(1999). Rates of ESBL production by *K. pneumoniae* have been as low as 5% in Japan, Lewis et al.,(1999) and 20 to 50% elsewhere in Asia, Bell et al., (2002); Du et al., (2002)and Yu et al., (2002). ESBLs have also been documented in Israel, Borer et al., (2002), Saudi Arabia El-Karsh et al., (1995) and a variety of North African countries AitMhand et al., (2002) and Neuhauser et al., (2003).

Risk factors for acquisition of ESBLs including; recent surgery, De Chambers (2005) and Heavy antibiotic use Lautenbach et al.,(2001). Several studies have found a relationship between third-generation cephalosporin use and acquisition of a ESBLs-producing strain**,**Lautenbach et al.,(2001);Du et al.,(2002)and Lee et al.,(2004).The present study reported an overall high incidence of antimicrobial resistance in our department, probably due to inappropriate scheme of antimicrobial usage in our hospital.

Although we have some limitations in this study such as small sample size and incomplete post discharge surveillance (patients have difficulty assessing their own wounds for infection). this study was considered one of the few studies that survey SSIs in orthopedic department in Egypt.

We concluded that incidence of SSIs in orthopedic patients in Egypt is higher than that reported in some developing countries. *S. aureus* is the most common pathogens associated with orthopedic SSIs. ORSA, VA-resistant Enterococcus species, ESBLs producing *Klebsiella* species and *P. aeruginosa*, as well as fluoroquinolone resistant *P. aeruginosa* and carbapenem resistant *K. pneumonia* posed an ongoing and increasing challenge to the antimicrobial policy in our hospital. In orthopedic department risk factors for SSIs that may represent points of intervention including; Limiting the number of personnel entering the operating room, Improving NNIS index of patients by proper management of surgical wound to prevent contamination, identifying and treating all infections remote to the surgical site before operation. Also, adherence to excellent surgical technique through proper training of surgeons and nurses may reduce duration of surgery. In the era of restricted hospital budgets and increased bacterial resistance, long-term surveillance of SSIs rates and follow-up of compliance may provide a way to improve performance at low costs.

5-References

Alicia I. H., J. R. Edwards, M. J. Patel, et al. 2008. Antimicrobial-Resistant Pathogens Associated With Healthcare-Associated Infections: Annual Summary of Data Reported to the National Healthcare Safety Network at the Centers for Disease Control and Prevention, 2006–2007. Infect. Control Hosp. Epidemiol.; 29:996-1011

AitMhand, R., Soukri A., Moustaoui N., et al. 2002. Plasmid-mediated TEM-3 extended-spectrum beta-lactamase production in Salmonella typhimuium in Casablanca. J. Antimicrob. Chemother. 49:169–172.

Barber G. R. , Miransky J., Brown A.E. ,etal. **1995**. Direct observations of surgical wound infections at a comprehensive cancer center. Arch. Surg.;130(10):1042-7.

Bradford P. A., Bratu S., Urban C., et al. 2004. Emergence of carbapenem-resistant Klebsiella species possessing the class A carbapenem-hydrolyzing KPC-2 and inhibitor-resistant TEM-30 b-lactamases in New York City. Clin. Infect. Dis.;39:55–60

Bell, J. M., Turnidge J. D., Gales A. C., et al. 2002. Prevalence of extended spectrum beta-lactamase (ESBL)-producing clinical isolates in the Asia-Pacific region and South Africa: regional results from SENTRY Antimicrobial Surveillance Program (1998–99). Diagn. Microbiol. Infect. Dis. 42:193–198.

Borer, A., Gilad J., Menashe G., et al. 2002. Extended-spectrum beta-lactamase-producing Enterobacteriaceae strains in community-acquired bacteremia in southern Israel. Med. Sci. Monit.8:CR44-47.

Centers for Disease Control and Prevention (CDC). 2007. The National Healthcare Safety Network (NHSN) Manual. Patient Safety Component Protocol. Division of Healthcare Quality Promotion. Available at: http://www.cdc.gov/ncidod/dhqp/pdf/nhsn/NHSN Manual_PatientSafetyProtocol_CURRENT.pdf.

Centers for Disease Control and Prevention. 1996. National Nosocomial Infections Surveillance (NNIS) report, data summary from October 1986-April 1996, issued May 1996: a report from the National Nosocomial Infections Surveillance (NNIS) system. Am J Infect Control.19;24:380-388.21.

Clinical and Laboratory Standards Institute. (2005). Performance standards for antimicrobial susceptibility testing. 15th informational supplement M100-S15. Clinical and Laboratory Standards Institute, Wayne, PA. USA.

Clinical and Laboratory Standards Institute. (2008). Performance standards for antimicrobial susceptibility testing: 16th informational supplement M100-S18. Clinical and Laboratory Standards Institute, Wayne, PA. USA.

Cullen D.J., G. Apolone, S. Greenfield, etal. 1994. Physical Status and age predict morbidity after three surgical procedures [comments]. Ann Surg.;220:3-9.

Chambers HF. 2005. Community-associated MRSA—resistance and virulence converge. N Engl J Med; 352:1485–1487

Du, B., Long Y., Liu H., etal. 2002. Extendedspectrum beta-lactamase-producing Escherichia coli and Klebsiella pneumoniae bloodstream infection: risk factors and clinical outcome. Intensive Care Med. 28:1718–1723

Deshpande L.M., Fritsche T. R., Moet G. J., etal. 2007. Antimicrobial resistance and molecular epidemiology of vancomycin-resistant enterococci from North America and Europe: a report from the SENTRY antimicrobial surveillance program. Diagn Microbiol Infect Dis; 58:163–170.

Devaney L and Rowell K.S.. 2004. Improved surgical wound classification-Why it matters. AORN j. ;80:208-9

De Champs, C., Sirot D., Chanal C., etal. 1991. Concomitant dissemination of three extended-spectrum betalactamases among different Enterobacteriaceae isolated in a French hospital. J. Antimicrob. Chemother. 27:441–457.

Esposito S and Leone S. 2007. Antimicrobial treatment for intensive care unit (ICU) infections including the role of the infectious disease specialist. Int J Antimicrob Agents; 29:494–500.

Edwards J.R., Peterson K. D., Andrus M. L., et al. 2008. National Healthcare Safety Network (NHSN) report, data summary for 2006 through 2007, issued November 2008. Am J. Infect Control.;36:609–26.

Eli N. P., Sands K. E., Cosgrove S. E., etal. 2003. Health and Economic Impact of Surgical Site Infections Diagnosed after Hospital Discharge. Emerging Infectious Diseases; 9 (2): 196-203

Estrada C.A., Young J. A., Nifong L.W.. 2003. Outcomes and perioperative hyperglycemia in patients with or without diabetes mellitus undergoing coronary artery bypass grafting. Ann Thorac Surg.;75:1392–1399.

El-Karsh, T., Tawfik A. F., Al-Shammary F., et al. 1995. Antimicrobial resistance and prevalence of extended spectrum beta-lactamase among clinical isolates of gram-negative bacteria in Riyadh. J. Chemother. 7:509–514

Ferraz E.M., Bacelar T.S., Aguiar J.L., etal. 1992. Wound infection rates in clean surgery; a potentially misleading risk classification. Infect. Control Hosp. Epidemiol;13:457-62

Graf. K, Sohr D., Haverich A., Ku¨hn C. , etal. 2009. Decrease of deep sternal surgical site infection rates after cardiac surgery by a comprehensive infection control program. icvts 9:282–286

Gastmeier P., Sohr D., Brandt C., etal. 2005. Redution of orthopedic wound infections in 21 hospitals. Arch. Orthop. Trauma Surg; 125:526-30

Green JW and Wenzel RP. 1977. Postoperative wound infection: a controlled study of the increased duration of hospital stay and direct cost of hospitalization. Ann Surg.;185:264-268.

Haley R.W., Culver D. H., White J. W., etal.1985. The efficacy of infection surveillance and control programs in preventing nosocomial infections in US hospitals. Am. J. Epidemiol. ;121:182-205.

Holley D. T., Toursarkissian B,, Vansconez H. C., etal. 1995. The ramifications of immediate reconstruction in the management of breast cancer. Am. Surg.;61(1):60-5.

He G. W., Ryan W.H., Acuff T. E., et al. 1994. Risk factors for operative mortality and sternal wound infection in bilateral internal mammary artery grafting. J. Thorac Cardiovasc Surg1994;107(1):196-202.

Hernandez K., Ramos E., Seas C., etal. 2005. Incidence of and risk factors for surgical-site infections in a Peruvian hospital. Infect. Control Hosp. Epidemiol;26:26-30

Hanberger, H., Garcia-Rodriguez J. A., Gobernado M.. 1999. Antibiotic susceptibility among aerobic gram-negative bacilli in intensive care units in 5 European countries. French and Portuguese ICU Study Groups. JAMA 281:67–71.

Jones M. E., Draghi D. C., Thornsberry C., et al. 2004. Emerging resistance among bacterial

pathogens in the intensive care unit—a European and North American surveillance study (2000–2002). Ann. Clin. Microbiol. Antimicrob.; 3:14.

Kasatpibal N., Jamulitrat S.,. M'-Irrazi V. M. B., Sellies J., Berrichi A., etal. 2005. Prospective study of operative site infections observed over four-year period: Analysis of 8811 orthopedic surgery procedures. J. of bone and joint Surgery – British Volume, Vol. 90-B Issue Supp_ll, 264.

Lilienfeld D.E., Vlahov D., Tenney J. H. 1988. Obesity and diabetes as risk factors for postoperative wound infections after cardiac surgery. Am J. Infect. Control.;16:3-6.

Lautenbach, E., Patel J. B. , Bilker W. B, et al. 2001. Extended-spectrum beta-lactamase-producing Escherichia coli and Klebsiella pneumoniae: risk factors for infection and impact of resistance on outcomes. Clin. Infect. Dis. 32:1162–1171.

Lee, S. O., Lee E. S., Park S. Y., etal. 2004. Reduced use of third-generation cephalosporins decreases the acquisition of extended-spectrum beta-lactamase-producing Klebsiella pneumoniae. Infect. Control Hosp. Epidemiol. 25:832–837.

Lewis J. S. 2nd, Herrera M., Wickes B., et al. 2007. First report of the emergence of CTX-M-type extended-spectrum b-lactamases (ESBLs) as the predominant ESBL isolated in a U.S. health care system. Antimicrob. Agents. Chemother.; 51:4015–4021.

Lewis, M. T., Yamaguchi K., Biedenbach D. J., etal. 1999. Invitro evaluation of cefepime and other broad-spectrum beta-lactams in 22 medical centers in Japan: a phase II trial comparing two annual organism samples. The Japan Antimicrobial Resistance Study Group. Diagn. Microbiol. Infect. Dis. 35:307–315

Maksimovic J., Markovic-Denic L., Bumbasirevic M., etal. 2008. Surgical Site Infections in Orthopedic Patients : Prospective Cohort Study. Croat Med. J;49(1): 58-65

Markovic D. I., Maksimovic J., Lesic A., Stefanovic S., Bumbasirevic M.. 2009. Etiology of surgical site infections at the orthopedic trauma units. Acta chir.lugosl;56(2):81-6

Madsen MS, Neumann L, Andersen JA. 1996. Penicillin prophylaxis in complicated wounds of hands and feet: a randomized, double-blind trial. Injury;27(4):275-8.

Moro M.L., Carrieri M. P., Tozzi A. E, etal. 1996. Risk factors for surgical wound infections in clean surgery: a multicenter study. Italian PRINOS Study Group. Ann. Ital. Chir.;67:13-9.

Mangram A.J., Teresa C. H., Pearson M. L., etal. 1999. Guidelines for prevention of surgical site infections. Hospital Infections Program National Center for Infectious Diseases, Centers for Disease Control and Prevention. Infection control and hospital epidemiology. Vol. 20(4): 256

M'-Irrazi M. B., J. Sellies, A. Berrichi, etal. 2005. Prospective study of operative site infections observed over four-year period: Analysis of 8811 orthopedic surgery procedures. J. of bone and joint Surgery – British Volume, Vol. 90-B Issue Supp_ll, 264.

Murray, P. R., Baron, E. J., Pfaller, M. A., Tenover, F. C. & Yolken, R. H. 1995. Manual of Clinical Microbiology, 5th edn. Washington, DC: American Society for Microbiology.

Nagachinta T, Stephens M., Reitz B., etal.1987. Risk factors for surgical wound infection following cardiac surgery. J Infect Dis.;156:967-73.

Neuhauser, M. M., Weinstein R. A., Rydman R., etal. 2003 . Antibiotic resistance among gram-negative bacilli in US intensive care units: implications for fluoroquinolone use. JAMA 289:885–888.

Schwaber MJ, Carmeli Y.2007. Mortality and delay in effective therapy associated with extended-spectrum b-lactamase production in Enterobacteriaceae bacteremia: a systematic review and meta-analysis. J Antimicrob. Chemother.; 60:913–920

Streit J. M., Jones R. N., Sader H. S., et al. 2004. Assessment of pathogen occurrences and resistance profiles among infected patients in the intensive care unit: report from the SENTRY Antimicrobial Surveillance Program (North America, 2001). Int J Antimicrob Agents 2004; 24:111– 118.

Scherrer M. 2003. Hygiene and room climate in the operating room. Minim. Invasive Ther. Allied Technol.;12:293-9

Saadatian-Elahi M., R. Teyssou, and P. Vanhems. 2008. Staphylococcus aureus, the major pathogen in orthopedic and cardiac surgical site infections. Int. J Surg;6(3):238-45

Soleto L., Pirard M., Boelaert M., et al. 2003. Incidence of surgical-site infections and the validity of the National Nosocomial Infections Surveillance System risk index in a general surgical ward in Santa Cruz, Bolvia. Infect. Control Hosp. Epidemiol;24:473-7

Tzelepi E, Giakkoupi P., Sofianou D., et al. 2000. Detection of extended-spectrum b-lactamases in clinical isolates of Enterobacter cloacae and Enterobacter aerogenes. J. Clin. Microbiol.; 38: 542–6.

Thu L.T., DibleyM.J., Ewald B., Tien N.P., Lam L.D. 2005. Incidence of surgical site infections and accompanying risk factors in Vietnamese orthopedic patients. J. Hosp. Infect.;60:360-7**.**

Taylor E.W., Duffy K., Lee K., et al. 2003. Telephone call contact for poat-discharge surveillance of surgical site infections. A pilot methodological study. J. Hosp. Infect;55:8-13

Vincent J. L., Bihari D. J., Suter P. M., et al. 1995. The prevalence of nosocomial infection in intensive care units in Europe. Results of the

European Prevalence of Infection in Intensive Care (EPIC) Study. EPIC International Advisory Committee. JAMA.; 274:639–644.

Winston K. R. 1992. Hair and neurosurgery. Neurosurgery;31(2):320-9.

Wenzel R. P. 1985. Nosocomial infections, diagnosis-related groups, and study on the efficacy of nosocomial infection control: economic implications for hospitals under the prospective payment system. Am J Med.1985;78:3-7

Yu, Y., Zhou W., Chen Y., etal. 2002. Epidemiological and antibiotic resistant study on extended-spectrum beta-lactamase-producing Escherichia coli and Klebsiella pneumoniae in Zhejiang Province. Chin Med. J. (Engl.) 115:1479–1482.

4/9/2010

A Hybrid Approach for Minimizing Spurious Trips in Hard Real-Time Systems

[1]Mahmood Ahmed, Dr. [1]Muhammad Shoaib.
[1]Department of Computer Science & Engineering
[1]University of Engineering and Technology
Lahore, Pakistan
mahmoodahmedmughal@gmail.com; shoaib_uet@hotmail.com

Abstract: In this paper a hybrid neural network and rule based approach for spurious trips minimization in hard real time systems such as nuclear reactor power plants is proposed. This approach is a hybrid or a mix of rule base and neural network. The purpose is to learn from experience in the same way as humans learn from their past experience in operation of nuclear power plant. The approach would use artificial neural network as well as a rule based approach for intelligent decision-making. The patters of data will be taken from the modern control systems like DCS, PLC etc. via OPC and is fed to the trained ANN. The output of the algorithm will be a optimized decision. The operator can improve his decision making based on suggested values by the Algorithm. [Journal of American Science 2010;6(7):281-286]. (ISSN: 1545-1003).

Keywords: Spurious trips, Hard Real time system, OPC, rule base, Backpropagation.

1 Introduction

Whenever accidents occur in nuclear power plants [12], operators will attempt to detect the seriousness by observing drifts of parameters presented on HMIs to obtain first hand information of plant's current status which may steer towards accident [10]. The shift operators are unaware of whole data statistics about all parameters and only have a partial future trend behavior so, it is extremely hard for operators to forecast the development of the proceedings by just looking at time-based **tendency** of some important variables on huge sized mimics in the main control room [7], [8]. Also, in this brief time abnormality, the operators will face hundreds of instrument readings that show some typical patterns of that momentary transient [33] , [26]. In most of the situations for severe accidents of nuclear power plants operators should be able to accurately forecast transient scenarios[33], so that they can make accurate decisions regarding safety of personnel as well as reliable operation of the plant [12]. Normally the operators always go for easy decisions like shutting down the power plant. Shutting down a nuclear power plant always costs a huge revenue loss to owner as well as power shortage to countries, already facing energy crisis, like Pakistan [15]. Unlike thermal power plants nuclear power plants always take more time to operational state again. So it is the need of the hour to efficiently operate the plant and to minimize nuclear power plant shutdowns. This can be achieved by taking advantage of latest research trends [4]. Lots of power plants in the world are using artificial intelligence techniques to improve the reliability and to minimize the plant outages. Alexander *G.* Parlos & Benito Fernandez, used Artificial Neural Networks for System Identification and Control of Nuclear Power Plant Components [14], [17]. Lots of artificial intelligence techniques comprising of neural networks and fuzzy inference methods have been successfully applied to numerous nuclear engineering regions such as optimal fuel loading [29], [30], [25] & [26], plant diagnostics [27], [28] , power plant control [31], signal validation [24], event identification [23], [32], [33], and so on. A few more applications of neural networks to nuclear power plant's engineering structures can also be found in the references [18], [19], [20], [21], and [22].

2 Background of the problem

The KANUPP (Karachi NUclear Power Plant), which is a CANDU type reactor [5], [3], was in total control of Pakistani engineers and scientists after Canadians left Pakistan. The plant has faced numerous challenges during its operation. Following the withdrawal of vendor technical assistance and imposition of embargoes by major nuclear countries in 1976 [15], the plant some times has been shutdown for longer durations to carry out maintenance, modifications or repair. A committed self-reliance program by PAEC and KANUPP, however, kept the plant operational throughout the difficult period [15]. Throughout its operational history although there is no major accident occurred but plant faced many spurious shutdowns, which could have been avoided through better decision-making. These spurious shutdown decisions have caused PAEC a great amount of revenue loss over its operational history [9], [15]. So the task is to minimize spurious shutdowns by using artificial intelligence techniques

that will assist the operators towards better decision-making. Monitoring of the overall plant status is conducted from a central control room. The control room for a single-unit CANDU station consists of an open room approximately 20 meters square. Instrumentation panels occupy two walls of the room. The control room also contains a central console that serves as the primary work area for the control room operator and his assistant [34]. From this central seated position, the operator coordinates all aspects of plant operation. In monitoring overall plant operation, the operator uses information from several information systems and sources. The primary source of plant status is drawn from the information displayed at console workstations and panel locations. The plant operator has to keep an eye on numerous parameters before taking a major decision (such as shutdown) in abnormal condition. These days KANUPP is not operated at full power (i.e 137Mwe). It is operated only at 90 MWe these days. Table 1 displays the list of only important parameters [9], [15].

Still there are lots of parameters not shown. So taking a decision based on that much number of parameters is a difficult task. Some times an abnormal shift in the value of a parameter can be ignored if some other parameter values are normal and some time only a single parameter value (e.g PHT outlet temperature 580 F) becomes so important that the operator takes an important decision. Because the abnormal situations arises less in the operational history so data patterns noted and the corresponding decisions taken are in less number. Therefore the task is to achieve higher accuracy with small training data samples for and ANN [6], [1].

3 The Proposed hybrid Methodology

The proposed methodology is actually a hybrid of two AI methodologies. This is neural network plus rule-based [6]. The desired patterns of data collected from the power plant operational history data are used as the training the artificial neural network using Backpropagation algorithm [13], [6], [16], [11], [2]. Then that trained artificial neural network in combination with rule based approach is used in the final decision making in plants shutdown. This methodology has been proposed to solve the spurious reactor trips problem in the KANUPP [9]. The purpose of introducing this hybrid methodology is to improve the decision making ability of the power plant operators. This will ultimately help in minimizing the spurious reactor trips and therefore the loss of revenue.

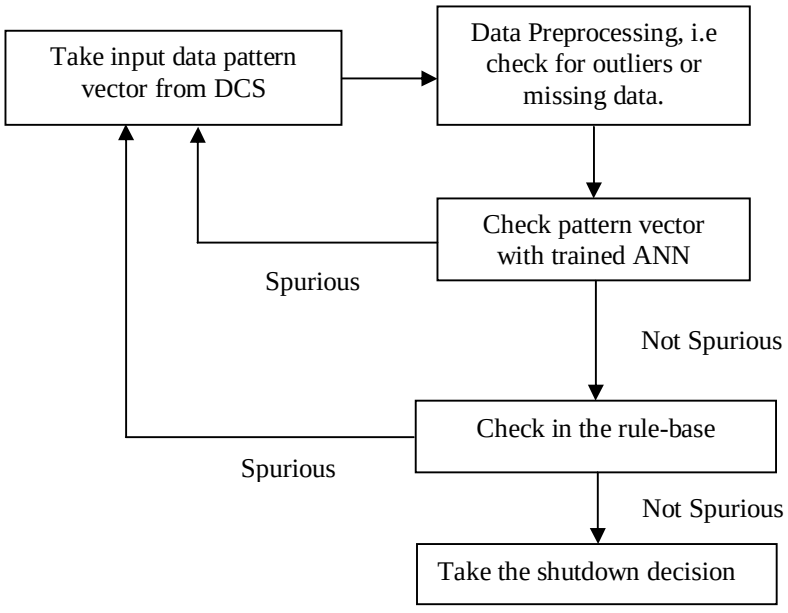

Figure 1: The proposed hybrid approach

4 Case Study

As a case study we considered the operational data of KANUPP. There are hundreds of the parameters in the nuclear power plant [9], we mention some of the variables used as input to the artificial neural network are listed in table 1 shown below.

Table 1: List of some parameters used in the training data

SN	Parameters	Normal operating values
1	Electrical Power (MWe)	90
2	Moderator Level	182
3	Moderator temp (F)	140
4	PHT inlet temperature (F)	478
5	PHT outlet temperature (F)	535
6	Steam Pressure (psi)	550
7	Steam Temp (F)	474
8	Calendria spray flow (igpm)	1500
9	Boiler feed water pressure (psi)	900
10	Condensate water pressure (psi)	200
11	Turbine RPM	3000
12	Generator RPM	3000
13	Boiler feed water pressure (psi)	900
14	Condensate water pressure (psi)	200
15	Exhaust hood temp (F)	110
16	Charging tank level	127
17	Charging tank temp (F)	140
18	Generator hydrogen pressure (psi)	30
19	Turbine shell expansion (mil)	210
20	Hydrogen seal differential pressure (psi)	8.5

The values listed in table 1 are the normal operating values. The training data samples for transient or abnormal conditions have been generated through the simulator. The total number of training data samples generated through the simulator is 255 [35]. Data has been divided into training, validation, and test sets. Out of these samples 60% are used for training, 20% for testing and the remaining 20% for validation [16]. The validation set is used to ensure that there is no over-fitting in the final result. The test set provides an independent measure of how well the network can be expected to perform on data not used to train it.

5 Results & Discussion

5.1 Optimizing the Number of Hidden nodes

The optimized value for the number of hidden nodes for this specific problem is found through a series of experiments for the Levenberg-Marquardt backpropagation. The results are shown in the table 2.

Table 2: Results for different no. hidden nodes.

No. of Hidden Neurons	Execution time	Regression Coefficient	Epochs	Comments
14	41.432071	0.8668	27	Validation stop
15	42.502456	0.8733	24	Validation stop
16	61.86331	0.9736	32	Validation stop
17	41.658935	0.9512	19	Validation stop
18	36.618649	0.9794	15	Validation stop
19	33.517457	0.9943	12	Validation stop

20	16.929745	0.9976	5	Performance goal met
21	21.89272	0.9973	6	Performance goal met
22	20.199239	0.9977	5	Performance goal met
23	26.361702	0.9974	6	Performance goal met
24	27.891669	0.9977	6	Performance goal met
25	43.87587	0.9974	6	Performance goal met
26	32.988149	0.9973	6	Performance goal met
27	34.791656	0.998	6	Performance goal met
28	37.71092	0.9963	6	Performance goal met
29	40.136347	0.9984	6	Performance goal met
30	42.629025	0.9972	6	Performance goal met
31	46.077593	0.9967	6	Performance goal met

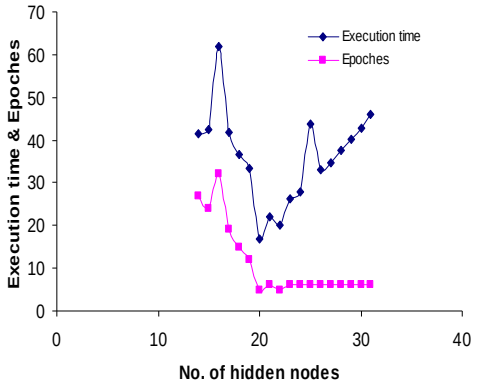

Figure 2: Plot of No. of hidden neurons against execution time & Epochs

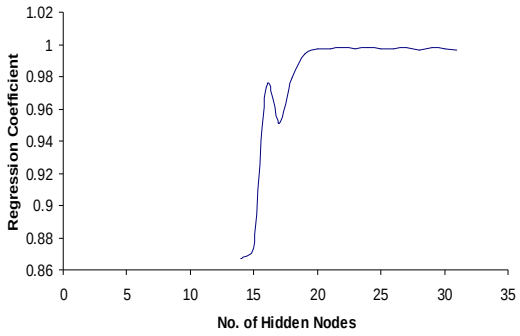

Figure 3: Plot of No. of hidden neurons against regression coefficient

From the table 2 it is clear that numbers of hidden nodes are insufficient up to 19. The performance goal was only met when the number of hidden neurons are 20 or above. From the figure 1 it is clear that the optimized numbers of hidden nodes are 20 for this specific problem. Below twenty there are not enough number of hidden neurons that are not sufficient to solve this problem. It means that the there are not enough number of nodes that can store all the features present in the input patterns. Hidden nodes are actually the feature detectors of the input pattern vectors. So as the size of the input pattern vector increases the required number of optimized hidden neurons also increases. It is also clear from the above figure that as we increase the no. of hidden neuron beyond the optimized number, the execution time increases. Also the storage requirement for hidden neurons is increased which in turn affects the system response time, and that will be fatal if you are dealing with a system that require a real time response.

Also from the figure 2 it is clear that regression coefficient has reached its maximum value when the no. of hidden nodes is 20. If we further increase the number of hidden nodes the regression is the same, i-e reached its maximum value. Value one mean a perfect match. Therefore it is useless to further increase the hidden nodes. Therefore it is the optimized number for this particular example.

5.2 Performance Comparison of different neural network training algorithms

Different backpropagation algorithms have been employed for the training of this nuclear power plant data [36]. The following table shows the results collected by implementing various algorithms. For this comparison case study the performance goal was set = 0.001, it is clear from the table 2 that the first three training algorithms were not able to meet the performance goal. The remaining training algorithms all met the performance goal. The algorithm that achieved the performance goal fastest is Conjugate Gradient with Powell/Beale Restarts (traincgb). The second algorithm that achieved the performance goal

with second minimum time is Variable Learning Rate Backpropagation (traingdx). But as the performance goal made further difficult i-e of the order of *1e-15*, then only algorithm that achieved the goal in minimum time was Levenberg-Marquardt (trainlm). Therefore whenever you need highest accuracy like in a nuclear power plant, this algorithm, Levenberg-Marquardt, is the most useful.

Table 2: Results for different training algorithms

Training Method	Execution time	Regression Coefficient	Comments
BFGS Quasi-Newton (trainbfg)	304.465443	0.9977	Validation stop
Fletcher-Powell Conjugate Gradient (traincgf)	4.520266	0.9961	Validation stop
Variable Learning Rate Backprop. (traingdx)	2.33319	0.9861	Validation stop
One Step Secant (trainoss)	10.050495	0.9978	Performance goal met
Resilient Backpropagation (trainrp)	6.204507	0.9966	Performance goal met
Conjugate Gradient with Powell/Beale Restarts (traincgb)	1.832672	0.9987	Performance goal met
Scaled Conjugate Gradient (trainscg)	3.128176	0.9965	Performance goal met
Levenberg-Marquardt (trainlm)	16.929745	0.9976	Performance goal met

6 Conclusion

The approach used in this paper was aimed towards the problem of spurious reactor trips. Human operators are always prone to errors. It is difficult for human operators to take accurate decisions by keeping an eye on enormous number of parameters and by analyzing a pattern of parameters. This approach assists the operators in their decision about reactor trip based on the past historical data. Nuclear plant operators can benefit from decision support system for improvement in their decision-making. This is one of the solutions to minimize revenue loss to the plant owner. The operator will not be bound to take decision suggested by the DSS; he will still be free to take decision of his own choice. The DSS will be there only for his support.

7 REFERENCES

[1] Ajith Abraham "Optimization of Evolutionary Neural Networks Using Hybrid Learning Algorithms" *School of Business Systems, Monash University*, Clayton, Victoria 3800, Australia

[2] Adam R. Klivans* Rocco A. Servedio "Toward Attribute Efficient Learning Algorithms" *arXiv:cs.LG/0311042 v1 27 Nov 2003*

[3] The most comprehensive educational and reference library on CANDU Technology. http://canteach.candu.org

[4] Corinna Cortes, Mehryar Mohri, Patrick Haffner, "Rational Kernels: Theory and Algorithms" *Journal of Machine Learning Research 5 (2004) 1035-1062*

[5] Canadian Nuclear Association, http://www.cna.ca/english/index.asp http://www.osti.gov/energycitations/searchresults.jsp?Author=Bartlett,%20E.B.

[6] Ernesto De Vito, Lorenzo Rosasco, Andrea Caponnetto, Umberto De Giovannini, Francesca Odone," Learning from Examples as an Inverse Problem." *Journal of Machine Learning Research* 6 (2005) 883–904

[7] Efraim Turban, Jay E. Aronson "*Decision Support Systems and Intelligent Systems*", Prentice-Hall of India, Sixth Edition 2003.

[8] IEEE Virtual Museum 2005 "*Panic at Three Mile Island*" http://www.ieee-virtual-museum.org/collection/event.php?id=3456831&lid=1

[9] KANUPP Research Staff, " Technical Up-gradation Documentation (TUP) ", *KANUPP Institute of Nuclear Power Engineering* Karachi, 2001.

[10] L-3 Communications MAPPS "*CANDU Plant Computer Systems*" http://www.cae.com/L3_MAPPS/Products_and_Services/Power_Systems_and_Simulation/Power_Solutions/candu.shtml

[11] Maureen Caudill and Charles Butler " *Understanding Neural Networks*", A Bradford Book The MIT Press Cambridge, Massachusetts London, England, 1996

[12] World Nuclear Association, Information and Issue briefs "*Chernobyl Accident*" September 2005. http://www.world-nuclear.org/info/chernobyl/inf07

[13] Michael Schmitt, "Some Dichotomy Theorems for Neural Learning Problems" *Journal of Machine Learning Research* 5 (2004) 891–912.

[14] Mario Marchand, Marina Sokolova "Learning with Decision Lists of Data-Dependent Features." *Journal of Machine Learning Research* 6 (2005) 427–451.

[15] Pakistan Atomic Energy Commission "Karachi Nuclear Power Plant" http://www.paec.gov.pk/kanupp/kanupp-index.htm
[16] Robert J. Schalkoff, *Clemson University* " *Artificial Neural Networks* ", MIT press and the McGraw-Hill Companies, International Editions 1997.
[17] Alexander *G.* Parlos, Benito Fernandez, "*Artificial Neural Networks Based System Identification and Control of Nuclear Power Plant Components"* Proceedings *of* the 29th Conference on Decision and Control Honolulu, Hawall December 1990.
[18] E. Eryurek and B.R. Upadhyaya, "Sensor validation for power plants using adaptive backpropagation neural network,' *IEEE Transactions on Nuclear Science,* Vo1.37, No. 2, pp1040-1047, April 1990.
[19] B.C. Hwang, M. Saif and M. Jamshidi, "Neural based fault detection and identification for a nuclear reactor," presented at the 12th World Congress of IFAC, Sydney, Australia, July18-23, 1993.
[20] S.R Naidu, E. Zafiriou and T.J. McAvoy, "Use of neural networks for sensor failure detection in a control system," *IEEE Control System Magazine,* Vol.10, pp49-55, April 1990.
[21] M.S. Roh, S.W. Cheon and S.H. Chang, "Thermal power prediction of nuclear power plant using neural network and parity space model," *IEEE Transactions on Nuclear Science,* Vo1.38, No. 2, pp866-872, April 1991.
[22] B.R Upadhyaya, E. Eryurek and G. Mathai, "Application of neural computing for signal validation," *Seventh Power Plant Dynamics, Control and Testing Symposium,* Vol.1, pp.27.01-27.18, May 1989.
[23] C. H. Roh, H. S. Chang, H. G. Kim, and S. H. Chang, "Identification of reactor vessel failures using spatiotemporal neural networks," *IEEE Trans. Nucl. Sci.*, vol. 43, pp. 3223–3229, Dec. 1996.
[24] J. W. Hines, D. J. Wrest, and R. E. Uhrig, "Signal validation using an adaptive neural fuzzy inference system," *Nucl. Technol.*, vol. 119, no. 2, pp. 181–193, Aug. 1997.
[25] P. Fantoni, S. Figedy, and A. Racz, "A neuro-fuzzy model applied full range signal validation of PWR nuclear power plant data," in *Proc. Int. Conf. Fuzzy Logic and Intelligent Technologies in Nuclear Science (FLINS'98),* Belgium, 1998.
[26] M. G. Na, Y. R. Sim, K. H. Park, S. M. Lee, D. W. Jung, S. H. Shin, B. R. Upadhyaya, K. Zhao, and B. Lu, "Sensor monitoring using a fuzzy neural network with an automatic structure constructor," *IEEE Trans. Nucl. Sci.*, vol. 50, pp. 241–250, Apr. 2003.
[27] E. B. Bartlett and R. E. Uhrig, "Nuclear power plant diagnostics using an artificial neural network," *Nucl. Technol.*, vol. 97, pp. 272–281, Mar. 1992.
[28] M. Marseguerra and E. Zio, "Fault diagnosis via neural networks: The Boltzmann machine," *Nucl. Sci. Eng.*, vol. 117, no. 3, pp. 194–200, July 1994.
[29] H. G. Kim, S. H. Chang, and B. H. Lee, "Optimal fuel loading pattern design using an artificial neural network and a fuzzy rule-based system," *Nucl. Sci. Eng*, vol. 115, no. 2, pp. 152–163, Oct. 1993.
[30] J. H. Lee, H. J. Sim, C. S. Jang, and C. H. Kim, "Incorporation of neural networks into simulated annealing algorithm for fuel assembly loading pattern optimization in a PWR," in *Proc. Int. Conf. Physics of Nuclear Science and Technology—American Nuclear Society*, vol. 1, Long Island, NY, Oct. 5–8, 1998, p. 75.
[31] M. G. Na, "Design of a genetic fuzzy controller for the nuclear steam generator water level control," *IEEE Trans. Nucl. Sci.*, vol. 45, pp. 2261–2271, Aug. 1998.
[32] S. W. Cheon and S. H. Chang, "Application of neural networks to a connectionist expert system for transient identification in nuclear power plants," *Nucl. Technol.*, vol. 102, no. 2, pp. 177–191, May 1993.
[33] Y. Bartal, J. Lin, and R. E. Uhrig, "Nuclear power plant transient diagnostics using artificial neural networks that allow "don't-know" classifications," *Nucl. Technol.*, vol. 110, no. 3, pp. 436–449, June 1995.
[34] Eric Davey, "Process Monitoring During Normal Operations At Canadian Nuclear Power Plants" Human Factors and Ergonomics Society 44th Annual Meeting San Diego, California, 2000 July 30 - August 04.
[35] CANDU Simulator, for training of Plant operators.
[36] MALAB Neural Network Tool Box Documentation version 5.0.

5/5/2010

Key factors for implementing the lean manufacturing system

Mohammad Taleghani
Department of Management, Islamic Azad University - Rasht Branch, IRAN.
Taleghani@iaurasht.ac.it

Abstract: The purpose of this paper is to provide a historical review for the role of management in implementation of lean thinking in a lean manufacturing environment. This paper begins with this subject who introduces the lean manufacturing as the combination of directions and a culture which managers could draw guidelines for achieving benefits through that. Two basic lines of lean manufacturing are “respect to the workforce" and "waste elimination" which is introduced in this paper and how these factors can cause an effective leadership during implementations. Then, it is described that h ow companies use the benefits of lean tools in their conception of lean implementations, and what factors involve managers with culture and leaderships issues. Also, this study implies that not only it is necessary to implement most of the technical tools but an organizations culture needs should change too. Furthermore, the alternatives which are needed could be implemented through an organizational value chain. Lean has a major strategic significance, though its implementation procedure. General approach to the supplier base viewing learns as a set of tactics rather than embracing it as a philosophy, because lean manufacturing has a strategic importance which the directions could be implemented through them. [Journal of American Science 2010;6(7):287-291]. (ISSN: 1545-1003).

Key words: Lean Management, Success and failure factors, Lean manufacturing

1. Introduction

While organizations try to remain profitable during periods of economic slowdown, many have accepted lean manufacturing as a tool to improve competitiveness. Some researchers utilize this culture as an important new management system that top managers of many manufacturing and service businesses now try to follow. Toyota's management system is variously referred to as "Toyota production System" (Ohno, 2008), "Toyota Management system" (Monden, 2008), "Lean Production" or "Lean Management"(Emiliani, 2003); It is also commonly referred to as "Lean manufacturing" due to its origins in production and operations management (Ohno, 2008). However, this description implies a narrow focus and is now recognized as incorrect because lean Principles and practices can be applied to any organization. Thus, the emergent preferred description for this management system for Toyota Motor Corporation is "Lean management" (Emiliani, 2006).

Lean implementation like many improvement tools have not succeeded universally in their application. Mora (2003), submits that "only some 10 per cent or less of companies succeed at implementing TPM and other lean manufacturing practices". Sohal and Eggleston (2004), advised "that only 10 per cent have the philosophy properly instituted". Repenning and Sterman (2001), advocated that companies use initiative almost as a passing style and submit that whilst the: "number of tools, techniques and technologies available to improve operational performance is growing rapidly, on the other hand, despite dramatic successes in a few companies most efforts to use them fail to produce significant results".

There are many possible failures that can occur while trying to implement lean manufacturing, these barriers fall into the following categories (Mejabi, 2003):

- Executive issues
- Cultural issues
- Management issues
- Implementation issues
- Technical issues

Mejabi (2003) stated that "each one of these categories is important and if taken into consideration can cause possible obstacles in the path to lean manufacturing ". All these issues have correlated points with each other. For example, executive issues occur when the company executives are not totally dedicated themselves to making the conversion to lean manufacturing and a sufficient knowledge of lean manufacturing principles.

The conversion process is difficult and if upper management is not board, it becomes even more difficult; in the other hand management issues are closely related to executive issues because management needs to be dedicated to the conversion

to lean manufacturing and have sufficient knowledge of lean manufacturing to bring about the change.

2. Literature review

The roots of Toyota's management system dates back to the early1890s, when self – taught inventor Sakichi Toyoda designed and patented a manually operated loom which automatically stop the machine when a thread broken in weaving cloth that greatly improved worker productivity and avoiding the production of defective cloth (Ford & Crowther, 2006). In part, as a result of these innovations, key objectives of Toyota's early management practice have been characterized as "production efficiency by consistently and thoroughly eliminating waste", and "the equally important respect for humanity" (Ohno, 2008).

Both Kiichiro Toyoda and Taiichi Ohno were greatly influenced by American industrialists and their Production and management practices (Ohno, 2008), but not by management theorists. By far the most influential person was Henry Ford, through his books My Life and My Work and Today and Tomorrow (Ford & Crowther, 2006). Another highly influential practice was the "Training Within Industry Service"(TWI),a structured four step program for training manufacturing workers – particularly supervisors (Huntzinger, 2003).

While the influence of western industrial management practice is clear, it is very important to recognize that it is also rather limited. Toyota managers have, over generations, purposefully made many important improvements to industrial management practice over time (Mejabi, 2003) consistent with the dual objectives of "production efficiency by consistently and thoroughly eliminating waste" and "the equally important respect for humanity" (Ohno, 2008). While these were the major drivers, Japanese business conditions and Japanese culture played recognizable but less significant roles (Ohno, 2008). In 2001, Toyota Motor Corporation published an internal document titled "The Toyota way 2001" (Taj & Berro, 2006), which presents these two objectives as top – level company principles: "continuous improvement" and "respect for people." The 13 page document provides a detailed description of these two principles and reveals explicit and implicit beliefs that have long guided management thinking. While this document is not publicly available, most of what appears in it can be found in a recent trade book (Liker, 2004). Publication of "The Toyota Way 2001" document helped to raise awareness of this principle external to Toyota Motor Corporation and its affiliated suppliers. The correct practice of Toyota's management system – Lean management – would require, at a minimum, acknowledgement and practice by management of both principles: "continuous improvement," and respect for people. However, most managers practice only the first principle, "continuous improvement", which greatly limits amount of improvement that can be achieved (Emiliani, 2006). It is the second principle, "respect for people," that enables the first principle. Simultaneous application of both principles results in the elimination of waste, called "muda," in Japanese. Lean means "manufacturing without waste" (Taj & Berro, 2006). Waste is defined as: activities (Ohno, 2008) and behaviors that add cost but do not add value as perceived by end – use customers (Womack & Jones, 2006).

2.1 Waste Elimination Practice

Eight distinct types of waste are recognized in the Lean manufacturing system cause effective implementation of Lean management results in the establishment of intra and inter organizational capability building routines and improve time – based competitiveness depends on the use of this Lean principles, structured processes and supporting tools (Imai, 2007).

The waste concept includes all possible defective work/ activities, not only defective products (Taj & Berro, 2006) also, the factors underlying poor quality and elementary management problems can cause these wastes (Hines & Taylor, 2000). Waste can be classified in eight categories (Womack & Jones, 2003):

(1) Motion: movement of people that does not add value.

(2) Waiting: idle time created when material, information, people or equipment is not ready.

(3) Correction: work that contains defects, errors, reworks mistakes or lacks something necessary.

(4) Over – processing: effort that adds no value from the customer's viewpoint.

(5) Over – production: Producing more than the customer needs right now.

(6) Transportation: movement of product that does not add value.

(7) Inventory: more materials, parts or products on hand than the customer needs.

(8) Knowledge: workforce is not confident about the best way to perform tasks.

2.1.1 Lean implementation leadership

In order to implement the concept of lean manufacturing successfully, many researchers emphasizes on commitment by top management (Alavi, 2003) and the companies should utilize strong leadership capability to exhibit excellent project management styles. In essence, these qualities would facilitate the integration of all infrastructures within an organization through strong leadership and management vision and strategy.

Good leadership ultimately promotes effective skills and knowledge enhancement among its workforce and minimizes the non – value activities in order to eliminate the wastes. Managers should also work to create interest in the implementation and communicate the change to everyone within the organization (Boyer & Sovilla, 2003), specifically; the needed information related to worker in shop floor should be updated respectfully.

2.1.2 Lean implementation procedures

Bhasin and Burcher (2006) agree that there is general lean procedure consistent to any company, but each one should find their way through their conceptions from lean manufacturing. Bicheno (2007) and Liker (2004) are strong in suggesting that a key component of lean thinking is to identify all the value adding time and reduce the non – value added activities. Bicheno (2007), claims that in batch production about 98 percent of time activities is not value adding time; in the USA, Sheridan (Sheridan, 2000), indicates that less than 2 per cent of all manufacturing jobs are in companies that are truly lean; that they have completed at least 80 percent of the conversion process. Also, Womack and Jones (Hines & Taylor, 2000) in their survey of automotive manufacturers suggested that only 41 percent were assessed as having a high level of lean adoption. So, having a comprehensive knowledge of lean tools and being familiar with lean culture in adoption of right implementation and changes through incremental improvements and step projects by the reciprocal cooperation with workers until the completion of implementation is essential.

2.2 Cultural Requirements

All companies may have the specific procedure to do the implementations, but the lean culture is needed to cause lean thinking in all actions the managers will take. The requirements in order to achieve the lean culture can be divided into two parts as bellow:

2.2.1 Intra – Organization improvements

(a) Develop a learning environment and training the employees, can provide an approximate efficiency and making the sense of more learning, encourage the organization's departments pursuing lean.

(b) Ensure that there is a strategy of change whereby the organization should understand and adapt their actions through the changes and communicates how the goals will be achieved. The managers through making effort to maximize stability in a changing environment should reduce schedule changes; program restructures; and procurement quantity changes.

(c) Assign responsibilities within the pilot program initially and ultimately within the whole organization whereby it is also clear who is supporting the program.

(d) Make decisions at the lowest level assessed by the number of organization level and promote lean leadership at all levels and evolution by the number of lean metrics.

(e) Control the conflicts and assess the fraction of an organization's employ operating under lean conditions.

2.2.2 Intra – Organization improvements

(a) Develop supplier relationships based on mutual trust and commitment; this could be assessed by the:

- Ø Number of years a relationship has existed with a supplier; and
- Ø Percentage of procurement purchased under long term supplier agreements.

(b) Systematically and continuously focus on the customer; one could receive a signal of this via the percentage of projects in which the customer was involved as intimated by Koenigsaecker (Koenigsaecker, 2000).

(c) Maintain the challenge of existing processes through, e. g. number of repeat problems and customer assistance to suppliers.

(d) Undeniably, as reiterated by Emiliani (2006) and liker (2004), lean requires a long – term commitment. A medium – sized company would need a minimum of three to five years to start pursuing the lean philosophy (According to the current British classifications) (Chase, 2004).

Lean philosophy also will be completed as the integration of various factors that the shortage of each factor causes some gaps in lean thinking.

2.3 Lean Thinking Issues

The managers within or outside the lean movement have rightly pointed to various gaps in lean thinking.This evolution is largely driven because of the shortcomings of lean that surfaced as organizations progressed on their learning curve, as well as the extension of lean thinking into new sectors, different settings and constraints (Hines, Holwe & Rich, 2004). Key aspects of this criticism are the lack of contingency and ability to cope with variability, the lack of consideration of human aspects, and the narrow operational focus on the shop- floor.

Ø Scope and lack of strategic perspective

Almost the complete lack of discussion of strategic level thinking in lean management as opposed to discussions of how to apply a series of different tools and techniques is one of the main shortages.

Ø Human aspects

It is further aspect that has high pressure on the shop floor workers.

Ø Lack of contingency

There is still a general misunderstanding of the contingent nature required to apply lean thinking.

Ø Coping with variability

Another most important part of the criticism was the ability of lean production systems and supply chains to cope with variability, a key aspect of the lean management.

3. Conclusion

This paper shows that one the major difficulties companies encounter in attempting to apply lean is not knowledge of particular tools and techniques, perhaps lack of comprehensive and suitable lean knowledge related to probable problems within the companies by the managers, direction, gap and a lack of recognition of lean culture in whole of the organization and planning cause the fails within the implementations. Additionally, some managers try to enhance the implementation by some of the lean tools and mostly try to only implement the "continuous improvement" and explicitly forget another basic lean principle, "respect for people".

The managers should know that lean thinking won't derive during a short time, and they should prepare the context of implementations before every decision making. Apply five or more of the technical tools simultaneously; install a continuous improvement viewpoint; and make numerous cultural changes embracing empowerment and sponsor the lean principles through – out the value chain are the other principles that the managers should focus during the implementations.

Acknowledgements:

Author is grateful to the Department of Management of Islamic Azad University support to carry out this work

Correspondence to:
Associate Professor Mohammad Taleghani
Department of Management, Islamic Azad University - Rasht Branch, IRAN
H/P: 00989111314029
Email: Taleghani@iaurasht.ac.it

References

[1] Alavi, S. (2003). "Learing the right way", Manufacturing Engineer, Vol. 82, No.3, pp.32–5.

[2] Boyer, M., & Sovilla, L. (2003). "How to identify and remove the barriers for a successful lean implementation", Journal of Ship Production. Vol. 19, No. 2, pp. 116 – 20.

[3] Bhasin, S., & Burcher, P. (2006). "Lean viewed as a philosophy", Journal of Manufacturing Technology and Management. Vol. 17, No. 1, pp. 56 – 72.

[4] Bicheno, J. (2007). "The New Lean Toolbox", Picsie, London. 2007.

[5] Chase, N. (2004). "Loose the waste – get lean. Quality", Vol. 38, 2004, pp. 2 – 6.

[6] Emiliani, M. L. (2006). "Linking leaders' beliefs to their behaviors and competencies". Management Decision. Vol. 41 No. 9, pp. 893 – 910.

[7] Emiliani, M. L. (2006). "origin of lean management in America: The role of Connecticut businesses". Journal of Management History. Vol. 12, No. 2, pp. 167 – 184.

[8] Ford, H., & Crowther, S. (2006) "Today and Tomorrow, Doubleday", Page & Co., New York, NY. 2006.

[9] Koenigsaecker, G. (2000). "Lean manufacturing in practice", Industry week, October, 2000, pp.1-8.

[10] Hines, P., Holwe, M., & Rich, N. (2004). "Learning to evolve: a review of contemporary lean thinking", *International Journal of Operations & Production Management*, Vol. 24 No.10, pp.994-1011.

[11] Hines, P., & Taylor, D. (2000). "Going Lean. Lean Enterprise Research Centre", Cardiff, 2000 , pp. 3 – 43.
[12] Huntzinger, J. (2003). "The roots of lean. Training within industry: the origin of Japanese management and Kaizen", Unpublished, 2003 , available at: www. lean. Org/ Community/ Resources/ Thinkers Corner. Cfm (accessed December 19, 2005).
[13] Imai , M. (2007). "Gemba Kaizen", Mc Graw – Hill, New York, NY. 2007.
[14] Liker, J. (2004). "The Toyota Way", McGraw – Hill, New York, NY. 2004.
[15] Monden, Y. (2008). "Toyota Production System", 3rd ed., Industrial Engineering and Management Press, Norcross, GA. 2008.
[16] Mora, E. (2003). "Management initiatives", Available at: www. m. e. umist. Ac. UK. 2005. (accessed 2 August 2003).
[17] Ohno, T. (2008). "Workplace Management", Productivity Press, Portland, OR . 2008b.
[18] Ohno, T. (2008). "Toyota Production System", Productivity Press, Portland, OR, 2008a, pp. xiii.
[19] Repenning, N. and Sterman, J. (2001), “Creating and sustaining process improvement”, California Management Review, Summer, pp. 1-8.
[20] Sheridan, J. (2000). "Growing with lean", Industry Week, October, 2000 , pp. 1-5.
[21] Sohal, A., & Eggleston, A. (2004). "Lean production Management", Vol. 14, pp. 1-17.
[22] Taj, S., & Berro, L. (2006). "Application of constrained management and lean manufacturing in developing best practices for productivity improvement in an auto-assembly plant", International Journal of Productivity and performance Management. Vol. 55, No. ¾ ,pp. 332 – 345.
[23] Womack, J., & Jones, D. (2006). "Lean Thinking", Simon & Schuster, New York, NY. 2006.
[24] Womack, J., & Jones, D. (2003). "Lean Thinking", Simon & Schuster, London. 2003.

28/5/2010

Mutageneic effects of *Kochia indica* extract on *Vicia faba* L.

Soliman A. Haroun*

Department of Botany, college of Science, Kafrelsheikh University 33511, Egypt
solimanharoun@yahoo.com

Abstract: The present study investigate the effect of *Kochia indica* extract using *Vicia faba* L assay. All parameters investigated were being affected. Four concentrations of 10, 20, 30 and 40% were applied for three time duration (6, 12, 24 h). The percentage of germination and plant height are dose and time dependent, probably due to alterations in cell cycle. Treated roots were highly affected compared to seed treatment. Low doses applied for short time show stimulatory effect on germination, growth and MI parameters. On the other hand high concentrations applied for long time gave rise to substation reduction for all parameters investigated. The percentage of mitotic and meiotic abnormalities increase as the concentration increase and time prolonged. Various types of abnormalities with special reference to micronuclei, laggards and bridges were observed at all concentrations but more frequent at higher doses. Following the same trend meiotic parameters of chromosome association, chiasma frequency and pollen fertility were being negatively affected and dose dependent. High concentrations show low chiasma frequency, pollen fertility and high percentage of abnormalities. Types of multivalents and univalents were also observed. The present studies recommend the use of this extract at concentrations up to 30% to minimize the side effects on plants as non target organism. It also encourages use of botanical extracts for biological control instead of synthetic chemicals. [Journal of American Science 2010;6(7):292-297]. (ISSN: 1545-1003).

Keywords: *kochia indica, Vicia faba*, mitosis, meiosis,chiasma,abnormalities

1. Introduction

Cytogenetic effects of synthetic chemicals used for plant protection have been well documented and previously investigated by many authors (Qureshi *et al*., 1988, Mekki 2008, Vyvyan, 2002, Badr *et al*., 1985, Mohammed, 1986). Almost all studies confirm the harmful effects of synthetic chemicals used in agriculture purposes and increase the environmental pollution which is a global problem. For these reasons many attempts were carried to find out alternative natural compounds for more ecological safety (Alam *et al* 1987, Panda & Sahu 1985, Shehab 1980, Abou elkheir 1992, Haroun & Al shehri 2001, Jose *et al* 2008, Abderrhman 1997, 1998, Adam & Rashad (1984) and Omari, *et al* 1996).

Aqueous extract of *Kochia indica* species (Chenopodiaceae) used in this study has been previously tested by Mahmoud (1998) as pest control. The study shows that the extract could be used as insecticide at certain concentrations, but completely ignores its side effect on crop plants as non target organism. These attract the attention to evaluate the effects of this extract on *Vicia faba* plants.

The aim of this study is to investigate the effect of this extract at different concentrations on the percentage of germination, plant growth (percentage of height of control), mitotic index, mitotic and meiotic aberrations, chromosome association and pollen fertility of *Vicia faba* L plants. This investigation is a part of programme study the potential effect of plant extracts as biological control instead of synthetic chemicals.

2. Material and Methods

Aqueous extract of *kochia indica* (shoot system) was prepared following Nassar (1995) and Mahmoud (1998). 250 g of fresh leaves and stems were ground into 500ml distilled water and left for extraction overnight at room temperature. The extract was filtered using whatman filter paper No1. Further extraction was carried out for more purification.

The elementary analysis of this extract was previously carried out by Mahmoud (1998) using ultraviolet spectroscopy (UV), infrared spectroscopy (IR), gas chromatography (GC) and mass spectrophotometer (MS). The analysis detect the active compound with proposed molecular formula C13 H14 Cl6 O4, molecular weight 447 and chemical structure, 1-phenyl 2,3,4,5,6 hexa chloro 2,3,4,5 tetra hydroxy heptane

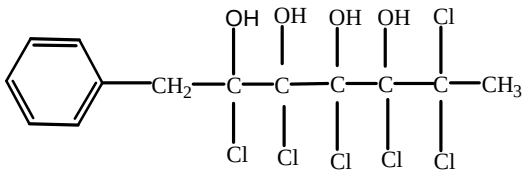

1-phenyl 2,3,4,5,6,6 hexa chloro 2,3,4,5 tetra hydroxy heptane.

For mitotic study, two types of treatments were carried out using seed soaking and root treatment experiment. Seeds of *Vicia faba* were presoaked in water for 24 h. and treated with four concentrations 10, 20, 30 and 40 % (same range of concentrations previously used as pesticides by Mahmoud 1998). All concentrations were applied for 6, 12 and 18 h of treatment. Treated seeds were planted in pots half filled with moist sand till germination. Young roots were excised and prepared for mitotic study. Percentage of germination and plant height were recorded at various concentrations relative to control.

For root treatment, fresh roots (1-2 cm) were subjected to the same concentration and time used in seed soaking experiment. Excised roots of both treatments were washed in distilled water and fixed in freshly prepared fixative solution (1:3 v/v acetic alcohol) for 24 hr. Squash technique using feulgen reagent was used for mitotic analysis. Mitotic index and percentage of abnormalities were counted using at least five slides freshly prepared for each concentration.

For meiotic analysis, growing plants (30 days old) were sprayed with the same concentrations applied for mitotic treatments. Young flower were collected before anthesis at early morning (9 am) and fixed in fresh fixative solution. Anthers were macerated in few drops of 2 % acetocarmine to study pollen mother cells (PMC's). Meiotic behavior as chromosome association and chiasma frequency were studied at diaknesis and metaphase I stages. Percentage of meiotic abnormalities and pollen fertility were also studied.

3. Results

The effects of *kochia indica* extract on percentage of germination and plant height (relative to control), mitotic index and percentage of abnormalities were recorded and summarized in table1.

Morphological data represented by percentage of germination and plant height revealed a significance decrease as the concentration increase and the time of treatment prolonged. It is evident from table 1 that low concentrations treatment (10 and 20% for 6hr) show a stimulatory effects compared to control. This result was previously reported by Haroun and Al shehri (2001), Anis and Wani (1997), Lamix and Gupta (1983), Katyayami *et al* (1980) and Abderrhman (1997). In the present study low concentrations induce growth is probably due to chemical components of chloride and phenol groups which might give hormonal effects and enhance plant growth and cell division.

The rest of data show gradual decrease in the percentage of germination and plant height as the concentration increase and the time prolonged recording values of 59.7 and 63.1 at 40% and 24hr for the two parameters respectively. This finding was agree with that previously recorded by Haroun and Al shehri (2001), Abou elkheir (1992), Panda & Sahu (1985) and Alam *et al* (1987).

Mitotic study

Inhibition of mitotic activities was often used for tracing cytotoxic substances. Cytotoxicity was defined as decrease in mitotic index revealed the mitodepressive effect of *Kochia indica* on mitotic index (MI) of *Vicia faba*. The mitotic index of 10 and 20 % concentrations is slightly increased compared to control, insure the relationship between this parameter and morphological characters as previously reported by Abderrhman (1998), Abou elkheir (1992), and Alam *et al* (1987). This increase may due to shorting the duration of mitotic cycle and enhance the interphase cells enter the subsequent division stages (Haroun & Al shehri 2001 and El Kodary 1980) or by induce the synthesis of DNA in dividing cells (Badr *et al* 1985 and Chand & Roy 1981).

The rest of treatments are significantly altered MI gradually as the concentration increased and time prolonged. Significance reduction in MI was recorded in root treatment insure the harmful effects of direct treatments on plants as previously stated by Marant (2003), Pavel & Creanga (2005), Jose *et al* (2008), Haroun and Al shehri (2001) and Banerjee (1992). The lowest values of MI were 2.7 and 2.5 recorded by 40% concentration at 24h for seed and root treatment respectively.

The percentage of mitotic aberrations recorded more or less follow the same trend of mitotic index. With no exception the percentage of aberrations increase as the concentration increase and time prolonged. The highest values recorded for this parameter were 20.7 and 31.9 for seed and root treatment respectively. This trend was previously recorded by Jose *et al* (2008), Pavel & Creanga (2005) and Alam *et al* (1987).

Table 1: Effects of different treatments of *Kochia indica* extract on percentage of germination, plant height (% of control), mitotic index and percentage of abnormalities for seed and root of treated *Vicia faba* L.

treatment	%germ.	% height. of cont.	Mitotic index ± SE		% abnormal. ± SE	
			Seed	root	Seed	root
6h Control	93.1±1.1		11.2±0.11	10.7±0.34	1.5±0.62	1.7±0.25
10	94.3±1.5	105.2	11.6±0.32	10.8±0.41	2.1±0.22	2.7±0.48
20	94.1±1.3	103.1	11.3±0.35	10.2±0.33	3.2±0.17	3.9±0.52
30	75.6±0.9	75.2	9.4 ±0.61	7.5±0.25	6.1±0.31	6.6±0.46
40	71.2±1.3	69.8	8.5±0.51	7.1±0.54	7.5 ±0.22	9.3±0.63
12h control	92.5±0.8		10.5±0.33	10.1±0.25	1.5±0.12	1.6±0.23
10	93.3±1.1	90.7	10.2±0.55	9.3±0.46	2.0 ±0.23	3.1±0.51
20	91.2±1.3	90.5	9.7±0.32	9.2±0.19	4.7±0.41	5.1±0.24
30	71.3±1.4	70.9	8.4±0.51	6.9±0.35	7.8 ±0.71	8.5±0.11
40	68.5±0.9	70.1	8.2±0.57	6.1±0.46	8.3 ±0.55	10.3±0.61
24h control	85.1±0.8		8.1±0.54	7.5±0.44	1.4 ±0.39	1.5±0.60
10	83.2±1.1	83.1	6.4±0.81	6.2±0.39	8.1 ±0.33	9.5±0.91
20	77.6±1.4	74.7	5.1±0.21	4.6±0.11	12.3±0.72	14.7±0.82
30	63.1±1.5	60.5	3.8±0.22	2.9±0.31	15.6±0.53	18.4±0.54
40	59.7±2.0	63.1	2.7±0.50	2.5±0.28	20.7±0.39	31.9±0.87

At higher doses more deleterious effects were observed and reduction in MI. values of 2.7 & 2.5 was recorded for seed and root treatment respectively. The percentage of mitotic abnormalities increased as the concentration increase and the time of treatments prolonged. Values of 31.9 and 20.7 were recorded for root and seed treatment at 40% concentration applied for 24h. This observation was previously stated by Haroun and Al shehri (2001) and Alam *et al* (1987).

Types of micronuclei were observed at various stages of mitosis (interphase, figure1-1; prophase figure1-2; telophase, figure1-4) in both treatments is the manifestation of chromosome damage and disturbance of the mitotic process. The micronucleus are almost acentric fragments, lagging chromosomes or from breakage of chromosomes failed to move to either pole during anaphase of mitosis (Gover and Kaur, 1999, Panda and Sahu, 1985). C-metaphase (figure1-3),C-anaphase (figure1-7), multipolar (figure 1-8), lagging chromosomes (figure1-5, 9), chromosome breaks,(figure1-6), bridges(figure 1-4,9) were observed at different treatments. Recording of some aberrations like lagging, bridges and breaks to some extend insure that the extract have more or less direct effect on chromosomes and spindle fiber apparatus (kong and Ma 1999). Not surprisingly that the percentage of abnormalities recorded is more frequent at high concentrations and root treatment as previously stated by Kabarity & Malallah (1980), Alam *et al (*1987), Jose *et al* (*2*008) and Haroun & Al shehri (2001).

Meiotic study

Number of pollen mother cells (PMC's), percentage of abnormal ones, chromosome association, chiasma frequency and percentage of pollen fertility were recorded and listed in table 2. Meiosis of control plants is normal showing 6.0 bivalents counts 2n = 12 as diploid number. Some abnormalities observed were probably due to squash technique. Value of 1.82 for chiasma frequency was recorded for control sample reflect the normal meiosis and complete pairing between chromosomes. High percentage of pollen fertility is recorded (97.5%) as a penalty of normal meiosis and high chiasma frequency.

Treated plants exhibit various degree of abnormalities more or less depends on concentrations applied. The percentage of abnormalities increase as the concentration increase (table 2). This trend was previously stated by Haroun and Alshehri (2001), Badr *et al* (1985) and Chand and Roy (1981). All treated plants show gradual decrease in chiasma frequencies and pollen fertility as the concentration increase. The lowest value recorded for these parameters are 1.12 and 80.4 at 40% concentration. No dough, there is a strong relationship between the last parameter and percentage of abnormalities and chiasma frequency as it is a penalty of abnormal meiosis and mispairing between chromosomes during meiosis.

For chromosome association, univalents were recorded in frequency ranged between 1.7 - 2.1 at all treatments. It seems to be more or less the material of abnormalities, which consequently affect paring and chiasma frequency. Bivalents association in form of ring type was observed (figure 2-1) and may affect chiasma frequency. The frequency of this parameter decrease as the concentration increase (table 2). Multivalent in forms of trivalent and quadrivalents were observed at diaknesis and metaphase I (figure 2-

1,2) and found more frequent at high concentrations. The formation of odd numbers pairing of chromosomes association as univalents and trivalents probably caused by cryptic structural changes in chromosomes forming genetic differences which restrict paring with other homologous as previously stated by Anis and Wani (1997) and Haroun and Al shehri (2001).

Some meiotic abnormalities were observed insure the harmful effects of this extract especially at high concentrations. Types of stickiness at metaphase I (figure 2-3), disturbed anaphase 11(figure 2-6) bridges at anaphase I and II (figure 2- 4,5) were observed and recorded more frequent at high doses following the same trend in mitotic study.

No dough meiotic disorders affect normal disjunction, pairing and chiasma frequency and subsequently affect crossing over which is the site of exchange genetic material during meiosis. This finaly lead to form abnormal and non functional gametes which can not compete any pollination or sexual reproduction as previously stated by Ramanna (1974) and Haroun and Al shehri (2001). Although the mechanism of mitotic and meiotic disturbance of this extract is not clear the possibility of genetic instability is insured especially at high doses.

The concentration of of 40% applied in the present study was previously recommended by Mahmoud (1998) as efficient potential insecticide and best control. The present data confirm the harmful effects of this concentration on plants as non target organism and recommend use of lower concentrations (ranged between 20-30%) which show low harmful effects on plants and significantly control insect fertility and reproduction.

Despite this extract is more or less chemical compound, but it is much safer than synthetic pesticides and highly recommended for biological control.

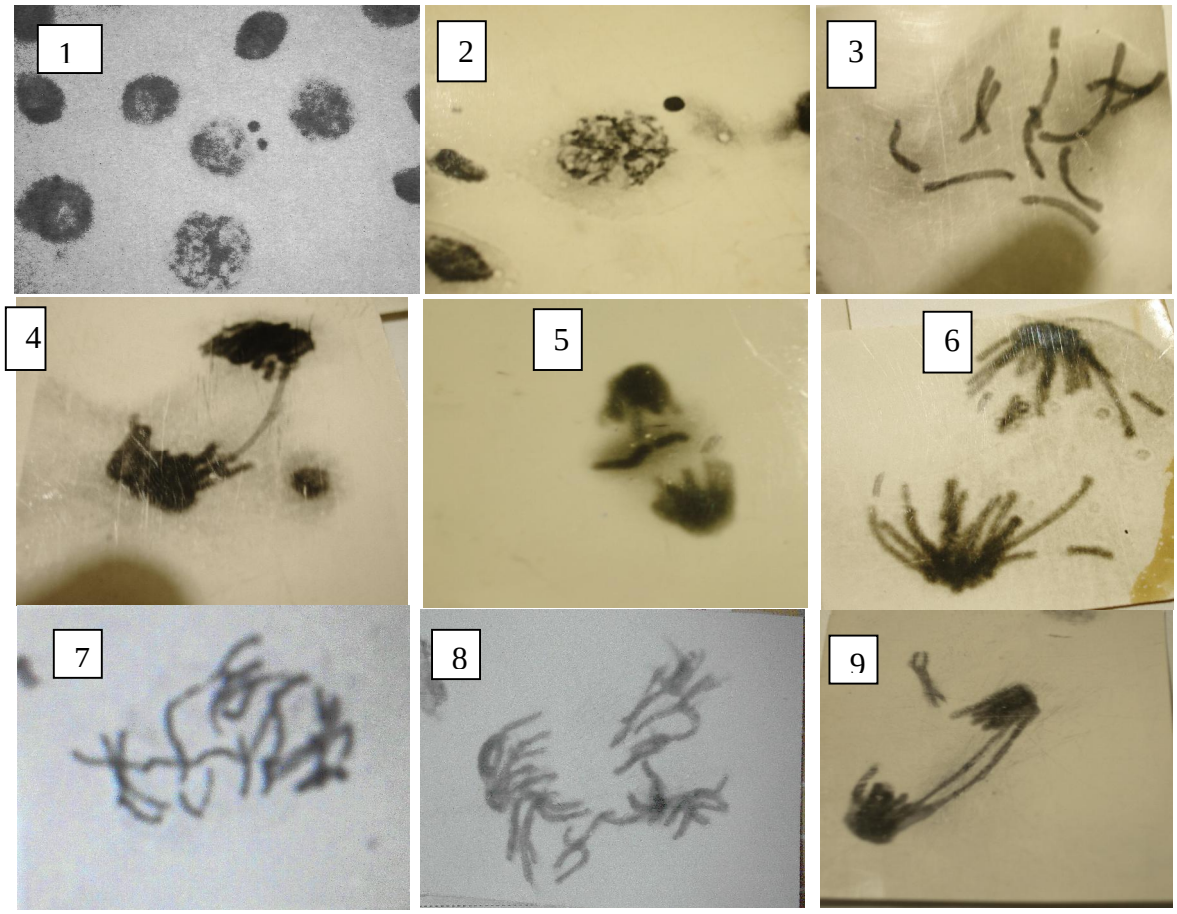

Figure 1: 1, miconuclei at interphase (x1000). 2, micronuclei at prophase (x1400). 3, c-metaphase (x1600). 4, micronuclei and bridge at telophase (x 1600). 5, lagging at telophase (x 1600). 6, breakes at anaphase (x 1600). 7, c-anaphase (x1600). 8, multipolar (x1600). 9, bridges and lagging (x1600).

Table 2: Effects of different concentrations of *Kochia indica* extract on percentage of abnormal pollen mother cells (PMC's), chromosome association, chiasma frequency and percentage of pollen fertility of *Vicia faba* L.

Treatment %	No.PMC,s examined	%abnorm. ±SE	Chromosome association I	II	III	IV	Chiasma frequency	%poll. Fert. ±SE
Contol	71	0.9±0.12	0.0	6.0	0.0	0.0	1.82	97.1±1.21
10	87	2.6±0.22	1.8	5.2	0.0	0.0	1.71	93.4±0.99
20	79	4.1± 0.31	2.1	4.8	0.0	0.0	1.53	89.3±1.10
30	68	4.5± 0.45	1.7	2.9	0.21	0.96	1.41	85.1±1.12
40	81	5.3± 0.33	1.8	2.7	1.91	0.22	1.12	80.4±1.39

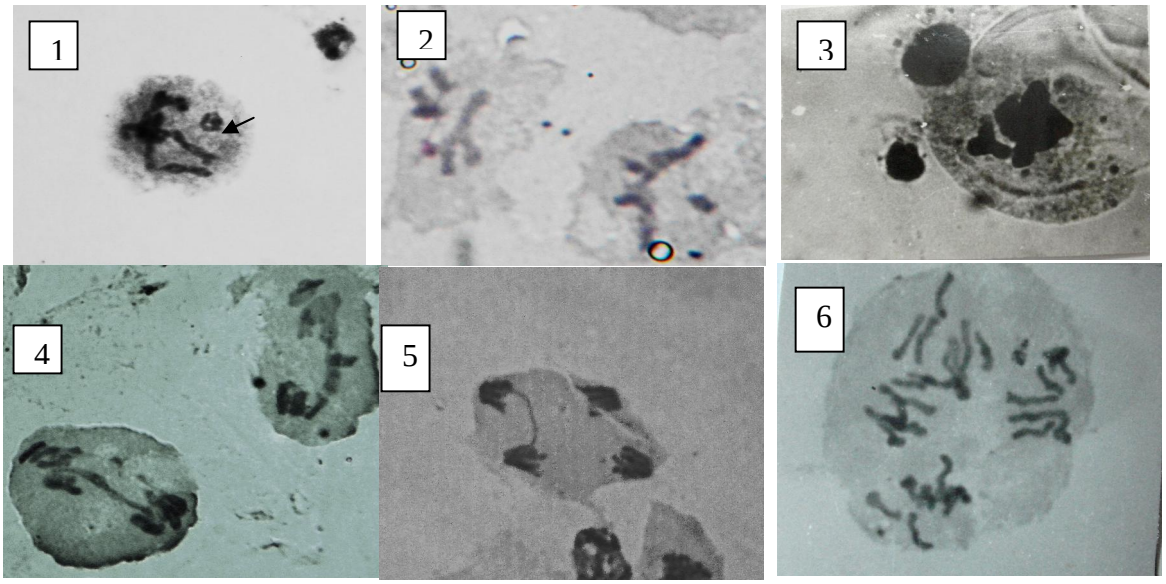

Figure 4: diplotene with ring bivalent arrow(1), diaknesis with multivalents (2), sticky metaphase I (3), bridges at anaphase I, and telophase II (4,5) , disturbed anaphase II (6) (x1600)

References

1. Abderrhman, S. M. Effects of *Peganum harmala* extract on root tips of *Allium cepa*. Cytologia.1997,90:171-174.
2. Abderrhman, S. M. Cytogenetic effects of *Peganum harmala* on Maize root tips. Cytologia. 1998, 63: 283-291.
3. Abou elkheir, Z.A. and Abou elkheir, G.M. Cytological effect of certain active constituents of *Peganum harmala*. 1. Effects of hormonal and harmine alkaloids on mitosis of *Allium cepa*. J. king Saud Univ. Science. 1992, 4. 37-45.
4. Adam, Z. M. and Rashad, T. R. Cytological effects of water extract of medical plants. Influence of *Ammi majus* extract on root tips of *Vicia faba*. Cytologia, 1984, 49: 265-271.
5. Alam, S. Golam, K., Amin, M., Islam, M. Mitotic effect of leaf extract of *Ipomoea carnea* on *Allium cepa*. Cytologia, 1987,52: 721-724
6. Anis, M. and Wani, A. A. Caffeine induced morpho-cytological ariability in Fennqrrek, *Trigonalla foenum*. Graecum L. Cytologia. 1997, 62: 343-349.
7. Badr, A. Hamoud, M. A. and Haroun, S. A. Effects of herbicide Gespax on mitosis, mitotic chromosomes and nucleic acid in *Vicia faba* L. root meristems. Proc. Saudi boil. 1985, Soc. 8: 359-369.
8. Banerjee, A. A time course study of the cytotoxicity effects of extract of different types of Tobacco on *Allium cepa* mitosis. Cytologia. 1992, 57: 315-320.
9. Chand, S. and Roy, S. C. Effects of herbicide 2, 4 dinitrophenol on mitosis, DNA, RNA and protein synthesis in *Nigella sativa* L. Biol. Plant. 1981, 23: 198-202.
10. Chauhan, L.K.S; Dikshith, T. S. S. and Sandararman, V. Effects of deltamethrin on plant cell I. cytological effects on the root meristems of *A. cepa*, Mut. Res; 1986, 171:25-30.
11. Grover, I. S. and Kaur, S. Genotoxicity of wastewater samples from sewage and industrial effluent detected by the *Allium* root anaphase aberration and micronucleus assays. Mutat. Res.

1999, 426 (2): 183-198.
12. Jose, M. S., David,L., Viccini,, G. S. Mitodepressive and clastogenic effects of aqueous extracts of the lichens *Myelochroa lindmanii* and *Canoparmelia texana* (Lecanorales, Parmeliaceae) on meristematic cells in plant bioassays. Genet. Mol. Biol. 2008, 31(1) 1-7.
13. Haroun, S.A. and Al shehri A.M. Cytogenetic effects of *Calotropis procera* extract on *Vicia faba*. Cytologia, 2001, 66: 337-378.
14. Kabarity A. and Mallah, G. Mitodepressive effect of Khat extract in the meristematic region of *Allium cepa* root tips. Cytologia . 1980, 45: 733-738.
15. Katyayami, A. Rao, E. M. and Rao, S. Induced growth patterns of *Trigonella foenum.* Graceum L. by hydrazide and ethyl methane sulphonate. J.Ind. Bot. Soc. 1980, 59: 144- 148.
16. Kong, M. S. and Ma, T. H. Genotoxicity of contaminated soil and shallow well water detected by plant bioassays. Mutat. Res. 1999, 426: (2): 221.
17. Lamix, V. and Gupta, M N. Ethyl methane sulphonate variability in *Trigonella foenum Gracum* L. Ind. Bot. Soc. 1983, 62: 305-311.
18. Mahmoud, N. A. Botanical extracts as potential insecticides. M.Sc. Thesis cairo University Egypt. 1998.
19. Marante, F. J. T., Castellano, A. G., Rosas, F.E., Aguiar, J.Q., Barreira, J.B. Identification and quantification of allelochemicals from the lichen *Lethariella canariensis*: Phytotoxicity and antoxidative activity. J. 2003, 29: 2049-2071.
20. Mekki, L. E. The effect of three agricultural chemicals on mitotic division and seed protein banding profiles of *Vicia faba*. I. J .Agric. Biol. 2008, 10 (5): 499-504.
21. Mohammed, I. F. Cytological effect of insecticide Cypermethorin on plants *Vicia faba* and *Allium cepa*. M.Sc. Thesis Ain Shams University Egypt. 1986.
22. Nassar, M. I. The potential of some Juvenoids, precocnes and botanical extracts for the control of *Muscina stabulanse* (Diptera-Muscidae). Ph.D. thesis, Entomology Dep. Fac. Sci. Cairo University Egypt. 1995.
23. Omari, Y. L., Shraideh, Z. A. and Abderrhman, S. M.Mitodepressive effect of Khat (*Catha edulis* on bone marrow of mice. Biomedical letters. 1996, 54: 64-72
24. Pavel, A. and Creanga, D. E. Chromosome aberrations in plants under magnetic fluid influence. Mater . 2005, 289: 469-472.
25. Panda, B. B. and Sahu, U. K. Induction of abnormal spindle function and cytokinesis inhibition in mitotic cells of *Allium cepa* by organophosphrous insecticide fensullothion, cytobios, 1985, 42:147-155
26. Qureshi, S., Tariq, M., Parmar, N. S. and Al-Meshal, I.A.Cytological effect of Khat (*Catha edulis*) in somatic and male germ cells of mice. Drug chem. Toxicol. 1988, 11: 151-165.
27. Ramanna, M. S. The origin of unreduced microspores due to aberrant cytokinesis in meiocytes of potato and its genetic significance. Euphytica 1974, 23: 20-30.
28. Shehab, A. S. Cytological effects of medical plants in Qutar. II. Mitotic effect of water extract of *Teucrium pilosam* on *Alium cepa*. Cytologia. 1980, 45: 57-64.
29. Vyvyan, J. R. Allelochemicals as leads for new herbicides and agrochemicals. Tetrahedron. 2002, 58: 1639-1646.

5/8/2010

Thermodynamic parameters of zinc sorption in some calcareous soils

F. Dandanmozd[1] and A.R. Hosseinpur[2]
[1].Soil Sci. Dep. College of Agri.Bu-Ali Sina Univ. Hamadan, Iran.
[2].Soil Sci. Dep. College of Agri. Shahrekord Univ. Shahrekord, Iran.
hosseinpur-a@agr.sku.ac.ir

Abstract: Sorption is one of the most chemical important process, in which determine micronutrients availability in soil. Sorption isotherms provide useful information about sorption capacity of soils. Sorption data can be used to determined sorption thermodynamic parameters. To evaluate the sorption of zinc (Zn) onto some soils, an experiment was conducted with ten calcareous soils of Hamadan province in the west of Iran. Half g soil samples were equilibrated at 25±1 and 45±1°C with 25 ml of 0.01M $CaCl_2$ containing 0 to 30 mg L^{-1} Zn as $ZnSO_4$. Suspensions were centrifuged, filtered and concentration of Zn in the clear extract solution was determined using atomic absorption spectrophotometer. Amount of Zn sorbed by the soil was calculated from difference between initial and final concentration of Zn in the equilibrium solution. Sorption of Zn was evaluated using adsorption isotherms. The thermodynamic parameters viz. K°, ΔG°, ΔH° and ΔS° were determined using sorption data and concentration of Zn in equilibrium solution at two different temperatures.The results showed that Zn Sorption was described by linear, Feeundlich, Temkin and D-R models. The values of K^{o} increased with rise in temperature from 25 to 45 °C in all the soils. The ΔG^{o} values at 25 °C and 45 °C were negative and ranged from -7.00 to -16.64 and -13.24 to -41.93 kJ mol^{-1}, respectively. The values of ΔH^{o} and ΔS^{o} were positive and ranged from 357.47 to 74.02 kJ mol^{-1} and 1255.97 to 281.79 J mol^{-1} K^{-1}**,** respectively. Evaluation of thermodynamic parameters provide an insight into mechanism of Zn sorption in the soils. The values of ΔG^{o} were found negative indicating Zn sorption was spontaneous and the values of ΔH^{o} were positive indicating Zn sorption was endothermic. Thermodynamic parameters revealed Zn sorption increased as the value of K^{o}, ΔG^{o}, ΔH^{o} and ΔS^{o} increased with temperature. Also the results showed that calcareous soils can sorb high amounts of Zn and that thermodynamic parameters are useful in describing Zn sorption. we suggest that such research be done in contaminated soils. Also we suggest that effect of thermodynamic sorption parameters on Zn uptake by plant be done using the pot experiment. [Journal of American Science 2010;6(7):298-304]. (ISSN: 1545-1003).

***Keywords*:** Sorption isotherm; Calcareous soil; Zinc; Thermodynamic parameter

1.Introduction

Adsorption is one of the most important chemical processes in soils. It determines the quantity of plant nutrients, metals, radionuclides, pesticides and other organic chemicals that are retained on soil surfaces and, therefore, it is one of the primary processes that affect transport of nutrients and contaminants in soils. Sorption also affects the electrostatic properties of suspended particles and colloids. The electrostatic properties affect coagulation and settling (Sparks 1995). Sorption reactions on soil mineral surfaces potentially attenuate toxic soil solution . Sorption isotherm analysis is a useful technique to study the retention of metals in soils. Sorption isotherms provide useful information about the soil retention capacity and the strength by which the sorbate is held onto the soil. Zinc sorption capacity correlates with soil contents of aluminosilicate clays, metal oxides, and carbonates (Kalbasi et al. 1978). Aluminosilicate clays affect Zn sorption mainly through their effects on soil cation exchange capacity (CEC) (McBride 1989). Soil pH, solution ionic strength, and solution ionic composition also affect Zn sorption. Increasing soil pH increases the total number of negative sites of clay minerals and organic matter (OM), and therefore increases the capacity for Zn sorption (Harter 1983; McBride 1989). For proper evaluation of the environmental threat posed by Zn, or its availability, it is necessary to supplement the individual sorption characteristics (Arias et al. 2006).

Zinc deficiency is common in calcareous soils. It is believed that this is a consequence reaction taking place between soluble Zn and soil solid phase leading to Zn reduced plant availability. Adsorption and or precipitation on surfaces of soil solids decrease the concentration of Zn in solution phase (Lindsay 1972).

Isothermal sorption batch experiments are very important in soil science research. Theoretically, maximum monolayer sorption, empirical adsorption constants, and other important adsorption parameters can be determined by this method. Cation exchange capacity of soils and soil components can also be quantified. Copper and Zinc are individually more soluble in acid soils than in calcareous soils, and their marked sorption hysteresis is most marked in the case of sorption by organic soil components (Wu et al. 1999).

Adsorption increase with increasing temperature due to the increase in number of active sites (Yavuz et al. 2003; Bouberka et al. 2005). To gain further insight into sorption process and

mechanisms, thermodynamic approach may be used to predict the final state of metal in the soil system from an initial non-equilibrium state (Jurinak and Bauer 1956; Sposito 1984). Evaluation of the free energy change corresponding to the transfer of element from bulk solution into the appropriate site of the double layer or clay mineral lattice are helpful to express the sorption process. Similarly, an understanding of change in enthalpy and entropy helps in determining the free energy change and disorders occurring during sorption process (Adhikari and Singh 2003). Adhikari and Singh (2003) showed that the high values of ΔG^o both for Pb and Cd indicated that both reactions are spontaneous. The values of ΔH^o were found to be negative for Cd and positive for Pb, indicating that Cd sorption reaction was exothermic while Pb sorption was endothermic reaction in all the soils. (Adhikari and Singh 2003). The values of ΔS° were found to be positive due to the exchange of the metal ions with more mobile ions present on the exchanger, which would cause increase in the entropy, during the adsorption process (Unlu and Ersoz 2006). Information about Zn sorption characteristics and sorption thermodynamic parameters (STP) are limited for the soils of Iran. The objectives of this research were to study the Zn sorption characteristics and determination of STP in ten surface soils of Hamadan province in the west of Iran.

2.Materials and Methods

We collected bulk samples of topsoils (0-30cm depth) from ten calcareous soils from Hamadan province in the west of Iran. All samples were air dried, crushed and sieved through a 2-mm sieve prior to soil analysis and sorption studies. Characteristics of the soils such as particle size distribution, pH, EC, CEC, organic C, and calcium carbonate equivalent were determined using standard analytical methods (Gee and Bauder 1986; Rhodes 1996; Summer and miller 1996; Nelson and Sommers 1996; Nelson, 1982). Concentration of available Zn in the soil samples was determined using DTPA method (Lindsay and Norvell 1978).

To study the sorption of Zn by soils, 0.5 g soil subsample from each soil was placed in a 100 ml plastic bottle and equilibrated with 25 ml of 0.01 M $CaCl_2$ solution containing levels of Zn, i.e. 0, 2, 5, 10, 15, 30 mg l^{-1} Zn as $ZnSO_4$ solution. Solutions were prepared in 0.01 M $CaCl_2$ to keep the ionic strength constant. Each sorption set, for Zn, was replicated three times. The soil suspensions were shaken for 30 min and equilibrated for 24 h at 25±1 and 45±1ºC in an incubator. Based on preliminary studies, an equilibrium period of 24 h and soil/solution ratio of 1:50 were found optimum beyond which no significant change in metal content of equilibrium solution was recorded. After equilibration time, the suspension was filtered, and concentration of Zn in the clear extract solution was determined using Varian Atomic Absorption Spectrophotometry. Amount of Zn sorbed by soils was calculated from the difference between the initial and final concentration of Zn in the equilibrium solution.

For studying the sorption relationship, the data were fitted to the following equations:

$C_e/q = 1/Kb + C_e/b$ Conventional Langmuir

$\log q = \log K_f + n \log C_e$ Freundlich equation

Where C_e is the Zn concentration in the equilibrium solution (mg/l), q is the amount of Zn sorbed by the soil (mg kg^{-1}), b is the sorption maxima (mg kg^{-1}), and K is the bonding energy coefficient (L mg^{-1}), K_f is the Freundlich distribution coefficient, and n is an empirical constant.

Langmuir and Freundlich isotherms don't give any idea about sorption mechanism but Dubinin-Radushkevich (D-R) isotherm describes sorption on a single type of uniform pores. In this respect, the D-R isotherm is analogus of Langmuir type but it is more general, because it does not assume a homogeneous surface or constant sorption potential (Unlu and Ersoz, 2006). In order to understand the adsorption type, D-R isotherms were determined. The D-R isotherm has the form:

$\ln q = \ln q_m - k\varepsilon^2$

and

$\varepsilon = [RT \ln (1 + (1/C_e))]$

where ε is Polanyi potential, q is the amount of Zn sorbed by the soil (mol g^{-1}), k is a constant related to the adsorption energy ($mol^2\ kJ^{-2}$) and q_m is the adsorption capacity (mol g^{-1}). The mean free energy of adsorption (E) was calculated from the k values using the equation:

$E = (-2k)^{-0.5}$

The magnitude of E is useful for estimating the type of adsorption process. If this value is between 8 and 16 kJ mol^{-1}, adsorption process can be explained by ion exchange (Unlu and Ersoz 2006).

Thermodynamic parameters were calculated from the variation of the thermodynamic equilibrium constant, K^o, computed by following the procedure outlined by Biggar and Cheung (1973). The value of K^o for adsorption reaction can be defined as:

$K^o = a_s/a_e = \gamma_s C_s/ \gamma_e C_e$

where a_s denotes activity of adsorbed metals, a_e is activity of metals in equilibrium solution, C_s is milligrams of metals adsorbed per litre of solution in contact with the adsorbent surface, C_e is milligrams of solute per litre of solution in equilibrium solution, γ_s is the activity coefficient of the sorbed metals and γ_e represents the activity coefficient of metals in equilibrium solution. Since at lower concentration activity coefficient approaches unity, Eq. 6 was reduced to:

$K^o = C_s/C_e$

The values of K^o were obtained by plotting ln (C_s/C_e) vs. C_s and extrapolating to zero C_s. The

standard free energy (ΔG^o) was calculated as follows:

$\Delta G^o = -RT \ln K^o$

The standard enthalpy (ΔH^o) was obtained from integrated form of the Vant Hoff equation:

$\ln K^o_2/K^o_1 = -\Delta H^o/R[1/T_2 - 1/T_1]$

The standard entropy (ΔS^o) was calculated as

$\Delta S^o = (\Delta H^o - \Delta G^o)/T$

3.Results and Discussion

Selected chemical and physical characteristics of the soils are presented in Table 1. The texture of the soil samples are clay loam to sandy clay loam. The calcium carbonate equivalent ranged from 5 to 53.8%. Organic matter content ranged from 0.68% to 2.40%. The pH of the soils varied from 7.44 to 8.20 which indicated that all of the soils were alkaline. The CEC ranged from 10 to 25.1 $cmol_c\ kg^{-1}$. The DTPA extractable Zn ranged from 0.49 to 4.15 $mg\ kg^{-1}$.

Table 1. Physicochemical properties of the experimental soils

Soil. No.	pH (1:2.5)	CEC	EC	O.M	Clay	Silt	CaCO3	Zn- DTPA
		$cmol(+)kg^{-1}$	$ds.m^{-1}$		%			$(mg\ kg^{-1})$
1	7.80	10.9	0.23	0.90	27.0	7.5	11.0	1.09
2	8.10	11.5	0.30	1.03	33.2	15.0	14.1	4.15
3	7.96	14.2	0.19	0.83	34.2	19.1	33.5	1.49
4	7.45	23.5	0.13	0.68	38.3	10.3	5.0	0.66
5	8.20	16.0	0.34	2.40	22.0	15.0	53.8	0.49
6	8.00	15.5	0.20	0.80	20.8	25.3	17.1	0.56
7	7.44	20.9	0.19	1.06	27.0	27.8	22.1	0.63
8	7.90	25.1	0.20	1.10	36.4	25.9	27.4	0.65
9	7.90	14.5	0.26	0.80	38.1	17.6	39.4	1.15
10	7.85	10.0	0.30	1.40	27.6	9.5	6.1	2.56

For proper evaluation of the environmental threat posed by Zn or its availability, it is necessary evaluate the Zn individual sorption characteristics. Langmuir, Freundlich and D-R equations were fitted to sorption data to predict the behaviour of Zn sorption by the soils (Tables 2). The Freundlich and D-R equations irrespective of the level of Zn added, gave better fit (R^2 = 0.92–0.99** and 0.88*- 0.99** respectively) than Langmuir equation (R^2 = 0.81*–0.99**). Elzinga et al. (1999) also evaluated batch sorption data and established general purpose Freundlich isotherms for various heavy metals in soils.

The values of the Langmuir constants b and k are presented in Table 2. The values of sorption maxima (b) ranged from 625 to 1250 $mg\ kg^{-1}$ soil (Table 2). The sorption maxima were related to the calcium carbonate equivalent (CCE) (r=0.927**), and other physicochemical properties such as OM, CEC and clay content did not significantly improve the relationship (Table 3). Reyhanitabar et al. (2007) studying Zn retention of 20 calcareous soils of central Iran, reported a significant relationship between Langmuir b with percentage of clay and CEC, but not CCE.

Trehan and Sekhon (1977) reported correlation between CCE and adsorption maxima, which is similar to our findings. Udo et al. (1970) reported the effect of soil clay on adsorption maxima (b). The effect of pH on b has also shown by other researchers (Karimian and Moafpourian 1999) but in our study this was not seen, perhaps due to the narrow range of pH of the studied soils (Table 1). Therefore CCE was the principle factor contributing to correlation with the Zn sorption maxima. The correlation of the sorption maxima with the CCE suggest that the soil carbonates sorbed the added Zn. The lack of relation between the zinc sorption maxima and CEC indicates that Zn^{2+} was sorbed through electrostatic as well as non-electrostatic processes. The cations competing with Zn^{2+} for adsorption were primarily calcium from the cation exchange complex and the dissolution of soil carbonates. The lack of correlation between the zinc sorption maxima with organic matter and clay content suggest that these two soil components were not responsible for the retention of native zinc in these calcareous soils. The affinity of metal bonding varied with soil types and metal concentration. All soils showed high affinity for Zn sorption. The bonding energy (k) ranged from 11.432 to 0.941 $L\ mg^{-1}$ (Table 2). Bonding energy showed a highly significant ($p<0.01$) relationship with percentage of O.M and significant ($p<0.05$) relationship with CCE. Reyhanitabar et. al. (2007) studying Zn retention of 20 calcareous soils of central Iran, reported a significant relationship between Langmuir k, percentage of clay and CCE which is in agreement with others reports (Karimian and Moafpourian 1999) and in case of CCE is similar to our findings. This could be used to partially explain the widespread Zn deficiency in plants grown on calcareous soils.

The applicability of the Freundlich sorption isotherm was also analyzed by plotting log q versus log C. Table 3 shows the Freundlich sorption isotherm constants and the correlation coefficients. Freundlich distribution coefficient (K_f) ranged from 225.5 to 1121.5 $l\ kg^{-1}$. Distribution coefficient

represents the sorption affinity of the metal cations in solution for the soil solid phase and can be used to characterize the mobility and retention of Zn in a soil system.

Table 2. Langmiur, Freundlich and D-R[a] constants of Zn sorption in experimental soils

Soil No.	Langmiur costants				Freundlich constants		
	b (mg kg^{-1})	k_L (l mg^{-1})	K_d=M	R^2	k_f (l kg^{-1})	n	R^2
1	769.23	1.30	1000.0	0.99**	292.89	2.23	0.97**
2	833.33	1.71	1428.6	0.99**	372.82	2.63	0.99**
3	1000.00	1.67	1666.7	0.98**	436.51	2.17	0.98**
4	769.23	1.86	1428.6	0.99**	357.03	2.49	0.97**
5	1250.00	11.43	14285.7	0.94**	1121.5	2.74	0.98**
6	769.23	1.08	833.3	0.98**	285.10	2.02	0.95**
7	1000.00	1.11	1111.1	0.81*	382.38	2.65	0.97**
8	1111.11	4.50	5000.0	0.85**	632.85	3.98	0.92**
9	1111.11	1.29	1428.6	0.95**	461.42	1.96	0.99**
10	625.00	0.94	588.2	0.98**	225.53	2.30	0.97**

Table 2.Continued

Soil No.	D-R constants			
	k (mol^{2}kJ^{-2})	q_m (mmolg^{-1})	E (kJmol^{-1})	R^2
1	-0.0033	-2.8824	12.3091	0.98**
2	-0.0026	-3.1530	13.867	0.99**
3	-0.0032	-2.5503	12.5000	0.99**
4	-0.0028	-3.0325	13.3631	0.98**
5	-0.0019	-2.7855	16.2221	0.95**
6	-0.0037	-2.5965	11.6248	0.97**
7	-0.0025	-3.1936	14.1421	0.95**
8	-0.0013	-3.6758	19.6116	0.88*
9	-0.0035	-2.3007	11.9523	0.98**
10	-0.0032	-3.1785	12.5000	0.98**

Table 3.Correlation coefficients between soil characteristics and D-R, Langmuir and Freundlich parameters of sorption for Zn

soil characteristics	Freundlich		Langmuir			D-R			
	n	K_f	q_m	K_a	K_d=M	S	K	q_m	E
CCE	0.12	0.84**	0.93**	0.71*	0.74*	0.93**	0.33	0.38	0.34
Clay	0.22	0.12	0.11	-0.30	-0.31	0.44	0.27	-0.13	0.35
Silt	0.35	-0.16	0.44	-0.004	0.02	0.11	0.13	-0.11	0.14
O.M	0.27	0.80**	0.45	0.88**	0.88**	0.45	0.50	-0.12	0.43
EC	-0.05	0.43	0.19	0.48	0.50	0.20	0.11	0.09	0.07
CEC	0.64*	0.26	0.38	0.19	0.18	0.38	0.60	-0.44	0.63

* Significant at the 0.05 probability level
** Significant at the 0.01 probability level

A distribution coefficient can be related to both plant uptake and environmental pollution. Low distribution coefficients indicate that most of the metals present in the system remain in the solution and are available for transport, chemical processes and plant uptake (Jalali and Moharami 2007).Whereas high values indicate lower mobility and higher retention of metal in the soil. So that Zn in soil no 5 had the lowest mobility and in soil no 10 had the highest mobility.

The order of sorption for Zn is similar to those found in case of Langmuir sorption equation. Freundlich K_f for Zn showed a highly significant ($p<0.01$) relationship with percentage of O.M and CCE. Reyhanitabar et. al. (2007) studying Zn retention of 20 calcareous soils of central Iran, reported a significant relationship between Freundlich K_f with percentage of clay, CEC and CCE but not with OM. Karimian and Moafpourian (1999) reported that in calcareous soils of the southern part of Iran Freundlich K_f showed a highly

significant relationship with soil pH and Clay but not with CEC, CCE and OM. Freundlich constant n which indicates adsorption intensity varied from 1.96 to 3.98. Freundlich n showed a significant ($p<0.05$) relationship with CEC. Reyhanitabar et al. (2007) reported a significant relationship between Freundlich n with percentage of clay. Elrashidi and O' Connor (1982) reported a significant relationship between Freundlich coefficients and percentage of clay, CEC and pH, but not with OM.

The values of q_m constant (D-R isotherm) which is the adsorption capacity (mol g^{-1}) ranged from -2.3007 to -3.6758 (Table 2). The values of k (D-R isotherm) which is a constant related to the adsorption energy (mol^2 kJ^{-2}) ranged from -0.0013 to -0.0037. This finding is similar to the results obtained from 1/n freundlich parameter. The magnitude of E which is calculated from D-R isotherm is useful for estimating the type of adsorption process. In this study, E values ranged from 11.62 to 19.61 kJ mol^{-1} (Table 2). Therefore it is possible to say that adsorption mechanism of Zn ions onto soils can be explained with an ion-exchange process.

Because the Langmuir adsorption isotherm was found to fit the Zn adsorption data of our soils (Table 2), its k and b values were used to calculate the distribution coefficient K_d as used by Bolt and Bruggenwert (1976), or to calculate maximum buffering capacity MBC, as used by Iengar and Raja (1983), Karimian and Moafpourian (1999) and Reyhanitabar et al. (2007):

K_d = MBC = Kb

The calculated K_d of soils (Table 2) ranged from 588.2 to 14258.7 L kg^{-1}. Karimian and Moafpourian (1999) and Reyhanitabar et al. (2007) reported a range of maximum buffering capacity, 309 to 3509 for the calcareous soils of southern Iran and 212.7 to 625.0 for the calcareous soils of central Iran. K_f were significantly correlated with OM and CCE. Reyhanitabar et al. (2007) studying Zn retention of 20 calcareous soils of central Iran, reported a significant relationship between K_f with percentage of clay, CEC and CCE.

Evaluation of thermodynamic parameters viz. Kº, ΔGº, ΔHº, ΔSº provide an insight into mechanism of Zn sorption in the soils. The data in Table 4 indicate that value of Kº increased with the rise in temperature from 25 to 45 ºC in all the soils. The ΔGº values for Zn were negative in all the soils (Tables 4). These negative values indicate that the sorption process is spontaneous. The ΔGº at 25 ºC and 45 ºC ranged from -7.00 to -16.64 and -13.24 to -41.93 kJ mol^{-1}, respectively. In all the soils, the free energy (ΔGº) of the Zn sorption was more negative at higher temperature which suggested that the spontaneity of the process increased with rise in temperature (Jurinak and Bauer 1956).

The values of isoteric heat (enthalpy) of Zn sorption (ΔHº) were positive and ranged from 74.02 to 357.47 kJmol^{-1} (Table 4). This indicates that sorption reaction was endothermic. Similar findings were also reported by Biggar and Chung (1973), Adhikari and Singh (2003), Dali-youcef et al. (2006) and Unlu and Ersoz (2006).

Values of ΔHº for heavy metals within the range of the enthalpy change of adsorption for ion exchange (i.e. 8.4 to12.6 kJ mol^{-1}) suggest that adsorption process is an ion exchange in nature (Helfferich 1962). The values of ΔHº in this study were greater than 12.6 kJ mol^{-1} suggesting the presence of other mechanism for the sorption of Zn in addition to ion exchange mechanism.

Table 4.Sorption thermodynamic parameters of Zn in soil studied

soil	Kº		ΔGº (KJ mol^{-1})		ΔHº	ΔSº (J mol^{-1})	
No.	25ºC	45ºC	25ºC	45ºC	(KJ mol^{-1})	25ºC	45ºC
1	26.80	1199.42	-8.06	-18.74	149.74	529.555	529.830
2	74.64	9542.58	-10.58	-24.22	191.09	676.737	677.098
3	50.58	2057.81	-9.62	-20.17	145.98	522.172	522.500
4	55.47	363.18	-9.85	-15.58	74.02	281.454	281.790
5	4384.80	3094076.39	-20.56	-39.51	258.38	936.083	936.785
6	48.05	149.83	-9.49	-13.24	44.79	182.187	182.511
7	47.98	19789.37	-9.49	-26.15	237.23	827.935	828.259
8	883.24	7709778.37	-16.64	-41.93	357.47	1255.400	1255.967
9	37.79	18508.771	-8.91	-25.97	244.00	848.693	848.997
10	17.38	249.56	-7.00	-14.59	104.96	357.714	375.953

The values of ΔSº for Zn sorption were positive and ranged from 281.79 to 1255.97 J mol^{-1} K^{-1} (The values of ΔSº at 25 and 45 ˚C were similar). The positive values of ΔSº indicates an increased randomness at solid-solution interface during the adsorption of Zn. The decrease in the degree of randomness leads to an increase in the adsorption capacity of the ion on the sorbent (Abou-Mesalam 2003).

The thermodynamic equilibrium constant (K^o) at 25°C significantly correlated with CCE and OM (Table 5). While K^o at 45°C did not correlate with soil physicochemical properties. Standard free energy (ΔG^o) at 25°C significantly ($p<0.05$)

correlated with CCE and OM, but ΔG^o at 45°C correlated ($p<0.05$) only with CCE. Standard entropy (ΔS^o) significantly correlated with CCE but standard enthalpy (ΔH^o) did not significantly correlated with soil physicochemical properties (Table 5).

Table 5.Correlation coefficients between soil characteristics and thermodynamic parameter

soil characteristics	K^o (25)	K^o (45)	ΔG^o (25)	ΔG^o (25)	ΔH^o (25)	ΔS^o (25)	ΔS^o (45)
CCE	0.71*	0.36	0.68*	0.70*	0.60	0.62*	0.62*
Clay	-0.37	0.13	-0.35	-0.09	0.25	0.24	0.24
Silt	-0.03	0.36	0.24	0.34	0.39	0.39	0.39
O.M	0.91**	0.35	0.73*	0.57	0.37	0.39	0.39
EC	0.54	0.04	0.32	0.31	0.25	0.27	0.27
CEC	0.10	0.57	0.41	0.43	0.37	0.38	0.38
pH	0.50	0.24	0.45	0.32	0.18	0.20	0.20

* Significant at the 0.05 probability level
** Significant at the 0.01 probability level

4. Conclusion

In this study the experimental data were better described by D-R and Freundlich isotherms than were by Langmuir isotherm. The most influential soil characteristics on Zn sorption in the studied soils are OM, CCE and CEC.

Thermodynamic studies revealed that Zn sorption reaction in all the soils were spontaneous and endothermic. This suggests that the sorption capacity of these soils enhanced with an increase in temperature. Therefore, in addition to soil properties and nature of pollutant, soil environment of factors particularly soil temperature needs to be considered when developing suitable strategies for proper management of heavy metal pollution.

Acknowledgement

The authors are grateful to Dr H. Beigi for critical review and editing on the manuscript.

Correspondence to:

A.R. Hosseinpur, Soil Sci. Dep.
Shahrekord, Univ. Shahrekord, Iran.

References

1. Abou-Mesalam MM. Sorption kinetics of copper, zinc, cadmium and nickel ions onsynthesized silico-antimonate ion exchanger. Colloids and surfaces A-physicochemical and engineering aspects. 2003;225: 85-94.
2. Adhikari T, Singh M.V. Sorption characteristics of lead and cadmium in some soils of India. Geoderma. 2003; 114: 81-92.
3. Arias M, Perez-Novo C, Lopez E, Soto B. Competitive adsorption and desorption of copper and Zinc in acid soils. Geoderma. 2006; 133: 151-159.
4. Biggar JW. Cheung MW. Adsorption of picloram (4-Amino-3,5,6-Trichloropicolinic Acid) on panoche, ephrata, and palouse soils: A thermodynamic approach to the adsorption mechanism. Soil Science Society of America Proceeding. 1973;37: 863- 868.
5. Bolt GH, Bruggenwert MGM. . Soil chemistry. Part A: Basic ellments. Elsevier. Amsterdam, the Netherlands, 1976.
6. Bouberka, Z, Kacha S, Kameche M, Elmaleh S, Derriche Z. Sorption study of an acid dye from an aqueous solutions using modified clays. Journal of Hazardous Materials. 2005;119:117-124.
7. Dali-youcef N, Oddane B, Drriche Z. Adsorption of zinc on natural sediment of Tafna River Journal of Hazardous Materials. 2006;137: 1263–1270.
8. Elrashidi CA, Oconnor GA. Influence of solution composition on sorption of zinc by soils. Soil Science Society of America Journal. 1982;46: 1153-1158.
9. Elzinga EJ, Van Grinsven JJM, Swartjes FA . General purpose Freundlich isotherms for cadmium, copper and zinc in soils. Eurasian Journal Soil Science. 1999;50: 139–149.
10. Gee GW, Bauder JW. Particle-size analysis. In: Klute A, ed. Methods of soil nalysis, ASA,SSSA, Madison, Wisconsin, USA. 1982;382-412.
11. Harter RD. Effect of soil pH on adsorption of lead, copper, zinc and nickel. Soil Science Society of America Journal. 1983;47: 47-51.
12. Helfferich F. Ion exchange. McGraw Hill, New York, USA. 1962
13. Iyengar BRV, Raja ME. Zinc adsorption as related to its availability in some soils of Karnataka. Journal of Indian Society Soil Science 1983;31: 432- 438.
14. Jalali M, Moharrami S. Competitive adsorption of trace elements in calcareous

soils of Western Iran. Geoderma. 2007;140: 156-163.
15. Jurinak JJ, Bauer N. Thermodynamics of zinc adsorption on calcite, dolomite and magnetite type minerals. Science Society of America Journal. 1956;20: 466– 471.
16. Kalbasi M, Racz GJ, Loewen-Rudgers LA. Mechanism of Zn sorption by iron and aluminium oxides. Soil Science. 1978;125: 146–150.
17. Karimian N, Moafpourian GR. Zinc adsorption characteristics of selected soil of Iran and their relationship with soil properties. Communication in Soil Science and Plant Analysis. 1999;30: 1722-1731.
18. Lindsay WL. Zinc in soils and plant nutrition. Advance in Agronomy. 1972;24: 147-186.
19. Lindsay WL, Norvell WA. Development of a DTPA soil test for zinc, iron, manganese, and copper. Science Society of America Journal. 1978;42: 421–428.
20. McBride MB.989. Reaction controlling heavy metal solubility in soils. Advance in Soil Science. 1989;10: 1-55.
21. Nelson DW, Sommers LE. Total carbon, organic carbon, and organic matter. In; Sparks DL, ed. Methods of soil analysis. ASA. SSSA. Madison, Wisconsin, USA. 1996;961-1010.
22. Nelson RE. Carbonate and gypsum. In: Page AL, ed. Method of soil analysis. ASA and SSSA, Madison, Wisconcin, USA. 1982;181-197.
23. Reyhanitabar A, Karimian N, Ardalan M, Savaghebi G, Ghannadha, M. Comparison of five adsorption isotherms for prediction of Zinc Retention in calcareous soils and the relationship of their coefficient with soil characteristics. Communication in Soil Science and Pant Analysis. 2007;38: 147-158.
24. Rhoades JD. Salinity: Electrical conductivity and total dissolved solids. In: Sparks DL, ed. Methods of soil analysis. SSSA. Madison, Wisconcin, USA. 1996;417-435.
25. Rouquerol F, Rouquerol J, Sing K. Adsorption by powders and porous solid. principles, methodology and applications. Academic press, London. 1999.
26. Sparks DL. Environmental soil chemistry. Academic Press, San Diego, CA. 1995.
27. Sposito G. The surface chemistry of soils. Oxford Univ. Press, New York, USA. 1984
28. Summer ME, Miller WP. Cation exchange capacity and exchange coefficient. In: Sparks DL, ed. Methods of soil analysis, SSSA Madison, Wisconsin, USA. 1996;1201-1231.
29. Trehan SP, Sekhon GT. Effects of clay, organic matter, and $CaCO_3$ content of zinc adsorption by soils. Plant and soil. 1977;46: 329-336.
30. Udo EJ, Bohn HL, Tucker, TC. Zinc adsorption by calcareous soils. Soil Science Society of America Proceeding. 1970;34: 405- 407.
31. Unlu N, Ersoz M. Adsorption characteristics of heavy metal ions onto a low cost biopolymeric sorbent from aqueous solutions. Journal of Hazardous Materials. 2006;136: 272–280.
32. Wu J, Laird DA, Thompson ML. Sorption and desorption of copper on soil clay components. Journal of Environmental Quality. 1999;28: 334–338.
33. Yavuz O, Altunkaynak Y, Guzel F. Removal of copper, nickel, cobalt and manganese from aqueous solution by kaolinite. Water Research. 2003;37: 948–952.

5/19/2010

Assessment Lake Nasser Egypt Within The Climatic Change

Elsayed Ahmed El Gammal
National Authority for Remote Sensing and Space Science- Cairo,Egypt
Email< egammal@hotmail.com >

Abstract-Changes of water level interacted with physical features in Lake Nasser to yield positive and negative geoenvironmental impct. In the current search, the problem postulated in two strangle portions in the course of the lake. First, El Madiq strangle zone where sands fall down and drifted on stream gradient to narrow course which exhibit shallow water on satellite imagery. Second, the entrance of the lake subjected to new delta initiation, with maximum thickness concentrated in a zone lies between Km 350 and 420 from the Dam. Two positive implications also determined, in Allaqui the difference in water area between 1987 and 2000 is 91.9 $km^{2.}$ and the difference in water extension is 25.54 km. Fine soil in an area about 30121 km^2 in the basin can be cultivate in Allaqui. The saturated water zone in Kurkur is closed to the land surface and subjected to transpiration and evapotranspiration. Kurkur vadose water can flow to the lake course and interflow water can also migrate back to the land surface to evaporate. An area of 392 km^2 ready for agriculture that can avoid Kurkur area from evaporation. [Journal of American Science 2010;6(7):305-312]. (ISSN: 1545-1003).

key words; Lake Nasser, strangle, sand drift and High Dam.

1- Introduction

The stored water in Lake Nasser, was, in a way, the multi mate testimony of the value of the High Dam to the welfare of Egypt, of River Nile flows and provides reserve from normal and above normal water years where the River Nile is only water source for Egypt. Lake Nasser extended in 500 km, 350 in Egypt and 150 in Sudan with average width about 12 km at water level 180 m. Lake Nasser mainly affected by climatic change on east Africa where the influences from the lake shore was neglected because the following functions; i-Geo-environment of the lake is a desert without vegetation or Human activities at the time of its formation. ii-The lake has one source of water, the River Nile because it has other few tributaries, precipitation iii- Only evaporation impact led to exciting changes on the lake due to the arid climate. Consequently, water level in Lake Nasser is a good indicator of the cycles of wet climate followed by droughts in East Africa. The main water supply sources are the Ethiopian Plateau, the equatorial lakes and Bahr El- Gazal water shed. The River Nile has under gone a wide variety of the floods over history, the inflow is ranging from a maximum value of 150 Bm3/year (1878-1879) to a minimum value of 42 Bm3/year (1913-1914).

The problems could be postulated down in two strangle portions detected in the course of River Nile. First, El Madiq portion strangled by sand encouragement inside the reservoir with help of physical features are main problem that reduce the reservoir capacity and affecting its useful life. After lake initiation, the water velocity decreased and the water go to narrow incised wadis in the Nile. Second, sedimentation of suspended materials coming from the Ethiopian plateau cause initiative a new delta in Halfa. Before the dam 1964), the suspended sediments were deposited along all the Nile valley to the Mediterranean Sea. And due to decrease of water velocity after lake foundation (1968), the suspended sediments were flushed down in the lake around the old Second Cataract and the water spillway in E-W small wadis. Therefore the total storage capacity of Lake Nasser in 1964 was 9115 Mm^3, in 1977 was 7904 Mm^3, 1988 was 7293 Mm^3, 2000 was 4930 Mm^3 and in 2006 it reduced to 4148 Mm^3.

Water level changes in Lake Nasser give another attraction to positive geoenvironmental implications in Kurkur area in the western side of the lake and Allaqui area in the eastern side. These wide areas have physical features promising for agricultural reclamation. For these reasons, this paper aim to asses the water fluctuations from water level 160 to 183 m within lake parts and monitor the causes of strangle problems on one side and the benefit areas for people on another.

2- Methodology

Use of remote sensing technique in change detection of water level in Lake Nasser required Landsat TM images in dates 1972, 1987, 2000, 2003 and 2008 using ARC-map program and Geographic Information system GIS (Fig.1). The water level changed (from 160m to 182 m), in different rates from part to another within the lake. There are high water fluctuations in Allaqui and Kurkur areas, consequently, the current search investigated their drainage basin characteristics and delineate new areas inside Kurkur and Allaqui basins for agricultural reclamation. Whilst there is

no fluctuation in El Madiq and Halfa portions. These multi-temporal Landsat TM images delineated the recent position of the El Madiq portion and the sand dunes morphology and concentration were interpreted from the satellite images and field work. Also we followed the sedimentation steps in the entrance of the lake (Halfa) on satellite imageries. The lithological characteristics, were extracted from the available geological maps of southern Egypt [2]. The geomorphological landforms were interpreted from integrating geological data with visual analyses of Landsat TM images and the spatially variable relief from the DEM and field verifications. Morphometric analyses of the lake shore and the stream gradient of the lake were necessary to understanding the impact of water level in the reservoir. Additionally, in El Madiq and Halfa portions, the E-W structural trends have thrown down the north flanks inside the River Nile before the lake foundation forming suddenly fall in stream gradient. Consequently, sedimentation retained within the reservoir bottom in both portions by lowering water velocity specially in the entrance of the lake. Moreover, the impact of changing hydro-climatic conditions in this region after the dam construction cause hazards in El Madiq as strangle zone due to sand encouragement and initiate a new delta in Halfa were also determined. The treatment of available data on the sedimentation in Halfa integrated with the Landsat TM images to delineate the volume and place of sedimentation. These measured hydraulic data collected from the Nile Research Institute reports [13] and other references before and after the High Dam construction. Overall, the satellite imagery and field work within hydro-climatic changes on east Africa developments will use in assessment
Lake Nasser.

3- Strangle Problems

3- a- El Madiq Strangle (Gorge) Zone

The shallow water gorge portion stretched from El Madiq to Kurusku in length 27.6 km and average width 2.7 km (including El Madiq strangle locality which has 1.1 km width and 4.6 km length) has been determined in the course of River Nile (Fig. 1). Before the High Dam the water velocity was high speed with more erosion in flanks and can pass toward the north. After the dam, the water velocity decreased and sand deposition increased due to change in global climate. And the water go to narrow incised wadis (khors) in eastern bank with altitude 150 m in trough periods (Fig. 2). These khors are traced in hard Nubia sandstone which already saturated by water and it
consider underground water reservoir before the dam construction.

The established natural hazards of sands on Lake Nasser from satellite imagery and field work delineate two sources of sands: First source, sand encouragement from Western Desert divided into two aeolian landforms; a- elongated dune fields (Figures 3 and 4) seem to have their source from a location found to the north [5]**.** b- sand sheet, Gurf Hussein on the western side of Lake Nasser as an example area covered by sand sheets on Landsat TM images (Fig. 5) and in the field (Fig.6). Second source is sand generated directly at the Lake's wall from the Nubia sandstones Kursku plateau in the eastern side and fall down inside the lake by gravity in this arid region (Fig.7). Workers investigated sand movements, but not study sand sources, and never study the second source. Unfortunately, the two sand sources are founded in "El Madiq" area therefore it can be regarded as danger area and the sands quantity calculated only for the first sand source.

Sand encouragement concentration

The amount of sand deposited in the Lake Nasser were estimated to be 1.5 million m^3/year [3]. El Gammal and Cherif [5] studied Ghurd Abu Muharik dune field (the biggest dune field dunes in Western Desert) and stated that the dunes increase in size down southwards and moves 17 m/year to the south. Afify [1] considered the main meteorological parameters related to wind and atmospheric conditions (barometric pressure and air temperature) which are playing essential part in the phenomenon of sand moving by wind and selected the wind action stations in Wadi El Arab and Adindan to consider the sand transport to the lake in wind modeling and concluded that there are 100 to 110 cm^3 /day in summer and spring in Wadi El Arab station at 2006 (in El Madiq zone, Fig. 2). Overall, the field work and Landsat TM images in multi-temporal dates (Fig.1) with the topographic map 1944 and 1980 [6&7], elucidated that "El Madiq" became more risk due to combining the following functions.

i- Topographic function

The western side of El Madiq zone has altitude range from 200 to 280 m covered by sands with about 10 m thick, these sands continuously supported by others from the north encouragement the lake. The strong wind from NNW to SSE pass on the western side and stopped by hills in eastern side to fall down inside the course of River Nile besides the suspended sediments coming from the Ethiopian plateau (Fig.3). The eastern side vertical scarped hills of Kurusku plateau has altitude range from 260 m and to 380 m. The course-shape in El Madiqu zone is thin incised water passage in the River Nile which restricted by NE and NW faults seen on Landsat images as shallow water part in Lake Nasser and there is no changes in water level through 40 years of lake initiation (Fig.1).

ii- Geomorphological landform and features

Yardangs and sand dunes landforms covered the western side of this portion. Yardangs are striking in NNW- SSE coincide with the wind direction in this region and separated from each others by corridors for mobile-sand dunes towards the lake. Yardang is an aeolian landform indicate to long time of wind action in this side in Quaternary arid periods (Fig.3). While in the eastern side there are short incised narrow wadis cutting the Kurusku dissected plateau and these wadis declined toward the lake from altitude 300m to 150 m (in drought periods) where the water collected from lateral movement within the dissected plateau together with the surface water in the lake.

iii- Stream gradient

Stream gradient is an important factor controls the stream's velocity, the downhill slope of the bed , if a river flows out of steep onto a flatter plain, the river 's gradient may change suddenly from steep to gentle, such a change in gradient causes the river to slow down , and the sudden loss of velocity can cause sediment deposition at the base of the steep slope [4]. Inside El Madiq portion (in the water), the sands drift from Wadi El Arab downward (>10m) passing on a NW-SE fault with northern downthrow the water velocity decrease and the sands deposited to the north of Wadi El Arab bottom in an area lies between Wadi El Arab and El Madiq locality causing more strangle in this portion.

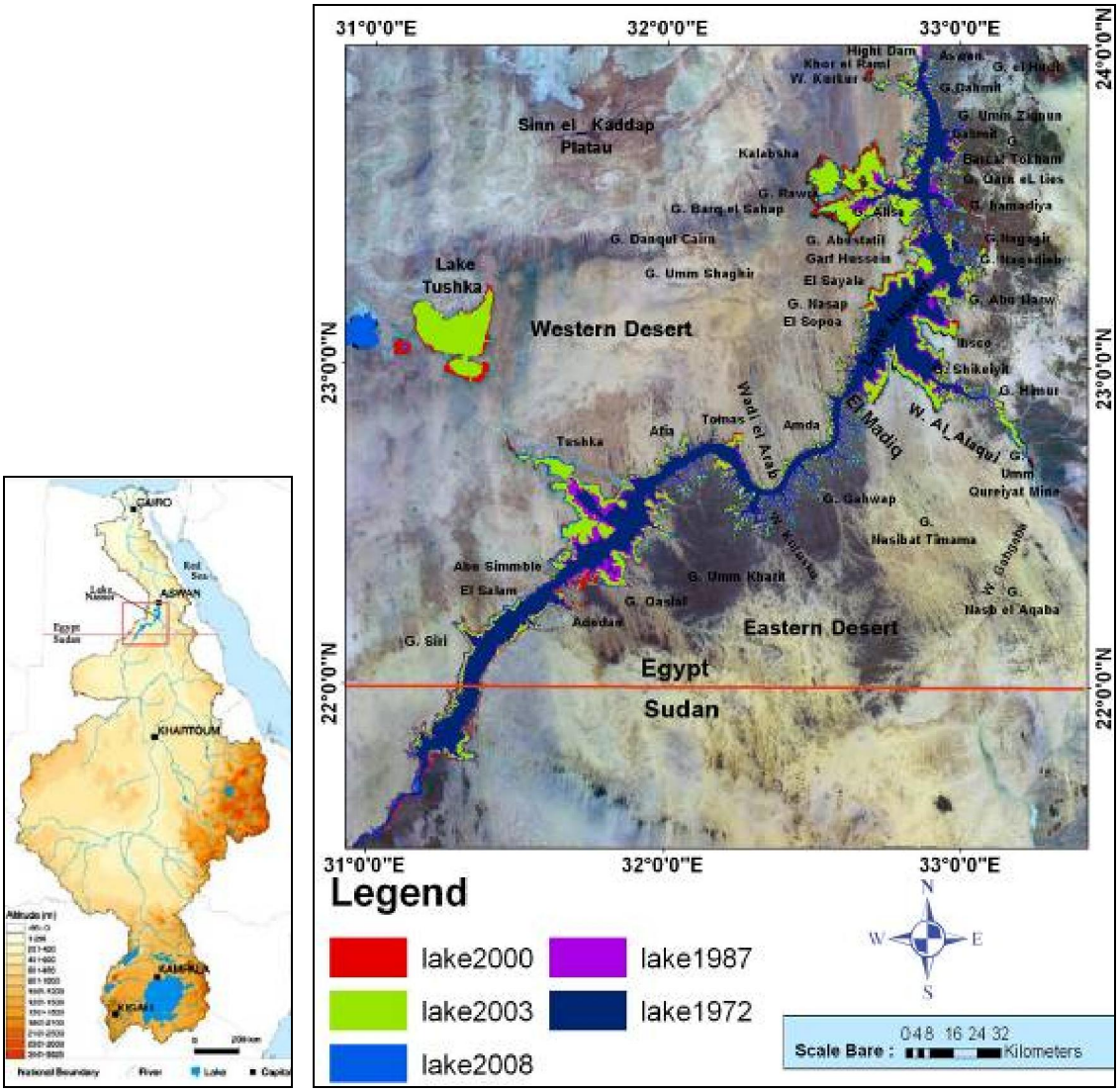

Figure 1. Change detection on Lake Nasser in multi temporal dates 1972, 1987, 2000, 2003 and 2008 using ARC-GIS, shows localities discussed in the text. Lake Nasser marked by frame in Nile Basin

3- b- New Delta Initiation in Lake Nuba

The suspended materials carried by the flood during the period 1929-1955 by weight are 30% fine sand fraction, 40% silt, and 30% clay but there is no presence of coarse sand [12]. The estimated Montnorillonite is so fine grains absorb water and swell then it consolidated in dry months forming bed.

Sediments Concentration

Before construction of the High Dam, in 1964, about 93% of the total average annual suspended load of 124 million tons/year was carried out to the Mediterranean Sea. After the High Dam construction, flood discharge of Nile downstream has been greatly modified and more than 98% of the total suspended load was retained within the reservoir and the total amount of sediment transported downstream the dam dropped to only 2.5 million tons/year due to decrease of water velocity. At year 2000 the average water velocity was 0.52 m/ sec at 487 km south the High Dam and at year 2001,it reduced to 0.46 m/sec in the entrance of the Lake to 0.04 [8].

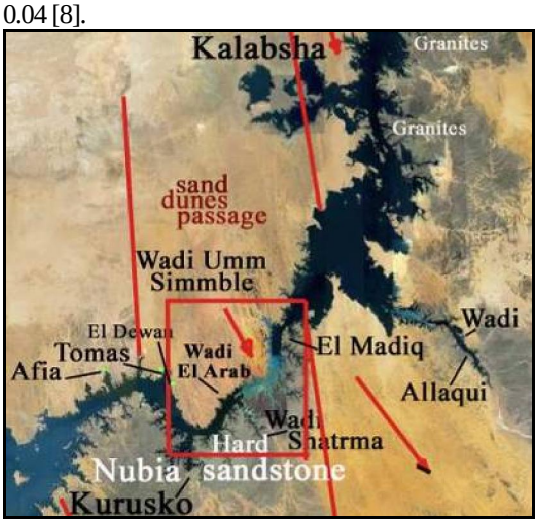

Figure 2. Sand encouragement on lake Nasser from the Western Desert, the arrow refer to the wind direction and sand movement. El Madiq shallow zone marked by frame

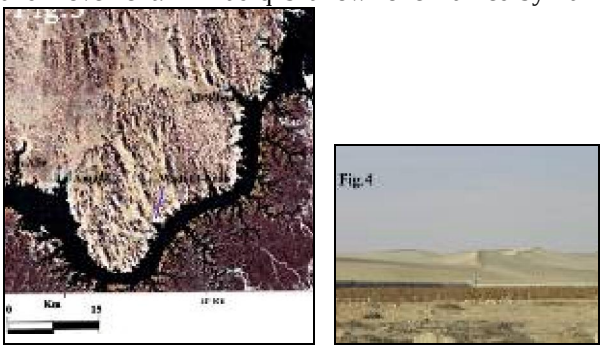

Figure 3. Landsat TM image shows sand and yardangs in the west and plateau in the east. Figure 4. Photograph shows elongated sand dune.

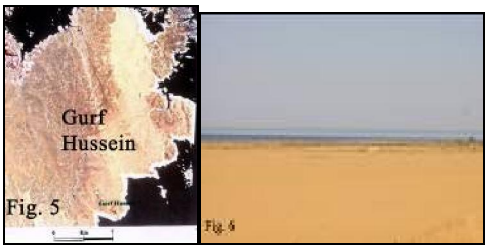

Figure 5. Landsat TM image shows sand sheet encouragement Gurf Hussein area. Figure 6. Photograph shows the sand sheet in Gurf Hussein.

Figure 7. Sand generation directly from the walls of the lake, derived from sandstone plateau

The deposited materials in Egyptian border equal to 56 Mm³ from February 2007 to March 2008 and the total sedimentation volume until March 2008 is 1123 M m³. While in Sudan, the sedimentation from February 2007 to March 2008 equal to 200Mm³ from Feb 2007 to Mar 2008 and the total sedimentation volume until March 2008 is 5161M m³ (Nile Research Institute reports 2000 and 2006). In the year 2006 at Halfa, the total volume of sedimentation 1.673 Bm³ at water level under 147 m and 3.345 Bm³ between water level 147 m to water level 175 m and no sedimentation above water level 175m. Consequently, the water can spillway to the north at 170m.

The total volume of sedimentation in the lake is 6284 million m^3 during 1964-2008 (18% in Egyptian and 83%, in Sudan), whilst in one cross section 26 (Second Cataract at 357 km from the High Dam, Figure 8) it is 1037.44 million m^3 during the same time in Halfa forming new delta from 1968 to 2008 in a zone including the following localities; 1- Gemi (372 km from the dam), the sedimentation thickness is 59.82 m. 2- Qengari 6 (394 km from the dam), the sedimentation thickness is 57.89 m. 3- Murshed 3(378.5 km from the dam), the sedimentation thickness is 54.49 m. 4- Old Second Cataract the sediment thickness is 52.10 m (Fig. 8). An estimated average of 160 million tons annual of sediment reached El-Gaafra Gauging Station (34 km to the north of the High Dam down stream) during the period from 1904 to 1963, the annual sediment load varied from 50 million tons to 228 million tons per year [13]. The suspended sediment concentration peaks at EL-Gaafra have dropped from 3000 ppm before lake initiation to only 50 ppm after the construction of the lake [9].

Stream Gradient

Stream gradient is an important factor controls a stream's velocity , the downhill slope of the bed, if a river flows out of steep onto a flatter plain, the river 's gradient may change suddenly from steep to gentle. Such a change in gradient causes the river to slow down, and the sudden loss of velocity can cause sediment deposition at the base of the steep slope lock-like that mentioned above in sand encouragement [4]. Inside Lake Nuba, the sediments drift from south to north downstream perpendicular on E-W fault (Fig.9**)** with northern downthrow (17m) forming delta. Hence, the water passage has been partially changed toward the east within E-W fault plain (Fig. 8 &9).

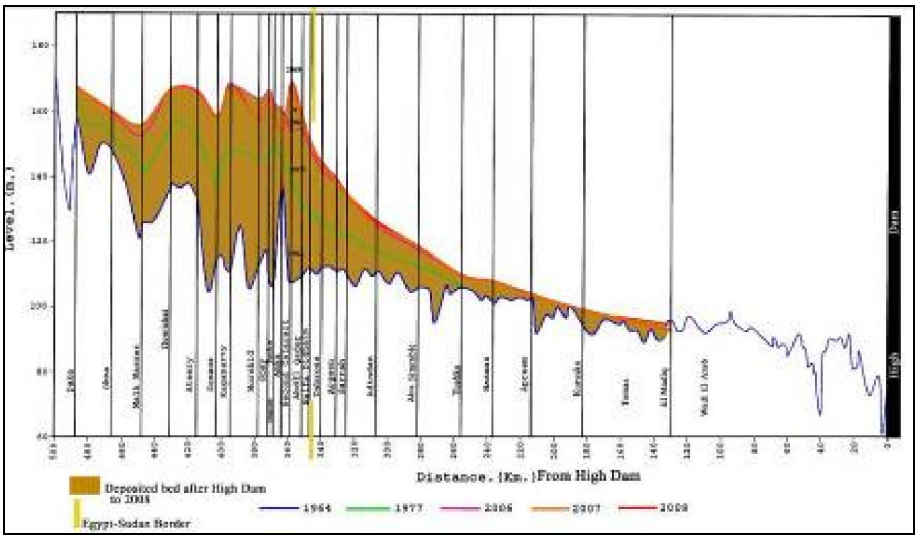

Figure 8. Diagram illustrates the deposited bed inside Lake Nasser prepared from data collection of the mentioned references.

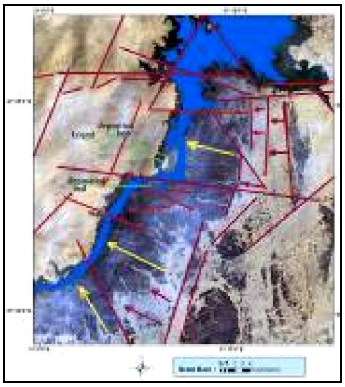

Figure 9. Lake Nuba physiographic map shows the structural elements (red lines) affecting in Halfa and slope directions (yellow lines).

Sediments on Satellite Images

However the water increase in some lake margins on Landsat TM images from 1972 to 2008 (Fig.1), there is a sharp demarcation line appears between the two kinds of water, the turbid brownish flood water in Sudan sector pushes the old green transparent water mass towards the north. Although the sedimentation can see northward until Wadi El Arab (170 km from the High Dam), the suspended materials had been deposited in a sector between 340 and 430 km from the dam (Figure 8), the new sediments formed in decreasing flood water parallel to the shore slightly emerged low dams separating the lotic and limnetic water masses indicating probably the shore of the future water-way in time to come in filling process of this part of the lake by sediment bed and the water spillway caused by shrinking volume of the lake due to mud deposits (Figure10).

After High Dam construction, firstly in year 1972, the water was go in restricted way without sedimentation (Fig.10). Then in year 2008 the deposition altitude reached up to 170 m at at Halfa, Abd El Qader and Ateery cross sections (between 347 km and 420 km from the Dam, measured at the lowest points of deposition in the lake), the same locality seen on the Landsat ETM images 1988 and 1998. In 1988, a year that the mud bed exposed when water level was 170 m in the lake and formed southern edge to Lake Nuba (Figure10). This mud bed merged by water in 2000 and 2003 (Fig.10) when the water elevated to 180 m and the water over-swell (spillway) on the mud bed in high flood only and in low flood there is no way for water to go to the north especially with the continuation of

suspended sediments. At the end of the gorge section to the wide confluence area near Amka, just above the old Second Cataract, the current speed was reduced at once to about 10 cm/sec. suspended matter started there forming a more than 1m thick new sediments layer year by year and this incredible sedimentation underwater and exposed forming new delta in Halfa appeared on Landsat images (Figure 10).

4. Useful Localities Detected With High Change Rate

Kurkur, Kalabsha Tushka and Al Alaqui areas show high water fluctuation. Several workers investigated Kalabsha and Tushka, there are several projects had been created in Tushka, Kalabsha and Garf Husein while Kurkur and Allaqui are seeking to scientific study and development projects. Here, Kurkur and Alaqui areas have been investigated in this study.

4-a- Kurkur Area

Kurkur drainage basin had been extracted from Landsat TM image equal to 988 km^2 divided into two parts, the lower stream part is nearly flat area with natural plants and fine soil, the second part is slightly slopping area (Fig.11). Kurkur Oases lies at the upper stream part of Kurkur drainage basin at the foot-slope of major scarp (220 m) of Sinn el Kaddab plateau (Fig.11). Kurkur Oases get the water from canyon karst inside the limestone Sinn el Kaddab plateau and from the quick runoff across the steep scarp. Because of the oases position in relative high topography upstream drainage inside the Kurkur basin, the oases not support by water from the lake (Fig.11). The water depth in Wadi Kurkur is ranging from 0.7m to 2 m seen in the field trip in wide area after high flood in September 2008 (Fig.12).This lead to high evaporation in temperature reach up to 50º in summer and in May 2009 the area was still wet fine soil where natural plants grown (Figure 12).

In Kurkur, there is a saturated zone where the water table appear in Kurkur Oases (pond and springs in local depression at the upstream parts) and interflow water is pulled downward by gravity known as gravity drainage [10] to downstream parts in Kurkur basin to the lake. Exposure of water bodies in Kurkur area far from the lake and occurrences of gypsum sands near to the tidal zone of water fluctuation in dry and wet periods (Fig.13) delineate the high ground water table in Kurkur basin. The aeolian deposition and wind deflation stopped at the Stocks's surface indicating to the ground water table [11].

This saturated water zone had been exposed to evaporation in high flood years (Fig.13), where the water nearly closed to the land surface in Kurkur subjected to transpiration and evapotranspiration in low flood years (Fig. 13). In 1984 the year that water diversion began the surface of Lake Nasser was 155 m when the lake elevation declined by 15 m to 1989 the year that surface area shrank to 180 m. One consequence of the reduction of the volume of Lake Nasser has been increase in salinity of the lake margins in Kurkur. Kurkur is a vadose zone (zone of aeration) in low floods the vadose water can flow to the lake course and in vadose zone the process known as interflow water in vadose zone can also migrate back to the land surface to evaporate.

4- b- Allaqui Area

The maximum perpendicular width (11.6 km) in Lake Nasser lies in it's conduction with Allaqui. Three dimensions elevation model (3DEM, Fig.14) illustrates big difference between year 1987 in drought period in east Africa and year 2000 in rain period where the water extended to 29.1 km 2000 in Wadi Allaqui course (Fig.14). The water area in Allaqui in 1987 was equal to 112 km^2 and the water extension (length) equal to 62.46 km. In 2000, water area 203.9 km^2 and the water extension (length) equal to 88 km. The difference in area between 1987 and 2000 equal to 91.9 $km^{2.}$ and the difference in water extended length between 1987 and 2000 equal to 25.54 km (Fig.14). In 2008, the water arm extended 26.2 km length and 2.1 km width wedged to .8 km width. An area of 91.9 km^2 water exceeded in the high flood periods on east Africa can be utilize in irrigate the fine soil in Allaqui. Wadi Allaqui have 250 km length and 2 km average width , it is a fifth order drainage channel inside the large basin extracted from Landsat TM image (Fig.15). Allaqui Basin area equal to 67868.12 km^2. Wadi fill in Allaqui composed of silt-size friable soil with depth reach up to 5 meters. Allaqui basin subjected two times annually to flash flood exceed than 25 cm. The igneous and metamorphic mountains in Allaqui basin reach up to 1148 (Gabal Eiqat and Gabal Seiga) and to 1152 m in Gabal Hileikonti with steep slopes and not infiltrate any precipitated water giving quick runoff to the course of Wadi Allaqui. The course of Wadi Allaqui declined from 600 m asl to 200 m inbetween the mountains then sloped to 150 m in the downstream trend with nearly horizontal surface in area about 30121 km^2 in the basin suitable for cultivation without the risk of flash flood (Fig.15) but it have ground water marked by playa exposure inside the Allaqui basin far from the tidal zone of high flood periods.

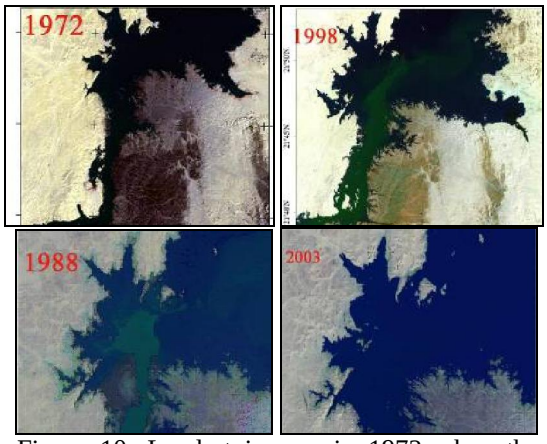

Figure 10. Landsat images in 1972 when the water has restricted passage with rare sedimentation, 1988 a year that the mud bed exposed when water level was <170 m in the lake and do southern margin end to the lake and 1998, this mud bed merged by water in 2003.

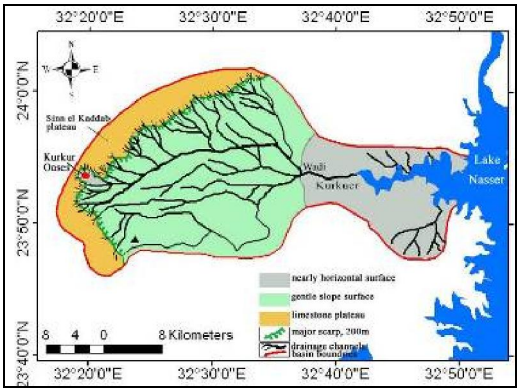

Figure 11. Kurkur drainage basin prepared from Landsat images and topographic maps using ARC

Figure 12. Natural plants and shallow water covering wide area in Wadi Kurkur.

Figure 13. Exposure of water bodies far from the lake (right) and wind deflation stopped at Stocks's surface in Kurkur area (left).

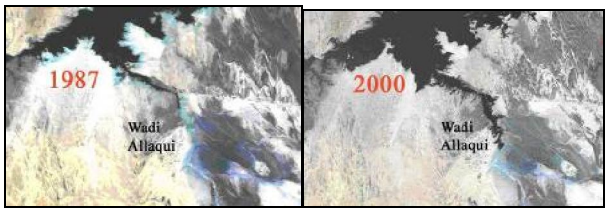

Figure14. The 3DEM in years 1987 and 2000 in Alaqui illustrates big difference in water extension.

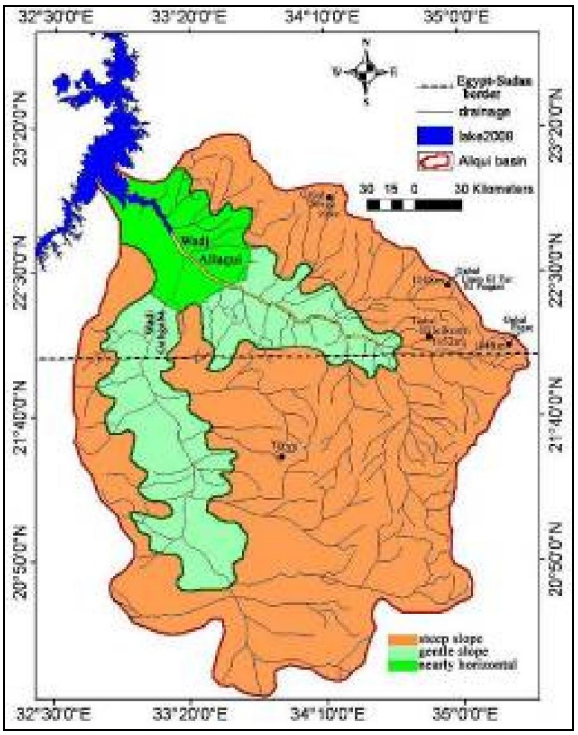

Figure 15. Allaqui drainage basin prepared from Landsat images using ARC-GIS.

5. Conclusion

Climatic changes on east Africa caused positive and negative geoenvironmental implications inside and around Lake Nasser. Inside El Madiq zone, 151, $2m^3$ sands accumulated only in Wadi El Arab and drifted on the stream gradient to more narrow zone in down stream trend due to E-W fault with 17 m northern down-throw. Then, this zone exhibit shallow water in the Lake course and have not water excess in high flood years. The entrance of the lake in Halfa is subjected to sedimentation of suspended materials forming new delta. The maximum sedimentation thickness is concentrated in a zone lies from Km 350 to 420 km from the High Dam. It produced a delta sediments with long 70 km and 60m thickness from altitude 105 to 170 m (till 2008) to elucidate that the best water level for avoid the sedimentation risk is 175-180 m suitable circumstance for less sedimentation and allow to water spillway on the

consolidated mud bed giving suitable storage capacity. The satellite images illustrated the strangles both in El Madiq and Halfa, coincided with the field observation and hydrologic data.

Kurkur basin can support the Nile course and ready for agriculture. The saturated water zone in Kurkur is nearly closed to the land surface subjected to transpiration and evapotranspiration in low flood years. Kurkur is a vadose zoe, water can flow to the lake course and the process known as interflow water can also migrate back to the land surface to evaporate. Consequently, cultivate 392 km^2 can avoid Kurkur area from evaporation In Wadi Allaqui, the difference in water area between 1987 and 2000 equal to91.9 $km^{2.}$ and the difference in water extention arm is 25.54 km. An area of 91.9km^2 water exceeded in the high flood periods can be utilize in irrigate the fine soil in nearly horizontal surface of about 30121 km^2 in Allaqui basin suitable for cultivation without the risk of flash flood but it have ground water marked by patches of playa inside the Allaqui basin before the construction of the High Dam.

References

[1] Afify, A., 2007, Emprical model for the estimation of Sand Transprt Rate In the vicinity of Nasser Lake, Meteorological Research Bulletin- ISSN 1687- 1014- vol.-22-2007.

[2] CONOCO Coral, and Egyptian General Petroleum Company, 1987. Geological map of Egypt scale 1:5,00,000, Cairo, Egypt.

[3] Dahab, A.H., 1992.The geomorphological effect of the desert sand drifting towards Lake Nasser. Inter. Conf. on Protections and development of the Nile Nile 2000, Cairo Feb. 3-5

[4] McGeary D. and Plummer.Ch.C., 1997. Earth Revealed. McGraw-Hill, New York , p359.

[5] El Gammal E.A. and Cherif,O. 2008. Use of remote sensing for the study the hazards impact of Ghurd Abu Muharik sand dune field Western Desert Egypt. International conference on environmental research and technology, 28-30 May 2008, Penang Malaysia. no.141, pp 710-715.

[6] Topographic map Aswan sheet scale 1: 500 000, Egyptian Survey 1944.

[7] Topographic map Aswan sheet scale 1: 500 000, Egyptian Survey 1980.

[8] El-Moattassem M., Abdel-Aziz T.M. and El Sersawy H., 2005. Modeling of sedimentation processes in Aswan High Dam reservoir , Ninth International Water Technology conf. Sharm El Sheikh, Egypt.

[9] El-Sersawy H. and Farid M. 2005. Overview of sediment transport evaluation and monitoring in the Nile Basin, Ninth International Water Technology conf. Sharm El Sheikh, Egypt.

[10] Fetter C. V. 1994. Applied Hydrogeology. Prentice Hall, New Jersey, pp. 30-35

[11] FrybergerS.G., Schenk,C.J. and Krystinik,L.F.,1988. Stokes surfaces and the effect of nearsurface groundwater-table on Aeolian deposition. Sedimentology Jour., 35: pp 21-41.

[12] Hurst, H.E. 1952. " The Nile" a general account of the River and the utilization of its water , pp. 237-279, Publisher Constable and Company LTD, London UK.

[13] Nile Research Institute (NRI), 2006. Annual reports from 2000 to 2006 Lake Nasser hydrology measurements in 1964 to 2008 Cairo, Egypt.

13-6-2010

Application of native excretory /secretory products from third larval instar of *Chrysomya megacephala* (Diptera:Calliphoridae) on an artificial wound

[1*]Nancy Taha, [2]Afaf Abdel-Meguid, [1]Ahmed El-ebiarie

1Department of Zoology and Entomology, Faculty of Science, Helwan University,
2Department of Entomology,Faculty of Science, Cairo, University, Egypt.
[*]nancyt0000@yahoo.com

Abstract: The analysis of native excretory/secretory products from third larval instar of *C.megacephala* using SDS-gel electrophoresis produces a band at 16KDa,a band between 16KDa and 23KDa and a broad band between 23 and 45KDa.This native excretory /secretory products cause the healing of an artificial wound in a rabbit. [Journal of American Science 2010;6(7):313-317]. (ISSN: 1545-1003).

.**Key Words***:* *Chrysomya megacephala*, mid-gut, excretory/secretory products, maggot therapy

1. Introduction

Numerous clinical reports have been published that describe the outstanding effects of maggot therapy, most notably on debridement, cleansing, disinfection and healing of indolent wounds, many of which have previously failed to respond to conventional treatment. Current day maggot therapy, with its multi-action approach to wound cleansing and healing, is highly successful Sherman *et al*.,(2004) . Zasloff (2002) reported that antimicrobial peptides (AMPs) are an evolutionarily conserved component of the innate immune response, which is the principal defense system for the majority of living organisms, and are found among all classes of life ranging from prokaryotes to humans. Maier *et al*.,(1999) stated that they represent a new family of antibiotics that have stimulated research and clinical interest The benefits associated with the use of insect larvae or maggots in the healing of wounds were first observed and recognized centuries ago but it is only recently, especially with the increase in antibiotic resistant micro-organisms, that such use, termed "biosurgery", has been readdressed and the renaissance of maggot therapy begun(Sherman *et al*.,2000). The larvae currently in clinical use are those of the green bottle fly *Lucilia sericata*.It is believed that larvae, or maggots, have a remarkable ability both to debride and to disinfect wounds. More recently it has been determined that this ability extends to the stimulation of tissue regeneration and to wound closure. Larvae are usable in the clinical setting to improve and to increase the rate of healing of many chronic wounds where conventional therapy such as antimicrobials, surgical debridement and wound drainage are unable to reduce or to stop the progressive tissue destruction (Mumcuolgu *et al*.,1999). Such chronic wounds originate from various conditions and include; diabetic foot ulcers, venous leg ulcers, infected surgical wounds, orthopedic wounds, osteomyelitis and pressure sores.

Despite of all these advantages of maggot debridement therapy (MDT), the utilization of MDT appears to be poor accepted by both patients and healthcare professionals. Social and cultural beliefs may initially hinder its use. There are other problems concerning the use of live maggots for MDT.Repeated changes are necessary because the life cycles of larvae are relatively short. Moreover, their limited shelf-life means that they need to be used soon after delivery. The most important problem is rearing these maggots in hospitals without smelling their bad odor, which is impossible even with very high sanitary conditions (Dominic *et al*., 2007)

The constituents of the larval excretory/secretory (ES) products are thought to be central to the way in which maggots promote wound healing with several mechanisms proposed to explain their actions. Debridement is thought to be partially achieved via the proteolytic action of collagenase and serine proteases present in the ES which degrade the necrotic tissue into a form which is ingestible to the larvae and which act to remove the slough from the wound surface (Beasley *et al*., 2004).

The stimulation of extra-cellular matrix (ECM) remodeling and closure has also been proposed to be attributable to the action of one or

more 'chymotrypsin-like,' serine protease/s present in the ES which acts to degrade fibronectin into bioactive peptides. It is thought that these bioactive peptides are then able to stimulate adhesion and migration of fibroblasts (Horobin *et al.*,2005)and are possibly responsible for the acceleration in healing(Horobin *et al.*,2003).The ES may also have an effect on fibroblast proliferation.

Chrysomya megacephala (F.), the Oriental latrine fly, is a common blow fly species of medical importance in many parts of the world, including Eygpt. Adults may feed on food sources including nectar, animal carcasses, garbage, and other filth materials, or even human food. Therefore, it is possible that mechanical transfer of potential disease causing pathogens, such as bacteria, viruses, protozoa, and helminth eggs, to human food may occur (Sukontason *et al.*, 2000). Larvae of this species are known to cause myiasis in several mammal species, including humans (Kumarasinghe *et al.*, 2000). Another facet of medical importance of this blow fly is its association with human corpses and its relevance to forensic entomology, *C. megacephala* were found connected with cases of human death (Sukontason *et al.*, 2005).

The aim of this paper,was to check the healing action of native excretory/secretory products from third larval instar of Chrysomya megacephala on a wound induced in a rabbit.

2. Material and Methods

The laboatory colony of *C. megacephala* used in this study was established in the Department of Entomology,Faculty of Science, Helwan University. *Chrysomya megacephala* was reared according to the method of Gaber *et al.,* (2005). Native excretions/secretions (nES) were collected by incubating third-instar larvae of *C.megacephala* in a small quantity(100 larvae per 1ml) of sterile distilled water for 1 h at 30 °C in darkness. The sterile liquid was siphoned from the containers and centrifuged at 10,000 × *g* for 5 min to remove particulate material, after which the supernatant was stored at 4°C for testing.

Male rabbit about 1.5 Kg weight,was used for this experiment.-Rabbit was kept in a big wooden box with wire.Water and food were daily given to the rabbit.The rabbit was partially anthesized. The upper thigh of the rabbit was shaved before induction of wound.

A drop of sulphuric acid was added to the skin to induce a severe wound.Photographs of the wound were taken with a digital camera 10 pixels.-The native excretory /secretory(nES) products was prepared with concentration 100 larvae per 1 ml distilled water.3-5ml nES was applied daily on the wound.-Daily observation of the changes in the wound were recorded and photographed.

3. Results

The analysis of native excretory/secretory products from third larval instar of *Chrysomya megacephala* produces a single band at 16KDa,a band between 16KDa and 23KDa and a broad band between 23KDa and 45KDa (Fig. 1). The tissue of the wound induced in the rabbit appeared to be dead (Fig.2).By applying the nE/S daily the tissue appears to be more healthy(Figs 3,4,5).Flow of blood can be seen and also the formation of collagen (Fig6).

4. Discussion

Proteolytic enzymes are a major component of the digestive process of parasites and are presumed to be released to interact with host tissues (Rhoads and Fetterer, 1997).

The analysis of native excretory/secretory products from third larval instar of *Chrysomya megacephala* produces a single band at 16KDa and a broad band between 23KDa and 45KDa. Insect trypsins have been characterized and purified from species of Coleoptera, Orthoptera, Lepidoptera and Diptera. Most insect trypsins are 20–30 kDa as determined by SDS-PAGE (Terra and Ferreira, 1994). These insect trypsins are most active at alkaline pH, are not activated by calcium ions, and are sensitive to natural trypsin inhibitors (Terra and Ferreira, 1994). Recently, workers in Nottingham, UK, demonstrated *in vitro* a range of enzymes secreted by *P. sericata* larvae (Chambers *et al.*,2003).

Four proteolytic enzymes, comprising two serine proteases, a metalloproteinase and an aspartyl proteinase, were detected, with molecular weights ranging from 20 to 40 kDa, with activity across a wide pH range. It is clear from the results of the present study that the wound healed in the rabbit may be due to the action of the proteolytic enzymes present in excretory/secretory products from third larval instars of *C.megacephala*. Research into the debridement mechanisms underlying maggot therapy has revealed that maggots secrete a rich soup of digestive enzymes while feeding, including carboxypeptidases A and B ,leucine aminopeptidase (Vistnes *et al.*,,1981), collagenase (Ziffern *et al.*,1953) and serine proteases (trypsin-like and chymotrypsin-like enzymes) (Casu,1994).

Enzymes can be produced from any living organism, either by extracting them from their cells or by recovering them from cell exudates (Lambert

and Meers 1983). The molecules involved in the beneficial effects of maggots are believed to be contained in their excretions/secretions (ES) (Mariena *et al*.,2007). Britland (2006) established the wound-healing capacity of "maggot juice" by applying extracts of the secretion to layers of cells that mimic skin. When they created artificial, circular "wounds" in the layers, the wounds healed fastest when exposed to the extracts. They suggest that protease enzymes in the juice enable repair cells to move more swiftly and freely within the wound site. "They all march in unison and fill the hole significantly quicker," says co-team leader, David Pritchard at the University of Nottingham in the UK. The researchers showed that the holes healed just as quickly whether the juice was applied directly or in a prototype gel which could be developed into a wound dressing.

Acknowledgements

I am grateful for my supervisor, Dr. Afaf Abdel-Meguid for her support cooperation and revising this manuscript. Deep thanks for my parents and my husband for supporting me both psychological and financial

Corresponding author
Nancy Taha,
Department of Zoology and Entomology, Faculty ofScience, Helwan University, Cairo, Egypt.
nancyt0000@yahoo.com

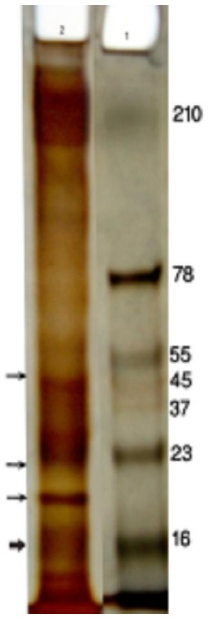

Fig(1): Electrophoretic pattern using SDS-gel electrophoresis.Lane(1) representing marker and lane(2) representing native excretory/secretory product produced from third larval instars of *Chrysomya megacepha*

Fig (2) The wound after adding sulphuric acid the tissue becomes dead.

Fig (3) The wound after one day from adding nES,the tissue starts healing.

Fig (4) The wound after 3 days fom adding nES,the tissue continue healing.

Fig (5) The wound after 5 days fom adding nES,the tissue.

Fig (6): The wound after 7 days fom adding n ES,the tissue starts healing.

5. References

1. Beasley W D, Hirst G,(2004). Making a meal of MRSA-the role of biosurgery in hospital acquired infection. *Journal of hospital infection*, 56, 6-9.
2. Britiland (2006). Pour on 'maggot juice' to help heal wounds.
3. Casu RE, Jarmey JM, Elvin CM, Eisemann CH, (1994). Isolation of a trypsin-like serine protease gene family from the sheep blow fly *L. cuprina*. *Insect Mol Biol*;3:159-70.
4. Chambers L, Woodrow S, Brown A P, Harris P D, Phillips D, Hall M, Church JCT, Pritchard Dl,(2003). Degradation of extracellular matrix components by defined proteinases from the green bottle larva *Lucilia sericata* used for the clinical debridement of non-healing wounds. *British Journal of Dermatology*, 148, 14-23.
5. Dominic CW Chan,Daniel HF Fong,June YY Leung,Patil NG,Gilberto KK Leung (2007). Maggot debridement therapy in chronic wound care.Hong Kong Med J Vol 13:382-6.
6. Horobin A J, Shakesheff K M, Woodrow S, Robinson C, Pritchard D I, (2003)**.** Maggots and wound healing: an investigation of the effects of secretions from *Lucilia sericata* larvae upon interactions between human dermal fibroblasts and extracellular matrix components. *British Journal of Dermatology*, 148, 923-933.
7. .Horobin AJ, Shakesheff KM, Pritchard Dl (2005) Maggots and wound healing: an investigation of the effects of secretions from *Lucilia sericata* larvae upon the migration of human dermal fibroblasts over a fibronectin- coated surface. *Wound Repair and Regeneration* 13 (4): 422-433.
8. -Kumarasinghe SPW, Karunaweera ND, Ihalamulla RL (2000) A study of cutaneous myiasis in Sri Lanka. *Int J Dermatol* 39:689–694
9. Lambert PW, Meers JL (1983) The production of industrial enzymes. Phil Trans R Soc Lond B300:263–282.
10. Maier M. Wu, Benz E., R. and Hancock R.E.W (1999).: "Mechanism of interaction ofdifferent classes of cationic antimicrobial peptides with planar bilayers and withthe cytoplasmic membrane of *Escherichia coli* ", *Biochemistry*, Vol. 38, , pp.7235–7242.
11. Mariena J.A. van der Plas a,b, Anne M. van der Does a, Mara Baldry a,Heleen C.M. Dogterom-Ballering a, Co van Gulpen a, Jaap T. van Dissel a,Peter H. Nibbering a,*,1, Gerrolt N. Jukema b,1(2007). Maggot xcretions/secretions inhibit multiple neutrophil pro-inflammatory responses. Microbes and Infection 9 , 507e514,
12. Mumcuoglu KY, Ingber A, Gilead L, Stessman J, Friedman R, Schulman H, et al., (1999). Maggot therapy for the treatment of intractable wounds. *Int J Dermatol.*;38:623–7.
13. Rhoads, M.L., Fetterer, R.H., (1997). Extracellular matrix: a tool for defining the extracorporeal function of parasite proteases. *Parasitol. Today* 13, 119–122.
14. Sherman RA, Hall MJR, Thomas S,(2000). Medicinal maggots: an ancient remedy for some contemporary afflictions. *Annu Rev Entomol*; 45:55-81.
15. Sherman RA, Shimoda KJ, (2004)**.** Presurgical maggot debridement of soft tissue wounds is associated with decreased rates of postoperative infection. *Clin Infect Dis.*;39:1067–70.
16. Sukontason K, Bunchoo M, Khantawa B, Piangjai S, Sukontason K, Methanitikorn R, Rongsriyam Y (2000). Mechanical carrier of bacterial enteric pathogens by *Chrysomya megacephala* (Diptera: Calliphoridae) in Chiang Mai, Thailand. Southeast *Asian J Trop Med Public Health* 31(Suppl 1):157–161.
17. Sukontason KL, Narongchai P, Sukontason K, Methanitikorn R, Piangjai S (2005). Forensically important fly maggots in a floating corpse: the first case report in Thailand. *J Med Assoc Thai* 88:1458–1461.
18. Vistnes L, Lee R, Ksander A(1981). Proteolytic activity of blowfly larvae secretions in experimental burns. *Surgery.*;90:835–41.
19. Zasloff M. (2002). "Antimicrobial peptides of multicellular organisms", *Nature*, Vol. 415, pp. 389–395.
20. Ziffren SE, Heist HE, May SC, Womack NA(. 1953). The secretion of collagenase by maggots and its implication. *Ann Surg*;138:932–4. [a floating corpse: the first case report in Thailand. *J Med Assoc Thai* 88:1458–1461.
21. Worachote Boonsriwong & Kom Sukontason & Jimmy K. Olson & Roy C. Vogtsberger & Udom Chaithong & Budsabong Kuntalue & Radchadawan Ngern-klun & Surasak Upakut & Kabkaew L. Sukontason (2007). Fine structure of the alimentary canal of the larval blow fly *Chrysomya megacephala* (Diptera: Calliphoridae) *Parasitol Res* 100:561–574.
22. Zumpt F (1965) Myiasis in man and animals in the old world.Butterworths, London Res., 22:149-154.

6/1/2010

Effect of Geometric Configuration of Quadratic Folded Plate Roofing Systems on Their Static and Dynamic Behavior.

[1]H. Elkady and [2]A. Hasan
[1]Civil Engineering Dept., National Research Center, Cairo, [2] Beni-suef University, Egypt.

Abstract: Some researchers proposed different analytical methods for presenting boundary conditions, and stiffeners effect in analytical solutions of folded plate slabs. This study investigates the effect of each of these factors to review the previous approximations range of validity for longer spans Quadratic Folded Plate (Q.F.P) slabs. The chosen elements are: Stiffness of end diaphragms, intermediate beams stiffness, and folded plates rise (height). Besides, the effectiveness of increasing the folded plates' thickness on the structural behavior of the system was investigated as well. Hence, the impact of such variance on the static and dynamic behavior of the system is studied. All previous parameters were applied on systems with three different spans 14, 20 and 26 meters. In order to achieve the previous objectives, 3-D Finite Elements Models (F.E.M) were adopted.to perform linear static analysis on the investigated systems, and the effect of each of the above mentioned parameters on deflections and stresses was studied and analyzed. The studied Q,F,P. rises varied from 90 cm to 180 cm. This doubling of rise reduced the roof deflection by 60% Increasing Q.F.P slab thickness from 8 to 12 cm limited this reduction in deflection to 15%. Stiffness of intermediate beams was another investigated factor, its original stiffness was increased up to six time. Tripling the intermediate beams original stiffness resulted in reducing slabs deflections by 17%. These parameters resulted in a similar trend in reduction of intermediate beams bending moments. As for reduction in end diaphragm bending moments due to changing Q.F.P rise, it reached 40% decrease on increasing the rise from 90 to 180 cm. Three Dimensional dynamic modal analyses were performed as well. The effect of different diaphragms, intermediate beams, and spans on the fundamental modes was investigated. From modal analysis, it was concluded that increasing the span from 14 to 20 meters did not have significant effect on the fundamental frequencies. On the other hand the 26 meters natural frequencies were lower by 27% from both spans. Increasing the roof rise from 90 to 180 cm increased the natural frequencies by 25%, this can be attributed to the increase in the stiffness of the system. Finally, the obtained results confirmed on the diffiecency in design that can result from approximate end conditions, or neglecting stiffners effect in analytical modeling, especially for Q.F.P. slabs with long spans. Consequently, elaborate numerical analysis is recommended in dealing with longer spans Q.F.P systems, as the geometric properties of each contributing element had obvious effect on the overall performance of the system. It is also concluded that folded plate rise is the most effective in the investigated parameters, while difference in folded plate thickness had the lowest effect on both static and dynamic behavior of the investigated system. [Journal of American Science 2010;6(7):318-326]. (ISSN: 1545-1003).

Key Words: Folded plates, height, end diaphragm, stiffness, and free vibrations.

1. Introduction

Folded plates are considered one of the very useful basic systems in engineering. Their applications can be found in various branches of engineering, such as in roofs, sandwich plate cores and cooling towers, etc. They are lightweight, easy to form, economical, and have much higher load carrying capacities than flat plates, which ensures their popularity and has attracted constant research interest since they were introduced. Early researchers solved folded plate problems approximately with the beam method or the theory that neglected relative joint displacement. However, these two methods meet difficulties in dealing with generalized folded plate problems. Computational approaches and numerical methods for folded plates offer more precise solutions. The methods of interest include finite strip methods [1-3], the combined boundary element-transfer matrix method [4], and finite element methods (FEM) [5-8]. From these methods, the FEMs are the most convenient because they can be applied to analyze large complex structures, and all kinds of boundary conditions and loadings can be easily implemented. Hence, almost all commercial software for structural analysis uses FEMs.

Q.F.P roofs is one of the most commonly used types of such roofing systems. Hence, it was chosen for this study. The presented study on the effect of geometric configuration of the systems main structural elements utilizes numerical analysis. Linear Static Three Dimensional F.E. analysis was performed. Effect of each parameter on slab deflection, end diaphragms moments, and intermediate beams maximum moments were reported. Hence, effect of applying real boundary conditions, and stiffeners is evaluated compared to

the accuracy of boundary conditions, and stiffeners approximation proposed in earlier literature [9,10,11].
As for free vibrations of Q.F.P slabs, most of the adopted analytical solutions uncouple the different modes of vibration, as the well known Naghdi shell equations [12,13]. These equations, when applied to plates, lead to a case where the transversal and the in plan deformation appear uncoupled.

Another analytical solution is available by Reissner–Mindlin equations [14], which are modeled by the elasticity equation, and does not depend on the thickness of the plate.

To evaluate the above mentioned approximations, and to estimate the effect of different structural elements including plates thickness, 3-D F.E. free vibration analysis was adopted in this study as well.

2. Finite Elements Analysis

2.1. Geometry and dimensions of investigated systems

All Q.F.P.slabs subjected to the presented studies had constant panels of 7.8 ms width (Fig.1a). Three different spans -14, 20, and 26 m- were investigated. A 3-D F.E. analysis was performed, in which the roof was modeled using 3-D quadratic shell elements (Fig.1b), while intermediate beams, end diaphragms, and columns were modeled as 3-D frame elements. The roof depth –or height- is referred to by the term "rise" throughout this study.

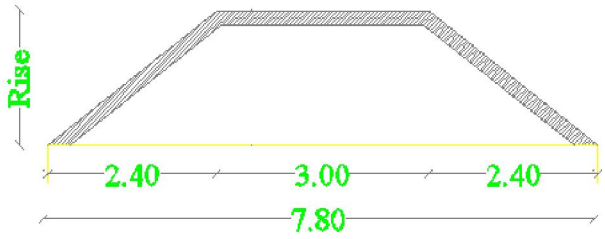

Figure 1a: Cross section dimensions of investigated models

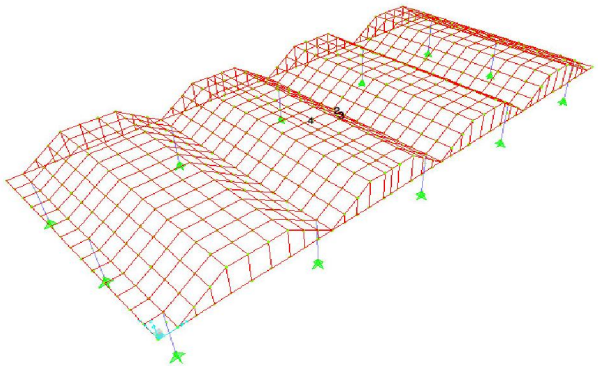

Figure 1b: 3-D model of investigated folded plates panels

2.2.Static Analysis of Q.F.P System

3-D Static linear F.E.analysis was performed. applying each of the parameters under study separately. In addition to the structure own weight, an imposed static load of 150 kg/sq.cm was applied on all models, as a make up for flooring and service. Throughout the analysis, the following straining actions and deformations are monitored and compared: Deflections and stresses at different locations of the folded plate are checked, maximum bending moments at diaphragms, and intermediate beams. The tested parameters effect is given below in details:

2.2.1. Effect of end diaphragm stiffness on .Q.F.P. system

2.2.1.1. End diaphragm stiffness effect on folded slab deflections.

The first investigated parameter was the end diaphragms stiffness, and its role in deflection control of the on Q.F.P. systems for each of the three chosen spans 14,20 and 26 metres. Variation in inertia was achieved by maintaining constant depth (70 cm) and changing diaphragm width from 10 to 150 cm.

Figure.2. displays the maximum deflection for Q.F.P.slabs versus end diaphragms with different widths. The Maximum deflection of the 26 m span slab with minimum diaphragm thickness (10 cm) was 13 mm, this value was reduced to 6mm when diaphragm width increased to 150 cm. This value presents a 54% reduction in slab deflection As for the system with the shortest span (14 meters) deflection values were 1.5 and 1 mm, for the 10 ,and 150 cm width diaphragm systems repsectively, in other words reduction of 33% in slab deflection

In common practice, end diaphragms width usually rangs from 40 to 80 cm, Increasing the end diaphragm width in the 26 meters span system from 40 to 8 cm, reduced Q.F.P. maximum deflection from 10.3 mm to 9 mm (13%). As for the shortest span -14 meters- the reduction in deflection was from1.15 mm to 1.05 mm(9%)

From the same figure it can be observed that the increase in diaphragm width over 80 cm in 14 meters span system did not enhance slab deflection. As for the 20 meters span deflection became constant when a diaphragm of 90 cm width or more is used. The slab deflection in the longest studied span -26 meters- did not reach a constant value, even on reaching an extreme diaphragm width of 1.5 meters.

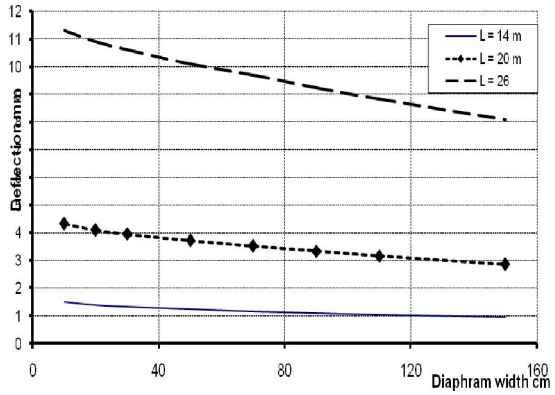

Fig. 2: Q.F.P. slabs maximum deflection versus different diaphragm widths.

2.2.1.2. End diaphragm stiffness effect on induced stresses inQ.F.P.slabs.

Stresses in folded slab roof are analyzed in two main directions: along the slab longitudinal axis, and perpendicular to it. Maximum compressive and tensile stresses were studied in both directions, and displayed in Figure 3.

Fig.3 (a) displays the maximum positive stresses in the Q.F.P. for the three studied spans. It can be observed that the resulting stresses in the 26 meters span are four times those in the 14 meters span slab., while the ratio of the length square –resulting from beam analysis is 3.45 times.

Increasing diaphragm width from 10 to 100 cm reduced the maximum stresses in the Q.F.P.slab of the 26 meters span system from 700 to 520 t/sq.m (25%). As for the compressive stresses (Fig3.b), the maximum variation in stresses sue to difference in end diaphragm stiffness was noticed in the 26 meters span system, as the stresses were reduced from 350 to 255 t/sq. meters (reduction of 28%) on increasing diaphragm width from 10 to 100 cms.

2.2.2.Effect of folded plate rise and intermediate beams stiffness on folded roof deflections.

Four possible rises for Q.F.P. slabs were considered in this study: 0.9, 1.2, 1.5 and, 1.8 meters. The original intermediate beams dimensions used in the study were 0.3*0.7 meters (width*depth respectively), triple (3I) and six times (6I) this stiffness was considered as well. Figure 4 gathers the effect of both: roof rise, and intermediate beams stiffnesses on slab deflection, each will be discussed separately as follows:

2.2.2.1..Effect of roof rise on the deflections of folded plate slabs with different spans.

For longest investigated span (26m) doubling folded plate depth (rise) from 0.9 m to 1.8 metres resulted in reducing deflections from 33mm to 12 mm (which can be interpreted to a reduction of 64% in deflection). This increase in folded plate depth (rise) for the 20 meters span resulted in reduction from 12.5 mm 5 mm (60%). As for the 14 m span slab deflection was reduced from 4.5 mm to 2 mm (56%), on using 1.8 meters depth (rise) instead of 0.9 meters.

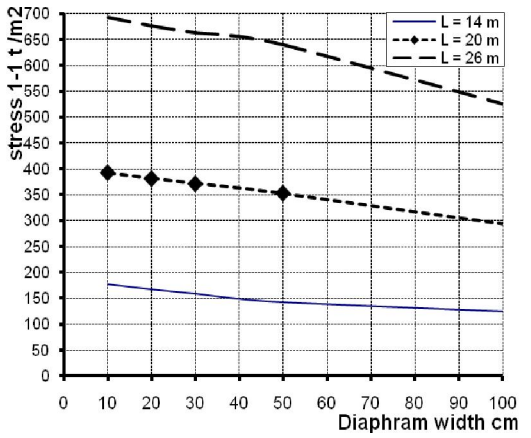

(a)

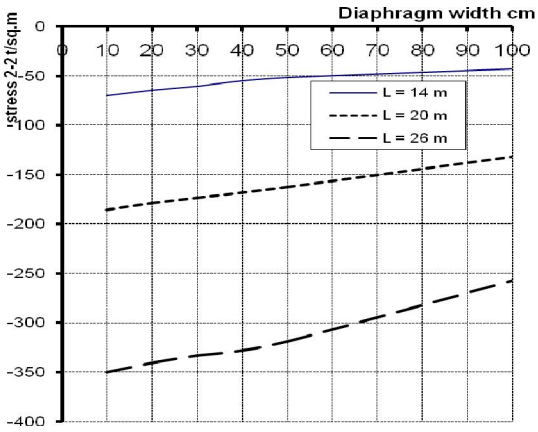

(b)

Fig.3: Folded plate stresses versus different diaphragm width.

2.2.2.2. Effect of intermediate beams stiffness on deflection of Q.F.P. with different spans.

From the above figure it can be seen that tripling the intermediate beam stiffness reduced deflection for Q.F.P 26 m span and 0.9 m rise from 33.4 to 28.5 (reduction of 17%), while tripling it another time reduced the deflection to 24.5 mm, which is the same percentage of reduction (17%) As for the Q.F.P 20 meters span deflection of 0.9 m roof was12.1 for the system with the original intermediate beams, decreased to 10.6 mm on tripling the intermediate beams stiffness (equivalent reduction of 14% in slab deflection), while another tripling of the beams inertia lead to a

maximum deflection of 9 mm (15%) . As for the shortest investigated Q.F.P.(14 meters span-0.9 m rise)) the original slabs deflection .was 4.5 mm, this deflection reduced to 4 , and 3.5 mms for 3 times, the six times the original intermediate beams stiffness respectively (percent of reduction in deflection did not exceed 14%).

2.2.3. Effect of folded plate rise on Q.F.P. intermidiate beams bending moments

The proposed heights for the system (0.9 to 1.8 meters) were applied. The effect of these heights on the intermidiate beams maximum moments is shown in Figure 5.

Increasing folded plate rise from 0.9 to 1.8 m for 26 meters span resulted in the reduction of intermediate beams moment from 16.8 m.ton to 4.6 m.ton (reduction of about 66%). This increase in rise enhanced the reduction in bending moments for 20 meters span from9.8 to 2.9 m.ton (71% reduction).

The highest reduction in intermediate beams moments due to increasing Q.F.P. rise was for the shortest (14 m) span, this reduction reached 73% on doubling the rise (from 0.9 to 1.8m).

From figure 4, the limited effect of changing the slab thickness from 8 to 12 cm on intermediate beams moments can be noticed clearly as well.

2.2.4. Effect of slab thickness, and rise of roof on end diaphragm moments

Figure 6 displays the values of the end diaphragm maximum bending moments versus different roof rises, and slab thicknesses for the three studied spans. Increasing the folded roof rise from 0.9 to 1.8 metres reduced diaphragm moments by 40% for 26 meters spans.39% for 20 metres, and 38.5% for 14m.

It is noticed that slab thickness did not have remarakable effect on diaphragm moments for spans equal to or less than 20 meters, as for 26 meters span its effect did not exceed 15%.

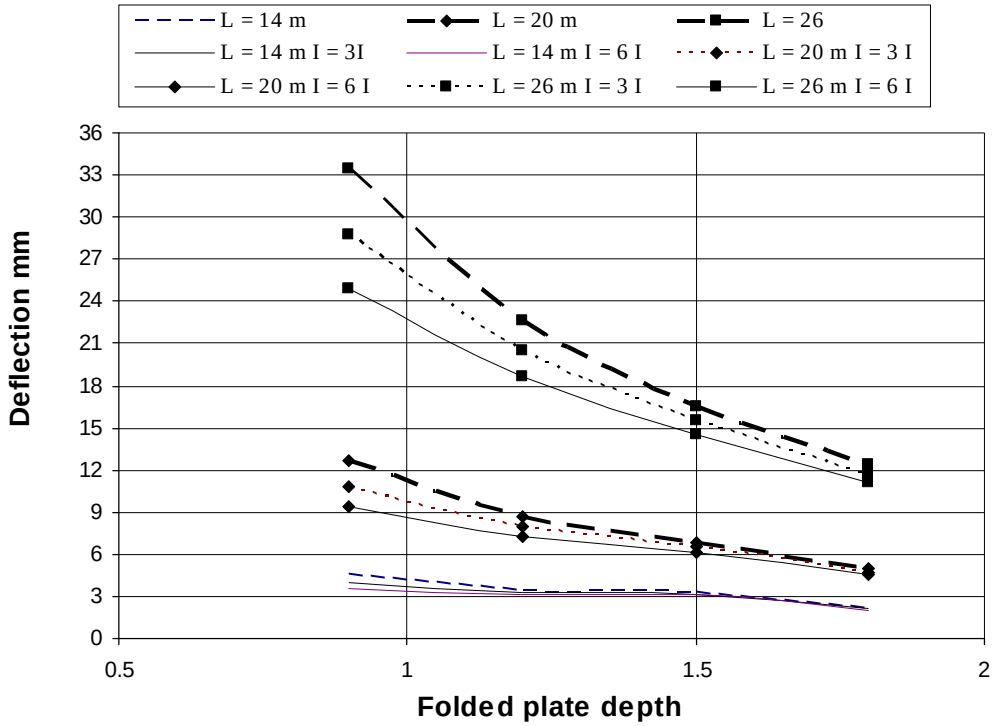

Figure 4: Effect of folded plate rise and intermediate beams stiffness on deflection of Q.F.P roofs with different spans.

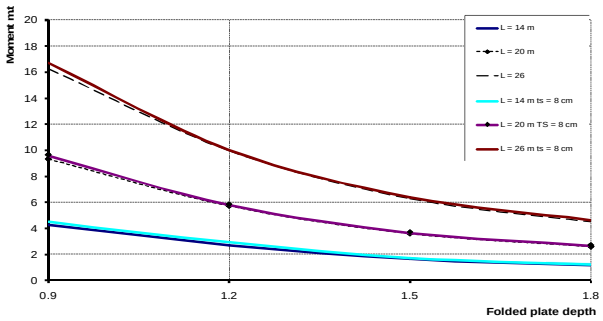

Fig.5: Intermediate beams maximum moments versus folded plate depth.

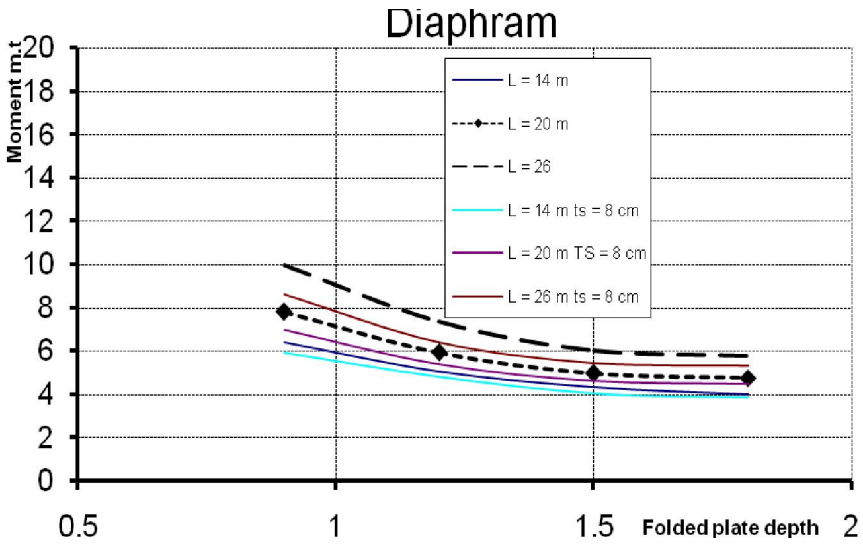

Fig 6: Effect of folded plate rise on the end diaphragms moment

2.3. Free vibrations analysis

Investigated systems were subjected to free vibrations analysis. Eigen values and Eigen vectors are adopted in the linear dynamic analysis. It was noticed - for the investigated spans, with different parameters - that the arrangement of mode shapes was consistent. Columns lateral displacements dominated the first three modes, and then roof deformations controlled the next ones. Figure .7. displays the roof modes, it can be seen that the dominating mode for the Q.F.P. slab is the intermediate symmetric bending mode The second mode was antisymmetric bending, followed by symmetric bending of the external spans. Alternative modes of antisymmetric, and symmetric plate bending follows.

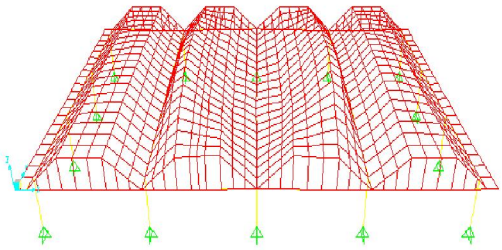

Q.F.P.slab First mode shape

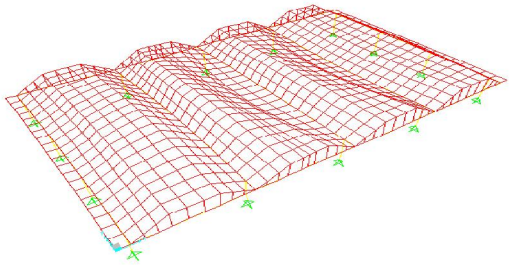

Q.F.P.slab second mode shape

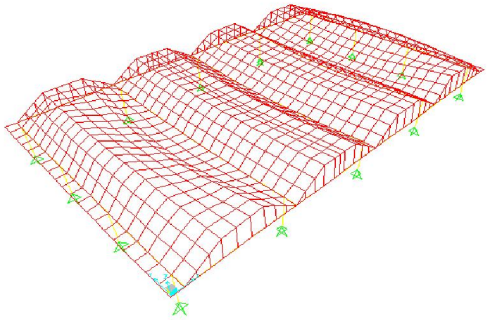

Q.F.P.slab third mode shape

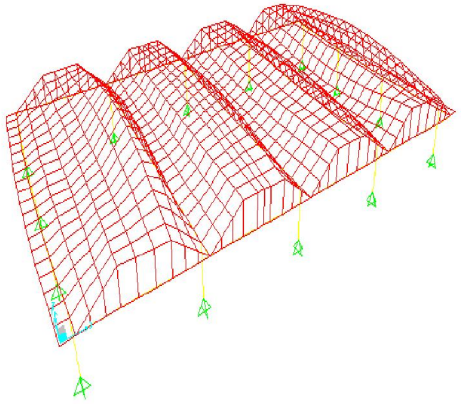

Q.F.P.slab fourth mode shape

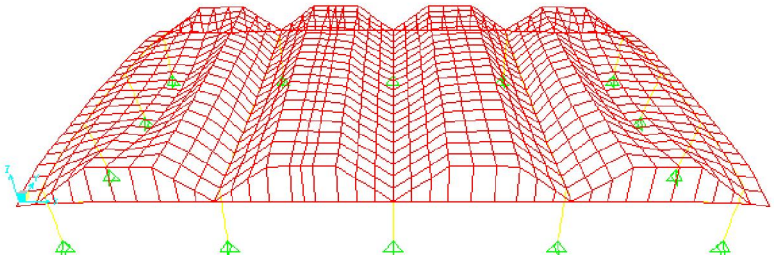

Q.F.P. slab fifth mode shape

Figure 7: Fundamental mode shapes of Q.F.P.slab.

In Figure 8 the fundamental frequencies of the system were given for Q.F.P. slabs with spans 14, 20 and 26 meters It is noticed that the frequencies of the first three modes were almost identical for all spans, these modes were the columns lateral displacements fundamental modes. Fundamental modes for the folded plate roof started from the fourth mode The frequency of three fundamental modes for the roof for 14 and 20 meters span were very close, while the Q.F.P. 26 meters span frequencies were 27% lower than them..

The effect of roof rise on the fundamental frequencies of the 20 meter span Q.F.P. system is shown on Figure 9. Two rises were investigated: 0.9, and 180 cm. It is observed that the system with higher rise (180 cm) has higher fundamental frequencies by 20%, which can be attributed to the higher stiffness of the system.

From Figure 10 the effect of using a slab of thickness 12 cm versus 8 cm on the fundamental mode frequencies is shown. It can be observed that the difference in fundamental frequencies due to change in slab thickness is variable, and reaches 16%. in some modes.

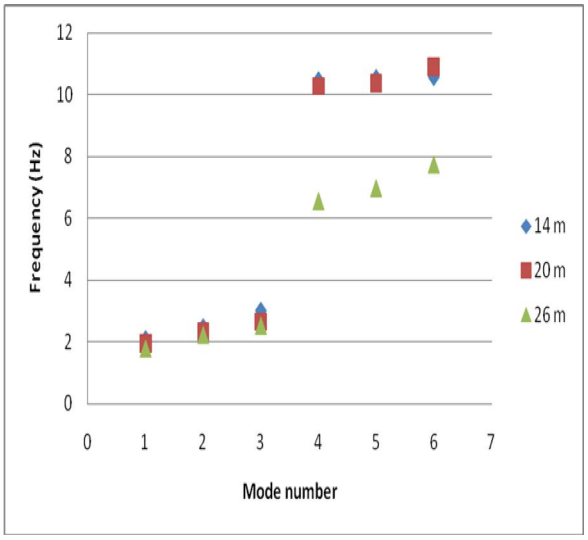

Fig. 8: Fundamental modes frequencies for folded plate roofs with different spans.

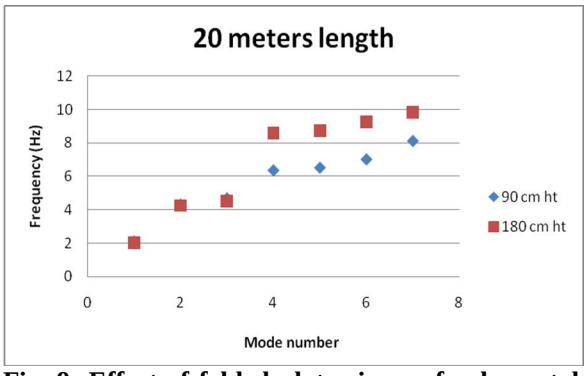

Fig. 9: Effect of folded plate rise on fundamental frequencies of 20 m span system.

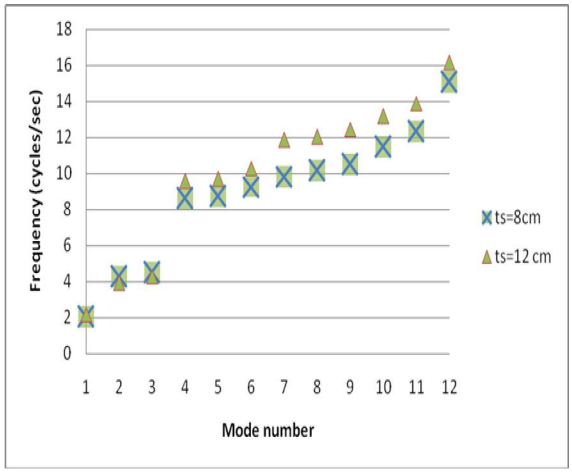

Fig.10: Fundamental modes of 20 meters span Q.F.P with different slab thicknesses.

3. Discussion of Results

For the longest Q.F.P system in the study (26 m span), increasing diaphragm stiffness by 15 times the original stiffness reduces Q.F.P. static deflections by 54%, while doubling the slab rise from 90 cm to 180 cm reduced this deflection by 64%.

Increasing end diaphragm stiffness had higher effect on static deflection control, than slab stresses, as increasing its stiffness by 10 times (increasing width from 10 to 100 cm) - in the longest system -reduced deflection by 38.5%, and corresponding reduction in maximum stresses in Q.F.P slab was 25%.

Increasing intermediate beams stiffness up to 6 times reduced the maximum deflection by a maximum of 17% for the longest investigated 26 meters span

The increase in rise was more significant in shorter spans. Maximum deflection in 14 meters span was less by 8% than 26 m span roof.

Mode shapes patterns arrangement was not affected by variation in spans from 14 to 26 meters. In other words, mode shapes came in the same order for all investigated spans.

Slab thickness in Q.F.P. systems has a variable effect on the free vibration analysis of the slabs. A difference reaching 16% in fundamental frequencies of the system was noticed on changing the slab thickness from 8 to 12 cm.

Doubling the roof rise (from 0.9 to 1.8 meters) increased the fundamental frequency of the Q.F.P. slab by 20%.

Spans between 14 to 20 meters had very close slabs fundamental frequencies. On the other hand difference widens significantly on reaching 26 meters spans.

4. Conclusion

Approximate static solutions that propose fixed boundary conditions at the end diaphragms for the Q.F.P slab ends [9,10,11] are not reliable for longer spans – especially for spans 20 meters or more. Thus, numerical modeling that takes into consideration their stiffness is recommended.

Previous literature neglected slab thickness in proposed analytical dynamic linear free vibrations solutions [14]. This study highlighted the possible loss in accuracy that reached 16% in some of the modes –of the investigated Q.F.P system- when the slab thickness varied from 12 to 8 cms.

Increasing folded plate rise was the most efficient factor among the investigated

parameters in the static analysis for deflection control.

On the other hand increasing the roof rise lead to an increase in the fundamental frequencies of the system.

Rise effect was most effective in shorter spans. Increasing folded plate rise enhanced the structural behavior of the overall Q.F.P. system than increasing intermediate beams stiffness.

Increasing stiffness of intermediate beams has limited effect on roofs with higher rises, and shorter spans.

Increasing folded plate thickness has limited effect on the change in static deflections, or straining actions of the system.

The static behavior of the system was slightly sensitive to increase in end diaphragm stiffness, especially in shorter spans.

Spans from 14 to 20 meters for the investigated Q.F.P. slabs had very close fundamental frequencies, this effect widens noticeably on analyzing longer spans.

Corresponding author
[1]H. Elkady
[1]Civil Engineering Dept., National Research Center, Cairo, Egypt

5. References

1. Cheung YK.,"Folded plate structures by finite strip method.", Jr of Struct Div ASCE 1969;95:2963–79.
2. Golley BW, Grice WA.,"Prismatic folded plate analysis using finite strip-element.", Comput Methods Appl Mech Eng 1989;76:101–18.
3. Eterovic AL, Godoy LA.," An exact-strip method for folded plate structures.", Comput Struct 1989;32(2):263–76.
4. Ohga M, Shigematsu T, Kohigashi S., "Analysis of folded plate structures by a combined boundary element-transfer matrix method", Jr. of Comput Struct 1991;41(4):739–44.
5. Liu WH, Huang CC.," Vibration analysis of folded plates.", Jr. of Sound Vibr 1992;157(1):123–37.
6. Perry B, Bar-Yoseph P, Rosenhouse G., " Rectangular hybrid shell element for analyzing folded plate structures.", Comput Struct 1992;44(1–2):177–85.
7. Duan M, Miyamoto Y. , "Effective hybrid/mixed finite elements for folded-plate structures.", J Eng Mech 2002;128(2):202–8.
8. Guha Niyogi A, Laha MK, Sinha PK., Finite element vibration analysis of laminated composite folded plate structures", . Jr. of Shock Vibr 1999;6:273–83.
9. Bar-Yoseph P, Hersckovitz I., "Analysis of folded plate structures.", Jr. of Thin-Walled Struct 1989;7:139–58.
10. Bandyopadhyay JN, Laad PK.,"Comparative analysis of folded plate structures.", Jr. of Comput Struct 1990;36(2):291–6.
11. Peng L.X, Kitipornchai S., Liew K.M. ,"Bending analysis of folded plates by the FSDT meshless method", Journal of thin walled str. 44, 2006, p 1138-1160.
12. Belytschko T, Lu YY, Gu L. ,"Element-free Galerkin methods", . Int J Numer Methods Eng 1994;37:229–56.
13. Liew KM, Ng TY, Wu YC.," Meshfree method for large deformation analysis—a reproducing kernel particle approach.", Eng Struct 2002;24(5):543–51.
14. Bernadou .M, "Finite Element Methods for Thin Shell Problems", J. Wiley & Sons, 1996.
15. Chapelle B, K.J. Bathe, " Fundamental considerations for the finite element analysis of shell structures", Comput. Struc. 66 (1998) 19–36.
16. Liew KM, Wu YC, Zou GP, Ng TY., "Elasto-plasticity revisited: Numerical analysis via reproducing kernel particle method and parametric quadratic programming", Int J Numer Methods Eng 2002;55(6):669–83.
17. Liew KM, Huang YQ, Reddy JN. "Moving least square differential quadrature method and its application to the analysis of shear deformable plates.", Int J Numer Methods Eng 2003;56(15):2331–51.
18. Liew KM, Zou GP, Rajendran S., " A spline strip kernel particle method and its application to two-dimensional elasticity problems.", Int J Numer Methods Eng 2003;57(5):599–616.
19. Liew KM, Chen XL., " Buckling of rectangular Mindlin plates subjected to partial in-plane edge loads using the radial point interpolation method", . Int J Solids Struct 2004;41(5–6):1677–95.
20. Liew KM, Cheng Y, Kitipornchai S., " Boundary element-free method (BEFM) for two-dimensional elastodynamic analysis using Laplace transform.", Int J Numer Methods Eng 2005;64(12):1610–27.
21. Liew KM, Ren J, Reddy JN., "Numerical simulation of the thermomechanical behaviour of shape memory alloys.", Int J Numer Methods Eng 2005;63(7):1014–40.
22. Liew KM, Cheng Y, Kitipornchai S.,

"Boundary element-free method (BEFM) and its application to two-dimensional elasticity problems.", Int J Numer Methods Eng 2006;65(8):1310–32.
23. Chen JS, Pan C, Wu CT, Liu WK., "Reproducing kernel particle methods for large deformation analysis of nonlinear structures.", Comput Methods Appl Mech Eng 1996;139:195–227.
24. Liew KM, Wang J, Tan MJ, Rajendran S. , "Postbuckling analysis of laminated composite plates using the mesh-free KP–Ritz method ", . Comput Methods Appl Mech Eng 2006;195(7–8):551–70.
25. Ren J, Liew KM. , "Mesh-free method revisited: two new approaches for the treatment of essential boundary conditions. ", Int J Comput Eng Sci 2002;3(2):219–33.
26. Wang J, Liew KM, Tan MJ, Rajendran S., " Analysis of rectangular laminated composite plates via FSDT meshless method.", Int J Mech Sci 2002;44:1275–93.
27. Liew KM, Lim HK, Tan MJ, He XQ. , "Analysis of laminated composite beams and plates with piezoelectric patches using the element-free Galerkin method.", Comput Mech 2002;29(6):486–97.

6/2/2010

Adsorption of $^{(152+154)}$Eu from Radioactive Waste Solution Using Modified Clay Polymer

M. Abdel Geleel[1], M.S. Sayed[2], and H.A. Omar[3]
[1]National Center for Nuclear Safety and Radiation Control, Cairo, [2]Radiation Protection Department, Hot Laboratory Center, [3]Radiation Protection Department, Nuclear Research Center, Atomic Energy Authority, Egypt
Magdass7@hotmail.com

Abstract: Removal of $^{(152+154)}$ Eu from it's liquid radioactive wastes using Aswan clay (C), Aswan clay/Polyacrylonitrile (C/P) and Polyacrylonitrile (PAN) was investigated. Factors affecting the polymer preparation as weight/ratio of clay to polymer, initiator percent (benzoyl peroxide) and temperature were tested. Characterization of the prepared matrices as surface area, swelling properties, FTIR and thermal properties were studied. The effect of pH, contact time, grain size, weight of the sorbent material and concentration of the initial adsorbent on the uptake percent of $^{(152+154)}$Eu from liquid radioactive waste were studied. The data followed the pseudo-first-order kinetic model. The equilibrium sorption data were described by the Langmiur and Freundlich isotherm models. The highest value of Langmiur maximum uptake Q_{max} was found to be 188.68, 155.58 and 70.92 $mg.g^{-1}$ for C, C/P and PAN respectively. The capacity of C/P to adsorb $^{152+154}$Eu was also determined by column technique and found to be 50.66 mg/g. [Journal of American Science 2010;6(7):327-333]. (ISSN: 1545-1003).

Key words: Radioactive wastes/ $^{(152+15)4}$Eu/ Clay/ Polyacrylonitrile/ Adsorption

1. Introduction

Removal of long lived radionuclide from nuclear waste effluent is an important environmental concern in nuclear waste management. Environmental radioactive contamination can be caused by the accidental emissions from any stage of nuclear fuel cycle or fallout from nuclear testing[(1)]. The sorption studies of radio contaminant on various materials were of great importance to evaluate the feasibility of using a particular material for waste treatment and disposal practices[(2,3)]. $^{(152+154)}$Eu is an important nuclear fission products present in the radioactive waste effluents resulting from the reprocessing of the nuclear fuels. It was chosen due to its biotoxicity, long half–life, higher solubility in aqueous systems and the possible recovery from the waste solution[(4)]. In principle, any solid material with a microporous structure can be used as an adsorbent e.g. clays, metal oxides or ash[(5-7)]. Surface area, structure and low cost are some properties necessary to select the adsorbent matrix[(8-10)]. Aswan clay C is available as a large deposits around the Egyptian deserts, this pale brown sedimentary clay consists principally of silica and alumina[(11)]. The most common preparation methods for reactive polymers have included chemical conversion of the existing reactive groups as in the acrylonitrile by coplymerization and grafting [(12, 13)].

In this work, Aswan clay mixed with polyacrylonitrile is prepared and characterized by FTIR and TGA. The adsorption properties, including effects of pH, time and initial ion concentration on uptake of $^{(152+154)}$Eu were investigated. Batch and column techniques were used as application of the desired matrix to adsorb radioerupium.

2. Materials and Methods

Chemicals and reagents

All reagent used in this work of AR grade chemicals and were used without further purification. Europium was supplied as europium (lll) nitrate from Sigma Aldrich Company, USA. The $^{(152+154)}$Eu was prepared by irradiating europium nitrate in the Second Egyptian Research Reactor, E & R2 at Inshas site. Aswan clay was obtained from natural deposits at upper Egypt. The chemical composition of clay was recommended from Project of Arab Ceramic Company and give the following constituents SiO_2 55%, Al_2O_3 25.8%, Fe_2O_3 2.4% and CaO 1.28%.

Clay / Polymer matrix preparation

Different percents of Aswan clay C as (100, 90, 80,70and 60 %) were added to different percents of PAN as (0, 10, 20, 30 and 40 %) respectively. The best mixtures were chosen at constant weight (0.02 wt %) of benzoyl peroxide as initiator and at 55^{o}C as constant preparation temperature to perform complete polymerization.

Characterization of the matrices

The specific surface areas of the studied matrices were determined using Nova SA instrument 3200. Swelling measurements were done by calculating the water uptake of a known weight of the prepared matrices. It was measured by immersing the samples in distilled water for at least two days. After wiping

with a cleaning tissue, the samples were weighted as quickly as possible. This procedure was repeated three times until satisfactory reproducibility was achieved. The water uptake onto dry samples was calculated according to:

Water uptake (%) = $[(W_w - W_o)/ W_o] \times 100$

Where: W_o, W_w are the weights of the dry and wet prepared samples, respectively.

A Fourier transform infrared (FTIR) spectrometer from Perkin Elmer 1600 was used to analyze the matrices in the wave number range 600 – 4000 cm^{-1}. Differential thermal analysis DTA and thermogravimetric analysis TGA were carried out by using TA 50 Shimadzu, Japan . Temperature was cycled at a constant rate of 10 ^oC/min from ambient temperature to 800 ^oC under nitrogen atmosphere.

Sorption kinetic measurements

Batch experiments with 315-500 µm were used to investigate parametric effects of the initial metal on the sorption process. Radio-europium samples were prepared by dissolving a known quantity of labeled Eu as stock solution. The kinetic behavior of Eu^{3+} on different matrices (C,C/P and PAN) were done by shaking the desired weight with 20 ml of 10^{-4}M of labeled europium (as LLW) in a polyethelyene vessels at speed 500 rpm in a thermoststic shaker for one hour at room temperature 25 ± 1^oC . Then a fixed value (2 ml) of the aliquot was pipetted out for determination of the amount of unsorbed radioeuropium. The activity of $^{(152+154)}Eu$ was determined radiometrically using NaI (Tl) scintillation detector. Sorption percentage (E %) of radioions removed from LLW were calculated from:

$$U\ \% = (A_i - A_e)/A_e \times 100$$

Where Ai and A_e are the activity of $^{(152+154)}Eu$ in solution initially and after equilibrium respectively.

The fixed bed column experiment was performed using a glass column of 1 cm diameter and 10cm long. 3gm of C/P matrix was transferred into the column with the aid of distilled water and adjusted at pH 7. The radioactive waste solution was then passed through the column with rate 1 ml/min. The effluent was collected in fractions (50 ml) for radioactive analysis.

3. Results and Discussion

Characterization of the studied matrices

The measured surface area of C, C/P and PAN were 281.59, 263.92 and 215.68 m^2g^{-1} respectively. Fig. (1) shows the swelling degree as a function of time and reach a certain limit after 60 min.. The maximum swelling degree reached by clay due to the presence of humic acid[14].

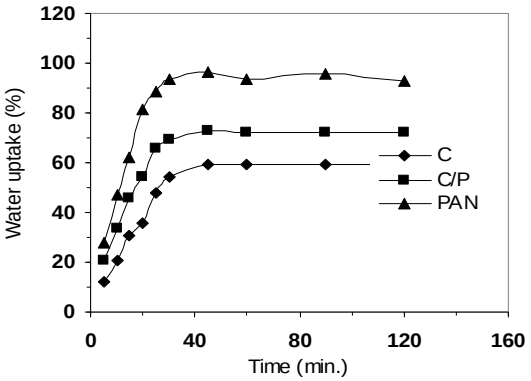

Fig.(1) Swelling behaviour of Aswan Clay (C), Aswan Clay/Polyacrylonitryle(C/p) and Polyacrylonitryl (PAN)

Understanding the mechanism of Eu^{+3} uptakes by C, PAN and C/P, infrared technique was used to evaluate the mechanism involved. Fig.(2) shows the IR spectra of the studied matrices, the main adsorption bands of C occurs at 3650, 1700 and 960 cm^{-1} due to the – OH stretching of the bonded OH groups of water molecule with intermolecular hydrogen bond[15]. Vibration bands at 1100, 900 and 650 cm^{-1} due to SiO_2 and Al_2O_3 presents as a main constituent of clay. The main adsorption bands pf PAN cleared at 2900, 1600, 1500 and 800 cm^{-1} due to C=C, C=N, N-O and amine oxide respectively [16]. IR spectrum of C/P shows more functional groups added to clay capable for forming more adsorption bonds.

Fig.(3) shows the DTA thermograms of the studied matrices. It was observed that a very small endothermic peak at 75-80 ^oC for C and C/P due to the dehydration process occurred by the libration of water molecules present in the samples [17]. On continues heating up to 400 ^oC an exothermic peak was observed for PAN and C/P samples due to gasification and decomposition of the polymer[18]. Table (1) shows the thermogravimetric analysis of the studied matrices at different temperature intervals. It was observed that continues weight loss for PAN and C/P with heating while C was approximately thermally stable up to 350^oC. From 350 – 550 ^oC a remarkable weight loss was observed for both PAN and C/P due to their thermal degradation[19].

Table (1) Thermogravimetric analysis of C, PAN and C/P

sample / ^oC	C	PAN	C/P
Ambint-350	0.4	8	3
350 – 550	1	75	30
550 – 800	8	100	40

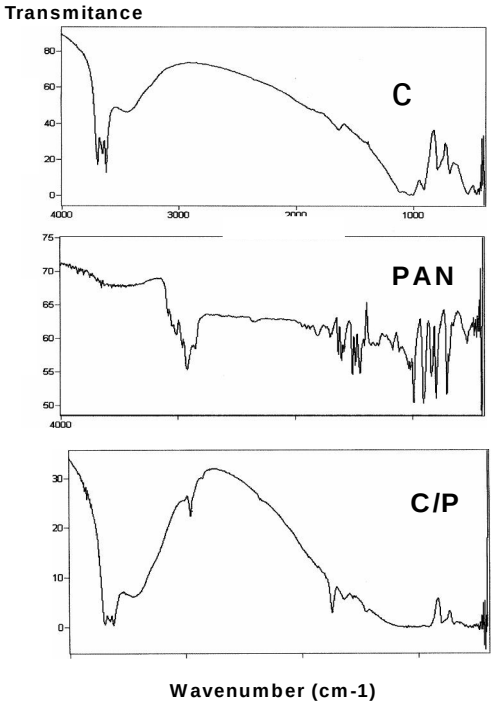

Fig. (2): IR spectra of C, PAN and C/P

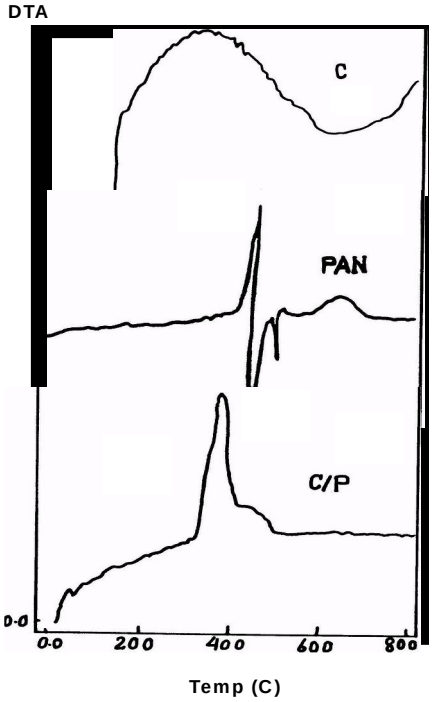

Fig.(3): DTA thermograms of C, PAN and C/P

Adsorption capacity of the studied matrices

Effect of pH

In Fig.(4), the uptake percent of Eu^{3+} by the studied matrices versus initial solution pH has been plotted. As can be seen europium ion uptake increases with increasing solution initial pH. At acidic initial pH <2, the uptake of Eu^{3+} ion was inhibited. This may be attributed to the increase of hydrogen ion concentration at this low pH which make repelling of Eu^{3+} ions from the surface of the adsorbrd matrices. At alkaline initial pH > 7, the uptake of Eu^{3+} ion was decreased due to starting of precipitation of Eu^{3+}. The highest uptake percent was observed at pH 7 [20].

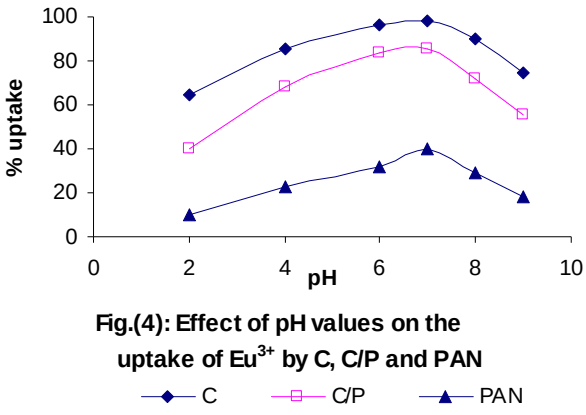

Fig.(4): Effect of pH values on the uptake of Eu^{3+} by C, C/P and PAN

Effect of contact time:

For an initial metal concentration around 1x 10^{-4} $molL^{-1}$, the results revealed that the uptake percent of Eu^{3+} ion at initial pH 7 by the studied matrices as a function of contact time seems to occur in two steps, Fig.(5). The first step increases rapidly within the first 30 minutes of contact, produce (90, 65 and 35%) adsorption for (C, C/P and PAN) respectively. The second

step, produce the uptake of Eu^{3+} ion to about (95, 85 and 40 %) for (C, C/P and PAN) respectively, and attained equilibrium by the end of contact time period of 120 minutes. The rapid uptake of Eu^{3+} ions by either (C, C/P and PAN) may be due to adsorption or exchange of ions with some ions on the surfaces of the matrices[21]. It should be noted that the diffusion of metal ions onto the clay lattice or polymer surface is a time dependant. Therefore, pseudo equilibrium is attained when the contact time is lengthened. Various models such as first–order, pseudo–first–order and pseudo–second order have been used to describe the kinetics of adsorption [22]. The pseudo-first-order rate equation is the most widely used for the adsorption of a solute from a liquid solution. The rate constant of Eu^{3+} adsorption on (C, C/P and PAN) were determined using the pseudo-first-order rate equation (Lagergren rate equation) shown below:

$$\text{Log}\,(q_e - q_t) = \log q_e - \frac{K_{ad}}{2.303}\, t$$

Where K_{ad} is the Lagergren rate constant and q_e and q_t are the amount of $Eu3^{+}$ ion sorbed (mg/g) at equilibrium and at time t, respectively. The straight line plot of Log (q_e - q_t) versus t for different matrices cleared in Fig. (6) indicate the applicability of the above equation to Eu^{3+} ion uptake on the studied matrices. The values of K_{ad} for uptake of Eu^{3+} ion on C and C/P were 0.068 min^{-1} and 0.0407 min^{-1} respectively.

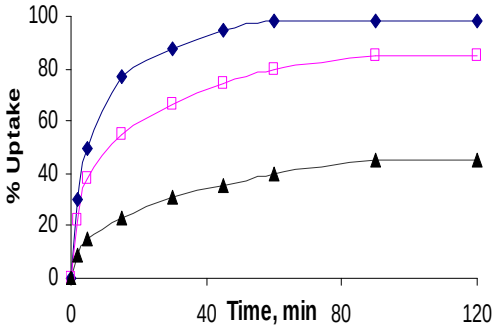

Fig. (5): Effect of shaking time on the uptake of Eu^{3+} by C, C/P and PAN

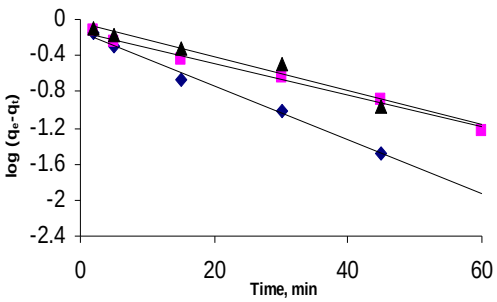

Fig. (6): Lagergren plot for uptake of Eu^{3+} on C, C/p, PAN

Effect of Sorbent Weight

The uptake of $^{(152+154)}$Eu using (C, C/P and PAN) as a function of sorbent weight is shown in Fig. (7). Sorbent weight was varied from 0.02 gm to 0.2 gm. It is clear that, with increase of the sorbent weight the Eu^{3+} sorption percent increases and reached a constant optimum value in all cases (C, C/P and PAN). This increase is possibly due to the ease of exchange of the Eu^{3+} ion with the easily removed ions on the surface of the sorbent matrix.

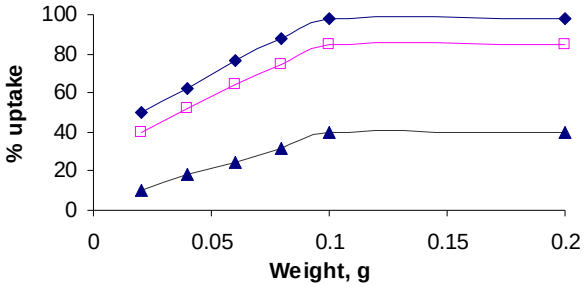

Fig. (7): Effect of dosage on the uptake of Eu^{3+} by C,C /P and PAN

Effect of Particle Sizes

The particle size effect was examined for two different particle sizes; >500 µm and 315-500 µm. Table (2) shows that both particle sizes can be compared with the uptake percent (98, 85 and 45 %) for (C,C/P and PAN) respectively at size 315-500 µm, while uptake percents was (92, 77

and 38 %) for the same matrices at size > 500 µm. So, it's cleared that Eu^{3+} uptake by the studied matrices particle sizes dependant. The smaller particle size matrix have more outer surface for contacting with the Eu^{3+} solution. Therefore, the size 315-500 µm was selected for all further studying

Table (2) Effect of particle size on Eu^{3+} uptake percent by C, C/P and PAN

Particle size	Uptake % C	C/P	PAN
315-500 µm	98	85	45
>500 µm	92	77	38

Effect of initial ion concentrations

The uptake of $^{(152+154)}Eu$ using the studied matrices as a function of different concentrations was investigated from $1x10^{-4}$ M to $2x10^{-2}$ M. The maximum uptake of Eu^{3+} about (95, 85 and 45 %) for (C, C/P and PAN) respectively. The Langmuir isotherm has been applied to many adsorption systems including organic[23] and inorganic[24] adsorbates. The batch equilibrium isotherm is fitted by both the Langmuir and Freundlich equations in the form:

$$C_s/q_e = 1/K_LQ_o + C_s/Q_o \quad \text{Langmuir}$$

$$\text{Log } q_e = \text{Log } K + 1/n \text{ Log } C_s \quad \text{Freundlich}$$

Where, Q_o (mg/g) is defined as the monolayer adsorbent capacity and K_L is Langmuir constant. C_s is the equilibrium concentration of europium ion in solution (mg/l). K and 1/n in Freundlich equation are constants related to the strength of adsorptive bond and heterogeneity factor respectively. Langmuir isotherm was found to fit only the concentration range of $1x10^{-4}$ to $1x10^{-2}$M of Eu^3. Fig. 8 shows the straight lines obtained for, C, C/P and C/PAN, when C_s/q_e is plotted versus C_s. The values of the constant K_L and Q_o are evaluated from the intercept and slope is represented in Table (3).

Fig. 9 shows the straight lines obtained, for C, C/P and C/PAN, when log q_e is plotted versus log C_s according to Freundlich equation. The values of the constants k and 1/n are evaluated from the intercept and slope and represented in Table (3). The value of 1/n lies between 0 and 1, the more heterogeneous the surface the closer value is to 0. The Freundlich equation was found to fit the data in the whole range of Eu^{3+} concentration[25].

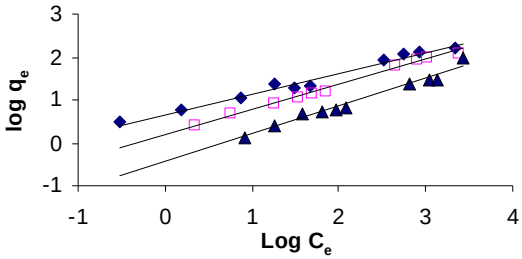

Fig. (8): Freundlich plot of Eu^{3+} sorption by C, C/P, PAN

◆ C □ C/P ▲ PAN

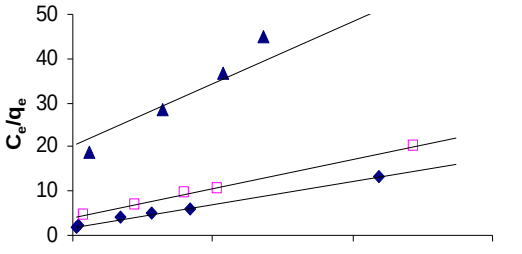

Fig.(9): Langmuir plot of Eu^{3+} by C, C/P, PAN

◆ C □ C/P ▲ PAN

Table (3):Langmuir and Freundlich isotherm parameters of Eu^{3+} ion sorbed onto C, C/P and C/PAN

Sample	Langmuir			Freundlich		
	Q_o(mg/g)	K_L(mg/L)	r^2	K	1/n	r^2
C	188.68	0.003	0.997	4.62	0.48	0.982
C/P	153.85	0.001	0.999	1.58	0.58	0.992
C/PAN	70.92	0.007	0.938	0.36	0.65	0.977

Column Studies

Fig.(10) shows that 3gm of C/P matrix was used into the column, effluent and influent samples are collected after a regular interval. All the sorption experiments were carried out at the room temperature of 25 ±2 ◦C and initial pH of 7.0. The residual activity of $^{(152+154)}$Eu was determined radiometrically using NaI (Tl) scintillation detector. As the adsorbate solution passes through column, the adsorption zone (where the bulk of adsorption takes place) starts moving out of the column and the effluent activity start rising with time. This is termed as break point.
The volume taken for the effluent activity to reach a specific breakthrough of interest is called the break though volume. The effluent activity (C) of $^{(152+154)}$Eu reached 50% of the feed solution (C_o). Breakthrough curve were plotted-giving ratio of effluent and feed (influent) activity (C/C_o) and volume, ml, for varying operating conditions.

Breakthrough capacity Q0.5 (at 50% or C/C_o = 0.5)

The maximum capacity under the condition of the experiment is calculated as 50.66 mg.g^{-1} [26]. The column was regenerated using 1M HCl and sorption-desorption studies were carried out for five cycles.

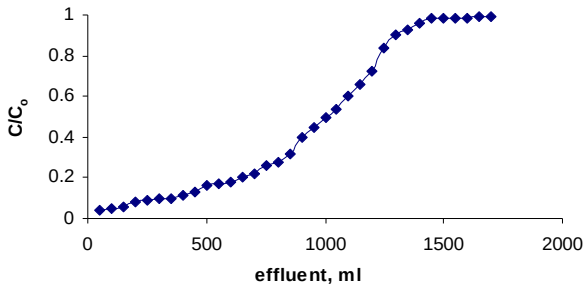

Fig. (10): Breakthrugh curve for Eu^{3+} on C/P

4. Conclusion

It could be generally concluded that the optimum condition of the preparation of clay/polymer ratio was C/P as 80:20, at weight percent of initiator was 0.02 and at temperature 55°C. The uptake percent of Eu^{3+} was 95, 85, 40 for C, C/P and PAN respectively, at pH 7, 120 min and 315-500 µm grain size. The rate constant of Eu^{3+} adsorption on C,C/P and PAN were determined using the pseudo-first-order rate equation (Lagergren rate equation). The Langmiur model is applicable in cases where only one molecular layer of adsorbate is formed at the adsorbent surface. Monolayer adsorption is distinguished by the fact that the amount adsorbed reaches a maximum value at a moderate concentration from 10^{-4} to 10^{-2}, this corresponds to complete coverage of the adsorbent surface by a monolayer of adsorbate. The simple Freundlich isotherm was able to describe the adsorption over all the concentration range used from $1x10^{-4}$ to $2x10^{-2}$ M. In Column tests, $^{(152+154)}$Eu removal by C/P reached about 100% and almost completely recovered with three to four times. Thus C/P matrix can be used to remove $^{(152+154)}$Eu as a heavy radioactive ion from aqueous wastes. Also coating the clay with PAN, avoiding the gel and swelling formation of the Aswan clay used.

5. References

1. M.V. Balarama Krishna, S.V.Rao, J. Arunachalam and M.S. Murali; Separation and Purification. Technology; 38, 149 (2004).
2. N.Fiol, I.Villaescusa and M.Martinez ; J. Separation and Purification Technology; 50, 132 (2006).
3. P.Pathak and G.Choppin; J. Radioanalytical and Nuclear Chemistry; (2), 270 (2001).
4. (4) W.Xiangke, D. Wenming and G.Yingchum; J. Radioanalytical and Nuclear Chemistry; (2), 250 (2001).
5. T.S.Anirudhan and M.Ramachandran; J Colloid and Interface Science, 299, 116 (2006).
6. M.A.M. Khraisheh, Y.S.Al-degs and W.A. M.Macminn; J. Chemical Engineering; 99, 177 (2004).
7. K.Shakir, K. Benyamin and M.Aziz; J. Radioanalytical and Nuclear Chemistry; Articles, 173 (1), 141 (1993).
8. S.Lowell and J.E.Shields; Powder Surface Area and Porosity; 2nd ed.; Chapman & Hall;New York (1984).
9. T.Kwolak, M.Hodorowiez and K.Stadnicko; J. Clays and Clay Minerals; 45,843 (1997).
10. P.S.Nayak and B.K.Singh; J. Desolivation; 207, 71 (2007).
11. S.Y.Lee and S.J.Kim; J.Clay and Clay Mineral; 38, 225 (2003).
12. A.Lezzi and S. Cobianco; J. Applied Polymer Science; 54, 889 (1994).
13. E.A.hegazy, H.Kamal, N.A.Kalifa and G.A.Mahmoud; J. Applied Polymer Science; 81, 849 (2001).
14. S.A.kyil, M.A.A.Aslani and M.Eral; J. Radioanalytical and Nuclear Chemistry;
15. 265(1), (2003).
16. B.Colthup, H.Daly and E.Wibereley; Academic Press, NewYork, (1990).
17. R.N.Nyquist and R.O.Kagel; Academic Press; New York; (1997).

18. F.Stengele and W.s.Kloss; J. of Thermal Analysis and Calorimetry; 51, 219 (1998).P.Dunn and B.C.Ennis; J. of Applied Polymer Science, 14 (7), 1795 (2003).
19. S.Yang, J.R.Castilleja, E.V.Sarrera and K.Lozano; J. Polymer Degradation and Stability; 23(3), 383 (2004).
20. R.Coşkun, C.Soykan and M.Saçak; J. Separation and Purification Technology; 94, 107 (2006).
21. A.A.El-Zahhar, H.M.Abdel-Aziz and T.Siyam; J. Radioanalytical and Nuclear Chemistry; 267 (3), 657 (2006).
22. S.Lagergren, B.K.Sevenska Handl; Water Research; 32 (3), 62 (1998).
23. H.A.Ferro-Garcia, J.Rivera-Utrille, I.Bautista-Toledo and C Moreno-Castille; Langmuir, 14, 1880 (1998).
24. V.P.Vinod and T.S.Anirudhan; J. Chem. Technol. Biotechnol, 77, 92 (2001).
25. S. Çay, A. Uyanik and A.Özasik; Separation and Purification Technology, 38, 273 (2004).
26. F. Šebesta; J. Radioanalytical and Nuclear Chemistry; 220(1), 77 (1997).

6/5/2010

Immobilization of Liquid Radioactive Wastes by Hardened Blended Cement - White Sand Pastes

M.S. Sayed[1] and Magdy M. Khattab[2*]

[1] Department of Safety and Radiation Protection, Hot Laboratory Center, Atomic Energy Authority,
[2]Department of Radiation Chemistry, National Center of Radiation Research, Atomic Energy Authority, Cairo, Egypt
Magdass7@hotmail.com

Abstract: A study was undertaken to determine the immobilization performance of blended cement pastes contains different ratios of white sand (WS) loaded with cesium and cobalt radioactive ions. The effect of different ratios of white sand namely 5%, 10% and 20% on the physico-mechanical of the prepared blended cement pastes was also studied. Particle size distribution, X-ray diffraction, thermal stability, and FT-IR analysis of the neat hardened blended cement (OPC) paste and with white sand as additive have been carried out. A pronounced increase of the compressive strength values were observed for the hardened blended cement pastes with different white sand ratios at different hydration time intervals 3, 7, 14, 28 and 90 days comparing to the hardened neat Portland cement (OPC) pastes. The cumulative pore volume becomes much smaller as the percent of white sand increases in the prepared blended cement pastes. The cumulative leach fraction (CLF) for ^{137}Cs and ^{60}Co radioactive ions from the hardened blended cement white sand pastes after 90 days were measured. The examination of the leaching data revealed that adding white sand to cement reduces the leach pattern as OPC+5% white sand < OPC+10% white sand < OPC+20% white sand < OPC only for the studied radionuclides. A simplified mathematical model for analyzing the migration of radioactive ions has been developed. [Journal of American Science 2010;6(7):334-341]. (ISSN: 1545-1003).

Keywords: Cement; white sand; immobilization of radioactive ions; leaching properties.

1. Introduction

Low and intermediated level radioactive wastes are produced from different application such as fuel processing plants, research reactors, activation analysis units, nuclear medicine in hospital as well as industrial activities [1]. The treatment of these wastes is needed to produce a waste product suitable for long term storage and disposal. Many diverse methods are used such as solidification, embedding or encapsulation to immobilize the radioactive wastes in a solidified form. These wastes must be structurally stable to ensure that they does not degrade and/or promote slumping, collapse or other failure [2]. Immobilization technique consists of entrapping within a solid matrix i.e cement, cement-based material, polymer or ceramic [3]. Immobilization in cement has many advantages such as its low volume reduction, compatibility with aqueous waste streams, good mechanical characteristics, radiation, thermal stability, low cost and relatively high leachability [4]. Studies on leaching of alkali metals from cement waste matrices confirm that the solubility of alkali metals are high enough at pH more than 7 [5]. Recently, an extensive array of leaching studies has been addressed to reduce the leachability of different radionuclides from immobilized waste matrices by mixing the cement with different materials having significant sorption capacity such as fly ash, silica fume, sand kaolina and zeolites [6-9]. Additive material is defined as a solid material in powder, granular or fibrous form that is added to cement system to reduce cost, modify the flow and hardness properties [10]. Additive materials have been previously treated for the purpose of removing hazardous ions found in variable wastes, e.g. sand was used as additive material to produce solidified grout with low cost and increasing the strength of this grout by increasing the binder aggregate ratio [11]. The sorptive behavior of different radionuclides as a model of monovalent and divalent cations has been investigated on sand [12]. The International Atomic Energy's (IAEA) standard leach method has been employed to study the leach radionuclides immobilized in cement matrices [13].

In the present work, white sand (WS) known as natural minerals has high sorptive property added to the cement pastes and used to determine their efficiency as cement- based material. The liquid low level radioactive waste (LLRW) used for this study contains ^{137}Cs and ^{60}Co with concentrations close to the discharge limits. Also, an evaluation of the cumulative leach fraction (CLF) of the immobilized ions was calculated

2. Experimental and Measurements

2.1. Materials

The materials used in the present work include a freshly powder of ordinary Portland cement (OPC) Type 1 which is provided by National Cement Company (NCC), Cairo, Egypt. The white sand (WS) is a powder material obtained from Sinai desert, Egypt with particles pass through the sieve size 140 i.e., particles smaller than 0.105mm (105μm); specific surface area was 195 $m^2.g^{-1}$ measured by surface area instrument, Nova, 2000. The chemical oxide compositions of the materials used are shown in Table 1

Table 1:Chemical oxide composition (%) of the materials used

Materials / Oxides	CaO	SiO_2	MgO	Na_2O	K_2O	Al_2O_3	SO_3	L.O.I
OPC	64.50	21.56	3.34	0.20	0.70	5.40	1.48	1.25
WS	0.04	99.30	0.005	0.009	0.0002	0.08	0.004	0.32

2.2. Preparation and measurements for the blended cement pastes

The hardened blended cement pastes were prepared by adding different ratios of (WS) namely 0, 5, 10 and 20 % by weight to a constant weight of fresh (OPC). The optimum water of consistency was selected and the resulting paste was moulded in cubic moulds (each mould with edge 2.5 cm diameter). The moulds with the specimens were placed at 100% relative humidity for 24 h at 20°C, then the specimens were moulded and cured under tape water for time interval of 3, 7, 28 and 90 days, the curing water changed every 7 days. All the samples are designated as OPC, OPC + 5%WS, OPC + 10%WS, OPC+ 20%WS respectively.

The compressive strength property was carried out on the hardened blended cement pastes according to the ASTM designation [14]. The particle size distributions of the selected specimens in this investigation were determined using a mercury intrusion porosimeter (MIP) technique. It has been supplied from Quantachrome Corp. Boynton Beach, Florida, USA. The effect of white sand (WS) addition on hydrated specimens was studied using X-ray diffraction analysis (XRD) technique. The oriented sample was analyzed using X-ray diffratometer (Shimadzu XRD 490) Japan with nickel filter and a Cu-K_α radiation**.** Infrared spectroscopy was measured using Perkin-Elmer 16 PC Fourier transform spectroscopy (FT-IR). The selected specimens were manually ground with mortar and pestle set inside the N_2 gas chamber and particles with diameter lower than (300-400 μm) were chosen. The spectra were traced in the range 4000- 400 cm^{-1} (wave number), and the band intensities were expressed in absorbance. The thermal stability of the prepared samples was carried out through studying the thermogravimetric analysis TGA and differential thermal analysis DTA which carried out using TA 50 (Shimadzu). The measurements were carried out from room temperature up to 800°C with heating rate 20°C min^{-1}.

For preparing the contaminated WS, a fixed bed column experiments was used through a glass column of 1 cm diameter and 10 cm long. Then, 10 gms of WS as sorbent materials were transferred into the column with the aid of distilled water and adjusted at pH 7 [15]. The radioactive solution was then passed through the column at rate 1 ml/min. The effluent was collected in fractions (5 ml) for radioactive analysis.

2.3 Static leach test

The IAEA standard leach test was applied to determine the leaching characteristic of ^{137}Cs and ^{60}Co radionuclides from the solidified waste [16]. The solidified waste grouts were immersed in beaker containing 300 ml-distilled water. Leachant was exchanged and analyzed for radioactivity after 1, 2, 3, 4, 5, 6, 7, and then after every week, month till 3 months. The ratio of leachant volume to the total exposed surface area of the grout was always kept constant at 10 cm [17]. A known volume was taken from the aqueous solution after contacting with the solid phase and its γ-activity was measured, using a well type NaI crystal connected to a multichannel analyzer which had 256 channel attached with preamplifier (Genee, 2000). All the leachate analyses were carried out on duplicate at room temperature. The cumulative leach fraction CLF (cm) was calculated according to the following equation:

$$CLF = (\sum A_t/A_o).\ (V/S)$$

where
A_o: initial activity on present in specimen at time zero,
A_t: activity leach out of sample after leaching time t,
t: duration of leaching renewal period (d),
V: volume of specimen, (cm^3) and,
S: surface area of specimen exposed to leachant

3. Results and Discussion

3.1. Compressive strength

On addition of water to blended cement containing different ratios of white sand namely 0, 5, 10 and 20%, the constituent of blended cement (calcium silicate) undergo hydrolysis and the products being less basic calcium silicate hydrate (C-S-H) gel and calcium hydroxide were formed. The final gel fills the spaces between the cement grains and form bridges between them, thereby causes stiffening of the paste and its subsequent hardening. The continuous formation of the gel gradually fills the capillary pores, the porosity of the paste decreased, and its strength is gradually increased which may be attributed to the cohesion force acting between the gel particles or to the inter growing of the crystals and the formation of more chemical bonds. The results also showed that at any hydration time, the compressive strength values of the blended cement pastes containing variable white sand ratios are higher than that of those for Portland cement only Fig.1. This may be due to the interaction between the fine particles of white sand particles and the free calcium hydroxide librated during the hydration process to form new kind of calcium silicate hydrate gel (C-S-H); this kind of gel is strongly hydraulic in nature which leads to an increase in the total content of binding centers leading to an increase in the compressive strength values [18].

3.2. Particle size distribution

Mercury intrusion porosimetry (MIP) is one of the widely methods used to estimate the pore size distribution [19]. It has been demonstrated that, the blended cement pastes contains different ratios of white sand have a lower cumulative intruded pore volume than the paste made of ordinary Portland cement only Fig.2. This may be ascribed due to the fact that, the formation of the new (C-S-H) gel leads to an increase in the total contents of the binding centers in the hardened blended cement paste. Therefore, the pore volume for all the hardened blended cement mixtures with white sand would be filled with the excess (C-S-H) gel, leading to a decrease in the pore diameter between the particles. As a result, the cumulative pore volume becomes much smaller so, the opportunity of mercury intrusion into the pore system becomes difficult.

3.3. X- ray diffraction

XRD was used to study the changes in the crystalline phases of the hardened blended cement pastes after 28 days of curing. The X- ray diffraction pattern of white sand (WS) and the hardened blended cement pastes with different addition of (WS) namely 5 and 20% respectively are shown in Fig.(3a, b). The peaks in Fig.(3a) indicate the main characteristic sharp peaks at 2 θ of 21^o and 26^o, which may be due to the presence of silica in the form of cristobalite and quartz form respectively. Whereas, the X-ray pattern shown in Fig. (3b) also, illustrated the main characteristic peaks of hydration products of cement, calcium silicate hydrate (C-S-H) gel at 2θ of 29.5^o, 32.6^o and 34.5^o respectively [20], and Portlanide phase(calcium hydroxide) was identified at 2θ of 18^o and 47.3^o. Also, it is clear that, as the (WS) content increases in the hardened blended cement pastes up to 20 %, the intensity of the main characteristic peak (C-S-H) gel phases increases. This mainly due to interaction takes place between the active silica in (WS) and $Ca(OH)_2$ librated during hydration process of OPC as a result, more hydrated products formed increasing the compressive strength values [21].

3.4. FT-IR

In Fig.4, the spectrum of white sand (WS) exhibits several strong sharp bands occurred at 3750, 1660, 1480, 1300, 1200, 970, 940 and 860 cm^{-1} respectively. The sharp band at 3750 cm^{-1} may be due to the free silonal group [22]. Also, the band at 1660 cm^{-1} referred to this silonal compound having a carbonyl group attached to the silicon, while the bands around 1300-1000 cm^{-1} means that different acetoxy groups attached to the silica atom. This also identified by a strong doublet band around 970-940 cm^{-1}. The FT-IR spectrum of the hardened blended cement pastes containing 5 and 20 % (WS) are shown in Fig. 4. The main characteristic band appeared around 3500-3200 cm^{-1} due to the hydrogen bond present in the active silica, as well as a strong band around 1600 cm^{-1} due to the consuming or cross linking that takes place between the silicon atom containing the silonal group and calcium silicate present in the hydrated cement phase leading to the formation of more calcium silicate hydrate (C-S-H) gel [23].

3.5. Thermal analysis

The thermal analysis of the tested hardened blended cement specimens with (WS) ratios 0, 5 and 20% was performed. It is considered that an endothermic peak in the temperature range 80-120°C display water loss from the cement gel phase was observed in Fig. (5) when studying the DTA curves. Another intense endothermic peak visible in all DTA curves within the temperature range of 450-485°C; corresponding to the released of trapped water in the crystalline gel form of the hydrated specimens at this temperature [24]. Based on TG curves Fig. (6), it can be stated that the content of water adsorbed on $Ca(OH)_2$ in the hardened cement paste and in the hardened cement paste with different (WS) admixture in the temperature range 80-120°C varied from 8-13% of the total weight of the original prepared specimens. As the percent of (WS) increased in the prepared specimens, the total weight loss percent decreased due to more consumption of the water of hydration to form more gel structure as cleared from the compressive strength tests.

3.6. Leaching Characteristics of ^{137}Cs and ^{60}Co radionuclides

The objective of measuring the cumulative leach fraction (CLF) is to predict the leaching rate of some radionuclides of potential concern from immobilized waste matrix under continuously saturated condition that represent the worst case. The addition of 5% (WS) to the hardened blended cement paste decrease the (CLF) for the studied radionuclides, this due to the low porosity of these constituent paste when compared with that of OPC Fig.(7,8). As the percent of the contaminated (WS) increase the (CLF) increase due to the high sorption capacity of this natural mineral for the studied radionuclides[25].

In general, the leaching character from the solidified material can be explained as a combination of both diffusion and dissolution mechanisms [26]. The value of the apparent diffusion coefficient (D) can be calculated from the slope (m) of the straight line of the plot of $(\sum A_t/A_o)$ versus $(t_n)^{1/2}$ as:

$$(\sum A_t/A_o) = 2\ (S/V)\ (Dt_n/\pi)^{1/2}$$

Where; ΣA_t = cumulative amount of radioactivity leached during cumulative time t_n. The value of the apparent diffusion coefficient (D) can be calculated from the slope (m) of the straight line when plot $(\sum A_t/A_o)$ against $(t)^{1/2}$ as

$$D = \pi\ (mV/2S)^2$$

Figure 9 and 10 represents the plotting of the fraction leached of ^{137}Cs and ^{60}Co from the prepared pastes versus the square root of leaching time. The results from the figures showed an initial fast leaching during the first period followed by slow leaching in the subsequent periods. According to this behavior, the diffusion coefficients D for the fast stages for the prepared pastes were found. The leaching fraction coefficients are listed in Table 2. From these data it was found that the diffusion coefficients values of the studied radionuclides were significantly reduced with (WS) addition of the studied pastes comparing with OPC paste [27]. The leachability index L is a material parameter of the leachability of diffusing species, which used to catalogue the efficiency of the matrix material to solidify a waste and is given by [28]:

$$L = -\log (D)$$

The value of 6 is the threshold to accept a given matrix as adequate for the immobilization of radioactive waste. Table 2, shows the mean leachability indices for the studied leached radionuclides from the prepared pastes and their range from 8.1 to 12 in case of ^{137} Cs and from 6 to 6.8 in case of ^{60} Co which exceed the value of 6. These values indicated that OPC/WS pastes can be used as efficient materials for immobilizing cesium and cobalt for the long term disposal.

Table(2) :The leaching coefficients (D) and the leachabilitiy indices (L) of ^{137}Cs and ^{60}Co radioactive ions from the blended cement pastes at different white sand (WS) ratios.

Prepared Pastes	^{137}Cs D	^{137}Cs L	^{60}Co D	^{60}Co L
OPC+ 5% (WS)	8.5×10^{-13}	12	1.5×10^{-7}	6.8
OPC+ 10% (WS)	1.98×10^{-9}	8.7	2.8×10^{-7}	6.5
OPC+ 20% (WS)	4.65×10^{-9}	8.3	3.9×10^{-7}	6.4
OPC	7.17×10^{-7}	8.1	4.2×10^{-7}	6

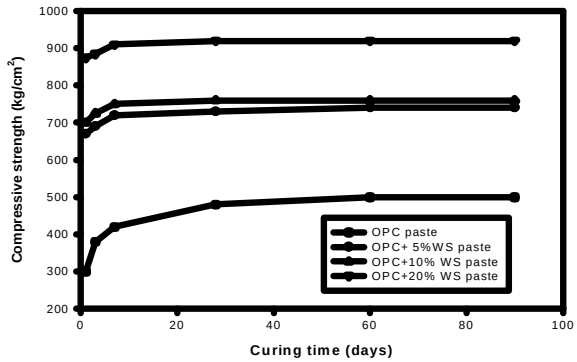

Fig.(1): Compressive strength versus curing time for the hardened blended cement pastes containing different white sand ratios

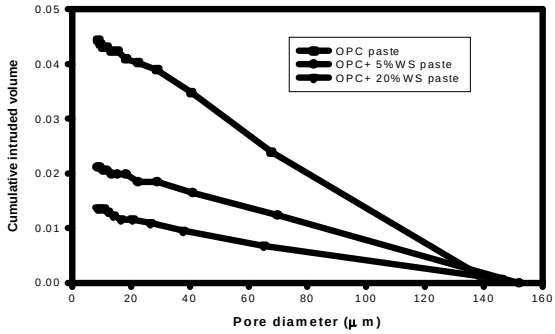

Fig.(2): Cumulative intruded volume versus pore diameter for the hardened cement paste and blended cement pastes contains 5% and 20% of white sand after 28 days of hydration.

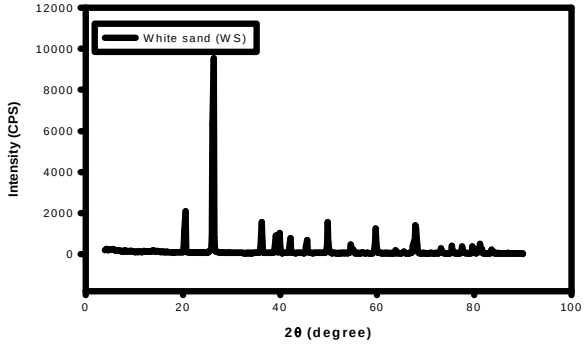

Fig.(3a): XRD pattern of white sand

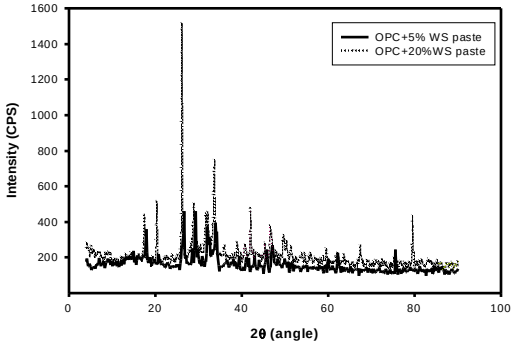

Fig.(3b): XRD patterns of the hardened blended cement pastes contains 5% and 20% white sand after 28 days of hydration.

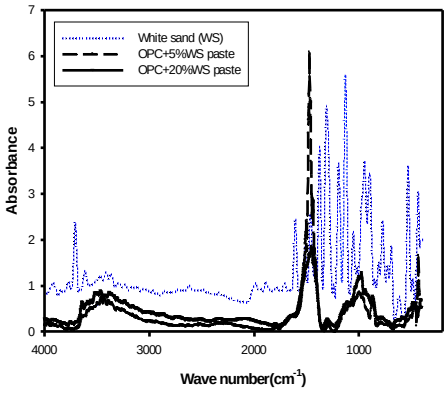

Fig.(4): FT-IR spectrum of white sand and the hardened blended cement pastes contains 5% and 20% white sand after 28 days of hydration.

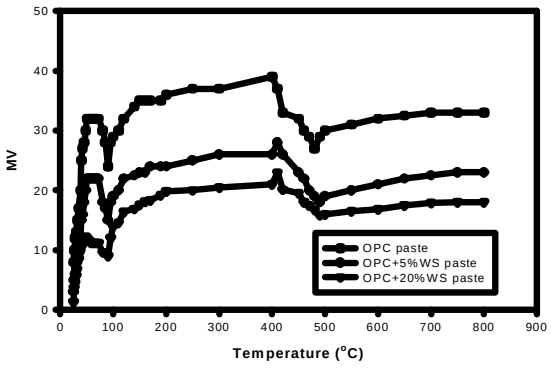

Fig.(5): DTA of the hardened blended cement at different white sand ratios

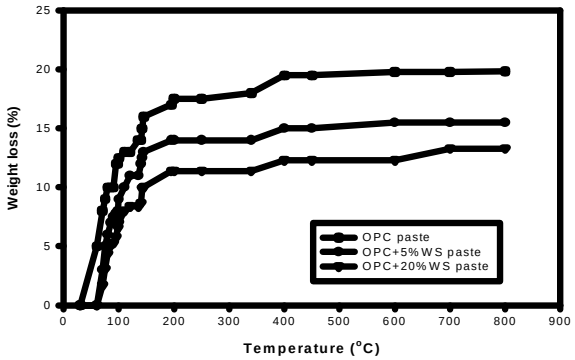

Fig.(6) Weight loss percent of the hardened blended cement pastes at different ratios of white sand.

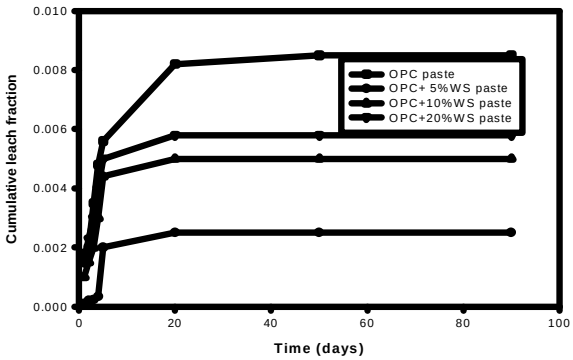

Fig.(7) Cumulative leach fraction of ^{137}Cs from the hardened blended cement pastes at different white sand ratios.

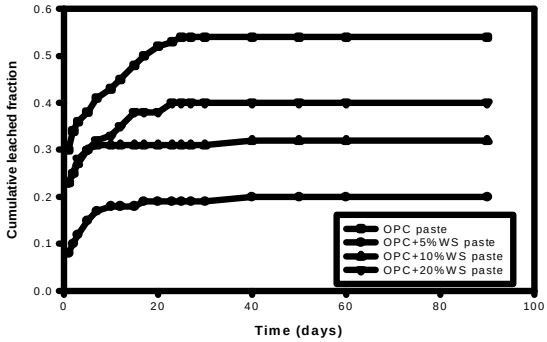

Fig.(8) Cumulative leach fraction of ^{60}Co from the hardened blended cement pastes at different white sand ratios.

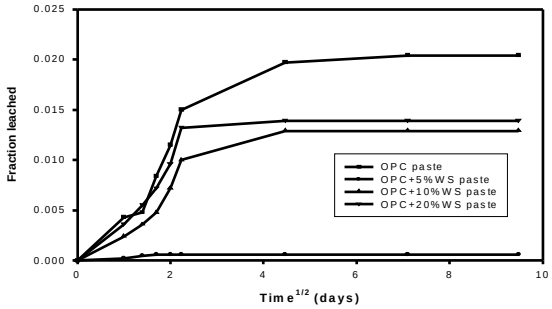

Fig.(9) Variation of fraction leached of ^{137}Cs from the hardened blended cement pastes at different white sand ratios.

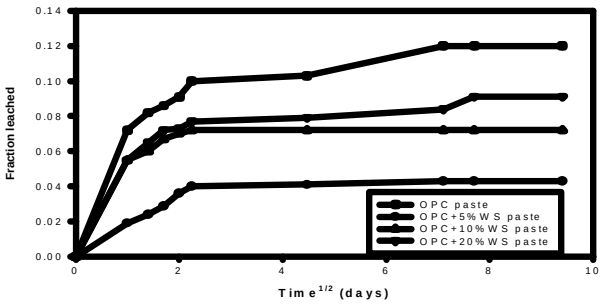

Fig.(10) Variation of fraction leached of ^{60}Co from the hardened blended cement pastes at different white sand ratios.

4. Conclusion

From the above mentioned results, it can be explain that:

- The addition of white sand up to 20% by weight to ordinary Portland cement increases the mechanical properties of the prepared blended cement pastes comparing to the neat ordinary Portland cement paste.
- The pore volume for all the hardened blended cement pastes containing white sand would be filled with the excess calcium silicate hydrate gel, leading to a decrease in the pore diameter between the particles. As a result, the cumulative pore volume becomes much smaller comparing to the neat ordinary Portland cement paste.
- Thermal stability behaviour shows that the hardened blended cement pastes containing white sand are lower in the loss of weight than that of the neat ordinary Portland cement paste.
- From XRD patterns, it has been observed that, the (WS) content increases in the hardened blended cement pastes up to 20 %, the intensity of the main characteristic peaks (C-S-H) gel phases increases. This is mainly attributed to the interaction which takes place between the active silica in (WS) and $Ca(OH)_2$ librated during hydration process of OPC.

Accordingly, The addition of 5% (WS) to the hardened blended cement paste decrease the (CLF), decrease the leaching coefficients (D) and increase the leachabilitiy indices (L) of ^{137}Cs and ^{60}Co radioactive ions from the prepared hardened blended cement pastes.

Corresponding author

Magdy M. Khattab[2*]

Department of Radiation Chemistry, National Center of Radiation Research, Atomic Energy Authority, Cairo, Egypt

5. References

1. El-Dessouky MI, El-Sourougy MR, Aly HF, Investigation on the treatment of low and medium level radioactive liquid waste. Isotopenpraxis 1990; 26: 608-611.
2. Burns RH, Solidification of low and intermediate level waste. At. Energy Rev. 1971; 9: 547-552.
3. Sakr K, Sayed MS, Hafez MB, Immobilization of radioactive waste in mixture of cement, clay and polymer. J. Radio. and Nucl. Chem. 2003; 256(2): 179- 184.
4. Philip J, Philip T, Long–term performance of surface and sub. Surface engineered barriers, US Nuclear Regulatory Commission, National Academy of Science, Washington DC, May 26 (2006).
5. I. Plecas, Dimovic S, Smiciklas I, Utilization of bentonite and zeolite in cementation of dry radioactive evaporator concentrate. Prog. Nucl. Energy 48 495-503 (2006).
6. Plecas IB, Pavlovic RS, Pavlovic SD, Leaching of ^{60}Co and ^{137}Cs from spent ion exchange resins in cement–bentonite clay matrix. Bull. Mater. Sci. 2003; 26(7): 699–701.
7. Osmanlioglu AE, Immobilization of radioactive waste by cementation with purified kaolina clay. Waste Management 2002; 22(5): 481-483.
8. Skripkiunas G, Sasnauskas V, Dauksys M, Dauksys D, Peculiarities of hydration of cement paste with addition of hydrosodalite. Materials Science 2007; 25(3): 627-635.
9. Polettini A, Pomi R, Sirini P, Testa F, Properties of Portland cement-stabilised MSWI fly ashes. J. Hazard. Mater. 2001; 88 (1): 123-138.
10. Koleva M, Vassilev V, Polymer composites containing waste dust from power production. Macedonian J.of Chemistry and Chemical Engineering 2008; 27(1): 47-52.
11. Shawabkeh RA, Solidification and stabilization of Cd^{2+} in sand-cement-clay mixture. J. Hazard. Mater. 2005; 125(1-3): 237-243.
12. Strkalj A, Malina J, Radenoic A, Waste mould sand potential low-cost sorbent for nickel and chromium ions from aqueous solution. Materials and Environment 2009; 56 (2): 118-125.
13. Plećas I, Perić A, Glodić S, Kostadinović A, Comparative leaching studies of ^{60}CO from spent radioactive ion-Exchange resin incorporated in cement**.** Cem. Concr. Res. 1995; 25(2): 314-318.
14. Ruiz MC, Irabien A, Environmental behavior of cement-based stabilized foundry sludge products incorporating additives. J. Hazard. Mater. 2004; 109(1-3): 45-52.
15. Guerrero A, Goñi S, Allegro VR, Efficiency of fly ash belite cement and zeolite matrices for immobilizing cesium. J. Hazard. Mater. 2006; 137(3): 1608-1617.
16. *Matsuzuru H, Moriyama N, Wadachi Y, Ito A,* Leaching behavior of cesium-137 in cement-waste composites. Health Phys. 1977; 32: 529-534.

17. Abdel Raouf MW, Nowier HG, Assessment of fossil fuel fly ash formulation in the immobilization of hazardous wastes. J. Environ. Eng. 2004; 130(5): 499-507.
18. Ruiz MC, Irabien A, Environmental behavior of cement-based stabilized foundry sludge products incorporating additives. J. Hazard. Mater. 2004; 109(1-3): 45-52.
19. Sohna, D, Johnson DL, Hardening process of cement-based materials monitored by the instrumented penetration test: Part 1: Neat cement paste and mortar. Cem. Concr. Res. 2002; 32(4): 557-563.
20. Shin-ichi Igarashi, Akio Watanabe, Mitsunori Kawamura, Evaluation of capillary pore size characteristics in high-strength concrete at early ages. Cem. Concr. Res. 2005; 35(3): 513-519.
21. Kantautas A, Palubinskaite D, Vaickelionis G, Synthesis and hardening of flouralinite cement. J. Materials Science 2006; 24(2): 385-393.
22. Turanli L, Uzal B, Bektas F, Effect of large amounts natural pozzolan addition on properties on of blended cement. Cem. Concr. Res. 2005; 35(6): 1106-1111.
23. Phenrat T, Marhaba TF, Rachakornkij M, Examination of solidified and stabilized matrices with Portland cement and lime. J. Environmental & Hazrdous Management 2004; 26(1): 65-75.
24. Ben-Dor L, Perez D, Sarig S, Thermal study of the effect of additives on the hydration of tri-calcium silicates. J. of American Ceramic Society 2006; 58(3-4): 87-89.
25. Veronica A, Bucharest SCN, The adaptation of natural (geological) barriers for radioactive low and intermediate level waste near surface disposal in Romania, WM'01 Conference, February 25-March 1, Tucson, AZ, Bucharest University (2001).
26. Plecas I, Immobilization of ^{137}Cs in Concrete. Acta Chim. Slov. 2003; 50(3): 597-600.
27. Abdel Rahman RO, Zaki AA, El-Kamash AM, Modeling the long-term leaching behavior of ^{137}Cs, ^{60}Co and ^{152,154}Eu radionuclides from cement-clay matrices. J. Hazard. Mater. 2007; 145(3): 372-380.
28. Shrivastav PO, Shrivastava R, Cation exchange application of synthetic tobermorite for the immobilization and solidification of cesium and strontium in cement matrix. Bullet. Mater. Soc. 2000; 23: 515-520.

6/6/2010

A Novel 3D Reconstruction Approach Based on Camera Perspectives

Muhammad Abuzar Fahiem and Abad Shah

Department of Computer Science and Engineering
University of Engineering and Technology, Lahore, Pakistan
abuzar@uet.edu.pk

Abstract: Engineering industry requires line drawings for manufacturing, machining and production of engineering equipments/objects. The generation of these paper-based drawings or computerized drawings is a complex and time consuming task. Conventionally, these drawings contain three two dimensional (2D) orthographic views, namely *top*, *front* and *side* of an object. Modern trends in engineering industry require three dimensional (3D) engineering drawings. Therefore, to fulfill this requirement the conversion of these 2D drawings to 3D drawings is essential. This conversion is referred to as the *reconstruction*. Various approaches have been proposed for the conversion/reconstruction using existing drawings. In this paper, we propose a novel 3D reconstruction approach which uses camera perspectives in the reconstruction process. Note that in the existing approaches this feature (camera perspective) is not used. Another salient feature of our approach is its underlying mechanism of tangential lines and hypothetical cuboid. Using our proposed approach, manufacturing cost and time can be saved, and it can also be helpful in technology transfer. [Journal of American Science 2010;6(7):342-352]. (ISSN: 1545-1003).

Keywords: 3D Reconstruction, Boundary Representation, Constructive Solid Geometry, Tangential Lines, Hypothetical Cuboid, 3D Modeling

1. Introduction

The area of computer vision deals with the representation, storage and retrieval of the real world objects as computer images. However, these computer images are generally two dimensional (2D) but the real world objects are three dimensional (3D). Therefore, to get real representation and impression of the real world objects, it is necessary to transform 2D computer images into 3D objects (Gingold et al., 2009). These transformations can be categorized into two broad domains; 3D modeling and 3D reconstruction.

The 3D modeling is used in a wide range of applications such as restoration of ancient sculptures, designing of ergonomically suitable costumes, development of aerodynamic vehicle profiles, generation of cockpit helmet designs, modeling of historical monument, and creation of 3D animated movies (Sparacino et al., 1995). It is based on raster images of objects from angle invariant multiple camera images but the main emphasis is on appearance of the 3D models of an object. Number of camera images may range from a few to some hundreds. Moreover, before proceeding to the 3D modeling, a proper view planning is required (Scott et al., 2004), and the 3D model acquisition pipeline needs to be established (Bernardini & Rushmeier, 2002).

The 3D reconstruction primarily focuses on the applications/objects related to engineering industry such as computer aided designing (CAD) and computer aided machining (CAM). The engineering objects are basically components that are composed of different geometric shapes such as triangle, rectangle, cuboid, cylinder, cone, pyramid, sphere, toroid etc. These objects are represented in the form of line drawings in engineering industry. As mentioned earlier that conventionally these drawings contain three 2D orthographic views namely *top, front* and *side* of an object. These drawings are either paper based, prepared manually by skilled draftsmen/engineers, or they are computerized, prepared using different CAD tools. With the advent of the modern engineering technologies like rapid prototyping (RP), and computerized numerically controlled (CNC) machines, there is an urgent need to convert these views of 2D drawings into 3D drawings to take full advantage of above technologies. This 2D to 3D conversion is technically termed as a *3D reconstruction*, and for this purpose various approaches have evolved (Wang & Grinstein, 1993; Company et al., 2005, Fahiem, 2009).

There are some situations where drawings of engineering objects are missing or incomplete. Such situations often occur with the third world countries where objects/equipments are supplied but their technology is not transferred in terms of engineering drawings. Redesigning or duplications of these engineering objects require manual reproduction of missing drawings which is a hectic, costly and time consuming job because it requires skilled human resources. The process of reproducing engineering

drawings of an object can be made convenient, cost and time effective by automating the job provided these objects are represented in some computerized vector format. For this automation, orthographic camera perspectives of the objects can be used. Then, the 2D drawings are extracted from these perspectives and 2D to 3D reconstruction of drawings is done.

In this paper, we propose a novel 3D reconstruction approach using 2D camera perspectives that makes our approach different from the existing approaches. This approach does not require already built engineering drawings. The prime focus of the proposed approach is on reconstruction and vectorization of these 2D camera perspectives into a 3D engineering drawing. The vectorization process is performed on the drawing exchange file (DXF) format which is recognized by the different CAD/CAM tools. This approach has potential to be helpful in the reverse engineering applications.

The remainder of this paper is organized as follows. A detailed survey of various 3D modeling and 3D reconstruction approaches is given in Section 2. In Section 3, we present our approach while Section 4 is dedicated to our concluding remarks.

2. Related Work

In this section, we give survey of various existing 3D modeling and 3D reconstruction approaches.

2.1. 3D Modeling Approaches

The existing 3D modeling approaches heavily depend on different types of hardware employed, and use of different light sources (Rusinkiewicz et al., 2002; Fleck et al., 2009). The hardware can be 3D cameras and scanners based on different principles. While the different light sources can be laser light, structured light or even an ambient light. In the following sections, more details of existing modeling approaches are given.

2.1.1. Time of Flight Approach

These approaches are based on 3D cameras/scanners that operate on the time of flight (ToF) principle of laser light (Blais et al., 2003). In this type of approaches, the produced laser beam reflects back to a laser detector after striking on the surface of an object. The trip time of the laser beam is recorded and the distance is calculated using Equation (1), c being the velocity of the light.

$$z = (c * t)/2 \quad (1)$$

These scanners suffer from a drawback that the measurement of so time for fast beam is very difficult. Cost of the measurement is directly proportional to accuracy of the results. Another problem with which these scanners encounter is; to get accurate results, it is necessary that the reflection of laser beam should be at a certain incident angle to the detector from the object surface. A deflection of the beam causes either no or wrong measurement of the time. These scanners are good for the modeling of far objects such as buildings etc.

2.1.2. Laser Triangulation Approach

This type of approaches is based on 3D cameras/scanners which operate on the laser triangulation (LT) principle (Xu et al., 1998). In the LT principle, a camera captures the laser dot position when the laser light strikes on an object surface. The laser source, the laser dot on object surface and the camera lens form a triangle (see Figure 1), and the distance z of a point on object surface from the laser source is calculated by solving this triangle using Equation (2).

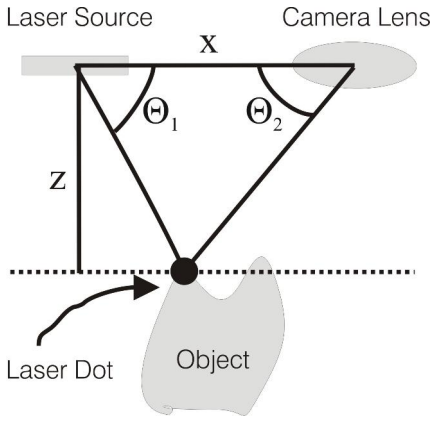

Figure 1: Laser Triangulation Principle

$$z = \frac{x}{1/\tan\theta_1 + 1/\tan\theta_2} \quad (2)$$

These systems of the scanners operating on the LT principle are accurate but they are expensive. These scanners are limited to a measurement of the distance in the order of a few meters. Moreover, these fail in the situations where deep narrow holes are present in object surface.

2.1.3. Structured Light Approach

Structured light (SL) is usually a strip or an array of strips of while halogen light produced from a projector. When these strips of light intersect with an object present in their path, they reflect back and produce a line of illumination on the surface of the object. A camera captures this line of illumination and the distance of a point on this line of illumination

from the camera is calculated through triangulation (Dipanda & Woo, 2004).

SL approach is suitable for retrieving protruded / projected shapes but is not useful in modeling holes/cavities because the line of illumination generated by SL may break or get invisible after striking with the holes/cavities.

2.1.4. Stereoscopy Approach

This type of approaches works on the human vision system and uses two cameras located at a known distance (Fofi et al., 2003). Correspondence of the pictures from both cameras is employed to retrieve the distance information. The correspondence is to find a set of pixels in one picture which can be identified as the same set of pixels in other picture, based upon the matching of certain common features overlapping in both the pictures. The distance information *z* can then be calculated by solving the triangle formed by two cameras and the corresponded pixels, using Equation (2) (see Figure 2).

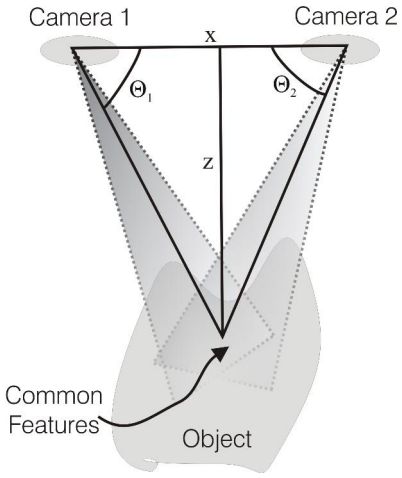

Figure 2: Stereoscopic Approach

This correspondence, itself, is a major problem in such scanners and they require heavy computational time and do not guarantee a reasonable accuracy because the correspondence is based on probabilistic matches of common features.

2. 2. 3D Reconstruction Approaches

The main theme of 3D reconstruction approaches is on vectorized modeling of a solid object from its 2D line drawings. These approaches employee algorithmic computations to generate a 3D solid object while on the other hand 3D modeling approaches are based on intense hardware support. Another major difference between these two kinds of approaches, 3D reconstruction and 3D modeling is that the former is a vector approach while the later is a raster approach. Moreover, 3D modeling is used for visual refinements while 3D reconstruction is used for industrial purposes especially in CAD/CAM industry.

The 3D reconstruction approaches can broadly be divided into two main categories; single-view approaches (discussed in Section 2.2.1) and multi-view approaches (discussed in Section 2.2.2).

2.2.1. Single-view Approach

The single-view approach checks sufficient and necessary conditions in the reconstruction of a 3D solid object from a single view in the drawing (Cooper, 2005; Martin et al., 2005; Feng et al., 2006; Kyratzi & Sapidis, 2009). This approach and its extensions are not 'reconstruction' approaches in the real sense because they do not actually perform any process of reconstruction. Rather they only provide labeling schemes to check the correctness of a line drawing or perceive a 3D solid object from 2D lines. These approaches do not meet the requirements of the engineering industry due to their poor accuracy. However, they are helpful in 3D visualization of free hand sketches and artistic strokes. These approaches can further be divided into following categories:

i) Labeling Approach
ii) Gradient Space (GS) Approach
iii) Linear Programming (LP) Approach
iv) Perceptual Approach
v) Primitive Identification (PI) Approach

Labeling approach marks each line in a drawing with either of three labels; convex, concave or occluding (Huffman, 1971; Clowes, 1971). These provide the necessary conditions for a drawing to be reconstructed into a 3D solid object and do not actually perform the 3D reconstruction. Gradient space approach develops a relationship between gradient of a face and slope of a line present in a drawing (Mackworth, 1973). This approach marks the lines with convex or concave labels depending upon its slope with respect to gradient. This approach, like labeling approach, provides only the necessary conditions for a drawing to be reconstructed into a 3D solid object. Linear programming approach provides necessary as well as sufficient conditions for 3D reconstruction of a solid object from its drawing and provides a system of linear equations to perform reconstruction (Sugihara, 1986). Perceptual approach uses adjacency graph along with the labeling scheme to perceive a 3D solid object from the lines in a drawing (Lamb & Bandopadhay, 1990). This approach is capable of correcting the slight roughness in line drawings. The primitive identification approach reconstructs a 3D solid on the basis of some basic primitives (prism,

cylinder, sphere) identified in a line drawing (Wang & Grinstein, 1989).

2.2.2. Multi-view Approach

This type of approaches performs the 3D reconstruction process from three orthographic views of an object. These approaches are conceptually different from single-view approaches as these collect the geometric information from multiple views of an object and correlate these pieces of information with each other to form a 3D solid object. On the other hand, single-view approaches try to perceive/realize the third dimension from a single set of geometric information gathered from a view. Multi-view approaches can be further divided into two categories as listed below:

i) Constructive Solid Geometry (CSG) Approach
ii) Boundary Representation (B-Rep) Approach

Both B-Rep and CSG approaches are described in the next two sections.

2.2.2.1. Constructive Solid Geometry

The constructive solid geometry (CSG) approach tries to construct a solid object by applying set operations (Union, Intersection, and Difference) on some basic primitives/shapes (Aldefeld, 1983). It is just like combining different pieces of a puzzle to generate a desired shape. The basic primitives may be cuboid, pyramid, cylinder, cone, sphere, toroid, etc. The basic primitives are represented at leaf nodes and the set operations are performed at parent/internal nodes of a binary tree (see Figure 3). One set operation is performed at a time on two basic primitives/shapes, so a binary tree is constructed and by performing the set operations recursively in bottom up parsing manner, yields a solid object at the root of the tree.

The CSG representations of solid objects always produce either a solid object or an empty set (i. e., a set having no solid object) because intersection of two non-interacting shapes would produce a null object.

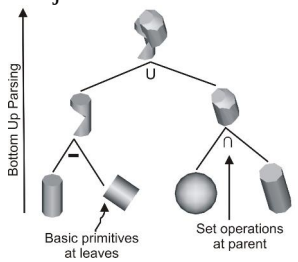

Figure 3: CSG Primitives, Set Operations and Bottom up Parsing

The CSG approaches always suffer from a major drawback because the topological information is not stored in the nodes of the tree. This drawback is inherent in these approaches because they can not predict the relative position of the primitives while performing the set operations. The binary tree, although contains the possible sequence of the set operations to be performed on the primitives during bottom up parsing, but it does not contain or can not compute the position of these primitives with respect to each other. This position information is important to build the desired shape otherwise same primitives may generate different solid objects (see Figure 4). In this Figure, the Union operation on the primitives cone and cuboid is performed at different positions relative to one another and the resultant solid objects are different although the primitives and the operation is same.

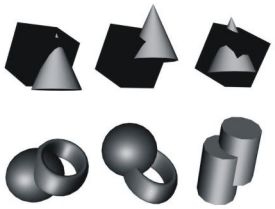

Figure 4: Missing Topological Information in CSG

There is another problem with the CSG approaches that the set operations do not hold the closure property over the CSG domain of primitives.

Aldefeld initially started work on the 3D reconstruction using CSG but this approach is able to handle isolated objects only and requires heavy user interaction (Aldefeld 1983). Then Aldefeld and Richter enhanced Aldefeld's previous approach by eliminating the restriction of isolated objects (Aldefeld & Richter,1984)). Cicek and Gulisen further enhanced the previous approaches by permitting the drawings with hidden lines (Cicek & Gulisen, 2004). This approach made provisions to reconstruct holes and cavities. Dimri and Guromoorthy performed the reconstruction from drawings with sectional views (Dimri & Guromoorthy, 2005).

2.2.2.2. Boundary Representation Approach

In the boundary representation (B-Rep) approach, a solid object is represented by its bounding surfaces (Idesawa, 1973). This approach uses two types of information for the boundary representation, which are topology and geometry. The main topological parameters that are used by this approach are faces, edges and vertices, while the geometry parameters include surfaces, curves and points, which are shown in Figure 5. A face is a bounded portion of a surface, an edge is a bounded piece of a curve, and a vertex is a point. The topology

records connectivity of the faces, edges and vertices, while the geometry describes the exact shape and position of each edge, face and vertex. The geometry of a vertex is its position in the space as by its (x, y, z) coordinates. Edges can be straight lines or curves which can be approximated in poly-lines. A face is represented by a set of close curves on a surface. Several curves may lie on a face to represent cavities in a solid object. Different faces interact with each other at the common vertices to inscribe the whole object. It is just like a volume comprising of a set of faces having associated topological information that defines the relationship between these faces.

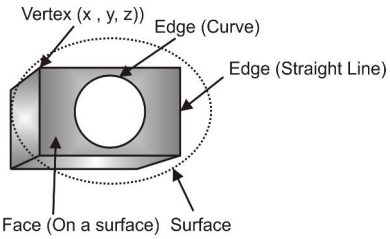

Figure 5: Topological and Geometrical Information in a B-Rep

There are four (4) major steps involved in the B-Rep approach, which are listed as follows:
i) Identification of vertices,
ii) Correspondence of these vertices to form an edge,
iii) Registration of these edges to form a face,
iv) Correspondence of these faces on a surface to form a volume

Idesawa has provided mathematical foundations to the B-Rep, and has set different criteria on the basis of which 3D reconstruction could be performed. But the major problem with this approach is that it can generate ghost figures (Idesawa, 1973). The problem of ghost figures was resolved by Wesley and Markowsky and they formalized the Idesawa's approach with algorithms (Wesley & Markowsky, 1981). Their approach is limited to polyhedrons only. Sakurai extended Wesley and Markowsky's work by incorporating cylinders and cones in addition to polyhedrons but these objects are handled with specific orientation (Sakurai, 1983). This approach is limited to cylinders and cones with axes parallel to one of the coordinate axes only. Moreover, this approach is unable to handle intersecting objects. Gu et al further extended Sakurai's approach to add more orientations of cylinders and cones with the condition that the axis should be parallel to one of the coordinate planes (Gu et al 1986). Their approach is also capable of handling ellipses, parabolas and fourth order curves. Another power of this approach is that it can handle intersecting objects, as well. Liu et al proposed an approach which is independent of orientation, and it can also incorporate quadrics (Liu et al, 2000). Cohen has used undirected graphs for 3D reconstruction but their approach requires heavy storage (Cohen, 2007). Suh and McCasland have reconstructed 3D solid objects from isometric views (Suh & McCasland, 2009).

3. Proposed Reconstruction Approach

In Figure 6, overall working of the proposed approach is shown. There are three (3) main steps in the approach, and they are: *2D Operations, 2D to 3D Transformations,* and *DXF Conversion* (see Figure 6).

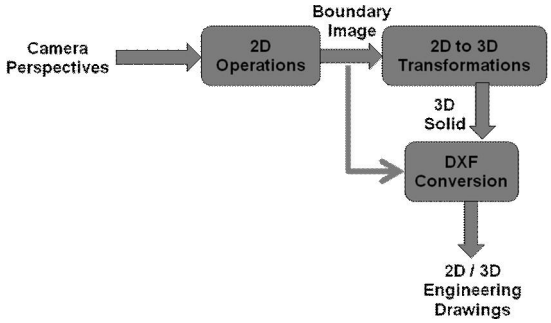

Figure 6: Block Diagram of Proposed Approach

Step 1 (2D Operations) performs the 2D operations on a camera perspective to get an image

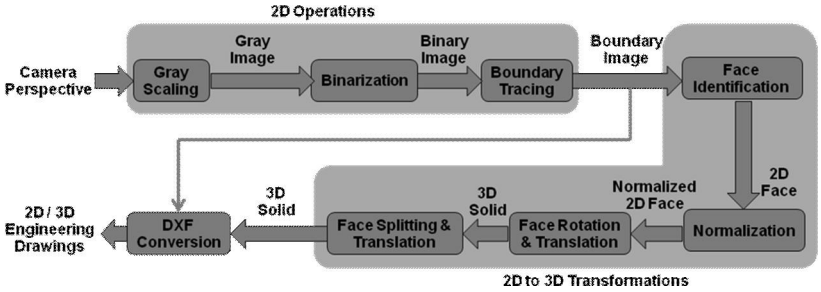

Figure 7: Detailed working of the Proposed Approach

with boundaries, and the image is referred to as a boundary image. Note that three (3) views (i.e., top, front and side) of an engineering object are captured as three corresponding boundary images in Step 1. Step 2 (2D to 3D Transformations) transforms the three boundary images (output of Step 1) of an engineering object into a 3D solid object. Step 3 (DXF Conversion) performs one of the two functions, a single boundary image (from Step 1) is vectorized to generate a 2D engineering drawings, or a 3D solid object (form Step 2) is vectorized to generate a 3D engineering drawing. The detailed working of these three main steps is further shown in Figure 7.

3.1. Step 1: 2D Operations

This step performs three (3) tasks, which are referred to as Gray Scaling, Binarization, and Boundary Tracing. The working of these three tasks we give in the next three (3) sections.

3.1.1. Task 1: Gray Scaling

As it has been mentioned earlier that the proposed approach starts its working by capturing camera perspectives (2D orthographic projections of the object in x-y plane) for each view (*top*, *front* and *side*) of an engineering object (see Figure 8 (a)), and these three views are converted into gray scale images using weighted average of red (R), green (G) and blue (B) colors for each pixel using Equation (3).

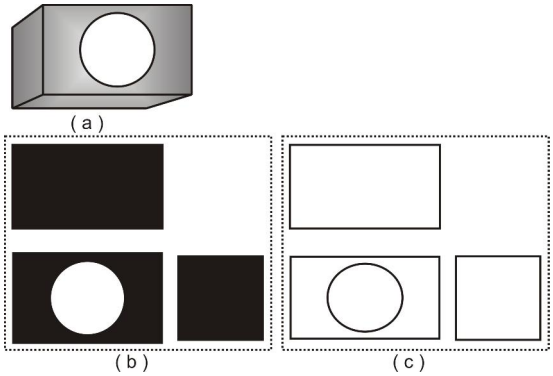

Figure 8: Binarization and Boundary Tracing (a) Engineering Object (b) Binarization (c) Boundary Tracing

$$Gray = 0.3R + 0.59G + 0.11B \quad (3)$$

3.1.2. Task 2: Binarization

The gray images (from Task 1) are then, binarized to get pure black and white binary images as shown in Figure 8 (b). The algorithm used to perform this task (Binarization) is given in Figure 9.

```
Function Binarize (GrayImage): BinaryImage
{
for each row of GrayImage a: i
    for each column of GrayImage a: j
        if a[i][j] <=threshold
        then b[i][j]=0
        else b[i][j]=255
return b
}
Call Binarize for each GrayImage
```

Figure 9: Algorithm for Binarization

3.1.3. Task 3: Boundary Tracing

This task traces the boundaries from the binary image (from Task 2) to get a boundary image. Figure 8 (c) shows these boundary images corresponding to each of the top, front and side views. These boundary images are vectorized using Step 3 of the proposed approach to generate a 2D engineering drawing, or these images are further processed (Step 2 - Task 1) to identify faces for the 3D reconstruction so that 3D engineering drawings can be generated. 2D engineering drawings are useful for the conventional CAD/CAM applications while on the other hand, 3D engineering drawings are needed in the case of CNC machines and RP applications. This makes the proposed approach useful for a wide range of the engineering industry applications.

3.2. Step 2: 2D to 3D Transformations

This step consists of four (4) tasks; i.e., Face Identification, Normalization, Face Rotation and Translation, and Face Splitting and Translation. The working of all these tasks is explained in the next four sections.

3.2.1. Task 1: Face Identification

This task identifies faces from boundary images extracted in Step 1 of the proposed approach (see Section 3.1). Before we proceed with the description of this step (Face Identification), it is necessary to mention that the previous approaches identify faces in a three step process which makes these approaches computationally expensive (Wang & Grinstein, 1993; Fahiem, 2009). The three steps in previous approaches are; identification of vertices, correspondence of these vertices to form an edge, and registration of these edges to form a face.

To reduce the computations, we collect the faces directly in our Face Identification step instead of collecting vertices, edges and faces (as is in previous approaches). For that, we use the concept of tangential lines (Fahiem, 2008). Tangential lines are basically straight lines of infinite length which scan

the image from each side (left, top, right and bottom) in the search of a black pixel. We need four tangential lines (TL_1, TL_2, TL_3, and TL_4), one for each of the four sides of a view. These lines start scanning the image row-wise as well as column-wise. The line TL_1 starts scanning the image column-wise from the left most column in the search of a black pixel. If a black pixel is found, then the scanning stops otherwise the line TL_1 scans the next column to the right of previous column in the search of a black pixel. This process continues until a black pixel is encountered. Similarly, the line TL_3 scans the image column-wise from the right most column in the search of a black pixel. It moves to the left until a black pixel is found. The lines TL_2 and TL_4 scan the image row-wise from top and bottom in the search of a black pixel, respectively. The line TL_2 moves towards bottom and the line TL_4 moves towards top until a black pixel is encountered. When this scanning process completes, the tangential lines intersect each other and form a bounding box on a view inscribing a 2D face, as shown in Figure 10. The intersection of TL_1 and TL_2 determines the upper-left corner of the bounding box. Similarly TL_2 and TL_3, TL_3 and TL_4, and TL_4 and TL_1 determine the upper-right, bottom-right, and bottom-left corners of the bounding box, respectively. Now the face is identified by the (x, y) coordinates produced by the intersections of the tangential lines (see Figure 10).

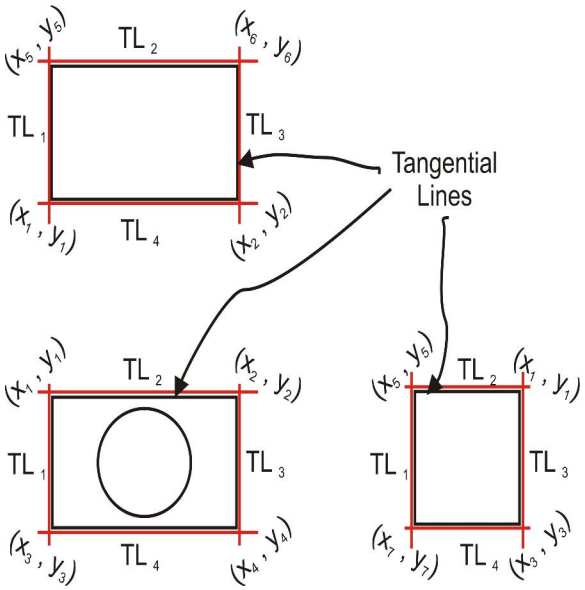

Figure 10: Face Identification using Tangential Lines

The working of Task 1: Face Identification in an algorithm is given in Figure 11.

```
Function FaceIdentify (BoundaryImage): 2DFace
{
BoundaryImage b
while PIXEL!=BLACK
        move TL1 on b from LEFT
        move TL2 on b from TOP
        move TL3 on b from RIGHT
        move TL4 on b from BOTTOM
Mark upper-left corner of bounding box at intersection of TL1 and TL2
Mark upper-right corner of bounding box at intersection of TL1 and TL2
Mark bottom-right corner of bounding box at intersection of TL1 and TL2
Mark bottom-left corner of bounding box at intersection of TL1 and TL2
Collect 2D face inscribed in bounding box
return 2DFace
}
Call FaceIdentify for each BoundaryImage
```

Figure 11: Algorithm for Face Identification

3.2.2. Task 2: Normalization

After the 2D faces identification (see Step 2 - Task 1), these faces are normalized so that a correct alignment of these faces with each other can be carried out, and it is done in the next step (Step 2 – Task 3). Three parameters, i.e., size, angle and perspective, of the 2D faces are normalized to make them size, angle and perspective invariant as it is explained in the following paragraph.

For the size normalization, the faces are scaled such that length of the top face is equal to length of the front face; width of the top face is equal to length of the side face; and width of the side face is equal to width of the front face. The faces are made angle and perspective invariant by adjusting the orientation of these faces such that the tangential lines TL_1 and TL_3 are parallel to y-axis and the tangential lines TL_2 and TL_4 are parallel to x-axis. The algorithm for this step is given in Figure 12.

```
Function Normalization (2DFace): Normalized2DFace
{
2DFace Top, Front, Side
scale Top, Front, Side such that
        TopLength=FrontLength
        TopWidth=SideLength
        SideWidth=FrontWidth
rotate & shear Top, Front, Side such that
                TL1 & TL3 // y-axis
                TL2 & TL4 // x-axix
return Normalized2DFace
}
```

Figure 12: Algorithm for Normalization

3.2.3. Task 3: Face Rotation and Translation

The normalized 2D faces produced by the previous step are still in the 2D x-y plane as the original projections (*top*, *front* and *side*) were. Before we do the reconstruction process of the 3D solid object, it is necessary that the top face should be in x-z plane and the side face should be in the y-z plane so that these faces could be aligned with the sides of the hypothetical cuboid (HC). To achieve this objective, the top face is rotated at -90^0 about the x-axis to transforms it into the x-z plane from the x-y plane.

Similarly, the side face is rotated at -90^0 about the z-axis to transform it into the y-z plane from the x-y plane. These rotations of the top and side faces are performed using Equation (4) and Equation (5), respectively (Gonzales & Woods, 2008).

$$x' = x\cos\theta - y\sin\theta \quad , \quad z' = x\sin\theta + y\cos\theta \qquad (4)$$

$$y' = x\cos\theta - y\sin\theta \quad , \quad z' = x\sin\theta + y\cos\theta \qquad (5)$$

Moreover, we introduce the third dimension as well, by setting the x, y and z coordinates to 0 for the side, top and front faces, respectively. At this stage, although the reconstructed solid object has 3D coordinates but the object lacks in the depth as the third dimension is 0.

The above process converts the 2D faces into 3D faces (see Figure 13(a)). This figure shows the top, front and side faces of the object after rotations and the introduction of the third dimension.

Now the dimensions of HC are determined. The length (L_{HC}), height (H_{HC}) and depth (D_{HC}) of HC are determined by Equation (6), Equation (7) and Equation (8), respectively.

$$L_{HC} = |x_2 - x_1| \qquad (6)$$

$$H_{HC} = |y_3 - y_1| \qquad (7)$$

$$D_{HC} = |z_5 - z_1| \qquad (8)$$

After determining and setting the dimensions of the HC, the faces are translated to align the sides of HC so that a 3D solid object can be reconstructed. To do this, the top face is translated into x-z plane along x-axis and y-axis of the HC using Equation (9). The side face is translated in y-z plane along y-axis of the HC using Equation (10) (Gonzales & Woods, 2008).

$$x' = x - x_{1(top)} \quad , \quad y' = y + y_{1(front)} \qquad (9)$$

$$y' = (y - y_{1(side)}) + y_{1(front)} \qquad (10)$$

In this way, the coordinates (0, y_1, z_1), (x_1, y_1, 0), (x_1, 0, z_1) of the top, front and sides faces (without depth – third dimension) are aligned with each other to produce a 3D coordinate (x_1, y_1, z_1) with the depth. Similarly, other 3D coordinates (without depth) are also aligned with each other and 3D coordinates (with depth) are generated for whole of the solid (see Figure 13 (b)). The algorithm of this task (Face Rotation and Translation) is given in Figure 14.

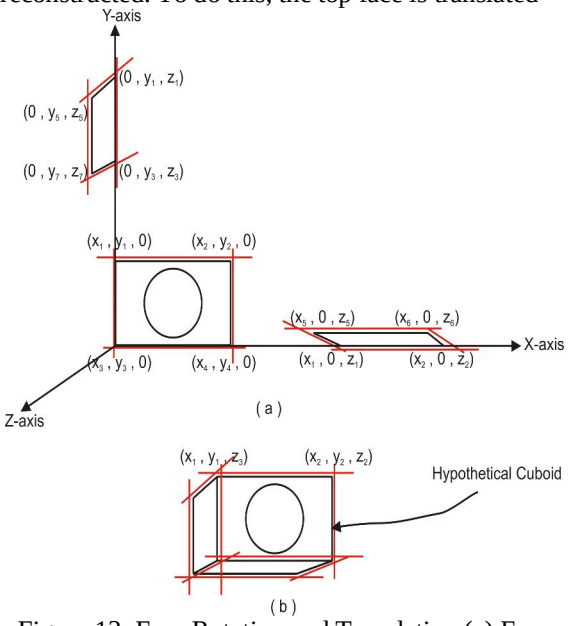

Figure 13: Face Rotation and Translation (a) Face Rotations (b) Face Translations on Hypothetical Cuboid

```
Function FaceRT (Normalized2DFace):
3DSolid
{
Normalized2DFace Top, Front, Side
rotate Top at -90^0 about x-axis
rotate Side at -90^0 about z-axis
translate Top in x-z plane along x-axis of HC
translate Top in x-z plane along y-axis of HC
translate Side in y-z plane along y-axis of HC
return 3DSolid
}
```

Figure 14: Algorithm for Face Rotation and Translation

3.2.4. Task 4: Face Splitting and Translation

The 3D solid object that has been reconstructed by the previous task (Step 2 – Task 3) may not be a true 3D solid because it may contain protruding faces. A protruding face is basically a part of a face which is projected beyond its plane as shown in Figure 15(a). Here right hand parts of top and front faces are basically protruding from their planes. Due to these protruding faces, the 3D solid object reconstructed in the previous task (Step2 – Task 3) is not a true 3D solid (see Figure 15(b)). These protruding faces are not translated to their correct positions and are hanging just like a cantilever beam. We will call such protruding hanging faces as simply a 'hanging face'. A hanging face is splitted and translated to the next edge of the front face to form a true 3D solid object (see Figure 15(c)) using algorithm of 'Face Splitting and Translation' as presented in Figure 16.

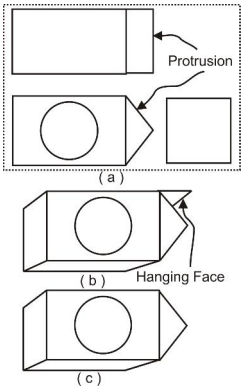

Figure 15: Face Splitting and Translation (a) 2D Faces (b) 3D Solid with Hanging Face (c) 3D Solid Object after Face Splitting and Translation

```
Function FaceST (Normalized2DFace, 3DSolid): 3DSolid
{
Normalized2DFace Top, Front, Side
3DSolid S
subtract Top from x-z plane of S
translate remaining in y-direction to next edge
subtract Front from x-y plane of S
translate remaining in z-direction to next edge
Subtract Side from y-z plane of S
translate remaining in x-direction to next edge
return 3DSolid
}
```

Figure 16: Algorithm for Face Splitting and Translation

This algorithm (see Figure 16) takes normalized 2D top, the front and side faces (from Step 2 – Task 2) and 3D solid (from Step 2 – Task 3) as input, and subtracts these faces from this solid object, and splits the hanging faces from the base face. These hanging faces, after splitting, are translated to the next edge. The top hanging face is translated to the next edge of front face of the 3D solid object. Similarly, other hanging faces (front and side) are also translated to the next edge of the 3D solid object. The output of the proposed algorithm is a complete 3D solid object.

3.3. Step 3: DXF Conversion

In the last step of the proposed approach, the 3D solid object is vectorized to generate a 3D engineering drawing. The vectorization is performed in drawing exchange file (DXF) format recognized by most of the CAD tools (Fahiem & Farhan, 2007). Typically, the DXF format comprises of eight (8) sections as it has been described in Table 1.

Table 1: Sections in DXF Format

Section	Description
Header	Contains the drawing's general information
Classes	Contains the application specific class definitions
Tables	Contains the information about Layer, Line type, etc.
Blocks	Contains the information about blocks
Entities	Contains drawing entities such as Line
Objects	Contains the application specific data
Thumbnail Image	Contains the preview image for the DXF
End of File	Marks the end of DXF

In our proposed approach, the vectorization process needs 'Line Entity' to model different shapes in a 3D solid object with 3D coordinates (generated in Step 2). Different entities in DXF format are specified by their numeric codes and the code for 'Line Entity' is 6. A line is specified by two 3D points with numeric codes for (x, y, z) coordinates of the starting and ending points. These codes are shown in Table 2.

Table 2: Numeric Codes for Line Starting and Ending Points

Point	Coordinate	Numeric Code
Starting	x	10
	y	20
	z	30
Ending	x	11
	y	21
	z	31

A typical line with (x_1, y_1, z_1) and (x_2, y_2, z_2) coordinates is represented as 6 10 x_1 20 y_1 30 z_1 11 x_2 21 y_2 31 z_2 in DXF format. We have converted the 3D solid object with the 3D coordinates generated in Step 2 in the DXF format using 'Line Entity'.

The output of this step is an ASCII file in DXF format containing the numeric values of 3D coordinates corresponding to different lines forming a 3D solid object. This file can be loaded in a CAD tool to regenerate a 3D engineering drawing automatically, from the numeric values corresponding to 3D coordinates of a 3D solid object stored in the file.

4. Conclusion

The novelty of the proposed 3D reconstruction approach is its reconstruction of 3D solid objects form 2D camera perspectives of engineering objects. This feature is new and is not available in the existing approaches (Wang & Grinstein, 2008). This approach is useful in reconstructing and redesigning of engineering objects when 2D drawings are not available for some reason. The approach is a reverse engineering process and

helpful in technology transfer, and is effective in terms of cost and time. This can also be helpful to engineering industry as it supports modern trends in manufacturing, machining and production of engineering equipments.

Corresponding Author:
Muhammad Abuzar Fahiem
Department of Computer Science and Engineering
University of Engineering and Technology
Lahore 54000, Pakistan
E-mail: abuzar@uet.edu.pk

References

1. Gingold, Y., Igarashi, T., and Zorin, D. 2009. Structured Annotations for 2D-to-3D Modeling. ACM Transactions on Graphics. 28(5): 1-9.
2. Sparacino, F., Wren, C., Pentland, A., and Davenport, G. 1995. HyperPlex: a World of 3D Interactive Digital Movies. Proceedings of International Joint Conference on Artificial Intelligence.
3. W. R., Roth, G., and Rivest, J. F. 2003. View Planning for Automated Three-Dimensional Object Reconstruction and Inspection. ACM Computing Surveys. 35(1): 64-96.
4. Bernardini, F., and Rushmeier, H. 2002. The 3D Model Acquisition Pipeline. Computer Graphics Forum. 21(2): 149-172.
5. Wang, W., and Grinstein, G. G. 1993. A Survey of 3D Solid Reconstruction from 2D Projection Line Drawings. Computer Graphics Forum. 12 (2): 137-158.
6. Company, P., Piquer, A., Contero, M., and Naya, F. 2005. A Survey on Geometrical Reconstruction as a Core Technology to Sketch-Based Modeling. Computers and Graphics. 29 (6): 892-904.
7. Fahiem, M. A. 2009. 3D Reconstruction of Solid Models from 2D Camera Perspectives. Lecture Notes in Electrical Engineering. 27: 241-250.
8. Rusinkiewicz, S., Hall-Holt, O., and Levoy, M. 2002. Real-Time 3D Model Acquisition. ACM Transactions on Graphics. 21(3): 438-446.
9. Fleck, S., Busch, F., Biber, P., and Strasser, W. 2009. Graph Cut Based Panoramic 3D Modeling and Ground Truth Comparison with a Mobile Platform – The Wagele. Image and Vision Computing. 27: 141–152.
10. Blais, F., Beraldin, J. A., El-Hakim, S., and Godin, G. 2003. New Developments in 3D Laser Scanners: From Static to Dynamic Multi-Modal Systems. Proceedings of 6th Conference on Optical 3-D Measurement Techniques.
11. Xu, Y., Xu, C., Tian, Y., Ma, S., and Luo, M. 1998. 3-D Face Image Acquisition and Reconstruction System. Proceedings of IEEE Instrumentation and Measurement Technology Conference.
12. Dipanda, A., and Woo, S. 2004. Structured Light System Configuration Determination for Efficient 3D Surface Reconstruction. Proceedings of International Conference on Image Processing.
13. Fofi, D., Salvi, J., and Mouaddib, E. M. 2003. Uncalibrated Reconstruction: An Adaptation to Structured Light Vision. Pattern Recognition. 36(7): 1631-1644.
14. Cooper, M. C. 2005. Wireframe Projections: Physical Realisability of Curved Objects and Unambiguous Reconstruction of Simple Polyhedra. International Journal of Computer Vision. 64 (1): 69-88.
15. Martin, R. R., Suzuki, H., and Varley, P. A. C. 2005. Labeling Engineering Line Drawings Using Depth Reasoning. Journal of Computing and Information Science in Engineering. 5(2): 158-167.
16. Feng, D., Lee, S., and Gooch, B. 2006. Perception-Based Construction of 3D Models from Line Drawings. Proceedings of ACM SIGGRAPH International Conference on Computer Graphics and Interactive Techniques.
17. Kyratzi, S., and Sapidis, N. 2009. Extracting a Polyhedron from a Single-View Sketch: Topological Construction of a Wireframe Sketch with Minimal Hidden Elements. Computers and Graphics. 33(3): 270-279.
18. Huffman, D. A. 1971. Impossible Objects as Nonsense Sentences, Machine Intelligence. 6: 295-323.
19. Clowes, M. B. 1973. On Seeing Things. Artificial Intelligence. 2(1): 79-116.
20. Macworth, A. K. 1973. Interpreting Pictures of Polyhedral Scenes. Artificial Intelligence. 4(2): 121-137.
21. Sugihara, K. 1986. Machine Interpretation of Line Drawings. The MIT Press.
22. Lamb, D., and Bandopadhay, A. 1990. Interpreting a 3D Object from a Rough 2D Line Drawing. Proceedings of the 1st IEEE conference on Visualization.
23. Idesawa, M. 1973. A System to Generate a Solid Figure from Three Views. Bulletin of Japan Society of Mechanical Engineers. 16(92): 216-255.
24. Wesley, M. A., and Markowsky, G. 1981. Fleshing out Projections. IBM Journal of Research and Development. 25(6): 934-954.

25. Sakurai, H. 1983. Solid Model Input Through Orthographic Views. Computer Aided Design. 17(3): 243-252.
26. Gu, K., Tang, Z., and Sun, J. 1986. Reconstruction of 3D Objects from Orthographic Projections. Computer Graphics Forum. 5(4): 317-323.
27. Liu, S., Hu, S., Tai, C., and Sun, J. 2000. A Matrix-Based Approach to Reconstruction of 3D Objects from Three Orthographic Views. Proceedings of 8th Pacific Conference on Computer Graphics and Applications.
28. Cohen A. B. 1995. Mechanical Engineering in the Information Age. Mechanical Engineering. 117(12): 66-70.
29. Suh, Y. S., and McCasland, J. 2009. Interactive Construction of Solids from Orthographic Multiviews for an Educational Software Tool. Computer-Aided Design and Applications. 6(2): 219-229.
30. Fahiem, M. A. 2008. A Deterministic Turing Machine for Context Sensitive Translation of Braille Codes to Urdu Text. Lecture Notes in Computer Science. 4958: 342-351.
31. Gonzalez, R. C., and Woods, R. E. 2008. Digital Image Processing. Prentice Hall.
32. Aldefeld, B. 1983. Automatic 3D Reconstruction from 2D Geometric Part Descriptions. Proceedings of IEEE Conference on Computer Vision and Pattern Recognition.
33. Aldefeld, B., and Richter, H. 1984. Semiautomatic Three-Dimensional Interpretation of Line Drawings. Computer-Aided Design. 8(4): 371-380.
34. Cicek, A., and Gulesin, M. 2004. Reconstruction of 3D Models from 2D Orthographic Views Using Solid Extrusion and Revolution. Journal of Material Processing Technology. 152(3): 291-298.
35. Dimri, J., and Gurumoorthy, B. 2005. Handling Sectional Views in Volume-Based Approach to Automatically Construct 3D Solid from 2D Views. Computer-Aided Design. 37(5): 485-495.
36. Fahiem, M. A., and Farhan, S. 2007. Representation of Engineering Drawings in SVG and DXF for Information Interchange. Proceedings of 6th WSEAS International Conference on Circuits, Systems, Electronics, Control & Signal Processing.
37. Wang, W., and Grinstein, G. G. 2008. A Survey of 3D Solid Reconstruction from 2D Projection Line Drawings. Computer Graphics Forum. 12(2): 137-158.

6/18/2010

Anti-inflammatory, Analgesic and Antiparkinsonism Activities of Some Novel Pyridazine Derivatives

Naif O. Al-Harbi [1], Saleh A. Bahashwan [2], Khalid A. Shadid [3]
[1.] Pharmacy Department, College of Health Sciences, King Saud University, Riyadh, Saudi Arabia
[2-3.] Pharmacy Department, College of Health Sciences, Taibah University, Medina Monawarah, Saudi Arabia
drnaifalharbi@yahoo.com

Abstract: Six compounds of pyridazine derivatives 1-6 have been pharmacological screening. The pharmacological screening showed that many of these compounds have a good anti-inflammatory, analgesic and antiparkinsonism activities comparable to reference drugs. The compounds 1a, 1b, 1c, 2a, 2b, and 5 were found more potent than Prednisolone (prednisolone)® and the inhibition of plasma PGE2 for these compounds were found more potent than prednisolone (prednisolone)®. The analgesic activities of all compounds were more potent than Valdecoxib (Bextra)®. Also, the compounds 1b, 2a, and 3b are the most potent antiparkinsonism agent comparable to Benzatropine (Benzotropene)®. The pharmacological properties are reported. [Journal of American Science 2010;6(7):353-357]. (ISSN: 1545-1003).

Keywords: Pyridazine; Anti-inflammatory; Analgesic; Antiparkinsonism.

1. Introduction

Pyridazine derivatives are currently being developed for the treatment of chronic inflammatory pain associated with osteoarthritis, rheumatoid arthritis and chronic lower back pain **[1,2]**, pyridazines retaing activity in the glia cell based screen for concentration dependent suppression of 1L/B production **[3,4]**. Pyridazine derivatives were found as anti-proliferative and anti-viral activity **[5]**, antinuclear and anti-bacterial action against *Helicobacter pylori* **[6]**, NMDA and AMPA receptor antagonistic action, anti-microbial and anti fungal activity **[7]**. In view of these observations used some novel pyridazine derivatives 1-6 which synthesized according Ref. **[8]**, tested their anti-inflammatory, analgesic and antiparkinsonism activities in comparison to some reference drugs.

2. Material and Methods

Determination of Acute Toxicity (LD_{50}): The LD_{50} for compounds were determined by injected different gradual increased doses of the tested compounds to adult male albino rats, then calculating the dose corresponding to 50 % animal death, according to Austen et al. **[9]**. (Table 1)

Anti-inflammatory Activity

(Carrageenan)®-induced Edema (Rats Paw Test): Groups of adult male albino rats (150-180gm), each of eight animals were orally dosed with tested compounds at a dose level of 25–50 mg/kg one hour before (carrageenan)® challenge. Foot paw edema was induced by subplantar injection of 0.05 cm^3 of 1% suspension of (carrageenan)® in saline into the plantar tissue of one hind paw. An equal volume of saline was injection to the other hand paw and served as control. Four hours after drug administration the animals were decapitated, blood was collected and the paws were rapidly excised. The average weigh of edema was examined for the treated as well as the control group and the percentage inhibition of weight of edema was also evaluated. (Prednisolone)® (5mg/kg) was employed as standard reference against which the tested compounds were compared. (Table 2).

Table 1: Acute toxicity (LD_{50}) of the selected compounds

Compound No.	LD_{50} [mg/kg]
1a	2.068±0.012
1b	2.478±0.013
1c	2.100±0.012
2a	2.150±0.013
2b	1.820±0.011
3a	1.914±0.012
3b	2.561±0.011
4	2.705±0.011
5	2.681±0.012
6	1.185±0.011
Prednisolone® (ref.)	1.618±0.016

Estimation of plasma prostaglandin E2 (PGE2)

Heparinized blood samples were collected from rats (n=8),plasma was separated by centrifugation at 12,000g for 2 min. at 40 °C, immediately frozen and stored at 20 °C until use. The design correlate EIA prostaglandin E2 (PGE2) kit

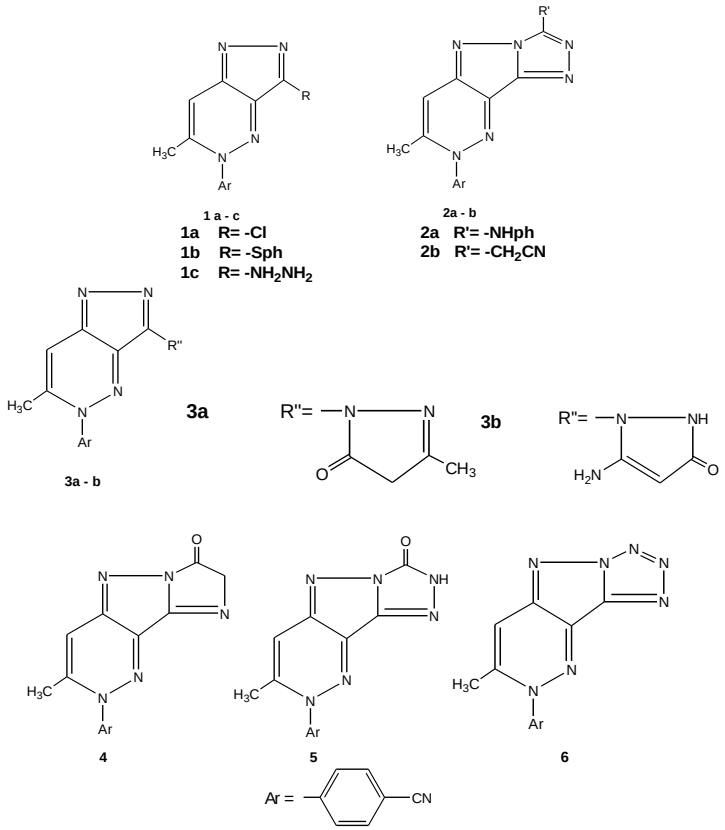

(Aldrich ,Steinheim ,Germany) is a competitive immuno assay for the quantitative determination of PGE2 in biological fluids. The kit uses a monoclonal antibody to PGE2 to bind, in a competitive manner, the PGE2 in the sample after a simultaneous incubation at room temperature. The excess reagents were washed away and the substrate was added, after a short incubation time the enzyme reaction was stopped and the yellow color generated was read on a micro plate reader DYNATech, MR5000 at 405nm (Dynatech Industries Inc., Mclean,VA, USA).The intensity of the bound yellow color is inversely proportional to the concentration of PGE2 in either standard or samples.

Analgesic Activity

Sixty Webster mice of both sexes weighting 20-25 gm were divided into 10 groups. One group was kept as control (received saline), the second group received vehicle (Gum acacia) and the third one received Valdecoxib (Bextra)® as a reference drug, where as the other groups received the test compounds (SC administration). Mice were dropped gently in a dry glass beaker of 1dm^{3}capacity maintained at 55-55.5 °C. Normal reaction time in seconds for all animals was determined at time in seconds for all animals was determined at time intervals of 10, 20, 30, 45, 60, 90 and 120 minutes. This is the interval extending from the instant the mouse reaches the hot beaker till the animals licks its feet or jump out of the beaker (dose 5mg/kg) [10]. The relative potencies to Valdecoxib (Bextra)® were determined (Table 3)

Antiparkinsonism Activity

The muscarinic agonists Tremorine and Oxotremorine induce parkinsonisim like signs such as tremor, ataxia, spasticity, salivation, lacrimation and hypothermia. These signs are antagonized by antiparkinsonism agents. Groups of eight mail mice (18-20g) were used. They were dosed orally with the tested compounds (5mg/kg) or the standard Benzatropine [(Benzotropene)® mesilate,5mg/kg] [11] 1h.prior the administration of 0.5mg/kg of Oxotremerine S.C.Rectal temperature was measured before administration of the compounds and 1h. after (Oxotremerine) dosage. The scores for the recorded signs are zero (absent), one(slight), two(medium), and three (high). (Table 4) .

Table 2: Anti-inflammatory activities of some new synthesized compounds

Compound No.	Dose[mg / kg]	Protection against carrageenan-induced edema[%]*	Inhibition of plasma PGE2 [%]*
1a	25 50	87.16±0.058 98.41±0.072	84.61±0.0110 95.16±0.0120
1b	25 50	93.65±0.080 95,10±0.076	78.62±0.096 82 .66±0.087
1c	25 50	92.12±0.066 93.15±0.075	77.41±0.088 81.56±0.086
2a	25 50	91.58±0.090 97.16±0.082	95.55±0.110 92.33±0.087
2b	25 50	90.16±0.077 96.18±0.075	81.16±0.088 91.62±0.100
3a	25 50	63.86±0.065 84.10±0.067	53.11±0.088 73.82±0.079
3b	25 50	55.70±0.069 74.13±0.070	50.99±0.100 71.00±0.098
4	25 50	65.80±0.076 87.16±0.081	48.16±0.028 79.77±0.079
5	25 50	93.44±0.086 96.18±0.083	89.44±0.085 92.96±0.094
6	25 50	38.14±0.054 55.22±0.052	31.16±0.076 43.18±0.088
Prednisolone®(ref.)	25 50	81.00±0.100 93.01±0.082	77.00±0.084 91.00±0.087

Table 3: Analgesic Activities of some novel selected compounds

Compound No.	Comparative analgesic potency to valdecoxib after time in minutes			
	1 10min	30min	60min	120min
1a	0.46±0.01	0.51±0.04	0.68±0.06	1.30±0,08
1b	0.42±0.01	0.46±0.04	0.56±0.05	1.11±0.07
1c	0.74±0.03	0.98±0.09	1.23±0.11	2.20±0.20
2a	0.46±0.01	0.62±0.06	0.76±0.07	1.63±0.06
2b	0.44±0.01	0.51±0.05	0.60±0.06	1.28±0.16
3a	0.50±0.01	0.80±0.07	0.86±0.08	1.89±0.08
3b	0.46±0.02	0.58±0.05	0.73±0.07	1.58±0.04
4	0.46±0.01	0.96±0.08	1.01±0.01	2.15±0.18
5	0.54±0.01	0.85±0.05	0.96±0.08	2.22±0.21
6	0.65±0.02	0.80±0.07	1.12±0.14	2.40±0.14
Valdecoxib (ref.)	1.00	1.00	1.00	1.00

All results were significantly different from the standard and normal control value at p=0.05

Table 4: Antiparkinsonism activity of several compounds as compared with Benzatropine

Compound No.	Salivation and lacrimation score		Tremors score		% decrease from oxotremerine rectal temp.		Relative potency to Benzatropine	
Control	0	1	0	1	0	1	0	1
Benzatropine								
1a	2		2		28		0.45	
1b	2		2		28		0.83	
1c	1		1		13		0.61	
2a	2		2		19		0 .82	
2b	1		1		12		0.54	
3a	2		2		16		0.71	
3b	3		3		21		0.83	
4	3		3		18		0.42	
5	2		2		5		0.18	
6	3		3		4		0.15	

3. Results and Discussions

Three pharmacological activities namely, anti-inflammatory, analgesic and antiparkinsonism were tested despite their different biological receptors. Yet both are of neurological origin. Ten representative compounds 1-6 were studies with respect to their anti-inflammatory, analgesic and antiparkinsonism activities.

Anti-inflammatory Activity

Purpose and Rational: For the determination of the antiphogi-stic potency of the compounds, two standard tests were realized at 25 and 50 mg / kg rat body weight namely, the protection against (Carrageenan)® induced edema according Winter et al. [12] and the inhibition of plasma PGE2. The later is known as a good confirming indicator for the (Carrageenan)® induced rat paw edema [13]. Regarding the protection against (Carrageenan)® induced edema, six compounds namely 1a, 1b, 1c, 2a, 2b and 5 were found more potent than (Prednisolone)®.Where, their protection percentage against (Carrageenan)® induced edema at two dose levels 25 and 50mg/kg are 87.16±0.058/98.41±0.072, 93.65±0.080/95.10±0.076,92.12±0.066/ 93.15±0.075, 91.68±0.090/97.16±0.082,90.16±0.077/ 96.18±0.075, and 93.44±0.086/69.18±0.083 respectively [(Prednisolone)® 81.00-0.010/93.01±0.082]. On the other hand, the inhibition of plasma PGE2 for the compounds 1a, 1b, 1c, 2a, 2b and 5 were found more potent than (Prednisolne)® at two tested doses levels 25 and 50mg/kg. The inhibition percentage for the latter compounds were found as: 84.61±0.110/ 95.16±0.120,78.62±0.096/82.66±0.087, 77.41±0.088/ 81.56±0.086,95.55±0.110/92.33±0.087, 81.16±0.088/ 91.62±0.0100, and 89.44±0.085/92.96±0.094 respectively. (Table 1)

Analgesic Activity

All tested compounds exhibited analgesic activity in a hot plate assay. Interestingly, the analgesic activities of the all compounds were more potent than Valdecoxib (Bextra)® as a reference drug (Table3). Compounds 1a, 1b, 2a, 2b, 3a and 3b are arranged in descending order of analgesic potency. Compound 1c, 4, 5 and 6 showed more twice times the activity of Valdecoxib (Bextra)® after two hours .

Antiparkinsonism Activity

Compounds 1a, 1c, 2b, 3a and 4 showed moderate activity relative potencies to Benzatropine [(Benzotropene)® 0.45, 0.61, 0.54, 0.71 and 0.42]. Compounds 1b, 2a and 3b are the most potent antiparkinsonic agents (0.83, 0.82 and 0.83 relative potencies). But compounds 5 and 6 are weak activity (relative potencies 0.18 and 0.15) (Table 4).

Pharmacological screening

All animals were obtained from the Animal House Colony, Initially the acute toxicity of the compounds was assayedvia the determination of their LD50. All compounds were interestingly less toxic than the reference drug (Prednisolone)®. (Table1) Then the newly compounds were screened pharmacologically for their anti-inflammatory, analgesic and antiparkinsonism activities using male albino rats. (Tables 2,3 and 4).

Acknowledgements:

The Kind help of Dr. Ahmed A .S .Fayed, Pharmacy department, College of Health Sciences, Taibah Univeristy, for carrying out the synthesis chemical compounds are acknowledged [8].

Corresponding Author:
Dr. Naif O. Al-Harbi
Pharmacy Department
College of Health Sciences
King Saud University 106150, Kingdom of Saudi Arabia
E-mail: drnaifalharbi@yahoo.com

References

1. Beswick p. ,Bingham S. ,Boutra C. and Brown T. Bio. Org. Med. Chem. Lett. , 21 , 445 (2004).
2. Whitehead A.J. ,Ward R.A. and Jons M.F. ,Tetrahedron lett. ,48, 911 (2007).
3. Rolay Ronaivo H. ,Craft J.M.,Hu W. and Wing L.K.,Neurosci . , 26, 662 (2006).
4. Hu W. ,Ranaivo H.R. and Wing L.K. ,Bio. Med. Chem. Lett. , 17, 414 (2007).
5. Meade E.A. ,Wortin L.L. ,Drach J.C. and Town S.L. ,J. Med. Chem. , 40, 794 (1997).
6. Hagihara M. ,Shibakowan N. and Keiichi I. ,PCT Int. Appl. Wo 2000077003 AI.21Dec.2000 ,42PP,C.A. ,13456679F (2001).
7. Malinkaw W. ,Redzicka A. and Lozach O. , IL. Farmaco , 59, 457 (2004).
8. Fayed A.S. ,Flefel E.M. ,Sabry N.M. and Hosni H.M. ,W.J. Chem., 4, 66, (2009).
9. Austen K.F. and Brocklehurst W.E. ,J. Exp. Med. , 113, 521, (1961).
10. Tgolsen A. ,Rofland G. H. ,Berge O.G. and Hole K. , J. Pharmacol. ,Ter. , 25, 241 (1991).
11. Vieweg H. ,Leistner S. and Wanger G. ,Pharmazie , 43, 358, (1988).
12. Winter C.A. ,Risely E.A. and Nuss G.W. ,Proc. Soc. Exp. Bio. Med. , 111, 541 (1962).
13. Herrmann F. ,Lindemann A. ,Gamass J. and Mertelsmann R., Eur. J. Immunol. , 20, 2513, (1999).

6/20/2010

Numerical Simulation of the Mass Flow of Leachate in a Municipal Solid Waste Fill (Part 2) - Vertical Flow Systems

Olayiwola Ademola Gbolahan Oni PhD

University of Ado-Ekiti, Ado Ekiti, Nigeria, West Africa
Current Address: Proworks Ltd., 13 Newman Street, Southampton, UK
onilayi@gmail.com

Abstract: A numerical simulation of the mass of leachate solute in a vertical flow system in a waste fill has been undertaken. The simulation technique involves dividing the waste body into refuse layers of equal and constant volumes and iterating with different time-steps. The principle of mass conservation in steady flow continuity has been applied to replicate the characteristics of the measured solute in saturated and oversaturation conditions of vertical flow in a waste fill. Comparison of modeled and the actual measurements shows a reasonable fit, indicating that the simulation model and underlying principles are suitable for simulating the solute mass flux. [Journal of American Science 2010:6(7):358-366]. (ISSN: 1545-1003).

Keywords: municipal waste, leachate solute, simulation, vertical flow, waste layers

1. Introduction

The negative consequence of the practice of waste landfill has been the driving force for continuous effort to minimise the volume of biodegradable and recyclable components of the stream of municipal waste sent to landfill sites in the developing nations of the world. In the UK, despite the bottom position of "landfilling" in the waste management hierarchy, and the utmost priority given to composting and waste recycling, landfill sites still remain the final destination of 85% of municipal solid waste (Price, 2001). A lot of well documented investigations have shown that leachate emissions, especially from old landfills (Kjeldsen, 1993; Kjeldsen et al., 1998; Looser *et al*., 1999; Baun *et al.*, 2000), which have existed prior to the promulgation of stringent laws that require engineering of landfills, can pollute groundwater resources. In an era of worldwide fiscal austerity and lean resources for avoidable calamities, there has been a lot of governmental funding into the understanding of the formation and containment of leachate, which is the potential pollution by-product of the landfill of waste. For instance, in the UK, the tax credit scheme enables landfill site operators to contribute money to enrolled Environmental Bodies (EBs) to undertake works and waste researches which, are included in the approved environmental projects contained in the Landfill Tax Regulations (ENTRUST, 2010). Although leachate is often referred to the leached wastewater exiting landfill sites; in reality, leachate is the leached water within the landfill, starting from the topmost layers to the basal layers.

Whereas the early investigations on waste were undertaken on the bulk waste quantity and chemical composition of the contaminant solute inherent in the leached water (Farquhar, 1973; Thompson and Zandi, 1976; Berger *et al*., 1996, Reinhart and Al-Yousfi, 1996), recent investigations have focused more on the leachate quantity in the waste lifts (Bleiker, 1995; Oni, 2000; Oni and Richard, 2004; Oni and Okunade, 2009) and the characteristics of the mass flux of the solute in the bulk waste (Rosqvist and Bendz, 1999; Rosqvist and Destouni 2000; Beaven and Hudson, 2003; Beaven et al., 2005; Rosqvist *et al*., 2005). Ever since the foremost classic investigations on waste by Farquhar and Rovers (1973) and Sowers (1973, it has been acknowledged that waste is complex in occurrence, formation, nature, emplacement. The heterogeneity of waste varies within site, and from site to site. Therefore, there has not been any formulated model that has been able to universally or exactly model the physical and chemical properties of waste fills (El Fadel *et al.*, 1997). Bearing this in mind, any large-scale experiment or model that can reasonably replicate the in situ properties of waste is an accomplishment.

Numerical modelling is common for simulating the characteristic of porous material, especially soils (Narasimhan and Witherspoon, 1978; Indraratna and Redana, 2000; Hatami and Bathurst, 2006); however there has not been any known significant work undertaken on the solute mass flow in various layers of the waste fills. In most cases, the simulation on the solute of the leached water in waste fills has been stochastically undertaken to estimate the volumetric content of the inherent water participating in the bulk volume of the waste fill.

In this paper, the modelling of the mass flow of leachate in various layers of a waste fill has been undertaken using a formulated simulation model. In

the first part of the series of this topic, the fundamentals of simulation technique as applied to steady flow in a recycling flow pattern in waste fills was explicitly described. In this paper fundamentals, as applied to vertical flow systems is described and used for the 2-dimesional visualisation of various simulation's assumed conditions. As the majority of reported investigations on landfill leachate has been on vertical flow systems, this study will be of interest to stakeholders in the Waste industry. Efforts have been made not to literarily repeat many aspects that have been well described in Part 1.

2. Methodology

2.1 Experimental data

A mass flow model has been formulated and used to simulate the mass flow (concentration flux) in the vertical flow in a waste fill located in large-scale test cell reported by Oni (2009). A diagrammatic description of the tests is depicted in Figure 1. The test procedure has been well described in a previous paper (Oni, 2009). Tracers were used to trace the movement of the leachate solute thus enabling the mass flux to be monitored via the concentration measurements. In the oversaturated condition, tracers, Lithium (30mg/l), Bromide (345mg/l), Coomassie Brilliant Blue (0.1g/) and Sodium Chloride (5g/l) were introduced into the surface pond overlying a waste fill in a steady flow condition. The tracers were inputted in "top hat" pulses at 1l/h and sprinkling on the waste in pulses continued for 48 hours following which the sprinkling reverted to water to washout the inherent tracer in the waste. The tests ended when there was evidence that the majority of the tracers have been flushed out through the continuous measurement of the concentration of the outflow from the base of the waste fill, via the gravel bed. The same procedure was undertaken for the saturated flow tests except for not having a surface pond. The tracer and water input in this condition was directly on the surface of the bare waste. In this study, however only the test data for the non-reactive tracer -Sodium Chloride was used for validating the simulation model. It is worth to note that the word "oversaturated" has been used to distinguish the vertical flow with or without surface pond. The enormous side wall flow observed in the vertical flow with surface pond in a previous study (Oni, 2009) perhaps justifies this term.

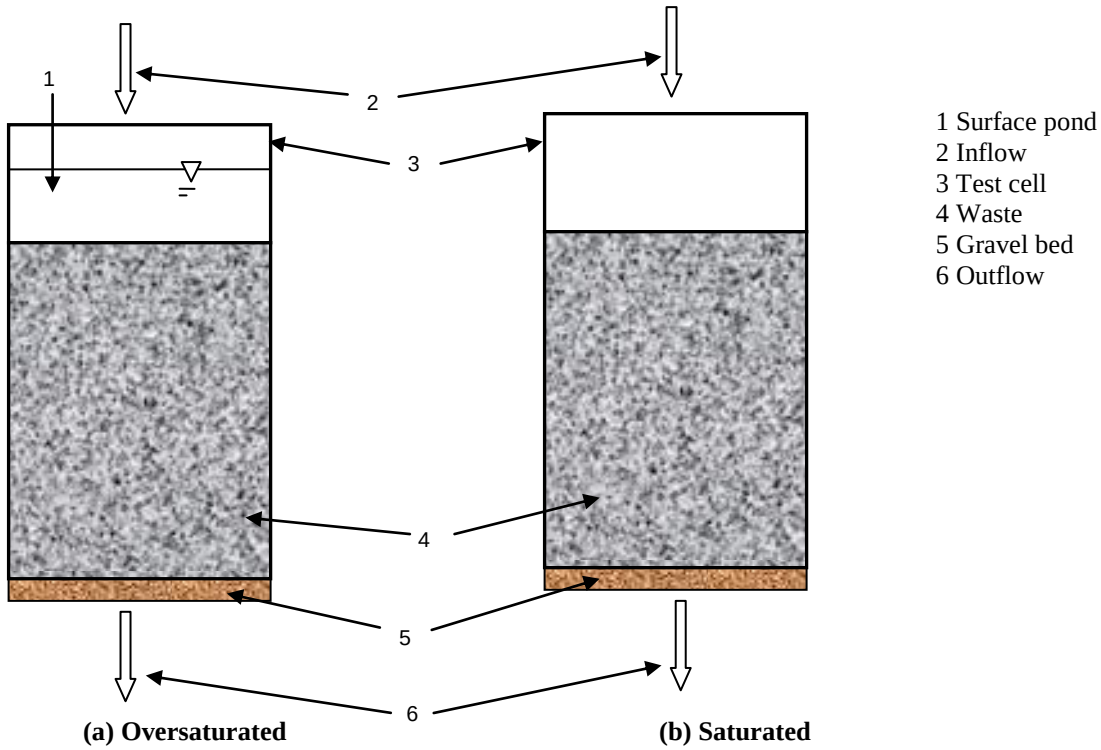

Figure 1: The vertical flow test.

2.2 Simulation process

The waste fill is divided into layers of equal and constant volume. The waste thickness of each layer is not the same due to the heterogeneity of waste. Owing to the variability of waste properties within an emplaced fill, it is assumed that this approach will minimise errors that would have occurred if the waste fill is divided into small grids, commonly used for soils, which are predominantly homogenous. Moreover, there is no acceptable model that can reasonably describe the horizontal and vertical components of flow within a waste grid. The simulation model is conceptualised on conservation of mass for an elemental volume in water flow continuity. It is derived such that there is a mass balance in the flow system of waste layers and adjoining gravel bed and surface pond and is made dimensionless by division by the original concentration of the tracer as follows. The relative concentration is an effective numerical measure of the leachate mass in waste flows and is thus given as:

$$\frac{C_i}{C_o} = \left(\frac{1}{C_o V}\right) \times \left((M_{i-1} + \Delta M) - \left(\left(\frac{M_{i-1} + \Delta M}{V + \Delta V} \right) \times \Delta V \right) \right)$$

[1]

where:

C_i = concentration of the tracer (solute) in an elemental volume at time i

C_o= initial (maximum) concentration of the tracer (solute) at source

V =constant volume of an elemental volume

M_{i-1} = the mass of the tracer (solute) in an elemental volume at time i-1

ΔM = incremental mass of the tracer (solute) added to an elemental volume from time i-1 to time i

ΔV = incremental volume of the tracer (solute) added to an elemental volume from time i-1 to time i.

The flow diagram for the solution technique is similar to the one which has been well depicted in Part 1 of this topic. It consists of the division of the waste fill into layers and applying the simulation model (Equation 1) to the waste pond, waste layers and the basal gravel layer in the iteration pattern described as in Figure 2.

The symbols in the diagram above are defined in the form below:

$\Delta M1_{in}$ = mass of the tracer (solute) input to the layer 1 from time i-1 to time i

$\Delta M1_{out}$ = mass of the tracer (solute) output from layer 1 from time i-1 to time i

n = the number of layers; gb= gravel layer; sp= surface pond

It is worth to note that for any time-step - time i-1 to time i, that:

$\Delta Msp_{out} = \Delta M1_{in}$; $\Delta M1_{out} = \Delta M2_{in}$; $\Delta M2out = \Delta M3_{in}$; $\Delta Mn_{out} = \Delta Mgl_{in}$; ΔMgb_{out} is the measured mass of solute out of the gravel bed.

Whereas the iterations are undertaken for various time-steps and number of waste layers, the volume of each waste layer is limited to a maximum that is equivalent to the pore volume of the basal gravel, which has been measured to be approximately 31. Consequently, the time-step is also limited to a maximum, which is equivalent to time that will enable the maximum volume to pass through an elemental volume under a steady flow condition.

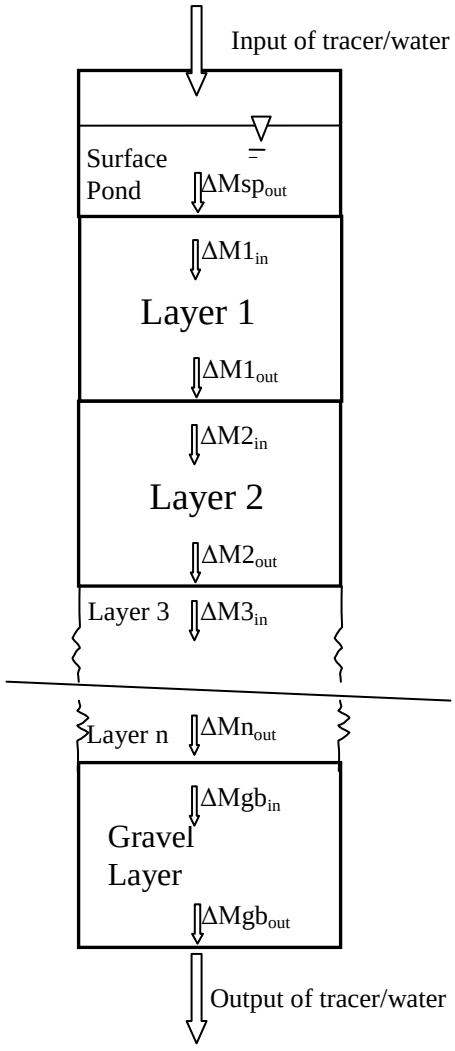

Figure 2: Schematics of the pattern of the simulation's iteration.

3. Results

The simulation in this study has been undertaken for both the saturation and oversaturation conditions of the vertical flow in the waste fill whose

hydro-physical properties were determined and shown in Table 1. The saturated discharge has been previously determined prior to the solute tests to give a full saturation (100%) flow through the waste fill. The oversaturated discharge was made higher to enable steady gravitational flow through the waste using the water head (potential) of the surface pond.

Table 1: Hydro-physical properties of the waste fill

Waste properties	Dry density of waste (kg/m^3)	Volume of surface pond (l)	Pore volume of waste (l)	Pore volume of gravel (l)	Effective porosity-(%)	Discharge rate - saturated (l/h)	Discharge rate -oversaturated (l/h)	Saturated hydraulic conductivity (m/s)
Measured values)	722	11.76	35.17	3.0	7.5	0.547	1.0	1.65×10^{-6}

The simulation has been undertaken for different time-steps and waste layer volumes. The depiction of the breakthrough curve (BTC) for each waste layer and the gravel bed in the saturated conditions of the waste fill using various conditions are shown in Figures 3-6. In general, the trend of the BTC appears relatively similar, consisting of a rise to a peak concentration from an initial zero and then reducing gradually to insignificant values with a long tail end, in all waste layers and gravel bed in varied conditions.

In order to further investigate the influence on the chosen time-step and elemental volume of waste on simulation result, modelling with the maximum allowable pore volume of waste layer with varying time-steps were undertaken and are depicted in Figures 4-6. It is observed that the maximum obtained concentration in each waste layer and gravel bed decreases as the time spread is increased and consequently the BTC becomes more spread out. Comparison of the various modelled BTCs obtained from various assumed conditions with the real BTC from actual measurement (Figure 7) shows that the BTC obtained for the maximum allowable time-step and elemental volume (Layer = 3l; Time-step = 5.5h) is the best replicate, and thus chosen for the simulation.

The simulated and real BTC of Sodium Chloride in the saturated condition is shown in Figure 7. Although the shape of the simulated and real BTC is a bit different, the general characteristics trend of the temporal leachate solute flux is reasonably similar, with both having a maximum BTC of approximately 0.6. Similarly, the simulated BTCs for the layers of oversaturated waste fill in various modelled conditions are shown in Figures 8-10. As in the saturated condition, the characteristic behaviour of the waste appears the same for various simulation conditions and the division of the waste into too many layers (Figure 8) appears to minimise the characteristic differences in the mass flow in different waste layers, thereby nullifying such condition for realistic simulation results. Furthermore, increasing the time-step and elemental volume appears to minimise the error incurred in simulation, as the quantity of temporal mass averaged in each layer during a time-step is increased. The BTC of the leachate solute obtained through simulation and measurements in the surface pond and outflow from the waste fill in the oversaturated condition is shown in Figure 11.

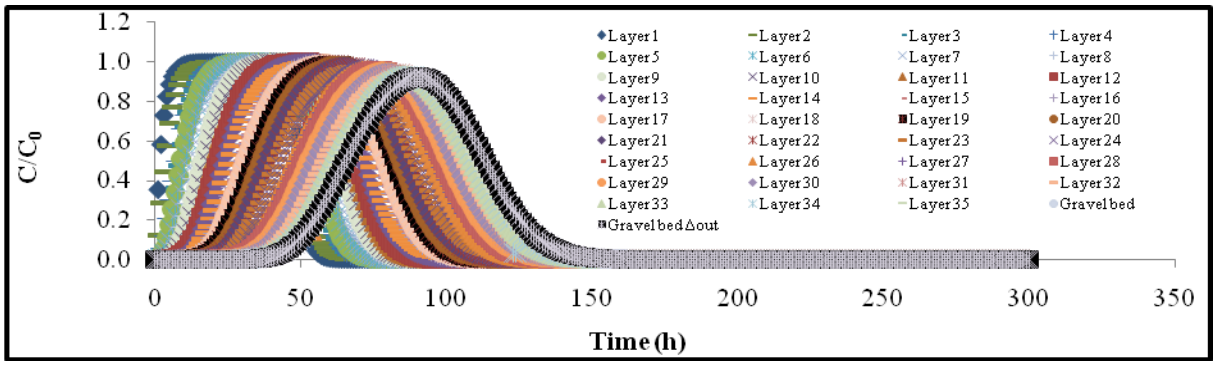

Figure 3: Simulated BTC of Solute Tracer -Sodium Chloride in a Saturated Vertical Flow (Layer = 1l; Time-step = 1h).

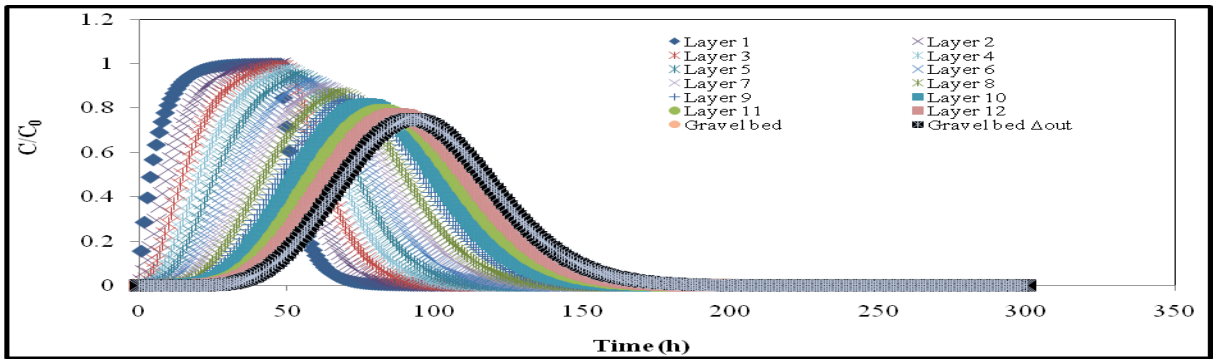

Figure 4: Simulated BTC of Solute Tracer -Sodium Chloride in a Saturated Vertical Flow (Layer = 3l; Time-step = 1h)

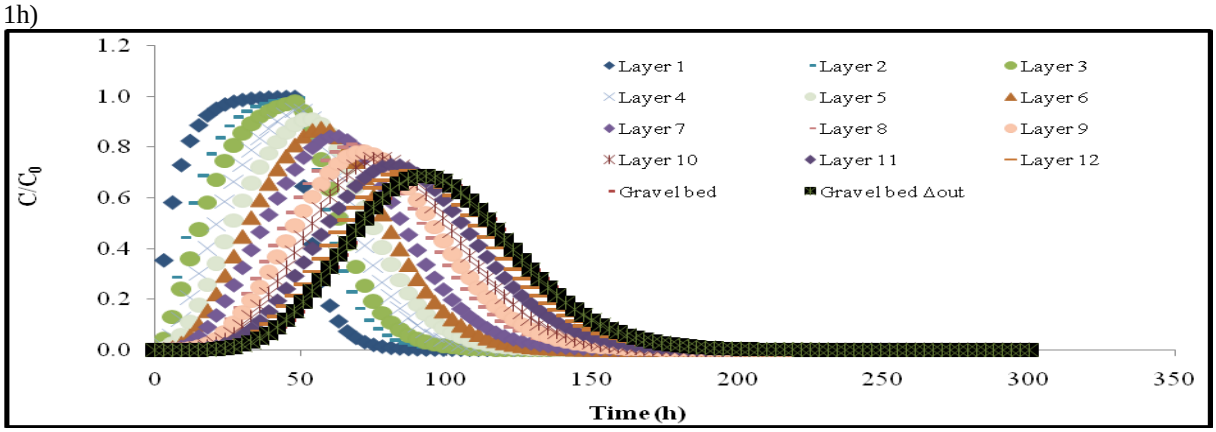

Figure 5: Simulated BTC of Solute Tracer -Sodium Chloride in a Saturated Vertical Flow (Layer = 3l; Time-step = 3h)

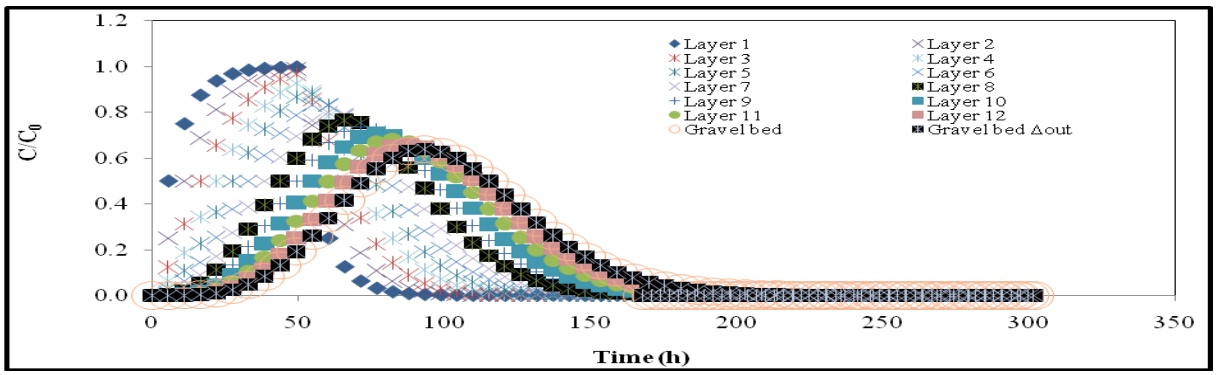

Figure 6: Simulated BTC of Solute Tracer -Sodium Chloride in a Saturated Vertical Flow (Layer = 3l; Time-step = 5.5h)

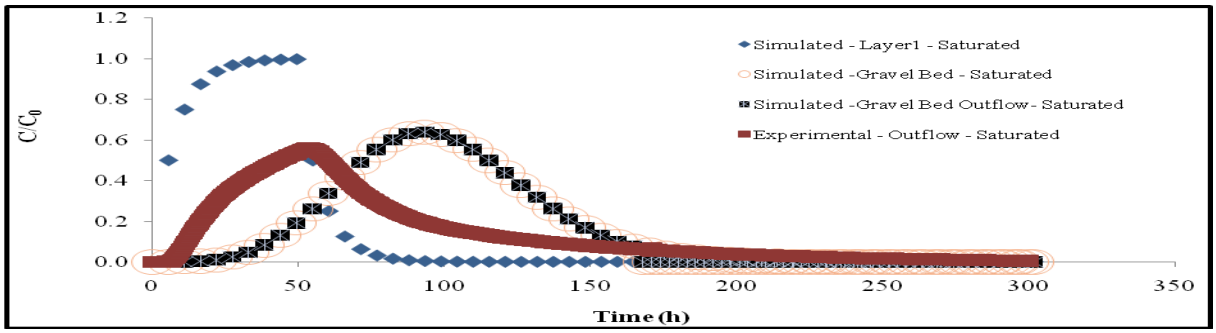

Figure 7: Comparison of Simulated and Real BTC of Solute Tracer -Sodium Chloride in a Saturated Vertical Flow

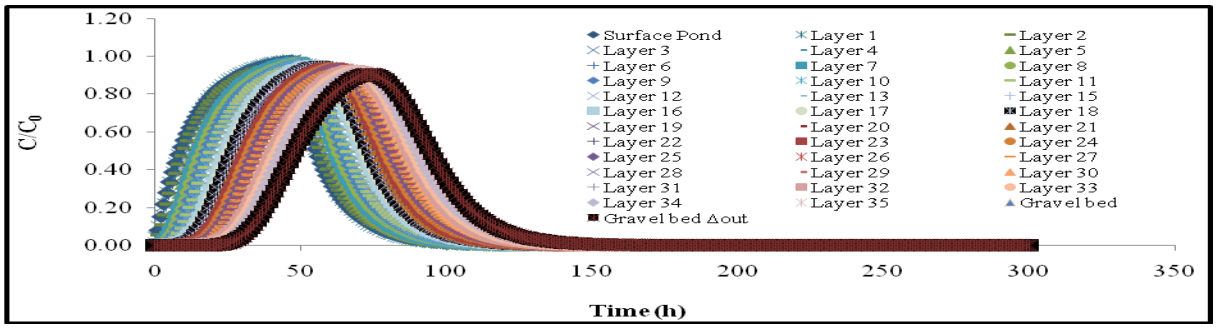

Figure 8: Simulated BTC of Solute Tracer -Sodium Chloride in an Oversaturated Vertical Flow (Layer = 1l; Time step = 1h)

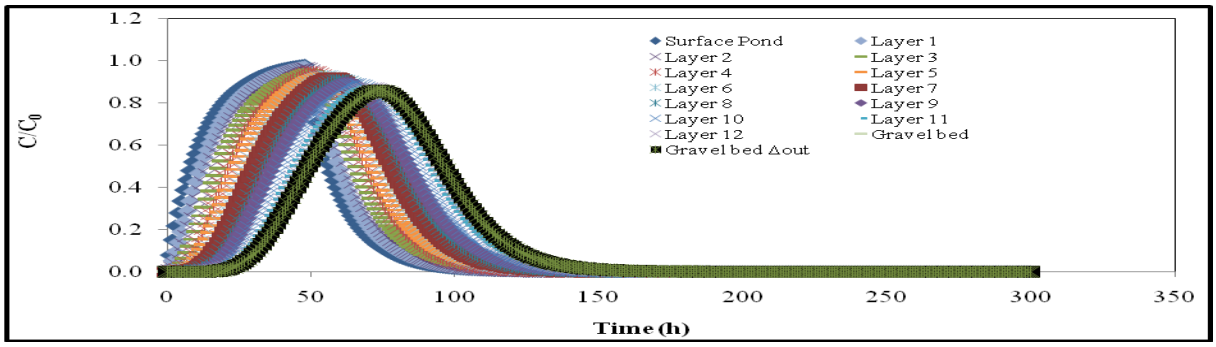

Figure 9: Simulated BTC of Solute Tracer -Sodium Chloride in an Oversaturated Vertical Flow (Layer = 3l; Time-step = 1h)

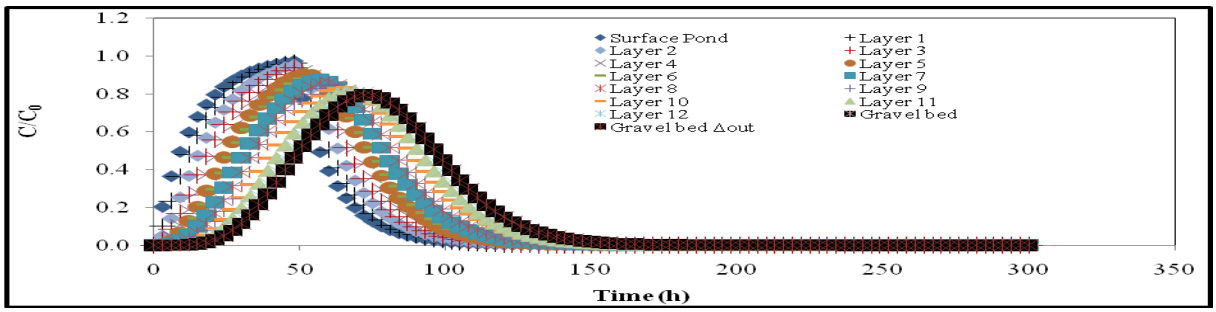

Figure 10: Simulated BTC of Solute Tracer -Sodium Chloride in an Oversaturated Vertical Flow (Layer = 3l; Time-step = 3h)

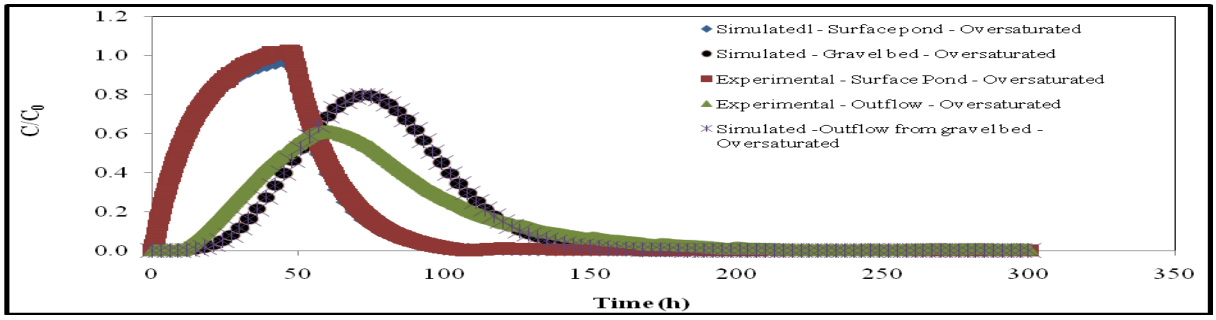

Figure 11: Comparison of Simulated and Real BTC of Solute Tracer -Sodium Chloride in an Oversaturated Vertical Flow

4. Discussion

In general, the shape of the BTC varies gradually from the topmost waste layer to the gravel bed; with the maximum concentration in the waste layers closest to the topmost layer. This could be probably explained in terms of dilution of solute in the waste layers as the solute is being transported away from source input/contact, which is the surface of the topmost waste layer. An increase in the number of the waste layers appeared to smooth the difference in the characteristics of each owing to the averaging method of estimation used in the simulation, as seen in Figure 3. However, the rate of change in the waste layers becomes more defined as the time-step and volume of the waste layers chosen are increased. Similarly, the BTC curve becomes more dispersed as the distance of the waste layer from the topmost layer increases. In fact the maximum concentration attained in the gravel bed appears to decrease as the time-step and layer volume is increased. This is owing to minimisation of errors due to the increased mass of solute being used to average the concentration in each waste layer in the simulation process.

The concentration of the temporal volume of leachate out of each waste layer has been computed, although not depicted herein, and are similar to the concentration existing in each layer, as can be seen for the basal gravel bed. This is expected and shows that the simulation technique is correct as it is based on average values of the fast and slow components the mass flow of the inherent leachate flux in each waste layer, gravel bed and the surface pond.

The quick attainment of the maximum concentration in the real BTC compared to the simulated values in Figure 7 is owing to the fast advective solute, and the relatively long tail is due to the relatively slow portion of the solute during tracer inflow and the water washout periods. As earlier stated, dilution becomes more significant as the position of the waste layers from the source of solute input decreases. The basis of the simulation technique is based on full dilution in each waste layer, and the similarity of the real BTC with that of the first layer showed that dilution of the inputted solute with the inherent water in each waste layer and the gravel bed is not 100% owing the relative fast velocity of the solute in preferential flow paths. It thus appears that the real shape of the BTC in the waste layers will be similar to that of the first layer and not smoothen out, as simulated using the average values. However, the simulation has well represented the average characteristic trend of the mass flux in the waste layers of the saturated fill.

In the oversaturated condition, there has been a very good match between the BTC for the surface pond using the measured data and by simulation (Figure 11), and there has been a good match between the simulated and real BTC for the outflow from the waste fill via the grave bed, in comparison to the saturated conditions in Figure 7. In particular, the shape and dispersion of the simulated and real BTC of the outflow appears reasonably similar, compared to saturated conditions. The reason appears obvious. In the oversaturated flow condition, the inputted tracer is thoroughly mixed with the inherent water and thus the solute mass that infiltrates into the waste fill at the topmost layer is well diluted and thus significantly reduces the effect of the fast advective component of the leachate solute in a mass flow through subsequent layers and the basal gravel layer. In saturated layer, the tracer is inputted into the bare waste surface in sprinkles and thus the infiltrating undiluted solute may be transported through a preferential path and thus not fully mixed within each waste layer.

Although the simulation technique appears more suited to the mass flow in the waste fill with overlying pond, the average characteristic trend of temporal leachate mass in the waste fill in varying saturated conditions has been reasonably replicated with the numerical simulation used in this study. Moreover, the individual solute mass within each waste lift has been depicted quantitatively therefore enabling a good visualisation and understanding of leachate flux within a waste fill subjected to a steady state vertical flow. This type of numerical simulation will be quite effective when assessing alternate designs or operation of a landfill system as these require basically the prediction of average flux characteristics under varying flow patterns in the waste fill. In general, this study has shown that numerical simulation is a very effective way of understanding the hydro-physical processes in a vertical flow in a waste fill.

5. Conclusion

Numerical simulation has been successfully used in this study for estimating and visualising the temporal mass of leachate solute in individual layers of a waste fill and the gravel bed under a steady flow state. This has been undertaken by depicting the BTC of saturated and oversaturated flows in a refuse fill

The simulation technique may be useful in assessing and predicting solute flux in varying flow conditions in municipal solid waste fills.

Acknowledgement: The author expresses his profound gratitude to Dr Richard Beaven and Prof David Richards, both of the School of Civil Engineering and the Environment, University of Southampton UK for the financial assistance and

opportunity to be involved in investigations on the hydro-physico mechanics of waste in the world- class Waste group of the school, following the completion of his doctoral studies. This kind gesture has been reciprocated with the global dissemination of the quality knowledge acquired through the publication of this paper and other quality papers by the author on municipal waste fills.

Corresponding Author:
Olayiwola Ademola Gbolahan Oni PhD
University of Ado-Ekiti, Ado Ekiti, Nigeria
Current Address: Proworks Ltd., 13 Newman Street, Southampton, SO16 4FL, UK
E-mail: onilayi@gmail.com

References

1. Price JL. The landfill directive and the
2. challenge ahead: demands and pressures on the UK householder. Resources, Conservation and Recycling 2001; 32(3-4):333-348.
3. Kjeldsen P. Groundwater pollution source characterisation of an old landfill, Journal of Hydrology1993; 412:349-371.
4. Kjeldsen P, Grundtvig A, Winther P, Andersen JS. Characterization of an old municipal landfill (Grindsted, Denmark) as a groundwater. pollution source: landfill history and leachate composition. Waste Management & Research 1998; 16(1):3-13.
5. Looser MO, Parriaux IA, and Bensimon M. Landfill underground pollution detection and characterization using inorganic traces. Water Research 1999; 33 (17):3609-3616.
6. Baun, A., Jensen SD, Bjerg PL, Christensen TH, Nyholm N. Toxicity of organic chemical. pollution in groundwater downgradient of a landfill (Grindsted, Denmark), Environ. Sci. Technol. 2000; 34:1647-1652.
7. ENTRUST, 2010. The Landfill Communities Fund (LCF). http://www.entrust.org.uk/home/lcf. Accessed Novemenber 18 2010.
8. Thompson B, Zandi I. Future of sanitary landfill. Journal of Environmental Engineering Division, ASCE 1975; 101 (EE1):41-53.
9. Berger K, Melchior S, Miehlich G. Suitability of hydrologic evaluation of landfill performance (HELP) model of the US Environmental Protection Agency for the simulation of the water balance of landfill cover systems. Environmental Geology 1996; 28 (4): pp. 181–189.
10. Reinhart DR, Al-Yousfi AB. The impact of leachate recirculation on municipal solid waste landfill operating characteristics. Waste Mangement Research 1996; 14:337-346.
11. Bleiker DE, Farquhar G, McBean E. Landfill settlement and the impact on site capacity and refuse hydraulic conductivity. Waste Management and Research 1995; 13:533-534.
12. Oni, O. A. An investigation into the impact of sequential filling on properties of emplaced waste lifts and moisture stored in a municipal solid waste landfill. PhD Thesis 2000. University Of Southampton, Southampton.
13. Oni OA, Richards DJ. Estimating moisture volume in a municipal solid waste landfill during refuse infill. In Proceedings of the 19th International conference on solid waste technology and management, Philadelphia 2004; 446-455.
14. Oni OA, Okunade E. A basic investigation into the hydro-physical properties of emplaced waste lifts in a MSW landfill". Australian Journal of Basic and Applied Science 2009; 3(2):628-643.
15. Rosqvist H, Bendz D. An experimental evaluation of the solute transport volume in biodegraded municipal solid waste. HESS 3 1999; 429–438.
16. Rosqvist H, Destouni G. Solute transport through preferential pathways in municipal solid waste. Journal of Contaminant Hydrology 2000; 46 (1-2): 39-60.
17. Beaven R P, Hudson A P. Description of a tracer test through waste and application of a dual porosity model. Ninth International Waste Management Symposium, Sardinia 2003.
18. Beaven RP, Dollar L, Oni OA, Woodman ND. A laboratory scale saturated and unsaturated tracer test through waste. HPML International Workshop, University of Grenoble, France 2005; 4p.
19. Rosqvist H, Dollar LH, and Fourie AB, Preferential flow in municipal solid waste and implications for long-term leachate quality: valuation of laboratory-scale experiments. Waste Management & Research 2005; 23 (4):367-380.
20. Farquhar GJ, Rovers FA. Gas production during refuse decomposition. Water, Air, and Soil Pollution 1973; 2:483-495.
21. Sowers GF. Settlement of Waste Disposal Fills. In Proceedings of the 8th International Conference on Soil Mechanics and Foundation Engineering 1973.
22. El-Fadel M, Findikakis AN, Leckie JO. Environmental impacts of solid waste landfilling. Journal of Environmental Management 1997; 50:1-25.
23. Narasimhan T, Witherspoon PNumerical Model for Saturated - Unsaturated Flow in Deformable Porous Media 3. Applications, Water Resources Research 1978, 14(06):1017-1034.

24. Indraratna B,. Redana IW. Numerical modelling of vertical drains with smear and well resistance installed in soft clay. Canadian. Geotechnical Journal 2000; 37:132-145.
25. Hatami K, Bathurst RJ. Numerical Model for Reinforced Soil Segmental Walls under Surcharge Loading. J. Geotech. and Geoenvir. Engrg. 2006;132 (6):673-684.
26. Oni, OAG. Studying Pollutant Solute Transport in Saturated MSW using Multi-Tracer Tests. Australian Journal of Basic and Applied Sciences 2009; 2(4):3727-3740.

14/6/10

The Journal of American Science

ISSN: 1545-1003

The international academic journal, "***The Journal of American Science*"** (ISSN: 1545-1003)**,** is registered in the United States, and invites you to publish your papers.

Any valuable papers that describe natural phenomena and existence or any reports that convey scientific research and pursuit are welcome, including both natural and social sciences. Papers submitted could be reviews, objective descriptions, research reports, opinions/debates, news, letters, and other types of writings that are nature and science related. All the manuscripts will be processed in a professional peer review. After the peer review, the journal will make the best efforts to publish all the valuable works as soon as possible.

Here is a new avenue to publish your outstanding reports and ideas. Please also help spread this to your colleagues and friends and invite them to contribute papers to the journal. Let's work together to disseminate our research results and our opinions.

Papers in all fields are welcome, including articles of natural science and social science.

Please send your manuscript to editor@americanscience.org;
sciencepub@gmail.com;
americansciencej@gmail.com

For more information, please visit http://www.americanscience.org;
http://www.sciencepub.net; http://www.sciencepub.org

Marsland Press
PO Box 180432, Richmond Hill, New York 11418, USA
The United States
Telephone: 347-321-7172; 718-404-5362; 517-349-2362
Email: editor@americanscience.org;
sciencepub@gmail.com;
americansciencej@gmail.com
Website: http://www.americanscience.org
http://www.sciencepub.net; http://www.sciencepub.org

The Journal of American Science

ISSN 1545-1003

Marsland Press

2158 Butternut Drive
Okemos, Michigan 48864
The United States
Telephone: (517) 349-2362

Emails: editor@americanscience.org;
americansciencej@gmail.com

Websites: http://www.americanscience.org;
http://www.sciencepub.net

ISSN 1545-1003